WHO Drug Information

Volume 38 • Number 4 • 2024

Proposed INN: List 132

International Nonproprietary Names for Pharmaceutical Substances

World Health Organization

WHO Drug Information

WHO Drug Information provides an overview of topics relating to medicines development, regulation, quality and safety. The journal also publishes and reports on guidance documents and includes lists of International Nonproprietary Names for Pharmaceutical Substances (INN), ATC/DDD classification and monographs for The International Pharmacopoeia. It presents and describes WHO policies and activities while reflecting on technical and pharmaceutical topics of international and regional interest.

WHO Drug Information is published four times a year and can be ordered from:
WHO Press, World Health Organization, 1211 Geneva 27, Switzerland.
e-mail: bookorders@who.int or on line at http://www.who.int/bookorders

WHO Drug Information can be viewed at:
https://www.who.int/our-work/access-to-medicines-and-health-products/who-drug-information

---

WHO Drug Information, Vol. 38, No. 4, 2024

ISBN 978-92-4-010703-8 (electronic version)
ISBN 978-92-4-010704-5 (print version)
ISSN 1010-9609

WHO Drug Information

Contents

Abbreviations and websites

CHMP	Committee for Medicinal Products for Human Use (https://www.ema.europa.eu/en/committees/committee-medicinal-products-human-use-chmp)
EMA	European Medicines Agency (www.ema.europa.eu)
EU	European Union (https://european-union.europa.eu/index_en)
FDA	U.S. Food and Drug Administration (www.fda.gov)
Health Canada	Federal department responsible for health product regulation in Canada (www.hc-sc.gc.ca)
HPRA	Health Products Regulatory Authority, Ireland (www.hpra.ie)
HSA	Health Sciences Authority, Singapore (www.hsa.gov.sg)
ICDRA	International Conference of Drug Regulatory Authorities (https://www.who.int/teams/regulation-prequalification/regulation-and-safety/regulatory-convergence-networks/icdra)
ICH	International Council for Harmonisation of Technical Requirements for Pharmaceuticals for Human Use (www.ich.org)
IGDRP	International Generic Drug Regulators Programme (https://www.igdrp.com)
INN	International Nonproprietary Names (https://www.who.int/teams/health-product-and-policy-standards/inn)
MHLW	Ministry of Health, Labour and Welfare, Japan (https://www.mhlw.go.jp/english/)
MHRA	Medicines and Healthcare Products Regulatory Agency, United Kingdom (www.mhra.gov.uk)
Medsafe	New Zealand Medicines and Medical Devices Safety Authority (www.medsafe.govt.nz)
Ph. Int	*The International Pharmacopoeia* (https://digicollections.net/phint/2022/index.html#p/home)
PMDA	Pharmaceuticals and Medical Devices Agency, Japan (https://www.pmda.go.jp/english/)
Swissmedic	Swiss Agency for Therapeutic Products (https://www.swissmedic.ch/swissmedic/en/home.html)
TGA	Therapeutic Goods Administration, Australia (https://www.tga.gov.au/)
WHO	World Health Organization (www.who.int)
WHO MHP	WHO Access to Medicines and Health Products Division (https://www.who.int/our-work/access-to-medicines-and-health-products)
WHO RPQ	WHO Regulation and Prequalification Department (https://www.who.int/teams/regulation-prequalification)
WHO PQT	WHO Prequalification Unit (https://extranet.who.int/prequal)
WHO HPS	WHO Health Product Policy and Standards Department (https://www.who.int/teams/health-product-policy-and-standards)

Note: The online version of this issue is available at *https://www.who.int/our-work/access-to-medicines-and-health-products/who-drug-information*

INTERNATIONAL CONFERENCE OF DRUG REGULATORY AUTHORITIES (ICDRA)

14 – 18 OCTOBER 2024

The 19th International Conference of Drug Regulatory Authorities (ICDRA) was held in New Delhi, India from 14 to 18 October 2024. The event was hosted by Central Drugs Standard Control Organization (CDSCO) of India in collaboration with the World Health Organization (WHO).

Close to 700 delegates from regulatory authorities of WHO Member States participated in the 19th ICDRA. The recommendations as presented at the end of the conference are set out on the following pages. They are reproduced here after having been finalized after the conference. Feedback, particularly from non-participating authorities, is welcome.

The first two days of the Conference (pre-ICDRA: 14-15 October 2024) were open to all interested stakeholders. The last three days (main ICDRA: 16-18 October 2024) were exclusive to representatives of national and regional regulatory authorities for medical products.

The theme of the Conference was "*Smart Regulation: Delivering Quality Assured Medical Products for All*".

For any feedback regarding the below recommendations, please contact ICDRA's Secretariat at icdra@who.int.

- 19th ICDRA website: https://icdra2024.in/ICDRA/Homepage
- Information on past ICDRA conferences is available at: https://www.who.int/teams/regulation-prequalification/regulation-and-safety/regulatory-convergence-networks/icdra

ICDRA RECOMMENDATIONS

PRE-ICDRA

THEME: *Smart Regulation: The New Era of WHO Listed Authorities (WLA) and Increased Reliance*

Recommendations to Member States and other stakeholders

1. Promote and advocate for the use of WHO Listed Authorities (WLA) framework, including reliance in all relevant regulatory functions.

Recommendations to WHO

1. Encourage additional National Regulatory Authorities (NRAs) to join the WLA framework and promote transparency in regulatory oversight activities.
2. Work towards expanding the scope of WLA for other types of medical products.

THEME: *Sustainable Local Production of Quality Assured Medical Products*

Recommendations to Member States

1. As an outcome of ecosystem assessment, Member States should tailor their production strategies to meet local health needs effectively, encouraging innovation while addressing the specific demand within their regions.
2. Establish public-private partnerships that streamline national and regional regulatory processes, facilitate harmonization, and address specific local regulatory challenges.

Recommendations to WHO

1. Support hands-on practical education programmes for manufacturers in low- and middle-income countries (LMICs), focusing on Good Manufacturing Practices (GMP), best practices in manufacturing and testing operations, and regulatory compliance, consistent with WHO international standards.
2. Encourage the establishment of training and technology transfer hubs within regions that lack advanced manufacturing capabilities that could also serve as centres of excellence providing regulatory technical assistance and support, training and resources necessary to upscale local production.

THEME: *Strengthening Regulatory Systems Through Partnerships: Coalition of Interested Parties (CIP)*

Recommendations to Member States

1. Share benchmarking outcomes with the CIP Network members to enhance targeted technical and financial support for regulatory system strengthening.

Recommendations to WHO

1. Expand the scope of CIP Network activities to include medical devices, including *in vitro* diagnostics (IVDs).
2. Continue the support to improve communication and coordination among partners and between partners and NRAs to enhance the impact of the targeted interventions.

THEME: *Building Bridges for effective Pharmacovigilance (PV) Systems*

Recommendations to Member States

1. When developing communication plans, strategies and approaches, engage relevant stakeholders and incorporate their inputs into national PV documents to ensure a harmonized approach.
2. Work together, with in-country stakeholders, to integrate pharmacovigilance into public health programmes by fostering interagency cooperation through joint task forces, regular meetings, cross-training, and establishing clear communication channels for consistent data sharing and coordination.
3. Invest in training and development programmes to equip PV professionals with the necessary skills and knowledge.

Recommendations to WHO

1. Provide guidance including tools and appropriate technologies (core variables, relevant forms, performance indicators, e-tools) to ensure harmonized data collection and sharing taking into consideration the current landscape and the unique challenges.

THEME: *Substandard and Falsified (SF) Medical Products: Need and Viability for Global Track and Trace Technologies*

Recommendations to Member States

1. Promote use of harmonized and interoperable global standards for medical product traceability.
2. Update regulatory frameworks to enable and enforce traceability of medical products.

Recommendations to WHO

1. Update and expand WHO guidance on harmonized product identification, labelling and data exchange standards.
2. Facilitate traceability gap analysis and promote best practices through knowledge exchange.

THEME: *Access to Medical Products: Collaborative Registration Procedure (CRP), Facilitated Regulatory Pathways (FRP), Joint Assessment Procedures*

Recommendations to Member States

1. Maximize the use of reliance approaches for post-authorization changes.
2. Consider joining the WHO Collaborative Registration Procedure, if not yet participating.

Recommendations to WHO

1. Advocate for high level of transparency for regulatory functions and sharing unredacted evaluation and inspection reports between regulators.
2. Promote more convergence and risk-based management of post-authorization changes.

Recommendations to other stakeholders

1. Share information on planned and conducted post-authorization changes (PAC) reliance pilots in order to inform new reliance PAC models.

THEME: *Quality of Pharmaceutical Starting Materials*

Recommendations to Member States

1. Improve the regulatory framework to monitor and control excipient supply chain and ensure enforcement.
2. Promote and/or recognize the use of independent third-party accreditation to ensure excipient quality.

Recommendations to WHO

1. Promote awareness on the need and support increased responsibility of the industry to ensure quality and safety of excipients.
2. Encourage regulatory reliance mechanisms based on convergence of requirements.

Recommendations to other Stakeholders

1. All stakeholders in the excipient supply chain to take responsibility and be accountable for the quality and safety of excipients, including production, distribution, storage and use.

THEME: *Regulation of Advanced Therapy Medicinal Products*

Recommendations to Member States

1. Continue working on the implementation of the principles outlined in the WHO Considerations' document (WHO TRS 1048, Annex 3) into regulatory practice. This includes working towards establishing a regulatory framework for cell and gene therapies if none exists or improving on an existing framework to address gaps.

Recommendations to WHO

1. Continue developing guidance and organizing implementation workshops to facilitate the establishment of regulatory frameworks, focusing on taking a risk-based regulatory approach and emphasizing the importance of regulatory convergence and collaboration among countries.

THEME: *Replacing, Reducing and Refining dependence on animal studies (3Rs)*

Recommendations to Member States

1. Engage with cross-sector initiatives that are focused on the development, validation and implementation of non-animal methods and incorporate relevant technological/ methodology advances into new or updated guidelines or legislation and adopt reliance practices where appropriate.
2. Have robust discussions with sponsors to critically evaluate routine control strategies that include animal methods to ensure that their use is scientifically appropriate and that no appropriate alternative method is available.

Recommendations to WHO

1. Publish 3Rs guideline and, where necessary, revise individual product recommendations where advances in technology/methodology can significantly reduce the need for animal use.
2. Provide technical guidance through workshops or training initiatives and develop measurement standards that will support implementation and use of new non-animal methods.

THEME: *African Medicines Agency – from Concept to Reality*

Recommendations to Member States

1. Put in place frameworks, processes, and resources to ensure timeous and consistent implementation of continental and regional regulatory recommendations at country level as well as reliance on other trusted institutions.
2. Ratify the African Medicines Agency Treaty to strengthen the operationalization of a strong continental regulatory system and review legislations to ensure that at a minimum, provisions in the African Union Model Law on Medical Products Regulation are addressed.

Recommendations to WHO

1. Support the African Medicines Agency in establishing a robust foundation to become a trusted agency operating at an equal level of ML3/4 agency and eventually a WLA.
2. Reinforce regulatory systems strengthening, capacity building, including training interventions at national and regional levels.

THEME: *Improving Access to Medical Devices (including IVDs) Through Prequalification and Reliance*

Recommendations to Member States

1. Ensure that reliance principles are embedded in regulatory frameworks and systems for medical devices.
2. Unpack challenges slowing down the implementation of reliance.
3. Continue strengthening collaboration among NRAs at regional and global level.

Recommendations to WHO

1. Continue supporting Member States and Regional initiatives in their efforts to build efficient and effective regulatory systems for medical devices, aligned with international standards and best practices.
2. Expand the CRP for IVDs to products beyond the Prequalification (PQ) scope.

THEME: *Prequalification of Medical Products*

Recommendations to Member States

1. Member states should continue to harmonize their regulatory requirements with those of WHO Prequalification (PQT) and other international requirements for faster access to prequalified products in countries.
2. Member states and other stakeholders should continue to collaborate with PQT and provide the additional capacity required to expand PQT's scope to include new therapeutic areas.

Recommendations to WHO

1. With more NRAs becoming WLAs and others maturing to ML3 and ML4, WHO prequalification should develop a framework for reliance on the work by these agencies or use their work to facilitate prequalification.
3. Continue expanding the scope of prequalification to enable additional procurement and reliance activities.
4. Facilitate greater advocacy by increasing transparency and streamlining of approaches as well as continued dialogue with stakeholders to ensure fit-for-purpose PQT Programme.

ICDRA

THEME: *Effective Regulatory Harmonization and Convergence Through Regional/Continental Networks*

Recommendations to Member States

1. Consider and engage in existing opportunities and multilateral with other regulators in order to execute and implement best practices, to draw lessons, contributing to global efforts to promote public health.

Recommendations to WHO

1. Facilitate the connections and complementarity between the different harmonization initiatives, *"harmonize the harmonization initiatives".*
2. Continue as pivotal interlocutor to assist in connecting the different regions and international initiatives with National Regulatory Authorities.

THEME: *Good Regulatory Practices: a Journey from Global Benchmarking Tool (GBT) to WLAs*

Recommendations to Member States

1. Enhance regulatory systems through WHO Regulatory Systems Strengthening (RSS)'s five-step capacity-building programme that can utilize reliance as an important strategy.

Recommendations to WHO

1. Update the GBT and the methodology used for benchmarking based on experience gained through extensive use of the GBT, and to address new challenges.
2. Expand WLA scope to other health products, such as medical devices.
3. Increase awareness about the WLA framework to promote reliance and facilitate the smooth transition from the Stringent Regulatory Authority (SRA) concept to WLA.

THEME: *Regulation of Medical Devices (Including IVDs): Global, Regional and Country Trends*

Recommendations to Member States

1. Encourage the use of reliance mechanisms as a useful resource to increase efficiency in regulatory decision making and capacity building.
2. Develop/strengthen regulatory systems for medical devices including in vitro diagnostics using the Global Benchmarking Tool Plus Medical Devices (GBT+MD) (once fully operational) and the Global Model Regulatory Framework for Medical Devices including in Vitro Diagnostics at different levels of regulatory controls and maturity.

Recommendations to WHO

1. Accelerate and make available the GBT+MD Tool as a useful resource along with the WHO Global Model Regulatory Framework to elevating the regulatory standards for medical devices including diagnostics at the earliest.
2. Consider revising and expanding the scope of WLA policy to include medical devices and IVDs in line with the roll out of GBT+MD.
3. Coordinate the creation of global training programmes for regulatory professionals, focusing on harmonized approaches to medical device regulation, including engaging and collaborating with regional and global regulatory and training platforms such as collaborating centres.

THEME: *Strengthening and Promoting Networking of National (Quality) Control Laboratories*

Recommendations to Member States

1. Regulatory bodies in each of the member states to advocate their National Quality Control Laboratories to become members of WHO global networks, as well as regional networks and to ensure that the legal provisions are in place to facilitate reliance and recognition amongst National Control Laboratories in the network.
2. National Quality Control Laboratories to promote sharing of information, namely about equipment, analytical techniques, existing competencies and testing data with the WHO networks.

Recommendations to WHO

1. Enhance the role of WHO National Control Laboratory Network for Biologicals (WHO-NNB) and WHO Global Network of Quality Control Laboratories for Pharmaceuticals (WHO-GNP) in advancing the quality of testing in National Quality Control Laboratories, through strengthening the capacity building activities on the several requirements of WHO Good Practices of Quality Control Laboratories (WHO TRS 1052 Annex 4), including auditing.
2. Support the development of best practices on the implementation of a risk-based lot release process for human vaccines.

THEME: *Clinical Trials: from WHA Recommendations to Action*

Recommendations to Member States

1. Improve information sharing and transparency in clinical trial oversight (as per GBT), harmonize regulatory and ethical review framework and implement risk-based approach and appropriate reliance mechanisms for regulatory and ethical review at national and regional levels via Ethics Committees networks.
2. Enhance engagement with patients and their communities/representative groups throughout the research and clinical trial process and address inclusion of under-represented populations in clinical trials such as children, pregnant and lactating individuals and older adults so as to not preclude access to interventions for these populations.
3. Support for academic and public health institutions in acting as leaders and sponsors of multi-Centre and multinational clinical trials is an important initiative needed to build an effective clinical trial ecosystem.

Recommendations to WHO

1. Enhance best practices in clinical trials support by implementation of relevant WHO and other internationally acceptable guidelines (e.g., WHO guidance for best practices for clinical trials 2024), including respective ICH Guidelines (e.g., ICH E6 (R3)) and Declaration of Helsinki (R10), and to encourage starting parallel regulatory and ethics review for clinical trials applications.
2. Facilitate Member States' participation in appropriate platforms for the collection, aggregation, and analysis of safety data in clinical trials and implementation innovative information technologies in clinical trial oversight.

THEME: *Advancements in Regulation of Traditional Medicines: Challenges and Opportunities*

Recommendations to Member States

1. Augment the regulatory infrastructure for making available quality, safe, and effective Traditional Medicine products.
2. Consider collaboration with international or regional regulatory initiatives to support adoption of common standards and reduce regulatory burden.

Recommendations to WHO

1. Support the Member States in developing or adapting regulatory frameworks related to enabling the availability of quality, safe, and effective Traditional Medicine products.
2. Support the Member States in establishing, implementing and augmenting standards of quality, safety and effectiveness of Traditional Medicine products.

THEME: *Quality Management Systems (QMS) for Regulators and Inspectorates*

Recommendations to Member States

1. Leverage digital tools and automation to enhance QMS efficiency and transparency.
2. Invest on QMS consistent implementation and maintenance with a focus on a risk-based approach for continuous improvement and decision-making process.

Recommendations to WHO

1. WHO should regularly update and publicize the examples and practices document on QMS for regulators by incorporating more models of QMS.
2. WHO should consider training and capacity building activities in the area of QMS for regulators through learning opportunities as well as connection and cooperation among national regulatory authorities.

THEME: *Norms and Standards for Medical Products: Efficient Management of post-approval changes*

Recommendations to Member States

1. Reliance and recognition - explore and implement reliance and recognition mechanisms to avoid duplication of efforts and streamline post approval changes processes.
2. Trust building among Member States - identify agencies they feel comfortable relying on and build trust with those agencies for reliance purposes.
3. Alignment of timelines - work towards aligning timelines for post approval changes to reduce variability and improve efficiency.

Recommendations to WHO

1. Framework for Post Approval Changes - develop a comprehensive framework for post approval changes that serves the needs of Member States addressing both pharmaceutical and biological products.
2. Advocacy and training - enhance advocacy and training on existing guidelines to ensure their application and implementation by Member States.
3. Communication and management of Post Approval Changes - establish a clear communication and management process for post approval changes, including a repository of information for Member States.

THEME: *SF Medical Products: Artificial Intelligence (AI), Machine Learning (ML) and Barcodes: The Time for Global Use?*

Recommendations to Member States

1. Investigate the role and acceptability for web trawling tools based on AI/ML that detect illegal or SF medical products.
2. Prioritize a return-on-investment analysis for implementation of AI in regulatory processes.

Recommendations to WHO

1. Conduct mapping on how AI can contribute to efficient regulatory practices.
2. Develop guiding principles for use of AI in regulatory practices.

THEME: *How to best regulate medicines for children and pregnant & lactating individuals*

Recommendations to Member States

1. Support broad implementation of the ICH E11A guideline across all WHO Regions so that paediatric extrapolation can be used to increase the efficiency of development of medicines for children.
2. Consider joining international cooperative efforts, such as WHO Paediatric Regulatory Network, International Council for Harmonisation of Technical Requirements for Pharmaceuticals for Human Use (ICH).

Recommendations to Member States and WHO

1. Work towards further work-sharing and global alignment for development of medicines for children.
2. Encourage inclusion of under-represented populations into clinical trials such as pregnant and lactating individuals in order to generate useful evidence for labelling information.

THEME: *Best practices regarding reliance on different Good Practices (GxP) inspections*

Recommendations to Member States

1. Effectively implement a risk-based approach, including working closely with various agencies/authorities to conduct more joint inspections or co-inspections for a prompt decision-making process.
2. Leverage digital tools and automation to minimize duplication of on-site inspections. At the same time, the Member States are to maintain their skill sets and utilize the reliance process.

Recommendations to WHO

1. Consider providing capacity building including hands-on training on reliance and recognition principles in GxP inspections, giving real-life examples and encouraging agencies and inspectorates to follow suit. The focus should not be limited to Good Manufacturing Practices (GMP) only and should include Good Clinical Practices

(GCP), Good Laboratory Practices (GLP), Good Distribution Practices (GDP), Good Storage Practices (GSP), Good Pharmacovigilance Practices (GVP), etc. In addition, WHO should organize training activities for the Member States on risk-based inspections, a subset of the reliance process.
2. Consider developing a database for information sharing of all GxP inspections accessible by the agencies and inspectorates. The access to information through the database would assist the respective agencies and inspectorates in the decision-making process. It is important for the WHO to ensure skill sets are not compromised during the reliance process.

THEME: *Information Management System (IMS) for Regulators (including the role of AI)*

Recommendations to Member States

1. Prioritize the implementation and maintenance of a regulatory IMS to improve decision-making, transparency, and communication with all stakeholders.

Recommendations to WHO

1. Support member states by developing guidance to facilitate the development, implementation and maintenance of regulatory IMS.
2. Support member states by developing a regulatory hub for NRAs to come together to share experiences and good regulatory practices in developing and maintaining regulatory IMS.

THEME: *Regulators' Role in Containing Antimicrobial Resistance (AMR)*

Recommendations to Member States

1. Strengthen national regulatory frameworks, facilitate global scientific research and alignment on new and preserve existing antimicrobials for human and veterinary use.
2. Expand networking and partnerships with stakeholders, including patients and Animal owners organizations under the "One Health" approach.
3. Scale up awareness of AMR among the general public and human and animal health professionals.
4. Enhance information and data sharing to promote Antimicrobial Stewardship and improve access to safe, effective, and quality Antimicrobials.

Recommendations to WHO

1. In collaboration with other members of the "Quadripartite" group (FAO, WOAH, and UNEP) WHO should strengthen its technical support and guidance to member states in implementing the call for action of the 1st Global Joint Summit and the Political Declaration of the United Nations General Assembly High-Level session on AMR.
2. Consider environmental aspects when addressing the specificities of the use of antibiotics for human use.

THEME: *Regulatory Preparedness and Response: Lessons Learned from COVID-19 Pandemic*

Recommendations to Member States

1. Establish adequate mechanisms for sharing regulatory information on medical countermeasures, including manufacturing oversight data, to facilitate reliance on harmonized international regulatory standards and practices.
2. Consider introducing new tools, such as simulations and artificial intelligence, that will allow for quicker response in emergency situations.

Recommendations to WHO

1. Update and expand the scope of current guidelines and tools for timely regulatory approval and post-approval medical countermeasures.
2. Continue efforts on regulatory preparedness capacity building, including training.

***

ESTABLISHMENT OF THE SPECIFIC ABSORBANCE VALUES FOR ALBENDAZOLE AND ATAZANAVIR SULFATE AND THE APPLICATION THEREOF IN THE QC TESTING OF MEDICINES

Danike de Villiers[1], Ilene Brits[2] and Marius Brits[1*]

[1]Faculty of Health Sciences, Centre of Excellence for Pharmaceutical Sciences (Pharmacen™), Potchefstroom, South Africa.
[2]Research Institute for Industrial Pharmacy* Incorporating CENQAM*, North-West University, Potchefstroom, South Africa.

Abstract

Efficient Quality Control (QC) testing of medicines is key to identifying and isolating Substandard and Falsified (SF) medicines to ultimately safeguard the overall health and safety of patients. Ultraviolet / Visible (UV/Vis) spectrophotometric analysis and the use of specific absorbance ($A_{1cm}^{1\%}$) values may benefit the identification of such products by means of procedures that are easy to execute, cost-effective and generates rapid results. Specific absorbance is defined as the absorbance measured at a specific wavelength of a 1% (w/v) sample while using a 1.0 cm pathlength cell. These specific absorbance values are commonly used in the pharmaceutical industry for the identification or quantification of Active Pharmaceutical Ingredients (APIs) in Finished Pharmaceutical Products (FPPs). However, the application of such values is reliant on the quality assured establishment and validation thereof. Concerns have been expressed with regards to the accuracy and validity of specific absorbance values reported in the available literature. This study aims to establish the specific absorbance values of albendazole and atazanavir sulfate and apply these accurate and validated values in the QC testing of FPPs containing these respective APIs. Furthermore, specific absorbance values established and published for zidovudine was used for the QC testing of zidovudine capsules to illustrate the implementation of these newly established and validated specific absorbance values in the quality testing of medicines. This study furthermore assessed the accuracy and validity of the $A_{1cm}^{1\%}$-values reported in *The International Pharmacopoeia* for the mentioned three APIs.

Keywords

Specific absorbance, Quality Control, post-market surveillance, albendazole, atazanavir sulfate, zidovudine.

ESTABLISHMENT OF THE SPECIFIC ABSORBANCE VALUES FOR ALBENDAZOLE AND ATAZANAVIR SULFATE AND THE APPLICATION THEREOF IN THE QC TESTING OF MEDICINES

Introduction

Ultraviolet / Visible (UV/Vis) spectrophotometric analysis is an analytical technique commonly employed for the qualitative and quantitative analysis of medicines.[1,2] This analytical technique allows for rapid and cost-effective generation of results with relative ease of execution compared to other pharmaceutical analytical techniques.[3,4] Specific absorbance values of Active Pharmaceutical Ingredients (APIs) are commonly used in pharmacopoeial monographs during the Quality Control (QC) testing of medicines especially for identification (ID), assay and dissolution testing thereof.[2,5,6] Clarke's Analysis of Drugs and Poisons defines specific absorbance ($A_{1cm}^{1\%}$) as the measured absorbance of a sample with a concentration of 1% (w/v) at a specified wavelength when measured through a 1.0 cm pathlength.[1,2,4,6,7] These reliable and accurate values are a cost-effective means of analysis to deliver rapid results and is relatively simple to execute.

The use of $A_{1cm}^{1\%}$-values may thus be of great benefit to QC laboratories in the testing of medicines to assist in the rapid identification of Substandard and Falsified (SF) medicinal products. SF medicines are medicinal products that do not comply with the defined quality specifications and result in the reporting of out of specification (OOS) results or deliberately misrepresent the content or indication for use thereof.[8,9,10] The prevalence of SF medicines has a direct impact on the health and safety of the patient as well as public health,[11] it is thus critical that the prompt identification of these SF medicines is facilitated by efficient and reliable QC testing procedures.[10] Cost-effective analytical techniques and providing guidance to National Quality Control Laboratories (NQCLs) may aid with the early detection of SF medicines and ultimately benefit the health and safety of the public especially in lower- and middle-income countries.[11,12,13] However, to reap the benefits of using these values in the QC testing of medicines the accuracy and validity of these values need to be established or proven. Concerns have been raised with regards to the validity of $A_{1cm}^{1\%}$-values published in current literature and needs expressed for the establishment of such values are not available in literature.[14,15,16]

In this study $A_{1\,cm}^{1\,\%}$-values for albendazole and atazanavir sulfate have been established using a framework published by De Villiers *et al.*[14] (summarised in Figure 1) to ensure the suitability of the established values for their intended uses (i.e. identification, assay or dissolution testing of medicines). These $A_{1\,cm}^{1\,\%}$-values have been compared to those values previously published, where

available. This study aimed to assess the accuracy and validity of $A_{1cm}^{1\%}$-values published by *The International Pharmacopoeia (Ph.Int.)* for three APIs (i.e. zidovudine, albendazole and atazanavir sulfate). Thereafter the established values were used in the QC testing of zidovudine capsules, albendazole chewable tablets and atazanavir capsules that were commercially available in South Africa in a post-market surveillance (PMS) study.

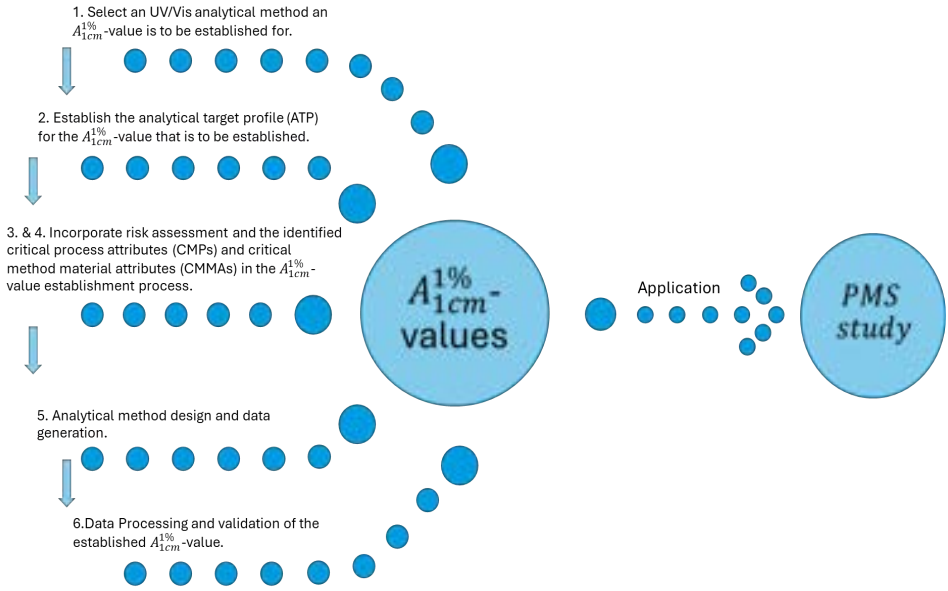

Figure 1: Summary of the systematic framework developed by De Villiers *et al.* to establish specific absorbance values.[14]

The three APIs used in this study are all listed in the World Health Organization (WHO) and South African Essential Medicines Lists (EML) as first line treatment options for their respective therapeutic indications.[17,18] $A_{1\,cm}^{1\,\%}$-values are reported in the specific monographs of *The International Pharmacopoeia* of these respective APIs for QC tests like identification, assay and dissolution. The QC tests that have reported $A_{1\,cm}^{1\,\%}$-values in *Ph.Int.* are summarised in Table 1.

The reliable and efficient QC testing of these API containing products may benefit consumer safety in these regions. The chemical properties of these APIs (i.e. zidovudine, albendazole and atazanavir sulfate) are summarised in Table 1.

Table 1: Summary of the chemical properties of zidovudine, albendazole and atazanavir sulfate

	Zidovudine	Albendazole	Atazanavir sulfate	Reference
Chemical structure	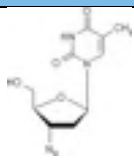 *	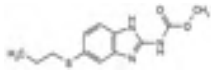 *	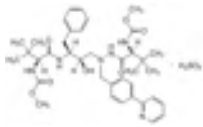 *	
Molecular formula	$C_{10}H_{13}N_5O_4$	$C_{12}H_{15}N_3O_2S$	$C_{38}H_{52}N_6O_7 \bullet H_2SO_4$	
Molecular mass (g/mol)	267.2	265.3	802.9	
Therapeutic classification	Antiretroviral	Antiretroviral	Anthelminthic	
UV maxima (UV_{max}) specified in the respective monographs	ID: 267 nm Assay: 267 nm Dissolution: 266 nm	ID: 308 nm and 231 nm Assay: 308 nm Dissolution: 291 nm	ID: 250 nm and 280 nm Assay: 250 nm Dissolution: 250 nm	(19, 20, 21, 22)
$A_{1\,cm}^{1\,\%}$-value for identification purposes	Yes	None	None	
$A_{1\,cm}^{1\,\%}$-value for assay purposes	Yes	Yes	Yes	
$A_{1\,cm}^{1\,\%}$-value for dissolution testing	None	Yes	Yes	

Materials

Zidovudine (with a purity of 99.2%) and atazanavir sulfate (with a purity of 99.8%) ICRS reference standards were purchased from WHO (EDQM, France). Albendazole secondary reference standard (with a purity of 98.9%) that is traceable to the WHO primary reference standard was purchased from Supelco (Merck, Germany). All solvents used were purchased from ACE Chemicals (ACE Chemicals, South Africa) and LabChem (LabChem, South Africa). Dizovin 100 mg capsules, Zentel 400 mg and Wormadole 400 mg chewable tablets and Atazor 200 mg capsules were procured from a local pharmacy in Potchefstroom, South Africa.

Instruments

Analytical balances from Sartorius research (Sartorius, Germany) and a ScienTech ultrasonic cleaner from Selectech Scientific (Selectech, South Africa) were used. Matching quartz cells with a 1.0 cm cell pathlength from Agilent Technologies (Agilent Technologies, USA) were used. A PerkinElmer UV/Vis Lambda 365 UV/Vis spectrophotometer (PerkinElmer, USA) with UV WinLab ES software (version 6.40) (PerkinElmer, USA) were used. A Labindia DS 800 dissolution apparatus (Labindia, India) was used for the dissolution test studies.

Methodology

Establishment of specific absorbance values

The $A_{1\ cm}^{1\ \%}$-values of albendazole ($C_{12}H_{15}N_3O_2S$) and atazanavir sulfate ($C_{38}H_{52}N_6O_7$) were established utilising the systematic framework for the establishment of the specific absorbance values of an API developed.[14] The $A_{1\ cm}^{1\ \%}$-values for the identification, assay and dissolution testing of both these APIs were established following the six (6) steps in the mentioned framework. The $A_{1\ cm}^{1\ \%}$-values of the prototype API (zidovudine) was also included in this study to illustrate the application of the established values in the QC testing of zidovudine capsules. The pharmacopoeial procedures described in the specific monographs of albendazole chewable tablets[19] and atazanavir capsules[20] were used in establishing the $A_{1\ cm}^{1\ \%}$-values suited for the intended purpose thereof.

Step 1: Selection of UV/Vis analytical method for which the specific absorbance value should be established

The analytical methods, published in the specific monographs of the *Ph.Int.,* for the ID and quantification of albendazole in albendazole chewable tablets, and for the quantification of atazanavir sulfate in atazanavir capsules were selected.[19,20]

Step 2: Establishment of the Analytical Target Profile (ATP)

The ATPs describing the intended use and purpose of the $A_{1cm}^{1\%}$-values were established for identification and quantification purposes of both albendazole and atazanavir sulfate. The required validation parameters for the established $A_{1cm}^{1\%}$-values were defined based on guideline published by De Villiers *et al.*[14]

Steps 3 & 4: Risk assessment, critical method parameters (CMPs) and critical method material attributes (CMMAs) identification

The risk assessment as well as identification of CMPs and CMMAs for establishing $A_{1cm}^{1\%}$-values for UV/Vis spectrophotometric analytical methods as identified by De Villiers *et al.* were considered and all applicable mitigatory steps described were implemented.[14]

Step 5: Analytical method design and data generation

Instrument qualification

The UV/Vis spectrophotometer used was qualified and in good working order. A performance qualification of the instrument was performed each time prior to use thereof to ensure that the instrument was in acceptable working order. A-grade volumetric glassware was used to prepare analytical solutions, and the analytical balances used were suitably qualified as required by international standards.[23]

Environmental conditions

All storage conditions specified by the suppliers of the APIs used in this study, were adhered to. Furthermore, the environmental conditions under which this study took place was controlled and recorded.

Cuvette qualification

The cuvette test was performed on the matching pair quartz cuvettes selected for use in this study. The absorbance of purified water against air was measured at 220 and 240 nm as specified by De Villiers *et al.*[14] The difference in the absorbance measured for purified water before and after a 180°rotation of the cuvette should not be more than 0.005. The transmittance should be at least 85% and 88% at 220 and 240 nm respectively for the cuvette to be considered suitable for use.

Solvent test

The solvent test as described in the framework was performed for all solvents, solvent ratios and dissolution media used to establish $A_{1\ cm}^{1\ \%}$-values for albendazole and atazanavir sulfate.[14] The absorbance of these solvents was measured at the monograph specified wavelength of maximum absorption (UV_{max}) and should not exceed 0.4 in order to be considered suitable for use.

Reference standard solution preparation for the establishment of the specific absorbance values

Reference standard solutions of albendazole and atazanavir sulfate were prepared in triplicate by three independent analysts as required by the framework.[14] Firstly, stock solutions were prepared using suitable reference standard materials of albendazole and atazanavir sulfate as described by the pharmacopoeial analytical procedures.[19,20] A stock solution containing either albendazole or atazanavir sulfate was prepared for each analytical procedure (i.e. ID, assay or dissolution testing) the $A_{1\ cm}^{1\ \%}$-values were to be established for. The method used by Vignaduzzo

et al. was utilised for the preparation of albendazole reference solutions for use in establishing the dissolution testing $A_{1\,cm}^{1\,\%}$-value.[24] A sulfuric acid / methanol mixture was prepared by adding 2 mL of sulfuric acid (98% w/v) to cooled methanol over ice, 5 mL of this mixture was then used to dissolve the albendazole secondary standard before making up to volume with the solvent indicated in the specific monograph method. Then, aliquots of the prepared stock solutions were diluted using the solvents specified in the respective monographs to obtain seven (7) standard solutions from which calibration curves were to be constructed for the three analysts. The concentration ranges and subsequent target concentrations of the standard solutions prepared are summarised in Table 2.

Table 2: Concentration ranges of reference standard solutions prepared for the establishment of the $A_{1cm}^{1\%}$-values

	Albendazole		Atazanavir sulfate		
	ID- and Assay $A_{1\,cm}^{1\,\%}$-value standard solution concentrations	Dissolution $A_{1\,cm}^{1\,\%}$-value standard solution concentrations	ID $A_{1\,cm}^{1\,\%}$-value standard solution concentrations	Assay $A_{1\,cm}^{1\,\%}$-value standard solution concentrations	Dissolution $A_{1\,cm}^{1\,\%}$-value standard solution concentrations
Experimental concentrations	6.40–9.60 (µg/mL)	7.11–21.33 (µg/mL)	9.11–13.67 (µg/mL)	91.12–136.98 (µg/mL)	50.62–151.86 (µg/mL)
Target concentrations	8.00 (µg/mL)	17.78 (µg/mL)	11.39 (µg/mL)	113.90 (µg/mL)	126.55 (µg/mL)

Blank solutions were prepared to contain solvent ratios similar to those used by the analysts in the preparation of the standard solutions (Table 3). The prepared blank solutions were subjected to the solvent test previously described.

UV spectrum recording of the target concentration standard solution

The UV spectra of the standard solutions containing API at the target concentrations (Table 2) specified by each analytical procedure were recorded over the range of 200–400 nm.
The UV_{max} identified should not differ by more than ± 2 nm from that specified in the specific monograph (Table 1) to be considered suitable for further analysis.

Standard solutions analysis

The absorbance of the seven (7) standard solutions (for each API, and its respective application) prepared by three independent analysts were measured at UV_{max}.

Step 6: Data processing and validation of established specific absorbance values

6.1 Data processing of the results reported by the three analysts

Data processing and evaluation was performed in accordance with that described by De Villiers *et al.* in the developed framework for establishment of $A_{1\,cm}^{1\,\%}$-values.[14] Thereafter the $A_{1\,cm}^{1\,\%}$-values were calculated for each API and the respective analytical procedures. To calculate the $A_{1cm}^{1\%}$-values linear calibration curves were constructed for each of the three individual data sets generated by the analysts. Linear regression analysis was performed for these data sets and the linearity was assessed ($r^2 \geq 0.99$). After linearity was deemed suitable the similarity of slopes and

intercepts were evaluated for the three data sets using multiple regression analysis (a p-value of > 0.5 was considered suitable). Once homogeneity of slopes and intercepts were found the data was pooled resulting in a regression equation with one common slope and intercept. However, if homogeneity of slopes were proven but not homogeneity of intercepts – a pooled regression equation was established having one common slope, but the individual intercepts were applied. The $A_{1cm}^{1\%}$-values were then calculated using the regression parameters of the pooled regression data. These values were then validated and assessed to illustrate the suitability for the intended use thereof as described in the framework.[14]

6.2 Validation of established specific absorbance values

The established $A_{1cm}^{1\%}$-values were assessed for compliance to the validation criteria specified in the developed ATPs. The following validation parameters were considered:

Specificity

The specificity of the $A_{1cm}^{1\%}$-value was ensured by utilising a high purity secondary standard of albendazole that was traceable to the WHO ICRS and an atazanavir sulfate ICRS primary reference standard. During analysis of the prepared standard solutions the instrument was blanked with a prepared blank solution that consisted of the solvent system or medium specified in the albendazole chewable tablets and / or atazanavir capsules monographs for the relevant procedure. The composition of the blank solutions used are summarised in Table 3.

Table 3: Summarised composition of the prepared blank solutions

	Albendazole		Atazanavir sulfate	
	$A_{1cm}^{1\%}$-value for ID and assay testing	$A_{1cm}^{1\%}$-value for dissolution testing	$A_{1cm}^{1\%}$-value for ID and assay testing	$A_{1cm}^{1\%}$-value for dissolution testing
Blank solution	Sodium hydroxide (0.1 mol/L)	Hydrochloric acid (~ 10 g/L)	Methanol	Dissolution buffer pH 2.5

Linearity over the reportable / working range

The linearity was assessed for the data generated by the three individual analysts by assessing the relationship between the instrument response and the concentrations of the prepared standard solutions over the reportable / working range as described in the methodology of the mentioned framework.[14] The working range linearity for ID and assay testing was 80–120% of the target concentration of the specific API (i.e. albendazole or atazanavir sulfate) in the applicable monograph. The working range for dissolution testing was 40–120% of the target concentrations of API specified in the applicable monograph.

The linearity was assessed by constructing a linear calibration curve and subjecting the data to least squares linear regression analysis to evaluate the significance of the regression and intercept of the linear equation. Acceptable linearity was indicated if a correlation coefficient (r^2) of ≥ 0.99 was found. Furthermore, non-significance of the intercept (i.e. the intercept did not differ statistically significant from zero) was indicated by a p-value of > 0.05.
The pooled regression line was also assessed for linearity and significance of the intercept(s) using the same criteria stated for assessing calibration curves reported by the three analysts.

Accuracy

The accuracy of the established $A_{1cm}^{1\%}$-value was evaluated by performing a recovery study. Three standard solutions (with known theoretical concentrations) were prepared and analysed; the standard solutions contained target concentrations of the APIs (Table 2) as specified in the analytical procedure of the pharmacopoeial monograph. For assay testing a % recovery that ranged between 98–102% and for dissolution testing that ranged between 95–105% was considered acceptable. The % recovery from the three standard solutions were calculated using the established $A_{1cm}^{1\%}$-value as single-point calibrator to determine the experimental concentration:

$$\%Recovery = \frac{Experimental\ concentration}{Theoretical\ concentration} \times 100$$

Intermediate precision

The intermediate precision of the $A_{1cm}^{1\%}$-value was assessed by considering the variation introduced to the $A_{1cm}^{1\%}$-value when it was established by different analysts on different days. This was assessed by calculating the relative standard deviation (RSD) of three $A_{1cm}^{1\%}$-values calculated from data reported by three individual analysts on different days. An RSD ≤ 1% is considered acceptable.

Application of the newly established specific absorbance values in the QC testing of commercially available medicines

ID, assay and dissolution tests were performed on zidovudine, albendazole and atazanavir sulfate containing products procured locally in Potchefstroom, South Africa. These tests were performed following the procedures described in *Ph.Int.*[19–22] The compliance of these products with the acceptance criteria in the mentioned monographs were assessed using the newly established $A_{1\ cm}^{1\ \%}$-values. The QC tests performed on the respective Finished Pharmaceutical Products (FPPs) are summarised in Table 4.

Table 4: Summary of QC tests performed on medicine products

Test performed	Products tested		
	Zidovudine capsules	Albendazole chewable tablets	Atazanavir sulfate capsules
Visual inspection	X	X	X
Uniformity of weight	X	X	X
ID	X	X	X
Assay	X	X	X
Dissolution testing	X	X	X

Results and discussion

Establishment of specific absorbance values

The results generated in the 6-Step process for the establishment of the $A_{1cm}^{1\%}$-values for application in the QC testing of albendazole chewable tablets and atazanavir capsules are presented and discussed in this section.

Step 1: Analytical method selection

The $A_{1cm}^{1\%}$-values were established for the analytical procedures described by the *Ph.Int.* in the monographs of albendazole chewable tablets and atazanavir capsules.[19,20]

Step 2: ATP for the specific absorbance values that are to be established

The established ATPs for the $A_{1cm}^{1\%}$-values suitable for use in the ID, assay and dissolution testing of albendazole chewable tablets and atazanavir capsules are described in Tables 5–7.

Table 5: ATP for the $A_{1cm}^{1\%}$-value to be utilised in the ID testing

ATP component	Description	
	Albendazole	Atazanavir sulfate
Intended use of method and $A_{1cm}^{1\%}$-value to be established	This $A_{1cm}^{1\%}$-value that is to be established will be used in the identification of albendazole ($C_{12}H_{15}N_3O_2S$) present in chewable tablets using UV/Vis spectrophotometric analysis. A range covering 90–110% of the specified target concentration should be used for the established of the $A_{1cm}^{1\%}$-value for ID-purposes. The UV-spectrum of the albendazole test sample should be recorded and compared to the two reference values reported in the method of analysis. These reported maxima are at about 231 nm and 308 nm with an absorbance of about 0.59 at 308 nm. The test sample with a nominal concentration of 8.00 µg/mL albendazole is prepared by dissolving a powdered sample of the tablets containing approximately 20 mg of albendazole in 50 mL of a 0.01 mol/L hydrochloric acid:methanol solution. Then 1.0 mL of this solution is further diluted to 50 mL with 0.1 mol/L sodium hydroxide. The absorbance of this prepared test sample should be measured using a UV/Vis spectrophotometer using a 1 cm quartz cell. The monograph states that albendazole exhibits two UV maxima at about 231 nm and 308 nm when observed between 220–340 nm with an absorbance value of about 0.59 at 308 nm. The UV-spectrum of the test sample should show similar properties to that specified for albendazole.	This $A_{1cm}^{1\%}$-value that is to be established will be used in the identification of atazanavir sulfate ($C_{38}H_{52}N_6O_7 \cdot H_2O_4S$) present in hard gelatine capsules using UV/Vis spectrophotometric analysis. A range covering 90–110% of the specified target concentration should be used for the established of the $A_{1cm}^{1\%}$-value for ID-purposes. The UV-spectrum of the atazanavir sulfate test sample should be recorded and compared to the two reference values reported in the method of analysis. The absorption maxima for atazanavir sulfate are reported to be of similar intensity and are at about 250 nm and 280 nm. The test sample with a nominal concentration of 11.39 µg/mL atazanavir sulfate is prepared by dissolving a powdered sample of the capsule content containing approximately 22.78 mg of atazanavir sulfate in 20 mL of methanol. Then 1.0 mL of this solution is further diluted to 100 mL with the same solvent. The absorbance of this prepared test sample should be measured using a UV/Vis spectrophotometer using a 1 cm quartz cell. The monograph states that atazanavir sulfate exhibits two UV maxima of similar intensity at about 250 nm and 280 nm when observed between 230–340 nm. The UV-spectrum of the test sample should show similar properties to that specified for atazanavir sulfate.

Table 5: ATP for the $A_{1cm}^{1\%}$-value to be utilised in the ID testing (continued)

ATP component	Description	
	Albendazole	Atazanavir sulfate
Validation parameters and associated acceptance criteria	<u>Specificity:</u> The solvent used during the identification should not present interactions that affect the results obtained by the analytical procedure. The procedure must be able to identify albendazole over the range of 80–120% (6.40–9.60 µg/mL) of the label claim of the product. The target concentration of the test solution is ~ 8.00 µg/mL. <u>Linearity and working range:</u> The procedure must demonstrate linearity ($r^2 \geq 0.99$) over the working range of 80–120% (6.40–9.60 µg/mL) relative to the label claim of the product. <u>Accuracy:</u> Accuracy is proven by means of a recovery study. The acceptable recovery ranges between 98–102%. <u>Intermediate precision:</u> Intermediate precision could be illustrated by evaluating the variability of the established $A_{1cm}^{1\%}$-values when determined by three independent analysts on different days. An RSD ≤ 1% is considered acceptable.	<u>Specificity:</u> The solvent used during the identification should not present interactions that affect the results obtained by the analytical procedure. The procedure must be able to identify atazanavir sulfate over the range of 80–120% (9.11–13.67 µg/mL) of the label claim of the product. The target concentration of the test solution is ~ 11.39 µg/mL. <u>Linearity and working range:</u> The procedure must demonstrate linearity ($r^2 \geq 0.99$) over the working range of 80–120% (9.11–13.67 µg/mL) relative to the label claim of the product. <u>Accuracy:</u> Accuracy is proven by means of a recovery study. The acceptable recovery ranges between 98–102%. <u>Intermediate precision:</u> Intermediate precision could be illustrated by evaluating the variability of the established $A_{1cm}^{1\%}$-values when determined by three independent analysts on different days. An RSD ≤ 1% is considered acceptable.

Table 6: ATP for the $A_{1cm}^{1\%}$-value to be utilised in the assay testing

ATP component	Description	
	Albendazole	Atazanavir sulfate
Intended use of method and $A_{1cm}^{1\%}$-value to be established	This $A_{1cm}^{1\%}$-value that is to be established will be used in the quantitation of the albendazole ($C_{12}H_{15}N_3O_2S$) present in chewable tablets using UV/Vis spectrophotometric analysis. A test sample with a nominal concentration of 8.00 µg/mL albendazole is prepared by dissolving a powdered sample of the tablets containing approximately 20 mg of albendazole in 50 mL of a 0.01 mol/L hydrochloric acid:methanol solution. Then 1.0 mL of this solution is further diluted to 50 mL with 0.1 mol/L sodium hydroxide. The absorbance of this prepared test sample should be measured using a UV/Vis spectrophotometer at about 308 nm using a 1 cm quartz cell. The $A_{1cm}^{1\%}$-value to be established should then be used to determine the amount of albendazole present in the test sample and expressed as % assay relative to the label claim of the tested medicine product. The acceptance criteria for the assay states that the chewable tablets should contain not less than 90.0% and not more than 110% of the amount of albendazole stated on the product label.	This $A_{1cm}^{1\%}$-value that is to be established will be used in the quantitation of the atazanavir sulfate ($C_{38}H_{52}N_6O_7{\cdot}H_2O_4S$) present in hard gelatine capsules using UV/Vis spectrophotometric analysis. A test sample with a nominal concentration of 113.9 µg/mL atazanavir sulfate is prepared by dissolving a powdered sample of the capsule contents containing approximately 22.78 mg of atazanavir sulfate in 20 mL of a methanol. Then 1 mL of this solution is further diluted to 10 mL with the same solvent. The absorbance of this prepared test sample should be measured using a UV/Vis spectrophotometer at about 250 nm using a 1 cm quartz cell. The $A_{1cm}^{1\%}$-value to be established should then be used to determine the amount of atazanavir sulfate present in the test sample and expressed as % assay relative to the label claim of the tested medicine product. The acceptance criteria for the assay states that the capsules should contain not less than 90.0% and not more than 110% of the amount of atazanavir stated on the product label.

Table 6: ATP for the $A_{1cm}^{1\%}$-value to be utilised in the assay testing (continued)

ATP component	Description	
	Albendazole	Atazanavir sulfate
Validation parameters and associated acceptance criteria	**Specificity:** The solvent used during the assay test should not present interactions that affect the results obtained by the analytical procedure. The procedure must be able to quantify albendazole over the range of 80–120% (6.40–9.60 µg/mL) of the label claim of the product. The target concentration of the test solution is ~ 8.00 µg/mL. **Linearity and working range:** The procedure must demonstrate linearity ($r^2 \geq 0.99$) over the working range of 80–120% (6.40–9.60 µg/mL) relative to the label claim of the product. **Accuracy:** Accuracy is proven by means of a recovery study. The acceptable recovery ranges between 98–102%. **Intermediate precision:** Intermediate precision could be illustrated by evaluating the variability of the established $A_{1cm}^{1\%}$-values when determined by three independent analysts on different days. An RSD ≤ 1% is considered acceptable.	**Specificity:** The solvent used during the assay test should not present interactions that affect the results obtained by the analytical procedure. The procedure must be able to quantify atazanavir sulfate over the range of 80–120% (91.12–136.98 µg/mL) of the label claim of the product. The target concentration of the test solution is ~ 113.9 µg/mL. **Linearity and working range:** The procedure must demonstrate linearity ($r^2 \geq 0.99$) over the working range of 80–120% (91.12–136.98 µg/mL) relative to the label claim of the product. **Accuracy:** Accuracy is proven by means of a recovery study. The acceptable recovery ranges between 98–102%. **Intermediate precision:** Intermediate precision could be illustrated by evaluating the variability of the established $A_{1cm}^{1\%}$-values when determined by three independent analysts on different days. An RSD ≤ 1% is considered acceptable.

Table 7: ATP for the $A_{1cm}^{1\%}$-value to be utilised in the dissolution testing

ATP component	Description	
	Albendazole	Atazanavir sulfate
Intended use of method and $A_{1cm}^{1\%}$-value to be established	The established $A_{1cm}^{1\%}$-value is to be used to quantify of the amount of albendazole ($C_{12}H_{15}N_3O_2S$) released from 400 mg chewable tablets after dissolution using UV/Vis spectrophotometric analysis. The amount of albendazole released when subjected to dissolution testing in 900 mL hydrochloric acid (~ 10 g/L) after 30 minutes should be determined. According to the analytical method, albendazole exhibits a UV_{max} at about 291 nm in the specified dissolution medium. The suitably diluted test sample with a nominal concentration of ~ 17.78 µg/mL albendazole in hydrochloric acid (~ 10 g/L) is prepared. The absorbance of this test sample should be measured using a UV/Vis spectrophotometer at about 291 nm using a 1 cm quartz cell. The reported $A_{1cm}^{1\%}$-value should be used to determine the amount of albendazole present in the test sample as % dissolution relevant to the label claim of the tested medicine product. The acceptance criteria for the dissolution states that 80% (Q) of the declared albendazole should be released from the chewable tablets at the stated time.	The established $A_{1cm}^{1\%}$-value is to be used to quantify of the amount of atazanavir sulfate ($C_{38}H_{52}N_6O_7{\cdot}H_2O_4S$) released from hard gelatine capsules after dissolution using UV/Vis spectrophotometric analysis. The amount of atazanavir sulfate released when subjected to dissolution testing in 900 mL dissolution buffer pH 2.5 after 45 minutes should be determined. According to the analytical method, atazanavir sulfate exhibits a UV_{max} at about 250 nm in the specified dissolution medium. The suitably diluted test sample with a nominal concentration of ~ 110 µg/mL atazanavir in dissolution buffer pH 2.5 is prepared. The absorbance of this test sample should be measured using a UV/Vis spectrophotometer at about 250 nm using a 1 cm quartz cell. The reported $A_{1cm}^{1\%}$-value should be used to determine the amount of atazanavir sulfate present in the test sample as % dissolution relevant to the label claim of the tested medicine product. The acceptance criteria for the dissolution states that 75% (Q) of the declared atazanavir sulfate should be released from the capsules at the stated time.

Table 7: ATP for the $A_{1cm}^{1\%}$-value to be utilised in the dissolution (continued)

ATP component	Description	
	Albendazole	Atazanavir sulfate
Validation parameters and associated acceptance criteria	<u>Specificity:</u> The solvent used during the dissolution test should not present interactions that affect the results obtained by the analytical procedure. The procedure must be able to quantify albendazole over the range of 40–120% (7.11–21.33 µg/mL) of the label claim of the product. The target concentration of the test solution is ~ 17.78 µg/mL. <u>Linearity & working range:</u> The procedure must demonstrate linearity ($r^2 \geq 0.99$) over the working range of 40–120% (7.11–21.33 µg/mL) relative to the label claim of the product. <u>Accuracy:</u> Accuracy is proven by means of a recovery study. The acceptable recovery ranges between 95–105%. <u>Intermediate precision:</u> Intermediate precision could be illustrated by evaluating the variability of the established $A_{1cm}^{1\%}$-values when determined by three independent analysts on different days. An RSD ≤ 1% is considered acceptable.	<u>Specificity:</u> The solvent used during the dissolution test should not present interactions that affect the results obtained by the analytical procedure. The procedure must be able to quantify atazanavir sulfate over the range of 40–120% (50.62–151.86 µg/mL) of the label claim of the product. The target concentration of the test solution is ~ 126.55 µg/mL. <u>Linearity & working range:</u> The procedure must demonstrate linearity ($r^2 \geq 0.99$) over the working range of 40–120% (50.62–151.86 µg/mL) relative to the label claim of the product. <u>Accuracy:</u> Accuracy is proven by means of a recovery study. The acceptable recovery ranges between 95–105%. <u>Intermediate precision:</u> Intermediate precision could be illustrated by evaluating the variability of the established $A_{1cm}^{1\%}$-values when determined by three independent analysts on different days. An RSD ≤ 1% is considered acceptable.

Steps 3 & 4: Risk assessment and identification of CMPs and CMMAs

The results of the risk assessment and identification of CMPs and CMMAs as performed by De Villiers *et al.* were considered while executing the volumetric analysis to establish the $A_{1cm}^{1\%}$-values in this study.[14] All required mitigatory steps stated in the mentioned publication were implemented to reduce the impact of the identified risks.

Step 5: Analytical method design and data generation

All instruments and equipment used to establish $A_{1cm}^{1\%}$-values in this study were suitably qualified and deemed to be in good working order before use. Environmental conditions were controlled, and ambient temperature did not exceed 25°C. The suitability for use of the cuvette selected as well as the solvents used during this study was investigated and confirmed. The results for the cuvette test performed are summarised in Table 8.

Table 8: Results of the cuvette qualification

	Albendazole			Atazanavir sulfate		
	Absorbance values	%Transmission values		Absorbance values	%Transmission values	
	240 nm	240 nm	220 nm	240 nm	240 nm	220 nm
Position 1	0.0197	105	95	0.0218	105	93
Position 2 (180˚ rotation)	0.0194	105	94	0.0201	105	93
Difference: (Specification)	0.0003 (NMT 0.005) Result complies	- (NLT 88%) Results comply	- (NLT 85%) Results comply	0.0017 (NMT 0.005) Result complies	- (NLT 88%) Results comply	- (NLT 85%) Results comply

* NMT represents not more than and NLT represents not less than

The differences between the measured absorbance values of purified water before and after a 180˚ rotation of the cuvette were found to be not more than 0.005. The % transmittance at 220 nm ranged between 93–95% and was 105% at 240 nm thus confirming the cleanliness and suitability of the cuvettes for use. The suitability of the solvent was then investigated using the qualified cuvette. The results of the solvent tests performed are tabulated in Table 9.

Table 9: Results of the solvent tests performed

Solvent test for ID and assay $A_{1cm}^{1\%}$-values establishment										
	Albendazole					Atazanavir sulfate				
	- 2 nm	- 1 nm	UV_{max}	+ 1 nm	+ 2 nm	- 2 nm	- 1 nm	UV_{max}	+ 1 nm	+ 2 nm
Wavelength	306 nm	307 nm	308 nm	309 nm	310 nm	248 nm	249 nm	250 nm	251 nm	252 nm
Absorbance: (Specification)	0.0073 (NMT 0.4) Result complies	0.0073 (NMT 0.4) Result complies	0.0072 (NMT 0.4) Result complies	0.0074 (NMT 0.4) Result complies	0.0077 (NMT 0.4) Result complies	0.1199 (NMT 0.4) Result complies	0.1198 (NMT 0.4) Result complies	0.1197 (NMT 0.4) Result complies	0.1231 (NMT 0.4) Result complies	0.1223 (NMT 0.4) Result complies
	✓	✓	✓	✓	✓	✓	✓	✓	✓	✓
Solvent test for dissolution testing $A_{1cm}^{1\%}$-values establishment										
	Albendazole					Atazanavir sulfate				
	- 2 nm	- 1 nm	UV_{max}	+ 1 nm	+ 2 nm	- 2 nm	- 1 nm	UV_{max}	+ 1 nm	+ 2 nm
Wavelength	289 nm	290 nm	291 nm	292 nm	293 nm	289 nm	290 nm	291 nm	292 nm	293 nm
Absorbance: (Specification)	0.0271 (NMT 0.4) Result complies	0.0273 (NMT 0.4) Result complies	0.0272 (NMT 0.4) Result complies	0.0272 (NMT 0.4) Result complies	0.0274 (NMT 0.4) Result complies	0.0271 (NMT 0.4) Result complies	0.0273 (NMT 0.4) Result complies	0.0272 (NMT 0.4) Result complies	0.0272 (NMT 0.4) Result complies	0.0274 (NMT 0.4) Result complies
	✓	✓	✓	✓	✓	✓	✓	✓	✓	✓

The measured absorbance values at UV_{max} ± 2 nm for all solvents used in this study was not greater than 0.4. These solvents were thus considered suitable for use to prepare reference standard solutions for analysis. The UV_{max} values of albendazole and atazanavir sulfate were then determined by three analysts by recording the absorbance spectra of the reference standard solutions nominally containing target concentrations of the applicable reference standard. Examples of the recorded spectra are presented in Figure 2. The results of the UV_{max} values reported by the three independent analysts are summarised in Table 10.

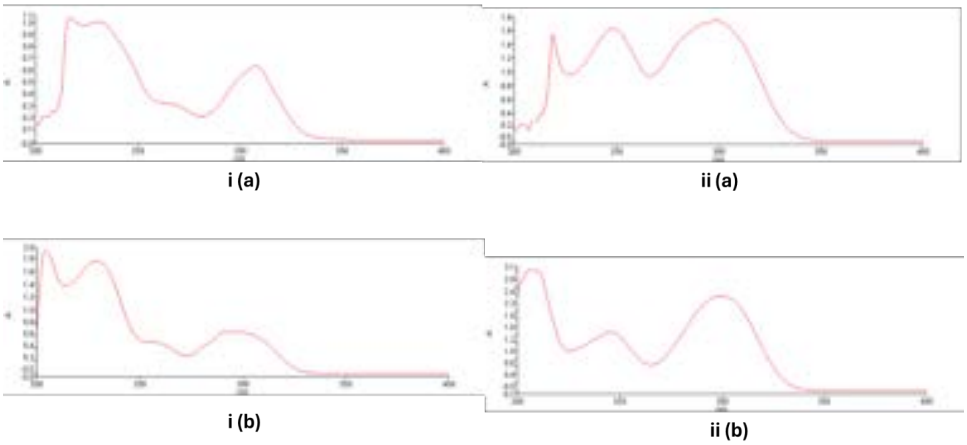

Figure 2: UV spectra for: (i) albendazole and (ii) atazanavir sulfate where (a) is the spectra for the assay $A_{1cm}^{1\%}$-value establishment and (b) for dissolution $A_{1cm}^{1\%}$-value establishment.

From Table 10 it can be seen that the UV_{max} values obtained for albendazole in both solvents did not differ by more than 2 nm from the theoretical UV_{max} values as specified in the applicable monograph. The UV_{max} values for atazanavir sulfate for the establishment of an $A_{1cm}^{1\%}$-value suitable for assay testing did not differ by more than 2 nm from the theoretical UV_{max} value, however, the UV_{max} values reported for the establishment of a $A_{1cm}^{1\%}$-value suitable for dissolution testing differed by 4 nm. This change in UV_{max} may be due to the aqueous dissolution medium and the pH thereof. Literature shows that the UV_{max} of atazanavir sulfate moves to a shorter wavelength in a more aqueous environment compared to that observed in methanol.[25–29] This shift was shown by the prepared reference standard solutions and confirmed by the test samples prepared from atazanavir capsules. The absorbance of seven standard solutions prepared by three independent analysts (as described in section 2.3 – Step 5) were then measured at the experimentally determined UV_{max} values. The absorbance values reported by the analyst were processed in Step 6 and the resulting $A_{1cm}^{1\%}$-values are validated.

Table 10: Results for the experimentally measured UV_{max} values of albendazole and atazanavir sulfate solutions

	Albendazole						Atazanavir sulfate					
	ID and Assay			Dissolution			Assay			Dissolution		
Analyst	**1**	**2**	**3**	**1**	**2**	**3**	**1**	**2**	**3**	**1**	**2**	**3**
Theoretical UV_{max}	308 nm	308 nm	308 nm	291 nm	291 nm	291 nm	250 nm	250 nm	250 nm	250 nm	250 nm	250 nm
Experimental UV_{max}	308 nm	308 nm	308 nm	291 nm	291 nm	291 nm	249 nm	248 nm	249 nm	246 nm	246 nm	246 nm
Absolute Difference: (Specification)	0 (NMT 2) Result complies	0 (NMT 2) Result complies	0 (NMT 2) Result complies	0 (NMT 2) Result complies	0 (NMT 2) Result complies	0 (NMT 2) Result complies	2 (NMT 2) Result complies	2 (NMT 2) Result complies	1 (NMT 2) Result complies	4 (NMT 2) Result does not comply	4 (NMT 2) Result does not comply	4 (NMT 2) Result does not comply
	✓	✓	✓	✓	✓	✓	✓	✓	✓	!	!	!

Step 6: Data processing and validation of established specific absorbance values

6.1 Data processing of the results reported by the three analysts for albendazole and atazanavir sulfate ICRS

The reported absorbance values and the corresponding linear regression analysis results for each analyst (for use to establish the $A_{1cm}^{1\%}$-value suitable for ID and assay testing) for both albendazole and atazanavir sulfate are summarised in Table 11. All individual data sets for albendazole and atazanavir sulfate showed acceptable linearity ($r^2 < 0.99$) as seen by the linear regression results reported in Table 11. The poolability of the three data sets was then investigated by assessing the similarity of the slopes and intercepts. The results of the comparison of slopes and intercepts are summarised in Figure 3.

OVERALL FIT

Regression Statistics	
Multiple R	0,998895675
r^2	0,997992358
Adjusted r^2	0,997323144
Standard Error	0,00408031
Observations	21

ANOVA

	df	*SS*	*MS*	*F*	*Significance F*
Regression	5	0,124141936	0,02482839	1491,2905	1,14268E-19
Residual	15	0,000249734	1,6649E-05		
Total	20	0,12439167			

	Coefficients	*Standard Error*	*t Stat*	*P-value*	*Lower 95%*	*Upper 95%*
Intercept	-0,0098	0,0127	-0,7709	0,4527	-0,0368	0,0173
m_1 Exp. Con (µg/mL)	0,0755	0,0016	48,2804	0,0000	0,0721	0,0788
m_2 d_1	0,0102	0,0179	0,5700	0,58	-0,0280	0,0485
m_4 d_1X	-0,0003	0,0022	-0,1397	0,89	-0,0050	0,0044
m_3 d_2	-0,0365	0,0179	-2,0325	0,06	-0,0747	0,0018
m_5 d_2X	0,0047	0,0022	2,1427	0,05	0,0000	0,0095

(a)

OVERALL FIT

Regression Statistics	
Multiple R	0,995970766
r^2	0,991957766
Adjusted r^2	0,989277021
Standard Error	0,020954471
Observations	21

ANOVA

	df	*SS*	*MS*	*F*	*Significance F*
Regression	5	0,812383624	0,16247672	370,03068	3,75508E-15
Residual	15	0,006586348	0,00043909		
Total	20	0,818969972			

	Coefficients	*Standard Error*	*t Stat*	*P-value*	*Lower 95%*	*Upper 95%*
Intercept	0,0016	0,0652	0,0250	0,9804	-0,1372	0,1405
m_1 Exp. Con (µg/mL)	0,0144	0,0006	25,5883	0,0000	0,0132	0,0156
m_2 d_1	0,1534	0,0921	1,6654	0,12	-0,0429	0,3498
m_4 d_1X	-0,0012	0,0008	-1,4982	0,15	-0,0029	0,0005
m_3 d_2	0,0224	0,0921	0,2432	0,81	-0,1740	0,2188
m_5 d_2X	-0,0001	0,0008	-0,1770	0,86	-0,0018	0,0016

(b)

Figure 3: Results for the comparison of slopes and intercepts of the reported data for use in establishing a $A_{1cm}^{1\%}$-values for use in ID and assay testing of (a) albendazole chewable tablets and (b) atazanavir capsules.

From Figure 3 it is seen that the slope coefficient m_4 indicates the similarity of slopes between analysts 1 and 2, since the slope coefficient m_4 does not differ significantly from zero as indicated by the p-value > 0.05. Similarly, the slope coefficient m_5 does also not differ significant from zero as the p-value > 0.05. Since $m_4 \approx 0 \approx m_5$, it can be concluded that the slopes of the regression lines derived by analysts 2 and 3 could be considered being similar. Next, the homogeneity of the intercepts was evaluated. The intercepts of the calibration curves produced by analysts 1 and 2 are compared by evaluating the intercept coefficient m_2. m_2 does not differ significantly from zero as indicated by the p-value > 0.05, thus the intercepts of analysts 1 and 2 do not differ. Similarly, the intercept coefficient m_3 also does not differ significantly from zero as the p-value is > 0.05, thus the intercepts of analysts 1 and 3 do not differ. Since $m_2 \approx 0 \approx m_3$, it can be concluded that the intercepts of the regression lines derived by analysts 2 and 3 could be considered being similar.

Table 11: Data generated by the three independent analysts for the establishment of the $A_{1cm}^{1\%}$-values for use in ID and / or assay testing of albendazole chewable tablets and atazanavir sulfate capsules

Albendazole						Atazanavir sulfate					
Analyst 1		Analyst 2		Analyst 3		Analyst 1		Analyst 2		Analyst 3	
Experimental Concentration (µg/mL)	Absorbance	Experimental Concentration (µg/mL)	Absorbance	Experimental Concentration (µg/mL)	Absorbance	Experimental Concentration (µg/mL)	Absorbance	Experimental Concentration (µg/mL)	Absorbance	Experimental Concentration (µg/mL)	Absorbance
6.447	0.4798	6.570	0.4912	6.425	0.4677	91.9358	1.3378	92.2152	1.3684	91.4966	1.3492
7.253	0.5340	7.391	0.5591	7.228	0.5295	103.428	1.5142	103.742	1.5310	102.934	1.4716
7.655	0.5644	7.802	0.5890	7.629	0.5667	109.174	1.5607	109.506	1.5811	108.652	1.5683
8.058	0.6014	8.213	0.6153	8.031	0.6043	114.920	1.6255	115.269	1.7021	114.371	1.6654
8.461	0.6315	8.623	0.6461	8.432	0.6345	120.666	1.7309	121.032	1.7710	120.089	1.7185
8.864	0.6550	9.034	0.6842	8.834	0.6568	126.412	1.8005	126.796	1.8077	125.808	1.8127
9.670	0.7217	9.855	0.7384	9.637	0.7252	137.904	2.0118	138.323	1.9819	137.245	1.9972
Regression parameters	**Analyst 1**		**Analyst 2**		**Analyst 3**		**Analyst 1**		**Analyst 2**		**Analyst 3**
r^2:	0.9982		0.9984		0.9974		0.990		0.992		0.994
Linear regression equation:	y = 0.0755x – 0.0098		y = 0.0751x – 0.0004		y = 0.0802x – 0.0463		y = 0.0142x + 0.0170		y = 0.0132x + 0.1551		y = 0.0143x + 0.0240
Significance of intercept p-value:	0.44		0.97		0.03		0.83		0.05		0.68
Regression parameters when c = 0	**Analyst 1**		**Analyst 2**		**Analyst 3**		**Analyst 1**		**Analyst 2**		**Analyst 3**
r^2:	1.0000		1.0000		0.9999		0.9998		0.9998		0.9999
Linear regression equation:	y = 0.0743x		y = 0.0752x		y = 0.0745x		y = 0.0144x		y = 0.0145x		y = 0.0145x
$A_{1cm}^{1\%}$-value:	743		752		745		144		145		145

The data generated by the three analysts for use in the ID and / or assay testing of albendazole chewable tablets and atazanavir capsules could thus be considered similar and are suitable to be pooled resulting in a regression equation with one common slope and intercept as depicted in Figure 4.

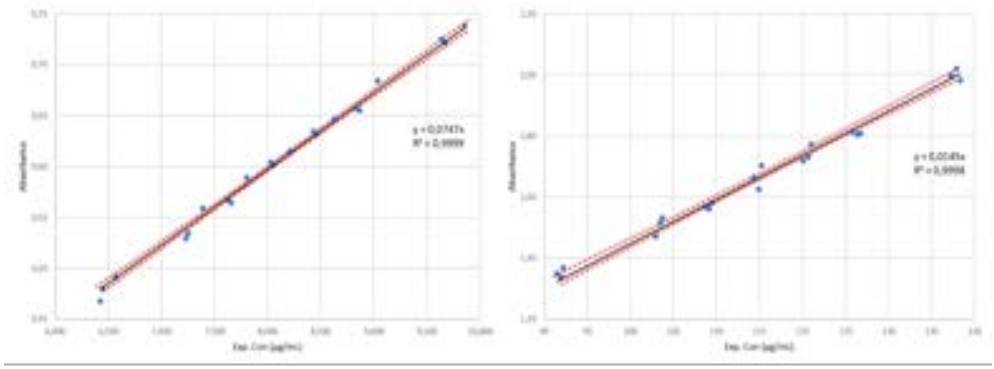

Figure 4: Calibration curve of the pooled data used to establish the $A_{1cm}^{1\%}$-value for use in the ID and / or assay testing of (a) albendazole chewable tablets and (b) atazanavir capsules. Dashed lines represent the calculated 95% CI of the regression lines.

Linear regression analysis was performed for the pooled data generated for albendazole and atazanavir sulfate. These results showed that the intercepts of the linear regression line obtained when the data reported by the three (3) analysts are pooled – did not differ statistically significant from zero ($p > 0.05$). The pooled data sets were thus subjected to linear regression analysis again, setting the intercept to zero resulting in a correlation coefficient (r^2) = 0,9999 and 0.9998 for the pooled regression data of albendazole and atazanavir sulfate respectively. The averaged $A_{1cm}^{1\%}$-value intended for use in the ID and / or assay testing of albendazole chewable tablets was calculated as 747 and 145 for atazanavir capsules using the regression parameters seen in Figure 4.

When considering the individual data sets reported for albendazole in Table 11 the intercept calculated for analyst 3 was not greater than 0.05 but considering that the overall intercept for the pooled data does not differ significantly from zero the effects of the intercept on the individual $A_{1cm}^{1\%}$-value could be voided. The data was subjected to linear regression analysis again, setting the intercept to zero. The individual $A_{1cm}^{1\%}$-values were then calculated using the resulting regression parameters.

It is important to note that the $A^{1\%}_{1\,cm}$-value established as 145 may only be used for the assay testing of atazanavir capsules as the concentration range required for use in the identification of atazanavir sulfate yielded absorbance values of below 0.2, which is not considered suitable for quantitative or semi-quantitative analysis.[30] Thus, from this point forward only the results for the establishment of an $A^{1\%}_{1\,cm}$-value suitable for use in the assay testing of atazanavir sulfate are presented and discussed. If the *Ph.Int.* should wish to establish a $A^{1\%}_{1\,cm}$-range that may be used for the identification of atazanavir sulfate, it is recommended that the pharmacopoeia should increase the nominal concentration of the test solution to at least 55.2 µg/mL to obtain an absorbance value of at least 0.8.

The data reported by the three analysts that were used to establish the $A^{1\%}_{1cm}$-values suitable for use during the dissolution testing of albendazole chewable tablets and atazanavir capsules were processed the same as previously described for the $A^{1\%}_{1cm}$-value suitable for ID and assay testing. The reported absorbance values and linear regression analysis results are summarised in Table 12.

Table 12: Data generated by the three independent analysts for the establishment of the $A_{1cm}^{1\%}$-values for use in dissolution testing of albendazole chewable tablets and atazanavir capsules

Albendazole						Atazanavir sulfate					
Analyst 1		Analyst 2		Analyst 3		Analyst 1		Analyst 2		Analyst 3	
Experimental Concentration (µg/mL)	Absorbance	Experimental Concentration (µg/mL)	Absorbance	Experimental Concentration (µg/mL)	Absorbance	Experimental Concentration (µg/mL)	Absorbance	Experimental Concentration (µg/mL)	Absorbance	Experimental Concentration (µg/mL)	Absorbance
7.0670	0.2503	7.3202	0.2563	7.1113	0.2550	50.6385	0.6032	50.6585	0.6027	50.4589	0.6140
8.8337	0.3068	9.1502	0.3302	8.8891	0.3163	63.2982	0.7539	63.3231	0.7736	63.0736	0.7607
10.6005	0.3719	10.9803	0.3852	10.6670	0.3842	75.9578	0.9238	75.9877	0.9277	75.6883	0.9043
12.3672	0.4346	12.8103	0.4600	12.4448	0.4422	88.6174	1.0629	88.6523	1.0730	88.3030	1.0786
14.1340	0.4909	14.6404	0.5146	14.2226	0.5011	101.2770	1.2244	101.3170	1.2091	100.9178	1.2213
17.6675	0.6347	18.3005	0.6666	17.7783	0.6312	126.5963	1.4565	126.6462	1.4680	126.1472	1.4533
21.2010	0.7614	21.9605	0.7865	21.3339	0.7551	151.9156	1.7517	151.9754	1.7767	151.3766	1.7677
Regression parameters	**Analyst 1**		**Analyst 2**		**Analyst 3**		**Analyst 1**		**Analyst 2**		**Analyst 3**
r^2:	0.9991		0.9987		0.9998		0.9974		0.9985		0.9977
Linear regression equation:	y = 0.0364x – 0.0140		y = 0.0364x – 0.0088		y = 0.0351x – 0.0053		y = 0.0112x + 0.0536		y = 0.0113x + 0.0510		y = 0.0113x + 0.0542
Significance of intercept p-value:	0.10		0.34		0.14		0.08		0.05		0.08
Regression parameters when c = 0	**Analyst 1**		**Analyst 2**		**Analyst 3**		**Analyst 1**		**Analyst 2**		**Analyst 3**
r^2:	0.9998		0.9998		1.0000		-		-		-
Linear regression equation:	y = 0.0355x		y = 0.0358x		y = 0.0355x		-		-		-
$A_{1cm}^{1\%}$-value:	355		358		355		112		113		113

The intercepts calculated for each of the data sets reported by the analysts when measuring the absorbance values of standard solutions containing albendazole were found to be non-significant (i.e. do not differ statistically significant from zero) as the p-values thereof were found to be greater than 0.05. The data was subjected to linear regression analysis again, setting the intercept to zero. The individual $A_{1cm}^{1\%}$-values were then calculated using the resulting regression parameters. However, for the data sets reported after the analysis of standard solutions containing atazanavir sulfate ICRS no further linear regression analysis was performed and the individual $A_{1cm}^{1\%}$-values were calculated using the regression parameters including the effect of the intercept. The poolability of the three data sets was then investigated by assessing the similarity of the slopes and intercepts (Figure 5).

OVERALL FIT

Regression Statistics	
Multiple R	0,999590716
r^2	0,9991816
Adjusted r^2	0,998908799
Standard Error	0,005710026
Observations	21

ANOVA

	df	*SS*	*MS*	*F*	*Significance F*
Regression	5	0,597098654	0,11941973	3662,6874	1,3668E-22
Residual	15	0,000489066	3,2604E-05		
Total	20	0,59758772			

	Coefficients	*Standard Error*	*t Stat*	*P-value*	*Lower 95%*	*Upper 95%*
Intercept	-0,0140	0,0065	-2,1478	0,0485	-0,0279	-0,0001
m_1 Exp. Con (µg/mL)	0,0364	0,0005	77,8982	0,0000	0,0355	0,0374
m_2 d_1	0,0052	0,0092	0,5667	0,58	-0,0144	0,0248
m_4 d_1X	-0,0001	0,0007	-0,1241	0,90	-0,0015	0,0013
m_3 d_2	0,0192	0,0092	2,0912	0,05	-0,0004	0,0389
m_5 d_2X	-0,0013	0,0007	-1,9882	0,07	-0,0027	0,0001

(a)

OVERALL FIT

Regression Statistics	
Multiple R	0,998927554
r^2	0,997856258
Adjusted r^2	0,997141677
Standard Error	0,020452033
Observations	21

ANOVA

	df	*SS*	*MS*	*F*	*Significance F*
Regression	5	2,920516772	0,58410335	1396,4222	1,8685E-19
Residual	15	0,006274285	0,00041829		
Total	20	2,926791056			

	Coefficients	*Standard Error*	*t Stat*	*P-value*	*Lower 95%*	*Upper 95%*
Intercept	0,0556	0,0233	2,3843	0,0308	0,0059	0,1053
m_1 Exp. Con (µg/mL)	0,0112	0,0002	47,9811	0,0000	0,0107	0,0117
m_2 d_1	-0,0046	0,0330	-0,1386	0,89	-0,0748	0,0657
m_4 d_1X	0,0001	0,0003	0,3831	0,71	-0,0006	0,0008
m_3 d_2	-0,0014	0,0330	-0,0433	0,97	-0,0717	0,0688
m_5 d_2X	0,0001	0,0003	0,2746	0,79	-0,0006	0,0008

(b)

Figure 5: Results for the comparison of slopes and intercepts of the reported data for use in establishing a $A_{1cm}^{1\%}$-values for use in dissolution testing of (a) albendazole chewable tablets and (b) atazanavir capsules.

The slope coefficients m_4 and m_5 for both the albendazole and atazanavir sulfate data do not differ statistically significant from zero, as indicated by the p-values > 0.05. Furthermore, since $m_4 \approx 0 \approx m_5$, it may be concluded that the slopes of the three analysts are similar and may be pooled. The homogeneity of the three intercepts was then evaluated. The p-values of the intercept coefficients m_2 and m_3 indicated no significant difference from zero. It is thus true that $m_2 \approx 0 \approx m_3$, it may thus be concluded that the three intercepts for the respective albendazole and atazanavir sulfate data sets are similar and may be pooled.

The individual data sets proven to be suitably similar were the pooled resulting in the regression equation with one common slope and intercept as depicted in Figure 6.

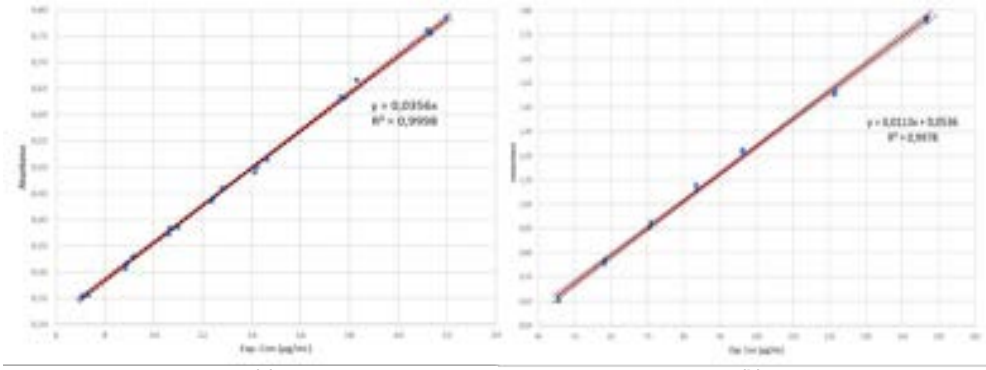

(a) (b)

Figure 6: Calibration curve of the pooled data used to establish the $A_{1cm}^{1\%}$-value for use in the dissolution testing of (a) albendazole chewable tablets and (b) atazanavir capsules. Dashed lines represent the calculated 95% CI of the regression lines.

Linear regression analysis was then performed using the pooled data. These results showed that the intercept for the albendazole pooled regression line did not differ statistically significant from zero ($p > 0.05$). The data was then subjected to linear regression analysis again, setting the intercept to zero. This resulted in a $r^2 = 0{,}9998$ and the $A_{1cm}^{1\%}$-value intended for use in the dissolution testing of albendazole chewable tablets was calculated to be 356 using the resulting regression parameters. These same considerations were made for the linear regression analysis results of the atazanavir sulfate pooled regression line obtained from the individual analysts. The linear regression results showed that the intercept for the pooled regression line differed significantly from zero (p-value < 0.05). The $A_{1cm}^{1\%}$-values for the individual data sets (Table 12) as well as the newly established $A_{1cm}^{1\%}$-value was thus calculated from the regression parameters and included the effect of the intercept. The regression analysis results of the pooled regression line showed a $r^2 = 0.9978$ and the $A_{1cm}^{1\%}$-value intended for use in the dissolution testing of atazanavir capsules was calculated as 113 using the regression parameters showed in Figure 6.

6.2 Validation of established specific absorbance values for albendazole and atazanavir sulfate ICRS

The established $A_{1\,cm}^{1\,\%}$-values were then validated by determining the accuracy and intermediate precision thereof. The results of the accuracy evaluation of the established $A_{1\,cm}^{1\,\%}$-values (using recovery studies) are summarised in Table 13. Intermediate precision was then assessed for the established $A_{1\,cm}^{1\,\%}$-values by calculating the RSD for the $A_{1\,cm}^{1\,\%}$-values of the individual analysts. The results for the assessment of intermediate precision of the individual values are tabulated in Table 14.

Table 13: Accuracy results for the newly established $A_{1\,cm}^{1\,\%}$-values

	Albendazole							Atazanavir sulfate						
	ID and assay				Dissolution			Assay			Dissolution			
	Theoretical concentration [µg/mL]	Experimental concentration [µg/mL]	% recovery	Theoretical concentration [µg/mL]	Experimental concentration [µg/mL]	% recovery	Theoretical concentration [µg/mL]	Experimental concentration [µg/mL]	% recovery	Theoretical concentration [µg/mL]	Experimental concentration [µg/mL]	% recovery
STD_1	7.9595	7.7848	98	17.7150	17.7191	100	113.9217	114.7494	101	126.4965	131.5811	104
STD_2	7.9713	7.8019	98	17.6596	17.5983	100	114.0215	114.6000	101	126.3967	129.8702	103
STD_3	7.9436	7.8224	98	17.6873	17.6587	100	113.8718	115.7517	102	126.4466	129.6047	102
		Average	98		Average	100		Average	101		Average	103
		Standard deviation	0.0		Standard deviation	0.0		Standard deviation	0.6		Standard deviation	1.0
		RSD (%)	0.0		RSD (%)	0.0		RSD (%)	0.6		RSD (%)	1.0

* STD_X represents the prepared standard solution subjected to testing where x = 1,2 or3

Table 14: Intermediate precision results for the newly established $A_{1\,cm}^{1\,\%}$-values

	Albendazole		Atazanavir sulfate	
	ID and assay	Dissolution	Assay	Dissolution
Established $A_{1cm}^{1\%}$-value	747	356	145	113
$A_{1cm}^{1\%}$-value$_1$	743	355	144	112
$A_{1cm}^{1\%}$-value$_2$	752	358	145	113
$A_{1cm}^{1\%}$-value$_3$	745	355	145	113
Average	747	356	145	113
Standard deviation	4.73	1.73	0.58	0.58
RSD (%)	0.63	0.49	0.40	0.51

The % recovery of standard solutions prepared in triplicate to nominally contain target concentration of albendazole or atazanavir sulfate was determined and shown in Table 13. The % recovery calculated for $A_{1\,cm}^{1\,\%}$-values intended for use in the ID and assay testing was found to range between 98–102%. The $A_{1\,cm}^{1\,\%}$-values established for the ID and / or assay of albendazole chewable tablets and atazanavir capsules could thus be considered sufficiently accurate. The % recovery calculated for $A_{1\,cm}^{1\,\%}$-values intended for use in dissolution testing was calculated to be with the range of 95–105% and could thus also be considered sufficiently accurate. The calculated intermediate precision of the established $A_{1\,cm}^{1\,\%}$-values an RSD of ≤ 1% was considered acceptable. The calculated RSDs shown in Table 14 could thus be considered acceptable.

The established and validated $A_{1\,cm}^{1\,\%}$-values for use in QC testing of albendazole (400 mg) chewable tablets and atazanavir capsules and are summarised in Table 15. Also included in this table are the published $A_{1\,cm}^{1\,\%}$-values reported for zidovudine.[14]

Table 15: Summary of newly established $A_{1\,cm}^{1\,\%}$-values for zidovudine, albendazole and atazanavir sulfate

	Zidovudine	Albendazole	Atazanavir sulfate
Established ID and assay testing $A_{1\,cm}^{1\,\%}$-values	372	747	145*
Pharmacopoeial ID and assay testing $A_{1\,cm}^{1\,\%}$-values	380	742	145*
Established dissolution testing $A_{1\,cm}^{1\,\%}$-values	368	356	113
Pharmacopoeial dissolution testing $A_{1\,cm}^{1\,\%}$-values	No value reported	376	114

* The $A_{1\,cm}^{1\,\%}$-values established as 145 for atazanavir sulfate should only be used in the assay testing of atazanavir capsules and is not intended for use in the identification thereof.

Table 15 allows for the comparison of the newly established and validated $A_{1\ cm}^{1\ \%}$-values with that published in the specific monographs for zidovudine capsules, albendazole chewable tablets and atazanavir capsules in the *Ph.Int.* The difference between the newly established values and the reported pharmacopoeial values for use in the ID and / or assay testing of these APIs ranges from 0.7–2.1% and range from 0.9–5.3% for dissolution testing where values have been reported. Based on the proven acceptable accuracy and intermediate precision of the established $A_{1\ cm}^{1\ \%}$-values it is recommended that these values be incorporated into the relevant *Ph.Int.* monographs. This may benefit the specificity of these QC tests as well as aid NQCLs in the identification, assay and dissolution testing of these FPPs, especially in the case of dissolution testing of zidovudine capsules as no $A_{1\ cm}^{1\ \%}$-value is currently reported in this monograph.

The $A_{1cm}^{1\%}$-values established for use in the ID and assay or dissolution testing of albendazole (Table 15) differ by 52%. Albendazole is classified as an ampholyte where the pK_a^{acidic} (10.26) > pK_a^{basic} (2.80) and may thus exist in solution as an anion, unionised form or cation depending on the pH of the solvent, rendering this API more susceptible to pH-induced spectral changes.[31,32] Atazanavir sulfate is classified as a zwitterionic ampholyte where the pK_a^{acidic} (3.36) < pK_a^{basic} (4.88), allowing it to exist in solution as an anion, zwitterion or cation depending on the pH of the solvent.[31,33] Since the difference in the pK_a-values of the two groups is much smaller (< 2 pH units) the ionisation behaviour thereof is more complex allowing overlapping of two equilibria thus making it less susceptible to pH-induced spectral changes (difference in $A_{1cm}^{1\%}$-values = 20%).

Zidovudine is a weak acid API with a pK_a = 9.8, thus existing in either the ionised or unionised state.[34] From the pH-ionisation profile of zidovudine it can be derived that the solvents used in the ID, assay and dissolution tests having pH-values ranging between 1–7 would not introduce significant changes in the degree of ionisation thereof. This could explain the small difference (difference in $A_{1cm}^{1\%}$-values = 1.1%) observed in the $A_{1cm}^{1\%}$-values established for zidovudine.

Application of the established specific absorbance values in the QC testing of commercially available medicinal products in South Africa

The $A_{1cm}^{1\%}$-values tabulated in Table 15 were used in a post-market surveillance (PMS) study of locally procured medicinal products. Products procured and subjected to testing included: zidovudine capsules, albendazole chewable tablets and atazanavir capsules. The results of the PMS study are summarised in Table 16.

Table 16: Summary of the results obtained during the QC testing of zidovudine capsules, albendazole chewable tablets and atazanavir capsules

Tests	Zidovudine capsules	Albendazole chewable tablets Product 1	Albendazole chewable tablets Product 2	Atazanavir sulfate capsules
1. Appearance	A size '3' hard gelatine that is white to off-white and opaque with 'ML 21' printed on the cap and '100' on the body with black ink. The capsules are filled with white to off-white powder.	A pale orange, mottled tablet that is rounded, oblong and biconvex in shape and has a fruity odour. The tablets are embossed with 'ALB 400' on one side and have a score line on the other. These tablets are about 6.95 mm thick, 18.49 mm long and 9.40 mm across.	A cream or buff coloured tablet that is oblong and biconvex in shape and has a fruity odour. These tablets are about 6.14 mm thick, 20.93 mm long and 8.58 mm across.	A size '0' hard gelatine capsule with a grey cap, 'ATV 200' printed in white and a white body with 'ATV 200' printed in black. The capsules are filled with white to yellow granules that may appear as powder
Photograph				
2. Label claim	Each capsule contains 100 mg zidovudine per capsule	Each tablet contains 400 mg albendazole per tablet	Each tablet contains 400 mg albendazole per tablet	Each capsule contains atazanavir sulfate equivalent to 200 mg atazanavir per capsule

Table 16: Summary of the results obtained during the QC testing of zidovudine capsules, albendazole chewable tablets and atazanavir capsules (continued)

Tests	Zidovudine capsules	Albendazole chewable tablets Product 1	Albendazole chewable tablets Product 2	Atazanavir sulfate capsules
3. Average unit mass (n = 20) (RSD)	214.4 mg/capsule (2.71%)	1 021.9 mg/tablet (1.01%)	976.6 mg/tablet (1.16%)	367.5 mg/capsule (0.98%)
4. Uniformity of mass specification	For capsules with an average mass < 300 mg a minimum of 18 of the 20 capsules should not deviate with more than ± 10%, and no capsule should deviate more than ± 20% from the average capsule fill mass.	For tablets with an average mass > 250 mg a minimum of 18 of the 20 tablets should not deviate with more than ± 5%, and no tablet should deviate more than ± 10% from the average tablet mass.	For tablets with an average mass > 250 mg a minimum of 18 of the 20 tablets should not deviate with more than ± 5%, and no tablet should deviate more than ± 10% from the average tablet mass.	For capsules with an average mass > 300 mg a minimum of 18 of the 20 capsules should not deviate with more than ± 7.5%, and no capsule should deviate more than ± 15.0% from the average capsule fill mass.
Tolerance ranges	**10%:** 192.96–235.84 mg **20%:** 171.52–257.28 mg	**5%:** 970.81–1 072.995 mg **10%:** 919.71–1 124.09 mg	**5%:** 927.77–1 025.43 mg **10%:** 878.94–1 074.26 mg	**7.5%:** 339.94–395.06 mg **15%:** 312.38–422.63 mg
Results	No capsules varied with more than 5% from the average capsule fill mass.	No tablets varied in mass with more than 5% from the average tablet mass.	No tablets varied in mass with more than 5% from the average tablet mass.	No capsules varied with more than 7.5% from the average capsule fill mass.

Table 16: Summary of the results obtained during the QC testing of zidovudine capsules, albendazole chewable tablets and atazanavir capsules (continued)

Tests	Zidovudine capsules	Albendazole chewable tablets Product 1	Albendazole chewable tablets Product 2	Atazanavir sulfate capsules
5. ID specification	Zidovudine displays one absorption maximum at about 267 nm when observed between 210 nm and 300 nm, the $A^{1\%}_{1\,cm}$-value ranges between 361–399.	Albendazole exhibits two absorption maxima at about 231 nm and 308 nm with an absorbance of about 0.59 at 308 nm.	Albendazole exhibits two absorption maxima at about 231 nm and 308 nm with an absorbance of about 0.59 at 308 nm.	Atazanavir exhibits two absorption maxima of similar intensity at about 250 nm and 280 nm when observed between 230–340 nm.
Results	The test sample displayed an absorption maximum at 266 nm with an absorbance value of 0.7511. The experimental $A^{1\%}_{1\,cm}$-value was found to be 375.	The test sample displayed absorption maxima at 308 nm with an absorbance value of 0.5952 and another at 231 nm with an absorbance value of 0.9439. The experimental $A^{1\%}_{1\,cm}$-value at 308 nm was found to be 747.	The test sample displayed absorption maxima at 307 nm with an absorbance value of 0.5650 and another at 232 nm with an absorbance value of 0.9183. The experimental $A^{1\%}_{1\,cm}$-value at 308 nm was found to be 706.	The test sample displayed absorption maxima at 249 and 280 nm with respective absorbance values of 0.2069 and 0.1912.
UV spectra				

Table 16: Summary of the results obtained for the QC testing of zidovudine capsules, albendazole chewable tablets and atazanavir capsules (continued)

Tests	Zidovudine capsules	Albendazole chewable tablets Product 1	Albendazole chewable tablets Product 2	Atazanavir sulfate capsules
6. Assay Specification	The capsules should contain not less than 90.0% and not more than 110.0% zidovudine when the absorbance is measured at about 267 nm.	The tablets should contain not less than 90.0% and not more than 110.0% albendazole when the absorbance is measured at about 308 nm.	The tablets should contain not less than 90.0% and not more than 110.0% albendazole when the absorbance is measured at about 308 nm.	The capsules should contain not less than 90.0% and not more than 110.0% atazanavir when the absorbance is measured at about 250 nm.
Results	100.4% 98.5% 98.3% **Average:** 99.1% **RSD:** 1.2%	98.8% 98.3% 97.4% **Average:** 98.1% **RSD:** 0.7%	94.0% 95.2% 95.1% **Average:** 94.8% **RSD:** 0.7%	102.3% 99.9% 99.8% **Average:** 100.2% **RSD:** 1.2%

Table 16: Summary of the results obtained for the QC testing of zidovudine capsules, albendazole chewable tablets and atazanavir capsules (continued)

Tests	Zidovudine capsules	Albendazole chewable tablets Product 1	Albendazole chewable tablets Product 2	Atazanavir sulfate capsules
7. Dissolution Specification	The amount of zidovudine released from each capsule should be not less than 75% (Q) after 45 minutes. The content zidovudine should be calculated using the $A_{1\ cm}^{1\%}$-value 368.	The amount of albendazole released from each tablet should be not less than 80% (Q) after 30 minutes. The content albendazole should be calculated using the $A_{1\ cm}^{1\%}$-value 356.	The amount of albendazole released from each tablet should be not less than 80% (Q) after 30 minutes. The content albendazole should be calculated using the $A_{1\ cm}^{1\%}$-value 356.	The amount of atazanavir released from each capsule should be not less than 75% (Q) after 45 minutes. The content atazanavir should be calculated using the $A_{1\ cm}^{1\%}$-value 113.
Results	1. 105%	1. 90%	1. 7%	1. 102%
	2. 99%	2. 96%	2. 6%	2. 102%
	3. 97%	3. 99%	3. 5%	3. 106%
	4. 104%	4. 94%	4. 6%	4. 103%
	5. 94%	5. 93%	5. 6%	5. 105%
	6. 99%	6. 96%	6. 7%	6. 103%
	Average: 100%	**Average:** 95%	**Average:** 6%	**Average:** 104%
	RSD: 4.2%	**RSD:** 3.3%	**RSD:** 9.1%	**RSD:** 1.6%

The appearance of all products was assessed and compared to that stated in the Patient Information Leaflet (PIL) issued by the respective manufacturer of the product. All products complied with the appearance specifications indicated. The PIL of the albendazole chewable tablets – Product 2 stated that the tablet is capsule shaped and is buff or cream coloured as the only description thereof,[35] it is clear from the appearance that the tablet can also be described as being oblong and biconvex in shape and has a fruity odour. Uniformity of mass was investigated using 20 randomly selected units from each of the respective products. All products assessed showed an acceptable amount of variation in mass of the individual units relative to the average mass of the sample.

The three APIs were suitably identified in the respective FPPs by means of UV/Vis analysis using the *Ph.Int.* specifications. The zidovudine capsules monograph is the only ID procedure that includes using an $A_{1\ cm}^{1\ \%}$-value in the positive identification of zidovudine in zidovudine capsules. The albendazole monograph requires confirming two UV maxima with the latter having an absorbance value of about 0.59,[19] the atazanavir capsules monograph requires confirming two UV maxima of about the same intensity to be suitably identified.[20] It may be beneficial to include $A_{1\ cm}^{1\ \%}$-ranges in the requirements for identification to improve the specificity of this QC test. The ranges intended for use established for the identification of zidovudine and albendazole were 335–409 and 672–822 respectively. The results obtained for the assay testing in all the products tests were found to comply with the specification of 90.0–110.0% of the labelled amount of API as required by the *Ph.Int.* monographs.[19-21]

Lastly, the results for the dissolution tests of the four FPPs showed that albendazole chewable tablets – Product 2 did not meet the dissolution specifications as described in the *Ph.Int.* The chewable tablets were still largely intact after the allocated time. Comparing the excipients included in the formulation of the albendazole chewable tablets Product 1 and Product 2, it was found that Product 1 contained microcrystalline cellulose, maize starch, croscarmellose sodium (a rapid disintegrant), povidone and sodium lauryl sulfate that may aid the disintegration and dissolution process.[36] Product 2 only contained microcrystalline cellulose, maize starch and colloidal anhydrous silica as potential disintegrants.[35] Furthermore, the PIL of Product 1 stated that the tablet may be swallowed whole with water, chewed with a little water or crushed and mixed with food,[36] whereas that of Product 2 indicated that the tablet may be chewed or crushed and mixed with food.[35] The albendazole chewable tablets specific monograph in *Ph.Int.* requires the product to state that the tablet may be chewed, swallowed whole or crushed and mixed with food in the case of small children.[19] The *Ph.Int.* policy for chewable tablets also defines the tablets as being able to be chewed, swallowed whole or crushed and should undergo QC testing procedures for conventional tablets.[37]

The labels of both products state that it is chewable tablets where Product 2 additionally indicates that it may be chewed or crushed.[35,36] If Product 2 is not intended to be swallowed both the Package Insert (PI) and the Patient Information Leaflet (PIL) should clearly state that the product should not be swallowed whole but chewed and only then swallowed. If this is neglected to be mentioned and the product is swallowed, as may be done by the definition of a chewable tablet, disintegration and subsequent dissolution may not occur as shown by the results presented in Table 16. This may result in a sub-therapeutic effect due to the incomplete release of the API from the dosage form.

Conclusion

Specific absorbance values were established for albendazole and atazanavir sulfate that were suitably validated for an intended use being either for the identification, assay or for the dissolution testing of these respective APIs in an FPP. These established and validated $A_{1\,cm}^{1\,\%}$-values jointly with the $A_{1\,cm}^{1\,\%}$-values reported for zidovudine by De Villiers *et al.* were applied in the quality testing of zidovudine capsules, albendazole chewable tablets and atazanavir capsules by performing a PMS study on these commercially available medicine products using the criteria stated in the specific monographs of *The international Pharmacopoeia* to conclude on the quality thereof. From the PMS study it can be concluded that the respective APIs were suitably identified within the tested products. All products tested were furthermore within the content specification limits of the respective specific monographs as determined by assay testing. One of the two albendazole chewable tablet products however did not meet the criteria of the dissolution testing specifications for albendazole chewable tablets, while all other products adhered to their respective dissolution testing specifications.

The $A_{1\,cm}^{1\,\%}$-values established and validated in this study and the application thereof may also be beneficial to NQCLs in the QC testing of FPPs containing these APIs and to identify SF medicines. From this study, the following recommendations are proposed:

1. The $A_{1\,cm}^{1\,\%}$-values currently reported in the specific monographs of the *Ph.Int.* should be replaced with the newly established $A_{1\,cm}^{1\,\%}$-values.
2. The newly established $A_{1\,cm}^{1\,\%}$-value suitable for use in the dissolution testing of zidovudine capsules should be incorporated into the *Ph.Int.* zidovudine capsules monograph – which will allow for the cost-effective and rapid analysis of dissolution test samples.
3. An $A_{1\,cm}^{1\,\%}$-range (672–822) should be included in the identification test C of the *Ph.Int.* albendazole chewable tablets monograph.
4. The atazanavir capsules identity test B of the Ph.Int. should be revised to increase the concentration of the test sample to enable the establishment of an $A_{1\,cm}^{1\,\%}$-value – this will increase the selectivity of the mentioned test.
5. The manufacturer of Product 2 should clearly indicate that this product must be chewed or crushed – but not swallowed whole – to ensure that disintegration and ultimate release of the API from the solid dosage form is achieved.

References

1. **Cordonnier J & Schaep J.** 32 Ultraviolet, visible and fluorescence spectrophotometry. In: Moffat A.C., Osselton M.D. & Widdop B. (eds.). Clarke's analysis of drugs and poisons, 3rd ed., Vols. I and II. The Pharmaceutical Press: London; England. 2004. Available from: https://www-medicinescomplete-com.nwulib.nwu.ac.za/#/content/clarke/clk214308?hspl=specific&hspl=absorbance#content%2Fclarke%2Fclk214308%23c32-bbs-0001 Date of access: 08 January 2023.

2. **BP (British Pharmacopoeia).** Appendix II B. Ultraviolet and visible absorption spectrophotometry, British Pharmacopoeia. 2024. https://www-pharmacopoeia-com.nwulib.idm.oclc.org/bp-2024/appendices/appendix-02/appendix-ii-b--ultraviolet-and-visible-absorption-spectrophotome.html?date=2024-07-01
Date of access: 26 September 2024.

3. **Karakurt S & Karakurt S.** Measurement uncertainty of spectrophotometric determination of hexavalent chromium in water. Science Bulletin, 2017; 79(4):181–194. https://www.researchgate.net/publication/321731757_Measurement_uncertainty_of_spectrophotometric_determination_of_hexavalent_chromium_in_water
Date of access: 11 July 2023.

4. **Pedersen-Bjergaard S, Gammelgaard B & Halvorsen T G.** Introduction to pharmaceutical analytical chemistry, 2nd ed. Chichester; Wiley. 2019.

5. **EDQM (European Directorate for the Quality of Medicines & HealthCare).** Technical guide for the elaboration of monographs. 8th ed., Strasbourg; France. 2022. Available from edqm.eu: https://www.edqm.eu/documents/52006/66555/02-technical-guide-elaboration-monographs-8th-edition-2022.pdf/46b07f46-779d-687d-1455-74d8a9a515ee?t=1656321894803 Date of access: 13 February 2023.

6. ***Ph.Int.* (The international pharmacopoeia).** 1.6 Spectrophotometry in the visible and ultraviolet regions. *The International Pharmacopoeia*, 11th ed., Geneva. 2022. World Health Organization; Licence: CC BY-NC-SA 3.0 IGO. Available at: https://digicollections.net/phint/2022/index.html#d/b.7.1.6 Date of access: 22 May 2023.

7. **Østergaard J.** UV/Vis Spectrophotometry and UV imaging. In Müllertz A., Pierre Y. & Rades T. (eds.). Analytical techniques in the pharmaceutical sciences, advances in delivery science and technology. New York; Springer. 2016, Pp. 3–27. DOI: 10.1007/978-1-4939-4029-5

8. **Hauk C, Hagen N & Heide L.** Identification of Substandard and Falsified Medicines: Influence of Different Tolerance Limits and Use of Authenticity Inquiries. The American Journal of Tropical Medicine and Hygiene, 2021; 104(5):1936–1945. DOI: 10.4269/ajtmh.20-1612

9. **WHO (World Health Organization).** Counterfeit Drugs: Guidelines for the Development of Measures to Combat Counterfeit Drugs. 1999. Available at: https://iris.who.int/bitstream/handle/10665/65892/WHO_EDM_QSM_99.1.pdf Date accessed: 24 July 2024.

10. **WHO (World Health Organization).** A study on the public health and socioeconomic impact of substandard and falsified medical products. 2020. https://www.who.int/publications/i/item/9789241513432 Date of access: 30 June 2023.

11. **Rahman M S, Yoshida N, Tsuboi H, Tomizu N, Endo J, Miyu O, Akimoto Y & Kimura K.** The health consequences of falsified medicines - A study of the published literature. Tropical Medicine & International Health, 2018; 23:1294–1303. https://doi.org/10.1111/tmi.13161 Date of access: 30August 2024.

12. **Bakker-'t Hart I M E, Ohana D & Venhuis B J.** Current challenges in the detection and analysis of falsified medicines. Journal of Pharmaceutical and Biomedical Analysis, 2021; 197. https://doi.org/10.1016/j.jpba.2021.113948. Date of access: 30 August 2024.

13. **WHO (World Health Organization).** A study on the public health and socioeconomic impact of substandard and falsified medical products. 2017. World Health Organization License: CC BY-NC-SA 3.0 IGO. https://iris.who.int/handle/10665/331690 Date of access: 30 August 2024.

14. **De Villiers D, Brits I & Brits M.** A framework for the establishment of specific absorbance values for qualitative and quantitative analysis of medicines. World Journal of Pharmacy and Pharmaceutical Sciences, 2024; 13(9):1125–1173. DOI: 10.20959/wjpps20249-28200

15. **Tran C V & Vargas J R.** 2020. Determination of specific absorbance (A¦) for six psychoactive drugs encountered in forensic toxicology. Journal of Analytical Toxicology, 2020; 44(6):531–540. DOI: 10.1093/jat/bkz091

16. **Anderson D T & Elbogen J L.** Determination of specific absorbance (A¦) for Zaleplon (Sonata®) by Spectrophotometry. Journal of Analytical Toxicology, 2009; 33:478–480. DOI: https://doi.org/10.1093/jat/33.8.478

17. **NDoH (National Department of Health).** Standard Treatment Guidelines and Essential Medicines List for South Africa. 2020. https://knowledgehub.health.gov.za/elibrary/primary-healthcare-phc-standard-treatment-guidelines-and-essential-medicines-list-south Date of access:15 June 2023.

18. **WHO (World Health Organization).** WHO model list of essential medicines. 2024. Available at WHO electronic EML at: https://list.essentialmeds.org/ Date of access: 10 September 2024.

19. ***Ph.Int.* (The international pharmacopoeia).** Albendazole chewable tablets (Albendazoli compressi manducabili). *The International Pharmacopoeia*, 11th ed., Geneva. 2022. World Health Organization; Licence: CC BY-NC-SA 3.0 IGO. Available at: https://digicollections.net/phint/2022/index.html#d/b.6.2.2.6 Date of access: 11 July 2023.

20. ***Ph.Int.* (The international pharmacopoeia).** Atazanavir capsules (Atazanaviri capsulae). *The International Pharmacopoeia*, 11th ed. Geneva. 2022. World Health Organization; Licence: CC BY-NC-SA 3.0 IGO. Available at: https://digicollections.net/phint/2022/index.html#d/b.6.2.2.19 Date of access: 11 July 2023.

21. ***Ph.Int.* (The international pharmacopoeia).** Zidovudine capsules (Zidovudini capsulae). *The International Pharmacopoeia*, 11th ed. Geneva. 2022. World Health Organization; Licence: CC BY-NC-SA 3.0 IGO. Available at: https://digicollections.net/phint/2022/index.html#d/b.6.2.2.143 Date of access: 11 July 2023.

22. **WHO (World Health Organization).** Zidovudine capsules (Zidovudini Capsulae): Draft proposal for revision in *The International Pharmacopoeia*, 2024. https://cdn.who.int/media/docs/default-source/medicines/norms-and-standards/current-projects/2024-07-31-zidovudinecapsules-qas22-933-forpubcon.pdf?sfvrsn=5880643f_3 Date of access: 15 October 2024.

23. ***Ph.Int.* (The international pharmacopoeia).** 1.1 Measurement of mass. *The International Pharmacopoeia*, 11th ed., Geneva. 2022. World Health Organization; Licence: CC BY-NC-SA 3.0 IGO. Available at: https://digicollections.net/phint/2022/index.html#d/b.7.1.1 Date of access: 29 August 2024.

24. **Vignaduzzo S E, Operto M A & Castellano P M.** Development and Validation of a Dissolution Test Method for Albendazole and Praziquantel in Their Combined Dosage Form. Journal of the Brazilian Chemical Society, 2015; 26(4):729–735. DOI:10.5935/0103-5053.20150033

25. **Adusumalli K R & Kumar A C.** Novel Sensitive UV Spectrophotometric Method for the Determination of Atazanavir. Journal of Applicable Chemistry, 2019; 8(6):2411–2416. http://www.joac.info/ContentPaper/2019/1-15-8-6-21.pdf Date of access: 09 October 2024.

26. **Ghante M R, Kadam M M, Sawant S D & Shelar R S.** Development and validation of UV spectrophotometric methods for estimation of atazanavir sulphate in bulk and tablet dosage form. International Journal of Pharmacy and Pharmaceutical Sciences, 2014; 6(7):351–353. https://journals.innovareacademics.in/index.php/ijpps/article/view/2031/9669 Date of access: 09 October 2024.

27. **Konidala S K & Sujana K.** Development and validation of UV spectroscopic method for determination of atazanavir sulphate in bulk and formulation. International Journal of Pharmacy and Pharmaceutical Sciences, 2012; 4(3):614–617. https://www.innovareacademics.in/journal/ijpps/Vol4Issue3/4187.pdf Date of access: 09 October 2024.

28. **Valli Purnima B, Santha Kumari M, Ramu G, Vijaya Bhaskara Reddy T & Ramachandran D.** Simultanious estimation of cobicistat and atazanavir sulphate in bulk and combined dosage form by UV-spectrophotometric method. World Journal of Pharmaceutical Research, 2016; 5(10):914–932. DOI: 10.20959/wjpr201610-7148

29. **Soundarya K, Hemant Kumar T & Manjunath S Y.** New UV Spectrophotometric Method for the Estimation of Atazanavir Sulfate in Bulk and Pharmaceutical Dosage Form. Scholars Academic Journal of Pharmacy, 2020; 9(11):296–300. DOI: 10.36347/sajp.2020.v09i11.002

30. **USP–NF (United States Pharmacopeia – National Formulary).** <1857> Ultraviolet-visible spectroscopy—theory and practice, United States Pharmacopoeia, 2023. DOI: https://doi.org/10.31003/USPNF_M5513_02_01

31. **Attwood D & Florence A T.** FASTtrack Physical Pharmacy. The Pharmaceutical Press: London; England. 2008. Available at: http://ndl.ethernet.edu.et/bitstream/123456789/91148/1/FASTtrack_Physical%20Pharmacy-David%20Attwood_Alexander%20T%20Florence-Pharmaceutical%20Press-2008-1.pdf Date of access: 24 October 2024.

32. **Jung H, Medina L, García L, Fuentes I & Moreno-Esparza R.** Absorption studies of albendazole and some physicochemical properties of the drug and its metabolite albendazole sulphoxide. Journal of Pharmacy and Pharmacology, 1998; 50(1):43–8. DOI: https://doi.org/10.1111/j.2042-7158.1998.tb03303.x Date of access: 24. October 2024.

33. **Wishart DS, Knox C, Guo AC, Shrivastava S, Hassanali M, Stothard P, Chang Z, Woolsey J.** Drugbank: Atazanavir Sulafte. 2024 (5.1.12). Available at: https://go.drugbank.com/salts/DBSALT000426 Date of access: 24 October 2024.

34. **Checa A, Soto V G, Cassou S H & Saurina J.** Fast determination of pKa values of reverse transcriptase inhibitor drugs for AIDS treatment by using pH-gradient flow-injection analysis and multivariate curve resolution. Analytica Chimica Acta; 2005, 554(1-2):177–183. DOI: https://doi.org/10.1016/j.aca.2005.08.084 Date of access: 24 October 2024.

35. **Dezzo Trading 392 (Pty) Ltd.** Wormadole: (Chewable Tablets): Package Insert. Lenasia, South Africa. 2017.

36. **GSK.** Zentel 400: Package Insert – Patient Information Leaflet. 1997. Epping, South Africa.

37. ***Ph.Int.*** **(The international pharmacopoeia).** Tablets. *The International Pharmacopoeia,* 11th ed., Geneva. 2022. World Health Organization; Licence: CC BY-NC-SA 3.0 IGO. Available at: https://digicollections.net/phint/2022/index.html#p/home Date of access: 15 October 2024.

***

WORLD HEALTH ORGANIZATION
EXTERNAL QUALITY ASSURANCE SCHEME
PHASE 11

Marius Brits[1], Luther Gwaza[2]

[1]North-West University, Faculty of Health Sciences, Centre of Excellence for Pharmaceutical Sciences (Pharmacen™) Potchefstroom, South Africa (Marius.Brits@nwu.ac.za)
[2]Norms and Standards for Pharmaceuticals, Health Products Policy and Standards Department, World Health Organization, Geneva, Switzerland (gwazal@who.int)

WORLD HEALTH ORGANIZATION
EXTERNAL QUALITY ASSURANCE SCHEME
PHASE 11

Introduction

The importance of participation in proficiency testing schemes for Pharmaceutical Quality Control Laboratories (PQCLs) has once again been highlighted in the most recent revision of the WHO Good Practices for Pharmaceutical Quality Control Laboratories (WHO GPPQCL).[1]

Proficiency testing activities form an integral part of the Quality Management System (QMS) of a PQCL in that it provides the laboratory with an independent overview of the overall technical performance (i.e. sample receipt, storage, testing capabilities, results processing, review and approval) of the laboratory. By participating in proficiency testing activities the laboratory is able to demonstrate compliance with the requirements set forth in WHO GPPQCL chapters 3.50, 4.3, 4.17, 5.3 and 6.72.[1] Furthermore, participation in Proficiency testing activities allows PQCLs the opportunity to use the proficiency testing data to estimate bias and check measurement of uncertainties. Participation in proficiency testing activities is a requirements for testing and calibration laboratories that are ISO 17025 accredited in order to illustrate their competence.[2]

The WHO External Quality Assurance Assessment Scheme (EQAAS) is an internationally recognised proficiency testing scheme which provides PQCLs the opportunity to evaluate their quality control testing performance against that of international PQCLs. EQAAS provides the PQCL the opportunity to identify its strengths, weaknesses and opportunities to continuously improve and strengthen its' QMS, and ultimately promote the safety of medicines.

The EQAAS has been organised by WHO with the assistance of the European Directorate for the Quality of Medicines and HealthCare (EDQM) since 2000. Continuous participation in this scheme enables PQCLs to monitor their performance over time to identify potential trends.

Laboratories across WHO's six regions have participated in the past external assessment studies and more than 1 452 studies involving 41 different tests were carried out to date.

Description of EQAAS Phase 11

In EQAAS Phase 11, laboratories were provided with the opportunity to evaluate their performance on five procedures using metronidazole tablets and metronidazole solution for injection common test samples. The five procedures executed during this phase are depicted in Figure 1.

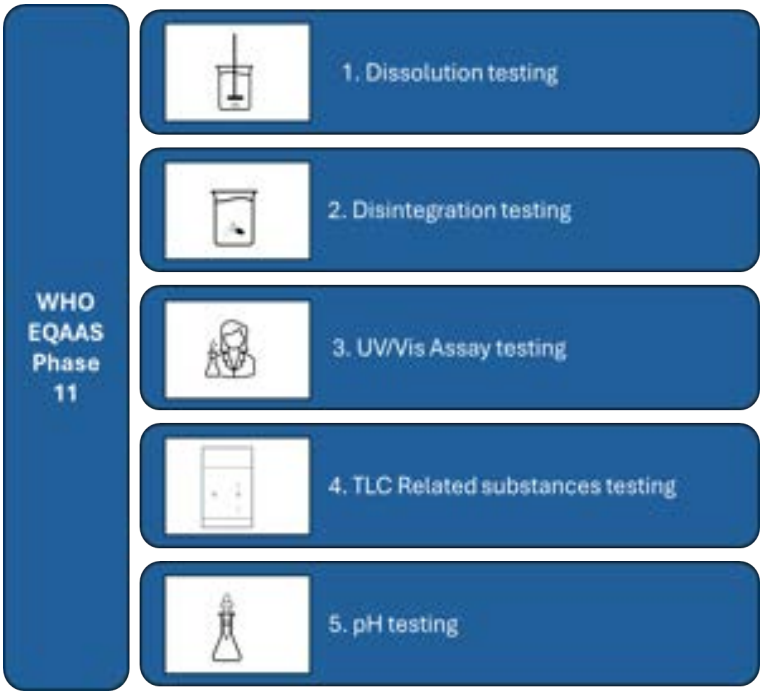

Figure 1: Schematic presentation of analytical procedure bouquet incorporated into EQAAS Phase 11.

▪ **Procedure 1:** This procedure aimed to assess the performance of the laboratories with regard to the dissolution testing on tablets containing 200 mg and 500 mg metronidazole. The percentage of metronidazole released from the tablets after 30 minutes was determined using the dissolution method described in the metronidazole tablets monograph of *The International Pharmacopoeia* (11th edition) published by WHO.[3]

▪ **Procedure 2:** This procedure aimed to assess the performance of the laboratories with regard to the disintegration testing of the mentioned metronidazole tablets. Laboratories were requested to confirm whether or not the tablets disintegrated within 10 minutes, according to general method 5.3, Disintegration test for tablets and capsules (Test A) of *The International Pharmacopoeia* (11th edition) published by WHO.[4]

▪ **Procedure 3:** This procedure aimed to assess the performance of the laboratories with regard to the assay testing of a 5 mg/mL metronidazole solution for injection. The laboratories were requested to determine the content of metronidazole in the solution for injection by UV/Vis spectrophotometry as described in the metronidazole injection monograph of *The International Pharmacopoeia* (11th edition) published by WHO.[5]

▪ **Procedure 4:** This procedure aimed to assess the performance of the laboratories with regard to the execution of a related substances test on a 5 mg/mL metronidazole solution for injection. The laboratories were requested to confirm whether or not the sample complied with the requirement: "the spot obtained with solution B is more intense than any spot obtained with solution A". The related substances test was to be performed as described in the metronidazole injection monograph of *The International Pharmacopoeia* (11th edition) published by WHO.[5]

▪ **Procedure 5:** This procedure aimed to assess the performance of the laboratories with regard to the determination of the pH of a 5 mg/mL metronidazole solution for injection. The laboratories were requested to measure and report the pH of the supplied sample as described in the metronidazole injection monograph of *The International Pharmacopoeia* (11th edition) published by WHO.[5]

Statistical methods

In the case of quantitative analysis (Procedures 1, 3 and 5), the assigned values were established based on the determined consensus value using robust statistics (e.g. the median value, mean interquartile range, Huber's robust mean) to avoid the influence of "outliers" on the overall mean. The target standard deviation values (TSD) were set based on experience, reported or expected precision of techniques and according to fitness for purpose.

A Cochran's test was performed to check for high standard deviations followed by a Grubb's test to identify outlying means. Outliers were isolated from the data sets to limit the unreasonable impact thereof on the calculation of certain statistics (e.g. the overall mean and the overall standard deviation). Standard deviations or relative standard deviations (RSD) identified as outliers are only to indicate that these values are high compared to the RSDs found in other laboratories, but they do not necessarily imply that they are unacceptable. RSDs provide participants with comparative material so that they can interpret their data in the light of the performances of other laboratories and draw their own conclusions.

For the quantitative tests, Z-scores were calculated as a bias estimate of the results reported by the various PQCLs. An absolute z-score of less than 2 is considered acceptable. A zone of doubtful performance exists for an absolute z-score ranging between 2–3. An absolute z-score of 3 or more is interpreted as an unacceptable performance, and corrective actions should be implemented by the PQCL. Corrective actions should also be triggered by the PQCL when the z-scores are frequently in the doubtful zone.

The z-score for each PQCLs was calculated using the following equation:

$$z - score = \frac{\bar{x} - \hat{x}}{TSD}$$

Where $\bar{x}$ is the unrounded mean value calculated by EDQM based on the reported results of the individual laboratory,
$\hat{x}$ is the assigned value,
TSD is the target value for the standard deviation.

In the following section, a brief overview will be provided of how the assigned values and target standard deviation (TSD) values – where applicable – were determined.

Procedure 1: Metronidazole tablets (200 mg & 500 mg) dissolution tests

Assigned value for procedure 1

The assigned value for the amount (%) of metronidazole released after 30 minutes was the consensus value obtained when calculating the Huber's robust mean which is equal to 98.0% for the 200 mg tablets and 97.0% for the 500 mg tablets.

Target standard deviation for procedure 1

The TSD for procedure 1 was set at 3% for both tablet strengths. EDQM indicated that the uncertainties of the assigned values (0.44% for the 200 mg tablets and 0.61% for the 500 mg tablets) were found to be negligible compared with the TSD and could thus be ignored in the interpretation of the performance scores.

Procedure 2: Metronidazole tablets (200 mg & 500 mg) disintegration test

Since the participants only reported if disintegration occurred within the specified time with a Yes/No-answer, no consensus value or z-score was determined and no statistical evaluation of the data *sensu stricto* was carried out by EDQM. Both strengths of the metronidazole tablets were tested in the feasibility study and were found to be compliant with the disintegration test, meaning all six units disintegrated within 10 minutes.

Procedure 3: Metronidazole injection assay by UV/Vis-spectrophotometry test

Assigned value for procedure 3

The assigned value for the assay (%) of the metronidazole injection was the consensus value obtained when calculating the Huber's robust mean which is equal to 101.3%.

Target standard deviation for procedure 3

The TSD for procedure 3 was set at 1%. EDQM indicated that the uncertainty of the assigned value (0.27%) was found to be negligible compared with the TSD and could thus be ignored in the interpretation of the performance scores.

Procedure 4: Metronidazole injection related substances test employing TLC

Since the participants only reported a Yes/No-answer, no consensus value or z-score was determined and no statistical evaluation of the data *sensu stricto* was carried out by EDQM. The metronidazole injection sample tested during the feasibility study was found to be compliant with the related substances test, meaning that the spot obtained with solution B was more intense than any spot obtained with solution A.

Procedure 5: Metronidazole injection pH test

Assigned value for procedure 5

The assigned value for the pH of the metronidazole injection was the consensus value obtained when calculating the Huber's robust mean which is equal to 5.0.

Target standard deviation for procedure 5

The TSD for procedure 1 was set at 0.15. It was reported by EDQM that the uncertainty of the assigned value is 0.01 and was found to be negligible compared with the TSD. The uncertainty of the assigned value could thus be ignored in the interpretation of the performance scores.

DISCUSSION OF THE RESULTS REPORTED FOR EQAAS Phase 11

A total of forty-four (44) laboratories participated in the WHO EQAAS Phase 11. Detailed reports were issued to all participants to allow them to evaluate and compare their performance against the other international participants. In the following section, a summarised overview will be provided of the outcomes of this phase.

Procedure 1: Metronidazole tablets (200 mg & 500 mg) dissolution tests

Only forty-two (42) of the participants reported their results – the results are summarised in Table 1.

Table 1: Summary of the outcomes of procedure 1

	Acceptable results	Doubtful results	Unacceptable results
200 mg tablets	39/42 (93%)	2/42 (5%)	1/42 (2%)
500 mg tablets	39/42 (93%)	1/42 (2%)	2/42 (5%)

The z-scores of the participants in procedure 1 with the 200 mg and 500 mg tablets are depicted in Figure 2. The black dots indicate the respective z-scores. For the dissolution testing of the 200 mg tablets, thirty-nine (39) of the laboratories (93%), reported satisfactory results ($|z\text{-score}| < 2$). Two (2) laboratories reported doubtful results ($2 < |z\text{-score}| > 3$) and one (1) laboratory reported unsatisfactory results ($|z\text{-score}| \geq 3$). The mean dissolution value reported by one (1) laboratory was found to be an outlier based on Grubbs' test. Three (3) laboratories reported high variability between the individual dissolution values (i.e. high standard deviation values) and were found to be outliers according to Cochran's test.

For the dissolution testing of the 500 mg tablets, again, thirty-nine (39) of the laboratories (93%), reported satisfactory results. One (1) laboratory reported doubtful results, and two (2) laboratories reported unsatisfactory results. The mean dissolution values reported by two (2) laboratories were found to be outliers based on Grubbs' test, and one (1) laboratory reported high variability between the individual dissolution values, which was found to be an outlier according to Cochran's test.

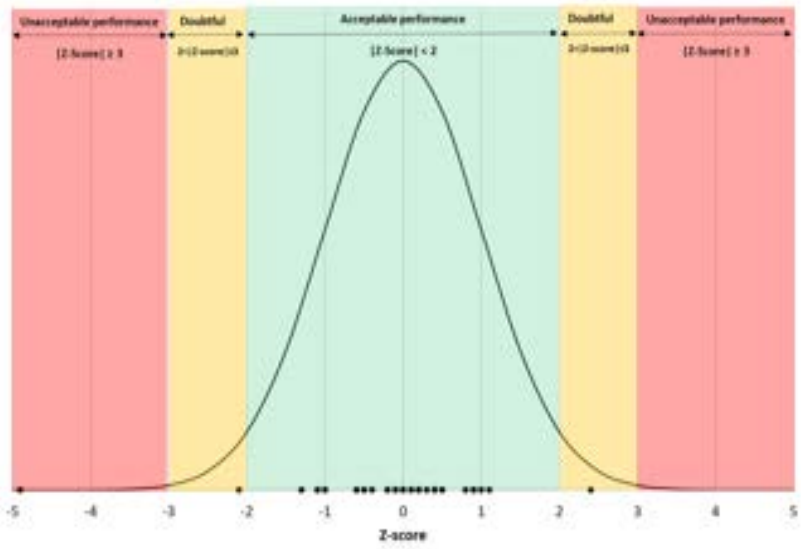

(a)

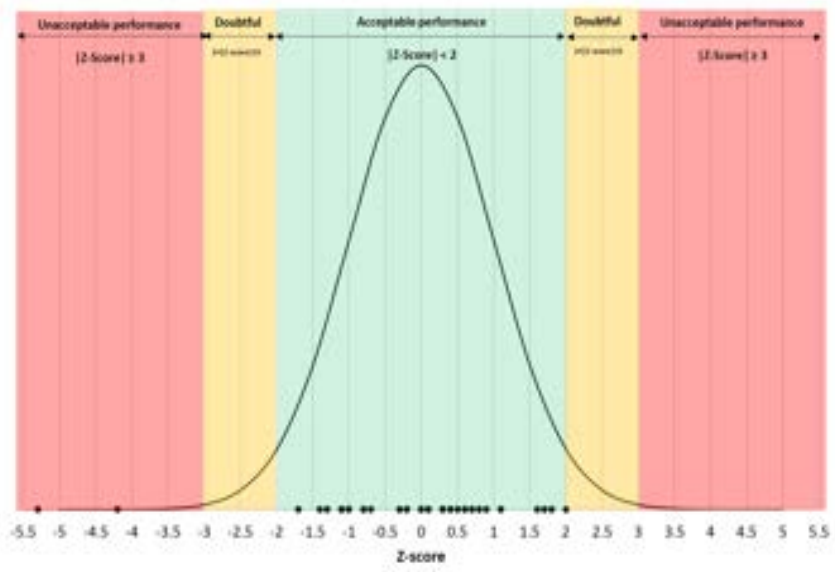

(b)

Figure 2: The z-scores of the participants in Procedure 1 for: (a) 200 mg metronidazole tablets and (b) 500 mg metronidazole tablets.

To conclude ninety-three percent (93%) of the laboratories reported satisfactory results for procedure 1. It was recommended that four (4) of the laboratories should to investigate their procedures and take the necessary actions to improve their performance. Points which may be considered as potential sources of errors included (but are not limited to): weighing errors, dilution errors, incorrect calibration/qualification of equipment used, composition- volume or temperature of dissolution media, incorrect speed of rotation, formation of bubbles in dissolution media, potential interferences with filters used and or calculation/reporting errors.

Procedure 2: Metronidazole tablets (200 mg & 500 mg) disintegration test

During WHO EQAAS Phase 10 a high failure rate (52%) was observed for the disintegration test.[6] WHO decided to provide technical support (Post-EQAAS Phase 10 Assistance Programme) to those PQCLs who expressed interest in identifying and resolving the issues which resulted in reporting failing/unacceptable results. It was decided to include disintegration tests again in the WHO EQAAS Phase 11 to evaluate the performance of PQCLs post-support.

During the feasibility study, it was found that all six (6) units of the metronidazole tablets (both strengths) disintegrated within 10 minutes. Figure 3 provides a schematic presentation of the disintegration results reported by the participants for the metronidazole tablets (both strengths).

(a) (b)

Figure 3: Schematic presentation of the disintegration results reported by the participants in Procedure 2 for: (a) 200 mg metronidazole tablets and (b) 500 mg metronidazole tablets.

Forty-one (41) of the laboratories reported results for the disintegration tests performed on the 200 mg metronidazole tablets. All the laboratories (100%) indicated that the tablets were fully disintegrated within 10 minutes, and thus reported acceptable results.

Forty-two (42) of the laboratories reported results for the disintegration tests performed on the 500 mg metronidazole tablets. Again, all the laboratories (100%) indicated that the tablets were fully disintegrated within 10 minutes, and thus reported acceptable results.

It can thus be concluded that all laboratories (100%) provided acceptable results and that the post-EQQAS assistance provided resulted in a significant increase in the abilities of PQCLs to deliver acceptable disintegration test outcomes.

Procedure 3: Metronidazole injection assay by UV/Vis-spectrophotometry test

During procedure 3, the laboratories performed a UV/Vis spectrophotometric assay on the issued metronidazole injection sample. The z-scores of the participants in procedure 3 are depicted in Figure 4. The black dots indicate the respective z-scores.

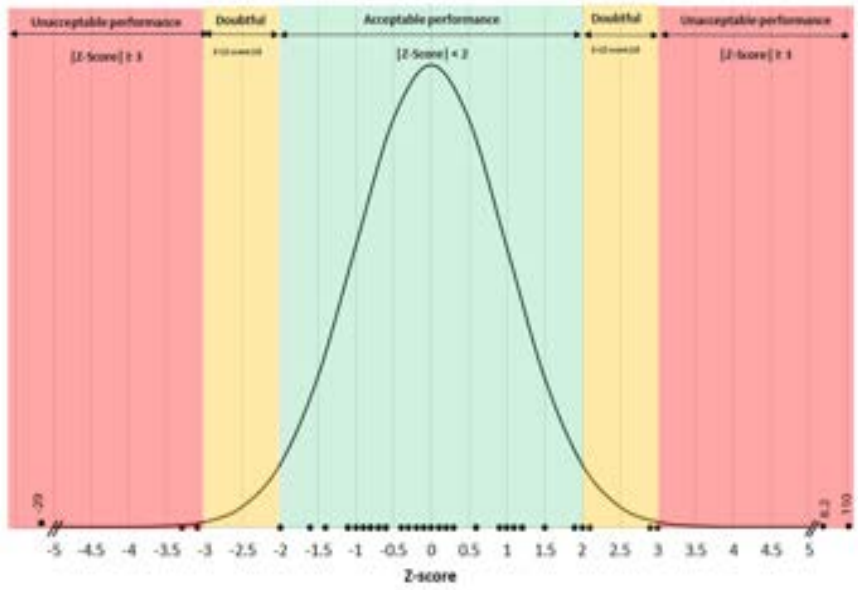

Figure 4: The z-scores of the participants in Procedure 3.

Forty-two (42) participants submitted assay results of which thirty-four (34) laboratories (81%) reported acceptable results. Three (3) laboratories reported doubtful results ($2 < |Z\text{-score}| < 3$), and five (5) reported unsatisfactory results ($|Z\text{-Score}| \geq 3$). The Grubb's test indicated that the mean assay values reported by three (3) laboratories were outliers. Four (4) laboratories reported incorrect standard deviation values.

It was recommended that eight (8) of the laboratories need to investigate their procedures and take the necessary actions to improve their performance. Points which may be considered as potential sources of errors included (but are not limited to): weighing errors, dilution errors, inappropriate handling of samples/solutions, incorrect calibration/qualification of equipment used, measurements were not performed at the specified wavelengths, use o inappropriate slit-width and calculation/reporting errors.

Procedure 4: Metronidazole injection related substances test employing TLC

During this procedure, the laboratories were requested to confirm whether or not the metronidazole injection sample complied with the related substances requirement "the spot obtained with solution B is more intense than any corresponding spot obtained with solution A", according to the method in *The International Pharmacopoeia* monograph on metronidazole injection.[5] During the feasibility study it was found that the sample complied with the mentioned requirement – thus an answer of "Yes" is correct. Figure 5 provides a schematic presentation of the results of the related substance reported by the participants for the metronidazole injection.

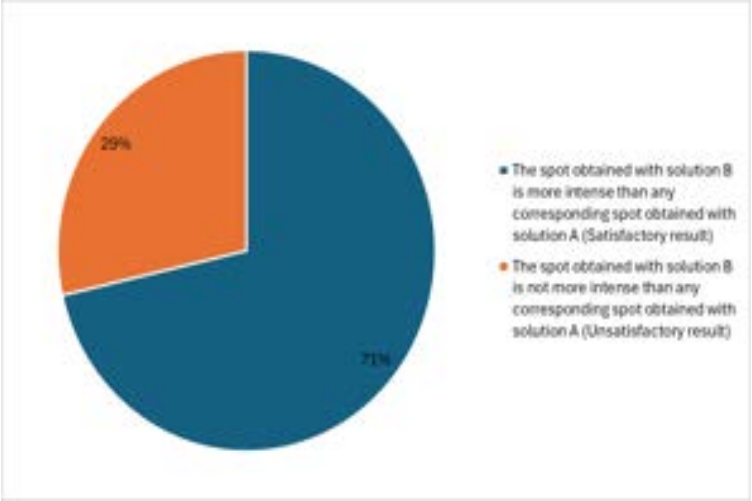

Figure 5: Schematic presentation of the results of the related substance tests reported by the participants in procedure 4 for the metronidazole injection.

Forty-two (42) of the participants provided results. Only thirty (30) of the participants (71%) reported satisfactory results for this procedure. Three (3) of the twelve (12) participants who reported unsatisfactory results, indicated in their comments on the preliminary report, that the reason for their failure could be attributed to either wrong interpretation of the monograph specification or the use of the incorrect TLC plate.

It was recommended that twelve (12) of the laboratories need to investigate their procedures and take the necessary actions to improve their performance. Points which may be considered as potential sources of errors included (but are not limited to): solution preparation errors, errors in sample volume spotted onto the TLC plate, period between deposit and development of the TLC plate being too long, positioning of the TLC plate during development and visualisation is not correct and reporting errors.

Procedure 5: Metronidazole injection pH test

All forty-four (44) of the participants submitted results for procedure 5. The z-scores of the participants in procedure 5 are depicted in Figure 6 where the black dots indicate the respective z-scores.

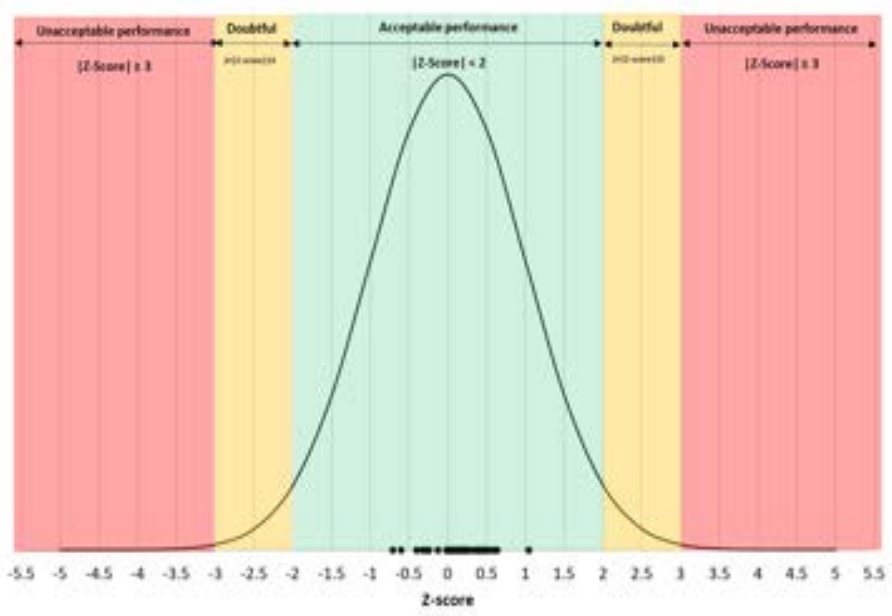

Figure 6: The z-scores of the participants in Procedure 5.

All the laboratories (100%) reported satisfactory results (|z-score| < 2). Two (2) of the laboratories showed high variability between the individual pH results that they reported and were found to be outliers for the standard deviation according to Cochran's test. One (1) laboratory reported an incorrect standard deviation value.

Given the overall results reported for this procedure, the TSD could potentially be lowered in future pH-studies.

Post-EQAAS Phase 11 Assistance Program

Laboratories that produced unacceptable results are recommended to investigate their procedures to identify the root causes that contributed to the reporting of these results. As for EQAAS phases 9 & 10, a Post-EQAAS Phase 11 Assistance Program (PEP-11-AP) will be launched by WHO to assist such laboratories. An invitation to participate in the PEP-11-AP will be forwarded to all laboratories. Participation in this assistance program will be voluntary and free of cost.

References

1. **WHO.** WHO Good practices for pharmaceutical quality control laboratories. WHO Technical Report Series, No: 1052: Annexure 4. 2024. Online: https://www.who.int/publications/m/item/who-good-practices-for-pharmaceutical-quality-control-laboratories.

2. **ISO.** ISO/IEC 17025:2017 – General requirements for the competence of testing and calibration laboratories.

3. **WHO**. 2022. Metronidazole tablets. International Pharmacopoeia. Online: https://digicollections.net/phint/2022/index.html#d/b.6.2.2.86.

4. **WHO.** 2022. Disintegration test for tablets and capsules. International Pharmacopoeia. Online: https://digicollections.net/phint/2022/index.html#d/b.7.5.4.

5. **WHO**. 2022. Metronidazole injection. International Pharmacopoeia. Online: https://digicollections.net/phint/2022/index.html#d/b.6.2.2.84.

6. **BRITS, M & ESTEVÃO CORDEIRO, S.** 2022. World Health Organization External Quality Assurance Assessment Scheme Phase 10. WHO Drug Information, 36(3):595-608.

***

QUALITY OF IMMEDIATE RELEASE SOLID ORAL HYDROCHLOROTHIAZIDE TABLETS IN SOUTH AFRICA

Jenaé Van Wyk, Joe M. Viljoen and Marius Brits*

*North-West University, Faculty of Health Sciences, Centre of Excellence for Pharmaceutical Sciences (Pharmacen™) Potchefstroom, South Africa

Abstract

Hydrochlorothiazide (HCTZ) is a thiazide diuretic that is used globally for the treatment of hypertension and oedema. It is the most commonly prescribed antihypertensive drug worldwide, where more than 134.1 million prescriptions for HCTZ were written in the United States during 2008. However, there have been global concerns regarding the quality of HCTZ, as several studies have reported the presence of substandard and/or falsified HCTZ products on the international market during surveillance studies conducted in recent years. In addition to the high prevalence of HCTZ substandard and/or falsified products, a study indicated the public's diminished perception of the quality of generic products compared to innovator products in South Africa. Therefore, the aim of this study is to evaluate the quality of commercially available HCTZ products in South Africa and to evaluate them according to the specifications stated in the British Pharmacopeia monograph for HCTZ tablets. In addition, the visual inspection of commercially available products was evaluated using a novel proposed panoramic, four-tier visual inspection method, which contributed to the enhanced assessment of the quality and safety of these products. Furthermore, the results obtained in this study concluded that both products indeed contained HCTZ, and that the quality of the generic product was comparable to that of the innovator product, as both products were of acceptable quality.

Keywords

Hydrochlorothiazide, quality, substandard, falsified, generic, comparable.

QUALITY OF IMMEDIATE RELEASE SOLID ORAL HYDROCHLOROTHIAZIDE TABLETS IN SOUTH AFRICA

Introduction

Hydrochlorothiazide (HCTZ) is a thiazide diuretic that is used globally for the treatment of hypertension and edema.[1] Its mechanism of action occurs in the distal convoluted tubules, where it inhibits sodium chloride reabsorption, resulting in increased excretion of water, sodium, potassium, and hydrogen ions, which consequently leads to diuretic action.[1] HCTZ is part of the Essential Medicine List of the World Health Organization (WHO) and is considered relatively safe.[2] Studies have shown that HCTZ is the most commonly prescribed antihypertensive drug worldwide, where more than 134.1 million prescriptions were written for HCTZ in the United States during 2008.[3] Although HCTZ is the most commonly prescribed antihypertensive, there have been global concerns regarding the quality of HCTZ, as several studies have reported the presence of substandard and/or falsified HCTZ products on the international market. Moreover, a medical product alert reported by WHO confirmed the presence of a falsified HCTZ product in the African region that has been found to contain glibenclamide instead of HCTZ.[4] In addition, the Central Drug Standards Control Organisation in India, flagged more than 50 substandard drug products in 2024 where HCTZ were among the flagged products.[5] Furthermore, substandard HCTZ were found during a quality control study conducted in Western Cameroon and the Northeast Democratic Republic of Congo.[6] During the period of 2018 to 2021, a recall of substandard and falsified medicinal products occurred in Zambia, where HCTZ products were, again, among the samples that were identified.[7] In a study by de Oliveira et al. it was indicated that several quality concerns (including pharmaceutical non-equivalence and drug-excipient incompatibilities) were identified within pharmaceutical formulations containing HCTZ that were available on the Brazilian market.[8] A similar concern was reported by Varillas et al. where one of the generic HCTZ products failed to show similar in vivo dissolution behaviour when it was compared to the innovator product.[9]

A study by Patel et al. indicated a diminished perception by the public concerning the quality of generic products compared to the innovator products in South Africa.[10] Therefore, with the high prevalence of substandard and/or falsified HCTZ products globally, as well as the diminished perception regarding the quality of generic products, it amplifies the need to investigate the quality of HCTZ products in South Africa, as the presence of substandard and/or falsified HCTZ products can lead to the inaccessibility to safe and efficacious medicines to the public.

The aim of this study is to evaluate the quality of commercially available HCTZ products in South Africa, as well as to confirm their authenticity, according to the specifications stated in the British Pharmacopeia for conventional solid oral dosage forms.[11]

Materials and Methods

Materials

HCTZ raw material (purity of 99.5%) was generously sponsored by Aspen Pharmacare, South Africa. Commercially available tablets containing 25 mg HCTZ were procured from local pharmacies in Potchefstroom, South Africa. Only two products could be procured in South Africa, namely: Hexazide 25 mg (Sandoz, Germany; batch number: MT1629; expiry date: 08/2025) and Ridaq 25 mg (Aspen Pharmacare, South Africa; batch number: A907151; expiry date: 11/2024). Ridaq 25 mg – the South African innovator product, was labelled as Product 1 and Hexazide 25 mg as Product 2.

Methods

Visual inspection of the obtained solid oral dosage forms

The quality of a finished pharmaceutical product (FPP) is limited not only to the quality of the dosage form that is to be administered to the patient but also to the quality of the packaging and information provided with the product. The quality of packaging may influence the chemical, physical, and biological stability of an FPP. Furthermore, the quality of the information provided with the product should promote safe administration to the patient. Unfortunately, the focus of visual inspection methods for solid oral dosage forms (SODs), as described in the pharmacopoeias, is mainly on the appearance of the SODs without considering other properties that may affect the quality and safety of an FPP. Due to the absence of such a panoramic visual inspection method, a four-tier approach (Figure 1) has been developed and will be applied in this study.

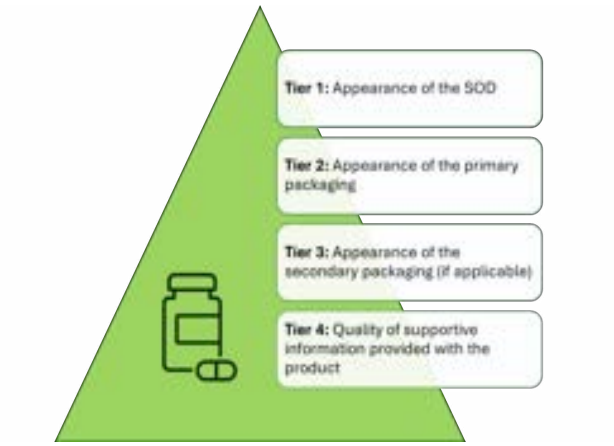

Figure 1: Four-tier visual inspection procedure for inspection of SODs.

Tier one (1) focusses on the appearance of the SOD which includes physical aspects such as: colour, shape, thickness, diameter, coating, scoring, engravement or printing, and the presence of visible defects. The compliance of the solid oral dosage form with the physical aspects specified by the manufacturer in the product information leaflet is evaluated. In tier two (2) the appearance of the primary packaging of the product is compared to that specified by the manufacturer. Parameters to be considered include type of packaging, presence of visual defects, tamper-evident features, and print quality on the primary packaging. In tier three (3) the appearance of the secondary packaging (if applicable) is evaluated where the same parameters as for the primary packaging are considered. In the last tier, the package insert(s) and content are evaluated. The compliance of the package insert information with the applicable (local) medicines regulatory authority requirements should be evaluated. In this study, compliance with the requirements of the South African Health Products Regulatory Authority (SAHPRA) was evaluated. [11] Tier one (1) inspection was performed on twenty (20) randomly selected tablets from each product.

Identification of HCTZ using thin-layer chromatography (TLC)

The presence of HCTZ in the products was confirmed using the thin-layer chromatographic (TLC) method specified in the HCTZ tablet monograph of the British Pharmacopoeia (BP). [12] A test solution was prepared by triturating a quantity of the HCTZ tablet powder equivalent to 10 mg of HCTZ with 10 mL of acetone. A standard solution containing 0.1% (w/v) of HCTZ was prepared in acetone. A sample of 5 µL of each of the solutions was applied to a TLC plate coated with silica gel GF_{254}. The TLC plate was developed to 15 cm using ethyl acetate as the mobile phase. Following, the TLC plate was inspected under ultraviolet light with a radiation wavelength of 254 nm. The presence of HCTZ in the products is confirmed by the appearance of a principal spot in the chromatogram from the test solution that is similar in position, shape, and intensity to the spot observed in the chromatogram obtained with the standard solution.

Assay

To determine the amount of HCTZ present in both products, an assay was performed according to the HCTZ tablet monograph of the BP. [12] Subsequently, twenty (20) tablets from each product were randomly selected, weighed, and powdered using a mortar and pestle. Thereafter, 50 mL of 0.1 N sodium hydroxide (NaOH) was added to a quantity of tablet powder containing approximately 30 mg of HCTZ. The sample was shaken for 20 min to allow the HCTZ to dissolve. Following, the sample solution was diluted to a final volume of 100 mL with 0.1 N NaOH. The mixed sample solution was subsequently filtered using a 0.45 µm polyvinylidene fluoride (PVDF) syringe filter (Microsep, South Africa) and 5 mL of the filtrate was diluted to a final volume of 100 mL using purified water.

The absorbance of the resulting test solution was determined at a wavelength of approximately 273 nm using the Lamba 365 UV/Vis spectrophotometer (Perkin Elmer, United Kingdom) and the HCTZ content ($C_7H_8ClN_3O_4S_2$) was calculated considering the specific absorbance of the solution ($A_{1cm}^{1\%}$) as 520 and 273 nm using Equation (1):

$$\%\ HCTZ\ per\ tablet = \frac{A_{sample} \times Mass_{STD} \times LC \times 100}{A_{STD} \times AVG \times 150} \quad (1)$$

Where:

% HCTZ per tablet	=	Percentage HCTZ in tablet relative to the label claim
A_{sample}	=	Absorbance of sample solution
$Mass_{STD}$	=	Mass of HCTZ standard used (for $A_{1cm}^{1\%}$ = 1000 mg)
LC	=	Label claim of the product (i.e., 25 mg/tablet)
A_{STD}	=	Absorbance of standard solution (for $A_{1cm}^{1\%}$ = 520 nm)
AVG	=	Average tablet mass of the product reported in mg

According to the BP monograph HCTZ tablets should contain an amount of HCTZ equivalent to 92.5 to 107.5% of the stated amount on the product label.[11]

Uniformity of dosage form (weight variation)

The uniformity of the drug present in a single-dose dosage form plays an important role in ensuring that the final product is safe and effective for use. The uniformity of the HCTZ content in the immediate release tablets was investigated using the weight variation test described in the BP.[12] Ten (10) tablets were randomly selected from each product and individually weighed. Thereafter, the acceptance value (AV) was calculated using the assay results obtained for each product. Subsequently, the individual estimated tablet content (x_i) was calculated using Equation (2):

$$x_i = w_i \times \frac{A}{\bar{W}} \quad (2)$$

Where:

$X_1, X_2, \ldots X_n$	= individual estimated contents of the tablets tested
$W_1, W_2, \ldots W_n$	= induvial masses of the tablets tested
A	= content of the HCTZ (percentage of label claim) obtained using the assay method
$\bar{W}$	= mean of individual masses

The calculated individual estimated content (x_i) was used to calculate the mean individual content ($\bar{X}$) using Equation (3):

$$\bar{X} = \frac{\sum_{i=1}^{n} x_i}{n} \quad (3)$$

Where:

$\bar{X}$	= mean of individual content values
x_i	= individual estimated contents of the tablets tested
n	= number of tablets tested = 10

The calculated individual estimated content (x_i) was used to calculate the sample standard deviation (s) using Equation (4):

$$s = \sqrt{\frac{\sum_{i=1}^{n}(x_i - \bar{X})^2}{n-1}} \quad (4)$$

Where:

s = Sample standard deviation
$\bar{X}$ = mean of individual content values
x_i = individual estimated content of the tablets tested
n = number of tablets tested = 10

The acceptance values (AV) were calculated using Equation (5):

$$AV = |M - \bar{X}| + ks \quad (5)$$

Where:

AV = Acceptance value
M = Reference value, where $M = \bar{X}$ if 98.5 % ≤ $\bar{X}$ ≤ 101.5% or M = 98.5% if $\bar{X}$ < 98.5% or M = 101.5% if $\bar{X}$ > 101.5%
$\bar{X}$ = mean of individual content values
k = Acceptability constant if n = 10, then k = 2.4
s = Sample standard deviation

The test product showed acceptable variability in weight if the calculated AV-value is not greater than 15.0.[12]

Average tablet mass

The average tablet mass was determined according to the specifications of the BP.[12] Twenty (20) tablets of each product were randomly selected and individually weighed. The average mass of the tablets was calculated using Equation (6):

$$Average\ tablet\ mass\ (in\ mg) = \frac{Sum\ of\ individual\ tablet\ massses\ (mg)}{20} \quad (6)$$

Tablet dimensions and hardness

The dimensions and hardness of the tablets were measured according to the methodology described in the BP.[12] The mechanical hardness and dimensions of the tablets were determined using an Erweka TBH 425 series tablet hardness tester (Erweka, Germany). Ten (10) tablets of each product were randomly selected and placed onto the equipment in a clockwise direction. Following, the measurement sequence of the instrument was initiated to automatically measure the diameter, hardness, and thickness of each individual tablet.

Friability

Tablet friability was established using the procedure specified in the BP. [12] As the individual tablet mass was less than 650 mg for both products, a sample corresponding to 6.5 g was selected. Each tablet was carefully dedusted to remove any residue powder prior to weighing the tablets. Next, the tablets of the specific product were transferred to the rotary drum of an Erweka TAR 220 friabilitator (Erweka, Germany) and rotated at 25 rpm for 4 min. The tablets were removed from the rotary drum and any traces of residue powder were brushed off. The tablets were consequently weighed to calculate the % mass loss, using Equation (7):

$$\%\ Mass\ loss = \frac{Mass\ of\ tablets\ after\ tumbling}{Mass\ of\ tablets\ prior\ to\ tumbling} \times 100 \quad (7)$$

According to the BP, the percentage mass loss may not exceed 1% (m/m).

Disintegration

Six (6) tablets of both products were randomly selected and subjected to the disintegration test as described in the BP [12] using an Erweka ZT 320 series disintegration tester (Erweka, Germany). One (1) tablet was placed in each of the six (6) tubes of the basket assembly and the immersion fluid (purified water), was maintained at 37 ± 2^{0}C. The instrument was started by allowing the basket-rack assembly to periodically submerge the tubes (containing the tablets) into the immersion fluid. After 15 min, the basket-rack was lifted from the fluid for observation to determine if all the tablets completely disintegrated. If one (1) or two (2) tablets failed to disintegrate within the set time, the test was repeated on an additional twelve (12) tablets. The test could be deemed unsuccessful if fewer than sixteen (16) of the eighteen (18) tablets failed to disintegrate within the set 15 min.

Comparative dissolution studies of commercially available HCTZ tablets

Comparative dissolution studies were performed on 12 tablets from each of the HCTZ innovator and generic products. The testing method was based on the SAHPRA and the WHO multisource pharmaceutical product guidelines on comparative dissolution testing. [13–14] BCS dissolution media (i.e., 0.1 N hydrochloric acid pH 1.2, acetate buffer pH 4.5, and phosphate buffer pH 6.8) were used. The medium volume was 900 mL with an agitation speed of 75 rpm maintained with the paddle method (USP apparatus II) at a temperature of 37.0 ± 0.5°C. Samples of 10 mL were withdrawn at the following intervals: 10, 15, 30, 45, and 60 min. After each withdrawal, 10 mL of preheated medium (maintained at 37.0 ± 0.5°C) was replaced in each vessel to maintain sink conditions during the dissolution studies. The amount of HCTZ released from the tablets was determined using a validated UV-spectrophotometric method. [15] Aliquots sampled at the various time intervals were diluted using the respective dissolution medium to obtain an approximate target concentration of 13.8 µg/mL. The UV absorbances of the samples were measured at the maximum absorbance wavelength of 271 nm, as established in the validated method. [15] Standard solutions containing approximately 13.8 µg/mL HCTZ in the respective dissolution media were used to quantify the amount of HCTZ released from the tablets at the various time intervals. Finally, the dissolution profile of the generic product was compared to the profile of the innovator product.

Results and Discussion

Each product was visually inspected using the newly proposed four-tier visual inspection procedure against the specifications stated in the product-specific patient information leaflet (PIL).[16-17]

Table 1: Visual inspection results of Products 1 and 2

Tier 1: Appearance of the tablet		
Properties	**Product 1**	**Product 2**
Colour	Pale peach	White to off-white
Shape	Round, flat-faced, bevelled edge and bisected on one side tablet	Round, biplanar tablet with a face
Average tablet thickness (mm) ± standard deviation	2.21±0.03	2.41±0.02
Average diameter (mm) ± standard deviation	6.47±0.01	7.83±0.01
Coating status	Uncoated tablets	Uncoated tablets
Tablet scoreline	One visible scoreline on one side	Cross-score notch on one side
Engraving on tablet	Absent	Absent
Tablet defect visible	None detected	None detected
Tier 2: Appearance of primary packaging		
Packaging type	Polypropylene container	Polyvinylchloride blister pack with aluminium backing
Visual defects	None detected	None detected
Tamper-evident features	White rayon sealed with low density polyethylene cap	Foil lamination
Print quality	Clear and legible	Clear and legible
Tier 3: Appearance of secondary packaging		
Packaging type	Only primary packaging	Cardboard carton
Visual defects	N/A	None detected
Tamper-evident features	N/A	None present
Print quality	N/A	Clear and legible
Product indication displayed	N/A	None indicated
Unique feature	N/A	None indicated
Tier 4: Quality of supportive product information		
Professional information presented	Yes	Yes

Patient information leaflet included	Yes	Yes
Product information (name, active ingredient, dosage form)	Yes	Yes
Therapeutic indication displayed	Yes	Yes
Dosage regimen included	Present	Present
Legibility of printed materials	Good	Good
Route of administration indicated	Yes	Yes
Contraindications indicated	Yes	Yes
Warnings and precautions indicated	Yes	Yes
Drug interactions indicated	Yes	Yes
Pregnancy and lactation information provided	Yes	Yes
Storage instructions indicated	Yes	Yes
Shelf life indicated	Yes On primary packaging	Yes On primary and secondary packaging
Manufacturing information displayed	Yes	Yes

Both products complied with the minimum specified requirements for the four-tier visual inspection, contributing to the quality and safety of the products. The presence of HCTZ in the products was confirmed using the TLC method specified in the BP. Figure 2 illustrates the TLC chromatogram obtained for the two test solutions (Solutions B & C) and the reference solution (Solution A).

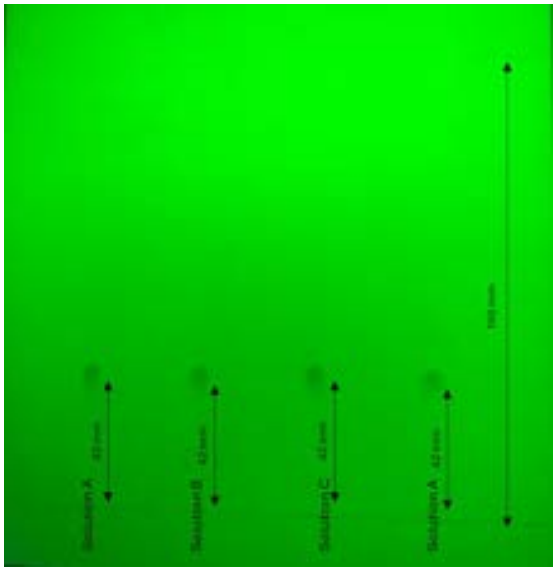

Figure 2: TLC chromatogram obtained of the HCTZ reference solution (Solution A), Product 1 test solution (Solution B) and Product 2 test solution (Solution C).

The principal spots observed for the two test solutions (Solutions B and C) on the TLC chromatogram were found to be similar in position (R_f-values of all spots observed = 0.28), shape, and intensity compared to the spot obtained with the standard solution (Solution A). Therefore, the presence of HCTZ in the commercially available products could be confirmed. Furthermore, no secondary spots were observed on the TLC chromatogram for any of the solutions.

The physical properties (i.e., friability, disintegration, and crushing strength) and performance results (i.e., disintegration and dissolution) of both products are summarised in Table 2.

Table 2: Physical properties and product performance results of Products 1 and 2

Properties evaluated	Product 1	Product 2
Average tablet mass (mg)	107.65	162.88
Friability (%)	0.10	0.61
Crushing strength (N)	45.0	64.5
SD:	4.16	3.75
%RSD:	9.25	5.80
Disintegration time (min & sec)	0 min and 6 sec	0 min and 3 sec
SD:	0.84	0.19
%RSD:	14.59	5.76

The average tablet hardness of Products 1 and 2 was 45 N and 64.5 N, respectively. This is indicative of a lower mechanical strength since it falls outside the range recommended by Krisch and Drennen of 90–120 N.[18] Nonetheless, both products complied with the friability test requirements in that the % friability did not exceed 1%.

The disintegration data indicate that both products exhibited complete disintegration within the set specification of 15 min for immediate release tablets. To evaluate the impact of rapid disintegration on the dissolution behaviour of the products, comparative dissolution studies were performed. The dissolution profiles attained from Products 1 and 2 are illustrated in Figure 3. Both products displayed very rapid dissolution, where the % dissolution was greater than 85% of the label claim within 15 min in all three-dissolution media. The RSD values at all withdrawal intervals (i.e.,15–60 min) were less than 10%. Therefore, it can be concluded that the dissolution profiles of these two products (in all three BCS dissolution media) could be considered similar based on the requirements set out by the WHO.[4]

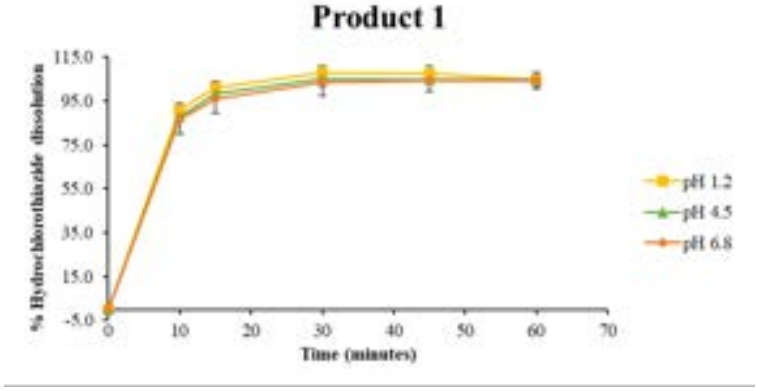

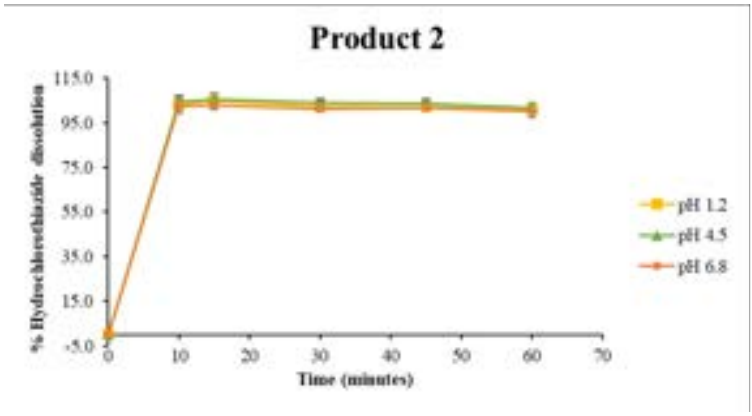

Figure 3: Dissolution profiles of HCTZ Products 1 and 2 in respective dissolution media (pH 1.2, 4.5 and 6.8) and the associated 95% confidence intervals.

Given that HCTZ is classified as a BCS Class III drug, the risk of non-bioequivalence of these two products could be considered being low, thus supporting the interchangeability thereof.

Following, the HCTZ content in Products 1 and 2 was determined using the UV/Vis spectrophotometric method of the BP. The results obtained are summarised and presented in Table 3.

Table 3: The assay results of Products 1 and 2

Sample number	% Assay	
	Product 1	Product 2
1	97.7	95.1
2	98.1	97.2
3	95.8	97.2
Average:	97.2	96.6
SD:	1.2	1.4
%RSD:	1.2	1.4

According to the BP, the equivalent HCTZ content should range from 92.5 to 107.5% relative to the label claim. [11] The product labels of both products claim that the tablets contain 25 mg HCTZ per tablet. Therefore, the assay results of both products comply with the pharmacopeial specification seeing that the average HCTZ content for Product 1 and Product 2 was 97.2% and 96.6%, respectively. Furthermore, a t-test (95% CI) indicated that there is statistically no significant difference between the HCTZ content of the two products (p-value > 0.05).

To evaluate the uniformity of the HCTZ distribution in the tablets, the weight variation test was performed. The AV-values calculated for Products 1 and 2 were 3.0 and 3.5, individually. These results conclude that both products show acceptable variability in HCTZ content, since both AV-values were found to be less than 15.0.

Conclusion

Due to the high prevalence of substandard and/or falsified HCTZ products worldwide, as well as the growing public concern with regard to the quality of generic products, the need to perform a post-market surveillance study of commercially available HCTZ immediate release products available in South Africa was identified.

Visual inspection of the commercially available products using the newly proposed four-tier, panoramic visual inspection method confirmed the acceptability of the FPPs with the specifications defined by the manufacturer in the PI/PIL. In addition, the identification test results confirmed the presence of HCTZ in both products.

The physical properties of both products indicated acceptable product performance that ensured the rapid release of HCTZ from both immediate-release dosage forms, thus supporting their reliable performance. Moreover, the uniformity of HCTZ in single dosage units of both products was illustrated. This will ensure accurate and consistent delivery of HCTZ doses upon administration to patients. Furthermore, being classified as a BCS Class III drug, the risk of non-bioequivalence of these products could be considered low, therefore supporting their interchangeability.

In conclusion, based on the outcome of the QC tests, no substandard and/or falsified HCTZ products were detected on the South African market. The quality of the generic product could be considered comparable to that of the innovator product. It is thus recommended that pharmacists and regulators educate the public to address their concerns and perceptions regarding the quality and safety of generic products in South Africa.

References

1) Hydrochlorothiazide, compilation prepared by National Library of Medicine. (https://www.ncbi.nlm.nih.gov/books/NBK430766/, accessed 23 October 2024).

2) WHO Model Lists of Essential Medicines, compilation prepared by World Health Organization (https://www.who.int/groups/expert-committee-on-selection-and-use-of-essential-medicines/essential-medicines-lists, accessed 23 October 2024).

3) Messerli FH, Makani H, Benjo A, Romero J, Alviar C, Bangalore S. Antihypertensive efficacy of Hydrochlorothiazide as evaluated by ambulatory blood pressure monitoring: A meta-analysis of randomised trials. JACC Journals. 2011; 57(5)590-600.5. (doi: 10.1016/j.jacc.2010.07.053, accessed 23 October 2024).

4) WHO. Medicinal product alert N˚ 6/2019: Falsified hydrochlorothiazide. 2019. Compilation prepared by WHO.(https://www.who.int/news/item/17-04-2019-medical-product-alert-n-6-2019-(english-version), accessed 23 October 2024).

5) The times of India. 50 commonly used drugs found substandard, companies say prodycts spurious, not theirs. 2024. Compilation prepared by The Times of India. (https://timesofindia.indiatimes.com/india/50-commonly-used-drugs-found-substandard-companies-say-products-spurious-not-theirs/articleshow/113679248.cms, accessed 23 October 2024).

6) Schäferman S, Hauk C, Wemakor E, Neci R, Mutombo G, Ndze EN, Cletus T, Nyaah F, Pattinora M, Wistuba D, Helmi I, Häfeleabah C, Gross H, Heide L. Substandard and falsified antibiotics and medicines against noncommunicable diseases in Western Cameroon and Northeastern Democratic Republic of Congo. The American Journal of Tropical Medicine and Hygiene. 2020; 103(2)894-908. (doi: 10.4269/ajtmh.20-0184, accessed 23 October 2024).

7) Chabalenge B, Jere E, Nanyangwe N, Hikaambo C, Mudenda S, Banda M, Kalungia A, Matafwali S. Substandard and falsified medicinal product recalls in Zambia from 2018 to 2021 and implications on the quality surveillance systems. The Journal of Medicine Access. 2022; 6:27550834221141767. (doi: 10.1177/27550834221141767, accessed 23 October 2024).

8) de Oliveira MA, Yoshida MI, Silva DC. Quality evaluation of pharmaceutical formulations containing hydrochlorothiazide. Molecules. 2014;19(10):16824-16836. (doi: 10.3390/molecules191016824, accessed 23 October 2024).

9) Varillas MA, Brevedan MIV, Gonzalez Vidal NL. Pharmaceutical Equivalence of Hydrochlorothiazide tablets in Argentina. Diss Tech, 2018; 25(4):22-27. (doi: 10.1055/s-0042-111434, accessed 23 October 2024).

10) Patel A, Guald R, Norris P, Rades T. Quality of generic medicines in South Africa: Perceptions versus reality- A qualitative study. BMC Health Services Research. 2012; 12:1-8, 297. (doi: 10.1186/1472-6963-12-297, accessed 23 October 2024).

11) SAHPRA. Guideline for professional information for human medicines (Categories A and D). 2019. Compilation prepared by SAHPRA (https://www.sahpra.org.za/wp-content/uploads/2020/02/2.16_Guideline-for-Professional-Information-for-Human-Medicines-Categories-A-and-D_Jul19_v2-1.pdf, accessed 24 October 2024).

12) BP (British Pharmacopeia). 2024 Compilation prepared by BP (https://www-pharmacopoeia-com.nwulib.idm.oclc.org/bp-2024/appendices/contents-of-the-appendices-1.html?date=2024-07-01, accessed 24 October 2024).

13) WHO. Multisource (generic) pharmaceutical products: guidelines on registration requirements to establish interchangeability. 2017. (https://www.who.int/publications/m/item/annex-6-trs-1003, accessed 24 October 2024).

14) Quality and bioequivalence guideline compilation prepared by SAHPRA (https://www.sahpra.org.za/wp-content/uploads/2020/02/2.02_Quality-and-Bioequivalence-Guideline_Jul19_v7-1.pdf , accessed 24 October 2024).

15) Van Wyk J, Viljoen JM, Brits M. Validated BCS Comparative dissolution method for hydrochlorothiazide tablets. World Journal of Pharmacy and Pharmaceutical Sciences. 2024; 13(9)1208-1223.

16) Ridaq. Compilation prepared by South African Health Products Regulatory Authority.(https://pi-pil-repository.sahpra.org.za/wp-content/uploads/2023/05/RIDAQ_Comb_Tab_ZA_RIDATAB_2303_00_EPIL_2023.03.04.pdf, accessed 25 October 2024).

17) Hexazide 25mg. Compilation prepared by South African Health Products Regulatory Authority. (https://medsinfoportal.sahpra.org.za/pil/79d49ebd9fc6bb9d8fcc5d395f345ece.pdf, accessed 25 October 2024).

18) Krisch J, Drennen J. Determination of film-coated tablet parameters by near-infrared spectroscopy. Journal of Pharmaceutical and Biomedical analysis. 1995; 13(10):1273-1281. (doi: 10.1016/0731-7085(95)01562-y, accessed 25 October 2024).

***

BCS-BASED BIOWAIVER MONOGRAPH FOR HYDROCHLOROTHIAZIDE

Jenaé Van Wyk, Joe M. Viljoen and Marius Brits*

*Faculty of Health Sciences, Centre of Excellence for Pharmaceutical Sciences (Pharmacen™) Potchefstroom, South Africa

Abstract

The Biopharmaceutical Classification System (BCS) is used to classify a drug substance based on its solubility and intestinal permeability. This system forms the basis for the development of a risk-based tool for international medicines regulatory authorities (MRAs), which is used when considering the waiver of in vivo bioequivalence studies during the development of generic formulations. Since the BCS classification of a drug substance is the primary precursor when considering a biowaiver, it is of utmost importance that a drug is classified correctly. However, after an in-depth literature review on the BCS classification of hydrochlorothiazide (HCTZ), several inconsistencies have been detected, with the primary inconsistency being the classification thereof. It has been found to be classified as a Class I, II, III, and/or IV drug. Furthermore, another detected inconsistency was the agreement of the polymorphic behaviour of HCTZ. Therefore, the focus of this publication was to evaluate the eligibility of HCTZ in immediate release (IR) solid oral dosage forms to qualify for a BCS-based biowaiver based on the available literature and additional generated experimental data, with the focus of this risk assessment being on solubility, permeability, dissolution, excipient impact, therapeutic window, dosage form and polymorphic behaviour of HCTZ. In this study, a proposed classification for HCTZ was given based on quality assured experimental data, as well as an in-depth literature review. In addition, the potential risk of the polymorphism of HCTZ to alter the bioavailability, product performance, and stability of HCTZ was explored. Additionally, the risk associated with the waiver of in vivo bioequivalence studies was explored and a recommendation was made. Finally, a computational simulation was performed using GastroPlus® to evaluate the impact of the experimentally determined solubility on the BCS classification of HCTZ, with respect to the intestinal permeability after the administration of different doses. This simulation presented results that were remarkably comparable to those obtain in vivo.

KEYWORDS

Hydrochlorothiazide, biopharmaceutical classification system, solubility, permeability, biowaiver, dissolution, excipients.

BCS-BASED BIOWAIVER MONOGRAPH FOR HYDROCLHOROTHIAZIDE

Introduction

The Biopharmaceutical Classification System (BCS) is used to classify a drug substance based on its solubility and intestinal permeability. This system forms the basis for the development of a risk-based regulatory tool for international medicines regulatory authorities (MRAs), which is used when considering the waiver of in vivo bioequivalence studies during the development of generic formulations. [1] The World Health Organization (WHO), the European Medicines Agencies (EMA), and the United States Food and Drug Administration (US-FDA) have established guidelines to which a drug substance must adhere to in order to be eligible for a biowaiver. [2–4] These guidelines are commonly applicable to immediate release (IR) solid oral dosage forms (fixed dose combinations can apply) that are classified in either Class I (high solubility; high permeability) or Class III (high solubility; low permeability) according to the BCS. [5] Therefore, it is of the utmost importance that a drug is classified correctly. After an extensive literature review on the BCS classification of hydrochlorothiazide (HCTZ), several inconsistencies in the classification of HCTZ were found. HCTZ has been classified as a Class I, II, III, and/or IV drug, as seen in Table 1. In addition, the primary inconsistency detected could be attributed to the fact that the solubility of HCTZ over the pH range of 1.2–6.8 has not been confirmed in the available literature. Most of the BCS classifications that have been performed were done based on its water solubility. [6]

Another concern that may influence the eligibility of the biowaiver is the disagreement with regard to the polymorphic behaviour of HCTZ. Some authors disagree on the number of anhydrous polymorphic forms of the HCTZ, whereas other researchers disagree completely with the existence of different anhydrous crystal forms of HCTZ. [7]

In order to be considered for a BCS-based biowaiver, a drug must not only be Class I/III, but it must adhere to the in vitro dissolution criteria, where the drug substance in both test and reference samples should dissolve either rapidly: where no less than 85% of the sample dissolves within 15 min; or rapidly where no less than 85% of the sample dissolves within 30 min (Class I), or not less than 85% of the test sample and reference sample dissolve in 15 min (Class I/III). In addition, the excipients of the test and innovator products must be qualitatively identical and quantitatively similar. Furthermore, the influence of polymorphism must be investigated. [2-4]

The purpose of this article is to evaluate the eligibility of HCTZ in IR solid oral tablets to qualify for a BCS-based biowaiver founded on the available literature and additional experimental data generated, with the focus of this risk assessment being on solubility, permeability, dissolution, excipient impact, therapeutic window, dosage form and polymorphic behaviour of HCTZ (Figure 1). This evaluation is not applicable to any fixed-dose combination products of HCTZ.

Table 1: The BCS classification of HCTZ in available literature

Class	Year	Reference
Provisional I	2016	(7)
II	2015	(8)
II	2019	(9)
II	2021	(10)
Provisional III	2003	(11)
III	2004	(12)
III	2014	(13)
III	2016	(14)
III	2018	(15)
III & IV	2005	(16)
IV	2011	(17)
IV	2015	(18)
IV	2016	(19)
IV	2016	(20)
IV	2017	(21)
IV	2017	(22)
IV	2017	(23)
IV	2017	(24)
IV	2018	(25)
IV	2020	(26)
IV	2022	(27)

Figure 1: Factors considered during the risk assessment with regards to the BCS classification of HCTZ.

MATERIALS AND METHODS

Literature research

A review of available online literature was performed by searching the World Wide Web, Pharmaceutical abstracts, PubMed, Science Direct, websites of medicine regulatory agencies of various countries (to obtain the PIL information of HCTZ products), the National Centre for Biotechnological information, Springer, and Scopus with the following keyword/s and combinations thereof: hydrochlorothiazide, BCS, solubility, permeability, stability, dissolution, bioavailability, bioequivalence, biowaiver, polymorphism, metabolism, pharmacokinetics, mechanism of action, dosage forms. The information obtained was evaluated according to the guidelines set by international organisations such as WHO, US-FDA, EMA and ICH. [2-4, 28]

Materials

HCTZ raw material (purity of 99.5%) was generously sponsored by Aspen Pharmacare, South Africa. Commercially available tablets containing 25 mg HCTZ were procured from local pharmacies in Potchefstroom, South Africa. The products obtained included: Hexazide 25 mg (Sandoz, Germany; batch number: MT1629; expiration date: 08/2025) and Ridaq 25 mg (Aspen Pharmacare, South Africa; batch number: A907151; expiration date: 11/2024). Ridaq 25 mg, the South African innovator product, was labelled as Product 1 and Hexazide 25 mg as Product 2.

All chemicals and reagents used were of analytical grade. Hydrochloric acid 32%, sodium dihydrogen orthophosphate 97%, sodium hydroxide 98.5%, and glacial acetic acid 97% were commercially obtained from ACE Chemicals (ACE Chemicals, South Africa).

Solubility

Solubility studies of HCTZ were conducted in accordance with the WHO-specified guidelines. [29] The solubility of HCTZ was determined in the following buffers: 0.1 N HCl (pH 1.2), acetate buffer (pH 4.5), and phosphate buffer (pH 6.8). Approximately 50 mg of HCTZ raw materials were weighed and transferred to test tubes. In addition, 100 mg glass beads (Sigma-Aldrich, USA) were added to each of the test tubes to promote good mixing and prevent formation of agglomerates. A sample of 10 mL of each buffer was transferred to the respective test tubes. Thereafter, the test tubes were sealed and fixed to sample holders in a temperature-controlled water bath, which was maintained at 37 ± 0.2^{0}C. The samples rotated at 62 rpm, where sample withdrawal occurred at 2 h, 4 h, 8 h, 24 h, 48 h, and 72 h to allow the construction of a solubility profile. After each sample withdrawal, the samples were filtered using Millipore® 0.45 µm polyvinylidene difluoride (PVDF) membrane filters (Microsep, South Africa) and appropriately diluted prior to high performance liquid chromatographic (HPLC) analysis. The stability-indicative HPLC method published by Bhagwate et al. was used to quantify the amount of HCTZ in the aliquots. [30]

Polymorphism

HCTZ raw material was subjected to recrystallisation studies as discussed in the available literature in an attempt to obtain Forms I and II. In the endeavour to obtain Form I, HCTZ was recrystallised from a 1:4 mixture of tetrahydrofuran and water using slow evaporation. [31] Furthermore, attempting to obtain Form II, the modified precipitation method was applied, where acetone solutions of HCTZ were added to distilled water containing hydroxypropyl methylcellulose under agitation. The precipitate that formed was immediately isolated by membrane filtration [32] and the recrystallised samples were subjected to X-ray powder diffraction analysis (XRPD) as well as scanning electron microscopy (SEM) analysis to characterise the solid-state form(s) obtained.

- XRPD
  A PANalytical Empyrean diffractometer (PANalytical, The Netherlands) was used to record XRPD patterns. The following conditions were applicable: target, Cu; voltage, 40 kV; current, 30 mA; divergence slit, 2 mm; anti-scatter slit, 0.6 mm, detector slit, 0.2 mm; monochromator; scanning speed, 2°/min with a step size of 0.025° and a step time of 1.0 sec.

- SEM
  An FEI Quanta 200 FEG scanning electron microscope (SEM) with an X-Max 20 EDS system (FEI, USA) was used to obtain micrographs of the crystalline forms of HCTZ. The powdered samples were adhered to a small piece of carbon tape, which was mounted onto a metal stub. The mounted samples were coated with a gold-palladium film using a suitable ion coater (Eiko Engineering ion Coater IB-2, United States).

Powder dissolution studies

HCTZ powder dissolution studies in three different dissolution media (0.1 N HCl – pH 1.2; acetate buffer – pH 4.5; and phosphate buffer – pH 6.8) were conducted according to the technique described by Lötter et al. [33] Samples weighing approximately 50 mg were accurately transferred into test tubes containing approximately 25 mg glass beads (with a diameter of 0.1 mm) (Sigma Aldrich, Johannesburg, South Africa). 10 mL volumes of the dissolution medium were transferred into each test tube. The suspended samples were agitated using a Vortex Genie shaker (Scientific Industries Inc., Bohemia, New York) for approximately 1 min before they were rinsed into the respective dissolution vessels. Samples were withdrawn at 10, 15, 30, 45, and 60 min. Following each withdrawal, 10 mL of pre-heated medium (maintained at 37.0 ± 0.5°C) was replaced in each vessel to maintain sink conditions during the dissolution studies. These samples were filtered with Millipore® 0.45 µm nylon syringe filters (Labfil, China) before UV-spectrophotometric analysis, using a Lamba 365 UV/Vis spectrophotometer (Perkin Elmer, United Kingdom) and UV Winlab explorer software (Perkin Elmer, United Kingdom) in matching pair quartz cells (Agilent, United States of America) with pathlengths of 1 cm. The aliquots sampled during the various time intervals were diluted using the respective dissolution medium to obtain an approximate target concentration of 13.8 µg/mL. The UV absorbances of the samples were measured at the maximum absorbance of 271 nm, as determined during method validation. [34] Standard solutions containing approximately 13.8 µg/mL of HCTZ in the respective dissolution media were subsequently used to quantify the % dissolution of HCTZ at the various time intervals.

Comparative dissolution studies of commercially available HCTZ tablets

Comparative dissolution studies were performed on 12 tablets from each of the HCTZ innovator and generic products that are commercially available in South Africa. As mentioned, the samples were procured from a local pharmacy within Potchefstroom, South Africa. The testing method was based on the South African Health Products Regulatory Authority (SAHPRA) and the WHO multisource pharmaceutical product guidelines on comparative dissolution testing. [4, 35] The three BCS dissolution media used included: 0.1 N hydrochloric acid pH 1.2, acetate buffer pH 4.5, and phosphate buffer pH 6.8. The medium volume was 900 mL with an agitation speed of 75 rpm maintained with the paddle method (USP apparatus II) at a temperature of 37.0 ± 0.5°C. Samples of 10 mL were withdrawn during the following time intervals: 10, 15, 30, 45, and 60 min. Following each withdrawal, 10 mL of pre-heated medium (maintained at 37.0 ± 0.5°C) was replaced in each vessel to maintain sink conditions during the

dissolution studies. The amount of HCTZ released from the tablets was determined using a validated UV-spectrophotometric method. [34] The dissolution profiles of the generic product were compared to the profile of the innovator product. The aliquots sampled at the various time intervals were diluted using the respective dissolution medium to obtain an approximate target concentration of 13.8 µg/mL. The UV absorbances of the samples were measured at the maximum absorbance of 271 nm as established in the validated method. [34] Standard solutions containing approximately 13.8 µg/mL HCTZ in the respective dissolution media were subsequently used to quantify the amount of HCTZ released from the tablets at the various time intervals. Finally, the dissolution profiles of Product 1 and Product 2 were also compared to the profile of the HCTZ raw material product by determining the similarity factor (f_2) first described by Moore and Flanner using Equation (1). [36]

$$f_2 = 50 \log \left\{ \left[1 + \frac{1}{n} \sum_{t=1}^{n} (R_t - T_t)^2 \right]^{-0.5} \times 100 \right\} \quad (1)$$

Where:

R_t = % of reference sample dissolved

T_t = % of test sample dissolved

n = number of dissolution time points

A similarity factor ranging between 50–100% is indicative of comparable dissolution behaviour. [36]

Particle size analysis

The particle size distribution of the HCTZ raw material sample was determined using a Malvern® particle size analyser (Malvern® Instruments, United Kingdom). The particle size distribution was determined while the particles were suspended in purified water.

In silico intestinal permeability of HCTZ predicted using GastroPlus®9.7

GastroPlus®9.7 is a bottom-up, whole-body physiologically based pharmacokinetic (PBPK) model that utilises the Advanced Compartmental Absorption Transit (ACAT) mechanistic absorption model to mimic the human intestinal absorption of oral formulations from the gastro-intestinal tract. [37] This software was used to predict the compartmental absorption, dissolution behaviour, and the permeability (indicative of the fraction absorbed observed in humans (F_a)) of HCTZ, when administered as an IR tablet, over the range from the lowest formulation strength (i.e., 12.5 mg) to the highest therapeutic dose (i.e., 100 mg) for HCTZ.

RESULTS AND DISCUSSION

General characteristics

HCTZ is a widely prescribed diuretic, belonging to the sulfonamide derivatives of the benzothiazine class. It is also known as 6-Chloro-3,4-dihydro-2H-1,2,4-benzothiadiazine-7-sulfonamide 1,1-dioxide ($C_7H_8ClN_3O_4S_2$), and the chemical structure is depicted in Figure 1. HCTZ is an amphiprotic drug with two dissociation constant (pK_a) values of 7.0 and 9.2. [39] It has been reported that amphoteric molecules exhibit the lowest solubility at their isoelectric point. [40] The solubility of a drug at this pH is referred to as the intrinsic solubility (S_0) of the said API. [40] The isoelectric point (pI) of HCTZ has been calculated using the following equation: [41]

$$pI = \frac{pK_{a1}+pK_{a2}}{2} \quad (2)$$

The pI of HCTZ was calculated as 12.5, which is significantly higher than the pH of the gastrointestinal tract. Moreover, HCTZ presents as a white or almost white crystalline powder that is practically odourless with a slight bitter taste. [42–43] The melting point of this API has been reported to range between 273 and 275°C; and it exhibits polymorphism. [42, 44] The opposing views regarding its polymorphic behaviour, as stated in the available literature, will be discussed in the next sections.

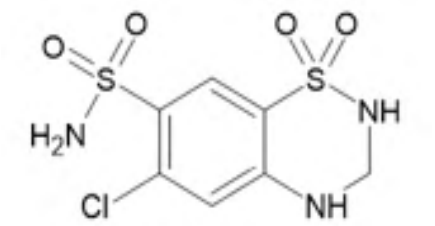

Figure 2: Chemical structure of hydrochlorothiazide. [42]

Additionally, HCTZ has a described partition coefficient, Log P (n-octanol/water), of –0.1. [39] Furthermore, the Log D value for HCTZ at pH 6.5 is –2.85. These values were established in a study that concluded that HCTZ possesses poor jejunal permeability once measured against the internal standard. [45]

Therapeutic uses, therapeutic index, adverse effects, and drug interactions

The mechanism of action of HCTZ occurs in the distal convoluted tubules where it inhibits sodium chloride reabsorption, resulting in increased excretion of water, sodium, potassium, and hydrogen ions. [46] The inhibition of the sodium chloride cotransporter induces both a natriuresis and a diuresis effect, which in turn, causes an initial decrease in blood pressure due to volume loss. [47] Furthermore, HCTZ has the ability to sustain a reduction in blood pressure by means of vasodilation, as well as a reduction in peripheral vascular resistance. [46-48] Due to HCTZ being effective in reducing blood pressure, it has become one of the primary treatments for early-onset hypertension. [46] It is also used in the treatment of peripheral oedema, related to heart failure, oestrogen therapy, corticosteroids, or nephrotic syndromes. [47]

HCTZ is commercially available in tablet or capsule form for oral administration with strengths of 12.5 mg, 25 mg and 50 mg per tablet/capsule. [46] The recommended initial dose of HCTZ for the treatment of hypertension in adult patients is 12.5 to 25 mg daily, where the dose can be increased, if deemed necessary, to a maximum dose of 50 mg daily. [48] The HCTZ dose-response curve for the treatment of hypertension is known to be flat. [48] A comparative study conducted where HCTZ strengths of 3, 6, 12.5, 25 mg, and a placebo, were compared in 111 patients with moderate hypertension, demonstrated that 12.5 mg produced a borderline anti-hypertensive effect, whereas 25 mg had a definite anti-hypertensive effect. The administration of 3 and 6 mg of HCTZ did not have an anti-hypertensive effect. Therefore, an initial dose of 12.5 to 25 mg HCTZ daily is considered satisfactory. [49]

The initial dose recommended for the management of peripheral oedema is 25 to 50 mg once or twice daily with a maximum daily dose of 200 mg. [48] HCTZ can furthermore be used in conjunction with other antihypertensive drugs, which include calcium channel blockers, betablockers, angiotensin converting enzyme (ACE) inhibitors, and any other diuretics. [46] HCTZ is generally well tolerated, however, it has been associated with adverse effects. In some cases, patients may develop an electrolyte imbalance, leading to conditions such as hypokalaemia, hyponatremia, hypomagnesemia, hypercalcemia, and hyperchloremic that occur because of the inhibition of the sodium chloride cotransporter. Electrolyte imbalance can manifest with neurological symptoms which include fatigue, weakness, and paralysis (due to hypomagnesemia). [50] Hyperglycaemia has been associated with the treatment of HCTZ that normally presents as thirst and recurrent urinary tract infections. Gout flares can be precipitated by hyperuricemia, caused by the diuretic effect of HCTZ that leads to increased uric acid reabsorption. [51] Thiazide therapy has also been shown to cause dyslipidaemia, where a study demonstrated that the total cholesterol in patients increased with 10%. [52] Allergic reactions due to a sulfonamide allergy can present in minor cases as a dermatological skin rash or, in worst case scenarios, cause anaphylaxis. [53] In rare cases, HCTZ has been associated with ocular disturbance, where treatment of HCTZ developed in acute angle-closure glaucoma and myopia. [54]

HCTZ is contraindicated in cases of anuria; sulfonamide allergies; patients with hepatic impairment, as it may result in hepatic encephalopathy; patients that have gout, as HCTZ decreases the urea clearance resulting in hyperuricemia; and in patients with systemic lupus erythematosus, as HCTZ worsens this disease. [46] Moreover, there are potentially hazardous interactions that can occur when combined with HCTZ treatment. These interactions include combinations with anti-cancer drugs, such as thiazide diuretics, which may potentiate bone marrow suppression; and lithium, since HCTZ causes volume depletion, resulting in an increased lithium absorption. [44, 46] Because HCTZ is commonly known to cause hypokalaemia, it is furthermore prone to cause interactions with cardiac glycosides, corticosteroids, and tubocurarine. In addition, nonsteroidal anti-inflammatory (NSAIDS) drugs may attenuate HCTZ anti-hypertensive effects. Carbamazepine used in conjunction with HCTZ can also result in hyponatremia and cholestyramine may reduce the absorption of HCTZ. [44, 46]

PHYSICOCHEMICAL PROPERTIES

Polymorphism

As stated in the previous section, the BP states that HCTZ exhibits polymorphism. [42] Studies in the early 1980s indicated the ability of HCTZ to recrystallise into four potentially different polymorphic forms. [55] However, in a more recent study conducted by Johnston et al., the existence of these four polymorphs was disputed and small differences observed in the XRPD patterns were attributed to misinterpretation of the preferred orientation effects in the data generated during the original study conducted by Kim and Kim. [56] Johnston et al. concluded that only two forms (Form I & Form II) of HCTZ exist. [56] Forms I and II have been characterised as anhydrous polymorphs of HCTZ, where Form I is the thermodynamically stable form, and Form II the metastable form. [31, 56–57]. It has also been indicated that Form II is not commercially available due to its significant thermodynamic instability. [31] The water solubility of Form I was determined as 0.79 mg/mL, while that of Form II is 0.73 mg/mL, thus not having a significant difference. [6, 32] However, the literature has again reported conflicting statements in which Aceves-Hernández et al. disagreed on the existence of polymorphs for HCTZ. The possible structural modifications at different temperatures illustrated that conformers presented with similar structural parameters, infrared vibration frequencies, reactive indexes, and dipole moments, which are indicative of similar polarities and similar interactions with polar solvents. Based on the information discussed, it was concluded that the molecular structure of HCTZ exhibits thermodynamic stability. [58–59]

In an attempt to confirm the existence of Forms I and II, the recrystallisation methods described by Chadha et al. and Florence were performed, and the isolated crystals were subjected to XRPD analysis. [31–32] The XRPD patterns (Figure 3) of the HCTZ raw material and recrystallised samples depicted diffraction peaks at the same 2θ˚positions, however, the intensities of these peaks differed. These differences in intensities could be attributed to the preferred orientation of the crystalline samples. [60] To investigate this, the morphology of the samples was examined using SEM studies. The SEM analysis (Figure 3) illustrated that the particles in the raw material (C) were isotropic in nature in that the dimensions of the particles in all directions were found to be comparable. However, the dimensions of the recrystallised samples (A & B) showed differences in all directions (i.e. monoclinic plate-like formations), which are characteristic of anisotropic solids. Seeing that the external shape of crystals plays a critical role in achieving randomness in the orientation, anisotropic crystals will result in a distinctly non-random orientation when subjected to powder packing for XRPD analysis, which will introduce distortions in the scattering intensities, explaining the significant differences in the intensities of the observed diffraction peaks. [60] Therefore, it can be concluded that differences in the habits of HCTZ result in a preferred orientation, as stated by Johnston et al. [56]

Furthermore, the XRPD patterns found in studies by Aceves-Hernández et al. and El-Gizawy et al. were comparable to the commercially available raw material used in South Africa. [58, 61] In addition, de Salvi et al. indicated that the commercially available products in Brazil exhibited the same XRPD pattern as Form I, which was also comparable to the raw material analysed in this study. [57] Therefore, it can be concluded that Form I is internationally available and is used to manufacture solid oral dosage forms comprising HCTZ, whereas Form II presents significant thermodynamic instability. [31] Seeing that there are no markable differences in the aqueous solubility of Forms I and II, and the rapid conversion of Form II into the thermodynamically stable Form I, it can be concluded that the polymorphic behaviour of HCTZ does not appear to introduce a significant risk to the bioavailability, drug product performance, and stability of HCTZ. The ICH guideline for specifications for test procedures and acceptance criteria for new drug substances and new drug products (ICH Q6A) states that polymorphic forms should only be monitored and controlled when their existence introduces a risk to the bioavailability, drug product performance, and stability of the drug. [62] The absence of any specifications to monitor and control the polymorphic form in the HCTZ drug substance and drug products in international pharmacopoeia supports this conclusion. [28, 42]

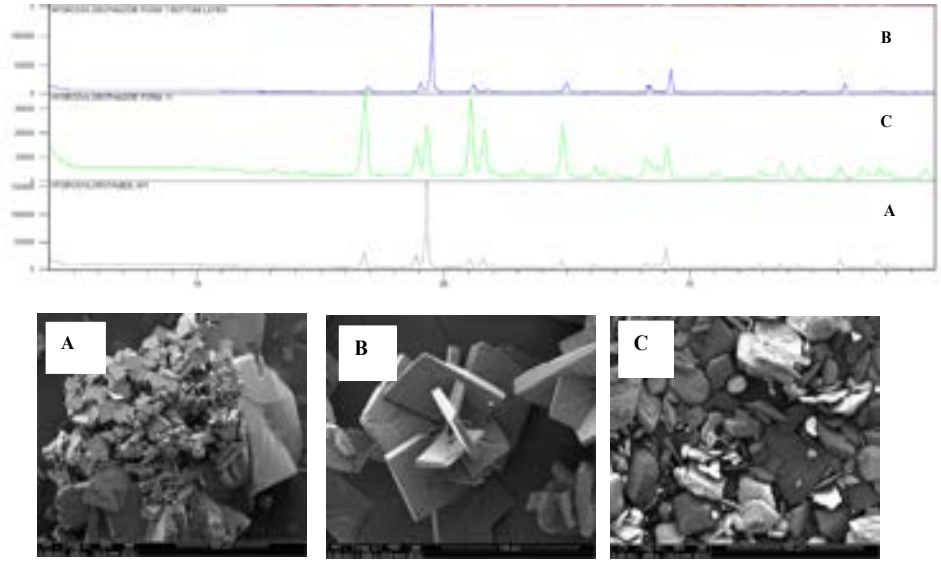

Figure 3: Overlay of XRPD pattern of: (A) HCTZ raw material, (B) HCTZ recrystallised using method described for Form I, and (C), HCTZ recrystallised using method described for Form II.

Over the last few decades, there have been multiple attempts to enhance the solubility, dissolution, and permeability characteristics of HCTZ. In a recent study, HCTZ nanoparticles were produced by means of top-spray coating, coated onto micro-sized microcrystalline cellulose particles. [63] Here, the coated particles exhibited a 3-fold increase in the dissolution rate of HCTZ compared to pure HCTZ. In addition, the nanoparticles produced an enhanced rate of permeability across the dialysis membrane. [63] In another study, multiple component crystals of HCTZ with nicotinic acid, 4-aminobenzioic acid, succinimide, and resorcinol were prepared. Except for nicotinic acid and succinimide, all co-crystals displayed improved solubility rates in a buffer solution with a pH of 7.4. Enhanced solubility was furthermore achieved with co-crystals of HCTZ with the water soluble coformers, 4-dimethyalaminopyridine and picolinamide. [23] HCTZ was formulated with the use of hot melt extrusion; this process includes the melting and forcing of polymers, additives, and drugs through an orifice within controlled temperatures, pressure, screw speed, and feeding rates. In this study, HCTZ existed within the formulation as either a dispersion within the polymer or as an amorphous solid. In addition, a significant increase was achieved in the dissolution profile as well as in the intestinal absorption. [64] The intestinal absorption was tested on 12 rabbits where it was established that the absorption of HCTZ in the presence of polymers increased from 37.9% to 75.2% in the jejunum; and from 21.7% to 79.9% in the ileum. [64] The potential for new salts of HCTZ with nicotinic acid (HCTZ-NA) and 2-picolinic acid (HCTZ-PIC) was also explored in an attempt to improve the solubility, dissolution, and therapeutic efficacy. It was subsequently found that the solubility (in water after 24 h) increased from 0.79 mg/mL to 1.42 mg/mL and 1.16 mg/mL for HCTZ-PIC and HCTZ-NA, respectively. An enhanced dissolution rate was achieved, with a six-fold increase after 10 min for both HCTZ-NA and HCTZ-PIC. Moreover, therapeutic efficacy was tested in four salt-induced hypertensive rats, where HCTZ-NA decreased the systolic pressure more than HCTZ and demonstrated the same safety, when reviewing the histological evidence of the rats. Therefore, it was concluded that of the two salt formations, HCTZ-NA displayed greater solubility, dissolution, therapeutic efficiency, and safety. [31]

Solubility

HCTZ is very slightly soluble in water (1000 to 10,000 parts of solvent per 1 part of the solute), soluble in acetone, and sparingly soluble in ethanol (from 30 to 100 parts of solvent per 1 part of the solute), where it dissolves in dilute solutions of alkali hydroxides. [42] However, because of the absence of BCS solubility data, additional studies were conducted on HCTZ in accordance with the WHO guidelines. [29]

The solubility of HCTZ in 0.1 N HCl pH 1.2, acetate buffer pH 4.5 and phosphate buffer pH 6.8 was determined experimentally. The respective solubility profiles are illustrated in Figure 4. A clear plateau was reached in the HCTZ solubility after 24 h in each of the respective buffer solutions, indicating the solubility equilibrium. Furthermore, the concentration of HCTZ did not deviate by more than 10% between the sequential measurements (as specified by the WHO), supporting the observation that HCTZ has reached its solubility equilibrium. [29]

Table 2 summarises the average solubility values of HCTZ in each of the buffer solutions and the corresponding dose/solubility ratios of the highest therapeutic dose of HCTZ (i.e., 25 mg according to the WHO guidelines) and the highest single dose for HCTZ (i.e., 50 mg as per the EMA guideline).[29, 65] This was done to determine whether a difference in the HCTZ dose would lead to a different conclusion on the classification of the solubility of HCTZ. The solubility of HCTZ in the three (3) media was found to be greater than 1 mg/mL, which translates into a solubility ratio of less than 30 mL based on the highest available therapeutic dose of 25 mg HCTZ and with a solubility ratio of less than 60 mL based on the highest available dose of 50 mg.

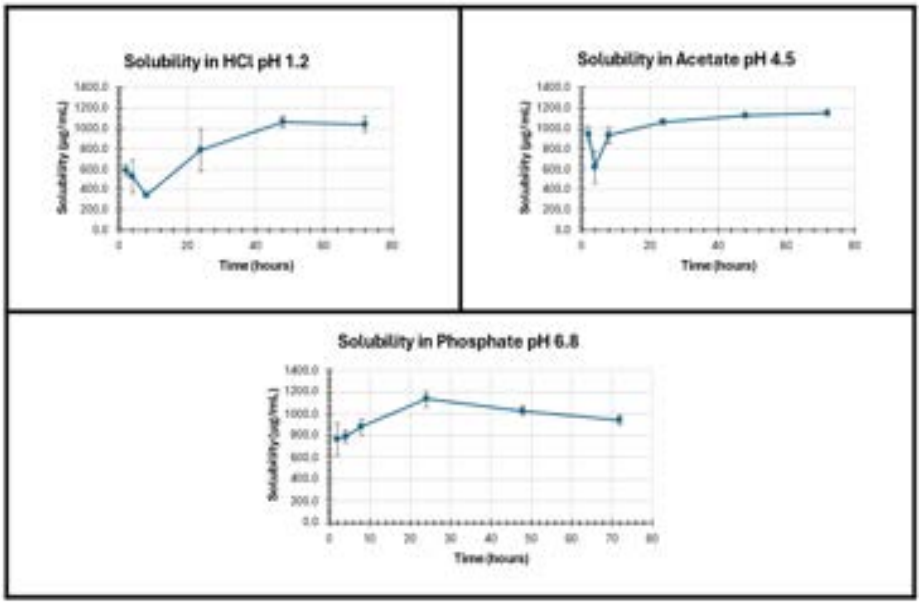

Figure 4: HCTZ solubility profiles in 0.1 N HCl pH 1.2, acetate buffer pH 4.5, and phosphate buffer pH 6.8. 95%. Confidence intervals are indicated by the error bars.

Table 2: Solubility (C_s) of HCTZ at 37˚C and the corresponding dose/solubility (D/S) ratios for D = 25 mg and D = 50 mg

Buffer / Solvent	C_s ± 95% CI (mg/mL)	$D/S_{25\ mg}$ (mL)	$D/S_{50\ mg}$ (mL)
1. 0.1 N HCl pH 1.2	1.058±0.144 mg/mL	23.6 mL	47.3 mL
2. Acetate buffer pH 4.5	1.113±0.067 mg/mL	22.5 mL	44.9 mL
3. Phosphate buffer pH 6.8	1.060±0.173 mg/mL	23.6 mL	47.2 mL

Performing an analysis of variance (ANOVA) test at 95% CI, it was confirmed that there was no statistically significant difference between the solubility of HCTZ in the three buffer solutions as a p-value > 0.05 was obtained. The results achieved thus support the findings of Leon et al., where it was illustrated with the use of the potentiometric titration method that there was no significant change in the solubility of HCTZ across the physiological pH range. [66]

PHARMACOKINETIC PROPERTIES

Absorption and bioavailability

Following oral administration, little to none of HCTZ is absorbed in the stomach. Absorption occurs predominantly in the duodenum and jejunum. [48] HCTZ is eliminated primarily unchanged through the kidneys and is not metabolised by the human body; therefore, the absorption of HCTZ should be close to the amount recovered in the urine. For this reason, most studies conducted to obtain the bioavailability of HCTZ were based on the percentage of urinary recovery. [67]

The influence of food on the absorption of HCTZ has been presented with conflicting statements, as one study stated that the absorption was increased, whereas another indicated that it was reduced in the presence of food compared to the fasting state. [68–69] It was however determined that the difference in the two studies could have been as a result of the difference between the fasting states during the two experiments. The presence of food could delay the passage through the small intestine, as a study conducted on patients with shunt surgery showed an accelerated intestinal passage, which caused reduced absorption of HCTZ. [70]
Peak plasma concentrations are normally achieved after 2 to 4 h post dosing, with a duration of activity of 6 to 12 h. [67] The absorption efficiency of HCTZ is independent of the dose, however, plasma levels as well as urinary excretion are dose proportional. [48, 67] This was confirmed in a study, after the administration of HCTZ, with strengths ranging from 12.5 to 75 mg. The mean plasma levels obtained in this study presented with a C_{max} averaging 70 to 376 $ng.mL^{-1}$ and an area under the curve (AUC) averaging 351 to 1923 $ng.h.mL^{-1}$. Peak plasma levels of HCTZ, as well as the AUC are correlated with the dose administered in that urinary recovery averaged between 65 and 72%, suggesting a mean oral absorption of 70%. [68] This correlation had further been supported in a study conducted on HCTZ tablets with the strengths of 12.5 and 25 mg. The plasma levels and AUC obtained for the 12.5 mg were 75 $ng.mL^{-1}$ and 436 $ng.h.mL^{-1}$, respectively; and increased significantly to 182 $ng.mL^{-1}$ and 1042 $ng.h.mL^{-1}$, correspondingly, when the dose of 25 mg HCTZ was administered. Urine recovery averaged between 60 and 73%, thus, again suggesting a mean oral absorption of approximately 70%. [71] Furthermore, a bioavailability study performed in 14 patients, in which 14 different HCTZ products were administered to the 14 subjects (in the fasting state) over a period of 14 weeks, revealed that the total urinary recovery of the 14 products ranged from 62 to 70% after 24 h; and 70 to 79% after 48 h. [72]

The effect of renal impairment on HCTZ absorption was investigated, and it was found that the mean peak plasma levels increased from 183 ng.mL^{-1} in patients with normal renal function to 415 ng.mL^{-1} in those with moderate to severe renal insufficiency. In addition, the AUC was higher in the subjects with impaired renal function than in the controls. Nonetheless, the more severe the renal impairment became, the more the excretion rate of HCTZ was reduced; consequently, the urinary recovery obtained decreased from 51% in patients with normal renal function to 15.8% in those with severe renal insufficiency. [73]

Permeability

A study carried out on Caco-2 cells that were seeded at high density in 96-well plates was used during drug permeability studies. For this study, any drug that showed an apparent permeability coefficient (P_{app}) lower than 10 x 10^{-6} cm.s^{-1} was considered having a low permeability. HCTZ revealed a P_{app}-value of 0.42 x 10^{-6} cm.s^{-1}, which indicated that it is poorly permeable. [74] In another study, the intestinal permeability of 92 commercially available drugs was tested, with HCTZ being one of them. From this study, it was concluded that HCTZ exhibits poor permeability, as it depicted a P_{app}-value of 0.51 x 10^{-6} cm.s^{-1} (which was lower than the internal standard of 10 x 10^{-6} cm.s^{-1} for poorly permeable drugs). [75] HCTZ was considered to have very good repeatable permeability characteristics, so the authors recommended its use as an internal standard for pH-independent poorly permeable drugs to evaluate Caco-2 cell permeability. [76]

Research was furthermore done on the effect of excipients on the permeability of poorly permeable drugs (including HCTZ), where it was concluded that most excipients did not have a significant influence on the permeability of any of the selected drugs, with the exception of sodium lauryl sulphate that increased the permeability 1.53, 1.27, and 1.42-fold of all drugs when added to the apical compartment. In addition, Tween® 80 significantly increased the permeability of HCTZ with a magnitude 2.5 times higher than that of the control. A control transport study was performed that tested the permeability ratio in the apical to basolateral direction, as well as the basolateral to the apical direction, where the obtained ratio was 1.88. With the addition of Tween® 80, the ratio reduced to 0.92. It could thus be concluded that HCTZ was a substrate for an efflux system, and that Tween® 80 had the ability to inhibit this efflux system. [77]

Furthermore, it was found that once a formulation of HCTZ containing Tween® 80 was administered to healthy volunteers, the percentage urinary recovery increased, therefore, HCTZ with the addition of Tween® 80 results in an enhanced absorption and, in turn, an enhanced bioavailability. [78] Another study was carried out to determine the in vivo proximal jejunum efflux (P_{eff}) in humans based on a single-pass perfusion approach at pH 6.5 under isotonic conditions of various drugs. The P_{eff} value obtained for HCTZ was 0.04 x10^{-4} cm s^{-1}, which, again, is indicative of a poorly permeable drug. [79]

Distribution, metabolism and elimination

The volume of distribution for HCTZ has been reported as 1–3 $L.kg^{-1}$. [48] Plasma protein binding is 40–60%, with a reduced protein binding reported in patients with renal impairment, since tubule secretions are competitively inhibited by endogenous acid metabolites and exogenous weak acids. [48] HCTZ accumulates in erythrocytes where equilibrium is reached between the plasma and blood cells, 4 h after oral administration. [68] It readily crosses the human placenta, where the plasma levels in the umbilical cord are equivalent to those obtained in the maternal circulation; however, plasma levels found in the amniotic fluid are higher. [69] While HCTZ has the ability to reach the foetal circulation at plasma levels equal to those of the maternal circulation, it is not detected in breast milk. [80]

As previously mentioned, HCTZ is not metabolised by the human body and is excreted almost entirely unchanged in the urine. [67] Renal clearance has been reported at 300 $ml.min^{-1}$, indicating a combination of glomerular filtration and proximal renal tubular secretion. [69] Moreover, HCTZ has a biphasic elimination, where the alpha phase plasma has a half-life of 2.5 h, and the beta phase displays a half-life of 8–12 h. [48] The half-life of HCTZ increases significantly in patients with severe renal impairment as a result of the adaptive non-renal excretion mechanism (still unidentified) because the kidneys represent the primary elimination pathway in normal patients. [48] During a study conducted, the elimination half-life of HCTZ increased from a mean value of 6.4 h. to 11.5 h in patients with a mean creatine clearance of 60 $mL.min^{-1}$, to 21 h in patients that had a mean creatine clearance of 19 $mL.min^{-1}$. [73] Furthermore, research showed that 14 patients demonstrated a mean half-life of approximately 5.5 h, which was derived from urine excretion data after the administration of both 25 and 50 mg HCTZ tablets. [72]

DOSAGE FORM PERFROMANCE

Bioequivalence studies

A bioequivalence study was performed on two commercially available 50 mg HCTZ tablets in 39 healthy volunteers. The HCTZ test and reference formulations were administered to the volunteers in a single-blind, randomised, fasting, 2 x 2 crossover study. Blood samples were taken 48 h after initial administration. The average C_{max} values obtained were 280.81 ng/mL and 267.81 ng/mL for the reference product and test product, individually. Moreover, the authors demonstrated that there was no statistically significant difference between the two formulations, since both formulations are within the 90% confidence interval that is in accordance with the Chilean National Regulatory Authority, which stated that if a 90% confidence interval is obtained, bioequivalence is accepted. [82]

The influence of HCTZ administration in the form of tablets and suspensions (with varying strengths of 25, 50, 100 and 200 mg) on the pharmacokinetic parameters, was investigated. The results summarised in Table 3 indicate that the plasma levels obtained from tablets and suspensions did not differ significantly, illustrating that the mean plasma levels are independent of the formulation but proportional to the dose size. [83] Another study on two different 50 mg HCTZ tablets demonstrated that there was no significant difference between the absorption of these two products, with both products having a mean peak concentration of 290 $ng.mL^{-1}$ after 2 h post dosing, as well as urinary recovery of 74.4% and 76.8%, respectively, after 24–48 h. Therefore, it can be concluded that these HCTZ products do not differ significantly from each other. [69]

Table 3: Mean HCTZ pharmacokinetic parameter values following single 25, 50 100 and 200 mg p.o tablet and suspension doses

	Dose (mg)			
	25	**50**	**100**	**200**
Tablet formulation:				
C_{max} ($ng.mL^{-1}$)	127	280	437	-
T_{max} (h)	2.4	2.1	2.3	-
AUC ($ng.g.mL^{-1}$)	978	1968	3354	-
48h urinary recovery (%)	63	55	50	54

Table 3: Mean HCTZ pharmacokinetic parameter values following single 25, 50 100 and 200 mg p.o tablet and suspension doses (continued)

	Dose (mg)			
	25	**50**	**100**	**200**
Suspension formulation:	**25**	**50**	**100**	**200**
C_{max} ($ng.mL^{-1}$)	134	270	490	-
T_{max} (h)	2.4	1.8	1.8	-
AUC ($ng.g.mL^{-1)}$	1038	1910	3993	-
48h urinary recovery (%)	60	54	59	57

Excipient profiles

Solid oral IR dosage forms are commonly used to deliver a drug very rapidly and effectively into the systemic circulation. Therefore, it is formulated with the aid of excipients to promptly disintegrate and release the drug for fast absorption and, in turn, to deliver a rapid therapeutic effect. The excipients included in these solid oral IR dosage forms may influence the dissolution, solubility, and permeability of a drug. [84] Table 4 contains an extensive list of excipients included in HCTZ solid oral IR products registered in different countries.

When reviewing the excipients in the aforementioned table, it can be deduced that most of the excipients pose no risk to the quality of HCTZ, however, surfactants have been included into some HCTZ products and, as stated by the MRAs, this remains the responsibility of generic manufactures to identify and include a detailed description how these excipients will not alter the absorption of the API upon the application of a BCS-based biowaiver. [2-4]

Table 4: Excipient list of HCTZ IR solid oral dosage drug products registered in various countries.

Excipient	Drug product containing excipient with a marketing authorization by the named country	Reference
Lactose monohydrate	United States, Czech Republic, Greece, Finland, Sweden, Norway, South-Africa, Canada, Germany	(85-95)
Magnesium stearate	United States, Czech Republic, Greece, Finland, Sweden, Norway, South Africa, Canada, Germany	
Aluminium stearate	Czech Republic	
Talc	Czech Republic, Finland, Greece, Sweden	
Diphasic calcium phosphate dihydrate	United States, Czech Republic, France, Canada	
Colloidal silicon dioxide	United States, Czech Republic, Greece, Finland, Sweden, Norway, South Africa, Canada, Germany	
Microcrystalline cellulose	United States, Norway, South Africa, Germany	
Gelatine	Czech Republic, Finland	
Stearic acid	United States	
Corn starch	United States, Czech Republic, France, Sweden, Canada	
Maize starch	Greece, South Africa, Germany	
Pregelatinized starch	United States, France, Canada	
Potato starch	Finland, South Africa	
Carboxymethyl starch sodium	Germany	
Sodium starch glycolate	United States, South Africa	
Povidone	Finland, Norway, Germany	
Croscarmellose sodium	Norway, Germany	
Polysorbate	South Africa	

Dissolution profiles

A comparative dissolution study was conducted on four commercially available HCTZ products in Argentina. [15] The dissolution study was carried out according to the specifications set in the Argentine Pharmacopeia, where it states that not less than 60% (Q) of the labelled amount of HCTZ should be released from the tablets within 60 min in 0.1 N HCl. The results concluded that two out of the three multisource products had a dissolution profile similar to that of the reference product that exhibited either very rapid dissolution or rapid dissolution according to the WHO guidelines. One multi-source product portrayed a significantly lower dissolution profile. The authors found that the excipients present in all four products differed, illustrating the discriminatory ability of the dissolution test. [15]

Another study confirmed the discriminatory capability of 0.1 N HCl dissolution medium for products containing HCTZ, where the dissolution profiles of 16 different products comprising HCTZ, and that are available in Taiwan, were investigated. The dissolution behaviour was examined in 0.1 N HCl and in a pH 7.4 buffer using USP apparatus I at 100 rpm. [96] The results indicated that the dissolution profiles of only 9/16 products in 0.1N HCl and 6/16 products in pH 7.4 buffer were comparable to the dissolution profile of the reference product in the respective media. [88] A different dissolution study was performed on three different HCTZ containing products (with different excipient compositions) in Salvador, Brazil, using dissolution apparatus 1 (basket) in 900 mL 0.1 HCl at 100 rpm. Again, differences were observed in the dissolution profiles of the three products. [97]

It is known that different manufacturing conditions may impact the quality and release of a drug from solid oral IR dosage forms. Shah et al. prepared four different HCTZ formulations by means of direct compression and wet granulation, with varying hardness due to differences in compaction forces. Dissolution studies using dissolution apparatus 1 (basket) at 50, 100, and 150 rpm in 0.1 N HCl illustrated statistically significant differences in the dissolution behaviour of tablets produced by means of wet granulation versus direct compression manufacturing methods. [98] Furthermore, Shah et al. also conducted in vivo studies with the four formulations to evaluate the correlation between the in vitro dissolution (in 0.1 N HCl) and in vivo urinary recovery results. These formulations were administered to six healthy volunteers where the cumulative urinary HCTZ excretion was determined. Statistically significant correlations were found between in vitro and in vivo results at 95% CI. [99] Based on the information presented, it can be concluded that 0.1 N HCl could be considered the most suitable and biorelevant dissolution medium for HCTZ tablets. This was confirmed in that the dissolution medium used by international pharmacopoeias (Table 5) is indeed 0.1 N HCl.

Table 5: The dissolution methodology used by various pharmacopoeias

Pharmacopeia	Specification	Dissolution media	Volume	Apparatus Agitation speed	Reference
United States Pharmacopeia	NLT 60% (Q) within 60 min	0.1 N HCl	900 mL	Apparatus 1 (Basket) 100 rpm	(38)
Argentina Pharmacopeia	NLT 60% (Q) within 60 min	0.1 N HCl	900 mL	Apparatus 1 (Basket) 100 rpm	(15)
Brazilian Pharmacopeia	NLT 75% (Q) within 30 min	0.1 N HCl	900 mL	Blades 50 rpm	(99)
Indian Pharmacopeia	NLT 60% (Q) within 45 min	0.1 N HCl	900 mL	Apparatus 1 (Basket) 100 rpm	(100)
Chinese Pharmacopeia	NLT 60% (Q) within 30 min	0.1 N HCl	900 mL	Apparatus 1 (Basket) 100 rpm	(101)

NLT = Not less than

To evaluate the dissolution behaviour of HCTZ raw material and that of HCTZ in two commercially available solid oral IR dosage forms in South Africa, comparative dissolution studies were performed. The dissolution studies were carried out in 900 mL of the BCS media: 0.1 N HCl pH 1.2, acetate buffer pH 4.5, and phosphate buffer pH 6.8, according to the WHO guidelines. (4)

The dissolution profiles of the HCTZ raw material in the mentioned media are depicted in Figures 5 and 6. After 60 min, 85% of the HCTZ was dissolved in 0.1 N HCl pH 1.2. Within 60 min, 87% and 91% of the HCTZ were dissolved in the acetate pH 4.5 and phosphate pH 6.8 media, respectively. To compare the dissolution behaviour of HCTZ raw material in the different BCS media, similarity factors were calculated. As mentioned previously, the absorption process of HCTZ occurs predominantly in the duodenum and jejunum, where the pH ranges between 6 and 7.5, thus, the dissolution profiles of the HCTZ raw material in 0.1 N HCl pH 1.2 and the acetate buffer pH 4.5 were compared with the results obtained in the phosphate buffer pH 6.8. The calculated similarity factors (Table 6) were greater than 50, indicating that the dissolution behaviour of HCTZ in the BCS media could be considered similar.

Table 6: f_2-similarity factor for HCTZ raw material dissolution studies in 0.1 N HCl and acetate buffer when compared to that in in phosphate buffer

0.1 N HCl pH 1.2 f_2-similarity factor	Acetate buffer pH 4.5 f_2-similarity factor
58.0	59.7

The dissolution profiles of commercially available products in South Africa in the BCS media were evaluated and are presented in Figures 7 and 8. Both products showed very rapid dissolution, where the % dissolution was found to be more than 85% of the label claim within 15 min in all three-dissolution media. The RSD-values at all withdrawal intervals (i.e.15–60 min) were less than 10%. It can thus be concluded that the dissolution profiles of these two products are equivalent according to the requirements set out by the WHO. [4]
Considering the dissolution results of the available literature and those presented in Figures 7 and 8, it is strongly recommended that pharmacopeial bodies consider tightening the dissolution specifications of HCTZ IR tablets to not less than 80% (Q) in 30 min. Applying a more restricted specification will ensure the availability of quality-assured HCTZ tablets in the fight against substandard and/or falsified medical products. Interestingly, the dissolution profiles of the HCTZ raw material and those of the drug products in the three media differed significantly (Table 7). From the figures mentioned, it is clear that both the rate and extend of dissolution of the raw material were lower than those of the drug products. The HCTZ raw material illustrated 85% or more dissolution only after 60 min in the respective dissolution media.

Table 7: f_2-similarity factor for HCTZ raw material against Product 1 and Product 2 when compared to HCTZ raw material

Medium	Product 1 f_2-similarity factor	Product 2 f_2- similarity factor
0.1 N HCl pH 1.2	25.7	24.8
Acetate buffer pH 4.5	27.6	24.1
Phosphate buffer pH 6.8	28.6	25.5

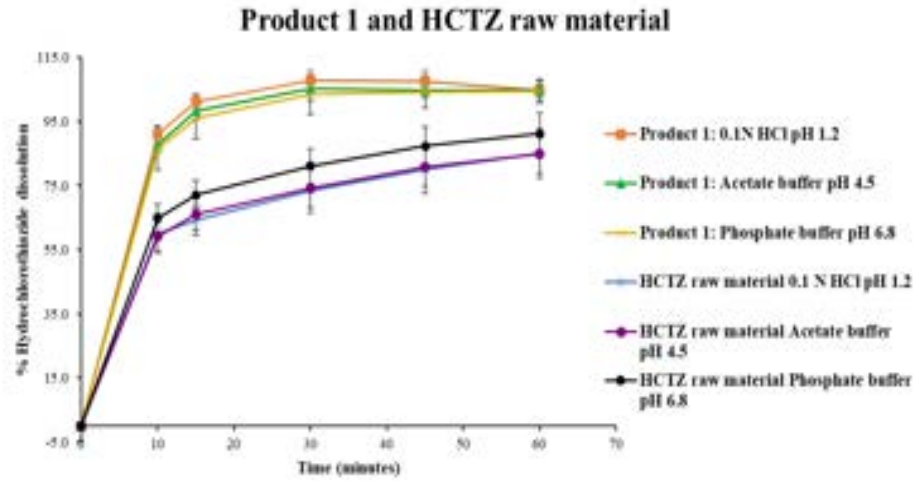

Figure 5: Dissolution profiles of HCTZ Product 1 and HCTZ raw material in respective dissolution media (pH 1.2, 4.5 and 6.8) with 95% confidence intervals indicated.

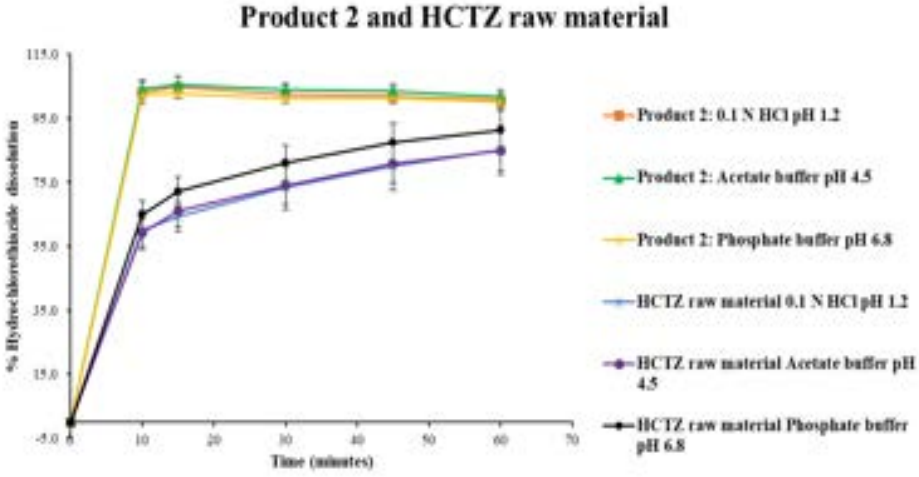

Figure 6: Dissolution profiles of HCTZ Product 2 and HCTZ raw material in respective dissolution media (pH 1.2, 4.5 and 6.8) with 95% confidence intervals indicated.

To explore potential reasons for the differences observed in the dissolution profiles, it is recognised that differences in the particle size of the HCTZ raw material may be a potential factor. However, the raw material used in this study (with a particle size d_{50}-value of 93.9705 µm) is the same material used in the manufacture of Product 1, indicating that particle size differences could not have been considered the reason for the observed differences. From the available literature, it has been illustrated that the inclusion of different excipients in the IR formulation may influence the dissolution behaviour of HCTZ. [15,96-97] The excipient list of both Product 1 and Product 2 is presented in Table 8.

Tabel 8: Excipients present in Product 1 and Product 2 [90 & 91]

Excipient	Product 1	Product 2
Lactose monohydrate	✓	✓
Magnesium stearate	✓	✓
Maize starch	-	✓
Microcrystalline cellulose	✓	✓
P/B orange dye	✓	-
Polysorbate	✓	-
Purified talc	✓	-
Sodium starch glycollate	✓	✓
Silica colloidal anhydrous	-	✓
Starch maize	✓	-

Both products contain sodium starch glycollate, which is a super-disintegrant. The available literature has indicated that the presence of sodium starch glycollate increases the apparent solubility of drugs containing a neutral aminic group, most probably due to the inhibition of drug agglomeration. [102] During the powder dissolution studies, agglomeration of the HCTZ raw material particles was observed, which could be attributed to the reduced dissolution rate of HCTZ. [103] The dissolution profiles of Products 1 and 2 both showed plateau formation, which is indicative of the complete dissolution of HCTZ in the dissolution media, however, the raw material depicted continuous dissolution for up to 60 min. In addition, literature indicated that when sodium starch glycolate was incorporated into HCTZ model formulations, it significantly increased the dissolution rate of the incorporated drugs due to the enhanced swelling capacity of the formulations. [104]

In silico intestinal permeability of HCTZ

Computational simulations were performed using GastroPlus® (Simulations Plus, Inc., Lancaster, CA) to evaluate the impact of the experimentally determined solubility values on the proposed BCS classification of HCTZ with regards to the intestinal permeability after the administration of different doses. These simulations were performed to evaluate the compartmental absorption, dissolution behaviour, and the permeability (indicative of the fraction absorbed observed in humans (F_a)) of HCTZ when administered as an IR tablet. Simulations were performed for different doses of HCTZ administered (12.5, 25, 50 and 100 mg), using the human fasting physiological model with an average body weight of 70 kg without enterohepatic recirculation and a default gastric transit time of 15 min. The input parameters for the Physiologically Based Pharmacokinetic (PBPK) modelling approach used are similar to that applied by Gigante et al. and are summarised in Table 9. [37]

Table 9: PBPK Simulation parameters used as model input variables in GastroPlus®

Input parameters	Values
Dosage form dose interval parameters	
Dose form	Immeditae release tablets
Dose	12.5, 25, 50 & 100 mg
Dose interval	0 (single dose administered)
Dose volume	250 mL
Particle and diffusion parameters	
Mean particle radius	25 µm
Mean precipitation time	900 sec
Diffusion coefficient	0.75 $cm^2/s \times 10^5$
Dissolution model	Johnson
Compartmental parameters	
PBPK model	Human fasted (male, 30 years, 70 kg)
ASF model	OptlogD Model SA/V6.1
Bile salt effect	Off
Small intestine transit time	3.2 h
Biliary clearance fraction	0
Simulation time	36 h
Paracellular model	Zhimin

The predicted compartmental absorption of HCTZ (Figure 7) revealed that following oral administration, absorption occurs predominantly in the duodenum, jejunum, and ileum, which was consistent with that reported by Dolery. [48] No absorption of HCTZ was found in the stomach.

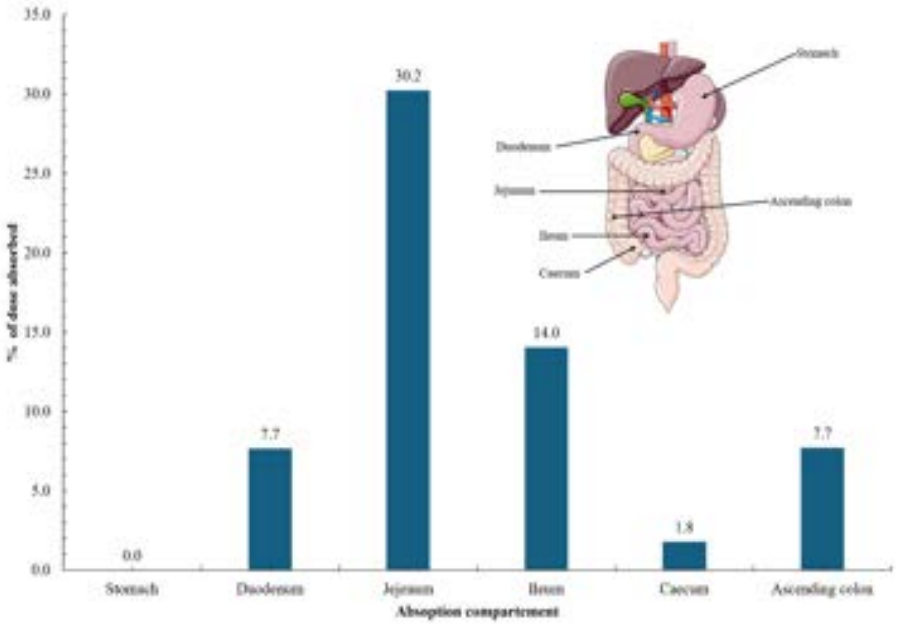

Figure 7: The predicted compartmental absorption of HCTZ following oral administration. The anatomical figure was drawn using a picture from Servier Medical Art. Servier Medical Art by Servier is licensed under a Creative Commons Attribution 4.0. (https://creativecommons.org/licenses/by/4.0/).

A prerequisite for the absorption of HCTZ from the IR tablet is that HCTZ should be released from the IR tablet and then dissolve in the gastrointestinal fluids before absorption in the gastrointestinal mucosa can occur. The predicted amounts of the HCTZ dissolved within the gastrointestinal fluids as a function of time after oral administration of varying doses (12.5, 25, 50 & 100 mg), are depicted in Figure 8(a). Complete dissolution occurred within 13.2 min for the 12.5 and 50 mg doses; and within 14.4 min for the 100 mg dose. The initial dissolution rate (IDR) for each of the doses were calculated and found to be between 1.571 and 11.373 mg/min as seen in Figure 8(b). The linear correlation between the IDR and the administered dose could be attributed to the greater concentration gradient that exists at the higher doses of HCTZ. [105]

(a)

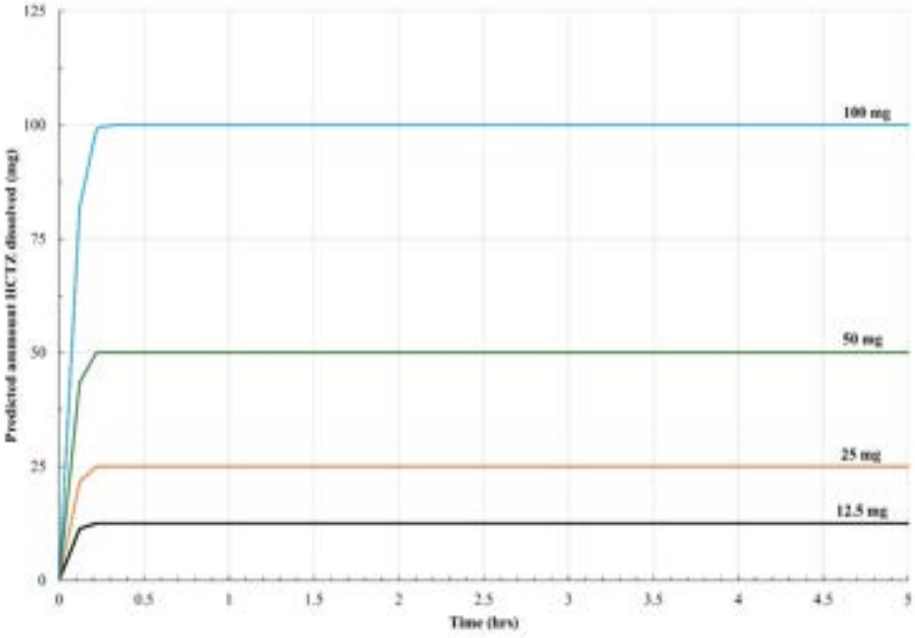

(b)

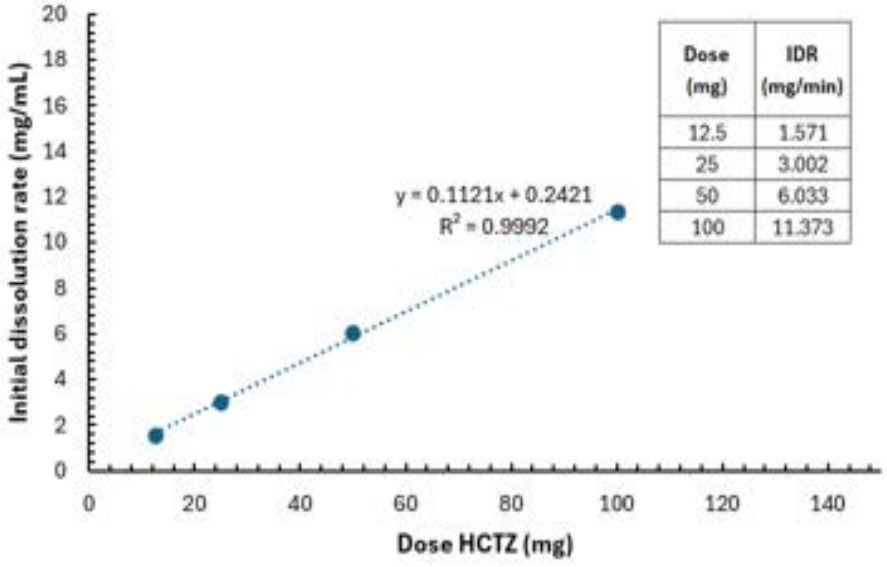

Dose (mg)	IDR (mg/min)
12.5	1.571
25	3.002
50	6.033
100	11.373

Figure 8: (a) The predicted amounts of the HCTZ dissolved within the gastrointestinal fluids as a function of time after oral administration of varying doses (12.5, 25, 50 & 100 mg). (b) Relationship between the initial dissolution rate and the HCTZ dose.

Once in solution, the absorption of HCTZ can occur, allowing it to reach the systemic circulation. The in-silico absorption-time predicted graphs of the different doses (Figure 9) of HCTZ illustrate two distinct phases namely, an initial absorption phase with a rapid high absorption rate followed by a continuously lower absorption phase. From these figures, it may seem as if the rate of the initial absorption phase of HCTZ ($t_{0\rightarrow 5\ hrs}$) differs after the administration of the different doses. Therefore, to quantify the absorption rates in these two phases, the data was subjected to a two-phase non-linear regression analysis with smooth transition model using GraphPad Prism 10 Software (GraphPad, Boston, MA).[106] Table 10 summarises the two-phase non-linear regression analysis results for the predicted in silico absorption data of HCTZ when administered as IR tablets with doses 12.5, 25, 50 and 100 mg. From this table it can be concluded that there is no significant difference in the absorption rate constants (K_{fast} = 0.01045–0.01047 min^{-1}) after the administration of different HCTZ doses, suggesting that the absorption of HCTZ is facilitated by means of passive diffusion.

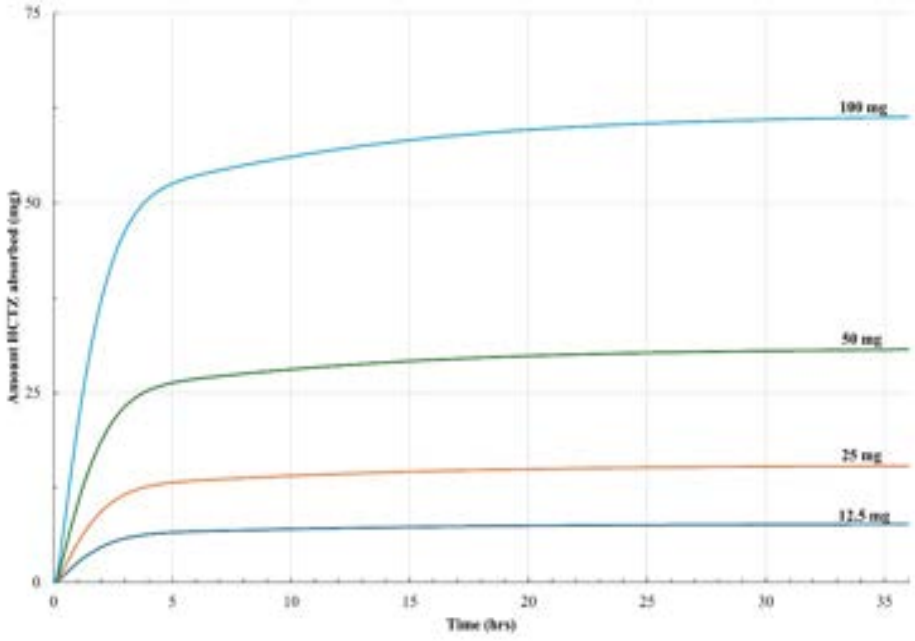

Figure 9: The in-silico absorption-time predicted graphs of HCTZ when administered as IR tablets with doses: 12.5, 25, 50 & 100 mg.

Table 10: Two-phase non-linear regression analysis results for the in silico predicted absorption data of HCTZ when administered as IR tablet with doses 12.5, 25, 50 and 100 mg

Two phase association best fit values				
	12.5 mg	**25 mg**	**50 mg**	**100 mg**
Plateau	7.92 min	15.84 min	31.59 min	63.33 min
Y_0	-0.7557 mg	-1.152 mg	-2.969 mg	-6.180 mg
K_{fast} ± 95% CI	0.01046 ± 0.00024 min^{-1}	0.01046 ± 0.00024 min^{-1}	0.01047 ± 0.00023 min^{-1}	0.01045 ± 0.00024 min^{-1}
K_{slow} ± 95% CI	0.0008695 ± 0.00016 min^{-1}	0.0008690 ± 0.00017 min^{-1}	0.0009208 ± 0.00015 min^{-1}	0.0008677 ± 0.00017 min^{-1}
Fast half-life	66.04 min	66.25 min	66.21 min	66.31 min
Slow half-life	797.1 min	797.6 min	752.8 min	798.9 min
Goodness of fit				
Degrees of freedom	316	316	316	316
r^2	0.998	0.998	0.998	0.998
Sums of square	1.821	7.328	25.72	119.4

The in silico predicted $\%F_a$ values, when varying the doses of HCTZ are administered as IR tablets, range between 61.3 and 61.4% (Figure 10). The predicted values compared well with those found in vivo. [68, 71-72] Therefore, it can be deduced that the $\%F_a$ values did not show significant differences, consequently suggesting that the biopharmaceutical properties remain relatively constant irrespective of the dose simulated. Furthermore, the linear correlation between the in silico predicted $AUC_{0\rightarrow 36hrs}$ and the administered doses (Figure 10) implies that gastrointestinal solubility and permeability of HCTZ remain unchanged within the different dose levels. This dose proportionality again supports the observation that the absorption of HCTZ is facilitated by means of passive diffusion. In a study by Patel et. al., it was illustrated that the mean plasma levels of HCTZ could be related to the dose size (25, 50 & 100 mg) when administered to patients. The authors mentioned reported that the mean urinary recovery of HCTZ accounted for 50–60% of the doses administered, which correlate well with the data predicted in this study. [83]

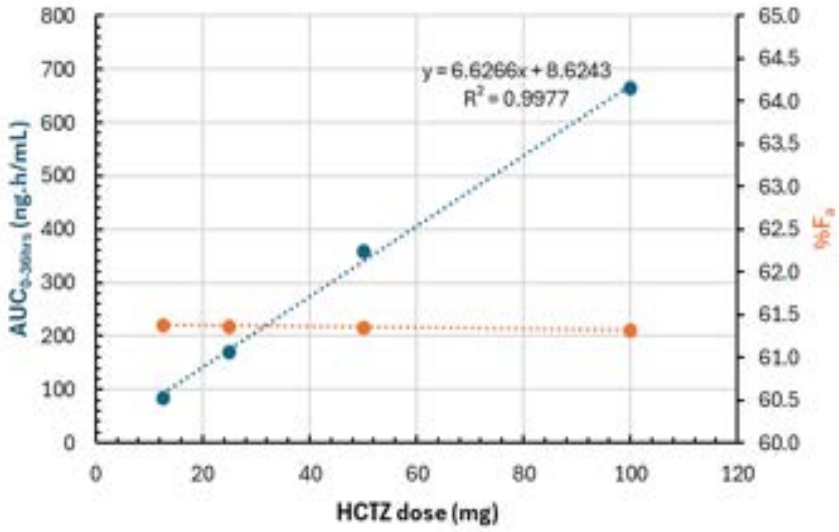

Figure 10: The in silico predicted $\%F_a$ and $AUC_{0\text{-}36\ hrs}$ values, when varying HCTZ doses (12.5, 25, 50 & 100 mg) are administered as IR tablets.

CONCLUSION

Solubility

According to the guidelines set out by the regulatory authorities, a drug substance is deemed highly soluble if the highest therapeutic dose or the highest single dose is soluble in less than 250 mL in a pH range of 1.2–6.8.[29, 60] Therefore, based on the experimental data obtained for HCTZ, the dose/solubility ratio indicated that in the pH range of 1.2–6.8, it does not exceed 30 mL for 25 mg, which is almost one-tenth of the 250 mL limit. Furthermore, it does not exceed 60 mL for 50 mg, which does not exceed the 250 mL limit. Therefore, HCTZ meets the requirements to be classified as a highly soluble drug according to the US-FDA, EMA, and the WHO, irrespective of the highest therapeutic dose and/or the highest single dose.[2–4] Due to the thermodynamic instability of the metastable form (Form II) and its rapid conversion into the stable form (Form I), as well as the similarity in the aqueous solubility of the two anhydrous forms, the risk of the polymorphic behaviour on the solubility of HCTZ could be considered low.

Permeability

A drug is classified as highly permeable if 85% or more of the dose administered is absorbed into the human body based on mass balance determinations.[29] HCTZ is absorbed within 2–4 h after dosing and is excreted unchanged in the urine. However, the bioavailability of HCTZ, according to the literature, ranges between 65 and 70%. HCTZ can thus be classified as a poorly permeable drug. Moreover, Caco-2 cell studies support the classification of HCTZ as a poorly permeable drug.

Excipients are generally considered inactive ingredients, yet there are excipients that influence the solubility, dissolution, and ultimately the bioavailability of a drug. The impact of absorption-modifying excipients (which do not necessarily affect the in vitro dissolution behaviour of the IR product) should be considered during the application for biowaiver submission. [107] BCS-based biowaiver guidelines clearly state that it remains the responsibility of the manufacturer to illustrate that the excipients included in the drug product should not adversely affect the bioavailability of the drug. Studies indicated that the presence of specific surfactants (e.g., sodium lauryl sulphate and Tween® 80) may potentiate the oral bioavailability from solid oral IR HCTZ dosage forms. Nonetheless, no indication could be found in the available literature of any excipients adversely affecting the bioavailability of HCTZ. Furthermore, none of the critical excipients known to affect the bioavailability (i.e., mannitol and sorbitol) was present in the HCTZ IR tablet formulations reviewed in this publication.

Classification

HCTZ demonstrates high solubility and low permeability. Therefore, according to the ICH M9 guidance on BCS-based biowaiver, HCTZ can be assigned to BCS Class III. [2]

Risk for BCS-based biowaiver

Regarding the classification of HCTZ and the clinical evidence reviewed, it is recommended to grant a BCS-based biowaiver for solid oral IR formulations containing HCTZ as a single drug, contingent on HCTZ meeting the following criteria: a) the data presented to support the approval of the BCS-based biowaiver were done according to the requirements stipulated by regulatory authorities; b) the innovator and generic products meet the specifications for the in vitro dissolution set out by the regulatory authorities; and c) the risks associated with excipients included have been adequately evaluated to illustrate that the excipients in the proposed product formulation are qualitatively the same and quantitatively similar to the innovator product.

Acknowledgements:

We express our deepest gratitude to Aspen Pharmacare (South Africa) for the generous donation of HCTZ raw material, Prof. Wilna Liebenberg (Pharmacen™, North West University, Potchefstroom, South Africa) for the XRPD analysis of the HCTZ samples performed, Mr. Neil Barnard (North West University, School of Pharmacy, Pharmaceutics, Potchefstroom, South Africa) for the particle size analysis performed, and SimulationsPlus Inc. for granting the academic license that enabled us to make use of GastroPlus®.

REFERENCES

1) Davit BM, Kanfer I, Tsang YC, Cardot JM. BCS Biowaivers: Similarities and Differences among EMA, FDA, and WHO requirements. The AAPS Journal, 2016;18(3):612-618. (doi: 10.1208/s12248-016-9877-2, accessed 12 April 2023).

2) US-FDA. M9 Biopharmaceutical Classification System based biowaiver. 2019. (https://www.fda.gov/regulatory-information/search-fda-guidance-documents/m9-biopharmaceutics-classification-system-based-biowaivers, accessed 12 April 2023).

3) EMA. Guideline on the investigation of bioequivalence. 2010. (https://www.ema.europa.eu/en/investigation-bioequivalence-scientific-guideline, accessed 08 July 2024).

4) WHO. Multisource (generic) pharmaceutical products: guidelines on registration requirements to establish interchangeability. 2017. (https://www.who.int/publications/m/item/annex-6-trs-1003, accessed 12 April 2023).

5) Amidon GL, Lennernäs H, Shah VP, Crison JR. A theoretical basis for biopharmaceutic drug classification. The colleration of in vitro drug product dissolution and in vivo bioavailability. Pharmaceutical Research, 1995*;* 12(3):413-420. (doi: 10.1208/s12248-014-9620-9, accessed 12 April 2023).

6) Ono A, Tomono T, Ogihara T, Terada K, Sugano K. Investigation of biopharmaceutical and physicochemical drug properties suitable for orally disintegrating tablets. ADMET & DMPK, 2016; 4(4):335-360. (doi: https://doi.org/10.1016/j.ejps.2014.08.003, accessed 12 April 2023).

7) Bakka E, Comer JEA, Takács-Novák K. Study of equilibrium solubility measurement by saturation shake-flask method using Hydrochlorothiazide as model compound. Journal of Pharmaceutical and Biomedical Analysis. 2008; 46(2):335-341. (doi: https://doi.org/10.1016/j.jpba.2007.10.030, accessed 12 April 2023).

8) Khan A, Iqbal Z, Shah Y, Ahmad L, Ismail, Ullah Z, Ullah A. Enhancement of dissolution rate of class II drugs (Hydrochlorothiazide); a comparative study of the two novel approaches; solid dispersion and liquid-solid techniques. Saudi Pharmaceutical Journal, 2015; 23(6):651. (doi: https://doi.org/10.1016/j.jsps.2015.01.025, accessed 12 April 2023).

9) Sharma S, Paliwal S, Singhai VD. In vitro drug release prediction of Hydrochlorothiazide modified release tablet using Wagner Nelson method and Deconvolution approach. International Journal of PharmTech Research, 2019;12(1):49-56. (doi: http://dx.doi.org/10.20902/IJPTR.2019.120107, accessed 13 April 2023).

10) Doloking H, Sartika AT, Tahar N. Formation of Hydrochlorothiazide- Para-aminobenzoic acid cocrystals by solvent evaporation method. Ad-Dawaa' Journal of Pharmaceutical Sciences, 2021;4(1):16-25. (doi: 10.24252/djps.v4il.21301, accessed 13 April 2023).

11) Kasim NA, Whitehouse M, Ramachandran C, Bermejo M, Lennernäs H, Hussain AS, … Amidon GL. Molecular properties of WHO Essential Drugs and Provisional Biopharmaceutical Classification. Molecular Pharmaceutics, 2003; 1(1):85-96. (doi: 10.1021/mp034006h, accessed 13 April 2024).

12) Lindenberg M, Kopp S, Dressman JB. Classification of orally administered drugs on the World Health Organization Model list of Essential Medicines according to the biopharmaceutical classification system. European Journal of Pharmaceutics and Biopharmaceutics, 2004; 58(2):265-278. (doi: 10.1016/j.ejpb.2004.03.001, accessed 13 April 2023).

13) Ono A, Sugano K. Application of the BCS biowaiver approach to assessing bioequivalence of orally disintegration tablets with immediate release formulations. European Journal of Pharmaceutical Science, 2014; 64:37-43. (doi: https://doi.org/10.1016/j.ejps.2014.08.003, accessed 13 April 2023).

14) Zaid AN, Ghanem M, Maqboul L, Zaid H, Mahasne A. Biowaiver eligibility of a lower strength Ramipril/Hydrochlorothiazide immediate release tablets using a new validated HPLC analytical method. Drug Research, 2016; 66(10):539-549. (doi: oi: 10.1055/s-0042-111434, accessed 13 April 2023).

15) Varillas MA, Brevedan MIV, Gonzalez Vidal NL. Pharmaceutical Equivalence of Hydrochlorothiazide tablets in Argentina. Diss Tech, 2018; 25(4):22-27. (doi: 10.1055/s-0042-111434, accessed 13 April 2023).

16) Wu CY, Benet, LZ. 2004. Predicting drug disposition via application of BCS: Transport/Absorption/Elimination Interplay and Development of a Biopharmaceutical Drug Disposition Classification System. Pharm Res, 2004; 22(1):11-23. (doi: 10.1007/s11095-004-9004-4, accessed 13 April 2023).

17) Reddy BBK, Karunakar A. Biopharmaceutics Classification System: A regulatory approach. Dissolution Technologies, 2011; 31-37.
(doi: dx.doi.org/10.14227/DT180111P31, accessed 15 April 2023).

18) Sanphui P, Devi VK, Clara D, Malviya N, Ganguly S, Desiraju GR. Cocrystals of Hydrochlorothiazide: Solubility and Diffusion/Permeability Enhancement through Drug-Coformer Interactions. Molecular Pharmaceutics,2015; 12(5):1615-1622.
(doi: 10.1021/acs.molpharmaceut.5b00020 , accessed 15 April 2023).

19) Onnainty R, Schenfeld EM, Petiti JP, Longhi MR, Torres A, Quevedo MA, Granero GE. Permeability profiles and intestinal toxicity assessment of Hydrochlorothiazide and its inclusion complex with B-Cyclodextrin loaded into Chitosan Nanoparticles. Molecular Pharmaceutics, 2016; 13(11):3736-3746.
(doi: https://doi.org/10.1021/acs.molpharmaceut.6b00532, accessed 15 April 2023).

20) Sorkhel AD, Chaudhari YS. Solubility enhancement study of poorly absorbable drugs. World Journal of Pharmaceutical Research, 2016; 5(3):933-964.

21) Park HJ, Yoon TJ, Kwon DE, Yu K, Lee YW. Coprecipitation of Hydrochlorothiazide/PVP for the dissolution rate improvement by precipitation with compressed fluid anti-solvent process. Journal of Supercritical Fluids,2017; 26:37-46.
(doi: https://doi.org/10.1016/j.supflu.2017.03.003, accessed 15 July 2023).

22) Ghadi R, Dand N. BCS class IV drugs: Highly notorious candidates for formulation development. Journal of Controlled Release, 2017; 248:71-95.
(doi: https://doi.org/10.1016/j.jconrel.2017.01.014, accessed 15 July 2023).

23) Ranjan S, Devarapalli R, Kundu S, Vangala VR, Ghosh A, Reddy CM. Three new hydrochlorothiazide cocrystals: Structural analyses and solubility studies. Journal of Molecular Structure, 2017; 1133:405-410.
(doi: https://doi.org/10.1016/j.molstruc.2016.12.019, accessed 16 July 2023).

24) Sultan AA, El-Gizawy SA, Osman A, El Maghraby GM. Self-dispersing mixed micelles forming systems for enhanced dissolution and intestinal permeability of Hydrochlorothiazide. Colloids and Surfaces B: Biointerfaces, 2017; 149(1):206-216. (doi: https://doi.org/10.1016/j.colsurfb.2016.10.028, accessed 16 July 2023).

25) Kumar S, Kaur R, Rajput R, Singh M. Bio Pharmaceutics Classifications System (BCS) Class IV drug nanoparticles: Quantum Leap to improve their therapeutic index. Advanced Pharmaceutical Bulletin, 2018; 8(4): 617-625. (doi: 10.15171/apb.2018.070, accessed 16 July 2023)

26) Ruponen M, Rusanen H, Laitinen R. Dissolution and permeability properties of co-amorphous formulations of Hydrochlorothiazide. Journal of Pharmaceutical Science, 2020; 109(7):2252-2261. (doi: https://doi.org/10.1016/j.xphs.2020.04.008, accessed 17 July 2024).

27) Parrish II R, Ashworth LD, Löbenberg R, Benavides S, Cies JJ, MacArthur RB. Compound non-sterile preparations and FDA-approved commercially available liquid products for children: A North American update. Pharmaceutics, 2022; 14(5):1032. (doi: 10.3390/pharmaceutics14051032, accessed 17 July 2024).

28) Validation of analytical procedures Q2(R2).1-34. Compilation prepared by the International Council of Harmonization. (https://www.fda.gov/media/152208/download, accessed 17 August 2023).

29) WHO. Protocol to conduct equilibrium solubility experiments for the purpose of Biopharmaceutical Classification System-based classification of active pharmaceutical ingredients for biowaiver. Compilation prepared by WHO. (https://www.who.int/docs/default-source/medicines/norms-and-standards/guidelines/regulatory-standards/trs1019-annex4-classification-system-based-classification-of-active-pharmaceutical-ingredients-for-biowaiver.pdf?sfvrsn=7ee2de7d_2, accessed 18 August 2023).

30) Bhagwate S, Gaikwad, NJ. Stability indicating HPLC method for the determination of hydrochlorothiazide in pharmaceutical dosage form. Journal of Applied Pharmaceutical Science, 2013; 2(02)88-92. (doi: 10.7324/JAPS.2013.30215, accessed 13 May 2024).

31) Chadha R, Bhandari S, Mandal SK, Jain DVS. Characterization and evaluation of multi-component crystals of Hydrochlorothiazide. Pharmaceutical Research, 2014; 31:2479-2489. (doi: https://doi.org/10.1007/s11095-014-1344-0, accessed 20 September 2023).

32) Florence A, Johnston A, Fernandes P, Shankland K, Stevens HNE, Osmundsen S, Mullen AB. Powder study of Hydrochlorothiazide form II. International Union of Crystallography,2015; 61(9)2798-2800.

33) Lötter A, Flanagan JR, Guillory JK. A simple reproducible method for determining dissolution rates of hydrophobic powders. Pharmaceutical Technology, 1983;7(4):56-66.

34) Van Wyk J, Viljoen JM, Brits M. Validated BCS Comparative dissolution method for hydrochlorothiazide tablets. World Journal of Pharmacy and Pharmaceutical Sciences. 2024; 13(9)1208-1223.

35) Quality and bioequivalence guideline compilation prepared by SAHPRA. (https://www.sahpra.org.za/wp-content/uploads/2020/02/2.02_Quality-and-Bioequivalence-Guideline_Jul19_v7-1.pdf, accessed 13 May 2024).

36) Moore JW, Flanner HH. Mathematical Comparison of curves with an emphasis on in vitro dissolution profiles. Pharmaceutical Technology. 1996; 20(6):64-74.

37) Gigante V, Pauletti GM, Kopp S, Xu M, Gonzalez-Alvarez I, Merino V, McIntosh MP, … Bermejo M. Global testing of a consensus solubility assessment to enhance robustness of the WHO biopharmaceutical classification system. ADMET & DMPK. 2021; 9(1): 23-39. (doi: https://dx.doi.org/10.5599/admet.850, accessed 18 July 2024).

38) USP. Hydrochlorothiazide. 2023. (United States Pharmacopeia). (https://online.uspnf.com/uspnf/document/2_GUID-44CC5E81-C0D8-44EB-9152-3C26ECB38FAF_40101_en-US?source=Search%20Results&highlight=Hydrochlorothiazide%20, accessed 13 May 2024).

39) Moffat AC, Osselton MD, Widdop B (eds). Hydrochlorothiazide. 3rd ed. Clarke's analysis of drugs and poisons; London:2004, pp.1109-1110.

40) Csicsák D, Borbás E, Kádár S, Tőzsér P, Bagi, P Pataki H, ... Völgyi G. Towards more accurate solubility measurements with real time monitoring: a carvedilol case study. New Journal of Chemistry. 2021; 45(26):11618-11625. (doi: 10.1039/d1nj01349a, accessed 16 May 2024).

41) Isoelectric point calculation - formula and equation. Compilation prepared by Study.com (https://study.com/academy/lesson/calculating-isoelectric-point-definition-formula.html#:~:text=At%20its%20pI%2C%20the%20molecule,are%20close%20to%20each%20other, accessed 16 May 2024).

42) BP. Hydrochlorothiazide. (British Pharmacopoeia). 2023.(https://www-pharmacopoeia-com.nwulib.idm.oclc.org/bp-2023/monographs/hydrochlorothiazide.html?date=2023-07-01&text=hydrochlorothiazide, accessed 20 August 2023).

43) Deppeler HP (ed). Hydrochlorothiazide In: Florey K.(ed) Analytical Profiles of Drug Substances. New York: Academic Press: 1981, pp.406-436.

44) O'Neil MJ, Smith A, Heckelman PE, Budavari S. THE MERCK INDERX. 13th edition. Whitehouse Station, NJ, USA: 2001. Merck & Co.

45) Kasim NA, Whitehouse M, Ramachandran C, Bermejo M, Lennernäs H, Hussain AS, … Amidon GL. Molecular properties of WHO Essential Drugs and Provisional Biopharmaceutical Classification. Molecular Pharmaceutics. 2003;1(1):85-96. (doi: 10.1021/mp034006h, accessed 5 September 2023).

46) Hydrochlorothiazide, compilation prepared by Medscape, (https://reference.medscape.com/drug/microzide-hydrodiuril-hydrochlorothiazide-342412#3, accessed 07 July 2024).

47) Hydrochlorothiazide, compilation prepared by National Library of Medicine, (https://www.ncbi.nlm.nih.gov/books/NBK430766/, accessed 28 June 2024).

48) Dollery C (eds). Hydrochlorothiazide. 2nd ed. Therapeutic drugs. London: 1999, pp. H52-H57.

49) Journela AJ, Lilja M, Lumme J. Relation between low dose hydrochlorothiazide, antihypertensive effect and adverse effects. Blood Pressure 3, 1994:231-235. (doi:10.3109/08037059409102262, accessed 28 June 2024).

50) Kuller L, Farrier N, Caggiula A, Borhani N, Dunkle S. Relationship of diuretic therapy and serum magnesium levels among participants in the multiple risk factor intervention trial. American Journal of Epidemiology, 1985; 122(1045-1059). (doi: 10.1093/oxfordjournals.aje.a114186, accessed 28 June 2024).

51) Choi HK, Soriano LC, Zhang Y, Rodríguez LA. Antihypertensive drugs and risk of incident gout among patients with hypertension: population-based case-control study. BMJ, 2012; 344:1-9. (doi: 10.1136/bmj.d8190, accessed 29 June 2024).

52) Ames R. Effect of diuretic drugs on lipid profile. Drugs 36 (Suppl.2), 1988;33-40. (doi: 10.2165/00003495-198800362-00007, accessed 29 June 2024).

53) Sullivan TJ. Cross-reactions among furosemide hydrochlorothiazide, and sulfonamides. JAMA, 1991; 265(1):120-121. (doi: 10.1001/jama.265.1.120, accessed 29 June 2024).

54) Chen SH, Karanjia R, Chevrier RL, Marshall DL. Bilateral acute angle closure glaucoma associated with hydrochlorothiazide induced hyponatraemia. BMJ, 2014; 2014:1-3. (DOI: 10.1136/bcr-2014-206690, accessed 29 June 2024).

55) Kim BH, Kim JK. Pharmaceutical studies on the polymorphism of Hydrochlorothiazide. Archives of Pharmaceutical Research, 1984; 7(1):47-52. (doi: https://doi.org/10.1007/BF02856921, accessed 20 July 2023).

56) Johnston A, Florence AJ, Shankland N, Kennedy AR, Shankland K, Price SL. Crystallization and Crystal Energy Landscape of Hydrochlorothiazide. Crystal Growth & Design, 2007; 7(4):705-712. (doi: 10.1021/cg0606242, accessed 30 July 2023).

57) de Salvi STB, Tita DL, Pavia-Santos CO, Antonio SG. Characterization of Hydrochlorothiazide in solid formulations. Powder Diffraction, 2015; 30(1):127-128. (doi: 0885-7156/2015/30(S1), accessed 01 August 2023)

58) Aceves-Hernández JM, Agacino-Valdés E, Paz M, Hinojosa-Torres J. Experimental and theoretical study of the conformational analysis of Hydrochlorothiazide. Journal of Molecular Structure, 2006;786(1):1-8. (doi: https://doi.org/10.1016/j.molstruc.2005.09.019, accessed 01 August 2023).

59) Baka E, Comer JEA, Takács-Novák K. Study of equilibrium solubility measurement by saturation shake-flask method using Hydrochlorothiazide as model compound. Journal of Pharmaceutical and Biomedical Analysis, 2008; 46(2):335-341. (doi: https://doi.org/10.1016/j.jpba.2007.10.030, accessed 01 August 2023).

60) Pecharsky VK, Zavalij PY. Fundamentals of powder diffraction and structural characterization of materials. United States of America: 2005.

61) El-Gizawy SA, Osman MA, Arafa MF, Maghraby GME. Aerosil as a noval co-crystal co-former for improving the dissolution of hydrochlorothiazide. International Journal of Pharmaceutics. 2015; 773-778. (doi:10.1016/j.ijpharm.2014.12.037, accessed 30 June 2024).

62) ICH. Specifications: Test Procedures and Acceptance Criteria for New Drug Substances and New Drug Products: Chemical Substances. 2000. Compilation prepared by EMA (https://www.ema.europa.eu/en/documents/scientific-guideline/ich-q-6-test-procedures-and-acceptance-criteria-new-drug-substances-and-new-drug-products-chemical-substances-step-5_en.pdf, accessed 30 June 2024).

63) Verma V, Patel P, Ryan KM, Hudson S, Padrela L. Production of hydrochlorothiazide nanoparticles with increased permeability using top-spray coating process. The Journal of Superficial Fluids. 2023; 192. (doi:https://doi.org/10.1016/j.supflu.2022.105788, accessed 05 August 2024).

64) Essa E, Amin M, Sultan A, Arafa M, Maghraby GE, McConville C. Hot melt extrusion for enhanced dissolution and intestinal absorption of hydrochlorothiazide. Journal of Drug Delivery Science and Technology. 2023; 88:1-9. (doi: 10.1016/j.jddst.2023.104895, accessed 05 August 2024).

65) EMA. Guideline on the investigation of bioequivalence. Compilation prepared by EMA, (https://www.ema.europa.eu/en/investigation-bioequivalence-scientific-guideline, accessed 05 August 2024).

66) Leon RS, Issa MG, Duque MD, Daniel JSP, Ferraz HG. Development of a discriminative dissolution method, using in silico tool for Hydrochlorothiazide and Valsartan tablets. Pharmaceutics. 2023;15(6)1-20. (doi: 10.3390/pharmaceutics15061735, accessed 05 August 2024).

67) Journal of the American Pharmaceutical Association. Bioavailability Monograph Hydrochlorothiazide. 1961; 16(1):47-50. (doi: 10.1002/jps.2600730317, accessed 05 August 2024).

68) Beerman B, Groschinsky-Grind M. Pharmacokinetics of Hydrochlorothiazide in man. Eur. J. Clin. Pharmacol. 1978; (13):297-303. (doi: 10.1007/BF00607430, accessed 05 August 2024).

69) Barbhayia R H, Patel RB, Corrick-West HP. Comparative bioavailability and pharmacokinetics of Hydrochlorothiazide from oral tablet dosage forms, determined by plasma levels and urinary excretion. Biopharmaceutics and drug disposition, 1982; 3:329-366. (doi:10.1002/BDD.2510030406, accessed 06 August 2024).

70) Backman L, Beerman B, Groschinsky-Grind M, Hallberg D. Malabsorption of Hydrochlorothiazide following intestinal shunt surgery. Clinical Pharmackokinetics.1979; 4:63-68. (doi: 10.2165/00003088-197904010-00006, accessed 06 August 2024).

71) Jordo L, Johnsson G, Lundborgd P, Persson BA, Regardh CG, Ronn O. Bioavailability and disposition of metoprolol and hydrochlorothiazide combined in one tablet and of separate doses of hydrochlorothiazide. Br. J. clin. Pharmac. 1979; 7:563-567. (doi: 10.1111/j.1365-2125.1979.tb04643.x., accessed 06 August 2024).

72) Meyer MC, Melikian AP, Whyatt PL, Slywka GW. Hydrochlorothiazide bioavailability: an evaluation of thirteen products. Curr Ther Res Clin Exp. 1975; 17(6)570-577.

73) Niemeyer C, Hasenfulβ G, Wais U, Knauf H, Schäfer-Korting M, Mutschler E. Pharmacokinetics of Hydrochlorothiazide in relation to renal function. Eur J Clin Pharmacol, 1983;24:661-665. (doi: 10.1007/BF00542218, accessed 06 August 2024).

74) Alsenz J, Haenel E. Development of a 7-day, 96-well Caco-2 permeability assay with high-throughput direct UV compound analysis. Pharmaceutical Research. 2003; 20(12):1961-1969. (doi: 10.1023/b:pham.0000008043.71001.43, accessed 06 August 2024).

75) Zhu C, Jaing L, Chen TM, Hwang KK. A comparative study of artificial membrane permeability assay for high throughput profiling of drug absorption potential. Eur. J. Med. Chem. 37:399-407. (doi: 10.1016/s0223-5234(02)01360-0, accessed 06 August 2024).

76) Koljonen M, Hakala KS, Ahtola-Sätilä, Laitinen L, Kostiainen R, Kotiaho T, Kaukonen A, Hirvonen J. Evaluation of cocktail approach to standardise Caco-2 permeability experiments. Eur. J. Pharm and Biopharm. 2006; 64:379-387. (doi: https://doi.org/10.1016/j.ejpb.2006.06.006, accessed 06 August 2024).

77) Rege BD, YU LX, Hussain AS, Polli JE. Effect of common excipients on Caco-2 transport of low permeability drugs. Journal of Pharmaceutical Science. 2001; 90(11):1776-1786. (doi: 10.1002/jps.1127, accessed 06 August 2024).

78) Gala PG. Effects of Surfactants on the dissolution of Hydrochlorothiazide from tablets. University Microfilms international. 1984. (https://www.proquest.com/docview/303291152/fulltextPDF/B9EA66866E434EDFPQ/1?%20Theses&accountid=12865&sourcetype=Dissertations%20, accessed 07 August 2024).

79) Lennernäs, H. Intestinal permeability and its relevance for absorption and elimination. Xenobiotica. 2007; 37(10-11):1015-1051. (doi: 10.1080/00498250701704819, accessed 06 August 2024).

80) Welling PG. Pharmacokinetics of Thiazide diuretics. Biopharmaceutical & Drug Disposition. 1986; 7(6):501-535. (doi: https://doi.org/10.1002/bdd.2510070602, accessed 07 August 2024).

81) Beermann B, Fåhraeus L, Groschinsky-Grind M, Lindström B. Placental transfer of hydrochlorothiazide. Gynecol Obstet Invest. 1980; 11(1):45-48. (doi: 10.1159/000299817, accessed 07 August 2024).

82) Fierro H, Rojas R, Yanez S, Acuna P, Rosales K, Yevenes P, Yzoard M, Tapia C, Rivas V, Caba A, Copaja M, Jorge F. Bioequivalence study of two Hydrochlorothiazide formulations after oral administration in healthy Chilean volunteers. Journal of Pharmacy and Pharmacology. 2016; 4:679-685. (doi:10.17265/2328-2150/2016.12.004, accessed 07 August 2024).

83) Patel RB, Patel UR, Rogge MC, Shah VP, Prasad VK, Selen A, Welling PG. Bioavailability of Hydrochlorothiazide from tablets and suspensions. Journal of Pharmaceutical Sciences. 1984; 73(3):359-361. (doi: 10.1002/jps.2600730317, accessed 07 August 2024).

84) Tripathee B, Hussain K, Prajapati R. Review on excipients used in immediate release tablet formulations. International journal of novel research and development. 2023;8(7)c39-53.

85) Hydrochlorothiazide tablet, dailymed. Compilation prepared by National Library of Medicine (https://dailymed.nlm.nih.gov/dailymed/drugInfo.cfm?setid=8c868894-667e-4a51-906a-838d63e420ba, accessed 24 September 2024).

86) Hydrochlorothiazide. Compilation prepared by Sukl (https://prehledy.sukl.cz/prehled_leciv.html#/, accessed 24 September 2024).

87) Hydrochlorothiazide Orifarm 25 mg. Compilation prepared by Norwegian Medicinal Product Agency. (https://www.dmp.no/en/content-a-z, accessed 24 September 2024).

88) Hydrochlorothiazide Bluefish 25 mg tablet. Compilation prepared by Swedish Medical Product Agency. (https://www.lakemedelsverket.se/sv/sok-lakemedelsfakta/lakemedel/20170906000023/hydrochlorothiazide-bluefish-25-mg-tablett, accessed 24 September 2024).

89) Fimea. Compilation prepared by Finnish Medicines Agency. (https://fimea.fi/en/frontpage, accessed 24 September 2024).

90) Ridaq. Compilation prepared by South African Health Products Regulatory Authority. (https://pi-pil-repository.sahpra.org.za/wp-content/uploads/2023/05/RIDAQ_Comb_Tab_ZA_RIDATAB_2303_00_EPIL_2023.03.04.pdf, accessed 24 September 2024).

91) Hexazide 25mg. Compilation prepared by South African Health Products Regulatory Authority. (https://medsinfoportal.sahpra.org.za/pil/79d49ebd9fc6bb9d8fcc5d395f345ece.pdf, accessed 24 September 2024).

92) Hydrochlorothiazide arrow. Compilation prepared Vidal (https://www.vidal.fr/medicaments/gammes/hydrochlorothiazide-arrow-92688.html, accessed 24 September 2024).

93) Hydrochlorothiazide. Compilation prepared by National Organization for Medicines (https://www.eof.gr/web/guest;jsessionid=661b7cb2f40ba8996f1a5958b4f3, accessed 24 September 2024).

94) Hydrochlorothiazide Tablets USP. Compilation prepared by Pharma Science (https://www.pharmascience.com/wp-content/uploads/2023/07/pms-Hydrochlorothiazide-pm-e-2020-01-27.pdf , accessed 24 September 2024).

95) Hydrochlorothiazide tablets. Compilation prepared by the Federal Institute for Drugs and Medical Devices (https://portal.dimdi.de/amguifree/termsofuse.xhtml, accessed 24 September 2024).

96) Lee MS, Huang CL, Haung SH, Chen YP, Chen CJ, Wen KC. A comparative study on the dissolution profiles of commercial hydrochlorothiazide tablets. Journal of Food and Drug Analysis. 2002; 10(1). (doi: https://doi.org/10.38212/2224-6614.2772, accessed 27 September 2024).

97) Da Silva CV, Ferreria PMO, da Silva Ferreria M, Cardoso AST, Dias, VS, Schmidt CA, Junior AFS, Cazedey ECL. Quality evaluation and dissolution profile of hydrochlorothiazide tablets available in Salvador-BA Brazil. Rev. Colomb. Cienc. Quim. Farm. 52(1)59-77.

98) Shah KA, Needham TE. Correlation of Urinary Excretion with in vitro dissolution using several dissolution methods for Hydrochlorothiazide formulations. Journal of Pharmaceutical Sciences. 1979; 68(12)1486-1490. (doi: doi: 10.1002/jps.2600681206, accessed 27 September 2024).

99) Brazilian Pharmacopeia. Hydrochlorothiazide. (https://www.gov.br/anvisa/pt-br/assuntos/farmacopeia/farmacopeia-brasileira/insumos-farmaceuticos-e-especialidades-ate-2a-errata-p-pdf-com-capa.pdf, accessed 29 September 2024)

100) Indian Pharmacopeia. Hydrochlorothiazide. 2018. (https://ipc.gov.in/, accessed 29 September 2024).

101) Chinese Pharmacopeia. Hydrochlorothiazide. 2020. (https://baipharm.chemlinked.com/regulatorydb/view/93, accessed 29 September 2024).

102) Zarmpi P, Flanagan T, Meehan E, Mann J, Fotaki N. Biopharmaceutical understanding of excipient variability on drug apparent solubility based on drug physicochemical properties. Case study: Superdisintergrants. The APPS Journal. 2020; 22(46):1-16. (doi: 10.1208/s12248-019-0411-1, accessed 29 September 2024).

103) Xi Lu J, Tupper C, Guiterrez V, Murray J. Biochemistry, Dissolution and Solubility. Compilation prepared by National Library of Medicine (https://www.ncbi.nlm.nih.gov/books/NBK431100/#:~:text=The%20Noyes-Whitney%20equation%20represents%20the%20dissolution,rate%3A%20dm%2Fdt%20%3D%20D%2AA%2A%20%28Cs%20-%20C%29%2Fh, accessed 30 September 2024).

104) Souta C, Rodriguez A, Parajes S, Martinez-Pacheco. A comparative study of the utility of two superdisintegrants in microcrystalline cellulose pellets prepared by extrusion-spherization. European Journal of Pharmaceutics and Biopharmaceutics. 2005; 61(1-2):94-99. (doi: https://doi.org/10.1016/j.ejpb.2005.04.003, accessed 30 September 2024).

105) Dokoumetzidis A, Papadopoulou V, Macheras P. Analysis of Dissolution Data Using Modified Versions of Noyes–Whitney Equation and the Weibull Function. Pharm Res 23, 2006; 256–261. (doi: 10.1007/s11095-006-9093-3, accessed 19 October 2024).

106) Walkowiak R, Kala R. Two-phase nonlinear regression with smooth transition. Communications in Statistics - Simulation and Computation, 2000; 29(2): 385–397. (doi: https://doi.org/10.1080/03610910008813618, accessed 19 October 2024).

107) Metry M, Polli JE. Evaluation of excipient risk in BCS class I and III biowaivers. AAPS J. 2022; 24(1)20. (doi: 10.1208/s12248-021-00670-1, accessed 19 October 2024).

***

POTENCY TESTING OF WHOLE-CELL PERTUSSIS-CONTAINING VACCINES: RESULTS OF MULTILABORATORY ASSESSMENT OF THE PERTUSSIS SEROLOGICAL POTENCY TEST

Christina von Hunolstein[1], Tim Schofield[2], Arjen Sloots[3], Sunil Gairola[4], Irma Riyanti[5], Erti Resnawati[5], Pavlinka Stoyanova[6], Coenraad Hendriksen[7], Sivashen Cunden[8], Pradip Das[9], Muhammad Erdiansyah[10], Viktoriya Milanova[11], Pavel Mitrenga[11], Saveta Mladenova[11], Supaporn Phumiamorn[12], Maya Ramdas[13], Sreenivasulu B. Reddy[14], Sonia Pagliusi[8], Valentina Salvati[1], Suchita Sharma[15], Yojana Shinde[4], Gurbaksh Singh[16], Dionne Williams-David[3], Marcel Thalen[17] and Laura Viviani[8]

[1]Istituto Superiore di Sanità, Rome, Italy (christina.vonhunolstein@iss.it; valentina.salvati@iss.it)
[2]CMC Sciences, Germantown, United States of America (*US collaboration concerned preceded 20 January 2025*) (timothylschofield@gmail.com)
[3]Intravacc, Bilthoven, Kingdom of the Netherlands (asloots@gmail.com)
[4]The Serum Institute of India, Pune, India (sunil.gairola@seruminstitute.com; yojana.shinde@seruminstitute.com)
[5]BioFarma, Bandung, Indonesia (irma.riyanti@biofarma.co.id)
[6]Bulgarian Drug Agency, Sofia, Bulgaria (Pavlinka.Stoyanova@bda.bg)
[7]Utrecht University, Utrecht, Kingdom of the Netherlands (hendriksen.3rs@gmail.com)
[8]Developing Countries Vaccine Manufacturers Network, Nyon, Switzerland (Cunden.Sivashen@gmail.com; sonia_pagliusi@yahoo.com; lviviani@sciethiq.com)
[9]Biological E, Hyderabad, India (pradip.das@biologicale.com)
[10]National Control Laboratory for Biologicals Products, Jakarta, Indonesia (erdiansyah@pom.go.id)
[11]BulBio-NCIPD Ltd, Sofia, Bulgaria (pavel_mitrenga@hotmail.com; savimladenova@abv.bg; V.Milanova@bulbio.com)
[12]Institute of Biological Products, Bangkok, Thailand (supaporn.p@dmsc.mail.go.th)
[13] Panacea Biotec, Lalru, India (mayaramdas@PANACEABIOTEC.COM)
[14]Sanofi Healthcare India Private Limited, Hyderabad, India (sree.basireddy77@gmail.com)
[15]CDSCO, Kasauli, India (suchitakasauli@gmail.com)
[16]Bharat Biotech, Hyderabad, India (gurbaksh3875@bharatbiotech.com)
[17]BioLyo Technologies BV, Ghent, Belgium (marcel@biolyotech.com)

Corresponding author: Christina von Hunolstein christina.vonhunolstein@iss.it

POTENCY TESTING OF WHOLE-CELL PERTUSSIS-CONTAINING VACCINES: RESULTS OF MULTILABORATORY ASSESSMENT OF THE PERTUSSIS SEROLOGICAL POTENCY TEST

ABSTRACT

The Developing Countries Vaccine Manufacturing Network (DCVMN) coordinated a study to assess the feasibility of a serological test – the pertussis serological potency test (PSPT) – to control the potency of the active whole-cell pertussis (wP) component in vaccines. The test was performed by seven wP vaccine manufacturers, and three national control laboratories responsible for the national release of these vaccines. The multilaboratory study was funded by the United States National Institute for Innovation in Manufacturing Biopharmaceuticals. All laboratories shared common protocols for immunizing mice and for testing mouse sera by enzyme-linked immunosorbent assay (ELISA). Each laboratory used its own wP vaccines and the reference vaccine routinely used in the mouse protection test (MPT), which is required by regulatory authorities. All products were tested using the MPT and PSPT. While in all laboratories the PSPT showed a decrease in serum IgG levels in mice after immunization with subpotent batches of the wP vaccine compared to potent batches, some problems were encountered while carrying out the test, which prevented definitive conclusions being made on the test performance. However, the study provided participants with the opportunity to familiarize themselves with the PSPT protocols and indicated the next steps to be addressed to implement this test.

Keywords: pertussis vaccine; vaccines, combined; serologic tests; enzyme-linked immunosorbent assay; feasibility studies; animal testing alternatives.

1. Introduction

Since 1959, when Russel and Burch published their recommendation introducing the principle of the 3Rs (replacement, reduction and refinement) for the use of animals for scientific purposes, animal welfare has attracted the attention of legislators in European countries. In 1986, the European Convention for the protection of vertebrate animals used for experimental and other scientific purposes (CoE ETS 123) was signed. The principle of the Convention was incorporated into Directive 86/609/EEC on the protection of animals used for scientific purposes and regulated by Directive 2010/63/EU 2 *(1)*.

Since then, various organizations such as the Biological Standardization Programme of the European Directorate for the Quality of Medicines and Health Care, the European Centre for the Validation of Alternative Methods (ECVAM) and the World Health Organization (WHO) have funded studies to develop alternative methods to animal tests to be conducted in vitro for both potency and safety testing of vaccines; whenever in vitro tests could not be used, reductions and refinements of in vivo tests were proposed.

Efforts to move away from in vivo testing have been further strengthened by the institutionalization of new models of production and quality assurance, such as the reliance on Good Manufacturing Practices and the application of the consistency approach *(2–4)*. For older so-called legacy vaccines that have been on the market for many years and whose safety, potency and efficacy have been demonstrated, the use of alternative tests is envisaged once the consistency of production and quality control has been further confirmed on an ongoing basis. The potency assay, a vital quality attribute used to ensure the biological properties of vaccines, is associated with their efficacy. By replacing an in vivo potency test with an in vitro test, good results have been obtained for several viral vaccines that consist of purified antigens (for example, hepatitis and inactivated polio), which are quantified in the vaccine by immunoassays *(5,6)*. These new in vitro assays have been accepted for batch consistency control testing and have been included in international or national pharmacopoeias (for example, the European Pharmacopoeia) and in the WHO series of technical reports *(7,8)*.

For some bacterial vaccines, such as those against diphtheria and tetanus, in vitro potency tests are not yet available. The VAC2VAC consortium has developed promising in vitro tests, but these methods need to be further evaluated *(9)*. Therefore, to date, the only alternative potency test recognized for diphtheria and tetanus vaccines by the European Pharmacopoeia and WHO is a refinement of the current in vivo challenge test with a serological test *(10-12)*.

While the original potency test uses animal death as a measure, the serological method measures the vaccine's ability to induce specific protective antibodies in mice or guinea pigs. The presence of antibodies is determined in vitro using an appropriate immunochemical method, such as the enzyme-linked immunosorbent assay (ELISA). Diphtheria and tetanus vaccines are usually combined with pertussis vaccines. Acellular pertussis (aP) vaccines have been adopted by high-income countries, while whole-cell pertussis (wP) vaccines are still widely used for routine vaccination in low- and middle-income countries *(13)*.

Due to the increased incidence of pertussis in countries where aP is used in vaccination programmes *(14)* and the fact that wP vaccines provide better and longer lasting immunity *(15,16)* than aP vaccines, WHO recommends that a change from wP vaccines to aP vaccines for primary immunization of infants should only be considered if further periodic booster or maternal immunization is ensured and supported in national immunization programmes *(17)*. Therefore, wP vaccines are expected to remain the vaccine of choice in large parts of the world. wP vaccines consist of inactivated *Bordetella pertussis* bacteria, usually two or more strains in appropriate proportions. The potency of a wP vaccine is determined using the mouse protection test (MPT; also known as Kendrick's test). This compares the dose of vaccine required to protect mice from a lethal challenge dose of *B. pertussis* strain 18323 administered intracerebrally with the amount of a reference preparation, calibrated in international units (IU) *(18)*.

Although the MPT has been used for a long time, its use has been disputed for various reasons. The MPT generally has high variability and consequently often fails to meet the statistical validity criteria for acceptance of the test. When statistical validity criteria are not met, batches of vaccine have to be retested, costing time and at least 100 mice per test.

Since death is the measure of the test, the mice experience severe pain and distress during and after the intracerebral injection procedure. Furthermore, the intracerebral challenge is technically difficult to perform. Thus, from the point of view of both animal welfare and reproducibility of the assay, it is widely recognized that an alternative to MPT is needed. Several attempts have been made to develop an alternative potency test for wP vaccines to be applied for routine quality control by manufacturers and national control laboratories (NCLs). Compared with the respiratory challenge test and the nitric oxide induction test, which are too difficult and complicated to be used as routine tests *(19,20)*, the mouse pertussis serological potency test (PSPT) seems the most promising for this purpose *(21)*. This serological method was developed by van der Ark and colleagues as a refinement of the potency test for wP vaccines *(21)*.

It was observed that the survival of mice immunized with the wP vaccine in the MPT could be predicted from the concentration of antibodies present on the day of the challenge with *B. pertussis* strain 18323. Many of the antibodies were found to be raised against the surface antigens of the challenge strain. For this reason, the inactivated *B. pertussis* bacterium, strain 18323, was chosen as the coating antigen in the whole-cell ELISA, which forms a key part of the PSPT.

Therefore, PSPT, based on the in vivo IgG antibody response, mimics a specific element of the complex immune response that occurs in the MPT and can be used as a surrogate for protection to demonstrate the biological activity of wP vaccine products that already have a well-established safety and efficacy profile.

The suitability of the PSPT has been demonstrated in previous small-scale collaborative studies funded by some sponsors *(22,23)*. However, the evaluation of the PSPT by large-scale multicentre collaborative validation studies has never been done, as the wP vaccine is no longer produced by multinational companies in Europe.

Today, wP vaccines are mostly produced by member companies of the Developing Countries Vaccine Manufacturing Network (DCVMN). These vaccines are considered crucial for paediatric immunization in developing countries. In fact, many of these vaccines are prequalified by WHO and supplied to, for example, the United Nations Children's Fund and the Pan American Health Organization for the immunization campaigns these agencies support globally.

In light of the challenges posed by the MPT and the promising results obtained in previous PSPT studies, DCVMN manufacturers expressed their interest in evaluating its applicability for routine batch release testing of their wP vaccines. These are multivalent vaccines with wP combined with diphtheria and tetanus (trivalent vaccine, DTwP) and other types of antigens such as hepatitis B (tetravalent vaccine, DTwP-HepB), *Haemophilus influenzae* type b glycoconjugate (pentavalent vaccine, DTwP-HepB-Hib), or the hepatitis B, Hib and inactivated poliomyelitis vaccine (hexavalent vaccine, DTwP-HepB-Hib-IPV) in the presence of aluminium hydroxide/phosphate as an adjuvant *(24)*.

To explore the feasibility of the PSPT, a multilaboratory study was designed by the wP vaccine manufacturers and the NCLs, and facilitated by DCVMN and the scientific–technical support of a dedicated Steering Group. The project was named: International assessment of the PSPT in mice to replace the intracerebral-challenge MPT for wP. It was submitted to the National Institute for Innovation in Manufacturing Biopharmaceuticals and funded through its Global Health Fund *(25)*.

The aim of the project was to evaluate, in the laboratories of participating manufacturers and NCLs, the applicability of the PSPT to their multivalent vaccines, following a protocol that previous studies had developed but not validated *(21,22)*.

2. Methods

2.1 Project participants

Seven vaccine manufacturers and three NCLs participated in the PSPT study on a voluntary and non-remunerated basis. The participants are listed by organization and country in Appendix 1. They are referred to herein by a randomly allocated code number.

2.2 Project design

The project was conducted under the supervision of the appointed Steering Group. The project study included the analysis by the MPT and PSPT of a reference wP vaccine and three different batches of wP vaccine produced by the manufacturers, or designated by the NCLs. These are referred to throughout the manuscript as follows: FL1, FL2 tested twice in the PSPT (FL2A and FL2B), FL3 tested unaltered and FL3-Alt tested after heat treatment (see subsection 2.3). The FL1 vaccine was used not only as a test vaccine, but also as a proposed internal reference standard vaccine (see subsection 2.3). The intracerebral MPT was performed to verify that the vaccines used in the PSPT were compliant and that the altered FL3 vaccine had a reduced wP potency. The MPT was performed as described in subsection 2.5.

The PSPT was performed in each laboratory as indicated in the protocol provided (see subsections 2.6.1 and 2.6.2). Each laboratory was asked to select one of two study design options (Fig. 1) that could be used to assess the variability of the assay (within-run), the variability from batch to batch and the suitability of the PSPT to detect a decrease in the potency of a deliberately altered batch in each laboratory.

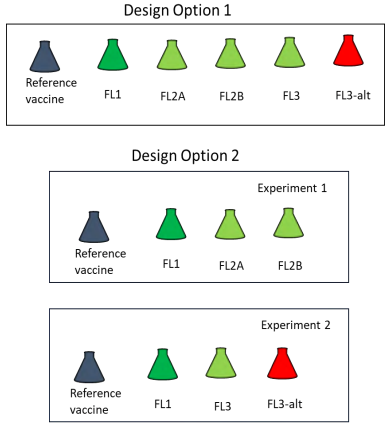

Fig 1. PSPT design options
PSPT: pertussis serological potency test.

Note: Design option 1 includes a reference vaccine (IPRS/20/PERT, RWRS 01/11, WHO-IS or in-house reference), batch FL1, FL2 tested twice as FL2A and FL2B, and FL3 tested unaltered and altered (FL3-Alt). Design option 2 includes the same batches tested over two separate experimental runs.

Replicate tests of FL2 (FL2A and FL2B) in design options 1 and 2 were used to obtain a preliminary assessment of within-run variability. Three batches produced and tested by participating manufacturers contributed to a preliminary assessment of batch variability (consistency in batch production). Variability of batches tested by NCLs was not considered in the inter batch variability assessment. The comparison of the results of the unaltered and altered batches (FL3 and FL3-Alt) was used to assess the ability to detect the decrease in potency measured with the PSPT in each laboratory.

2.3 Test and reference vaccines

Each participant used their own licensed wP-containing vaccine and the standard reference vaccine in use in the MPT (Table 1). The NCLs used vaccine batches received for batch release with the consent of the respective manufacturer.

Eight participants used batches of a pentavalent vaccine (DTwP-HepB-Hib), one participant used batches of a hexavalent vaccine (DtwP-HepB-IPV-Hib) and one participant used batches of a trivalent vaccine (DTwP). The wP content in terms of opacity units (OU) per mL of vaccine is indicated for each laboratory in Table 1.

Each manufacturer's laboratory tested three batches of its vaccine containing wP. NCL 1310 tested three batches from the same manufacturer, and NCL 7132 and 7452 tested vaccines of the same combination, but from three and two different manufacturers, respectively.
The batch designated as FL3 was altered by each participant according to a common protocol, with incubation at 43–45 °C for 21 days under gentle agitation. These conditions were chosen to reduce MPT potency by about 60% *(26,27)*.

Each participant was required to use the wP reference vaccine currently in use in the MPT (Table 1): (i) WHO's Fourth International Standard (IS4) for pertussis vaccine (lyophilized inactivated, *B. pertussis*, 40 IU/ampoule, 150 OU/ampoule, NIBSC code 94/532); (ii) the regional working reference standard for pertussis (RWRS 01/11, 63 IU/vial, 300 OU/vial); (iii) the national reference standard for pertussis (IPRS/20/PERT, potency of 75 IU/vial, 300 OU/vial) recognized by the Indian Pharmacopoeia; (iv) an in-house reference vaccine (STBF 2015-1, 62 IU/vial). RWRS, IPRS and the in-house reference were calibrated against WHO's Fourth International Standard in the MPT. The unitage of RWRS and IPRS was assigned based on collaborative studies by the Indian Pharmacopoeia. All reference vaccines are called external reference standard (ERS) or reference vaccine throughout the paper.

Table 1. Characteristics of whole-cell pertussis or reference vaccines used by each participating laboratory

Laboratory code	Test vaccine		External reference standard[a]		
	Components	OU/mL	Origin	Batch no./code	IU/vial
1310	DTwP-HepB-Hib	24	National	RWRS 01/11	63
2069	DTwP-HepB-Hib	24	National	IPRS/20/PERT	75
2673	DTwP-HepB-Hib	24	In-house	STBF 2015-1	62
4990	DTwP-HepB-Hib-IPV	30	National	IPRS/20/PERT	75
5544	DTwP	30	WHO IS	NIBSC 94/532	40
5980	DTwP-HepB-Hib	28	National	IPRS/20/PERT	75
7132	DTwP-HepB-Hib	24, 28, 32	National	IPRS/20/PERT	75
7452	DTwP-HepB-Hib	24, 28, 32	National	RWRS 01/11	63
9258	DTwP-HepB-Hib	32	National	IPRS/20/PERT	75
9525	DTwP-HepB-Hib	32	National	IPRS/20/PERT	75

OU: opacity units; IU: international units; D: diphtheria; T: tetanus; P: pertussis; Hep B: hepatitis B; Hib: *Haemophilus influenzae* type b glycoconjugate; IPV: inactivated poliomyelitis vaccine.

[a] The external reference standard contains only *Bordetella pertussis* plain whole cells.

2.4 Mice and their evaluation for absence of *Bordetella* spp.

Participants were recommended to use the mouse strain currently in use for the MPT also in the PSPT (Table 2).

Table 2. Characteristics of the mouse strains used in the mouse protection test and pertussis serological potency test

Laboratory code	Strain, sex and breeding of mouse	Laboratory code	Strain, sex and breeding of mouse
1310	ddY; male; outbred	7132	Swiss albino; male; outbred
2069	Swiss albino; male; outbred	7452	ICR; female; outbred
2673	ddYbf; male; outbred	9258	Swiss Webster; 50/50; outbred
4900	ICR; 50/50; outbred	5544	ICR; 50/50; outbred
5980	NIH Ola Hsd; 50/50; inbred	9525	Swiss albino; male; outbred

All mice were bread under specific pathogen free conditions, certified by the respective commercial breeder or manufacturer's breeding facility. The health status of the animals was recorded on arrival and monitored during the experiments by comparison with sentinel animals (data not shown). The sentinel mice (nine mice) belonged to the same cohort of animals used for the MPT and PSPT, were housed in the same animal room but were not immunized.

Before the start of the study, three of the nine sentinel animals were individually screened for the presence of pre-existing antibodies versus the ELISA coating antigen (see subsection 2.6.2) and/or the presence of *Bordetella* spp. infection (*B. pertussis, B. parapertussis and B. bronchiseptica*) by an appropriate method (polymerase chain reaction for *Bordetella* spp. on mouse serum, liver/lung/heart tissue or with commercial kits). If none of the mice was found positive, the batch of animals was considered suitable for the study. On the bleeding day (day 28; see subsection 2.6.1), the serum samples obtained from the remaining six sentinel mice/room were all tested in the PSPT-ELISA to determine the absence of wP-specific antibodies. The animal studies were reviewed and approved by the respective institutional animal ethics committees.

2.5 Intracerebral MPT

Vaccine batches were tested for pertussis potency by the intracerebral MPT. Each study participant performed the test according to routine wP batch potency determination in mice by challenge as per the relevant WHO manual *(18)*. Briefly, mice were randomly distributed across the dilution groups of the reference vaccine and test batches. After an acclimatization period, groups of animals, weighing 12–16 g, were immunized (16 mice/dilution group) intraperitoneally (i.p.) with 0.5 mL of a three- to five-fold dilution series of the wP vaccine under study and of a reference vaccine, respectively. Fourteen days after immunization, animals were challenged with a lethal dose of *B. pertussis*, strain 18323, by intracerebral route and monitored for clinical signs of pertussis and death up to day 28. Negative control (injected intracerebrally with casamino acids) and positive control (naive mice, injected with the challenge culture as a virulence check of challenge culture) animal groups were used to monitor the challenge procedure. The relative potency was expressed in IU calculated by comparing the effective dose of the test vaccine to the reference vaccine using parallel probit analysis. A batch passed the test if it had a potency of not less than 4.0 IU per single human dose and the lower fiducial limit ($P = 0.95$) of the estimated potency was not less than 2.0 IU per single human dose *(18)*.

2.6 PSPT

2.6.1 Immunization of mice and preparation of serum samples

The mouse PSPT was performed as previously described *(21)*. Briefly, groups of 12 mice (equal number of female and male animals, or animals of the same sex, and target weight 20–24 g), were randomly subdivided into four dose groups. Each group of animals was immunized at day 0 with one of the four doses of an ERS or test vaccine. Animals were immunized i.p. using a

2.5 mL syringe fitted with a Gx1 needle with a dose of 0.5 mL dilution/mouse. The ERS was administered at a dose of 5.0, 2.5, 1.25 and 0.625 IU/mouse in a total volume of 0.5 mL. Test vaccines (24–32 OU/mL) were injected as 10-fold (50 µL of vaccine + 450 µL diluent), 20-fold (25 µL of vaccine + 475 µL diluent), 40-fold (12.5 µL of vaccine + 487.5 µL diluent) and 80-fold (6.25 µL of vaccine + 493.8 µL diluent) dilutions in a total volume of 0.5 mL. Twenty-eight days after immunization, all animals were bled under anaesthesia (cardiac or retro-orbital puncture) and individual blood samples were collected, processed, divided in aliquots (200 µL) and stored at –20 °C. The protocol is available at the DCVMN website *(28)*.

2.6.2 PSPT whole-cell ELISA

The PSPT whole-cell ELISA to detect *B. pertussis*-specific IgG antibodies was performed on individual mouse sera obtained at 28 days after immunization *(21)*. Briefly, flat-bottomed polysorb microtitre plates were coated with 100 µL/well of a 0.25 OU/mL suspension of inactivated whole-cell *B. pertussis* strain 18323 in phosphate buffered saline (prepared ad hoc for this study, see subsection 2.7), and incubated at 37 °C overnight without a lid to allow the liquid to evaporate. Non-specific binding sites of the plates were blocked with a 1% solution of bovine serum albumin in phosphate buffered saline (150 µL/well) at 37 °C for 1 h and washed three times with a solution of 0.05 % Tween 80 in distilled water. Sera diluted in phosphate buffered saline with 0.5 % w/v bovine serum albumin and 0.05 % Tween 80 were added (100 µL/well) and incubated at 37 °C for 1 h. After washing, 100 µL of goat anti-mouse *horseradish peroxidase* IgG conjugate were added and plates were again incubated at 37 °C for 1 h. After washing, 100 µL of substrate (3,3′,5,5′-tetramethylbenzidine) was added. The plates were incubated at room temperature for 10 min. The detection reaction was stopped by addition of 100 µL of 0.2M sulfuric acid. Absorbance at 450 nm was measured with an automated microtitre plate reader. All plates included a blank, the absorbance of which was subtracted from the absorbance of positive and negative control sera (see subsection 2.8), sera of mice injected with the ERS and the test samples. Reagents, other than the whole-cell ELISA coating antigen, were from different brands and are therefore not indicated in this section.

A defined plate layout was provided to all participants as the absorbance values ($OD_{450\ nm}$ values) had to be imported into an Excel (Microsoft, Redmond, United States of America) spreadsheet designed during the project for calculating the serum IgG concentrations (antibody, ELISA Unit (EU)/mL; here also indicated as titre). Titres for individual mouse sera were determined by interpolation from a four parameter logistic fit to the concentration response data of the positive control. The concentration of the first positive control level was arbitrarily set to 100 EU/mL without loss of interpretability.

Dilutions of test sera which fell within the dynamic range of the positive control fit (20% to 80%, where 0% corresponds to the lower asymptote of the curve and 100% to the upper asymptote) were interpolated (calibrated) from the curve, dilution corrected, and the serum titre reported as the geometric mean of the resolved dilutions. The protocol is available at the DCVMN website *(28)*.

2.7 Whole-cell ELISA coating antigen

DCVMN provided all participating laboratories a standardized, thoroughly characterized batch of coating antigen of inactivated *B. pertussis* strain 18323 for their use in the PSPT study. BioLyo Technologies (Gent, Belgium) was contracted by DCVMN for the production of a large-scale batch of coating antigen. A total of 2080 lyophilized vials with inactivated *B. pertussis* strain 18323 (ATCC, code 9797), 25 OU/vial, were produced. Intravacc (Bilthoven, Kingdom of the Netherlands) was appointed by DCVMN for the characterization of this newly produced batch of coating antigen. Characterization showed that the overall protein content of the newly produced batch was comparable to a previously produced reference batch (made using a different process) and used in the earlier collaborative studies *(22, 23)* and the new batch included a wide range of virulence factors. The newly produced batch of coating antigen had similar IgG-binding properties as the previously tested batch which was able to distinguish sera induced by potent and subpotent vaccines generated in an earlier collaborative study (data not shown).

The coating antigen is now available in the product catalogue of the National Institute for Biological Standards and Control: *Bordetella pertussis* 18323 coating antigen, NIBSC code 23/150 *(29)*.

2.8 Preparation of pertussis positive and negative control sera for the whole-cell ELISA

The wP positive control serum was generated in each laboratory and consisted of a homologous pooled serum obtained by immunization (i.p.) of 15 mice with the highest dose of the particular ERS used by each laboratory. At 28 days after immunization, mice were bled and the serum of each animal was assayed in the whole-cell ELISA (see subsection 2.6.2). Individual mouse sera with similar high antibody concentrations were pooled and this positive control serum was stored in aliquots at –20 °C. In the PSPT whole-cell ELISA, the positive control serum was prediluted 1/400 and then further diluted two-fold through eight dilutions to obtain a standard curve. To the dilution in the first well of the dilution series, a value of 100 EU/mL was assigned.

The wP negative control serum was obtained from non-immunized mice of the same cohort for the study, after confirmation of absence of *Bordetella* spp. and/or coating antigen-specific antibodies in the whole-cell ELISA (see subsection 2.6.2). The negative control serum was aliquoted and stored at –20 °C. It was diluted at 1/400 in each run of the assay.

2.9 Statistical methods

Determination of mouse serum antibody content was carried out according to subsection 2.6.2 in a data collection and antibody determination Excel spreadsheet using the SOLVER function to fit the positive control data. Mouse sera below the lower limit of the dynamic range of 20% were judged to be negative and assigned an antibody concentration equal to 2.5 EU/mL. Individual mouse titres across doses of the reference and test vaccines were used to perform parallel line analysis using Combistats (EDQM, Strasbourg, France). Analyses were performed

using both the ERS (NRS/RWRS, in-house reference or the WHO IS) and an internal reference standard (IRS) vaccine (FL1) as reference vaccines. Data were manually screened and mouse responses ($OD_{450\,nm}$) below the value of the first dilution of the negative control were eliminated from the analyses and treated as non-responding mice (that is, negative). Doses showing non-monotonic behaviour relative to other doses in a concentration series, and low doses with a high proportion of negative responses (more than 6/12 mice) were likewise eliminated before performance of the parallel line analysis.

The model that was selected for parallel line analysis was:

$$ln(y_{ijk}) = \alpha_i + \beta \cdot ln(x_{ijk}),$$

where $ln(y_{ijk})$ and $ln(x_{ijk})$ are the natural logs of the mouse titres and vaccine doses, i is the standard or test vaccine, j is the dose, k is the mouse, α_i is the intercept for the i[th] vaccine (standard or test) and β is the common slope of the regression for the two vaccines. From this equation, the estimated relative potency ($\widehat{RP}$) is calculated as:

$$ln(\widehat{RP}) = \frac{\hat{\alpha}_T - \hat{\alpha}_S}{\hat{\beta}},\ \widehat{RP} = e^{ln(\widehat{RP})}.$$

Tests of assumptions (parallelism and linearity) were performed according to methods described in *Statistical analysis of results of biological assays and tests (30)*. A failure of an assumption is earmarked when the *P*-value is less than or equal to 0.05. A confidence interval scaled to the estimated relative potency was calculated according to the above-mentioned publication *(30)*, which was held to a provisional acceptance criterion of being within 50% to 200% (as per the requirement in the MPT).

Assay (within-run) and batch-to-batch variabilities were assessed using variance component analysis on natural log (ln) potencies obtained from samples tested using the design selected in each laboratory. The factor associated with vaccine batch was treated as a random effect in the analyses. Assay ($\hat{\sigma}^2_{Assay}$, from replicate testing of FL2) and batch ($\hat{\sigma}^2_{Batch}$, from the three batches in the manufacturing laboratories) variance component estimates were used to report assay and total ($\hat{\sigma}^2_{Total} = \hat{\sigma}^2_{Assay} + \hat{\sigma}^2_{Batch}$) variabilities for each laboratory. Results are reported as per cent geometric coefficient of variation (%GCV) as per the United States Pharmacopeia *(31)*:

$$\%GCV_{Assay} = 100 \cdot \left(e^{\hat{\sigma}_{Assay}} - 1\right)\%, and$$

$$\%GCV_{Total} = 100 \cdot \left(e^{\sqrt{\hat{\sigma}^2_{Assay} + \hat{\sigma}^2_{Batch}}} - 1\right)\%.$$

The ability to detect decreases in potency was measured from FL3-Alt versus FL3 as per cent reduction (%Red) in their relative potencies: $\%Red = 100(ratio - 1)\%$.

3. Results

3.1 Determination of wP vaccine induced IgG responses by whole-cell ELISA

No sentinel mouse sera were found positive for *Bordetella* spp. in any of the laboratories. Therefore, each laboratory carried out the whole-cell ELISA as specified in the study protocol and used the data collection and the Excel spreadsheet for antibody calculation. Initial testing of mouse sera resulted in a variety of positive control curve features. A sampling of curves by parallel line analysis and parameter estimates obtained early in this study are shown in Fig. 2.

Panel (a) shows a positive control curve with acceptable features, panel (b) shows an incomplete lower asymptote and a hook effect and panel (c) shows incomplete lower and upper asymptotes and a shallow slope. Many laboratories exhibited laboratory features that were not acceptable as compared to the curve in panel (a). While this may not have affected interpolation, it did yield inaccurate assessment of the dynamic range of the curve, and thus the reliability of interpolated values.

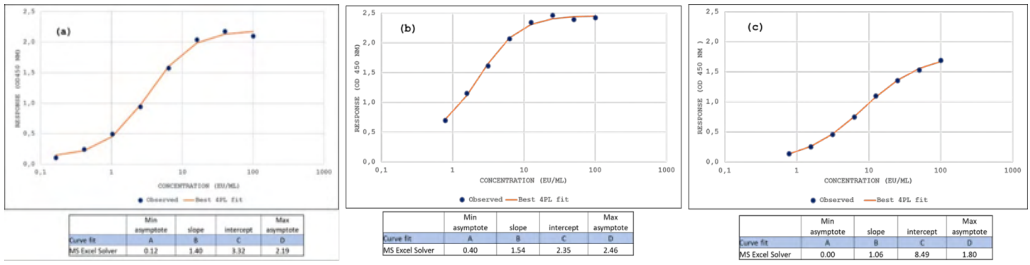

Fig. 2. ELISA positive control curves by parallel line analysis and parameter estimates illustrating: (a) acceptable properties; (b) incomplete lower asymptote and a hook effect; and (c) incomplete lower and upper asymptotes and a shallow slope.

Subsequent to these observations, interviews were conducted with each laboratory to suggest measures to optimize the performance of the whole-cell ELISA, including studies to identify an optimal conjugate dilution by titration and changes to the dilution series of the whole-cell ELISA positive control and the test samples. A number of features of an acceptable positive control curve were given: (i) at least two points on or near the lower and upper asymptotes; (ii) monotonically increasing dose response across the range of the curve (for example, no hook or prozone effects on the upper asymptote); and (iii) at least four points in the dynamic range.

3.2 Determination of relative potencies of wP vaccine batches by parallel line analysis

Parallel line analysis was performed on dose response of test batches of vaccines versus an ERS and an IRS (see subsection 2.9). Interpretation of the results reflects, in part, the mechanism by which parallel line analysis is used to determine relative potency (RP) of a test batch to a reference vaccine. Linear regression was used on log titre versus log dose for both the test and reference vaccines. The natural log (ln) of dose is used in the calculations. An ideal depiction of the calculation of relative potency is shown in Fig. 3.

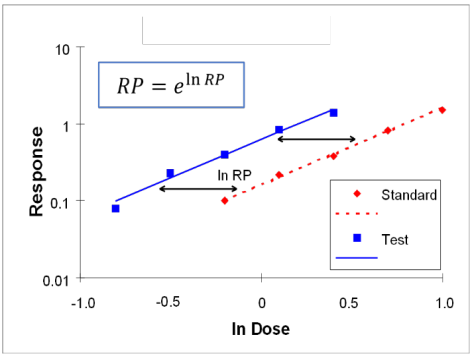

Fig. 3. Illustration of relative potency (RP) determination for a test vaccine relative to a reference vaccine in a parallel line analysis
Note: Each point shows the mean response at each dose.

The ln(RP) represents the horizontal shift of the test vaccine dose–response relationship from the reference vaccine dose–response relationship. The principle of RP is that a test batch acts as a dilution (shifted to the right) or a concentration (shifted to the left) of the standard. The RP is obtained by using the antilog of the log base used in the analysis, in this case the Napierian base, *e*. The assumptions for a valid RP are that the dose–response relationships are linear (that is, they can be fit with a simple linear equation) and the dose response profiles are parallel (that is, the profiles have equal slope coefficients). It should be noted that the underlying vaccine dose kinetics model is four parallel lines, the same as used in the whole-cell ELISA. This understanding and the fact that parallel line analysis is sensitive to the location on the full (four parallel lines) dose–response curves of the reference vaccine and test batches, are the basis for interpretation of the results of the parallel line analysis in the PSPT study.

In general, test batches seemed to be underdosed in relation to the particular ERS used. Underdosing was determined to be about five-fold to 12.5-fold lower than the target doses. This resulted in excessive numbers of negative sera at lower doses. A plot of the sum of the proportions of negative mice across laboratories (cumulative proportions in per cent - mostly based on 12 mice per dose when mice were not eliminated due to probable laboratory errors) is shown in Fig. 4.

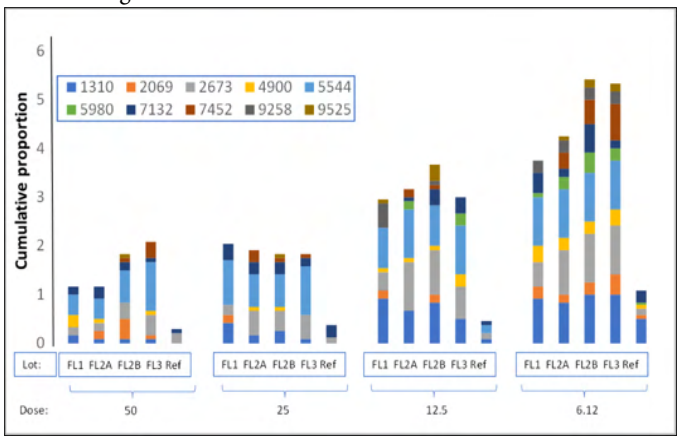

Fig.4. Cumulative proportion of negatives by dose for batches tested in the pertussis serological potency test project

This tendency for higher numbers of negative mice at lower doses resulted in frequent violations of the assumptions for parallel line analysis (linearity and parallelism) and excessively wide confidence intervals expressed around the estimated relative potency of test batches. Illustrations of the consequences of high proportions of negative mice on these assumptions and the variability, and therefore the width of the confidence interval, are shown in Fig. 5.

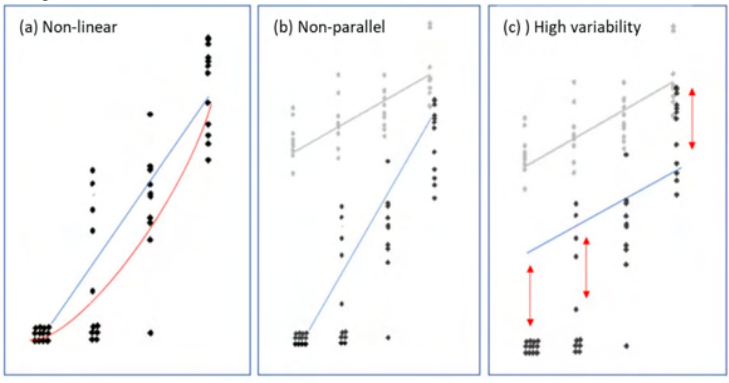

Fig.5. Illustrative examples of the consequences of high proportions of negatives (clusters of points at low doses)

Panel (a) non-linearity where clusters "bend" the dose–response; panel (b) non-parallelism where the slope of a low potency batch is drawn towards clusters; and panel (c) high variability (resulting in wide confidence intervals) where parallel lines are a poor fit to the data.

Statistical curvature (non-linear) is observed for a subpotent batch due to the negative boundary and abundance of points at lower doses. Non-parallelism is primarily due to a suboptimal (linear) fit where a slope is heavily influenced downward towards the clusters of negatives at lower doses. A poor fit results when the lines are forced to be parallel, resulting in large deviations between individual mouse responses and the fitted lines (arrows) and resultant wider confidence intervals. A summary of conformance to assumptions and conditions across laboratories when test batches were analysed together with an ERS is presented in Table 3.

Table 3. Failures of parallel line analysis assumptions and conditions when testing unaltered batches against an external reference standard[a]

Laboratory	No. of failures across batches (except FL3-Alt)		
	Parallelism	Linearity	CI of relative potency
1310[b]	1	1	0
2069	0	0	4
2673[c]	0	0	5
4900	0	0	4
5544	2	0	4
5980[c]	1	0	4
7132[b]	0	0	4
7452[b]	0	0	3
9258	0	0	2
9525	0	0	4

CI: confidence interval.

[a] External reference standard: RWRS/IPRS/20/PERT/WHO-IS/in-house reference STBF 2015-1.

[b] National control laboratory.

[c] Laboratory using study design option 2; all the others laboratory used study design option 1.

Conformance with the assumptions of linearity and parallelism was achieved in seven of the 10 laboratories. All, except one laboratory, failed to meet the 95% confidence intervals (50–200%) of the estimated potency. The width of the confidence interval signifies excess within-run variability (high proportions of negatives), which can result in false negative conclusions for parallelism and linearity. Hence, the variability is masking the underlying non-linearity and lack of parallelism between the test batches and the ERS, that is, the low failure rates for linearity and parallelism may be due to false negatives. Because of the underdosing (and

resulting high proportion of negatives at lower doses) a conclusion about the use of the ERS as a reference vaccine cannot be reached at this time.

A summary of conformance with assumptions and conditions across laboratories when test batches were analysed versus an internal homologous vaccine (IRS, FL1) used as reference vaccine is shown in Table 4.

Table 4. Failures in assumptions and conditions of parallel line analysis when testing unaltered batches against an internal reference vaccine

Laboratory	No. of failures across batches (except FL3-Alt)		
	Parallelism	Linearity	CI of relative potency
1310[a]	0	1	0
2069	0	2	0
2673[b]	1	0	1
4900	0	0	0
5544	0	0	2
5980[b]	0	0	0
7132[a]	0	0	1
7452[a]	1	0	1
9258	0	0	0
9525	0	0	0

CI: confidence interval.

[a] National control laboratory; the internal reference vaccine was not a homologous vaccine with other test batches, but of the same antigen composition.

[b] Laboratory using design option 2.

Conformance with the assumptions of linearity and parallelism when using an IRS was achieved in eight of the 10 laboratories. There were, in addition, fewer instances of a failure to meet the condition on the range of the confidence interval (four out of 10 laboratories). This is likely due to homology between the IRS (different batch of the same vaccine type) and test vaccines (except in two of the three NCLs that tested vaccines versus a vaccine with similar composition, but that was not homologous).

3.3 PSPT project results

The PSPT project goals were to assess: i) assay variability (within-run variability); ii) batch variability; and iii) the ability to detect decreases in potency across a panel of 10 laboratories. Evaluations were performed in accordance with the validity rules described in subsection 2.9 (Statistical methods). The additional condition that the confidence interval should lie within 50% to 200% of the estimated relative potency was evaluated as a preliminary assessment of the quality of the PSPT results.

3.3.1 Assay and batch variabilities

Assay variability from FL2A and FL2B and batch based on variability between manufactured batches FL1, FL2 and FL3 was assessed in each laboratory. Calculations were performed as described on subsection 2.9, and gave estimated variance components for assay $\left(\hat{\sigma}^2_{Assay}; within-run\right)$ and batch($\hat{\sigma}^2_{Batch}$), their total ($\hat{\sigma}^2_{Total} = \hat{\sigma}^2_{Assay} + \hat{\sigma}^2_{Lot}$), and their respective %GCV's for each laboratory (Table 5).

Table 5. Variance component estimates with measures (% GCV) of assay and total variabilities

Reference	Laboratory	GM[a]	$\hat{\sigma}^2_{Assay}$	$\hat{\sigma}^2_{Batch}$	$\hat{\sigma}^2_{Total} = \hat{\sigma}^2_{Assay} + \hat{\sigma}^2_{Batch}$	%GCV (assay)	%GCV (total)
External	1310[b]	2.22	0.0025	0.0936	0.0962	5.2	36.4
	2069	1.72	0.0005	0.0355	0.0360	2.3	20.9
	2673	0.06	1.3432	0.3595	1.7027	218.7	268.7
	4900	0.90	0.0000	0.0046	0.0046	0.3	7.0
	5544	0.14	1.5780	0.0000	1.5780	251.2	251.2
	5980	0.57	0.0834	0.0000	0.0834	33.5	33.5
	7132[b]	0.76	0.0013	NA	NA	3.7	NA
	7452[b]	1.12	0.0313	NA	NA	19.4	NA
	9258	1.38	0.0025	0.0129	0.0154	5.1	13.2
	9525	2.17	0.0245	0.0177	0.0422	16.9	22.8
Internal	1310[b]	1.48	0.0600	0.0381	0.0981	27.8	36.8
	2069	0.69	0.0007	0.0037	0.0044	2.7	6.9
	2673	0.62	0.0385	0.0598	0.0983	21.7	36.8
	4900	1.06	0.0001	0.0164	0.0165	0.8	13.7
	5544	1.11	0.2184	0.0000	0.2184	59.6	59.6
	5980	0.86	0.0004	0.0227	0.0231	2.1	16.4
	7132[b]	1.12	0.0127	NA	NA	11.9	NA
	7452[b]	NA	NA	NA	NA	NA	NA
	9258	1.37	0.0041	0.1080	0.1121	6.6	39.8
	9525	1.22	0.0057	0.0364	0.0421	7.9	22.8

GM: geometric mean; NA: not applicable

[a] GM of relative potency across batches FL1, FL2, FL3 in the case of manufacturers (four batches for design option 1 and five batches for design option 2), and FL2A and FL2B in the case of national control laboratories (two).

[b] National control laboratory; batches were from different manufacturers; batch variability not calculated.

Within-run variability was similar among laboratories, especially when comparing with the IRS FL1. For laboratories 2673 and 5544, the high results achieved when testing against the ERS are due to the use of non-optimal doses of test lots in the two laboratories.

The pattern of total variability is similar to that of within-run assay variability due to its large influence on total variability.

3.3.2 Detection of the altered batches by MPT and PSPT

The heat-treated vaccines, FL3-Alt, showed lower potency in the MPT as the lower confidence limit was less than 2 IU/single human dose, and were therefore tested as out of specification. However, the results of laboratories 2673 and 4900 for these vaccines were slightly higher than the lower confidence limit with values of 2.20 and 2.10, respectively.

The percentage in potency reduction is reported in the Table 6, for vaccines tested in MPT and PSPT. The potency decrease is evident also in PSPT. The percentage reductions in potency in the MPT and PSPT are not always in line. This finding can be related to underdosing of the test vaccines, and is demonstrated by the in-line results of participant 2673 that repeated the PSPT using optimal test vaccine doses. The potency value in the PSPT, in contrast, is not expected to be the same as that of the MPT, as the two assays are based on different measurement criteria, that is, protection (functional antibodies activity) versus antibody response (binding activity).

Table 6. Potency (IU/dose) and reduction in potency of the heat-treated versus the unaltered vaccines in MPT and PSPT

Laboratory	MPT potency (CI)			PSPT potency versus ERS (CI)			PSPT Potency versus IRS FL1 (CI)		
	FL3	FL3-Alt	% red	FL3	FL3-Alt	% red	FL3	FL3-Alt	% red
1310	6.29 (2.12–19.75)	2.93 (1.03–8.31)	53	3.0802 (1.804–4.589)	1.8998 (1.1556–2.7563)	38	1.9380 (1.1932–3.6533)	0.9312 (0.6408–1.3150)	52
2069	5.03 (2.34–10.96)	4.06 (1.78–9.32)	19	1.6492 (0.4429–3.3560)	0.7195 (0.0502–2.0298)	56	0.6456 (0.3918–0.9827)	0.3738 (0.1540–0.6675)	42
2673[a]	7.07 (2.80–9.22)	4.88 (2.20–10.80)	31	1.1070 (0.7561–1.6469)	0.7897 (0.5541–1.1035)	29	1.1703 (0.7384–1.8917)	0.7890 (0.5071–1.1724)	33
4900	7.60 (4.40–13.6)	5.18 (2.10–12.5)	32	0.9246 (0.2047–1.944)	0.6916 (0.0452–1.8851)	25	0.9410 (0.6104–1.426)	0.4774 (0.1395–1.1969)	49
5544	7.41 (2.71–3.38)	2.01 (0.46–6.72)	73	0.0301 (0.000–0.3280)	0.0196 (0.000–0.2507)	35	0.8790 (0.1123–2.3366)	0.4023 (0.0569–1.0258)	54
5980	5.18 (2.94–9.16)	3.12 (1.71–5.65)	40	0.5424 (0.1662–1.113)	0.4938 (0.1503–1.0230)	9	0.9900 (0.7308–1.3333)	0.7535 (0.5476–1.0150)	24
7132	8.10 (4.56–13.94)	0.69 (0.18–1.71)	91	0.9294 (0.1007–2.4381)	0.5131 (0.0633–1.3739)	45	1.4376 (0.7584–3.0630)	0.6549 (0.3428–1.1190)	54
7452	5.95 (2.59–14.12)	2.04 (0.87–4.59)	66	0.0533 (0.0025–0.2206)	0.0053 (0.0000–0.0367)	90	0.22 (0.1069–0.3585)	0.071 (0.0239–0.1353)	68
9258	7.41 (3.17–16.15)	3.13 (1.12–6.87)	58	1.4932 (0.6621–2.5552)	1.3631 (0.6518–2.2591)	9	1.8775 (1.3169–2.8592)	1.2291 (0.8874–1.7322)	35
9525	5.90 (3.40–10.6)	1.85 (0.80–3.70)	69	1.8450 (0.0094–5.834)	0.3086 (0.0000–2.1434)	83	1.4753 (0.8719–2.6497)	0.7025 (0.3099–1.2679)	52

PSPT: pertussis serological potency test; CI: 95% confidence intervals; MPT: mouse potency test; ERS: external reference standard; IRS: internal reference standard; red: reduction.

[a] Based on vaccination of a new set of animals for PSPT using optimal dosing.

4. Discussion

In the earlier smaller serological testing studies *(22,23)*, participants were provided with anonymized vaccine kits (reference and test samples), the main reagents for testing and the test protocols. In this study, the participants only received the protocols for immunizing the mice and testing the sera in ELISA, the coating antigen and the software for data processing.
In our study, each participating manufacturer tested its own licensed wP-containing vaccine as well as the reference standard vaccine used in the MPT; the NCLs used vaccine batches that they had received for batch release with the consent of the respective manufacturer. The manufacturers and the NCLs tested the products in accordance with their quality assurance system, including, animal husbandry, validation of instruments, and handling of raw materials and reagents.

The aim of our study was to test a serological method to replace the MPT which is currently required for routine testing of vaccines on the market. Our study showed that the serological method is in principle applicable to all wP-containing vaccines. However, it also demonstrated that the PSPT requires further product-specific optimization and validation.

The first step of our project was to organize a new, larger batch of the whole-cell ELISA coating antigen. This is the key reagent in the serological test and is not commercially available. The DCVMN Secretariat therefore commissioned BioLyo Technologies to produce a freeze-dried batch of the coating antigen. The overall protein profile and antigenic properties were characterized by Intravacc to show that the new batch was comparable to the coating material previously produced and used in the studies funded by the Dutch Platform for Alternatives to Animal Testing *(22)* and ECVAM *(23)*.

Problems were encountered in the procurement of materials, as some of the reagents specified in the protocols were not available in some countries. These were exacerbated by the complex logistical and supply issues associated with the coronavirus disease 2019 pandemic. This circumstance also led, among other factors, to an extension of the study duration from 18 to 24 months.

Throughout the project, there was close cooperation and exchange between the participating laboratories and the project steering committee. With this support, all laboratories were able to carry out the PSPT.

The suitability of the PSPT for testing the potency of different manufacturers' products was assessed by evaluating within-assay variability, interbatch wP potency variability, and the ability to discriminate between potent, MPT compliant batches and subpotent, MPT non-compliant batches.
Initial analyses showed an unexpectedly high proportion of negative serum responses in the whole-cell ELISA in low doses of the test vaccines, which resulted in difficulties in processing of

the parallel line analysis data and a wider uncertainty in the estimation of relative potency as measured by the confidence interval. This may indicate suboptimal dosing of the test vaccines used in this study.

The same dose range in a previous study did not cause a problem in the potency estimation. In our study, vaccine combinations from seven manufacturers were used in which the wP component was combined, not only with the usual DT antigens, but also with different active antigens, such as HepB, IPV or Hib components. These antigens were not always present in the wP vaccines tested in previous studies *(22,23)*.

It is noteworthy that the change in dose range by a participating laboratory performing a second run confirmed the need to establish the product-specific dose range before validation of the PSPT. In view of the time constraints and ethical concerns, only this laboratory repeated the immunization part of the test.

Another difference between our study and the earlier ones was the use of different reference standards: van der Ark et al. used an in-house plain *B. pertussis* whole-cell vaccine in their studies *(21,22)*, which contained the same strains as the DTwP-IPV vaccine, also produced in-house. However, our study required the use of the international WHO wP standard, a regional standard or a national Indian standard. These differences may be the reason why the dose range of test vaccines used in our study was suboptimal.

Since the full-dose response of the vaccines follows a sigmoid relationship between logarithmic dose and response (here logarithmic response due to the statistical properties of the whole-cell ELISA responses), the doses of the ERS and test batches must be chosen so that linear and parallel response series (mouse serum antibody concentrations) are generated for both the reference and test vaccines. The linear series is selected from a suitable part of the overall curve. This can be the middle of the sigmoid curve or the lower exponential part (called log-log, as designed and analysed in our study). In this setting, the test vaccines should be approximately equipotent to the reference vaccine to ensure that the dose–response relationships are linear and parallel.

The whole-cell ELISA method posed a challenge especially for laboratories that had little experience with the optimization and performance evaluation of ELISA-based methods. Thus, in addition to the close cooperation between the laboratories and the steering committee described above, one-on-one meetings were held with the laboratories to solve their individual problems. Following these discussions, the laboratories were advised how to improve the test by measures such as titrating the conjugate (to a level that gave symmetrical positive control curves), using a 2.5- or 2-fold dilution series of the positive control, and selecting a different initial dilution of the positive control and test samples. It is recommended that at least two points sit on or near the upper and lower asymptotes and at least four points sit in the middle of the dynamic range of the positive control curve *(31,32)*. ELISA results improved after

implementation of the recommended measures in some laboratories that were able to perform additional testing of sera (data not shown).

Due to the small number of batches and the use of suboptimal vaccine doses, the assessment of assay and inter batch variability cannot be conclusive. However, intra-assay variability was negligible across manufacturers, leading to the qualitative conclusion that batch potencies were consistent across manufacturers.

The use of vaccine batches of lower quality, and thus reduced potency, is essential when evaluating the suitability of a new method *(33)*. In our case, the degree of reduction in MPT potency after mild heat treatment *(27)* was not expected to be consistent across vaccines due to intrinsic differences in heat resistance between manufacturers' products and possible laboratory-specific differences in the implementation of the inactivation protocol. Nevertheless, the PSPT was able to detect a reduction in potency in the heat-treated vaccines, although not always in line with the MPT. This was because the assessment of potency against the ERS was also affected by the suboptimal dosing of both the used reference standard and the test vaccines.

It should also be borne in mind that wP vaccines and ERS vaccines may consist of different strains. This would mean that the antibody response against the surface antigens measured by serology could be different, which could affect parallelism, linearity and confidence interval in the serological method. Satisfactory criteria could be achieved if an in-house homologous vaccine was used as a reference standard, as it is analogous in antigen composition (FL1 in this study). This circumstance is already recognized by WHO, which allows the use of a product-specific reference vaccine with the same composition as the test vaccine in the case of serological potency tests for diphtheria, tetanus and acellular pertussis components *(12,34)*. The willingness of NCLs to participate in the PSPT project was recognized by the project sponsor as an added value for the study. Indeed, the interaction between manufacturers and NCLs is crucial to share experiences and discuss criteria that need to be met for regulatory approval. At the same time, the experience gained by the participating NCLs will facilitate collaboration with other members of the WHO National Control Laboratories Network for Biologicals *(35)* who are interested in implementing the PSPT for batch release control of wP vaccines for which consistency of production has already been demonstrated by the challenge method.

5. Conclusions

The MPT is an animal-based potency test which is variable, severe for the animals and requires qualified expertise to be successfully carried out. Efforts by researchers committed to replacing or improving the MPT to avoid intracerebral injections in mice have been underway for some time.

Establishing an alternative method to a compendial animal experiment is extremely time-consuming and costly. Challenges faced include the production of reference substances, setbacks in development and validation of methods, and regulatory requirements. Expert and multistakeholder collaboration are needed to design, coordinate and finalize a project with validation and collaborative studies. Our study is a good step in this direction. The results encourage further investments in the product-specific establishment of the serological method. Some of the manufacturers participating in the project have considered continuing the work on PSPT optimization for their own products.

Acknowledgements

The authors wish to acknowledge BioLyo Technologies for the production of the inactivated and lyophilized *B. pertussis* material used as coating antigen in the ELISA.
Special thanks to Ute Rosskopf (Lead, WHO National Control Laboratory Network for Biologicals, Access to Medicines and Health Products Division, World Health Organization, Geneva, Switzerland) for her expert advice on the project's goals and the need to produce enough coating antigen material for further studies, and to Johan van der Gun, former Bilthoven Biologicals (Bilthoven, Kingdom of the Netherlands) for expert advice and critical review of the study.

Declaration of interest

TS, CVH, VS, AS received funds from the Developing Countries Vaccine Manufacturers Network (DCVMN) as part of the grant awarded to DCVMN by the National Institute for Innovation in Manufacturing Biopharmaceutical (Project Call 3.1. Global Health – https://niimbl.force.com/s/current-projects).

Funding

This study was financially supported by the National Institute for Innovation in Manufacturing Biopharmaceuticals (NIIMBL, Project PC3.1-302).

Disclaimer

This manuscript and the views expressed herein are those of the authors, and do not necessarily represent the views, decisions or policies of WHO or any other organization.

References

1. Directive 2010/63/EU of the European Parliament and of the Council of 22 September 2010 on the protection of animals used for scientific purposes. Brussels: European Union; 2010 (https://eur-lex.europa.eu/eli/dir/2010/63/oj, accessed 28 September 2024).

2. Good manufacturing practice [internet]. Amsterdam: European Medicines Agency; 2024 (https://www.ema.europa.eu/en/human-regulatory-overview/research-development/compliance-research-development/good-manufacturing-practice, accessed 28 September 2024).

3. Hendriksen C, Arciniega JL, Bruckner L, Chevalier M, Coppens E, Descamps J, et al. The consistency approach for the quality control of vaccines. Biologicals. 2008;36(1):73–7. https://doi.org/10.1016/j.biologicals.2007.05.002

4. Dierick JF, Halder M, Jungbaeck C, Lorenz J, Préaud JM, Riou P, et al. The consistency approach for the substitution of in vivo testing for the quality control of established vaccines: practical considerations and progressive vision. Open Res Eur. 2022;2:116 https://doi.org/ 10.12688/openreseurope.15077.2

5. Kumar S, Singh MP, Bharti VK, Pandey RP. Quality control of vaccines: a journey from classical approach to 3Rs. Microbiol Curr Res. 2018;2(3):45–71.

6. Zhang X, Wu X, He Q, Wang J, Mao Q, Liang Z, et al. Research progress on substitution of in vivo method(s) by in vitro method(s) for human vaccine potency assays. Expert Rev Vaccines. 2023;22(1):270–7. https://doi.org/10.1080/14760584.2023.2178421

7. Recommendations to Assure the Quality, Safety and Efficacy of Recombinant Hepatitis B Vaccines, Annex 4, TRS No 978; 2013 (https://www.who.int/publications/m/item/recombinant-hep-b-A4-trs-978, accessed 25 October 2024)

8. Recommendations to assure the quality, safety and efficacy of poliomyelitis vaccines (inactivated), Annex 3, TRS No 99; 2015 (https://www.who.int/publications/m/item/poliomyelitis-vaccines-inactivated-annex-3-trs-no-993, accessed 25 October 2024)

9. VAC2VAC [internet]. Heidelberg: European Vaccine Initiative; 2023 (https://europevaccine.wixsite.com/vac2vac-eu, accessed 28 September 2024).

10. Assay of diphtheria vaccine, monograph 20707. In: European Pharmacopoeia, 11th edition. Strasbourg: Council of Europe; 2023.

11. Assay of tetanus vaccine, monograph 20708. In: European Pharmacopoeia, 11th edition. Strasbourg: Council of Europe; 2023.

12. Manual for quality control of diphtheria, tetanus and pertussis vaccines. Geneva: World Health Organization; 2013 (https://iris.who.int/handle/10665/80681, accessed 25 October 2024).

13. The Periscope Consortium. Periscope: road towards effective control of pertussis. Lancet Infect Dis. 2019;19(5):e179–e186. (http://dx.doi.org/10.1016/S1473-3099(18)30646-7, accessed 25 October 2024)

14. Esposito S, Stefanelli P, Fry NK, Fedele G, He Q, Paterson P, et al. Pertussis prevention: reasons for resurgence, and differences in the current acellular pertussis vaccines. Front Immunol. 2019;10:1344. (https://www.frontiersin.org/journals/immunology/articles/10.3389/fimmu.2019.01344/full accessed 25 October 2024)

15. Zerbo O, Bartlett J, Goddard K, Fireman B, Lewis E, Klein NP. Acellular pertussis vaccine effectiveness over time. Pediatrics. 2019; 144(1):e20183466. https://doi.org/10.1542/peds.2018-3466

16. Guiso N, Meade BD, Wirsing von König KH. Pertussis vaccines: the first hundred years. Vaccine. 2020;38:1271–6. https://doi.org/10.1016/j.vaccine.2019.11.022

17. Pertussis vaccines: WHO position paper – August 2015. Wkly Epidem Rec. 2015;90(35):433–58 https://iris.who.int/handle/10665/242413 (accessed 25 October 2024).

18. Testing for whole cell pertussis vaccine. In: Manual for quality control of diphtheria, tetanus and pertussis vaccines. Geneva: World Health Organization; 2013 https://iris.who.int/handle/10665/80681 (accessed 28 September 2024).

19. Canthaboo C, Xing D, Douglas A, Corbel, M. Investigation of an aerosol challenge model as alternative to the intracerebral mouse protection test for potency assay of whole cell pertussis vaccines. Biologicals. 2000;28(4):241–6.

20. Canthaboo C, Xing D, Corbel M. Development of a nitric oxide induction assay as a potential replacement for the intracerebral mouse protection test for potency assay of pertussis whole cell vaccines. Dev Biol Stand. 1999;101:95–103. https://www.sciencedirect.com/science/article/abs/pii/S104510560090263X (accessed 25 October 2024)

21. van der Ark A, van Straaten-van de Kappelle I, Akkermans A, Hendriksen C, van de Donk H. Development of pertussis serological potency test: serological assessment of response induced by whole cell vaccines as an alternative to mouse protection in an intracerebral challenge model. Biologicals. 1994;22(3):233–42. https://doi.org/10.1006/biol.1994.1034

22. van der Ark A, van Straaten-van de Kappelle I, Olander RM, Enssle K, Jadhav S, van de Donk H, et al. The pertussis serological potency test: collaborative study to evaluate replacement of the mouse protection test. Biologicals. 2000;28(2):105–18. https://doi.org/10.1006/biol.2000.0247

23. von Hunolstein C, Gomez Miguel MJ, Pezzella C, Scopetti F, Behr-Gross ME, Halder M, et al. Evaluation of the serological methods for potency testing of whole cell pertussis vaccines. Pharmeuropa Bio. 2008;2008(1):7–18. accessed 25 October 2024

24. List of vaccines [internet]. Nyon: Developing Countries Vaccine Manufacturers Network (DCVMN); 2024 (https://dcvmn.org/dcvaccines-list/, accessed 25 October 2024).

25. NIIMBL Launches Global Health Fund [internet]. Newark, DE: National Institute for Innovation in Manufacturing Biopharmaceuticals; 2019 (https://www.niimbl.org/projects/international-assessment-of-the-pspt-in-mice-to-replace-the-intracerebral-challenge-mouse-protection-test-mpt-for-whole-cell-pertussis-wp/ , accessed 25 October 2024)

26. Temperature sensitivity of vaccines. Geneva: World Health Organization; 2006 (https://iris.who.int/handle/10665/693872, accessed 28 September 2024).

27. Expanded Programme on Immunization. Heat stability of pertussis vaccine. Wkly Epidem Rec.1985;60(39):300–1.

28. PSPT consortium [internet]. Nyon: Developing Countries Vaccine Manufacturers Network (DCVMN); 2024 (https://dcvmn.org/pspt-consortium/, accessed 25 October 2024).

29. Bordetella Pertussis 18323 coating antigen 23/150 [internet]. Potter's Bar: National Institute for Biological Standards and Control; 2024 (https://nibsc.org/products/brm_product_catalogue/detail_page.aspx?catid=23/150, accessed 25 October 2024).

30. Statistical analysis of results of biological assays and tests. Strasbourg: Council of Europe; 2023 (https://www.edqm.eu/en/d/418688, accessed 28 September 2024).

31. ⟨1033⟩ Biological assay validation. Rockville, MD: United States Pharmacopeia; 2020. https://doi.org/10.31003/USPNF_M912_01_01

32. ⟨1032⟩ Design and development of biological assays. Rockville, MD: United States Pharmacopeia; 2022. https://doi.org/10.31003/USPNF_M1354_01_01

33. van den Biggelaar RHGA, Hoefnagel MHN, Vandebriel RJ, Sloots A, Hendriksen CFM, van Eden W, Rutten VPMG, et al. Overcoming scientific barriers in the transition from in vivo to non-animal batch testing of human and veterinary vaccines. Expert Rev Vaccines. 2021;20(10):1221–3. https://doi.org/10.1080/14760584.2021.1977628

34. Recommendations to assure the quality, safety and efficacy of acellular pertussis vaccines. Annex 4 of WHO Technical Report Series, No. 979, 2013. Geneva: World Health Organization; 2014 (https://www.who.int/publications/m/item/acellular-pertussis-vaccines-annex-4-trs-no-979, accessed 28 September 2024).

35. Prequalification of Medical Products. National Control Laboratories [internet]. Geneva: World Health Organization; 2023 (https://extranet.who.int/prequal/vaccines/national-control-laboratories, accessed 25 October 2024).

Appendix 1. List of participating organization

Participating organization	Type of organization	Country	Names *
Bharat Biotech	Manufacturer	India	Ganesh Dubey; Brunda Ganneru; Tarun Neha; Gopal Singh
Biological E	Manufacturer	India	Venugopal Bandameedi; Venkatarakesh Deevi
BB-NCIPD	Manufacturer	Bulgaria	Viktor Denev; Valentina Borisova; Elena Nikolova;
Central Drugs Standard Control Organization, Central Drugs Laboratory, Kasauli	National Control Laboratory	India	Sushil Sahu
Institute of Biological Products (IBP), Department of Medical Sciences	National Control Laboratory	Thailand	Apichai Supasansatorn; Wereyarmarst Jaroenkunathum
National Quality Control Laboratory of Drug and Food (NQCLDF)	National Control Laboratory	Indonesia	Anissa Wari Murti; Zulfa Noerhidayati; Ratih Pujilestari; Keti Yuliani
Panacea Biotec	Manufacturer	India	Bonny Sharma; Deepak Mahajan; Yashpal Kaushik; Maya Ramdas Rashi Saini
PT Bio Farma (Persero)	Manufacturer	Indonesia	Aini Qolbiyah Afgani; Dewi Dahlia Yuliarsih; Chairunnisaa Jabal Rahmah
Sanofi Healthcare India Private Limited	Manufacturer	India	Surender Reddy Battula; Sunil Reddy Dadhireddy
Serum Institute of India	Manufacturer	India	M. Anadkumar; Ghule Arvindkumar; Karegaonkar Ritesh;

[a] Names listed in alphabetical order.

***

ATC/DDD Classification (Temporary)

The following ATC codes and DDDs were agreed at the meeting of the WHO International Working Group for Drug Statistics Methodology in October 2024.

Comments or objections to the decisions from the meeting were forwarded to the WHO Collaborating Centre for Drug Statistics Methodology before 1 February 2025. The new ATC codes and DDDs that will have received no objections by 1 February 2025, will be considered final and included in the January 2026 version of the ATC/DDD Index.

New ATC 5th level codes:

New ATC code	ATC level name/INN
A05AA06	norucholic acid
A05AX08	linerixibat
A05BA11	resmetirom
A10AE57	insulin icodec and semaglutide
A10BD31	metformin, sitagliptin and dapagliflozin
A10BD32	glimepiride and dapagliflozin
A10BD33	pioglitazone and dapagliflozin
A12CB04	zinc orotate
A16AB28	verenafusp alfa
A16AX26	glepaglutide
A16AX27	apraglutide
A16AX28	sepiapterin
A16AX29	doxecitine and doxribtimine
B02BD18	arvenacogene sanparvovec
B02BX12	fitusiran
B06AC09	donidalorsen
B06AX06	lovotibeglogene autotemcel
B06AX07	mozafancogene autotemcel
C03EB03	torasemide and potassium-sparing agents
C09BB14	zofenopril and amlodipine
C10BA14	pitavastatin and fenofibrate
C10BX23	rosuvastatin, amlodipine and ramipril
C10BX24	rosuvastatin, amlodipine and telmisartan
D03AX17	diperoxochloric acid
D06BB13	berdazimer sodium
D11AA02	sofpironium bromide
G02CX07	elinzanetant
J01FA17	nafithromycin

New ATC code	ATC level name/INN
J07BB55	influenza and covid-19, RNA-based vaccine
J07BX07	chikungunya vaccines
L01EB12	firmonertinib
L01EC04	tovorafenib
L01EE06	tunlametinib
L01EH04	zongertinib
L01EK05	rivoceranib
L01EP03	savolitinib
L01EX29	vimseltinib
L01FF14	camrelizumab
L01FF15	envafolimab
L01FX37	linvoseltamab
L03AC03	nogapendekin alfa and inbakicept
L04AA61	nerandomilast
L04AC27	cendakimab
L04AF09	deuruxolitinib
L04AG18	sibeprenlimab
L04AG19	axatilimab
L04AL03	nipocalimab
N06BX53	piracetam and cinnarizine
N06DA06	benzgalantamine
N06DX06	blarcamesine
N06DX07	hydromethylthionine
N07XX26	pridopidine
P02CA53	albendazole and ivermectin
R03BX02	ensifentrine
R03DX12	depemokimab
S01BA17	clobetasol
V04CX13	pegulicianine
V09IX19	vidoflufolastat (^{18}F)

New ATC 4th and 3rd levels:

ATC code	New ATC level name
L01EP	Cellular-mesenchymal-epithelial transition factor (c-MET) kinase inhibitors
L04AL	Neonatal fragment crystallizable receptor (FcRn) inhibitors

ATC level alterations:

Previous ATC code	ATC level name	New ATC code
L01EX17	capmatinib	L01EP01
L01EX21	tepotinib	L01EP02
L04AA58	efgartigimod alfa	L04AL01
L04AG16	rozanolixizumab	L04AL02

ATC level name alterations:

ATC code	Previous ATC level name	New ATC level name
J07BX01	smallpox and monkeypox vaccines	smallpox and mpox vaccines

New DDDs:

ATC code	ATC level name	New DDD	Unit	Adm. route
A16AX19	fosdenopterin	63	mg	P
B01AD13	apadamtase alfa and cinaxadamtase alfa	200	U	P
C01EB22	meldonium	0.75	g	O
D11AH10	lebrikizumab	8.9	mg	P
J01DF51	aztreonam and beta-lactamase inhibitor	6	g	P
L01EB12	firmonertinib	80	mg	O
L01EJ04	momelotinib	0.2	g	O
L01EK04	fruquintinib	3.75	mg	O
L01EL05	pirtobrutinib	0.2	g	O
L02BX04	relugolix	0.12	g	O
L03AC03	nogapendekin alfa and inbakicept	12.5	mcg	intravesical
L04AE03	siponimod	2	mg	O
L04AE05	etrasimod	2	mg	O
L04AJ07	crovalimab	24.3	mg	P
N06BA14	solriamfetol	0.1	g	O

ATC/DDD Classification (Final)

The following ATC codes and DDDs were agreed at the meeting of the WHO International Working Group for Drug Statistics Methodology in March 2024.

These are considered as final and will be included in the **January 2025 version of the ATC/DDD Index.**

New ATC 5th level codes:

New ATC code	Substance name
A05AX07	seladelpar
A16AX25	nedosiran
B02BX11	marstacimab
B06AC08	sebetralstat
J05AX33	labuvirtide
L01EE05	mirdametinib
L01FX35	datopotamab deruxtecan
L01FX36	patritumab deruxtecan
L01XL12	obecabtagene autoleucel
L01XX82	darinaparsin
L01XX83	para-toluenesulfonamide
L01XX84	pelabresib
L01XX85	idroxioleic acid
L01XX86	calaspargase pegol
L01XY04	bifikafusp alfa and onfekafusp alfa
L03AX23	motixafortide
L03AX24	mavorixafor
L04AJ11	pozelimab
L04AX10	tegomil fumarate
M01AE20	pelubiprofen
N07XX25	omaveloxolone
R07AX33	deutivacaftor, tezacaftor and vanzacaftor
S01XA33	diquafosol

New ATC 4th and 3rd levels:

ATC code	New ATC level name
L01XU	Other antineoplastic agents (cont.)

ATC level name alterations:

ATC code	Previous ATC level name	New ATC Level name
L02BX53	abiraterone and prednisolone	abiraterone and corticosteroids

New DDDs:

ATC code	ATC level name	New DDD	Unit	Adm. route
C01EB24	mavacamten	5	mg	O
G02CX06	fezolinetant	45	mg	O
J05AX33	labuvirtide	45.7	mg	P
L04AF08	ritlecitinib	50	mg	O
M01AE20	pelubiprofen	90	mg	O
N02CD07	atogepant	60	mg	O

DDD alterations:

ATC code	ATC level name	Previous DDD	Unit	Adm. route	New DDD	Unit	Adm. route
J05AB16	remdesivir	0.1	g	P	0.12	g	P
L01EX08	lenvatinib	18	mg	O	20	mg	O
L01EX15	pexidartinib	0.8	g	O	0.5	g	O
L02BA03	fulvestrant	8.3	mg	P	16.7	mg	P
L04AJ02	ravulizumab	58.9	mg	P	70	mg	P

***

International Nonproprietary Names for Pharmaceutical Substances (INN)

Notice is hereby given that, in accordance with article 3 of the Procedure for the Selection of Recommended International Nonproprietary Names for Pharmaceutical Substances, ramantthe names given in the list on the following pages are under consideration by the World Health Organization as Proposed International Nonproprietary Names. The inclusion of a name in the lists of Proposed International Nonproprietary Names does not imply any recommendation of the use of the substance in medicine or pharmacy.

Lists of Proposed (1–117) and Recommended (1–78) International Nonproprietary Names can be found in *Cumulative List No. 17, 2017* (available in CD-ROM only). The statements indicating action and use are based largely on information supplied by the manufacturer. **This information is merely meant to provide an indication of the potential use of new substances at the time they are accorded Proposed International Nonproprietary Names**. WHO is not in a position either to uphold these statements or to comment on the efficacy of the action claimed. Because of their provisional nature, these descriptors will neither be revised **nor included in the Cumulative Lists of INNs**.

Dénominations communes internationales des Substances pharmaceutiques (DCI)

Il est notifié que, conformément aux dispositions de l'article 3 de la Procédure à suivre en vue du choix de Dénominations communes internationales recommandées pour les Substances pharmaceutiques les dénominations ci-dessous sont mises à l'étude par l'Organisation mondiale de la Santé en tant que dénominations communes internationales proposées. L'inclusion d'une dénomination dans les listes de DCI proposées n'implique aucune recommandation en vue de l'utilisation de la substance correspondante en médecine ou en pharmacie.

On trouvera d'autres listes de Dénominations communes internationales proposées (1–117) et recommandées (1–78) dans la *Liste récapitulative No. 17, 2017* (disponible sur CD-ROM seulement). Les mentions indiquant les propriétés et les indications des substances sont fondées sur les renseignements communiqués par le fabricant. **Elles ne visent qu'à donner une idée de l'utilisation potentielle des nouvelles substances au moment où elles sont l'objet de propositions de DCI**. L'OMS n'est pas en mesure de confirmer ces déclarations ni de faire de commentaires sur l'efficacité du mode d'action ainsi décrit. En raison de leur caractère provisoire, ces informations **ne figureront pas dans les listes récapitulatives de DCI.**

Denominaciones Comunes Internacionales para las Sustancias Farmacéuticas (DCI)

De conformidad con lo que dispone el párrafo 3 del "Procedimiento de Selección de Denominaciones Comunes Internacionales Recomendadas para las Sustancias Farmacéuticas", se comunica por el presente anuncio que las denominaciones detalladas en las páginas siguientes están sometidas a estudio por la Organización Mundial de La Salud como Denominaciones Comunes Internacionales Propuestas. La inclusión de una denominación en las listas de las DCI

Propuestas no supone recomendación alguna en favor del empleo de la sustancia respectiva en medicina o en farmacia.

Las listas de Denominaciones Comunes Internacionales Propuestas (1–117) y Recomendadas (1–78) se encuentran reunidas en *Cumulative List No. 17, 2017* (disponible sólo en CD-ROM). Las indicaciones sobre acción y uso que aparecen se basan principalmente en la información facilitada por los fabricantes. **Esta información tiene por objeto dar una idea únicamente de las posibilidades de aplicación de las nuevas sustancias a las que se asigna una DCI Propuesta**. La OMS no está facultada para respaldar esas indicaciones ni para formular comentarios sobre la eficacia de la acción que se atribuye al producto. Debido a su carácter provisional, esos datos descriptivos **no deben incluirse en las listas recapitulativas de DCI.**

Proposed International Nonproprietary Names: List 132

Comments on, or formal objections to, the proposed names may be forwarded by any person to the INN Programme of the World Health Organization within four months of the date of their publication in *WHO Drug Information*, i.e., for **List 132 of Proposed INN not later than 13 June 2025. Publication date:** 14.02.2025

Dénominations communes internationales proposées: Liste 132

Des observations ou des objections formelles à l'égard des dénominations proposées peuvent être adressées par toute personne au Programme des Dénominations communes internationales de l'Organisation mondiale de la Santé dans un délai de quatre mois à compter de la date de leur publication dans *WHO Drug Information*, c'est à dire pour la **Liste 132 de DCI Proposées le 13 juin 2025 au plus tard. Date de publication :** 14.02.2025

Denominaciones Comunes Internacionales Propuestas: Lista 132

Cualquier persona puede dirigir observaciones u objeciones respecto de las denominaciones propuestas, al Programa de Comunes Internacionales de la Organización Mundial de la Salud, en un plazo de cuatro meses, contados desde la fecha de su publicación en *WHO Drug Information*, es decir, para **la Lista 132 de DCI Propuestas el 13 de Junio de 2025 a más tardar.**
Fecha de publicación: 14.02.2025

Proposed INN (Latin, English, French, Spanish)	*Chemical name or description: Action and use: Molecular formula, Chemical Abstracts Service (CAS) registry number: Graphic formula*
DCI Proposée	*Nom chimique ou description: Propriétés et indications: Formule brute, Numéro dans le registre du CAS: Formule développée*
DCI Propuesta	*Nombre químico o descripción: Acción y uso: Fórmula molecular, Número de registro del CAS: Fórmula desarrollada*

abazistobartum # abazistobart	immunoglobulin G4-kappa, anti-[*Homo sapiens* PDCD1 (programmed cell death 1, PD-1, PD1, CD279)], chimeric and humanized monoclonal antibody;

	H-gamma4 heavy chain chimeric (1-444) [VH Musmus/Homsap (*Mus musculus* IGHV5-9*02 (85.6%) -(IGHD) -IGHJ1*01 (86.7%) A120>Q (109), T123>L (112)/*Homo sapiens* IGHV3-23*04 (84.5%) -(IGHD) -IGHJ4*01 (93.3%), CDR-IMGT [8.8.10] (26-33.51-58.97-106)) (1-117) -*Homo sapiens* IGHG4*01, *nG4m(a)* CH2 L92, 12-G4v5 h P10(CH1 (118-215), hinge 1-12 S10>P (225) (216-227), CH2 L92 (306) (228-337), CH3 (338-442), CHS (443-444)) (118-444)], (131-214')-disulfide with L-kappa light chain humanized (1'-214') [V-KAPPA (*Homo sapiens* IGKV3-11*01 (85.3%) -IGKJ1*01 (100%), CDR-IMGT [6.3.9] (27'-32'.50'-52'.89'-97')) (1'-107') -*Homo sapiens* IGKC*01 (100%) Km3 A45.1, V101 (C-KAPPA A45.1 (153'), V101 (191')) (108'-214')]; dimer (223-223'':226-226'')-bisdisulfide, produced in Chinese hamster ovary (CHO) cells, derived from the cell line CHO-K1, lacking the glutamine synthetase (GS-KO) gene, glycoform alfa *immunostimulant, antineoplastic*
abazistobart	immunoglobuline G4-kappa, anti-[*Homo sapiens* PDCD1 (protéine 1 de mort cellulaire programmée, PD-1, PD1, CD279)], anticorps monoclonal chimérique et humanisé; chaîne lourde H-gamma4 chimérique (1-444) [VH Musmus/Homsap (*Mus musculus* IGHV5-9*02 (85.6%) -(IGHD) -IGHJ1*01 (86.7%) A120>Q (109), T123>L (112)/*Homo sapiens* IGHV3-23*04 (84.5%) -(IGHD) -IGHJ4*01 (93.3%), CDR-IMGT [8.8.10] (26-33.51-58.97-106)) (1-117) -*Homo sapiens* IGHG4*01, *nG4m(a)* CH2 L92,12-G4v5 h P10(CH1 (118-215), charnière 1-12 S10>P (225) (216-227), CH2 L92 (306) (228-337), CH3 (338-442), CHS (443-444)) (118-444)], (131-214')-disulfure avec la chaîne légère L-kappa humanisée (1'-214') [V-KAPPA (*Homo sapiens* IGKV3-11*01 (85.3%) -IGKJ1*01 (100%), CDR-IMGT [6.3.9] (27'-32'.50'-52'.89'-97')) (1'-107') -*Homo sapiens* IGKC*01 (100%) Km3 A45.1, V101 (C-KAPPA A45.1 (153'), V101 (191')) (108'-214')]; dimère (223-223'':226-226'')-bisdisulfure, produit dans des cellules ovariennes de hamster chinois (CHO), dérivant de la lignée cellulaire CHO-K1, ne présentant pas le gène de la glutamine synthétase (GS-KO), glycoforme alfa *immunostimulant, antinéoplasique*
abazistobart	inmunoglobulina G4-kappa, anti-[*Homo sapiens* PDCD1 (proteína 1 de muerte celular programada, PD-1, PD1, CD279)], anticuerpo monoclonal quimérico y humanizado; cadena pesada H-gamma4 quimérica (1-444) [VH Musmus/Homsap (*Mus musculus* IGHV5-9*02 (85.6%) -(IGHD) -IGHJ1*01 (86.7%) A120>Q (109), T123>L (112)/*Homo sapiens* IGHV3-23*04 (84.5%) -(IGHD) -IGHJ4*01 (93.3%), CDR-IMGT [8.8.10] (26-33.51-58.97-106)) (1-117) -*Homo sapiens* IGHG4*01, *nG4m(a)* CH2 L92,12-G4v5 h P10(CH1 (118-215), bisagra 1-12 S10>P (225) (216-227), CH2 L92 (306) (228-337), CH3 (338-442), CHS (443-444)) (118-444)], (131-214')-disulfuro con la cadena ligera L-kappa humanizada (1'-214') [V-KAPPA (*Homo sapiens* IGKV3-11*01 (85.3%) -IGKJ1*01 (100%), CDR-IMGT [6.3.9] (27'-32'.50'-52'.89'-97')) (1'-107') -*Homo sapiens* IGKC*01 (100%) Km3 A45.1, V101 (C-KAPPA A45.1 (153'), V101 (191')) (108'-214')]; dímero (223-223'':226-226'')-bisdisulfuro, producido en las células ováricas de hámster chino (CHO), línea celular derivada de CHO-K1, en ausencia del gen glutamina sintetasa (GS-KO), forma glicosilada alfa *inmunoestimulante, antineoplásico*

3002062-67-8

acinterferonum alfa #

acinterferon alfa — human interferon α-14 (IFN-α-14, IFNA14, interferon α-H, interferon λ2-H), [N^{10}>G, N^{11}>S, R^{12}>K, M^{18}>L, R^{22}>G, R^{23}>K, P^{26}>L, M^{60}>L, M^{61}>I, N^{72}>E, T^{80}>G, E^{83}>D, Y^{86}>R, I^{87}>T, F^{90}>Y, Q^{91}>R, M^{93}>L, V^{100}>M, I^{101}>M, E^{114}>A, A^{146}>V, R^{164}>G]-variant, non-glycosylated, produced by *Escherichia coli*
immunostimulant, antiviral

acinterféron alfa — interféron α-14 humain (IFN-α-14, IFNA14, interféron α-H, interféron λ2-H), [N^{10}>G, N^{11}>S, R^{12}>K, M^{18}>L, R^{22}>G, R^{23}>K, P^{26}>L, M^{60}>L, M^{61}>I, N^{72}>E, T^{80}>G, E^{83}>D, Y^{86}>R, I^{87}>T, F^{90}>Y, Q^{91}>R, M^{93}>L, V^{100}>M, I^{101}>M, E^{114}>A, A^{146}>V, R^{164}>G]-variant, non-glycosylé, produit par *Escherichia coli*
immunostimulant, antiviral

acinterferón alfa — interferón α-14 humano (IFN-α-14, IFNA14, interferón α-H, interferón λ2-H), [N^{10}>G, N^{11}>S, R^{12}>K, M^{18}>L, R^{22}>G, R^{23}>K, P^{26}>L, M^{60}>L, M^{61}>I, N^{72}>E, T^{80}>G, E^{83}>D, Y^{86}>R, I^{87}>T, F^{90}>Y, Q^{91}>R, M^{93}>L, V^{100}>M, I^{101}>M, E^{114}>A, A^{146}>V, R^{164}>G]-variante, no glicosilado, producido por *Escherichia coli*
inmunoestimulante, antiviral

2941004-21-1

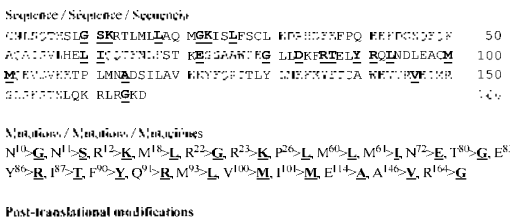

actinium (^{225}Ac) zadavotidum guraxetanum

actinium (^{225}Ac) zadavotide guraxetan

hydrogen (*N*-{(4*R*)-4-carboxylato-κ*O*-4-[4,7,10-tris(carboxylato-κ*O*-methyl)-1,4,7,10-tetraazacyclododecan-1-yl-κ^4*N*^{1},*N*^{4},*N*^{7},*N*^{10}]butanoyl}-3-iodo-D-tyrosyl-D-phenylalanyl-*N*^{6}-{8-[*N*^{2}-(L-glutamocarbonyl)-*N*^{6}-L-lysino]-8-oxooctanoyl}-D-lysine)(^{225}Ac)actinate(1−)
antineoplastic

actinium (^{225}Ac) zadavotide guraxétan

hydrogéno(*N*-{(4*R*)-4-carboxylato-κ*O*-4-[4,7,10-tris(carboxylato-κ*O*-méthyl)-1,4,7,10-tétraazacyclododécan-1-yl-κ^4*N*^{1},*N*^{4},*N*^{7},*N*^{10}]butanoyl}-3-iodo-D-tyrosyl-D-phénylalanyl-*N*^{6}-{8-[*N*^{2}-(L-glutamocarbonyl)-*N*^{6}-L-lysino]-8-oxooctanoyl}-D-lysine)(^{225}Ac)actinate(1−)
antinéoplasique

actinio (^{225}Ac) zadavotida guraxetán

hidrógeno(*N*-{(4*R*)-4-carboxilato-κ*O*-4-[4,7,10-tris(carboxilato-κ*O*-metil)-1,4,7,10-tetraazaciclododecan-1-il-κ^4*N*^{1},*N*^{4},*N*^{7},*N*^{10}]butanoil}-3-iodo-D-tirosil-D-fenilalanil-*N*^{6}-{8-[*N*^{2}-(L-glutamocarbonil)-*N*^{6}-L-lisino]-8-oxooctanoil}-D-lisina)(^{225}Ac)actinato(1−)
antineoplásico

$C_{63}H_{89}{}^{225}AcIN_{11}O_{23}$ 2901793-42-6

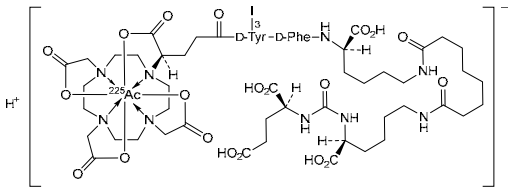

adezkibartum #

adezkibart

immunoglobulin G1-lambda2, anti-[*Homo sapiens* FLT3LG (fms related receptor tyrosine kinase 3 ligand)], *Homo sapiens* monoclonal antibody; H-gamma1 heavy chain *Homo sapiens* (1-449) [VH (*Homo sapiens* IGHV1-69*11 (89.7%) -(IGHD) -IGHJ5*01 (90.9%) L123>T (114), CDR-IMGT [8.8.12] (26-33.51-58.97-108)) (1-119) -*Homo sapiens* IGHG1*03, G1m3, nG1m1 CH1 R120, CH3 E12, M14, 6-G1v39 CH2 F1.3, E1.2, S116 (CH1 R120 (216) (120-217), hinge 1-15 (218-232), CH2 L1.3>F (236), L1.2>E (237), P116>S (333) (233-342), CH3 E12 (358), M14 (360) (343-447), CHS (448-449)) (120-449)], (222-216')-disulfide with L-lambda2 light chain *Homo sapiens* (1'-217') [V-LAMBDA (*Homo sapiens* IGLV6-57*01 (93.7%) -IGLJ2*01 (100%), CDR-IMGT [8.3.10] (26'-33'.51'-53'.92'-101')) (1'-111') -*Homo sapiens* IGLC2*01 (100%) (C-LAMBDA2) (112'-217')]; dimer (228-228":231-231")-bisdisulfide, produced in a cell line from Chinese hamster ovary (CHO) cells, derived from the cell line CHO-K1, glycoform alfa
immunosuppressant

adezkibart

immunoglobuline G1-lambda2, anti-[*Homo sapiens* FLT3LG (ligand du récepteur tyrosine kinase 3 apparenté au fms)], anticorps monoclonal *Homo sapiens*; chaîne lourde H-gamma1 *Homo sapiens* (1-449) [VH (*Homo sapiens* IGHV1-69*11 (89.7%) -(IGHD) -IGHJ5*01 (90.9%) L123>T (114), CDR-IMGT [8.8.12] (26-33.51-58.97-108)) (1-119) -*Homo sapiens* IGHG1*03, G1m3, nG1m1 CH1 R120, CH3 E12, M14, 6-G1v39 CH2 F1.3, E1.2, S116 (CH1 R120 (216) (120-217), charnière 1-15 (218-232), CH2 L1.3>F (236), L1.2>E (237), P116>S (333) (233-342), CH3 E12 (358), M14 (360) (343-447), CHS (448-449)) (120-449)], (222-216')-disulfure avec la chaîne légère L-lambda2 *Homo sapiens* (1'-217') [V-LAMBDA (*Homo sapiens* IGLV6-57*01 (93.7%) -IGLJ2*01 (100%), CDR-IMGT [8.3.10] (26'-33'.51'-53'.92'-101')) (1'-111') -*Homo sapiens* IGLC2*01 (100%) (C-LAMBDA2) (112'-217')]; dimère (228-228":231-231")-bisdisulfure, produit dans une lignée cellulaire des cellules ovariennes de hamster chinois (CHO), dérivant de la lignée cellulaire CHO-K1, glycoforme alfa
immunosuppresseur

adezkibart

inmunoglobulina G1-lambda2, anti-[*Homo sapiens* FLT3LG (ligando del receptor tirosina kinasa 3 acoplado al fms)], anticuerpo monoclonal *Homo sapiens*; cadena pesada H-gamma1 *Homo sapiens* (1-449) [VH (*Homo sapiens* IGHV1-69*11 (89.7%) -(IGHD) -IGHJ5*01 (90.9%) L123>T (114), CDR-IMGT [8.8.12] (26-33.51-58.97-108)) (1-119) -*Homo sapiens* IGHG1*03, G1m3, nG1m1 CH1 R120, CH3 E12, M14, 6-G1v39 CH2 F1.3, E1.2, S116 (CH1 R120 (216) (120-217), bisagra 1-15 (218-232), CH2 L1.3>F (236), L1.2>E (237), P116>S (333) (233-342), CH3 E12 (358), M14 (360) (343-447), CHS (448-449)) (120-449)], (222-216')-disulfuro con la cadena ligera L-lambda2 *Homo sapiens* (1'-217') [V-LAMBDA (*Homo sapiens* IGLV6-57*01 (93.7%) -IGLJ2*01 (100%), CDR-IMGT [8.3.10] (26'-33'.51'-53'.92'-101')) (1'-111') -*Homo sapiens* IGLC2*01 (100%) (C-LAMBDA2) (112'-217')]; dímero (228-228":231-231")-bisdisulfuro, producido en una línea celular de las células ováricas de hámster chino (CHO), línea celular derivada de CHO-K1, forma glicosilada alfa
inmunosupresor

2921564-55-6

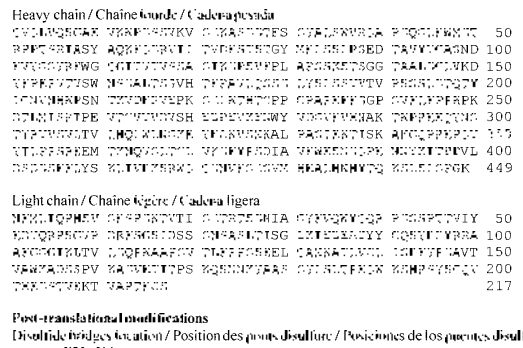

Heavy chain / Chaîne lourde / Cadena pesada

```
QVQLVQSGAE VKKPGASVKV SCKASGYTFS SYALSWVRQA PGQGLEWMGI  50
RPFGRTASY AQKFQGRVTI TVDKSTSTGY MELSSLRSED TAVYYCARGN 100
YYGSSYRFWG QGTLVTVSSA STKGPSVFPL APSSKSTSGG TAALGCLVKD 150
YFPEPVTVSW NSGALTSGVH TFPAVLQSSG LYSLSSVVTV PSSSLGTQTY 200
ICNVNHKPSN TKVDKRVEPK SCDKTHTCPP CPAPELFGGP SVFLFPPKPK 250
DTLMISRTPE VTCVVVDVSH EDPEVKFNWY VDGVEVHNAK TKPREEQYNS 300
TYRVVSVLTV LHQDWLNGKE YKCKVSNKAL PAPIEKTISK AKGQPREPQV 350
YTLPPSREEM TKNQVSLTCL VKGFYPSDIA VEWESNGQPE NNYKTTPPVL 400
DSDGSFFLYS KLTVDKSRWQ QGNVFSCSVM HEALHNHYTQ KSLSLSPGK  449

Light chain / Chaîne légère / Cadena ligera
NFMLTQPHSV SESPGKTVTI SCTRSSGNIA SYYVQWYQQR PGSSPTTVIY  50
EDNQRPSGVP DRFSGSIDSS SNSASLTISG LKTEDEADYY CQSYDSSYRA 100
AFGGGTKLTV LGQPKAAPSV TLFPPSSEEL QANKATLVCL ISDFYPGAVT 150
VAWKADSSPV KAGVETTTPS KQSNNKYAAS SYLSLTPEQW KSHRSYSCQV 200
THEGSTVEKT VAPTECS                                     217
```

Post-translational modifications

Disulfide bridges location / Position des ponts disulfure / Posiciones de los puentes disulfuro

```
Intra-H (C23-C104) 22-96   146-202   263-323   369-127
                   22"-96" 146"-202" 263"-323" 369"-127"
Intra-L (C23-C104) 22'-91'  139'-198'
                   22'"-91'" 139'"-198'"
Inter-H-L (h 5-CL 126) 222-216' 222"-216'"
Inter-H-H (h 11, h 14)  228-228" 231-231"
```

N-terminal glutaminyl cyclization / Cyclisation du glutaminyle N-terminal / Ciclación del glutaminilo N-terminal

```
Q > pyroglutamyl (pE, 5-oxoprolyl) / pyroglutamyle (pE, 5-oxoprolyl) / piroglutamilo (pE, 5-oxoprolilo)
H VH Q1: 1, 1"
```

N-glycosylation sites / Sites de N-glycosylation / Posiciones de N-glicosilación

```
H CH2 N84.4: 299, 299"
```

Fucosylated complex bi-antennary CHO-type glycans / glycanes de type CHO bi-antennaires complexes fucosylés / glicanos de tipo CHO biantenarios complejos fucosilados

C-terminal lysine clipping / Coupure de la lysine C-terminale / Recorte de lisina C-terminal

```
H CHS K2: 449, 449"
```

adimanebartum #

adimanebart — immunoglobulin G1-lambda2, anti-[*Homo sapiens* MUSK (muscle associated receptor tyrosine kinase)], humanized monoclonal antibody, agonist;
H-gamma1 heavy chain humanized (1-450) [VH (*Homo sapiens* IGHV3-23*01 (93.9%) -(IGHD) -IGHJ1*01 (100%), CDR-IMGT [8.8.14] (26-33.51-58.97-110)) (1-121) -*Homo sapiens* IGHG1*01, G1m17,1 CH1 K120, CH3 D12, L14, 6-G1v14 CH2 A1.3, A1.2 (CH1 K120 (218) (122-219), hinge 1-15 (220-234), CH2 L1.3>A (238), L1.2>A (239) (235-344), CH3 D12 (360), L14 (362) (345-449), CHS K2>del (450)) (122-450)], (224-217')-disulfide with L-lambda2 light chain humanized (1'-218') [V-LAMBDA (*Homo sapiens* IGLV8-61*01 (89.7%) -IGLJ2*01 (100%), CDR-IMGT [9.3.12] (26'-34'.52'-54'.91'-102')) (1'-112') -*Homo sapiens* IGLC2*01 (100%) (C-LAMBDA2) (113'-218')]; dimer (230-230":233-233")-bisdisulfide, produced in Chinese hamster ovary (CHO) cells, derived from the cell line CHO-K1, lacking the glutamine synthetase (GS-KO) gene, glycoform alfa
muscle associated receptor tyrosine kinase agonist, neuromuscular diseases

adimanebart — immunoglobuline G1-lambda2, anti-[*Homo sapiens* MUSK (récepteur tyrosine kinase associée aux muscles)], anticorps monoclonal humanisé, agoniste;
chaîne lourde H-gamma1 humanisée (1-450) [VH (*Homo sapiens* IGHV3-23*01 (93.9%) -(IGHD) -IGHJ1*01 (100%), CDR-IMGT [8.8.14] (26-33.51-58.97-110)) (1-121) -*Homo sapiens* IGHG1*01, G1m17,1 CH1 K120, CH3 D12, L14, 6-G1v14 CH2 A1.3, A1.2 (CH1 K120 (218) (122-219), charnière 1-15 (220-234), CH2 L1.3>A (238), L1.2>A (239) (235-344), CH3 D12 (360), L14 (362) (345-449), CHS K2>del (450)) (122-450)], (224-217')-disulfure avec la chaîne légère L-lambda2 humanisée (1'-218') [V-LAMBDA (*Homo sapiens* IGLV8-61*01 (89.7%) -IGLJ2*01 (100%), CDR-IMGT [9.3.12] (26'-34'.52'-54'.91'-102')) (1'-112') -*Homo sapiens* IGLC2*01 (100%) (C-LAMBDA2) (113'-218')]; dimère (230-230":233-233")-bisdisulfure, produit dans des cellules ovariennes de hamster chinois (CHO), dérivant de la lignée cellulaire CHO-K1, ne présentant pas le gène de la glutamine synthétase (GS-KO), glycoforme alfa
agoniste du récepteur de la tyrosine kinase associée aux muscles, maladies neuromusculaires

adimanebart — inmunoglobulina G1-lambda2, anti-[*Homo sapiens* MUSK (receptor tirosina kinasa asociada a los músculos)], anticuerpo monoclonal humanizado, agonista;
cadena pesada H-gamma1 humanizada (1-450) [VH (*Homo sapiens* IGHV3-23*01 (93.9%) -(IGHD) -IGHJ1*01 (100%), CDR-IMGT [8.8.14] (26-33.51-58.97-110)) (1-121) -*Homo sapiens* IGHG1*01, G1m17,1 CH1 K120, CH3 D12, L14, 6-G1v14 CH2 A1.3, A1.2 (CH1 K120 (218) (122-219), bisagra 1-15 (220-234), CH2 L1.3>A (238), L1.2>A (239) (235-344), CH3 D12 (360), L14 (362) (345-449), CHS K2>del (450)) (122-450)], (224-217')-disulfuro con la cadena ligera L-lambda2 humanizada (1'-218') [V-LAMBDA (*Homo sapiens* IGLV8-61*01 (89.7%) -IGLJ2*01 (100%), CDR-IMGT [9.3.12] (26'-34'.52'-54'.91'-102')) (1'-112') -*Homo sapiens* IGLC2*01 (100%) (C-LAMBDA2) (113'-218')]; dímero (230-230":233-233")-bisdisulfuro, producido en las células ováricas de hámster chino (CHO), línea celular derivada de CHO-K1, en ausencia del gen glutamina sintetasa (GS-KO), forma glicosilada alfa
agonista del receptor de la tirosina kinasa asociada a los músculos, enfermedades neuromusculares

3011838-77-7

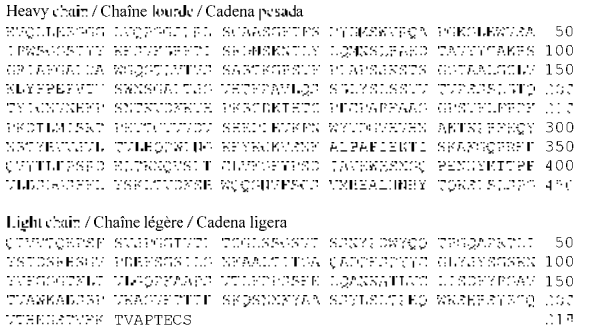

agazisiranum

agazisiran

O-[(2*R*,3*S*)-2-(hydroxymethyl)oxolan-3-yl] hydrogen *all-P-ambo*-3'-*O*-(2-{[(1-{17-[(2-acetamido-2-deoxy-β-D-galactopyranosyl)oxy]-3,6,9,12,15-pentaoxaheptadecan-1-yl}-1*H*-1,2,3-triazol-4-yl)methyl]amino}-2-oxoethyl)-2'-*O*-(2-{bis[(1-{17-[(2-acetamido-2-deoxy-β-D-galactopyranosyl)oxy]-3,6,9,12,15-pentaoxaheptadecan-1-yl}-1*H*-1,2,3-triazol-4-yl)methyl]amino}-2-oxoethyl)-*P*-thiouridylyl-(5'→5')-2'-*O*-methyl-*P*-thioguanylyl-(3'→5')-2'-*O*-methylguanylyl-(3'→5')-2'-*O*-methyladenylyl-(3'→5')-2'-*O*-methyladenylyl-(3'→5')-2'-*O*-methylguanylyl-(3'→5')-2'-*O*-methylguanylyl-(3'→5')-2'-*O*-methyladenylyl-(3'→5')-2'-deoxy-2'-fluorouridylyl-(3'→5')-2'-*O*-methyluridylyl-(3'→5')-2'-deoxy-2'-fluoroadenylyl-(3'→5')-2'-deoxy-2'-fluorouridylyl-(3'→5')-2'-deoxy-2'-fluorocytidylyl-(3'→5')-2'-deoxy-2'-fluorouridylyl-(3'→5')-2'-*O*-methylguanylyl-(3'→5')-2'-*O*-methylguanylyl-(3'→5')-2'-*O*-methyladenylyl-(3'→5')-2'-*O*-methyluridylyl-(3'→5')-2'-*O*-methylguanylyl-(3'→5')-2'-*O*-methyluridylyl-(3'→5')-2'-*O*-methylcytidylyl-(3'→5')-2'-*O*-methyl-*P*-thiouridylyl-(3'→5')-2'-*O*-methyl-*P*-thio-3'-adenylate duplex with *all-P-ambo*-2'-*O*-methyl-*P*-thiocytidylyl-(5'→3')-2'-*O*-methyl-*P*-thiocytidylyl-(5'→3')-2'-deoxy-2'-fluorouridylyl-(5'→3')-2'-*O*-methyluridylyl-(5'→3')-2'-deoxy-2'-fluorocytidylyl-(5'→3')-2'-*O*-methylcytidylyl-(5'→3')-2'-deoxy-2'-fluorouridylyl-(5'→3')-2'-*O*-methyladenylyl-(5'→3')-2'-deoxy-2'-fluoroadenylyl-(5'→3')-2'-*O*-methyluridylyl-(5'→3')-2'-deoxy-2'-fluoroadenylyl-(5'→3')-2'-*O*-methylguanylyl-(5'→3')-2'-deoxy-2'-fluoroadenylyl-(5'→3')-2'-*O*-methylcytidylyl-(5'→3')-2'-deoxy-2'-fluorocytidylyl-(5'→3')-2'-*O*-methyluridylyl-(5'→3')-2'-deoxy-2'-fluoroadenylyl-(5'→3')-2'-*O*-methylcytidylyl-(5'→3')-2'-deoxy-2'-fluoroadenylyl-(5'→3')-2'-*O*-methyl-*P*-thioguanylyl-(5'→3')-2'-deoxy-2'-fluoro-*P*-thioadenylyl-(5'→3')-2'-*O*-methyluridine

complement factor B synthesis reducer

agazisiran

tout-P-ambo-3'-*O*-(2-{[(1-{17-[(2-acétamido-2-désoxy-β-D-galactopyranosyl)oxy]-3,6,9,12,15-pentaoxaheptadécan-1-yl}-1H-1,2,3-triazol-4-yl)méthyl]amino}-2-oxoéthyl)-2'-*O*-(2-{bis[(1-{17-[(2-acétamido-2-désoxy-β-D-galactopyranosyl)oxy]-3,6,9,12,15-pentaoxaheptadécan-1-yl}-1H-1,2,3-triazol-4-yl)méthyl]amino}-2-oxoéthyl)-*P*-thiouridylyl-(5'→5')-2'-*O*-méthyl-*P*-thioguanylyl-(3'→5')-2'-*O*-méthylguanylyl-(3'→5')-2'-*O*-méthyladénylyl-(3'→5')-2'-*O*-méthyladénylyl-(3'→5')-2'-*O*-méthylguanylyl-(3'→5')-2'-*O*-méthylguanylyl-(3'→5')-2'-*O*-méthyladénylyl-(3'→5')-2'-désoxy-2'-fluorouridylyl-(3'→5')-2'-*O*-méthyluridylyl-(3'→5')-2'-désoxy-2'-fluoroadénylyl-(3'→5')-2'-désoxy-2'-fluorouridylyl-(3'→5')-2'-désoxy-2'-fluorocytidylyl-(3'→5')-2'-désoxy-2'-fluorouridylyl-(3'→5')-2'-*O*-méthylguanylyl-(3'→5')-2'-*O*-méthylguanylyl-(3'→5')-2'-*O*-méthyladénylyl-(3'→5')-2'-*O*-méthyluridylyl-(3'→5')-2'-*O*-méthylguanylyl-(3'→5')-2'-*O*-méthyluridylyl-(3'→5')-2'-*O*-méthylcytidylyl-(3'→5')-2'-*O*-méthyl-*P*-thiouridylyl-(3'→5')-hydrogéno-2'-*O*-méthyl-*P*-thio-3'-adénylate de *O*-[(2*R*,3*S*)-2-(hydroxyméthyl)oxolan-3-yle]
duplex avec *tout-P-ambo*-2'-*O*-méthyl-*P*-thiocytidylyl-(5'→3')-2'-*O*-méthyl-*P*-thiocytidylyl-(5'→3')-2'-désoxy-2'-fluorouridylyl-(5'→3')-2'-*O*-méthyluridylyl-(5'→3')-2'-désoxy-2'-fluorocytidylyl-(5'→3')-2'-*O*-méthylcytidylyl-(5'→3')-2'-désoxy-2'-fluorouridylyl-(5'→3')-2'-*O*-méthyladénylyl-(5'→3')-2'-désoxy-2'-fluoroadénylyl-(5'→3')-2'-*O*-méthyluridylyl-(5'→3')-2'-désoxy-2'-fluoroadénylyl-(5'→3')-2'-*O*-méthylguanylyl-(5'→3')-2'-désoxy-2'-fluoroadénylyl-(5'→3')-2'-*O*-méthylcytidylyl-(5'→3')-2'-désoxy-2'-fluorocytidylyl-(5'→3')-2'-*O*-méthyluridylyl-(5'→3')-2'-désoxy-2'-fluoroadénylyl-(5'→3')-2'-*O*-méthylcytidylyl-(5'→3')-2'-désoxy-2'-fluoroadénylyl-(5'→3')-2'-*O*-méthyl-*P*-thioguanylyl-(5'→3')-2'-désoxy-2'-fluoro-*P*-thioadénylyl-(5'→3')-2'-*O*-méthyluridine
réducteur de synthèse du facteur B du complément

agazisirán

todo-P-ambo-3'-*O*-(2-{[(1-{17-[(2-acetamido-2-desoxi-β-D-galactopiranosil)oxi]-3,6,9,12,15-pentaoxaheptadecan-1-il}-1H-1,2,3-triazol-4-il)metil]amino}-2-oxoetil)-2'-*O*-(2-{bis[(1-{17-[(2-acetamido-2-desoxi-β-D-galactopiranosil)oxi]-3,6,9,12,15-pentaoxaheptadecan-1-il}-1H-1,2,3-triazol-4-il)metil]amino}-2-oxoetil)-*P*-tiouridilil-(5'→5')-2'-*O*-metil-*P*-tioguanilil-(3'→5')-2'-*O*-metilguanilil-(3'→5')-2'-*O*-metiladenilil-(3'→5')-2'-*O*-metiladenilil-(3'→5')-2'-*O*-metilguanilil-(3'→5')-2'-*O*-metilguanilil-(3'→5')-2'-*O*-metiladenilil-(3'→5')-2'-desoxi-2'-fluorouridilil-(3'→5')-2'-*O*-metiluridilil-(3'→5')-2'-desoxi-2'-fluoroadenilil-(3'→5')-2'-desoxi-2'-fluorouridilil-(3'→5')-2'-desoxi-2'-fluorocitidilil-(3'→5')-2'-desoxi-2'-fluorouridilil-(3'→5')-2'-*O*-metilguanilil-(3'→5')-2'-*O*-metilguanilil-(3'→5')-2'-*O*-metiladenilil-(3'→5')-2'-*O*-metiluridilil-(3'→5')-2'-*O*-metilguanilil-(3'→5')-2'-*O*-metiluridilil-(3'→5')-2'-*O*-metilcitidilil-(3'→5')-2'-*O*-metil-*P*-tiouridilil-(3'→5')-hidrógeno-2'-*O*-metil-*P*-tio-3'-adenilato de *O*-[(2*R*,3*S*)-2-(hidroximetil)oxolan-3-ilo]
dúplex con *todo-P-ambo*-2'-*O*-metil-*P*-tiocitidilil-(5'→3')-2'-*O*-metil-*P*-tiocitidilil-(5'→3')-2'-desoxi-2'-fluorouridilil-(5'→3')-2'-*O*-metiluridilil-(5'→3')-2'-desoxi-2'-fluorocitidilil-(5'→3')-2'-*O*-metilcitidilil-(5'→3')-2'-desoxi-2'-fluorouridilil-(5'→3')-2'-*O*-metiladenilil-(5'→3')-2'-desoxi-2'-fluoroadenilil-(5'→3')-2'-*O*-metiluridilil-(5'→3')-2'-desoxi-2'-fluoroadenilil-(5'→3')-2'-*O*-metilguanilil-(5'→3')-2'-desoxi-2'-fluoroadenilil-(5'→3')-2'-*O*-metilcitidilil-(5'→3')-2'-desoxi-2'-fluorocitidilil-(5'→3')-2'-*O*-metiluridilil-(5'→3')-2'-desoxi-2'-fluoroadenilil-(5'→3')-2'-*O*-metilcitidilil-(5'→3')-2'-desoxi-2'-fluoroadenilil-(5'→3')-2'-*O*-metil-*P*-tioguanilil-(5'→3')-2'-desoxi-2'-fluoro-*P*-tioadenilil-(5'→3')-2'-*O*-metiluridina
reductor de la síntesis del factor B del complemento

$C_{534}H_{706}F_{15}N_{179}O_{329}P_{44}S_8$ 2985646-78-2

(3'-5')**U**=*G*=*G*-*A*-*A*-*G*-*G*-*A*-U-*U*-A-U-C-U-*G*-*G*-*A*-*U*-*G*-*U*-*C*-*U*=*A*=R_1

(5'-3')*C*=*C*=U-*U*-C-*C*-U-*A*-A-*U*-A-*G*-A-*C*-C-*U*-A-*C*-A-*G*=A=*U*

N : A,C,G,U
N : 2'-*O*-methyl-N / 2'-*O*-méthyl-N / 2'-*O*-metil-N
N : 2'-deoxy-2'-fluoro-N / 2'-désoxy-2'-fluoro-N / 2'-desoxi-2'-fluoro-N
– : –PO(OH)– =: –PO(SH)–

U= :

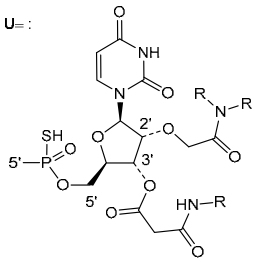

R :

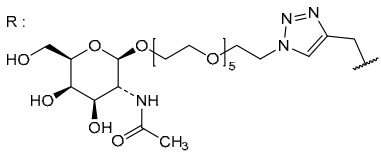

R1 :

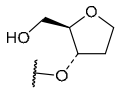

alixorextonum

alixorexton *N*-[7,10-*cis*-(4*S*,4a*R*)-17-oxo-1,2,3,4,4a,5,7,8,9,10,16,17-dodecahydro-7,10-ethanopyrido[1,2-*d*][1,7,4]benzodioxaazacyclotridecin-4-yl]methanesulfonamide
orexin-2 receptor agonist

alixorexton *N*-[7,10-*cis*-(4*S*,4a*R*)-17-oxo-1,2,3,4,4a,5,7,8,9,10,16,17-dodécahydro-7,10-éthanopyrido[1,2-*d*][1,7,4]benzodioxaazacyclotridécin-4-yl]méthanesulfonamide
agoniste du récepteur de l'orexine 2

alixorextón *N*-[7,10-*cis*-(4*S*,4a*R*)-17-oxo-1,2,3,4,4a,5,7,8,9,10,16,17-dodecahidro-7,10-etanopirido[1,2-*d*][1,7,4]benzodioxaazaciclotridecin-4-il]metanosulfonamida
agonista del receptor de la orexina 2

$C_{21}H_{30}N_2O_5S$ 2648347-56-0

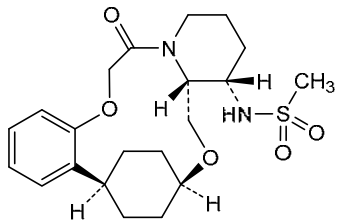

alnodesertibum

alnodesertib (*S*)-({2-(2-aminopyridin-4-yl)-6-[(3*R*)-3-methylmorpholin-4-yl]pyrimidin-4-yl}imino)(cyclopropyl)(methyl)-λ^6-sulfanone
serine/threonine kinase inhibitor, antineoplastic

alnodésertib (*S*)-({2-(2-aminopyridin-4-yl)-6-[(3*R*)-3-méthylmorpholin-4-yl]pyrimidin-4-yl}imino)(cyclopropyl)(méthyl)-λ^6-sulfanone
inhibiteur de sérine/thréonine kinases, antinéoplasique

alnodesertib

(*S*)-({2-(2-aminopiridin-4-il)-6-[(3*R*)-3-metilmorfolin-4-il]pirimidin-4-il}imino)(ciclopropil)(metil)-λ^6-sulfanona
inhibidor de la serina/treonina kinasa, antineoplásico

$C_{18}H_{24}N_6O_2S$ 2267316-76-5

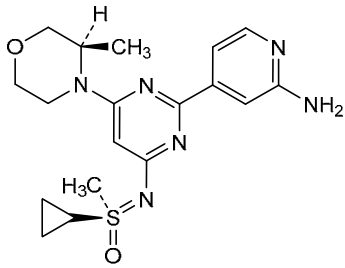

amdokitugum #

amdokitug

immunoglobulin G1-kappa, anti-[*Homo sapiens* IL17A (Interleukin 17A, IL-17)], monoclonal antibody;
H-gamma1 heavy chain (1-445) [VH (*Homo sapiens* IGHV3-23*04 (89.8%) -(IGHD) -IGHJ5*01 (100%), CDR-IMGT [8.7.9] (26-33.51-57.96-104)) (1-115) -*Homo sapiens* IGHG1*03v (100%) G1m3>G1m17, nG1m1 CH1 K120, CH3 E12, M14 (CH1 R120>K(212) (116-213), hinge 1-15 (214-228), CH2 (229-338), CH3 E12 (354), M14 (356) (339-443), CHS (444-445)) (116-445)], (218-214')-disulfide with L-kappa light chain (1'-214') [V-KAPPA Musmus/Homsap (*Mus musculus* IGKV13-85*01 (87.4%) -IGKJ4*01 (100%)/*Homo sapiens* IGKV1-NL1*01 (87.4%) -IGKJ2*02 (90.9%) Q120>S (100'), CDR-IMGT [6.3.9] (27'-32'.50'-52'.89'-97')) (1'-107') -*Homo sapiens* IGKC*01 (100%) Km3 A45.1, V101 (C-KAPPA A45.1 (153'), V101 (191')) (108'-214')]; dimer (224-224'': 227-227'')-bisdisulfide, produced in Chinese hamster ovary (CHO) cells, derived from the cell line CHO-K1, lacking the glutamine synthetase (GS-KO) gene, glycoform alfa
immunosuppressant, anti-inflammatory

amdokitug

immunoglobuline G1-kappa, anti-[*Homo sapiens* IL17A (interleukine 17A, IL-17)], anticorps monoclonal;
chaîne lourde H-gamma1 (1-445) [VH (*Homo sapiens* IGHV3-23*04 (89.8%) -(IGHD) -IGHJ5*01 (100%), CDR-IMGT [8.7.9] (26-33.51-57.96-104)) (1-115) -*Homo sapiens* IGHG1*03v (100%) G1m3>G1m17, nG1m1 CH1 K120, CH3 E12, M14 (CH1 R120>K (212) (116-213), charnière 1-15 (214-228), CH2 (229-338), CH3 E12 (354), M14 (356) (339-443), CHS (444-445)) (116-445)], (218-214')-disulfure avec la chaîne légère L-kappa (1'-214') [V-KAPPA Musmus/Homsap (*Mus musculus* IGKV13-85*01 (87.4%) -IGKJ4*01 (100%)/*Homo sapiens* IGKV1-NL1*01 (87.4%) -IGKJ2*02 (90.9%) Q120>S (100'), CDR-IMGT [6.3.9] (27'-32'.50'-52'.89'-97')) (1'-107') -*Homo sapiens* IGKC*01 (100%) Km3 A45.1, V101 (C-KAPPA A45.1 (153'), V101 (191')) (108'-214')]; dimère (224-224'': 227-227'')-bisdisulfure, produit dans des cellules ovariennes de hamster chinois (CHO), dérivant de la lignée cellulaire CHO-K1, ne présentant pas le gène de la glutamine synthétase (GS-KO), glycoforme alfa
immunosuppresseur, anti-inflammatoire

amdokitug

inmunoglobulina G1-kappa, anti-[*Homo sapiens* IL17A (interleukina 17A, IL-17)], anticuerpo monoclonal;
cadena pesada H-gamma1 (1-445) [VH (*Homo sapiens* IGHV3-23*04 (89.8%) -(IGHD) -IGHJ5*01 (100%), CDR-IMGT [8.7.9] (26-33.51-57.96-104)) (1-115) -*Homo sapiens* IGHG1*03v (100%) G1m3>G1m17, nG1m1 CH1 K120, CH3 E12, M14 (CH1 R120>K (212) (116-213), bisagra 1-15 (214-228), CH2 (229-338), CH3 E12 (354), M14 (356) (339-443), CHS (444-445)) (116-445)], (218-214')-disulfuro con la cadena ligera L-kappa (1'-214') [V-KAPPA Musmus/Homsap (*Mus musculus* IGKV13-85*01 (87.4%) -IGKJ4*01 (100%)/*Homo sapiens* IGKV1-NL1*01 (87.4%) -IGKJ2*02 (90.9%) Q120>S (100'), CDR-IMGT [6.3.9] (27'-32'.50'-52'.89'-97')) (1'-107') -*Homo sapiens* IGKC*01 (100%) Km3 A45.1, V101 (C-KAPPA A45.1 (153'), V101 (191')) (108'-214')]; dímero (224-224": 227-227")-bisdisulfuro, producido en las células ováricas de hámster chino (CHO), línea celular derivada de CHO-K1, en ausencia del gen glutamina sintetasa (GS-KO), forma glicosilada alfa
inmunosupresor, antiinflamatorio

3012586-05-6

Heavy chain / Chaîne lourde / Cadena pesada

```
EVQLVESGGG LVQPGRSLRL SCAASGFTFS SYDMSWVRQA PGKGLEWVAE   50
ISSGGSYTYY PDSVKGRFTI SRDNSKNTLY LQMNSLRAED TAVYYCARHE  100
YYGTWFAYWG QGTLVTVSSA STKGPSVFPL APSSKSTSGG TAALGCLVKD  150
YFPEPVTVSW NSGALTSGVH TFPAVLQSSG LYSLSSVVTV PSSSLGTQTY  200
ICNVNHKPSN TKVDKRVEPK SCDKTHTCPP CPAPELLGGP SVFLFPPKPK  250
DTLMISRTPE VTCVVVDVSH EDPEVKFNWY VDGVEVHNAK TKPREEQYNS  300
TYRVVSVLTV LHQDWLNGKE YKCKVSNKAL PAPIEKTISK AKGQPREPQV  350
YTLPPSRDEL TKNQVSLTCL VKGFYPSDIA VEWESNGQPE NNYKTTPPVL  400
DSDGSFFLYS KLTVDKSRWQ QGNVFSCSVM HEALHNHYTQ KSLSLSPGK   445
```

Light chain / Chaîne légère / Cadena ligera

```
DIQMTQSPSS LSASVGDRVT ITCRASQDIN NYLAWYQQKP GKAPKLLIYY   50
ATSLETGVPS RFSGSGSGTD YTLTISSLQP EDFATYYCQQ YWSTPFTFGQ  100
GTKLEIKRTV AAPSVFIFPP SDEQLKSGTA SVVCLLNNFY PREAKVQWKV  150
DNALQSGNSQ ESVTEQDSKD STYSLSSTLT LSKADYEKHK VYACEVTHQG  200
LSSPVTKSFN RGEC                                         214
```

Post-translational modifications
Disulfide bridges location / Position des ponts disulfure / Posiciones de los puentes disulfuro
Intra-H (C23-C104) 22-95 142-198 259-319 365-423
22"-95" 142"-198" 259"-319" 365"-423"
Intra-L (C23-C104) 23'-88' 134'-194'
23'"-88"' 134'"-194'"
Inter-H-L (h 5-CL 126) 218-214' 218"-214'"
Inter-H-H (h 11, h 14) 224-224" 227-227"

N-glycosylation sites / Sites de N-glycosylation / Posiciones de N-glicosilación
H CH2 N84.4; 295, 295"
Fucosylated complex bi-antennary CHO-type glycans / glycanes de type CHO bi-antennaires complexes fucosylés / glicanos de tipo CHO biantenarios complejos fucosilados

C-terminal lysine clipping / Coupure de la lysine C-terminale / Recorte de lisina C-terminal
H CHS K2: 445, 445"

amezalpatum

amezalpat

[8[4]-*tert*-butyl-1[4]-ethoxy-6[4]-ethyl-6[5]-oxo-6[4],6[5]-dihydro-6(3,1)-[1,2,4]triazola-1,8(1),2(1,3)-tribenzenaoctaphan-1[3]-yl]acetic acid
peroxisome proliferator-activated receptor alpha (PPARα) antagonist, antineoplastic

amézalpat

acide [8[4]-*tert*-butyl-1[4]-éthoxy-6[4]-éthyl-6[5]-oxo-6[4],6[5]-dihydro-6(3,1)-[1,2,4]triazola-1,8(1),2(1,3)-tribenzénaoctaphan-13-yl]acétique
antagoniste du récepteur alpha activé par les proliférateurs de peroxysomes (PPARα), antinéoplasique

amezalpat

ácido [8^4-*terc*-butil-6^4-etil-1^4-etoxi-6^5-oxo-6^4,6^5-dihidro-6(3,1)-[1,2,4]triazola-1,8(1),2(1,3)-tribencenaoctafan-1^3-il]acético
antagonista del receptor alfa activado por factores de proliferación de peroxisomas (PPARα), antineoplásico

$C_{34}H_{41}N_3O_4$ 1616372-41-8

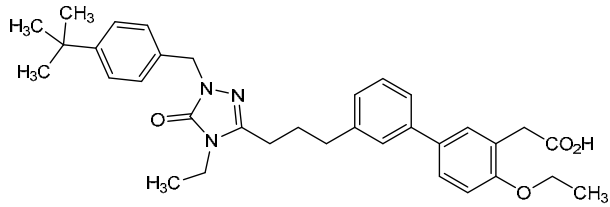

amrecibartum #

amrecibart

immunoglobulin G4-kappa, anti-[*Homo sapiens* F11 (coagulation factor 11, coagulation factor XI, FXI, plasma thromboplastin antecedent, PTA)], *Homo sapiens* monoclonal antibody;
H-gamma4 heavy chain *Homo sapiens* (1-450) [VH (*Homo sapiens* IGHV3-23*03 (91.8%) -(IGHD) -IGHJ3*02 (100%), CDR-IMGT [8.8.16] (26-33.51-58.97-112)) (1-123) -*Homo sapiens* IGHG4*01, *nG4m(a)* CH2 L92, 12-G4v5 h P10(CH1 (124-221), hinge 1-12 S10>P (231) (222-233), CH2 L92 (312) (234-343), CH3 (344-448), CHS (449-450)) (124-450)], (137-215')-disulfide with L-kappa light chain *Homo sapiens* (1'-215') [V-KAPPA (*Homo sapiens* IGKV1-39*01 (100%) -IGKJ5*01 (100%), CDR-IMGT [6.3.10] (27'-32'.50'-52'.89'-98')) (1'-108') -*Homo sapiens* IGKC*01 (100%) Km3 A45.1, V101 (C-KAPPA A45.1 (154'), V101 (192')) (109'-215')]; dimer (229-229'':232-232'')-bisdisulfide, produced in Chinese hamster ovary (CHO) cells, cell line CHO-K1, glycoform alfa
anticoagulant

amrécibart

immunoglobuline G4-kappa, anti-[*Homo sapiens* F11 (facteur de coagulation 11, facteur de coagulation XI, FXI, antécédent de la thromboplastine plasmatique, PTA)], anticorps monoclonal *Homo sapiens*;
chaîne lourde H-gamma4 *Homo sapiens* (1-450) [VH (*Homo sapiens* IGHV3-23*03 (91.8%) -(IGHD) -IGHJ3*02 (100%), CDR-IMGT [8.8.16] (26-33.51-58.97-112)) (1-123) -*Homo sapiens* IGHG4*01, *nG4m(a)* CH2 L92, 12-G4v5 h P10(CH1 (124-221), charnière 1-12 S10>P (231) (222-233), CH2 L92 (312) (234-343), CH3 (344-448), CHS (449-450)) (124-450)], (137-215')-disulfure avec la chaîne légère L-kappa *Homo sapiens* (1'-215') [V-KAPPA (*Homo sapiens* IGKV1-39*01 (100%) -IGKJ5*01 (100%), CDR-IMGT [6.3.10] (27'-32'.50'-52'.89'-98')) (1'-108') -*Homo sapiens* IGKC*01 (100%) Km3 A45.1, V101 (C-KAPPA A45.1 (154'), V101 (192')) (109'-215')]; dimère (229-229'':232-232'')-bisdisulfure, produit dans des cellules ovariennes de hamster chinois (CHO), lignée cellulaire CHO-K1, glycoforme alfa
anticoagulant

amrecibart

inmunoglobulina G4-kappa, anti-[*Homo sapiens* F11 (factor de coagulación 11, factor de coagulación XI, FXI, antecedente de la tromboplastina plasmática PTA)], anticuerpo monoclonal *Homo sapiens*;
cadena pesada H-gamma4 *Homo sapiens* (1-450) [VH (*Homo sapiens* IGHV3-23*03 (91.8%) -(IGHD) -IGHJ3*02 (100%), CDR-IMGT [8.8.16] (26-33.51-58.97-112)) (1-123) -*Homo sapiens* IGHG4*01, *nG4m(a)* CH2 L92, 12-G4v5 h P10(CH1 (124-221), bisagra 1-12 S10>P (231) (222-233), CH2 L92 (312) (234-343), CH3 (344-448), CHS (449-450)) (124-450)], (137-215')-disulfuro con la cadena ligera L-kappa *Homo sapiens* (1'-215') [V-KAPPA (*Homo sapiens* IGKV1-39*01 (100%) -IGKJ5*01 (100%), CDR-IMGT [6.3.10] (27'-32'.50'-52'.89'-98')) (1'-108') -*Homo sapiens* IGKC*01 (100%) Km3 A45.1, V101 (C-KAPPA A45.1 (154'), V101 (192')) (109'-215')]; dímero (229-229'':232-232'')-bisdisulfuro, producido en las células ováricas de hámster chino (CHO), línea celular CHO-K1, forma glicosilada alfa
anticoagulante

3008610-20-3

Heavy chain / Chaîne lourde / Cadena pesada

```
EVQLVESGGG LVQPGGSLRL SCAASGFTFS NYAMSWVRQA PGKGLEWVSV   50
IRSGGETTYY ADSVKGRFTI SRDNSKNTLY LQMNSLRAED TAVYYCAKVH  100
PSTWYGGDAF DIWGQGTMVT VSSASTKGPS VFPLAPCSRS TSESTAALGC  150
LVKDYFPEPV TVSWNSGALT SGVHTFPAVL QSSGLYSLSS VVTVPSSSLG  200
TKTYTCNVDH KPSNTKVDKR VESKYGPPCP PCPAPEFLGG PSVFLFPPKP  250
KDTLMISRTP EVTCVVVDVS QEDPEVQFNW YVDGVEVHNA KTKPREEQYN  300
STYRVVSVLT VLHQDWLNGK EYKCKVSNKG LPSSIEKTIS KAKGQPREPQ  350
VYTLPPSQEE MTKNQVSLTC LVKGFYPSDI AVEWESNGQP ENNYKTTPPV  400
LDSDGSFFLY SRLTVDKSRW QEGNVFSCSV MHEALHNHYT QKSLSLSLGK  450
```

Light chain / Chaîne légère / Cadena ligera

```
DIQMTQSPSS LSASVGDRVT ITCRASQSIS SYLNWYQQKP GKAPKLLIYA   50
ASSLQSGVPS RFSGSGSGTD FTLTISSLQP EDFATYYCQQ SYSTPPITFG  100
QGTRLEIKRT VAAPSVFIFP PSDEQLKSGT ASVVCLLNNF YPREAKVQWK  150
VDNALQSGNS QESVTEQDSK DSTYSLSSTL TLSKADYEKH KVYACEVTHQ  200
GLSSPVTKSF NRGEC                                        215
```

Post-translational modifications
Disulfide bridges location / Position des ponts disulfure / Posiciones de los puentes disulfuro
Intra-H (C23-C104) 22-96 150-206 264-324 370-428
22''-96'' 150''-206'' 264''-324'' 370''-428''
Intra-L (C23-C104) 23'-88' 135'-195'
23'''-88''' 135'''-195'''
Inter-H-L (CH1 10-CL 126) 137-215' 137''-215'''
Inter-H-H (h 8, h 11) 229-229'' 232-232''

N-glycosylation sites / Sites de N-glycosylation / Posiciones de N-glicosilación
H CH2 N84.4: 300, 300''
Fucosylated complex bi-antennary CHO-type glycans / glycanes de type CHO bi-antennaires complexes fucosylés / glicanos de tipo CHO biantenarios complejos fucosilados

C-terminal lysine clipping / Coupure de la lysine C-terminale / Recorte de lisina C-terminal
H CHS K2: 450, 450''

amsulostatum

amsulostat

(2*Z*)-3-fluoro-4-(quinolin-8-ylsulfonyl)but-2-en-1-amine
protein-lysine-oxidase (LOX) inhibitor, antifibrotic

amsulostat

(2*Z*)-3-fluoro-4-(quinolin-8-ylsulfonyl)but-2-én-1-amine
inhibiteur de la protéine-lysine-oxydase (LOX), antifibrotique

amsulostat

(2*Z*)-3-fluoro-4-(quinolin-8-ilsulfonil)but-2-en-1-amina
inhibidor de la proteína lisil oxidasa (LOX), antifibrítico

$C_{13}H_{13}FN_2O_2S$ 2409963-83-1

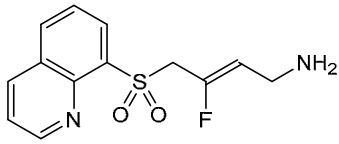

anbenitamabum repodatecanum #

anbenitamab repodatecan

immunoglobulin G1-kappa, anti-[*Homo sapiens* ERBB2 (epidermal growth factor receptor 2, receptor tyrosine protein kinase erbB-2, EGFR2, HER2, HER-2, p185c-erbB2, NEU, CD340)], humanized monoclonal antibody, bispecific biparatopic, tetravalent, conjugated at O-4 of the four terminal GlcNAc groups of the two branched glycans to a *repodatecan* group, consisting of a cleavable linker and a camptothecin derivative;
H-gamma1 heavy chain anti-ERBB2 domain II humanized (1-449) [VH (*Homo sapiens* IGHV3-66*01 (78.8%) -(IGHD) -IGHJ4*01 (100%), CDR-IMGT [8.8.12] (26-33.51-58.97-108)) (1-119) -*Homo sapiens* IGHG1*01, G1m17,1 CH1 K120, CH3 D12, L14, 14-G1v32 CH3 W22 (knob), 18-G1v82-4 CH3 A88(CH1 K120 (216) (120-217), hinge 1-15 (218-232), CH2 (233-342), CH3 D12 (358), L14 (360), T22>W (368), K88>A (411) (343-447), CHS (448-449)) (120-449)], (222-214')-disulfide with L-kappa light chain anti-ERBB2 humanized (1'-214') [V-KAPPA (*Homo sapiens* IGKV1-39*01 (86.3%) -IGKJ1*01 (100%), CDR-IMGT [6.3.9] (27'-32'.50'-52'.89'-97')) (1'-107') - *Homo sapiens* IGKC*01 (100%) Km3 A45.1, V101 (C-KAPPA A45.1 (153'), V101 (191')) (108'-214')];
H-gamma1 heavy chain anti-ERBB2 domain IV humanized (1''-450'') [VH (*Homo sapiens* IGHV3-66*01 (81.6%) -(IGHD) -IGHJ4*01 (100%), CDR-IMGT [8.8.13] (26''-33''.51''-58''.97''-109'')) (1''-120'') -*Homo sapiens* IGHG1*01, G1m17,1 CH1 K120, CH3 D12, L14, 14-G1v33 CH3 S22, A24, V86(hole), 18-G1v82-3 CH3 K85.1 (CH1 K120 (217'') (121''-218''), hinge 1-15 (219''-233''), CH2 (234''-343''), CH3 D12 (359), L14 (361) T22>S (369''), L24>A (371''), F85.1>K (408''), Y86>V (410'') (344''-448''), CHS (449''-450'')) (121''-450'')], (223''-214''')-disulfide with L-kappa light chain anti-ERBB2 humanized (1'''-214''') [V-KAPPA (*Homo sapiens* IGKV1-39*01 (86.3%) -IGKJ1*01 (100%), CDR-IMGT [6.3.9] (27'''-32'''.50'''-52'''.89'''-97''')) (1'''-107''') - *Homo sapiens* IGKC*01 (100%) Km3 A45.1, V101 (C-KAPPA A45.1 (153'''), V101 (191''')) (108'''-214''')]; dimer (228-229'':231-232'')-bisdisulfide, produced in Chinese hamster ovary (CHO) cells, glycoform alfa, substituted at O-4 of the four distal 2-acetamido-2-deoxy-β-D-glucopyranosyl groups of the two glycans at N-4 of the asparaginyl residues 299 and 300'' with 2-(2-{8-[(10*S*)-10-benzyl-1-{[(1*S*,9*S*)-9-ethyl-5-fluoro-9-hydroxy-4-methyl-10,13-dioxo-2,3,9,10,13,15-hexahydro-1*H*,12*H*-benzo[*de*]pyrano[3',4':6,7]indolizino[1,2-*b*]quinolin-1-yl]amino}-1,6,9,12,15,18,34-heptaoxo-3,21,24,27,30-pentaoxa-5,8,11,14,17,33-hexaazaheptatriacontan-37-oyl]-8,9-dihydro-1(*or* 3)*H*-dibenzo[*b*,*f*][1,2,3]triazolo[4,5-*d*]azocin-1(*or* 3)-yl}acetamido)-2-deoxy-β-D-galactopyranosyl (*repodatecan*) groups (introduced by enzymatic glycosylation with 2-(2-azidoacetamido)-2-deoxy-D-galactopyranose and subsequent reaction of the azido groups with the specific click reagent), resulting in a drug/antibody ratio of ~3.8 on average
antineoplastic

anbénitamab répodatécan	immunoglobuline G1-kappa, anti-[*Homo sapiens* ERBB2 (récepteur 2 du facteur de croissance épidermique, récepteur tyrosine-protéine kinase erbB2, EGFR2, HER2, HER-2, p185c-erbB2, NEU, CD340)], anticorps monoclonal humanisé, bispécifique biparatopique, tétravalent, conjugué en O-4 des quatre groupes terminaux GlcNAc des deux glycanes ramifiés à un groupe *répodatécan*, constitué d'un lieur clivable et d'un dérivé de camptothécine; chaîne lourde H-gamma1 anti-ERBB2 domaine II humanisée (1-449) [VH (*Homo sapiens* IGHV3-66*01 (78.8%) -(IGHD) -IGHJ4*01 (100%), CDR-IMGT [8.8.12] (26-33.51-58.97-108)) (1-119) -*Homo sapiens* IGHG1*01, G1m17,1 CH1 K120, CH3 D12, L14, 14-G1v32 CH3 W22 (knob), 18-G1v82-4 CH3 A88 (CH1 K120 (216) (120-217), charnière 1-15 (218-232), CH2 (233-342), CH3 D12 (358), L14 (360), T22>W (368), K88>A (411) (343-447), CHS (448-449)) (120-449)], (222-214')-disulfure avec la chaîne légère L-kappa anti-ERBB2 humanisée (1'-214') [V-KAPPA (*Homo sapiens* IGKV1-39*01 (86.3%) -IGKJ1*01 (100%), CDR-IMGT [6.3.9] (27'-32'.50'-52'.89'-97')) (1'-107') - *Homo sapiens* IGKC*01 (100%) Km3 A45.1, V101 (C-KAPPA A45.1 (153'), V101 (191')) (108'-214')]; chaîne lourde H-gamma1 anti-ERBB2 domaine IV humanisée (1''-450'') [VH (*Homo sapiens* IGHV3-66*01 (81.6%) -(IGHD) -IGHJ4*01 (100%), CDR-IMGT [8.8.13] (26''-33''.51''-58''.97''-109'')) (1''-120'') -*Homo sapiens* IGHG1*01, G1m17,1 CH1 K120, CH3 D12, L14, 14-G1v33 CH3 S22, A24, V86 (hole), 18-G1v82-3 CH3 K85.1 (CH1 K120 (217'') (121''-218''), charnière 1-15 (219''-233''), CH2 (234''-343''), CH3 D12 (359), L14 (361) T22>S (369''), L24>A (371''), F85.1>K (408''), Y86>V (410'') (344''-448''), CHS (449''-450'')) (121''-450'')], (223''-214''')-disulfure avec la chaîne légère L-kappa anti-ERBB2 humanisée (1'''-214''') [V-KAPPA (*Homo sapiens* IGKV1-39*01 (86.3%) -IGKJ1*01 (100%), CDR-IMGT [6.3.9] (27'''-32'''.50'''-52'''.89'''-97''')) (1'''-107''') - *Homo sapiens* IGKC*01 (100%) Km3 A45.1, V101 (C-KAPPA A45.1 (153'''), V101 (191''')) (108'''-214''')]; dimère (228-229'':231-232'')-bisdisulfure, produit dans des cellules ovariennes de hamster chinois (CHO), glycoforme alfa, substitué en O-4 des quatre groupes distaux 2-acétamido-2-désoxy-β-D-glucopyranosyle des deux glycanes en N-4 des résidus asparaginyle 299 et 300'' par des groupes 2-(2-{8-[(10*S*)-10-benzyl-1-{[(1*S*,9*S*)-9-éthyl-5-fluoro-9-hydroxy-4-méthyl-10,13-dioxo-2,3,9,10,13,15-hexahydro-1*H*,12*H*-benzo[*de*]pyrano[3',4':6,7]indolizino[1,2-b]quinoléin-1-yl]amino}-1,6,9,12,15,18,34-heptaoxo-3,21,24,27,30-pentaoxa-5,8,11,14,17,33-hexaazaheptatriacontan-37-oyl]-8,9-dihydro-1(*ou* 3)*H*-dibenzo[*b*,*f*][1,2,3]triazolo[4,5-*d*]azocin-1(*ou* 3)-yl}acétamido)-2-désoxy-β-D-galactopyranosyle (*répodatécan*) (introduits par glycosylation enzymatique avec le 2-(2-azidoacétamido)-2-désoxy-D-galactopyranose et réaction ultérieure des groupes azido avec le réactif click spécifique), ce qui donne un rapport médicament/anticorps d'environ 3,8 en moyenne *antinéoplasique*

anbenitamab repodatecán	inmunoglobulina G1-kappa, anti-[*Homo sapiens* ERBB2 (receptor 2 del factor de crecimiento epidérmico, receptor tirosina-proteína kinasa erbB2, EGFR2, HER2, HER-2, p185c-erbB2, NEU, CD340)], anticuerpo monoclonal humanizado, biparatópico biespecífico, tetravalente, conjugado en O-4 de los cuatro grupos GlcNAc terminales de los dos glicanos ramificados con un grupo *repodatecán*, que consta de un conector escindible y un derivado de camptotecina; cadena pesada H-gamma1 anti-ERBB2 dominio II humanizada (1-449) [VH (*Homo sapiens* IGHV3-66*01 (78.8%) -(IGHD) -IGHJ4*01 (100%), CDR-IMGT [8.8.12] (26-33.51-58.97-108) (1-119) -*Homo sapiens* IGHG1*01, G1m7,1, CH1 K120, CH3 D12, L14, 14-G1v32 CH3 W22 (knob), 18-G1v82-4 CH3 A88 (CH1 K120 (216) (120-217), bisagra 1-15 (218-232), CH2 (233-342), CH3 D12 (358), L14 (360), T22>W (368), K88>A (411) (343-447), CHS (448-449)) (120-449)], (222-214')-disulfuro con la cadena ligera L-kappa anti-ERBB2 humanizada (1'-214') [V-KAPPA (*Homo sapiens* IGKV1-39*01 (86.3%) -IGKJ1*01 (100%)) CDR-IMGT [6.3.9] (27'-32'.50'-52'.89'-97')) (1'-107') -*Homo sapiens* IGKC*01 (100%), Km3 A45.1, V101 (C-KAPPA A45.1 (153'), V101 (191')) (108'-214')]; cadena pesada H-gamma1 anti-ERBB2 domnio IV humanizada (1''-450'') [VH (*Homo sapiens* IGHV3-66*01 (81.6%) -(IGHD) -IGHJ4*01 (100%), CDR-IMGT [8.8.13] (26''-33''.51''-58''.97''-109'') (1''-120'') -*Homo sapiens* IGHG1*01, G1m7,1, CH1 K120, CH3 D12, L14, 14-G1v33 CH3 S22, A24, V86 (hole), 18-G1v82-3 CH3 K85.1 (CH1 K120 (217'') (121''-218''), bisagra 1-15 (219''-233''), CH2 (234''-343''), CH3 D12 (359), L14 (361) T22>S (369''), L24>A (371''), F85.1>K (408''), Y86>V (410'') (344''-448''), CHS (449''-450'')) (121''-450'')], (223''-214''')-disulfuro con la cadena ligera L-kappa anti-ERBB2 humanizada (1'''-214''') [V-KAPPA (*Homo sapiens* IGKV1-39*01 (86.3%) -IGKJ1*01 (100%)) CDR-IMGT [6.3.9] (27'''-32'''.50'''-52'''.89'''-97) ''' (1'''-107''') -*Homo sapiens* IGKC*01 (100%), Km3 A45.1, V101 (C-KAPPA A45.1 (153'''), V101 (191''') (108'''-214''')]; dímero (228-229'':231-232'')-bisdisulfuro, producido en las células ováricas de hámster chino (CHO), forma glicosilada alfa, sustituido en O-4 de los cuatro grupos distales 2-acetamido-2-desoxi-β-D-glucopiranosilo de los dos glicanos en N-4 de los residuos de asparaginilo 299 y 300'' con grupos 2-(2-{8-[(10*S*)-10-bencil-1-{[(1*S*,9*S*)-9-etil-5-fluoro-9-hidroxi-4-metil-10,13-dioxo-2,3,9,10,13,15-hexahidro-1*H*,12*H*-benzo[*de*]pirano[3',4':6,7]indolizino[1,2-*b*]quinolein-1-il]amino}-1,6,9,12,15,18,34-heptaoxo-3,21,24,27,30-pentaoxa-5,8,11,14,17,33-hexaazaheptatriacontan-37-oil]-8,9-dihidro-1(*o* 3)*H*-dibenzo[*b*,*f*][1,2,3]triazolo[4,5-*d*]azocin-1(*o* 3)-il}acetamido)-2-desoxi-β-D-galactopiranosilo (*repodatecán*) (introducidos por glicosilación enzimática con 2-(2-azidoacetamido)-2-desoxi-D-galactopiranosa y posterior reacción de los grupos azido con el reactivo clic específico), lo que da como resultado una relación fármaco/anticuerpo de ~3,8 en promedio *antineoplásico*

2923420-38-4

Heavy chain / Chaîne lourde / Cadena pesada : H-gamma1 anti-ERBB2 domain II (knob) (H)

```
EVQLVESGGG LVQPGGSLRL SCAASGFTFT DYTMDWVRQA PGKGLEWVAD  50
VNPNSGGSIY NQRFKGRFTL SVDRSKNTLY LQMNSLRAED TAVYYCARNL 100
GPSFYFDYWG QGTLVTVSSA STKGPSVFPL APSSKSTSGG TAALGCLVKD 150
YFPEPVTVSW NSGALTSGVH TFPAVLQSSG LYSLSSVVTV PSSSLGTQTY 200
ICNVNHKPSN TKVDKKVEPK SCDKTHTCPP CPAPELLGGP SVFLFPPKPK 250
DTLMISRTPE VTCVVVDVSH EDPEVKFNWY VDGVEVHNAK TKPREEQYNS 300
TYRVVSVLTV LHQDWLNGKE YKCKVSNKAL PAPIEKTISK AKGQPREPQV 350
YTLPPSRDEL TKNQVSLWCL VKGFYPSDIA VEWESNGQPE NNYKTTPPVL 400
DSDGSFFLYS ALTVDKSRWQ QGNVFSCSVM HEALHNHYTQ KSLSLSPGK  449
```

Heavy chain / Chaîne lourde / Cadena pesada : H-gamma1 anti-ERBB2 domain IV (hole) (H")

```
EVQLVESGGG LVQPGGSLRL SCAASGFNIK DTYIHWVRQA PGKGLEWVAR  50
IYPTNGYTRY ADSVKGRFTI SADTSKNTAY LQMNSLRAED TAVYYCSRWG 100
GDGFYAMDYW GQGTLVTVSS ASTKGPSVFP LAPSSKSTSG GTAALGCLVK 150
DYFPEPVTVS WNSGALTSGV HTFPAVLQSS GLYSLSSVVT VPSSSLGTQT 200
YICNVNHKPS NTKVDKKVEP KSCDKTHTCP PCPAPELLGG PSVFLFPPKP 250
KDTLMISRTP EVTCVVVDVS HEDPEVKFNW YVDGVEVHNA KTKPREEQYN 300
STYRVVSVLT VLHQDWLNGK EYKCKVSNKA LPAPIEKTIS KAKGQPREPQ 350
VYTLPPSRDE LTKNQVSLSC AVKGFYPSDI AVEWESNGQP ENNYKTTPPV 400
LDSDGSFKLV SKLTVDKSRW QQGNVFSCSV MHEALHNHYT QKSLSLSPGK 450
```

Light chain / Chaîne légère / Cadena ligera : L-kappa anti-ERBB2 (L', L'")

```
DIQMTQSPSS LSASVGDRVT ITCRASQDVN TAVAWYQQKP GKAPKLLIYS  50
ASFLYSGVPS RFSGSRSGTD FTLTISSLQP EDFATYYCQQ HYTTPPTFGQ 100
GTKVEIKRTV AAPSVFIFPP SDEQLKSGTA SVVCLLNNFY PREAKVQWKV 150
DNALQSGNSQ ESVTEQDSKD STYSLSSTLT LSKADYEKHK VYACEVTHQG 200
LSSPVTKSFN RGEC                                        214
```

Post-translational modifications

Disulfide bridges location / Position des ponts disulfure / Posiciones de los puentes disulfuro

Intra-H (C23-C104) 22-96 146-202 263-323 369-427
22"-96" 147"-203" 264"-324" 370"-428"
Intra-L (C23-C104) 23'-88' 134'-194'
23'"-88'" 134'"-194'"
Inter-H-L (h 5-CL 126) 222-214' 223"-214'"
Inter-H-H (h 11, h 14) 228-229" 231-232"

N-glycosylation sites / Sites de N-glycosylation / Posiciones de N-glicosilación
H CH2 N84.4: 299, 300"
Fucosylated complex bi-antennary CHO-type glycans / Glycanes de type CHO bi-antennaires complexes fucosylés / Glicanos de tipo CHO biantenarios complejos fucosilados
C-terminal lysine clipping / Coupure de la lysine C-terminale / Recorte de lisina C-terminal
H CHS K2: 449, 450"

Modified distal βdGlcNAc groups / Groupes βdGlcNAc distaux modifiés / Grupos βdGlcNAc distales modificados
*(*repodatecan*:mAb ~ 3.8:1)

Asn299, Asn300":

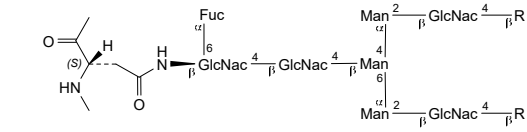

R:

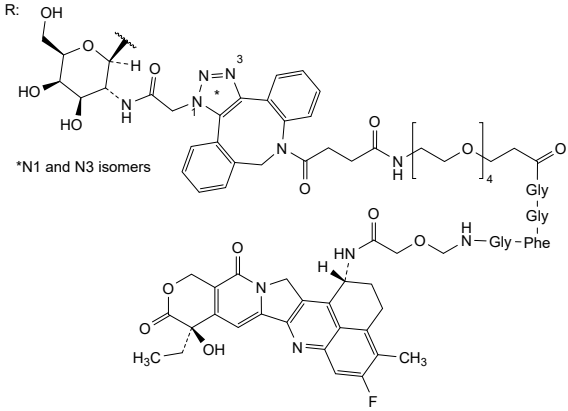

andamertinibum

andamertinib — *N*-(4-methoxy-2-[4-(3-methoxyazetidin-1-yl)piperidin-1-yl]-5-{[6-(1-methyl-1*H*-indazol-5-yl)pyrimidin-4-yl]amino}phenyl)prop-2-enamide
epidermal growth factor receptor tyrosine kinase inhibitor, antineoplastic

andamertinib — *N*-(4-méthoxy-2-[4-(3-méthoxyazétidin-1-yl)pipéridin-1-yl]-5-{[6-(1-méthyl-1*H*-indazol-5-yl)pyrimidin-4-yl]amino}phényl)prop-2-énamide
inhibiteur de la tyrosine kinase du récepteur du facteur de croissance épidermique, antinéoplasique

andamertinib — *N*-(5-{[6-(1-metil-1*H*-indazol-5-il)pirimidin-4-il]amino}-4-metoxi-2-[4-(3-metoxiazetidin-1-il)piperidin-1-il]fenil)prop-2-enamida
inhibidor de la tirosina kinasa del receptor del factor de crecimiento epidérmico, antineoplásico

$C_{31}H_{36}N_8O_3$ 2254145-43-0

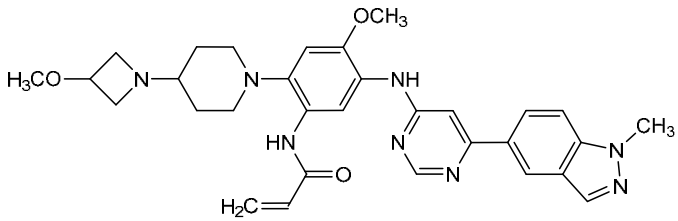

anvumetostatum

anvumetostat — (4-amino-1,3-dihydrofuro[3,4-*c*][1,7]naphthyridin-8-yl){(3*S*)-3-[4-(trifluoromethyl)phenyl]morpholin-4-yl}methanone
antineoplastic

anvumétostat — (4-amino-1,3-dihydrofuro[3,4-*c*][1,7]naphtyridin-8-yl){(3*S*)-3-[4-(trifluorométhyl)phényl]morpholin-4-yl}méthanone
antinéoplasique

anvumetostat — (4-amino-1,3-dihidrofuro[3,4-*c*][1,7]naftiridin-8-il){(3*S*)-3-[4-(trifluorometil)fenil]morfolin-4-il}metanona
antineoplásico

$C_{22}H_{19}F_3N_4O_3$ 2790567-82-5

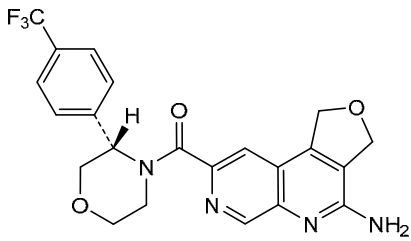

anzutresgenum autoleucelum #

anzutresgene autoleucel

autologous CD4+/CD8+ enriched T lymphocytes transduced with a self-inactivating, non-replicating lentiviral vector encoding a T cell receptor (TCR) specific for the preferentially expressed antigen in melanoma (PRAME). The TCR transgene consists of a TCRα and a TCRβ chain separated by a self-cleaving ribosome skipping sequence derived from porcine teschovirus (P2A) under the control of a murine stem cell virus (MSCV) promoter and a Woodchuck hepatitis virus post-transcriptional response element (WPRE). The viral vector backbone also comprises a packaging signal ψ (psi), residual *gag* sequence, a Rev response element (RRE), a central polypurine tract/central termination sequence (cPPT/CTS) and is flanked by 5' and 3' long terminal repeats (LTRs). The vector is pseudotyped with vesicular stomatitis virus G glycoprotein.
The leukapheresis material is enriched for CD4+ and CD8+ T lymphocytes by positive immunoselection prior to activation with CD3 and CD28 agonists in growth media containing interleukin 7 (IL-7) and interleukin 15 (IL-15). The cells are then transduced with a lentiviral vector and expanded in growth media containing human AB serum, IL-7 and IL-15. The cell suspension consists of CD3+ T lymphocytes (≥90%) of which >20% of the CD3+CD8+ cells express the PRAME-specific TCR. The transduced T lymphocytes release interferon gamma (IFN-γ) by co-culture with PRAME-expressing tumor cells *in vitro*
cell-based gene therapy (antineoplastic)

anzutresgène autoleucel

lymphocytes T autologues enrichis en CD4+/CD8+ transduits avec un vecteur lentiviral auto-inactivant et non réplicatif codant un récepteur de lymphocytes T (TCR) spécifique de l'antigène préférentiellement exprimé dans le mélanome (PRAME). Le transgène TCR est constitué d'une chaîne TCRα et d'une chaîne TCRβ séparées par une séquence auto-clivante de saut de ribosomes dérivée du teschovirus porcin (P2A), sous le contrôle d'un promoteur du virus des cellules souches murines (MSCV) et d'un élément de réponse post-transcriptionnelle du virus de l'hépatite de la marmotte (WPRE). Le squelette du vecteur viral comprend également un signal d'empaquetage ψ (psi), une séquence *gag* résiduelle, un élément de réponse Rev (RRE), un tractus polypurine central/une séquence de terminaison centrale (cPPT/CTS) et, il est flanqué de répétitions terminales longues (LTRs) en 5' et en 3'. Le vecteur est pseudotypé avec la glycoprotéine G du virus de la stomatite vésiculaire (VSV). Le matériel de leucaphérèse est enrichi en lymphocytes T CD4+ et CD8+ par immunosélection positive, avant activation avec des agonistes CD3 et CD28, dans un milieu de croissance contenant de l'interleukine 7 (IL-7) et de l'interleukine 15 (IL-15). Les cellules sont ensuite transduites avec un vecteur lentiviral et expansées dans un milieu de croissance contenant du sérum AB humain, de l'IL-7 et de l'IL-15. La suspension cellulaire est constituée de lymphocytes T CD3+ (≥90%) dont >20% des cellules CD3+CD8+ expriment le TCR spécifique de PRAME. Les lymphocytes T transduits libèrent de l'interféron gamma (IFN-γ) par co-culture avec des cellules tumorales exprimant PRAME *in vitro*
thérapie génique à base de cellules (antinéoplasique)

anzutresgén autoleucel

linfocitos T CD4+/CD8+ autólogos enriquecidos, transducidos con un vector lentiviral auto-inactivante, no replicativo, que codifica un receptor de células T (TCR) específico del antígeno preferentemente expresado en melanoma (PRAME). El transgén del TCR consiste en una cadena TCRα y una cadena TCRβ separadas por una secuencia de auto-escisión de salto ribosómico derivada del teschovirus porcino (P2A) bajo el control de un promotor del virus de células madre murino (MSCV) y un elemento regulador post-transcripcional del virus de la hepatitis de la marmota (WPRE). El esqueleto del vector viral también consta de una señal de empaquetamiento ψ (psi), una secuencia residual *gag*, un elemento de respuesta Rev (RRE), una secuencia de tracto de poli-purina central/terminación central (cPPT/CTS), y está flanqueado por repeticiones terminales largas (LTRs) en 5' y 3'. El vector está seudotipado con la glicoproteína G del virus de la estomatitis vesicular (VSV).
El material de leucoaféresis se enriquece en linfocitos T CD4+ y CD8+ mediante inmunoselección positiva, antes de la activación con agonistas de CD3 y CD28 en medio de crecimiento que contiene interleuquina 7 (IL-7) e interleuquina 15 (IL-15). Las células después se transducen con el vector lentiviral y se expanden más en medio de crecimiento que contiene suero AB humano, IL-7 e IL-15. La suspensión celular consiste en linfocitos T CD3+ (≥90%) de los cuales >20% de las células CD3+CD8+ expresan el TCR específico de PRAME. Los linfocitos T transducidos liberan interferón gamma (IFN-γ) mediante co-cultivo *in vitro* con células tumorales que expresan PRAME
terapia génica basada en células (antineoplásico)

apazunersenum

apazunersen

all-P-ambo-2'-*O*,4'-*C*-methylene-*P*-thioadenylyl-(3'→5')-2'-*O*,4'-*C*-methylene-*P*-thioguanylyl-(3'→5')-2'-*O*,4'-*C*-methylene-*P*-thioadenylyl-(3'→5')-2'-deoxy-*P*-thioadenylyl-(3'→5')-*P*-thiothymidylyl-(3'→5')-2'-deoxy-*P*-thioguanylyl-(3'→5')-2'-deoxy-*P*-thioguanylyl-(3'→5')-2'-deoxy-*P*-thiocytidylyl-(3'→5')-2'-deoxy-*P*-thioadenylyl-(3'→5')-2'-deoxy-*P*-thiocytidylyl-(3'→5')-2'-deoxy-*P*-thioadenylyl-(3'→5')-*P*-thiothymidylyl-(3'→5')-2'-deoxy-*P*-thiocytidylyl-(3'→5')-*P*-thiothymidylyl-(3'→5')-5-methyl-2'-*O*,4'-*C*-methylene-*P*-thiocytidylyl-(3'→5')-5-methyl-2'-*O*,4'-*C*-methylene-*P*-thiouridylyl-(3'→5')-5-methyl-2'-*O*,4'-*C*-methylene-*P*-thiouridylyl-(3'→5')-2'-*O*,4'-*C*-methyleneguanosine
ubiquitin protein ligase E3A-antisense transcript reducer (Angelman Syndrome)

apazunersen

tout-P-ambo-2'-*O*,4'-*C*-méthylène-*P*-thioadénylyl-(3'→5')-2'-*O*,4'-*C*-méthylène-*P*-thioguanylyl-(3'→5')-2'-*O*,4'-*C*-méthylène-*P*-thioadénylyl-(3'→5')-2'-désoxy-*P*-thioadénylyl-(3'→5')-*P*-thiothymidylyl-(3'→5')-2'-désoxy-*P*-thioguanylyl-(3'→5')-2'-désoxy-*P*-thioguanylyl-(3'→5')-2'-désoxy-*P*-thiocytidylyl-(3'→5')-2'-désoxy-*P*-thioadénylyl-(3'→5')-2'-désoxy-*P*-thiocytidylyl-(3'→5')-2'-désoxy-*P*-thioadénylyl-(3'→5')-*P*-thiothymidylyl-(3'→5')-2'-désoxy-*P*-thiocytidylyl-(3'→5')-*P*-thiothymidylyl-(3'→5')-5-méthyl-2'-*O*,4'-*C*-méthylène-*P*-thiocytidylyl-(3'→5')-5-méthyl-2'-*O*,4'-*C*-méthylène-*P*-thiouridylyl-(3'→5')-5-méthyl-2'-*O*,4'-*C*-méthylène-*P*-thiouridylyl-(3'→5')-2'-*O*,4'-*C*-méthylèneguanosine
réducteur de transcription antisens de l'ubiquitine protéine ligase E3A (syndrome d'Angelman)

apazunersén

todo-P-ambo-2'-*O*,4'-*C*-metileno-*P*-tioadenilil-(3'→5')-2'-*O*,4'-*C*-metileno-*P*-tioguanilil-(3'→5')-2'-*O*,4'-*C*-metileno-*P*-tioadenilil-(3'→5')-2'-desoxi-*P*-tioadenilil-(3'→5')-*P*-tiotimidilil-(3'→5')-2'-desoxi-*P*-tioguanilil-(3'→5')-2'-desoxi-*P*-tioguanilil-(3'→5')-2'-desoxi-*P*-tiocitidilil-(3'→5')-2'-desoxi-*P*-tioadenilil-(3'→5')-2'-desoxi-*P*-tiocitidilil-(3'→5')-2'-desoxi-*P*-tioadenilil-(3'→5')-*P*-tiotimidilil-(3'→5')-2'-desoxi-*P*-tiocitidilil-(3'→5')-*P*-tiotimidilil-(3'→5')-5-metil-2'-*O*,4'-*C*-metileno-*P*-tiocitidilil-(3'→5')-5-metil-2'-*O*,4'-*C*-metileno-*P*-tiouridilil-(3'→5')-5-metil-2'-*O*,4'-*C*-metileno-*P*-tiouridilil-(3'→5')-2'-*O*,4'-*C*-metilenoguanosina

reductor de la transcripción antisense de la ligasa E3A de la proteína ubiquitina (síndrome de Angelman)

$C_{184}H_{224}N_{67}O_{96}P_{17}S_{17}$ 2919324-01-7

(3'-5')*A*=*G*=*A*=dA=dT=dG=dG=dC=dA=dC=dA=dT=dC=dT=*C*=*U*=*U*=*G*

N : nucleoside / nucléoside / nucleósido
B : nucleobase / nucléobase / nucleobase
dN : 2'-deoxy-N / 2'-désoxy-N / 2'-desoxi-N
N : 2'-*O*,4'-*C*-methylene-N / 2'-*O*,4'-*C*-méthylène-N / 2'-*O*,4'-*C*-metileno-N
N : 5-methyl-N / 5-méthyl-N / 5-metil-N
= : -PO(SH)-

N :

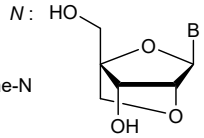

arumakimigum #

arumakimig

immunoglobulin (H-gamma1_L-lambda2)_(H-gamma1_L-kappa), anti-[*Homo sapiens* IL18 (interleukin 18, IL-18, interferon gamma-inducing factor, IGIF, interleukin-1 gamma, IL-1G, IL1F4)] and anti-[*Homo sapiens* IL1B (interleukin 1 beta, IL-1B, 1L1F2)], *Homo sapiens* monoclonal antibody, bispecific, bivalent;
H-gamma1 heavy chain anti-IL18 *Homo sapiens* (1-449) [VH (*Homo sapiens* IGHV1-69*01 (91.8%) -(IGHD) -IGHJ5*01 (92.9%), CDR-IMGT [8.8.12] (26-33.51-58.97-108)) (1-119) -*Homo sapiens* IGHG1*03, G1m3, nG1m1 CH1 R120, CH3 E12, M14, 6-G1-v14 CH2 A1.3, A1.2, 14-G1v74 CH3 C10, 14-G1v32 CH3 W22 (knob) (CH1 R120 (216) (120-217), hinge 1-15 (218-232), CH2 L1.3>A (236), L1.2>A (237) (233-342), CH3 S10>C (356), E12 (358), M14 (360), T22>W (368) (343-447), CHS (448-449)) (120-449)], (222-215')-disulfide with L-lambda2 light chain anti-IL18 *Homo sapiens* (1'-216') [V-Lambda (*Homo sapiens* IGLV1-40*01 (88.3%) -IGLJ2*01 (100%), CDR-IMGT [8.3.11] (26'-33'.51'-53'.90'-100')) (1'-110') -*Homo sapiens* IGLC2*01 (100%) (C-LAMBDA2) (111'-216')];
H-gamma1 heavy chain anti-IL1B *Homo sapiens* (1"-448") [VH (*Homo sapiens* IGHV3-30-5*03 (93.9%) -(IGHD) -IGHJ4*01 (100%), CDR-IMGT [8.8.11] (26"-33".51"-58".97"-107")) (1"-118") -*Homo sapiens* IGHG1*03, G1m3, nG1m1 CH1 R120, CH3 E12, M14, 6-G1v14 CH2 A1.3, A1.2, 14-G1v75 CH3 C5, 14-G1v33 CH3S22, A24, V86 (hole) (CH1 R120 (215") (119"-216"), hinge 1-15 (217"-231"), CH2 L1.3>A (235"), L1.2>A (236") (232"-341"), CH3 Y5>C (350"), E12 (357"), M14 (359"), T22>S (367"), L24>A (369"), Y86>V (408") (342"-446"), CHS (447"-448")) (119"-448")], (221"-214"')-disulfide with L-kappa light chain anti-IL1B *Homo sapiens* (1'-214"') [V-Kappa (*Homo sapiens* IGKV6-21*01 (98.9%) -IGKJ3*01 (100%), CDR-IMGT [6.3.9] (27"'-32"'.50"'-52"'.89"'-97"')) (1"'-107"') -*Homo sapiens* IGKC*01 (100%) Km3 A45.1, V101 (C-KAPPA A45.1 (153"'), V101 (191"')) (108"'-214"')]; dimer (228-227"':231-230")-bisdisulfide, produced in Chinese hamster ovary (CHO) cells, cell line CHO-K1, glycoform alfa

anti-inflammatory

arumakimig

immunoglobuline (H-gamma1_L-lambda2)_(H-gamma1_L-kappa), anti-[*Homo sapiens* IL18 (interleukine 18, IL-18, facteur inducteur d'interferon gamma, IGIF, interleukine-1 gamma, IL-1G, IL1F4)] et anti-[*Homo sapiens* IL1B (interleukine 1 bêta, IL-1B, 1L1F2)], anticorps monoclonal *Homo sapiens,* bispécifique, bivalent;
chaîne lourde H-gamma1 anti-IL18 *Homo sapiens* (1-449) [VH (*Homo sapiens* IGHV1-69*01 (91.8%) -(IGHD) -IGHJ5*01 (92.9%), CDR-IMGT [8.8.12] (26-33.51-58.97-108)) (1-119) -*Homo sapiens* IGHG1*03, G1m3, nG1m1 CH1 R120, CH3 E12, M14, 6-G1v14 CH2 A1.3, A1.2, 14-G1v74 CH3 C10, 14-G1v32 CH3 W22 (knob) (CH1 R120 (216) (120-217), charnière 1-15 (218-232), CH2 L1.3>A (236), L1.2>A (237) (233-342), CH3 S10>C (356), E12 (358), M14 (360), T22>W (368) (343-447), CHS (448-449)) (120-449)], (222-215')-disulfure avec la chaîne légère L-lambda2 anti-IL18 *Homo sapiens* (1'-216') [V-Lambda (*Homo sapiens* IGLV1-40*01 (88.3%) -IGLJ2*01 (100%), CDR-IMGT [8.3.11] (26'-33'.51'-53'.90'-100')) (1'-110') -*Homo sapiens* IGLC2*01 (100%) (C-LAMBDA2) (111'-216')];
chaîne lourde H-gamma1 anti-IL1B *Homo sapiens* (1''-448'') [VH (*Homo sapiens* IGHV3-30-5*03 (93.9%) -(IGHD) -IGHJ4*01 (100%), CDR-IMGT [8.8.11] (26''-33''.51''-58''.97''-107'')) (1''-118'') -*Homo sapiens* IGHG1*03, G1m3, nG1m1 CH1 R120, CH3 E12, M14, 6-G1v14 CH2 A1.3, A1.2, 14-G1v75 CH3 C5, 14-G1v33 CH3S22, A24, V86 (hole) (CH1 R120 (215'') (119''-216''), charnière 1-15 (217''-231''), CH2 L1.3>A (235''), L1.2>A (236'') (232''-341''), CH3 Y5>C (350''), E12 (357''), M14 (359''), T22>S (367''), L24>A (369''), Y86>V (408'') (342''-446''), CHS (447''-448'')) (119''-448'')], (221''-214''')-disulfure avec la chaîne légère L-kappa anti-IL1B *Homo sapiens* (1'-214''') [V-Kappa (*Homo sapiens* IGKV6-21*01 (98.9%) -IGKJ3*01 (100%), CDR-IMGT [6.3.9] (27'''-32'''.50'''-52'''.89'''-97''')) (1'''-107''') -*Homo sapiens* IGKC*01 (100%) Km3 A45.1, V101 (C-KAPPA A45.1 (153'''), V101 (191''')) (108'''-214''')]; dimère (228-227''':231-230''')-bisdisulfure, produit dans des cellules ovariennes de hamster chinois (CHO), lignée cellulaire CHO-K1, glycoforme alfa
anti-inflammatoire

arumakimig

inmunoglobulina (H-gamma1_L-lambda2)_(H-gamma1_L-kappa), anti-[*Homo sapiens* IL18 (interleukina 18, IL-18, factor inductor del interferón gamma, IGIF, interleukina-1 gamma, IL-1G, IL1F4)] y anti-[*Homo sapiens* IL1B (interleukina 1 beta, IL-1B, 1L1F2)], anticuerpo monoclonal *Homo sapiens,* biespecífico, bivalente;
cadena pesada H-gamma1 anti-IL18 *Homo sapiens* (1-449) [VH (*Homo sapiens* IGHV1-69*01 (91.8%) -(IGHD) -IGHJ5*01 (92.9%), CDR-IMGT [8.8.12] (26-33.51-58.97-108)) (1-119) -*Homo sapiens* IGHG1*03, G1m3, nG1m1 CH1 R120, CH3 E12, M14, 6-G1v14 CH2 A1.3, A1.2, 14-G1v74 CH3 C10, 14-G1v32 CH3 W22 (knob) (CH1 R120 (216) (120-217), bisagra 1-15 (218-232), CH2 L1.3>A (236), L1.2>A (237) (233-342), CH3 S10>C (356), E12 (358), M14 (360), T22>W (368) (343-447), CHS (448-449)) (120-449)], (222-215')-disulfuro con la cadena ligera L-lambda2 anti-IL18 *Homo sapiens* (1'-216') [V-Lambda (*Homo sapiens* IGLV1-40*01 (88.3%) -IGLJ2*01 (100%), CDR-IMGT [8.3.11] (26'-33'.51'-53'.90'-100')) (1'-110') -*Homo sapiens* IGLC2*01 (100%) (C-LAMBDA2) (111'-216')];
cadena pesada H-gamma1 anti-IL1B *Homo sapiens* (1''-448'') [VH (*Homo sapiens* IGHV3-30-5*03 (93.9%) -(IGHD) -IGHJ4*01 (100%), CDR-IMGT [8.8.11] (26''-33''.51''-58''.97''-107'')) (1''-118'') -*Homo sapiens* IGHG1*03, G1m3, nG1m1 CH1 R120, CH3 E12, M14, 6-G1v14 CH2 A1.3, A1.2, 14-G1v75 CH3 C5, 14-G1v33 CH3S22, A24, V86 (hole) (CH1 R120 (215'') (119''-216''), bisagra 1-15 (217''-231''), CH2 L1.3>A (235''), L1.2>A (236'') (232''-341''), CH3 Y5>C (350''), E12 (357''), M14 (359''), T22>S (367''), L24>A (369''), Y86>V (408'') (342''-446''), CHS (447''-448'')) (119''-448'')], (221''-214''')-disulfuro con la cadena ligera L-kappa anti-IL1B *Homo sapiens* (1'-214''') [V-Kappa (*Homo sapiens* IGKV6-21*01 (98.9%) -IGKJ3*01 (100%), CDR-IMGT [6.3.9] (27'''-32'''.50'''-52'''.89'''-97''')) (1'''-107''') -*Homo sapiens* IGKC*01 (100%) Km3 A45.1, V101 (C-KAPPA A45.1 (153'''), V101 (191''')) (108'''-214''')]; dímero (228-227''':231-230''')-bisdisulfuro, producido en las células ováricas de hámster chino (CHO), línea celular CHO-K1, forma glicosilada alfa
antiinflamatorio

3018901-76-0

Heavy chain / Chaîne lourde / Cadena pesada: FI-gammaI anti-IL18 (knob) (H')

```
EVQLVQSGAE VKKPGSSVKV SCKASGGTFS STAISWVRQA PGQGLEWMGR  50
IIPVLGTANY AQKFQGRVTI TADESTSTAY MELSSLRSED TAVYYCARAA 100
YHFLVEGNAV DYWGQGTLVT VSSASTKGPS VFPLAPSSKS TSGGTAALGC 150
LVKDYFPEPV TVSWNSGALT SGVHTFPAVL QSSGLYSLSS VVTVPSSSLG 200
TKTYTCNVDH KPSNTKVDKR VESKYGPPCP PCPAPEAAGG PSVFLFPPKP 250
KDTLMISRTP EVTCVVVDVS HEDPEVKFNW YVDGVEVHNA KTKPREEQYN 300
STYRVVSVLT VLHQDWLNGK EYKCKVSNKA LPAPIEKTIS KAKGQPREPQ 350
VYTLPPSREE TKNQVSLWCL VKGFYPSDIA VEWESNGQPE NNYKTTPPVL 400
DSDGSFFLYS KLTVDKSRWQ QGNVFSCSVM HEALHNHYTQ KSLSLSPGK  449
```

Light chain / Chaîne légère / Cadena ligera: L-lambda anti-IL18 (L')

```
DIVLTQPPSV SGAPGQRVTI SCTGSSSNIG AGYDVHWYQQ LPGTAPKLLI  50
YGNSNRPSGV PDRFSGSKSG TSASLAITGL QAEDEADYYC QSYDSSLSGY 100
VFGTGTKLTV LGQPKAAPSV TLFPPSSEEL QANKATLVCL ISDFYPGAVT 150
VAWKADSSPV KAGVETTTPS KQSNNKYAAS SYLSLTPEQW KSHRSYSCQV 200
THEGSTVEKT VAPTEC                                       216
```

Heavy chain / Chaîne lourde / Cadena pesada: FI-gammaI anti-IL1B (hole) (H")

```
QVQLVESGGG VVQPGRSLRL SCAASGFTFS SYAMHWVRQA PGKGLEWVAI  50
IWYDGSNKYY ADSVKGRFTI SRDNSKNTLY LQMNSLRAED TAVYYCARGL 100
FDFWSGYWWQ GTLVTVSSAS TKGPSVFPLA PSSKSTSGGT AALGCLVKDY 150
FPEPVTVSWN SGALTSGVHT FPAVLQSSGL YSLSSVVTVP SSSLGTQTYI 200
CNVNHKPSNT KVDKRVEPKS CDKTHTCPPC PAPELAAAPS VFLFPPKPKD 250
TLMISRTPEV TCVVVDVSHE DPEVKFNWYV DGVEVHNAKT KPREEQYNST 300
YRVVSVLTVL HQDWLNGKEY KCKVSNKALP APIEKTISKA KGQPREPQVC 350
TLPPSREEMT KNQVSLWCLV KGFYPSDIAV EWESNGQPEN NYKTTPPVLD 400
SDGSFFLVSK LTVDKSRWQQ GNVFSCSVMH EALHNHYTQK SLSLSPGK   448
```

Light chain / Chaîne légère / Cadena ligera: L-kappa anti-IL1B (L'")

```
EIVLTQSPDF QSVTPKEKVT ITCRASQSIG SDLHWYQQKP DQSPKLLIKY  50
ASQSFSGVPS RFSGSGSGTD FTLTINSLEA EDAAAYYCHQ SSSLPFTFGQ 100
GTKVEIKRTV AAPSVFIFPP SDEQLKSGTA SVVCLLNNFY PREAKVQWKV 150
DNALQSGNSQ ESVTEQDSKD STYSLSSTLT LSKADYEKHK VYACEVTHQG 200
LSSPVTKSFN RGEC                                         214
```

Post-translational modifications

Disulfide bridges location / Position des ponts disulfure / Posiciones de los puentes disulfuro

Intra-H (C23-C104) 22-96 146-202 263-321 369-427
22"-96" 145"-201" 262"-322" 368"-426"

Intra-L (C23-C104) 22'-89' 138'-197'
23'"-88'" 134'"-194'"

Inter-H-L (h 5-CL 126) 222-215' 221"-214'"

Inter-H-H (h 11, h 14) 228-227" 231-230"

Inter-H-H (CH3 C10-C5)* 356-350"

*variants 14-G1v74 (H CH3 C10) and 14-G1v75 (H" CH3 C5) creating an additional inter-H-H disulfide bond.

N-terminal glutaminyl cyclization / Cyclisation du glutaminyle N-terminal / Ciclación del glutaminilo N-terminal

Q > pyroglutamyl (pE, 5-oxoprolyl) / pyroglutamyle (pE, 5-oxoprolyle) / piroglutamilo (pE, 5-oxoprolilo)

H VH Q1: 1"

N-glycosylation sites / Sites de N-glycosylation / Posiciones de N-glicosilación

H CH2 N84.4: 299, 298"

Fucosylated complex bi-antennary CHO-type glycans / glycanes de type CHO bi-antennaires complexes fucosylés / glicanos de tipo CHO biantenarios complejos fucosilados.

C-terminal lysine clipping / Coupure de la lysine C-terminale / Recorte de lisina C-terminal

H CHS K2: 449, 448"

astepatidum

astepatide

L-tyrosyl-2-methylalanyl-L-α-glutamylglycyl-L-threonyl-L-phenylalanyl-L-threonyl-L-seryl-L-α-aspartyl-L-tyrosyl-L-seryl-L-isoleucyl-L-leucyl-L-leucyl-L-α-glutamyl-*N*^{6}-(*N*^{6}-{*N*^{6}-[*N*-(17-carboxyheptadecanoyl)-L-γ-glutamyl]-L-lysyl}-L-lysyl)-L-lysyl-L-glutaminyl-L-alanyl-L-alanyl-L-arginyl-L-α-glutamyl-L-phenylalanyl-L-isoleucyl-L-α-glutamyl-L-tryptophyl-L-leucyl-L-leucyl-L-alanylglycylglycyl-L-prolyl-L-seryl-L-serylglycyl-L-alanyl-L-prolyl-L-prolyl-L-prolyl-L-serine

gastric inhibitory polypeptide (GIP) receptor and glucagon-like peptide 1 (GLP-1) receptor agonist, antidiabetic

astépatide

L-tyrosyl-2-méthylalanyl-L-α-glutamylglycyl-L-thréonyl-L-phénylalanyl-L-thréonyl-L-séryl-L-α-aspartyl-L-tyrosyl-L-séryl-L-isoleucyl-L-leucyl-L-leucyl-L-α-glutamyl-*N*^{6}-(*N*^{6}-{*N*^{6}-[*N*-(17-carboxyheptadécanoyl)-L-γ-glutamyl]-L-lysyl}-L-lysyl)-L-lysyl-L-glutaminyl-L-alanyl-L-alanyl-L-arginyl-L-α-glutamyl-L-phénylalanyl-L-isoleucyl-L-α-glutamyl-L-tryptophyl-L-leucyl-L-leucyl-L-alanylglycylglycyl-L-prolyl-L-séryl-L-sérylglycyl-L-alanyl-L-prolyl-L-prolyl-L-prolyl-L-sérine
agoniste des récepteurs du peptide-1 similaire au glucagon (GLP-1) et du polypeptidique insulinotrope dépendant du glucose (GIP), antidiabétique

astepatida

L-tirosil-2-metilalanil-L-α-glutamilglicil-L-treonil-L-fenilalanil-L-treonil-L-seril-L-α-aspartil-L-tirosil-L-seril-L-isoleucil-L-leucil-L-leucil-L-α-glutamil-*N*^{6}-(*N*^{6}-{*N*^{6}-[*N*-(17-carboxiheptadecanoil)-L-γ-glutamil]-L-lisil}-L-lisil)-L-lisil-L-glutaminil-L-alanil-L-alanil-L-arginil-L-α-glutamil-L-fenilalanil-L-isoleucil-L-α-glutamil-L-triptofil-L-leucil-L-leucil-L-alanilglicilglicil-L-prolil-L-seril-L-serilglicil-L-alanil-L-prolil-L-prolil-L-prolil-L-serina
agonista de los receptores del péptido 1 similar al glucagón (GLP-1) y del polipéptido inhibidor gástrico (GIP), antidiabético

$C_{226}H_{348}N_{50}O_{68}$ 2959444-13-2

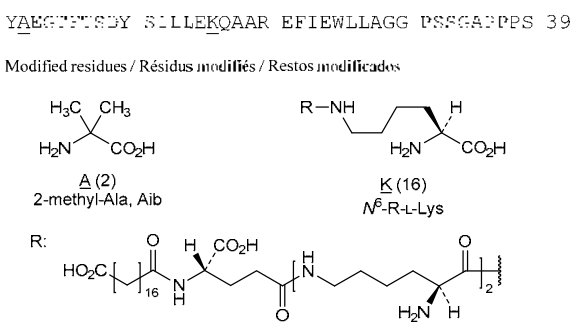

atebimetinibum

atebimetinib

4-[(dimethylamino)methyl]-3-({2-fluoro-3-[(methylsulfamoyl)amino]phenyl}methyl)-2-oxo-2*H*-1-benzopyran-7-yl dimethylcarbamate
MEK tyrosine kinase inhibitor, antineoplastic

atébimétinib

diméthylcarbamate de 4-[(diméthylamino)méthyl]-3-({2-fluoro-3-[(méthylsulfamoyl)amino]phényl}méthyl)-2-oxo-2*H*-1-benzopyran-7-yle
inhibiteur de la tyrosine kinase activée par un mitogène (MEK), antinéoplasique

atebimetinib

dimetilcarbamato de 4-[(dimetilamino)metil]-3-({2-fluoro-3-[(metilsulfamoil)amino]fenil}metil)-2-oxo-2*H*-1-benzopiran-7-ilo
inhibidor de la tirosina kinasa MEK, antineoplásico

$C_{23}H_{27}FN_4O_6S$ 2669009-92-9

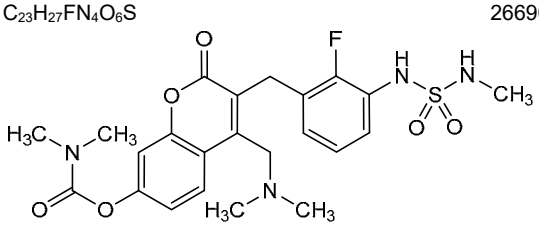

avicursenum

avicursen

all-P-ambo-2'-*O*-(2-methoxyethyl)-5-methyl-*P*-thiocytidylyl-(3'→5')-2'-*O*-(2-methoxyethyl)-5-methyl-*P*-thiouridylyl-(3'→5')-2'-*O*-(2-methoxyethyl)-*P*-thioguanylyl-(3'→5')-2'-deoxy-*P*-thioadenylyl-(3'→5')-2'-deoxy-*P*-thioguanylyl-(3'→5')-*P*-thiothymidylyl-(3'→5')-2'-deoxy-5-methyl-*P*-thiocytidylyl-(3'→5')-*P*-thiothymidylyl-(3'→5')-2'-deoxy-*P*-thioguanylyl-(3'→5')-*P*-thiothymidylyl-(3'→5')-*P*-thiothymidylyl-(3'→5')-*P*-thiothymidylyl-(3'→5')-2'-*O*-(2-methoxyethyl)-5-methyl-*P*-thiouridylyl-(3'→5')-2'-*O*-(2-methoxyethyl)-5-methyl-*P*-thiocytidylyl-(3'→5')-2'-*O*-(2-methoxyethyl)-5-methyl-*P*-thiocytidylyl-(3'→5')-2'-*O*-(2-methoxyethyl)-*P*-thioadenylyl-(3'→5')-2'-*O*-(2-methoxyethyl)-5-methyl-*P*-thiouridylyl-(3'→5')-2'-*O*-(2-methoxyethyl)-5-methyl-*P*-thiouridylyl-(3'→5')-2'-*O*-(2-methoxyethyl)-5-methyl-*P*-thiocytidylyl-(3'→5')-2'-*O*-(2-methoxyethyl)-5-methyluridine

integrin alpha-4 synthesis reducer, anti-inflammatory

avicursen

tout-P-ambo-2'-*O*-(2-méthoxyéthyl)-5-méthyl-*P*-thiocytidylyl-(3'→5')-2'-*O*-(2-méthoxyéthyl)-5-méthyl-*P*-thiouridylyl-(3'→5')-2'-*O*-(2-méthoxyéthyl)-*P*-thioguanylyl-(3'→5')-2'-désoxy-*P*-thioadénylyl-(3'→5')-2'-désoxy-*P*-thioguanylyl-(3'→5')-*P*-thiothymidylyl-(3'→5')-2'-désoxy-5-méthyl-*P*-thiocytidylyl-(3'→5')-*P*-thiothymidylyl-(3'→5')-2'-désoxy-*P*-thioguanylyl-(3'→5')-*P*-thiothymidylyl-(3'→5')-*P*-thiothymidylyl-(3'→5')-2'-*O*-(2-méthoxyéthyl)-5-méthyl-*P*-thiouridylyl-(3'→5')-2'-*O*-(2-méthoxyéthyl)-5-méthyl-*P*-thiocytidylyl-(3'→5')-2'-*O*-(2-méthoxyéthyl)-*P*-thioadénylyl-(3'→5')-2'-*O*-(2-méthoxyéthyl)-5-méthyl-*P*-thiouridylyl-(3'→5')-2'-*O*-(2-méthoxyéthyl)-5-méthyl-*P*-thiouridylyl-(3'→5')-2'-*O*-(2-méthoxyéthyl)-5-méthyl-*P*-thiocytidylyl-(3'→5')-2'-*O*-(2-méthoxyéthyl)-5-méthyluridine

réducteur de synthèse de l'intégrine alpha-4, anti-inflammatoire

avicursén

todo-P-ambo-5-metil-2'-*O*-(2-metoxietil)-*P*-tiocitidilil-(3'→5')-5-metil-2'-*O*-(2-metoxietil)-*P*-tiouridilil-(3'→5')-2'-*O*-(2-metoxietil)-*P*-tioguanilil-(3'→5')-2'-desoxi-*P*-tioadenilil-(3'→5')-2'-desoxi-*P*-tioguanilil-(3'→5')-*P*-tiotimidilil-(3'→5')-2'-desoxi-5-metil-*P*-tiocitidilil-(3'→5')-*P*-tiotimidilil-(3'→5')-2'-desoxi-*P*-tioguanilil-(3'→5')-*P*-tiotimidilil-(3'→5')-*P*-tiotimidilil-(3'→5')-*P*-tiotimidilil-(3'→5')-5-metil-2'-*O*-(2-metoxietil)-*P*-tiouridilil-(3'→5')-5-metil-2'-*O*-(2-metoxietil)-*P*-tiocitidilil-(3'→5')-5-metil-2'-*O*-(2-metoxietil)-*P*-tiocitidilil-(3'→5')-2'-*O*-(2-metoxietil)-*P*-tioadenilil-(3'→5')-5-metil-2'-*O*-(2-metoxietil)-*P*-tiouridilil-(3'→5')-5-metil-2'-*O*-(2-metoxietil)-*P*-tiouridilil-(3'→5')-5-metil-2'-*O*-(2-metoxietil)-*P*-tiocitidilil-(3'→5')-5-metil-2'-*O*-(2-metoxietil)uridina

inhibidor de la integrina alfa 4, antiinflamatorio

$C_{233}H_{327}N_{60}O_{129}P_{19}S_{19}$ 350263-41-1

m^5Cmoe=m^5Umoe=Gmoe=dA=dG=dT=m^5C_d=dT=dG=dT=dT=dT=m^5Umoe=m^5Cmoe=m^5Cmoe=Amoe=m^5Umoe=m^5Umoe=m^5Cmoe=m^5Umoe

N : nucleoside / nucléoside / nucleósido
m^5N : 5-methyl-N / 5-méthyl-N / 5-metil-N
dN & N_d : 2'-deoxy-N / 2'-désoxy-N / 2'-desoxi-N
Nmoe : 2'-*O*-methoxyethyl-N / 2'-*O*-méthoxyéthyl-N / 2'-*O*-metoxietil-N

=: -PO(SH)-

balekafuspum alfa #

balekafusp alfa

humanized immunoglobulin G1-kappa, anti-[human interleukin-2 (IL-2, T-cell growth factor, TCGF)] with an engineered kappa light chain, where a circular permuted form of human interleukin-2 is inserted within CDR-L1 between Y^{31} (Kabat L.27D) and D^{34} (Kabat L.30), Q^{32}>del (Kabat L.28), G^{33}>del (Kabat L.29) through ^{32}GGG^{34} and ^{167}GGGG^{170} linkers;
gamma 1 heavy chain (1-451) [VH (*Homo sapiens* IGHV5-51*01 -(IGHD) -IGHJ3*01, CDR-Kabat [5.17.12] (31-35.50-66.99-110)) (1-121) -*Homo sapiens* IGHG1*03 (CH1 (122-219), hinge (220-234), CH2 N>^{301}A (235-344), CH3 (345-449), CHS (450-451)) (122-451)]-disulfide with partial kappa light chain fused to a circular permuted form of human interleukin-2 (1'-355') [partial V-KAPPA (*Homo sapiens* IGKV1-39*01, CDR-Kabat [8] (partial CDR-L1: Kabat L.24-L.27D) (24'-31')) (1'-31')] fused via peptide linker $^{32'}$GGG$^{34'}$ to human interleukin-2 (IL-2, T-cell growth factor (TCGF)) in a permuted form (C-terminal fragment 77-133 (35'-91' in the current sequence) fused to the N-terminal fragment 2-76 (92'-166' in the current sequence)), variant (^{125}C>S$^{83'}$), fused via peptide linker $^{167'}$GGGG$^{170'}$ to a partial kappa light chain [V-KAPPA (*Homo sapiens* IGKV1-39*01 -IGKJ4*01, CDR-Kabat [5.7.9] (partial CDR-L1: Kabat L.30-L.34) (171'-175'.191'-197'.230'-238')) (171'-248') -*Homo sapiens* IGKC*01 (249'-355')]; dimer (230-230'':233-233'')-bisdisulfide, produced in Chinese hamster ovary (CHO) cells, cell line CHO-K1, glycoform alfa
antineoplastic

balékafusp alfa

immunoglobuline humanisée G1-kappa, anti-[interleukine-2 humaine (IL-2, facteur de croissance des lymphocytes T (FCLT)], avec une chaîne légère kappa recombinée, dans laquelle une forme circulaire permutée d'interleukine-2 humaine est insérée dans le CDR-L1 entre Y^{31} (Kabat L.27D) et D^{34} (Kabat L.30), Q^{32}>dél (Kabat L.28), G^{33}>dél (Kabat L.29) jusqu'aux coupleurs ^{32}GGG34 et ^{167}GGGG^{170};
chaîne lourde gamma 1 (1-451) [VH (*Homo sapiens* IGHV5-51*01 -(IGHD) -IGHJ3*01, CDR-Kabat [5.17.12] (31-35.50-66.99-110)) (1-121) -*Homo sapiens* IGHG1*03 (CH1 (122-219), charnière (220-234), CH2 N>^{301}A (235-344), CH3 (345-449), CHS (450-451)) (122-451)] -disulfure avec la chaîne légère partielle, fusionnée avec une forme circulaire permutée de l'interleukine-2 humaine (1'-355') [V-KAPPA partielle (*Homo sapiens* IGKV1-39*01, CDR-Kabat [8] (CDR-L1 partiel: Kabat L.24-L.27D) (24'-31')) (1'-31')] fusionnée à l'aide d'un coupleur peptidique $^{32'}$GGG$^{34'}$ au fragment de l'interleukine-2 humaine (IL-2, facteur de croissance des lymphocytes T (FCLT)), dans sa forme permutée (fragment C-terminal 77-133 (35'-91' dans la séquence en cours) fusionné au fragment N-terminal 2-76 (92'-166' de la séquence en cours)), variante (^{125}C>S$^{83'}$), fusionné à l'aide du coupleur peptidique $^{167'}$GGGG$^{170'}$ à la chaîne légère kappa partielle [V-KAPPA (*Homo sapiens* IGKV1-39*01 -IGKJ4*01, CDR-Kabat [5.7.9] (CDR-L1 partiel: Kabat L.30-L.34) (171'-175'.191'-197'.230'-238') (171'-248') -*Homo sapiens* IGKC*01 (249'-355')]; dimère (230-230'':233-233'')-bisdisulfure, produit dans des cellules ovariennes de hamster chinois (CHO), lignée cellulaire CHO-K1, glycoforme alfa
antinéoplasique

balekafusp alfa

inmunoglobulina humanizada G1-kappa, anti-[interleukina-2 humana (IL-2, factor de crecimiento de céulas T, TCGF)] con una cadena ligera kappa manipulada, donde una forma circular permutada de una interleukina-2 human se insera en CDR-L1 entre Y^{31} (Kabat L.27D) y D^{34} (Kabat L.30), Q^{32}>del (Kabat L.28), G^{33}>del (Kabat L.29) a través de enlaces ^{32}GGG^{34} y ^{167}GGGG^{170};
cadena pesada gamma 1(1-451) [VH (*Homo sapiens* IGHV5-51*01 -(IGHD) -IGHJ3*01, CDR-Kabat [5.17.12] (31-35.50-66.99-110)) (1-121) -*Homo sapiens* IGHG1*03 (CH1 (122-219), bisagra (220-234), CH2 N>^{301}A (235-344), CH3 (345-449), CHS (450-451)) (122-451)]-disulfuro con una cadena ligera kappa parcial fusionada a una forma permutada circular de interleukina-2 humana (1'-355') [parcial V-KAPPA (*Homo sapiens* IGKV1-39*01, CDR-Kabat [8] (parcial CDR-L1: Kabat L.24-L.27D) (24'-31')) (1'-31')] fusionada a través de un enlace peptídico $^{32'}$GGG$^{34'}$ a una interleukina-2 humana (IL-2, factor de crecimiento de células T (TCGF)) en una forma permutada (C-terminal fragmento 77-133 (35'-91' en la secuencia actual) fusionada al fragmento N-terminal 2-76 (92'-166' en la secuencia actual)), variante (^{125}C>S$^{83'}$), fusionada a través de enlace peptídico $^{167'}$GGGG$^{170'}$ a una cadena ligera kappa parcial [V-KAPPA (*Homo sapiens* IGKV1-39*01 -IGKJ4*01, CDR-Kabat [5.7.9] (parcial CDR-L1: Kabat L.30-L.34) (171'-175'.191'-197'.230'-238')) (171'-248') -*Homo sapiens* IGKC*01 (249'-355')]; dímero (230-230'':233-233'')-bisdisulfuro, producido en células ováricas de hamster Chino (CHO) K1, glicoforma alfa

antineoplásico

2866185-77-3

Sequence / Séquence / Secuencia

IgG1 heavy chain

```
EVQLVQSGAE VKKPGESLKI SCKGSGYAFT NYLIEWVRQM PGKGLEWMGV   50
INPGSGGTNY NEKFKGQVTI SADKSISTAY LQWSSLKASD TAMYYCARWR  100
GEGYYAYFDV WGQGTTVTVS SASTKGPSVF PLAPSSKSTS GGTAALGCLV  150
KDYFPEPVTV SWNSGALTSG VHTFPAVLQS SGLYSLSSVV TVPSSSLGTQ  200
TYICNVNHKP SNTKVDKRVE PKSCDKTHTC PPCPAPELLG GPSVFLFPPK  250
PKDTLMISRT PEVTCVVVDV SHEDPEVKFN WYVDGVEVHN AKTKPREEQY  300
ASTYRVVSVL TVLHQDWLNG KEYKCKVSNK ALPAPIEKTI SKAKGQPREP  350
QVYTLPPSRE EMTKNQVSLT CLVKGFYPSD IAVEWESNGQ PENNYKTTPP  400
VLDSDGSFFL YSKLTVDKSR WQQGNVFSCS VMHEALHNHY TQKSLSLSPG  450
K                                                        451
```

IgG1 light chain-permuted IL-2

```
AIRLTQSPSS FSASTGDRVT ITCKASQSVD YGGGNFHLRP RDLISNINVI   50
VLELKGSETT FMCEYADETA TIVEFLNRWI TFSQSIISTL TPTSSSTKKT  100
QLQLEHLLLD LQMILNGINN YKNPKLTRML TFKFYMPKKA TELKHLQCLE  150
EELKPLEEVL NLAQSKGGGG DSYMNWYQQK PGKAPKLLIY AASNLESGVP  200
SRFSGSGSGT DFTLTISSLQ SEDFATYYCQ QSNEDPYTFG GGTKVEIKRT  250
VAAPSVFIFP PSDEQLKSGT ASVVCLLNNF YPREAKVQWK VDNALQSGNS  300
QESVTEQDSK DSTYSLSSTL TLSKADYEKH KVYACEVTHQ GLSSPVTKSF  350
NRGEC                                                    355
```

Mutations / Mutations / Mutaciónes

N^{301}>A, $^{125'}$C>S$^{83'}$

Peptide linker / Peptide liant / Péptido de unión

$^{32'}$GGG$^{34'}$, $^{167'}$GGGG$^{170'}$

Post-translational modifications

Disulfide bridges location / Position des ponts disulfure / Posiciones de los puentes disulfuro

Intra IgG1 heavy chain: 22-96, 148-204, 265-325, 371-429,
22''-96'', 148''-204'', 265''-325'', 371''-429''

Intra IgG1 light chain-IL-2: 23'-229', 63'-148', 275'-335', 23'''-229''', 63'''-148''', 275'''-335'''

Inter IgG1 heavy chain-light chain-IL-2: 224-355', 224''-355'''

Inter IgG1 heavy chain-heavy chain: 230-233, 230''-233''

O-glycosylation sites / Sites de O-glycosylation / Posiciones de O-glicosilación

T93', T93'''

C-terminal lysine clipping / Coupure de la lysine C-terminale / Recorte de lisina C-terminal

IgG1 heavy chain: 451, 451''

balertatugum #

balertatug — immunoglobulin G1-kappa, anti-[*Homo sapiens* CD70 (tumor necrosis factor superfamily member 7, TNFSF7, CD27LG, CD27L)], monoclonal antibody;
H-gamma1 heavy chain (1-448) [VH (*Homo sapiens* IGHV1-2*02 (86.7%) -(IGHD) -IGHJ4*01 (92.3%) L123>T (113), CDR-IMGT [8.8.11] (26-33.51-58.97-107)) (1-118) -*Homo sapiens* IGHG1*01 (100%) G1m17,1 CH1 K120, CH3 D12, L14 (CH1 K120 (215) (119-216), hinge 1-15 (217-231), CH2 (232-341), CH3 D12 (357), L14 (359) (342-446), CHS (447-448)) (119-448)], (221-218')-disulfide with L-kappa light chain (1'-218') [V-KAPPA Musmus/Homsap (*Mus musculus* IGKV3-12*01 (84.8%) -IGKJ1*01 (83.3%) G120>Q (104') , L124>V (108')/*Homo sapiens* IGKV4-1*01 (79.2%) -IGKJ1*01 (100%), CDR-IMGT [10.3.9] (27'-36'.54'-56'.93'-101')) (1'-111') -*Homo sapiens* IGKC*01 (100%) Km3 A45.1, V101 (C-KAPPA A45.1 (157'), V101 (195')) (112'-218')]; dimer (227-227'':230-230'')-bisdisulfide, produced in a cell line from Chinese hamster ovary (CHO) cells, derived from the cell line CHO-K1, glycoform alfa
antineoplastic

balertatug — immunoglobuline G1-kappa, anti-[*Homo sapiens* CD70 (membre 7 de la superfamille du facteur de nécrose tumorale (TNF), TNFSF7, CD27LG, CD27L)], anticorps monoclonal;
chaîne lourde H-gamma1 (1-448) [VH (*Homo sapiens* IGHV1-2*02 (86.7%) -(IGHD) -IGHJ4*01 (92.3%) L123>T (113), CDR-IMGT [8.8.11] (26-33.51-58.97-107)) (1-118) -*Homo sapiens* IGHG1*01 (100%) G1m17,1 CH1 K120, CH3 D12, L14 (CH1 K120 (215) (119-216), charnière 1-15 (217-231), CH2 (232-341), CH3 D12 (357), L14 (359) (342-446), CHS (447-448)) (119-448)], (221-218')-disulfure avec la chaîne légère L-kappa (1'-218') [V-KAPPA Musmus/Homsap (*Mus musculus* IGKV3-12*01 (84.8%) -IGKJ1*01 (83.3%) G120>Q (104') , L124>V (108')/*Homo sapiens* IGKV4-1*01 (79.2%) -IGKJ1*01 (100%), CDR-IMGT [10.3.9] (27'-36'.54'-56'.93'-101')) (1'-111') -*Homo sapiens* IGKC*01 (100%) Km3 A45.1, V101 (C-KAPPA A45.1 (157'), V101 (195')) (112'-218')]; dimère (227-227'':230-230'')-bisdisulfure, produit dans une lignée cellulaire des cellules ovariennes de hamster chinois (CHO), dérivant de la lignée cellulaire CHO-K1, glycoforme alfa
antinéoplasique

balertatug — inmunoglobulina G1-kappa, anti-[*Homo sapiens* CD70 (miembro 7 de la superfamilia del factor de necrosis tumoral (TNF), TNFSF7, CD27LG, CD27L)], anticuerpo monoclonal;
cadena pesada H-gamma1 (1-448) [VH (*Homo sapiens* IGHV1-2*02 (86.7%) -(IGHD) -IGHJ4*01 (92.3%) L123>T (113), CDR-IMGT [8.8.11] (26-33.51-58.97-107)) (1-118) -*Homo sapiens* IGHG1*01 (100%) G1m17,1 CH1 K120, CH3 D12, L14 (CH1 K120 (215) (119-216), bisagra 1-15 (217-231), CH2 (232-341), CH3 D12 (357), L14 (359) (342-446), CHS (447-448)) (119-448)], (221-218')-disulfuro con la cadena ligera L-kappa (1'-218') [V-KAPPA Musmus/Homsap (*Mus musculus* IGKV3-12*01 (84.8%) -IGKJ1*01 (83.3%) G120>Q (104') , L124>V (108')/*Homo sapiens* IGKV4-1*01 (79.2%) -IGKJ1*01 (100%), CDR-IMGT [10.3.9] (27'-36'.54'-56'.93'-101')) (1'-111') -*Homo sapiens* IGKC*01 (100%) Km3 A45.1, V101 (C-KAPPA A45.1 (157'), V101 (195')) (112'-218')]; dímero (227-227'':230-230'')-bisdisulfuro, producido en una línea celular de las células ováricas de hámster chino (CHO), línea celular derivada de CHO-K1, forma glicosilada alfa
antineoplásico

3010940-29-8

Heavy chain / Chaîne lourde / Cadena pesada

```
QVQLVQSGAE VKKPGASVKV SCKASGYTFT NYGMNWVRQA PGQGLKWMGW  50
INTYTGEPTY ADAFKGRVTM TRDTSISTAY MELSRLRSDD TAVYYCARDY 100
GDYGMDYWGQ GTTVTVSSAS TKGPSVFPLA PSSKSTSGGT AALGCLVKDY 150
FPEPVTVSWN SGALTSGVHT FPAVLQSSGL YSLSSVVTVP SSSLGTQTYI 200
CNVNHKPSNT KVDKKVEPKS CDKTHTCPPC PAPELLGGPS VFLFPPKPKD 250
TLMISRTPEV TCVVVDVSHE DPEVKFNWYV DGVEVHNAKT KPREEQYNST 300
YRVVSVLTVL HQDWLNGKEY KCKVSNKALP APIEKTISKA KGQPREPQVY 350
TLPPSRDELT KNQVSLTCLV KGFYPSDIAV EWESNGQPEN NYKTTPPVLD 400
SDGSFFLYSK LTVDKSRWQQ GNVFSCSVMH EALHNHYTQK SLSLSPGK   448
```

Light chain / Chaîne légère / Cadena ligera

```
DIVMTQSPDS LAVSLGERAT INCRASKSVS TSGYSFMHWY QQKPGQPPKL  50
LIYLASNLES GVPDRFSGSG SGTDFTLTIS SLQAEDVAVY YCQHSREVPW 100
TFGQGTKVEI KRTVAAPSVF IFPPSDEQLK SGTASVVCLL NNFYPREAKV 150
QWKVDNALQS GNSQESVTEQ DSKDSTYSLS STLTLSKADY EKHKVYACEV 200
THQGLSSPVT KSFNRGEC                                    218
```

Post-translational modifications

Disulfide bridges location / Position des ponts disulfure / Posiciones de los puentes disulfuro

Intra-H (C23-C104) 22-96 145-201 262-322 368-426
22"-96" 145"-201" 262"-322" 368"-426"
Intra-L (C23-C104) 23'-92' 138'-198'
23'"-92'" 138'"-198'"
Inter-H-L (h 5-CL 126) 221-218' 221"-218'"
Inter-H-H (h 11, h 14) 227-227" 230-230"

N-terminal glutaminyl cyclization / Cyclisation du glutaminyle N-terminal / Ciclación del glutaminilo N-terminal

Q > pyroglutamyl (pE, 5-oxoprolyl) / pyroglutamyle (pE, 5-oxoprolyle) / piroglutamilo (pE, 5-oxoprolilo)

H VH Q1: 1, 1"

N-glycosylation sites / Sites de N-glycosylation / Posiciones de N-glicosilación

H CH2 N84.4: 298, 298"

Fucosylated complex bi-antennary CHO-type glycans / glycanes de type CHO bi-antennaires complexes fucosylés / glicanos de tipo CHO biantenarios complejos fucosilados

C-terminal lysine clipping / Coupure de la lysine C-terminale / Recorte de lisina C-terminal

H CHS K2: 448, 448"

balomenibum

balomenib — 4-methyl-1-{[(2*S*)-5-oxomorpholin-2-yl]methyl}-5-({2-[6-(2,2,2-trifluoroethyl)quinazolin-4-yl]-2,7-diazaspiro[3.5]nonan-7-yl}methyl)-1*H*-indole-2-carbonitrile
menin inhibitor, antineoplastic

baloménib — 4-méthyl-1-{[(2S)-5-oxomorpholin-2-yl]méthyl}-5-({2-[6-(2,2,2-trifluoroéthyl)quinazolin-4-yl]-2,7-diazaspiro[3.5]nonan-7-yl}méthyl)-1*H*-indole-2-carbonitrile
inhibiteur de la ménine, antinéoplasique

balomenib — 4-metil-1-{[(2S)-5-oxomorfolin-2-il]metil}-5-({2-[6-(2,2,2-trifluoroetil)quinazolin-4-il]-2,7-diazaespiro[3.5]nonan-7-il}metil)-1*H*-indol-2-carbonitrilo
inhibidor de la menina, antineoplásico

$C_{33}H_{34}F_3N_7O_2$ 2939850-17-4

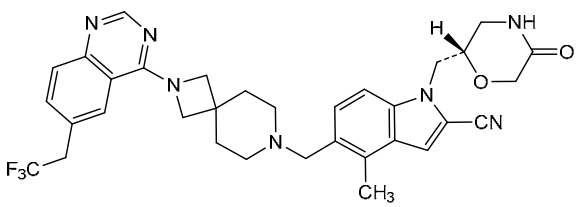

baloncibartum #

baloncibart	immunoglobulin G4-kappa, anti-[*Homo sapiens* NPR1 (natriuretic peptide receptor 1, natriuretic peptide receptor A, NPRA, atrionatriuretic peptide receptor A, ANPRA, guanylate cyclase A, GUCY2A)], *Homo sapiens* monoclonal antibody; H-gamma4 heavy chain *Homo sapiens* (1-447) [VH (*Homo sapiens* IGHV3-23*04 (89.6%) -(IGHD) -IGHJ4*01 (100%), CDR-IMGT [8.8.13] (26-33.51-58.97-109)) (1-120) -*Homo sapiens* IGHG4*01, *nG4m(a)* CH2 L92, 12-G4v5 h P10 (CH1 (121-218), hinge 1-12 S10>P (228) (219-230), CH2 L92 (309) (231-340), CH3 (341-445), CHS (446-447)) (121-447)], (134-214')-disulfide with L-kappa light chain *Homo sapiens* (1'-214') [V-KAPPA (*Homo sapiens* IGKV1-6*01 (93.7%) -IGKJ3*01 (100%), CDR-IMGT [6.3.9] (27'-32'.50'-52'.89'-97')) (1'-07') -*Homo sapiens* IGKC*01 (100%) Km3 A45.1, V101 (C-KAPPA A45.1 (153'), V101 (191')) (108'-214')]; dimer (226-226'':229-229'')-bisdisulfide, produced in Chinese hamster ovary (CHO) cells, cell line CHO-K1, glycoform alfa *antihypotensive*
baloncibart	immunoglobuline G4-kappa, anti-[*Homo sapiens* NPR1 (récepteur 1 du peptide natriurétique, récepteur A du peptide natriurétique, NPRA, récepteur A du peptide atrionatriurétique, ANPRA, guanylate cyclase A, GUCY2A)], anticorps monoclonal *Homo sapiens*; chaîne lourde H-gamma4 *Homo sapiens* (1-447) [VH (*Homo sapiens* IGHV3-23*04 (89.6%) -(IGHD) -IGHJ4*01 (100%), CDR-IMGT [8.8.13] (26-33.51-58.97-109)) (1-120) -*Homo sapiens* IGHG4*01, *nG4m(a)* CH2 L92, 12-G4v5 h P10 (CH1 (121-218), charnière 1-12 S10>P (228) (219-230), CH2 L92 (309) (231-340), CH3 (341-445), CHS (446-447)) (121-447)], (134-214')-disulfure avec la chaîne légère L-kappa *Homo sapiens* (1'-214') [V-KAPPA (*Homo sapiens* IGKV1-6*01 (93.7%) -IGKJ3*01 (100%), CDR-IMGT [6.3.9] (27'-32'.50'-52'.89'-97')) (1'-07') -*Homo sapiens* IGKC*01 (100%) Km3 A45.1, V101 (C-KAPPA A45.1 (153'), V101 (191')) (108'-214')]; dimère (226-226'':229-229'')-bisdisulfure, produit dans des cellules ovariennes de hamster chinois (CHO), lignée cellulaire CHO-K1, glycoforme alfa *antihypotenseur*
baloncibart	inmunoglobulina G4-kappa, anti-[*Homo sapiens* NPR1 (receptor 1 del péptido natriurético, receptor A del péptido natriurético, NPRA, receptor A del péptido atrionatriurético ANPRA, guanilato ciclasa A, GUCY2A)], anticuerpo monoclonal *Homo sapiens*; cadena pesada H-gamma4 *Homo sapiens* (1-447) [VH (*Homo sapiens* IGHV3-23*04 (89.6%) -(IGHD) -IGHJ4*01 (100%), CDR-IMGT [8.8.13] (26-33.51-58.97-109)) (1-120) -*Homo sapiens* IGHG4*01, *nG4m(a)* CH2 L92, 12-G4v5 h P10 (CH1 (121-218), bisagra 1-12 S10>P (228) (219-230), CH2 L92 (309) (231-340), CH3 (341-445), CHS (446-447)) (121-447)], (134-214')-disulfuro con la cadena ligera L-kappa *Homo sapiens* (1'-214') [V-KAPPA (*Homo sapiens* IGKV1-6*01 (93.7%) -IGKJ3*01 (100%), CDR-IMGT [6.3.9] (27'-32'.50'-52'.89'-97')) (1'-07') -*Homo sapiens* IGKC*01 (100%) Km3 A45.1, V101 (C-KAPPA A45.1 (153'), V101 (191')) (108'-214')]; dímero (226-226'':229-229'')-bisdisulfuro, producido en las células ováricas de hámster chino (CHO), línea celular CHO-K1, forma glicosilada alfa *antihipotensor*

2988795-75-9

Heavy chain / Chaîne lourde / Cadena pesada

```
EVQLVESGGG LVQPGGSLRL SCAASGFSFV SYVMGWVRQA PGKGLEWVSS  50
ISGSLTNTYY ADPVKGRFTI SRDNSKNTLY LQMNSLRAED TAAYYCVTYD 100
ILTGHLFDYW GQGTLVTVSS ASTKGPSVFP LAPCSRSTSE STAALGCLVK 150
DYFPEPVTVS WNSGALTSGV HTFPAVLQSS GLYSLSSVVT VPSSSLGTKT 200
YTCNVDHKPS NTKVDKRVES KYGPPCPPCP APEFLGGPSV FLFPPKPKDT 250
LMISRTPEVT CVVVDVSQED PEVQFNWYVD GVEVHNAKTK PREEQFNSTY 300
RVVSVLTVLH QDWLNGKEYK CKVSNKGLPS SIEKTISKAK GQPREPQVYT 350
LPPSQEEMTK NQVSLTCLVK GFYPSDIAVE WESNGQPENN YKTTPPVLDS 400
DGSFFLYSRL TVDKSRWQEG NVFSCSVMHE ALHNHYTQKS LSLSLGK    447
```

Light chain / Chaîne légère / Cadena ligera

```
AIQMTQSPSS LSASVGDRVT ITCRSSQGIR NDFGWYQQKP GKAPKLLIYA  50
ASRLQSGVPS RFSGSGSGTD FTLTINNLQP EDFATYYCLQ DYTYPFTFGP 100
GTKVDIKRTV AAPSVFIFPP SDEQLKSGTA SVVCLLNNFY PREAKVQWKV 150
DNALQSGNSQ ESVTEQDSKD STYSLSSTLT LSKADYEKHK VYACEVTHQG 200
LSSPVTKSFN RGEC                                        214
```

Post-translational modifications

Disulfide bridges location / Position des ponts disulfure / Posiciones de los puentes disulfuro

Intra-H (C23-C104) 22-96 147-203 261-321 367-425
22"-96" 147"-203" 261"-321" 367"-425"
Intra-L (C23-C104) 23'-88' 134'-194'
23'"-88'" 134'"-194'"
Inter-H-L (CH1 10-CL 126) 134-214' 134"-214'"
Inter-H-H (h 8, h 11) 226-226" 229-229"

N-glycosylation sites / Sites de N-glycosylation / Posiciones de N-glicosilación
H CH2 N84.4: 297, 297"
Fucosylated complex bi-antennary CHO-type glycans / glycanes de type CHO bi-antennaires complexes fucosylés / glicanos de tipo CHO biantenarios complejos fucosilados

C-terminal lysine clipping / Coupure de la lysine C-terminale / Recorte de lisina C-terminal
H CHS K2: 447, 447"

baluretgenum parvecum #

baluretgene parvec — recombinant non-replicating adeno-associated virus serotype 5 (rAAV5) vector encoding human photoreceptor-specific nuclear hormone receptor subfamily 2, group E member 3 (NR2E3) under control of the CAG promoter (CMV enhancer / chicken beta-actin (CBA) promoter / chimeric intron) and a simian virus 40 (SV40) polyadenylation signal; flanked by AAV2 inverted terminal repeats
gene therapy (Leber's hereditary optic neuropathy)

baluretgène parvec — vecteur recombinant de virus adéno-associé non réplicatif de sérotype 5 (rAAV5) codant le membre 3 du groupe E de la sous-famille 2 de récepteurs d'hormones nucléaires spécifiques aux photorécepteurs humains (NR2E3), sous le contrôle du promoteur CAG (amplificateur du CMV / promoteur de la bêta-actine de poulet (CBA) / intron chimérique), et un signal de polyadénylation du virus simien 40 (SV40); flanqué des répétitions terminales inversées AAV2
thérapie génique (neuropathie optique héréditaire de Leber)

baluretgén parvec — vector de virus adenoasociado del serotipo 5, recombinante (rAAV5), no replicativo, que codifica el miembro 3 del grupo E de la subfamilia 2 del receptor nuclear de hormona específico de fotorreceptores (NR2E3) humano bajo el control del promotor CAG (potenciador de CMV / promotor de la beta actina de pollo (CBA) / intrón quimérico) y una señal de poliadenilación del virus simio 40 (SV40); flanqueado por las repeticiones terminales invertidas del AAV2
terapia génica (neuropatía óptica hereditaria de Leber)

2964417-29-4

becondogrelum

becondogrel — methyl (*S*)-(2-chlorophenyl)[(7a*S*)-2-oxo-2,6,7,7a-tetrahydrothieno[3,2-*c*]pyridin-5(4*H*)-yl]acetate
platelet aggregation inhibitor

bécondogrel — (*S*)-(2-chlorophényl)[(7a*S*)-2-oxo-2,6,7,7a-tétrahydrothiéno[3,2-*c*]pyridin-5(4*H*)-yl]acétate de méthyle
antiagrégant plaquettaire

becondogrel — (*S*)-(2-clorofenil)[(7a*S*)-2-oxo-2,6,7,7a-tetrahidrotieno[3,2-*c*]piridin-5(4*H*)-il]acetato de metilo
inhibidor de la agregación plaquetaria

$C_{16}H_{16}ClNO_3S$ 1416696-44-0

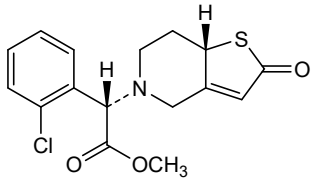

besufetamigum #

besufetamig — immunoglobulin (H-gamma1_L-kappa)_(H-gamma1_L-kappa), anti-[*Homo sapiens* PDCD1 (programmed cell death 1, PD-1, PD1, CD279)] and anti-[*Homo sapiens* CD3E (CD3 epsilon, Leu-4)], *Homo sapiens* monoclonal antibody, bispecific;
H-gamma1 heavy chain anti-PDCD1 *Homo sapiens* (1-456) [VH (*Homo sapiens* IGHV7-4-1*02 (90.8%) -(IGHD) -IGHJ3*01 (92.3%) M123>T (122), CDR-IMGT [8.8.20] (26-33.51-58.97-116)) (1-127) -*Homo sapiens* IGHG1*03 G1m3, nG1m1 CH1 R120, CH3 E12, M14, 6-G1v59-1 CH2 G1.2, R1.1, 14-G1v72 CH3 D7, E24 (CH1 R120 (224) (128-225), hinge 1-15 (226-240), CH2 L1.2>G (245), G1.1>R (246) (241-350), CH3 L7>D (361), E12 (366), M14 (368), L24>E (378) (351-455), CHS K2>del (456)) (128-456)], (230-214')-disulfide with common L-kappa light chain *Homo sapiens* (1'-214') [V-KAPPA (*Homo sapiens* IGKV1-39*01 (100%) -IGKJ1*01 (100%), CDR-IMGT [6.3.9] (27'-32'.50'-52'.89'-97')) (1'-107') -*Homo sapiens* IGKC*01 (100%) Km3 A45.1, V101 (C-KAPPA A45.1 (153'), V101 (191')) (108'-214')];
H-gamma1 heavy chain anti-CD3E *Homo sapiens* (1''-447'') [VH (*Homo sapiens* IGHV3-30-5*03 (88.8%) -(IGHD) -IGHJ5*02 (100%), CDR-IMGT [8.8.11] (26''-33''.51''-58''.97''-107'')) (1''-118'') -*Homo sapiens* IGHG1*03 G1m3, nG1m1 CH1 R120, CH3 E12, M14, 6-G1v59-1 CH2 G1.2, R1.1, 14-G1v73 CH3 K7, K22 (CH1 R120 (215) (119''-216''), hinge 1-15 (217'', 231''), CH2 L1.2>G (236''), G1.1>R (237'') (232''-341''), CH3 L7>K (352''), E12 (357''), M14 (359''), T22>K (367'') (342''-446''), CHS K2>del (447'')) (119''-447'')], (221''-214''')-disulfide with common L-kappa light chain *Homo sapiens* (1'''-214''') [V-KAPPA (*Homo sapiens* IGKV1-39*01 (100%) -IGKJ1*01 (100%), CDR-IMGT [6.3.9] (27'''-32'''.50'''-52'''.89'''-97''')) (1'''-107''') -*Homo sapiens* IGKC*01 (100%) Km3 A45.1, V101 (C-KAPPA A45.1 (153'''), V101 (191''')) (108'''-214''')]; dimer (236-227'': 239-230'')-bisdisulfide, produced in Chinese hamster ovary (CHO) cells, cell line CHO-DG44, glycoform alfa
immunosuppressant, antineoplastic

bésufétamig	immunoglobuline (H-gamma1_L-kappa)_(H-gamma1_L-kappa), anti-[*Homo sapiens* PDCD1 (protéine 1 de mort cellulaire programmée, PD-1, PD1, CD279)] et anti-[*Homo sapiens* CD3E (CD3 epsilon, Leu-4)], anticorps monoclonal *Homo sapiens*, bispécifique; chaîne lourde H-gamma1 anti-PDCD1 *Homo sapiens* (1-456) [VH (*Homo sapiens* IGHV7-4-1*02 (90.8%) -(IGHD) -IGHJ3*01 (92.3%) M123>T (122), CDR-IMGT [8.8.20] (26-33.51-58.97-116)) (1-127) -*Homo sapiens* IGHG1*03 G1m3, nG1m1 CH1 R120, CH3 E12, M14, 6-G1v59-1 CH2 G1.2, R1.1, 14-G1v72 CH3 D7, E24 (CH1 R120 (224) (128-225), charnière 1-15 (226-240), CH2 L1.2>G (245), G1.1>R (246) (241-350), CH3 L7>D (361), E12 (366), M14 (368), L24>E (378) (351-455), CHS K2>del (456)) (128-456)], (230-214')-disulfure avec la chaîne légère commune L-kappa *Homo sapiens* (1'-214') [V-KAPPA (*Homo sapiens* IGKV1-39*01 (100%) -IGKJ1*01 (100%), CDR-IMGT [6.3.9] (27'-32'.50'-52'.89'-97')) (1'-107') -*Homo sapiens* IGKC*01 (100%) Km3 A45.1, V101 (C-KAPPA A45.1 (153'), V101 (191')) (108'-214')]; chaîne lourde H-gamma1 anti-CD3E *Homo sapiens* (1''-447'') [VH (*Homo sapiens* IGHV3-30-5*03 (88.8%) -(IGHD) -IGHJ5*02 (100%), CDR-IMGT [8.8.11] (26''-33''.51''-58''.97''-107'')) (1''-118'') -*Homo sapiens* IGHG1*03 G1m3, nG1m1 CH1 R120, CH3 E12, M14, 6-G1v59-1 CH2 G1.2, R1.1, 14-G1v73 CH3 K7, K22 (CH1 R120 (215) (119''-216''), charnière 1-15 (217'', 231''), CH2 L1.2>G (236''), G1.1>R (237'') (232''-341''), CH3 L7>K (352''), E12 (357''), M14 (359''), T22>K (367'') (342''-446''), CHS K2>del (447'')) (119''-447'')], (221''-214''')-disulfure avec la chaîne légère commune L-kappa *Homo sapiens* (1'''-214''') [V-KAPPA (*Homo sapiens* IGKV1-39*01 (100%) -IGKJ1*01 (100%), CDR-IMGT [6.3.9] (27'''-32'''.50'''-52'''.89'''-97''')) (1'''-107''') -*Homo sapiens* IGKC*01 (100%) Km3 A45.1, V101 (C-KAPPA A45.1 (153'''), V101 (191''')) (108'''-214''')]; dimère (236-227'': 239-230'')-bisdisulfure, produit dans des cellules ovariennes de hamster chinois (CHO), lignée cellulaire CHO-DG44, glycoforme alfa *immunosuppresseur, antinéoplasique*
besufetamig	inmunoglobulina (H-gamma1_L-kappa)_(H-gamma1_L-kappa), anti-[*Homo sapiens* PDCD1 (proteína 1 de muerte celular programada, PD-1, PD1, CD279)] y anti-[*Homo sapiens* CD3E (CD3 épsilon, Leu-4)], anticuerpo monoclonal *Homo sapiens*, biespecífico; cadena pesada H-gamma1 anti-PDCD1 *Homo sapiens* (1-456) [VH (*Homo sapiens* IGHV7-4-1*02 (90.8%) -(IGHD) -IGHJ3*01 (92.3%) M123>T (122), CDR-IMGT [8.8.20] (26-33.51-58.97-116)) (1-127) -*Homo sapiens* IGHG1*03 G1m3, nG1m1 CH1 R120, CH3 E12, M14, 6-G1v59-1 CH2 G1.2, R1.1, 14-G1v72 CH3 D7, E24 (CH1 R120 (224) (128-225), bisagra 1-15 (226-240), CH2 L1.2>G (245), G1.1>R (246) (241-350), CH3 L7>D (361), E12 (366), M14 (368), L24>E (378) (351-455), CHS K2>del (456)) (128-456)], (230-214')-disulfuro con la cadena ligera común L-kappa *Homo sapiens* (1'-214') [V-KAPPA (*Homo sapiens* IGKV1-39*01 (100%) -IGKJ1*01 (100%), CDR-IMGT [6.3.9] (27'-32'.50'-52'.89'-97')) (1'-107') -*Homo sapiens* IGKC*01 (100%) Km3 A45.1, V101 (C-KAPPA A45.1 (153'), V101 (191')) (108'-214')];

cadena pesada H-gamma1 anti-CD3E *Homo sapiens* (1"-447") [VH (*Homo sapiens* IGHV3-30-5*03 (88.8%) -(IGHD) -IGHJ5*02 (100%), CDR-IMGT [8.8.11] (26"-33".51"-58".97"-107")) (1"-118") -*Homo sapiens* IGHG1*03 G1m3, nG1m1 CH1 R120, CH3 E12, M14, 6-G1v59-1 CH2 G1.2, R1.1, 14-G1v73 CH3 K7, K22 (CH1 R120 (215) (119"-216"), bisagra 1-15 (217", 231"), CH2 L1.2>G (236"), G1.1>R (237") (232"-341"), CH3 L7>K (352"), E12 (357"), M14 (359"), T22>K (367") (342"-446"), CHS K2>del (447")) (119"-447")], (221"-214'")-disulfuro con la cadena ligera común L-kappa *Homo sapiens* (1'"-214'") [V-KAPPA (*Homo sapiens* IGKV1-39*01 (100%) -IGKJ1*01 (100%), CDR-IMGT [6.3.9] (27'"-32'".50'"-52'".89'"-97'")) (1'"-107'") -*Homo sapiens* IGKC*01 (100%) Km3 A45.1, V101 (C-KAPPA A45.1 (153'"), V101 (191'")) (108'"-214'")]; dímero (236-227": 239-230")-bisdisulfuro, producido en las células ováricas de hámster chino (CHO), línea celular CHO-DG44, forma glicosilada alfa

3037124-22-1

Heavy chain / Chaîne lourde / Cadena pesada: H-gamma1 anti-PDCD1 (H)

```
QVQLVQSGSE LKQPGASVKV SCKASGYTFT HYALHWLRQA PGQGLEWMGW  50
LNTNTENPTF AQGFTGRFVF SLDTSVTTAY LQISSLKAED TAVYYCARGD 100
MVVPTTIWNY YHFMDVWGQG TTVTVSSAST KGPSVFPLAP SSKSTSGGTA 150
ALGCLVKDYF PEPVTVSWNS GALTSGVHTF PAVLQSSGLY SLSSVVTVPS 200
SSLGTQTYIC NVNHKPSNTK VDKRVEPKSC DKTHTCPPCP APELGRGPSV 250
FLFPPKPKDT LMISRTPEVT CVVVDVSHED PEVKFNWYVD GVEVHNAKTK 300
PREEQYNSTY RVVSVLTVLH QDWLNGKEYK CKVSNKALPA PIEKTISKAK 350
GQPREPQVYT DPPSREEMTK NQVSLTCEVK GFYPSDIAVE WESNGQPENN 400
YKTTPPVLDS DGSFFLYSKL TVDKSRWQQG NVFSCSVMHE ALHNHYTQKS 450
LSLSPG                                                 456
```

Heavy chain / Chaîne lourde / Cadena pesada: H-gamma1 anti-CD3E (H")

```
QVQLVQSGGG VVQPGRSLRL SCVASGFTFS SYGMHWVRQA PGKGLEWVAQ  50
IWYNARKQEY SDSVKGRFTI SRDNSKNTLY LQMNSLRAED TAVYYCTRGT 100
GYNWFDPWGQ GTLVTVSSAS TKGPSVFPLA PSSKSTSGGT AALGCLVKDY 150
FPEPVTVSWN SGALTSGVHT FPAVLQSSGL YSLSSVVTVP SSSLGTQTYI 200
CNVNHKPSNT KVDKRVEPKS CDKTHTCPPC PAPELGRGPS VFLFPPKPKD 250
TLMISRTPEV TCVVVDVSHE DPEVKFNWYV DGVEVHNAKT KPREEQYNST 300
YRVVSVLTVL HQDWLNGKEY KCKVSNKALP APIEKTISKA KGQPREPQVY 350
TKPPSREEMT KNQVSLKCLV KGFYPSDIAV EWESNGQPEN NYKTTPPVLD 400
SDGSFFLYSK LTVDKSRWQQ GNVFSCSVMH EALHNHYTQK SLSLSPG    447
```

Light chain / Chaîne légère / Cadena ligera: L-kappa common (L', L'")

```
DIQMTQSPSS LSASVGDRVT ITCRASQSIS SYLNWYQQKP GKAPKLLIYA  50
ASSLQSGVPS RFSGSGSGTD FTLTISSLQP EDFATYYCQQ SYSTPPTFGQ 100
GTKVEIKRTV AAPSVFIFPP SDEQLKSGTA SVVCLLNNFY PREAKVQWKV 150
DNALQSGNSQ ESVTEQDSKD STYSLSSTLT LSKADYEKHK VYACEVTHQG 200
LSSPVTKSFN RGEC                                        214
```

Post-translational modifications

Disulfide bridges location / Position des ponts disulfure / Posiciones de los puentes disulfuro

Intra-H (C23-C104) 22-96 154-210 271-331 377-435
22"-96" 145"-201" 262"-322" 368"-426"
Intra-L (C23-C104) 23'-88' 134'-194'
23'"-88'" 134'"-194'"
Intra-H-L (h 5-CL 126) 230-214' 221"-214'"
Inter-H-H (h 11, h 14) 236-227" 239-230"

N-terminal glutaminyl cyclization / Cyclisation du glutaminyle N-terminal / Ciclación del glutaminilo N-terminal
Q > pyroglutamyl (pE, 5-oxoprolyl) / pyroglutamyle (pE, 5-oxoprolyle) / piroglutamilo (pE, 5-oxoprolilo)
H VH Q1: 1, 1"

N-glycosylation sites / Sites de N-glycosylation / Posiciones de N-glicosilación
H CH2 N84.4: 307, 298"
Fucosylated complex bi-antennary CHO-type glycans / glycanes de type CHO bi-antennaires complexes fucosylés / glicanos de tipo CHO biantenarios complejos fucosilados.

betovumelinum

betovumeline — (1*R*,5*R*)-1-(3-methyl-1,2,4-oxadiazol-5-yl)-3-azabicyclo[3.1.0]hexane
muscarinic receptor agonist

bétovuméline — (1*R*,5*R*)-1-(3-méthyl-1,2,4-oxadiazol-5-yl)-3-azabicyclo[3.1.0]hexane
agoniste des récepteurs muscariniques

betovumelina — (1*R*,5*R*)-1-(3-metil-1,2,4-oxadiazol-5-il)-3-azabiciclo[3.1.0]hexano
agonista de los receptores muscarinicos

$C_8H_{11}N_3O$ 1314018-44-4

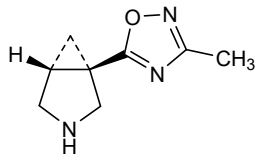

birelentinibum

birelentinib — [(2*S*,5*S*)-5-{4-amino-5-[4-(2,3-difluorophenoxy)phenyl]imidazo[5,1-*f*][1,2,4]triazin-7-yl}oxan-2-yl]methanol
tyrosine kinase inhibitor, antineoplastic

birélentinib — [(2*S*,5*S*)-5-{4-amino-5-[4-(2,3-difluorophénoxy)phényl]imidazo[5,1-*f*][1,2,4]triazin-7-yl}oxan-2-yl]méthanol
inhibiteur de tyrosine kinase, antinéoplasique

birelentinib — [(2*S*,5*S*)-5-{4-amino-5-[4-(2,3-difluorofenoxi)fenil]imidazo[5,1-*f*][1,2,4]triazin-7-il}oxan-2-il]metanol
inhibidor de la tirosina kinasa, antineoplásico

$C_{23}H_{21}F_2N_5O_3$ 2662512-15-2

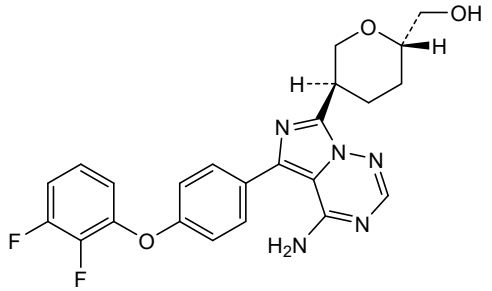

blixeprodilum

blixeprodil — (2*R*)-2-(4-fluorophenyl)-2-(methylamino)cyclohexan-1-one
N-methyl-D-aspartate (NMDA) receptor antagonist

blixéprodil — (2*R*)-2-(4-fluorophényl)-2-(méthylamino)cyclohexan-1-one
antagoniste des récepteurs du N-méthyl-D-aspartate (NMDA)

blixeprodil

(2*R*)-2-(4-fluorofenil)-2-(metilamino)ciclohexan-1-ona
antagonista del receptor de N-metil-D-aspartato (NMDA)

$C_{13}H_{16}FNO$ 2881017-49-6

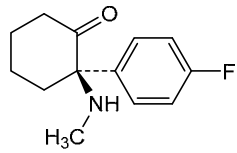

bocunebartum #

bocunebart

immunoglobulin G1-kappa, anti-[*Homo sapiens* ADCYAP1 (adenylate cyclase-activating polypeptide 1, pituitary adenylate cyclase-activating polypeptide, PACAP)], humanized monoclonal antibody;
H-gamma1 heavy chain humanized (1-442) [VH (*Homo sapiens* IGHV3-66*01 (81.4%) -(IGHD) -IGHJ1*01 (100%), CDR-IMGT [8.7.6] (26-33.51-57.96-101)) (1-112) -*Homo sapiens* IGHG1*03v, G1m3>G1m17, nG1m1 CH1 K120, CH3 E12, M14, 8-G1v29 CH2 A84.4 (CH1 R120>K (209) (113-210), hinge 1-15 (211-225), CH2 N84.4>A (292) (226-335), CH3 E12 (351), M14 (353) (336-440), CHS (441-442)) (113-442)], (215-216')-disulfide with L-kappa light chain humanized (1'-216') [V-KAPPA (*Homo sapiens* IGKV1-5*01 (85.4%) -IGKJ1*01 (90.0%) Q120>G (102'), CDR-IMGT [7.3.10] (27'-33'.51'-53'.90'-99')) (1'-109') -*Homo sapiens* IGKC*01 (100%) Km3 A45.1, V101 (C-KAPPA A45.1 (155'), V101 (193')) (110'-216')]; dimer (221-221'':224-224'')-bisdisulfide, produced in Chinese hamster ovary (CHO) cells, cell line CHO-DG44, non-glycosylated
anti-inflammatory

bocunebart

immunoglobuline G1-kappa, anti-[*Homo sapiens* ADCYAP1 (polypeptide 1 activant l'adénylate cyclase, polypeptide activant l'adénylate cyclase pituitaire, PACAP)]; anticorps monoclonal humanisé;
chaîne lourde H-gamma1 humanisée (1-442) [VH (*Homo sapiens* IGHV3-66*01 (81.4%) -(IGHD) -IGHJ1*01 (100%), CDR-IMGT [8.7.6] (26-33.51-57.96-101)) (1-112) -*Homo sapiens* IGHG1*03v, G1m3>G1m17, nG1m1 CH1 K120, CH3 E12, M14, 8-G1v29 CH2 A84.4 (CH1 R120>K (209) (113-210), charnière 1-15 (211-225), CH2 N84.4>A (292) (226-335), CH3 E12 (351), M14 (353) (336-440), CHS (441-442)) (113-442)], (215-216')-disulfure avec la chaîne légère L-kappa humanisée (1'-216') [V-KAPPA (*Homo sapiens* IGKV1-5*01 (85.4%) -IGKJ1*01 (90.0%) Q120>G (102'), CDR-IMGT [7.3.10] (27'-33'.51'-53'.90'-99')) (1'-109') -*Homo sapiens* IGKC*01 (100%) Km3 A45.1, V101 (C-KAPPA A45.1 (155'), V101 (193')) (110'-216')]; dimère (221-221'':224-224'')-bisdisulfure, produit dans des cellules ovariennes de hamster chinois (CHO), lignée cellulaire CHO-DG44, non-glycosylé
anti-inflammatoire

bocunebart

inmunoglobulina G1-kappa, anti-[*Homo sapiens* ADCYAP1 (polipéptido 1 activador de la adenilato ciclasa, polipéptido activador de la adenilato ciclasa pituitaria, PACAP)]; anticuerpo monoclonal humanizado;

cadena pesada H-gamma1 humanizada (1-442) [VH (*Homo sapiens* IGHV3-66*01 (81.4%) -(IGHD) -IGHJ1*01 (100%), CDR-IMGT [8.7.6] (26-33.51-57.96-101)) (1-112) -*Homo sapiens* IGHG1*03v, G1m3>G1m17, nG1m1 CH1 K120, CH3 E12, M14, 8-G1v29 CH2 A84.4 (CH1 R120>K (209) (113-210), bisagra 1-15 (211-225), CH2 N84.4>A (292) (226-335), CH3 E12 (351), M14 (353) (336-440), CHS (441-442)) (113-442)], (215-216')-disulfuro con la cadena ligera L-kappa humanizada (1'-216') [V-KAPPA (*Homo sapiens* IGKV1-5*01 (85.4%) -IGKJ1*01 (90.0%) Q120>G (102'), CDR-IMGT [7.3.10] (27'-33'.51'-53'.90'-99')) (1'-109') -*Homo sapiens* IGKC*01 (100%) Km3 A45.1, V101 (C-KAPPA A45.1 (155'), V101 (193')) (110'-216')]; dímero (221-221":224-224")-bisdisulfuro, producido en las células ováricas de hámster chino (CHO), línea celular CHO-DG44, no glicosilado

antiinflamatorio

2984605-64-1

Heavy chain / Chaîne lourde / Cadena pesada

```
EVQLVESGGG LVQPGGSLRL SCAASGFDLN SYYMTWVRQA PGKGLEWIGF  50
IDAGTDAYTA SWAKGRFTIS RDNSKNTVYL QMNSLRAEDT AVYFCARDLG 100
LWGQGTLVTV SSASTKGPSV FPLAPSSKST SGGTAALGCL VKDYFPEPVT 150
VSWNSGALTS GVHTFPAVLQ SSGLYSLSSV VTVPSSSLGT QTYICNVNHK 200
PSNTKVDKRV EPKSCDKTHT CPPCPAPELL GGPSVFLFPP KPKDTLMISR 250
TPEVTCVVVD VSHEDPEVKF NWYVDGVEVH NAKTKPREEQ YASTYRVVSV 300
LTVLHQDWLN GKEYKCKVSN KALPAPIEKT ISKAKGQPRE PQVYTLPPSR 350
EEMTKNQVSL TCLVKGFYPS DIAVEWESNG QPENNYKTTP PVLDSDGSFF 400
LYSKLTVDKS RWQQGNVFSC SVMHEALHNH YTQKSLSLSP GK         442
```

Light chain / Chaîne légère / Cadena ligera

```
DIQLTQSPST LSASVGDRVT ITCQSSESVY SNYLAWFQQK PGKAPKFLIY  50
EASKLESGVP SRFSGSGSGT EFTLTISSLQ PDDFATYYCA QGDISEDVAF 100
GGGTYVEIKR TVAAPSVFIF PPSDEQLKSG TASVVCLLNN FYPREAKVQW 150
KVDNALQSGN SQESVTEQDS KDSTYSLSST LTLSKADYEK HKVYACEVTH 200
QGLSSPVTKS FNRGEC                                      216
```

Post-translational modifications

Disulfide bridges location / Position des ponts disulfure / Posiciones de los puentes disulfuro

Intra-H (C23-C104) 22-95 139-195 256-316 362-420
22"-95" 139"-195" 256"-316" 362"-420"
Intra-L (C23-C104) 23'-89' 136'-196'
23'"-89'" 136'"-196'"
Inter-H-L (h 5-CL 126) 215-216' 215"-216'"
Inter-H-H (h 11, h 14) 221-221" 224-224"

No N-glycosylation sites / pas de sites de N-glycosylation / ningún posición de N-glycosilación
H CH2 N84.4>A (8-G1v29): 292, 292"

C-terminal lysine clipping / Coupure de la lysine C-terminale / Recorte de lisina C-terminal
H CHS K2: 442, 442"

bretisilocinum

bretisilocin	*N*-ethyl-2-(5-fluoro-1*H*-indol-3-yl)-*N*-methylethan-1-amine *serotonin (5-HT$_{2A}$) receptor agonist*
brétisilocine	*N*-éthyl-2-(5-fluoro-1*H*-indol-3-yl)-*N*-méthyléthan-1-amine *agoniste des récepteurs de la sérotonine (5-HT$_{2A}$)*
bretisilocina	*N*-etil-2-(5-fluoro-1*H*-indol-3-il)-*N*-metiletan-1-amina *agonista del receptor de serotonina (5-HT$_{2A}$)*

$C_{13}H_{17}FN_2$ 2698331-35-8

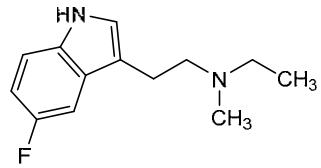

catadegbrutinibum

catadegbrutinib 3-*tert*-butyl-*N*-{(1*R*)-1-[1^3-methyl-8^2,8^4-dioxo-2^7*H*-2(4,6)-pyrrolo[2,3-*d*]pyrimidina-8(1)-[1,3]diazinana-4(1,4)-piperazina-3(5,2)-pyridina-6(4,1)-piperidina-1(1),7(1,4)-dibenzenaoctaphan-1^4-yl]ethyl}-1,2,4-oxadiazole-5-carboxamide
Bruton tyrosine kinase degrader, antineoplastic

catadegbrutinib 3-*tert*-butyl-*N*-{(1*R*)-1-[1^3-méthyl-8^2,8^4-dioxo-2^7*H*-2(4,6)-pyrrolo[2,3-*d*]pyrimidina-8(1)-[1,3]diazinana-4(1,4)-pipérazina-3(5,2)-pyridina-6(4,1)-pipéridina-1(1),7(1,4)-dibenzénaoctaphan-1^4-yl]éthyl}-1,2,4-oxadiazole-5-carboxamide
dégradeur de tyrosine kinase de Bruton, antinéoplasique

catadegbrutinib 3-*terc*-butil-*N*-{(1*R*)-1-[1^3-metil-8^2,8^4-dioxo-2^7*H*-2(4,6)-pirrolo[2,3-*d*]pirimidina-8(1)-[1,3]diazinana-4(1,4)-piperazina-3(5,2)-piridina-6(4,1)-piperidina-1(1),7(1,4)-dibencenaoctafan-1^4-il]etil}-1,2,4-oxadiazol-5-carboxamida
degradador de la tirosina kinasa de Bruton, antineoplásico

$C_{47}H_{54}N_{12}O_4$ 2736508-60-2

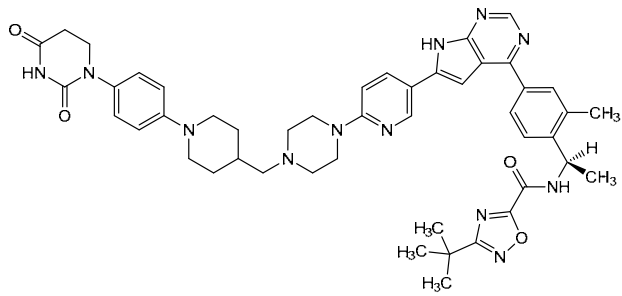

cendifensinum

cendifensine (3,4-dichlorophenyl)[(3*S*)-3-propylpyrrolidin-3-yl]methanone
monoamine reuptake inhibitor

cendifensine (3,4-dichlorophényl)[(3*S*)-3-propylpyrrolidin-3-yl]méthanone
inhibiteur de la recapture des monoamines

cendifensina (3,4-diclorofenil)[(3*S*)-3-propilpirrolidin-3-il]metanona
modulador de la recaptación de monoaminas

$C_{14}H_{17}Cl_2NO$ 1034048-49-1

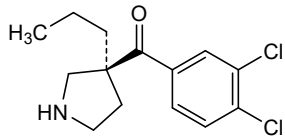

cenvacibartum #

cenvacibart	immunoglobulin G4-kappa, anti-[*Homo sapiens* F11 (coagulation factor 11, coagulation factor XI, FXI, plasma thromboplastin antecedent, PTA)], *Homo sapiens* monoclonal antibody; H-gamma4 heavy chain *Homo sapiens* (1-445) [VH (*Homo sapiens* IGHV3-11*01 (91.7%) -(IGHD) -IGHJ3*02 (100%), CDR-IMGT [8.8.11] (26-33.51-58.97-107)) (1-118) -*Homo sapiens* IGHG4*01, *nG4m(a)* CH2 L92, 12-G4v5 h P10(CH1 (119-216), hinge 1-12 S10>P (226) (217-228), CH2 L92 (307) (229-338), CH3 (339-443), CHS (444-445)) (119-445)], (132-214')-disulfide with L-kappa light chain *Homo sapiens* (1'-214') [V-KAPPA (*Homo sapiens* IGKV1-33*01 (95.8%) -IGKJ2*02 (100%), CDR-IMGT [6.3.9] (27'-32'.50'-52'.89'-97')) (1'-107') -*Homo sapiens* IGKC*01 (100%) Km3 A45.1, V101 (C-KAPPA A45.1 (153'), V101 (191')) (108'-214')]; dimer (224-224":227-227")-bisdisulfide, produced in Chinese hamster ovary (CHO) cells, cell line CHO-K1, glycoform alfa *anticoagulant*
cenvacibart	immunoglobuline G4-kappa, anti-[*Homo sapiens* F11 (facteur de coagulation 11, facteur de coagulation XI, FXI, antécédent de la thromboplastine plasmatique, PTA)], anticorps monoclonal *Homo sapiens*; chaîne lourde H-gamma4 *Homo sapiens* (1-445) [VH (*Homo sapiens* IGHV3-11*01 (91.7%) -(IGHD) -IGHJ3*02 (100%), CDR-IMGT [8.8.11] (26-33.51-58.97-107)) (1-118) -*Homo sapiens* IGHG4*01, *nG4m(a)* CH2 L92, 12-G4v5 h P10(CH1 (119-216), charnière 1-12 S10>P (226) (217-228), CH2 L92 (307) (229-338), CH3 (339-443), CHS (444-445)) (119-445)], (132-214')-disulfure avec la chaîne légère L-kappa *Homo sapiens* (1'-214') [V-KAPPA (*Homo sapiens* IGKV1-33*01 (95.8%) -IGKJ2*02 (100%), CDR-IMGT [6.3.9] (27'-32'.50'-52'.89'-97')) (1'-107') -*Homo sapiens* IGKC*01 (100%) Km3 A45.1, V101 (C-KAPPA A45.1 (153'), V101 (191')) (108'-214')]; dimère (224-224":227-227")-bisdisulfure, produit dans des cellules ovariennes de hamster chinois (CHO), lignée cellulaire CHO-K1, glycoforme alfa *anticoagulant*
cenvacibart	inmunoglobulina G4-kappa, anti-[*Homo sapiens* F11 (factor de coagulación 11, factor de coagulación XI, FXI, antecedente de la tromboplastina plasmática, PTA)], anticuerpo monoclonal *Homo sapiens*;

cadena pesada H-gamma4 *Homo sapiens* (1-445) [VH (*Homo sapiens* IGHV3-11*01 (91.7%) -(IGHD) -IGHJ3*02 (100%), CDR-IMGT [8.8.11] (26-33.51-58.97-107)) (1-118) -*Homo sapiens* IGHG4*01, *nG4m(a)* CH2 L92, 12-G4v5 h P10(CH1 (119-216), bisagra 1-12 S10>P (226) (217-228), CH2 L92 (307) (229-338), CH3 (339-443), CHS (444-445)) (119-445)], (132-214')-disulfuro con la cadena ligera L-kappa *Homo sapiens* (1'-214') [V-KAPPA (*Homo sapiens* IGKV1-33*01 (95.8%) -IGKJ2*02 (100%), CDR-IMGT [6.3.9] (27'-32'.50'-52'.89'-97')) (1'-107') -*Homo sapiens* IGKC*01 (100%) Km3 A45.1, V101 (C-KAPPA A45.1 (153'), V101 (191')) (108'-214')]; dímero (224-224":227-227")-bisdisulfuro, producido en las células ováricas de hámster chino (CHO), línea celular CHO-K1, forma glicosilada alfa

anticoagulante

3008610-21-4

Heavy chain / Chaîne lourde / Cadena pesada

```
QVQLVESGGG LVKPGGSLRL SCAASGFTFS DYSMNWIRQA PGKGLEWISY  50
ISFSGNSIYY ADSVKGRFTI SRDNAKNSLY LQMNSLRVED TAIYYCTSRD 100
WGYAFDIWGQ GTMVTVSSAS TKGPSVFPLA PCSRSTSEST AALGCLVKDY 150
FPEPVTVSWN SGALTSGVHT FPAVLQSSGL YSLSSVVTVP SSSLGTKTYT 200
CNVDHKPSNT KVDKRVESKY GPPCPPCPAP EFLGGPSVFL FPPKPKDTLM 250
ISRTPEVTCV VVDVSQEDPE VQFNWYVDGV EVHNAKTKPR EEQFNSTYRV 300
VSVLTVLHQD WLNGKEYKCK VSNKGLPSSI EKTISKAKGQ PREPQVYTLP 350
PSQEEMTKNQ VSLTCLVKGF YPSDIAVEWE SNGQPENNYK TTPPVLDSDG 400
SFFLYSRLTV DKSRWQEGNV FSCSVMHEAL HNHYTQKSLS LSLGK      445
```

Light chain / Chaîne légère / Cadena ligera

```
DIQMTQSPSF LSASLGDRVT ITCQASQDIS NYLNWYQVKP GKAPKLLIYD  50
ASNLETGVPS RFSGSGSGTD FTFTISSLQP EDIATYFCQQ YDNLPYIFGQ 100
GTKLEIKRTV AAPSVFIFPP SDEQLKSGTA SVVCLLNNFY PREAKVQWKV 150
DNALQSGNSQ ESVTEQDSKD STYSLSSTLT LSKADYEKHK VYACEVTHQG 200
LSSPVTKSFN RGEC                                        214
```

Post-translational modifications

Disulfide bridges location / Position des ponts disulfure / Posiciones de los puentes disulfuro

```
Intra-H (C23-C104)  22-96    145-201    259-319    365-423
                    22"-96"  145"-201"  259"-319"  365"-423"
Intra-L (C23-C104)  23'-88'    134'-194'
                    23'"-88'"  134'"-194'"
Inter-H-L (CH1 10-CL 126)  132-214'  132"-214'"
Inter-H-H (h 8, h 11)      224-224"  227-227"
```

N-terminal glutaminyl cyclization / Cyclisation du glutaminyle N-terminal / Ciclación del glutaminilo N-terminal

Q > pyroglutamyl (pE, 5-oxoprolyl) / pyroglutamyle (pE, 5-oxoprolyle) / piroglutamilo (pE, 5-oxoprolilo)

H VH Q1: 1, 1"

N-glycosylation sites / Sites de N-glycosylation / Posiciones de N-glicosilación

H CH2 N84.4: 295, 295"

Fucosylated complex bi-antennary CHO-type glycans / glycanes de type CHO bi-antennaires complexes fucosylés / glicanos de tipo CHO biantenarios complejos fucosilados

C-terminal lysine clipping / Coupure de la lysine C-terminale / Recorte de lisina C-terminal

H CHS K2: 445, 445"

cenzestotugum #

cenzestotug

immunoglobulin G1-kappa, anti-[*Homo sapiens* TNFRSF4 (tumor necrosis factor receptor (TNFR) superfamily member 4, OX40, CD134)], monoclonal antibody;

H-gamma1 heavy chain (1-443) [VH Musmus/Homsap (*Mus musculus* IGHV2-2*01 (80.4%) -(IGHD) -IGHJ4*01 (91.7%) S123>L (108)/*Homo sapiens* IGHV3-30-5*03 (76.5%) -(IGHD) -IGHJ4*01 (92.9%), CDR-IMGT [8.7.7] (26-33.51-57.96-102)) (1-113) -*Homo sapiens* IGHG1*03v (100%) G1m3>G1m17, nG1m1 CH1 K120, CH3 E12, M14 (CH1 R120>K (210) (114-211), hinge 1-15 (212-226), CH2 (227-336), CH3 E12 (352), M14 (354) (337-441), CHS (442-443)) (114-443)], (216-214')-disulfide with L-kappa light chain (1'-214') [V-KAPPA (*Homo sapiens* IGKV1-33*01 (87.4%) -IGKJ4*01 (81.8%) V124>L (104'), I126>V (106'), CDR-IMGT [6.3.9] (27'-32'.50'-52'.89'-97')) (1'-107') -*Homo sapiens* IGKC*01 (100%) Km3 A45.1, V101 (C-KAPPA A45.1 (153'), V101 (191')) (108'-214')]; dimer (222-222":225-225")-bisdisulfide, produced in Chinese hamster ovary (CHO) cells, cell line CHO-K1, glycoform alfa

immunostimulant, antineoplastic

cenzestotug

immunoglobuline G1-kappa, anti-[*Homo sapiens* TNFRSF4 (membre 4 de la superfamille des récepteurs des facteurs de nécrose tumorale (TNFR), OX40, CD134)]; anticorps monoclonal;

chaîne lourde H-gamma1 (1-443) [VH Musmus/Homsap (*Mus musculus* IGHV2-2*01 (80.4%) -(IGHD) -IGHJ4*01 (91.7%) S123>L (108)/*Homo sapiens* IGHV3-30-5*03 (76.5%) -(IGHD) -IGHJ4*01 (92.9%), CDR-IMGT [8.7.7] (26-33.51-57.96-102)) (1-113) -*Homo sapiens* IGHG1*03v (100%) G1m3>G1m17, nG1m1 CH1 K120, CH3 E12, M14 (CH1 R120>K (210) (114-211), charnière 1-15 (212-226), CH2 (227-336), CH3 E12 (352), M14 (354) (337-441), CHS (442-443)) (114-443)], (216-214')-disulfure avec la chaîne légère L-kappa (1'-214') [V-KAPPA (*Homo sapiens* IGKV1-33*01 (87.4%) -IGKJ4*01 (81.8%) V124>L (104'), I126>V (106'), CDR-IMGT [6.3.9] (27'-32'.50'-52'.89'-97')) (1'-107') -*Homo sapiens* IGKC*01 (100%) Km3 A45.1, V101 (C-KAPPA A45.1 (153'), V101 (191')) (108'-214')]; dimère (222-222":225-225")-bisdisulfure, produit dans des cellules ovariennes de hamster chinois (CHO), lignée cellulaire CHO-K1, glycoforme alfa
immunostimulant, antinéoplasique

cenzestotug

inmunoglobulina G1-kappa, anti-[*Homo sapiens* TNFRSF4 (miembro 4 de la superfamilia de los receptores de los factores de necrosis tumoral (TNFR), OX40, CD134)]; anticuerpo monoclonal;
cadena pesada H-gamma1 (1-443) [VH Musmus/Homsap (*Mus musculus* IGHV2-2*01 (80.4%) -(IGHD) -IGHJ4*01 (91.7%) S123>L (108)/*Homo sapiens* IGHV3-30-5*03 (76.5%) -(IGHD) -IGHJ4*01 (92.9%), CDR-IMGT [8.7.7] (26-33.51-57.96-102)) (1-113) -*Homo sapiens* IGHG1*03v (100%) G1m3>G1m17, nG1m1 CH1 K120, CH3 E12, M14 (CH1 R120>K (210) (114-211), bisagra 1-15 (212-226), CH2 (227-336), CH3 E12 (352), M14 (354) (337-441), CHS (442-443)) (114-443)], (216-214')-disulfuro con la cadena ligera L-kappa (1'-214') [V-KAPPA (*Homo sapiens* IGKV1-33*01 (87.4%) -IGKJ4*01 (81.8%) V124>L (104'), I126>V (106'), CDR-IMGT [6.3.9] (27'-32'.50'-52'.89'-97')) (1'-107') -*Homo sapiens* IGKC*01 (100%) Km3 A45.1, V101 (C-KAPPA A45.1 (153'), V101 (191')) (108'-214')]; dímero (222-222":225-225")-bisdisulfuro, producido en las células ováricas de hámster chino (CHO), línea celular CHO-K1, forma glicosilada alfa
inmunoestimulante, antineoplásico

3014361-58-8

Heavy chain / Chaîne lourde / Cadena pesada

```
QVQLVESGGG VVQPGRSLRI SCAVSGFSLT SYGVLWVRQA PGKGLEWLGV  50
IWSGGSTDYN AAFISRLTIS RDNSKSTVYF QMNSLRAEDT AVYYCAREEF 100
GYWGQGTLVT VSSASTKGPS VFPLAPSSKS TSGGTAALGC LVKDYFPEPV 150
TVSWNSGALT SGVHTFPAVL QSSGLYSLSS VVTVPSSSLG TQTYICNVNH 200
KPSNTKVDKK VEPKSCDKTH TCPPCPAPEL LGGPSVFLFP PKPKDTLMIS 250
RTPEVTCVVV DVSHEDPEVK FNWYVDGVEV HNAKTKPREE QYNSTYRVVS 300
VLTVLHQDWL NGKEYKCKVS NKALPAPIEK TISKAKGQPR EPQVYTLPPS 350
REEMTKNQVS LTCLVKGFYP SDIAVEWESN GQPENNYKTT PPVLDSDGSF 400
FLYSKLTVDK SRWQQGNVFS CSVMHEALHN HYTQKSLSLS PGK         443
```

Light chain / Chaîne légère / Cadena ligera

```
DIQMTQSPSS LSASVGDRVT ITCRASQDIN NYLNWYQQKP GGAVKLLIYY  50
TSRLHTGVPS RFSGSGSGTD FTLTISSLQP EDIATYYCQQ TNTLPWTFGG 100
GTKLEVKRTV AAPSVFIFPP SDEQLKSGTA SVVCLLNNFY PREAKVQWKV 150
DNALQSGNSQ ESVTEQDSKD STYSLSSTLT LSKADYEKHK VYACEVTHQG 200
LSSPVTKSFN RGEC                                        214
```

Post-translational modifications
Disulfide bridges location / Position des ponts disulfure / Posiciones de los puentes disulfuro
Intra-H (C23-C104) 22-95 140-196 257-317 363-421
22"-95" 140"-196" 257"-317" 363"-421"
Intra-L (C23-C104) 23'-88' 134'-194'
23'"-88'" 134'"-194'"
Inter-H-L (h 5-CL 126) 216-214' 216"-214'"
Inter-H-H (h 11, h 14) 222-222" 225-225"

N-terminal glutaminyl cyclization / Cyclisation du glutaminyle N-terminal / Ciclación del glutaminilo N-terminal
Q > pyroglutamyl (pE, 5-oxoprolyl) / pyroglutamyle (pE, 5-oxoprolyle) / piroglutamilo (pE, 5-oxoprolilo)
H VH Q1: 1, 1"

N-glycosylation sites / Sites de N-glycosylation / Posiciones de N-glicosilación
H CH2 N84.4: 293, 293"
Fucosylated complex bi-antennary CHO-type glycans / glycanes de type CHO bi-antennaires complexes fucosylés / glicanos de tipo CHO biantenarios complejos fucosilados

C-terminal lysine clipping / Coupure de la lysine C-terminale / Recorte de lisina C-terminal
H CHS K2: 443, 443"

ceperognastatum

ceperognastat — *N*-[4-fluoro-5-({(2*S*,4*S*)-2-methyl-4-[(5-methyl-1,2,4-oxadiazol-3-yl)methoxy]piperidin-1-yl}methyl)-1,3-thiazol-2-yl]acetamide
O-GlcNAcase (OGA) enzyme inhibitor

cépérognastat — *N*-[4-fluoro-5-({(2*S*,4*S*)-2-méthyl-4-[(5-méthyl-1,2,4-oxadiazol-3-yl)méthoxy]pipéridin-1-yl}méthyl)-1,3-thiazol-2-yl]acétamide
inhibiteur de l'enzyme O-GlcNAcase (OGA)

ceperognastat — *N*-[4-fluoro-5-({(2*S*,4*S*)-2-metil-4-[(5-metil-1,2,4-oxadiazol-3-il)metoxi]piperidin-1-il}metil)-1,3-tiazol-2-il]acetamida
inhibidor del enzima O-GlcNAcase (OGA)

$C_{16}H_{22}FN_5O_3S$ 2241514-56-5

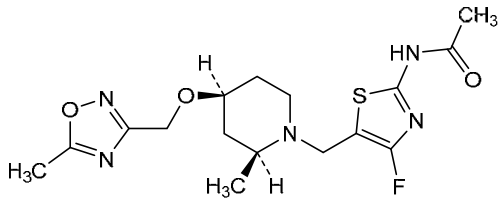

ciltistotugum #

ciltistotug — immunoglobulin G2-kappa, anti-[*Homo sapiens* CD40 (TNFRSF5, tumor necrosis factor receptor (TNFR) superfamily member 5, p50)], monoclonal antibody;
H-gamma2 heavy chain (1-441) [VH Musmus/Homsap (*Mus musculus* IGHV1-47-14*01 (84.7%) -(IGHD) -IGHJ2*01 (100%)/*Homo sapiens* IGHV1-2*02 (79.6%) -(IGHD) -IGHJ6*01 (90.9%) V124>L (111), CDR-IMGT [8.8.8] (26-33.51-58.97-104)) (1-115) -*Homo sapiens* IGHG2*01 G2m.. (100%) CH2 V45.1 (CH1 (116-213), hinge 1-12 (214-225), CH2 V45.1 (276) (226-334), CH3 (335-439), CHS (440-441)) (116-441)], (129-219')-disulfide with L-kappa light chain (1'-219') [V-KAPPA Musmus/Homsap (*Mus musculus* IGKV1-110*01 (88.0%) -IGKJ1*01 (91.7%) L124>V (109')/*Homo sapiens* IGKV2-30*02 (88.0%) -IGKJ4*01 (100%), CDR-IMGT [11.3.9] (27'-37'.55'-57'.94'-102')) (1'-112') -*Homo sapiens* IGKC*01 (100%) Km3 A45.1, V101 (C-KAPPA A45.1 (158'), V101 (196')) (113'-219')]; dimer (217-217":218-218":221-221":224-224")-tetrakisdisulfide, produced in Chinese hamster ovary (CHO) cells, cell line CHO-K1, glycoform alfa
immunostimulant, antineoplastic

ciltistotug — immunoglobuline G2-kappa, anti-[*Homo sapiens*CD40 (TNFRSF5, membre 5 de la superfamille des récepteurs des facteurs de nécrose tumorale (TNFR), p50)], anticorps monoclonal;
chaîne lourde H-gamma2 (1-441) [VH Musmus/Homsap (*Mus musculus* IGHV1-47-14*01 (84.7%) -(IGHD) -IGHJ2*01 (100%)/*Homo sapiens* IGHV1-2*02 (79.6%) -(IGHD) -IGHJ6*01 (90.9%) V124>L (111), CDR-IMGT [8.8.8] (26-33.51-58.97-104)) (1-115) -*Homo sapiens* IGHG2*01 G2m.. (100%) CH2 V45.1 (CH1 (116-213), charnière 1-12 (214-225), CH2 V45.1 (276) (226-334), CH3 (335-439), CHS (440-441)) (116-441)], (129-219')-disulfure avec la chaîne

légère kappa (1'-219') [V-KAPPA Musmus/Homsap (*Mus musculus* IGKV1-110*01 (88.0%) -IGKJ1*01 (91.7%) L124>V (109')/*Homo sapiens* IGKV2-30*02 (88.0%) -IGKJ4*01 (100%), CDR-IMGT [11.3.9] (27'-37'.55'-57'.94'-102')) (1'-112') -*Homo sapiens* IGKC*01 (100%) Km3 A45.1, V101 (C-KAPPA A45.1 (158'), V101 (196')) (113'-219')]; dimère (217-217'':218-218'':221-221'':224-224'')-tétrakisdisulfure, produit dans des cellules ovariennes de hamster chinois (CHO), lignée cellulaire CHO-K1, glycoforme alfa
immunostimulant, antinéoplasique

ciltistotug

inmunoglobulina G2-kappa, anti-[*Homo sapiens* CD40 (TNFRSF5, miembro 5 de la superfamilia de los receptores de los factores de necrosis tumoral (TNFR), p50)], anticuerpo monoclonal;
cadena pesada H-gamma2 (1-441) [VH Musmus/Homsap (*Mus musculus* IGHV1-47-14*01 (84.7%) -(IGHD) -IGHJ2*01 (100%)/*Homo sapiens* IGHV1-2*02 (79.6%) -(IGHD) -IGHJ6*01 (90.9%) V124>L (111), CDR-IMGT [8.8.8] (26-33.51-58.97-104)) (1-115) -*Homo sapiens* IGHG2*01 G2m.. (100%) CH2 V45.1 (CH1 (116-213), bisagra 1-12 (214-225), CH2 V45.1 (276) (226-334), CH3 (335-439), CHS (440-441)) (116-441)], (129-219')-disulfuro con la cadena ligera kappa (1'-219') [V-KAPPA Musmus/Homsap (*Mus musculus* IGKV1-110*01 (88.0%) -IGKJ1*01 (91.7%) L124>V (109')/*Homo sapiens* IGKV2-30*02 (88.0%) -IGKJ4*01 (100%), CDR-IMGT [11.3.9] (27'-37'.55'-57'.94'-102')) (1'-112') -*Homo sapiens* IGKC*01 (100%) Km3 A45.1, V101 (C-KAPPA A45.1 (158'), V101 (196')) (113'-219')]; dímero (217-217'':218-218'':221-221'':224-224'')-tetrakisdisulfuro, producido en las células ováricas de hámster chino (CHO), línea celular CHO-K1, forma glicosilada alfa
inmunoestimulante, antineoplásico

3014361-59-9

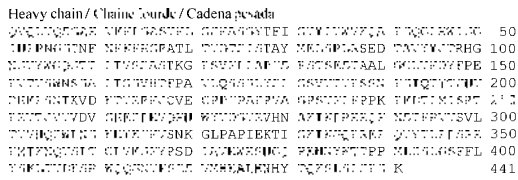

Heavy chain / Chaîne lourde / Cadena pesada

```
QVQLVQSGAE VKKPGASVKV SCKASGYTFT SYWMHWVRQA PGQGLEWMGE  50
IDPSNSYTNF NEKFKSRATL TVDKSTSTAY MELSSLRSED TAVYYCTRHG 100
NYYFGSSYWY FDVWGQGTTV TVSSASTKGP SVFPLAPSSK STSGGTAALG 150
CLVKDYFPEP VTVSWNSGAL TSGVHTFPAV LQSSGLYSLS SVVTVPSSSL 200
GTQTYICNVN HKPSNTKVDK KVEPKSCDKT HTCPPCPAPE AAGGPSVFLF 250
PPKPKDTLMI SRTPEVTCVV VDVSHEDPEV KFNWYVDGVE VHNAKTKPRE 300
EQYNSTYRVV SVLTVLHQDW LNGKEYKCKV SNKALPAPIE KTISKAKGQP 350
REPQVYTLPP SREEMTKNQV SLTCLVKGFY PSDIAVEWES NGQPENNYKT 400
TPPVLDSDGS FFLYSKLTVD KSRWQQGNVF SCSVMHEALH NHYTQKSLSL 441
SPGK
```

Light chain / Chaîne légère / Cadena ligera

```
DVVMTQTPLT LPVSLGDQAS ISCRSSQSLV HSNGNTYLHW YLQKPGQSPK  50
LLIYKVSNRF SGVPDRFSGS GSGTDFTLKI SRVEAEDLGV YFCSQSTHVP 100
WTFGGGTKVE IKRTVAAPSV FIFPPSDEQL KSGTASVVCL LNNFYPREAK 150
VQWKVDNALQ SGNSQESVTE QDSKDSTYSL SSTLTLSKAD YEKHKVYACE 200
VTHQGLSSPV TKSFNRGEC                                   219
```

Post-translational modifications
Disulfide bridges location / Position des ponts disulfure / Posiciones de los puentes disulfuro
Intra-H (C 23-C 104) 22-96 142-198 255-315 361-419
22"-96" 142"-198" 255"-315" 361"-419"
Intra-L (C 23-C 104) 23'-93' 139'-199'
23'"-93'" 139'"-199'"
Inter-H-L (CH1 10-CL 126) 129-219' 129"-219'"
Inter-H-H (h 4, h 5, h 8, h11) 217-217" 218-218" 221-221" 224-224"

N-terminal glutaminyl cyclization / Cyclisation du glutaminyle N-terminal / Ciclación del glutaminilo N-terminal
Q > pyroglutamyl (pE, 5-oxoprolyl) / pyroglutamyle (pE, 5-oxoprolyle) / piroglutamilo (pE, 5-oxoprolilo)
H VH Q1: 1, 1"

N-glycosylation sites / Sites de N-glycosylation / Posiciones de N-glicosilación
H CH2 N84.4: 291, 291"
Fucosylated complex bi-antennary CHO-type glycans / glycanes de type CHO bi-antennaires complexes fucosylés / glicanos de tipo CHO biantenarios complejos fucosilados

C-terminal lysine clipping / Coupure de la lysine C-terminale / Recorte de lisina C-terminal
H CHS K2: 441, 441"

cirtociclibum

cirtociclib

N-[5-(difluoromethoxy)-1*H*-pyrazol-3-yl]-1-[(oxan-4-yl)methyl]-1*H*-pyrazolo[3,4-*b*]pyrazin-6-amine
cyclin-dependent kinase inhibitor, antineoplastic

cirtociclib

N-[5-(difluorométhoxy)-1*H*-pyrazol-3-yl]-1-[(oxan-4-yl)méthyl]-1*H*-pyrazolo[3,4-*b*]pyrazin-6-amine
inhibiteur de la kinase cycline-dépendante, antinéoplasique

cirtociclib

N-[5-(difluorometoxi)-1*H*-pirazol-3-il]-1-[(oxan-4-il)metil]-1*H*-pirazolo[3,4-*b*]pirazin-6-amina
inhibidor de la kinasa dependiente de ciclinas, antineoplásico

$C_{15}H_{17}F_2N_7O_2$ 2888704-84-3

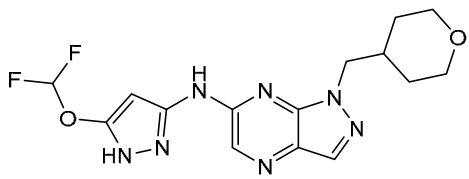

claseprubartum #

claseprubart

immunoglobulin G4-kappa, anti-[*Homo sapiens* C1S (complement C1s)], *Homo sapiens* monoclonal antibody;
H-gamma4 heavy chain *Homo sapiens* (1-443) [VH (*Homo sapiens* IGHV3-11*01 (96.9%) -(IGHD) - IGHJ1*01 (100%), CDR-IMGT [8.8.10] (26-33.51-58.97-106)) (1-117) -*Homo sapiens* IGHG4*01, *nG4m(a)* CH2 L92, 12-G4v5 h P10, 6-G4v3 CH2 E1.2, 9-G4v21 CH2 Y15.1, T16, E18 (CH1 (118-215), hinge 1-12 S10>P (225) (216-227), CH2 L1.2>E (232), M15.1>Y (249), S16>T (251), T18>E (253), L92 (306) (228-337), CH3 (338-442), CHS K2>del (443)) (118-443)], (131-214')-disulfide with L-kappa light chain *Homo sapiens* (1'-214') [V-KAPPA (*Homo sapiens* IGKV1-33*01 (95.8%) - IGKJ4*01 (100%), CDR-IMGT [6.3.9] (27'-32'.50'-52'.89'-97')) (1'-107') -*Homo sapiens* IGKC*01 (100%) Km3 A45.1, V101 (C-KAPPA A45.1 (153'), V101 (191')) (108'-214')]; dimer (223-223'':226-226'')-bisdisulfide, produced in Chinese hamster ovary (CHO) cells, cell line CHO-K1, glycoform alfa
immunosuppressant

claséprubart

immunoglobuline G4-kappa, anti-[*Homo sapiens* C1S (complément C1s)], anticorps monoclonal *Homo sapiens*;
chaîne lourde H-gamma4 *Homo sapiens* (1-443) [VH (*Homo sapiens* IGHV3-11*01 (96.9%) -(IGHD) - IGHJ1*01 (100%), CDR-IMGT [8.8.10] (26-33.51-58.97-106)) (1-117) -*Homo sapiens* IGHG4*01, *nG4m(a)* CH2 L92, 12-G4v5 h P10, 6-G4v3 CH2 E1.2, 9-G4v21 CH2 Y15.1, T16, E18 (CH1 (118-215), charnière 1-12 S10>P (225) (216-227), CH2 L1.2>E (232), M15.1>Y (249), S16>T (251), T18>E (253), L92 (306) (228-337), CH3 (338-442), CHS K2>del (443)) (118-443)], (131-214')-disulfure avec la chaîne légère L-kappa *Homo sapiens*

(1'-214') [V-KAPPA (*Homo sapiens* IGKV1-33*01 (95.8%) - IGKJ4*01 (100%), CDR-IMGT [6.3.9] (27'-32'.50'-52'.89'-97')) (1'-107') -*Homo sapiens* IGKC*01 (100%) Km3 A45.1, V101 (C-KAPPA A45.1 (153'), V101 (191')) (108'-214')]; dimère (223-223":226-226")-bisdisulfure, produit dans des cellules ovariennes de hamster chinois (CHO), lignée cellulaire CHO-K1, glycoforme alfa
immunosuppresseur

claseprubart

inmunoglobulina G4-kappa, anti-[*Homo sapiens* C1S (complemento C1s)], anticuerpo monoclonal *Homo sapiens*;
cadena pesada H-gamma4 *Homo sapiens* (1-443) [VH (*Homo sapiens* IGHV3-11*01 (96.9%) -(IGHD) -IGHJ1*01 (100%), CDR-IMGT [8.8.10] (26-33.51-58.97-106)) (1-117) -*Homo sapiens* IGHG4*01, *nG4m(a)* CH2 L92, 12-G4v5 h P10, 6-G4v3 CH2 E1.2, 9-G4v21 CH2 Y15.1, T16, E18 (CH1 (118-215), bisagra 1-12 S10>P (225) (216-227), CH2 L1.2>E (232), M15.1>Y (249), S16>T (251), T18>E (253), L92 (306) (228-337), CH3 (338-442), CHS K2>del (443)) (118-443)], (131-214')-disulfuro con la cadena ligera L-kappa *Homo sapiens* (1'-214') [V-KAPPA (*Homo sapiens* IGKV1-33*01 (95.8%) -IGKJ4*01 (100%), CDR-IMGT [6.3.9] (27'-32'.50'-52'.89'-97')) (1'-107') -*Homo sapiens* IGKC*01 (100%) Km3 A45.1, V101 (C-KAPPA A45.1 (153'), V101 (191')) (108'-214')]; dímero (223-223":226-226")-bisdisulfuro, producido en las células ováricas de hámster chino (CHO), línea celular CHO-K1, forma glicosilada alfa
inmunosupresor

2922766-89-8

Heavy chain / Chaîne lourde / Cadena pesada

```
EVQLVESGGG LVKPGGSLRL SCAASGFTFS DYYMSWIRQA PGKGLEWVSY  50
ISRSGSTKYY ADSVKGRFTI SRDNAKNSLY LQMNSLRAED TAVYYCARDS 100
NYALDNWGQG TLVTVSSAST KGPSVFPLAP CSRSTSESTA ALGCLVKDYF 150
PEPVTVSWNS GALTSGVHTF PAVLQSSGLY SLSSVVTVPS SSLGTKTYTC 200
NVDHKPSNTK VDKRVESKYG PPCPPCPAPE FLGGPSVFLF PPKPKDTLYI 250
TREPEVTCVV VDVSQEDPEV QFNWYVDGVE VHNAKTKPRE EQFNSTYRVV 300
SVLTVLHQDW LNGKEYKCKV SNKGLPSSIE KTISKAKGQP REPQVYTLPP 350
SQEEMTKNQV SLTCLVKGFY PSDIAVEWES NGQPENNYKT TPPVLDSDGS 400
FFLYSRLTVD KSRWQEGNVF SCSVMHEALH NHYTQKSLSL SLG         443
```

Light chain / Chaîne légère / Cadena ligera

```
DIQMTQSPSS LSASVGDRVT ITCQASQDIS NYLNWYQQKP GKAPKLLIYD  50
ASNLETGVPS RFSGSGSGTD FTFTISSLQP EDIATYYCQH YDDLPLTFGG 100
GTKVEIKRTV AAPSVFIFPP SDEQLKSGTA SVVCLLNNFY PREAKVQWKV 150
DNALQSGNSQ ESVTEQDSKD STYSLSSTLT LSKADYEKHK VYACEVTHQG 200
LSSPVTKSFN RGEC                                        214
```

Post-translational modifications
Disulfide bridges location / Position des ponts disulfure / Posiciones de los puentes disulfuro
Intra-H (C23-C104) 22-96 144-200 258-318 364-422
22"-96" 144"-200" 258"-318" 364"-422"
Intra-L (C23-C104) 23'-88' 134'-194'
23'"-88'" 134'"-194'"
Inter-H-L (CH1 10-CL 126) 131-214' 131"-214'"
Inter-H-H (h 8, h 11) 223-223" 226-226"

N-glycosylation sites / Sites de N-glycosylation / Posiciones de N-glicosilación
H CH2 N84.4: 294, 294"
Fucosylated complex bi-antennary CHO-type glycans / glycanes de type CHO bi-antennaires complexes fucosylés / glicanos de tipo CHO biantenarios complejos fucosilados

claturafenibum

claturafenib

N-{2-chloro-3-[(5-chloro-3-methyl-4-oxo-3,4-dihydroquinazolin-6-yl)amino]-4-fluorophenyl}-3-fluoroazetidine-1-sulfonamide
B-Raf (BRAF) inhibitor, antineoplastic

claturafénib

N-{2-chloro-3-[(5-chloro-3-méthyl-4-oxo-3,4-dihydroquinazolin-6-yl)amino]-4-fluorophényl}-3-fluoroazétidine-1-sulfonamide
inhibiteur de B-Raf (BRAF), antinéoplasique

claturafenib

N-{2-cloro-3-[(5-cloro-3-metil-4-oxo-3,4-dihidroquinazolin-6-il)amino]-4-fluorofenil}-3-fluoroazetidina-1-sulfonamida
inhibidor B-Raf (BRAF), antineoplásico

$C_{18}H_{15}Cl_2F_2N_5O_3S$ 2754408-94-9

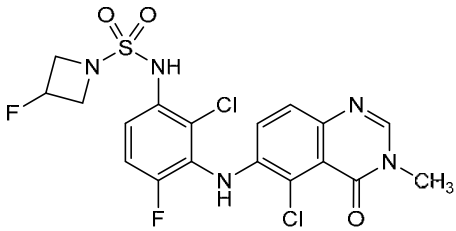

cliramitugum #

cliramitug

immunoglobulin G1-kappa, anti-[*Homo sapiens* TTR (transthyretin) amyloid], *Homo sapiens* monoclonal antibody; H-gamma1 heavy chain *Homo sapiens* (1-450) [VH (*Homo sapiens* IGHV4-39*01 (87.9%) -(IGHD) -IGHJ3*02 (100%), CDR-IMGT [10.7.12](26-35.53-59.98-109)) (1-120) -*Homo sapiens* IGHG1*03 (100%) G1m3, nG1m1 CH1 R120, CH3 E12, M14 (CH1 R120 (217) (121-218), hinge 1-15 (219-233), CH2 (234-343), CH3 E12 (359), M14 (361) (344-448), CHS (449-450)) (121-450)], (223-214')-disulfide with L-kappa light chain *Homo sapiens* (1'-214') [V-KAPPA (*Homo sapiens* IGKV1-39*01 (92.6%) -IGKJ1*01 (100%), CDR-IMGT [6.3.9] (27'-32'.50'-52'.89'-97')) (1'-107') -*Homo sapiens* IGKC*01 (100%) Km3 A45.1, V101 (C-KAPPA A45.1 (153'), V101 (191')) (108'-214')]; dimer (229-229":232-232")-bisdisulfide, produced in Chinese hamster ovary (CHO) cells, cell line CHO-K1, glycoform alfa
transthyretin inhibitor, amyloidosis

cliramitug

immunoglobuline G1-kappa, anti-[*Homo sapiens* TTR (transthyrétine) amyloïde], anticorps monoclonal *Homo sapiens*; chaîne lourde H-gamma1 *Homo sapiens* (1-450) [VH (*Homo sapiens* IGHV4-39*01 (87.9%) -(IGHD) -IGHJ3*02 (100%), CDR-IMGT [10.7.12] (26-35.53-59.98-109)) (1-120) -*Homo sapiens* IGHG1*03 (100%) G1m3, nG1m1 CH1 R120, CH3 E12, M14 (CH1 R120 (217) (121-218), charnière 1-15 (219-233), CH2 (234-343), CH3 E12 (359), M14 (361) (344-448), CHS (449-450)) (121-450)], (223-214')-disulfure avec la chaîne légère L-kappa *Homo sapiens* (1'-214') [V-KAPPA (*Homo sapiens* IGKV1-39*01 (92.6%) -IGKJ1*01 (100%), CDR-IMGT [6.3.9] (27'-32'.50'-52'.89'-97')) (1'-107') -*Homo sapiens* IGKC*01 (100%) Km3 A45.1, V101 (C-KAPPA A45.1 (153'), V101 (191')) (108'-214')]; dimère (229-229":232-232")-bisdisulfure, produit dans des cellules ovariennes de hamster chinois (CHO), lignée cellulaire CHO-K1, glycoforme alfa
inhibiteur de la transthyrétine, amylose

cliramitug

inmunoglobulina G1-kappa, anti-[*Homo sapiens* TTR (transtiretina) amieloide], anticuerpo monoclonal *Homo sapiens*;
cadena pesada H-gamma1 *Homo sapiens* (1-450) [VH (*Homo sapiens* IGHV4-39*01 (87.9%) -(IGHD) -IGHJ3*02 (100%), CDR-IMGT [10.7.12] (26-35.53-59.98-109)) (1-120) -*Homo sapiens* IGHG1*03 (100%) G1m3, nG1m1 CH1 R120, CH3 E12, M14 (CH1 R120 (217) (121-218), bisagra 1-15 (219-233), CH2 (234-343), CH3 E12 (359), M14 (361) (344-448), CHS (449-450)) (121-450)], (223-214')-disulfuro con la cadena ligera L-kappa *Homo sapiens* (1'-214') [V-KAPPA (*Homo sapiens* IGKV1-39*01 (92.6%) -IGKJ1*01 (100%), CDR-IMGT [6.3.9] (27'-32'.50'-52'.89'-97')) (1'-107') -*Homo sapiens* IGKC*01 (100%) Km3 A45.1, V101 (C-KAPPA A45.1 (153'), V101 (191')) (108'-214')]; dímero (229-229'':232-232'')-bisdisulfuro, producido en las células ováricas de hámster chino (CHO), línea celular CHO-K1, forma glicosilada alfa
inhibidor de transtiretina, amiloidosis

2965214-50-8

Heavy chain / Chaîne lourde / Cadena pesada

```
QLQLQESGPG LVKPSETLSL TCSVSGGSII SRSSYWGWIR QPPGKGLEWI  50
GGIYHSGNTY DNPSLKSRLT MSVDTSKNQF SLNLRSVTAA DTAVYYCARI 100
VPGGDAFDIW GQGTMVTVSS ASTKGPSVFP LAPSSKSTSG GTAALGCLVK 150
DYFPEPVTVS WNSGALTSGV HTFPAVLQSS GLYSLSSVVT VPSSSLGTQT 200
YICNVNHKPS NTKVDKRVEP KSCDKTHTCP PCPAPELLGG PSVFLFPPKP 250
KDTLMISRTP EVTCVVVDVS HEDPEVKFNW YVDGVEVHNA KTKPREEQYN 300
STYRVVSVLT VLHQDWLNGK EYKCKVSNKA LPAPIEKTIS KAKGQPREPQ 350
VYTLPPSREE MTKNQVSLTC LVKGFYPSDI AVEWESNGQP ENNYKTTPPV 400
LDSDGSFFLY SKLTVDKSRW QQGNVFSCSV MHEALHNHYT QKSLSLSPGK 450
```

Light chain / Chaîne légère / Cadena ligera

```
DIQMTQSPSS LSASVGDRVT IACRASQSVG TYLNWYQQKR GKAPKLLIFA  50
ASSLQSGVPS RFSGSGSGTD FTLTISSLQP EDFATYYCQQ SYSSPPTFGQ 100
GTKVEIKRTV AAPSVFIFPP SDEQLKSGTA SVVCLLNNFY PREAKVQWKV 150
DNALQSGNSQ ESVTEQDSKD STYSLSSTLT LSKADYEKHK VYACEVTHQG 200
LSSPVTKSFN RGEC                                        214
```

Post-translational modifications
Disulfide bridges location / Position des ponts disulfure / Posiciones de los puentes disulfuro
Intra-H (C23-C104) 22-97 147-203 264-324 370-428
22''-97'' 147''-203'' 264''-324'' 370''-428''
Intra-L (C23-C104) 23'-88' 134'-194'
23'''-88''' 134'''-194'''
Inter-H-L (h 5-CL 126) 223-214' 223''-214'''
Inter-H-H (h 11, h 14) 229-229'' 232-232''

N-terminal glutaminyl cyclization / Cyclisation du glutaminyle N-terminal / Ciclación del glutaminilo N-terminal
Q > pyroglutamyl (pE, 5-oxoprolyl) / pyroglutamyle (pE, 5-oxoprolyle) / piroglutamilo (pE, 5-oxoprolilo)
H VH Q1: 1, 1''

N-glycosylation sites / Sites de N-glycosylation / Posiciones de N-glicosilación
H CH2 N84.4: 300, 300''
Fucosylated complex bi-antennary CHO-type glycans / glycanes de type CHO bi-antennaires complexes fucosylés / glicanos de tipo CHO biantenarios complejos fucosilados

C-terminal lysine clipping / Coupure de la lysine C-terminale / Recorte de lisina C-terminal
H CHS K2: 450, 450''

colfoscerili miristas
colfosceril miristate

(2*R*)-2,3-bis(tetradecanoyloxy)propyl 2-(trimethylazaniumyl)ethyl phosphate
surfactant replacement

miristate de colfoscéril — phosphate de (2*R*)-2,3-bis(tétradécanoyloxy)propyle et de 2-(triméthylazaniumyl)éthyle
surfactant pulmonaire

miristato de colfoscerilo — fosfato de (2*R*)-2,3-bis(tetradecanoiloxi)propilo y 2-(trimetilazanioil)etilo
surfactante pulmonar

$C_{36}H_{72}NO_8P$ 18194-24-6

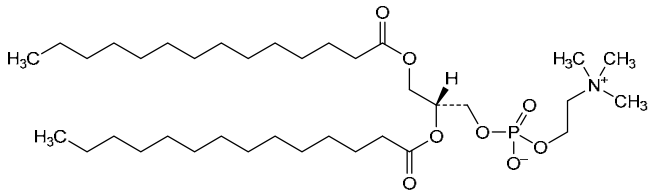

colulintidum

colulintide — *N*$^{2.1}$-acetyl-*N*$^{6.11}$-[(22*S*)-22,42-dicarboxy-10,19,24-trioxo-3,6,12,15-tetraoxa-9,18,23-triazadotetracontan-1-oyl]calcitonin [*Anguilla japonica* (Japanese eel)], [C^{1}>A, N^{3}>H, C^{7}>A, Q^{14}>2MeAla, Q^{20}>E, T^{21}>D, G^{30}>E, T^{31}>S]-variant;
N-acetyl-L-alanyl-L-seryl-L-histidyl-L-leucyl-L-seryl-L-threonyl-L-alanyl-L-valyl-L-leucylglycyl-N^{6}-({[N-(19-carboxynonadecanoyl)-L-γ-glutamyl]amino}-10-oxo-3,6,12,15-tetraoxa-9-azaheptadecanoic-1-oyl)-L-lysyl-L-leucyl-L-seryl-2-methylalanyl-L-α-glutamyl-L-leucyl-L-histidyl-L-lysyl-L-leucyl-L-α-glutamyl-L-α-aspartyl-L-tyrosyl-L-prolyl-L-arginyl-L-threonyl-L-α-aspartyl-L-valylglycyl-L-alanyl-L-α-glutamyl-L-seryl-L-prolylamide
amylin functional analogue, obesity

colulintide — *N*$^{2.1}$-acétyl-*N*$^{6.11}$-[(22*S*)-22,42-dicarboxy-10,19,24-trioxo-3,6,12,15-tétraoxa-9,18,23-triazadotétracontan-1-oyl]calcitonine [*Anguilla japonica* (anguille du Japon)], variant [C^{1}>A, N^{3}>H, C^{7}>A, Q^{14}>2MeAla, Q^{20}>E, T^{21}>D, G^{30}>E, T^{31}>S];
N-acétyl-L-alanyl-L-séryl-L-histidyl-L-leucyl-L-séryl-L-thréonyl-L-alanyl-L-valyl-L-leucylglycyl-*N*^{6}-({[*N*-(19-carboxynonadécanoyl)-L-γ-glutamyl]amino}-10-oxo-3,6,12,15-tétraoxa-9-azaheptadécanoïc-1-oyl)-L-lysyl-L-leucyl-L-séryl-2-méthylalanyl-L-α-glutamyl-L-leucyl-L-histidyl-L-lysyl-L-leucyl-L-α-glutamyl-L-α-aspartyl-L-tyrosyl-L-prolyl-L-arginyl-L-thréonyl-L-α-aspartyl-L-valylglycyl-L-alanyl-L-α-glutamyl-L-séryl-L-prolylamide
analogue fonctionnel de l'amyline, obésité

colulintida — *N*$^{2.1}$-acetil-*N*$^{6.11}$-[(22*S*)-22,42-dicarboxi-10,19,24-trioxo-3,6,12,15-tetraoxa-9,18,23-triazadotetracontan-1-oil]calcitonina (*Anguilla japonica*), variante [C^{1}>A, N^{3}>H, C^{7}>A, Q^{14}>2MeAla, Q^{20}>E, T^{21}>D, G^{30}>E, T^{31}>S];
N-acetil-L-alanil-L-seril-L-histidil-L-leucil-L-seril-L-treonil-L-alanil-L-valil-L-leucilglicil-*N*^{6}-({[*N*-(19-carboxinonadecanoil)-L-γ-glutamil]amino}-10-oxo-3,6,12,15-tetraoxa-9-azaheptadecanoic-1-oil)-L-lisil-L-leucil-L-seril-2-metilalanil-L-α-glutamil-L-leucil-L-histidil-L-lisil-L-leucil-L-α-glutamil-L-α-aspartil-L-tirosil-L-prolil-L-arginil-L-treonil-L-α-aspartil-L-valilglicil-L-alanil-L-α-glutamil-L-seril-L-prolilamida
análogo funcional de la amilina, obesidad

$C_{188}H_{309}N_{45}O_{62}$ 2891912-36-8

ASHLSTAVLG KLSAELHKLE DYPRTDVGAE SP 32

Modified residues / Résidus modifiés / Restos modificados

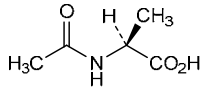

A (1)
N-Ac-L-Ala

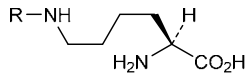

K (11)
N^6-R-L-Lys

R:

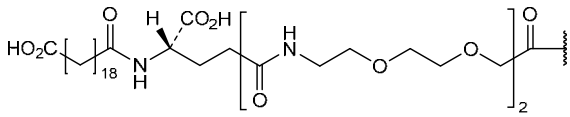

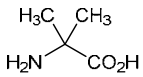

A (14)
2-methyl-Ala, Aib

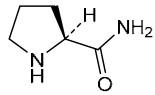

P (32)
L-Pro-NH_2

corabotasum #

corabotase

botulinum neurotoxin type A (BoNT/A, botA) [*Clostridium botulinum* strain Hall (ATCC 3502, NCTC 13319)], heavy chain fragment (HC 1-424), fused to botulinum neurotoxin type B (BoNT/B, botB) (*Clostridium botulinum* strain Okra), heavy chain, C-terminal fragment (HC 419-850, 425-856 in the final protein), variant (E^{750}>M^{756}, S^{758}>Y^{764}), (6-429')-disulfide with botulinum neurotoxin type A (BoNT/A, botA) [*Clostridium botulinum* strain Hall (ATCC 3502, NCTC 13319)], des-Met^0-light chain (LC 1'-437') (EC:3.4.24.69), produced by *Escherichia coli*
muscle relaxant

corabotase

neurotoxine botulique de type A (BoNT/A, botA) [*Clostridium botulinum*, souche Hall (ATCC 3502, NCTC 13319)], chaîne lourde, fragment (HC 1-424), fusionné à la neurotoxine botulique de type B (BoNT/B, botB) (*Clostridium botulinum*, souche Okra), chaîne lourde, fragment C-terminal (HC 419-850, 425-856 dans la protéine finale), variant (E^{750}>M^{756}, S^{758}>Y^{764}), (6-429')-disulfure avec neurotoxine botulique de type A (BoNT/A, botA) [*Clostridium botulinum*, souche Hall (ATCC 3502, NCTC 13319)], chaîne légère dés-Met^0 (LC 1'-437') (EC:3.4.24.69), produite par *Escherichia coli*
relaxant musculaire

corabotasa

neurotoxina botulínica tipo A (BoNT/A, botA) [*Clostridium botulinum* cepa Hall (ATCC 3502, NCTC 13319)], cadena pesada, fragmento (HC 1-424), fusionada a neurotoxina botulínica tipo B (BoNT/B, botB) (*Clostridium botulinum* cepa Okra), cadena pesada, fragmento C-terminal (HC 419-850, 425-856 en la proteína final), variante (E^{750}>M^{756}, S^{758}>Y^{764}), (6-429')-

disulfuro con neurotoxina botulínica tipo A (BoNT/A, botA) [*Clostridium botulinum* cepa Hall (ATCC 3502, NCTC 13319)], cadena ligera des-Met^{0} (LC 1'-437') (EC:3.4.24.69), producida por *Escherichia coli*
relajante muscular

2616765-46-7

Sequence / Séquence / Secuencia
Heavy chain / Chaîne lourde / Cadena pesada: **BoNT/A + BoNT/B**

ALNDLCIKVN NWDLFFSPSE DNFTNDLNKG EEITSDTNIE AAEENISLDL 50
IQQYYLTFNF DNEPENISIE NLSSDIIGQL ELMPNIERFP NGKKYELDKY 100
TMFHYLRAQE FEHGKSRIAL TNSVNEALLN PSRVYTFFSS DYVKKVNKAT 150
EAAMFLGWVE QLVYDFTDET SEVSTTDKIA DITIIIPYIG PALNIGNMLY 200
KDDFVGALIF SGAVILLEFI PEIAIPVLGT FALVSYIANK VLTVQTIDNA [illegible]
LSKRNEKWDE VYKYIVTNWL AKVNTQIDLI RKKMKEALEN QAEATKAIIN 300
YQYNQYTEEE KNNINFNIDD LSSKLNESIN KAMININKFL NQCSVSYLMN 350
SMIPYGVKRL EDFDASLKDA LLKYIYDNRG TLIGQVDRLK DKVNNTLSTD 400
IPFQLSKYVD NQRLLSTFTE YIKN[illegible] [illegible] [illegible] 450
[illegible] [illegible] [illegible] [illegible] [illegible] 500
[illegible] [illegible] [illegible] [illegible] [illegible] 550
FFEYNIREDI [illegible] [illegible] [illegible] [illegible] 600
[illegible] [illegible] [illegible] [illegible] [illegible] [illegible]
[illegible] [illegible] [illegible] [illegible] [illegible] 700
[illegible] [illegible] [illegible] [illegible] [illegible] 750
FKKEE**M**KLFL API**Y**DSDEFY [illegible] [illegible] [illegible] 800
[illegible] [illegible] [illegible] [illegible] [illegible] 850
DEGWTE 856

Light chain / Chaîne légère / Cadena ligera: BoNT/A
[illegible] [illegible] [illegible] [illegible] [illegible] 50
[illegible] [illegible] [illegible] [illegible] [illegible] 100
[illegible] [illegible] [illegible] [illegible] [illegible] 150
[illegible] [illegible] [illegible] [illegible] [illegible] 200
[illegible] [illegible] [illegible] [illegible] [illegible] [illegible]
[illegible] [illegible] [illegible] [illegible] [illegible] 300
[illegible] [illegible] [illegible] [illegible] [illegible] 350
[illegible] [illegible] [illegible] [illegible] [illegible] 400
[illegible] [illegible] [illegible] [illegible] 437

Mutations / Mutations / Mutaciónes
BoNT/B C-terminal fragment: E^{750}>**M**^{756}, S^{758}>**Y**^{764}

Post-translational modifications
Disulfide bridge location / Position du pont disulfure / Posición del puente disulfuro
6-429'

N-Glycosylation sites / Sites de N-glycosylation / Posiciones de N-glicosilación
none / aucun / ninguna

crusekitugum #

crusekitug

immunoglobulin G1-kappa, anti-[*Homo sapiens* IL17A (interleukin 17A, IL-17A)], humanized monoclonal antibody; H-gamma1 heavy chain humanized (1-450) [VH (*Homo sapiens* IGHV4-4*08 (79.4%) -(IGHD) -IGHJ1*01 (100%), CDR-IMGT [8.7.14] (26-33.51-57.96-109)) (1-120) -*Homo sapiens* IGHG1*01 (100%) G1m17,1 CH1 K120, CH3 D12, L14 (CH1 K120 (217) (121-218), hinge 1-15 (219-233), CH2 (234-343), CH3 D12 (359), L14 (361) (344-448), CHS (449-450)) (121-450)], (223-217')-disulfide with L-kappa light chain humanized (1'-217') [V-KAPPA (*Homo sapiens* IGKV1-12*01 (89.2%) -IGKJ4*01 (91.7%), CDR-IMGT [6.3.12] (27'-32'.50'-52'.89'-100')) (1'-110') -*Homo sapiens* IGKC*01 (100%) Km3 A45.1, V101 (C-KAPPA A45.1 (156'), V101 (194')) (111'-217')]; dimer (229-229'':232-232'')-bisdisulfide, produced in Chinese hamster ovary (CHO) cells, cell line CHO-S, glycoform alfa
immunosuppressant, anti-inflammatory

crusékitug

immunoglobuline G1-kappa, anti-[*Homo sapiens* IL17A (interleukine 17A, IL-17A)], anticorps monoclonal humanisé;

chaîne lourde H-gamma1 humanisée (1-450) [VH (*Homo sapiens* IGHV4-4*08 (79.4%) -(IGHD) -IGHJ1*01 (100%), CDR-IMGT [8.7.14] (26-33.51-57.96-109)) (1-120) -*Homo sapiens* IGHG1*01 (100%) G1m17,1 CH1 K120, CH3 D12, L14 (CH1 K120 (217) (121-218), charnière 1-15 (219-233), CH2 (234-343), CH3 D12 (359), L14 (361) (344-448), CHS (449-450)) (121-450)], (223-217')-disulfure avec la chaîne légère L-kappa humanisée (1'-218') [V-KAPPA (*Homo sapiens* IGKV1-12*01 (89.2%) -IGKJ4*01 (91.7%), CDR-IMGT [6.3.12] (27'-32'.50'-52'.89'-100')) (1'-110') -*Homo sapiens* IGKC*01 (100%) Km3 A45.1, V101 (C-KAPPA A45.1 (156'), V101 (194')) (111'-217')]; dimère (229-229'':232-232'')-bisdisulfure, produit dans des cellules ovariennes de hamster chinois (CHO), lignée cellulaire CHO-S, glycoforme alfa
immunosuppresseur, anti-inflammatoire

crusekitug

inmunoglobulina G1-kappa, anti-[*Homo sapiens* IL17A (interleukina 17A, IL-17A)], anticuerpo monoclonal humanizado;
cadena pesada H-gamma1 humanizada (1-450) [VH (*Homo sapiens* IGHV4-4*08 (79.4%) -(IGHD) -IGHJ1*01 (100%), CDR-IMGT [8.7.14] (26-33.51-57.96-109)) (1-120) -*Homo sapiens* IGHG1*01 (100%) G1m17,1 CH1 K120, CH3 D12, L14 (CH1 K120 (217) (121-218), bisagra 1-15 (219-233), CH2 (234-343), CH3 D12 (359), L14 (361) (344-448), CHS (449-450)) (121-450)], (223-217')-disulfuro con la cadena ligera L-kappa humanizada (1'-218') [V-KAPPA (*Homo sapiens* IGKV1-12*01 (89.2%) -IGKJ4*01 (91.7%), CDR-IMGT [6.3.12] (27'-32'.50'-52'.89'-100')) (1'-110') -*Homo sapiens* IGKC*01 (100%) Km3 A45.1, V101 (C-KAPPA A45.1 (156'), V101 (194')) (111'-217')]; dímero (229-229'':232-232'')-bisdisulfuro, producido en las células ováricas de hámster chino (CHO), línea celular CHO-S, forma glicosilada alfa
inmunosupresor, intiinflamatorio

2956768-50-4

Heavy chain / Chaîne lourde / Cadena pesada
```
EVQLQESGPG LVKPSETLSL TCTVSGIDLS DFYWSWIRQP PGKGLEWIGH  50
IHEVASITYA SWAKGRVTIS KDTSKNQFSL KLSSVTAADT AVYYCARSDY 100
FSRYFSPNIW GQGTLVTVSS ASTKGPSVFP LAPSSKSTSG GTAALGCLVK 150
DYFPEPVTVS WNSGALTSGV HTFPAVLQSS GLYSLSSVVT VPSSSLGTQT 200
YICNVNHKPS NTKVDKKVEP KSCDKTHTCP PCPAPELLGG PSVFLFPPKP 250
KDTLMISRTP EVTCVVVDVS HEDPEVKFNW YVDGVEVHNA KTKPREEQYN 300
STYRVVSVLT VLHQDWLNGK EYKCKVSNKA LPAPIEKTIS KAKGQPREPQ 350
VYTLPPSRDE LTKNQVSLTC LVKGFYPSDI AVEWESNGQP ENNYKTTPPV 400
LDSDGSFFLY SKLTVDKSRW QQGNVFSCSV MHEALHNHYT QKSLSLSPGK 450
```

Light chain / Chaîne légère / Cadena ligera
```
DIQMTQSPSS VSASVGDRVT ITCQASQNIY SSLAWYQQKP GKAPKLLIYH  50
ASSLASGVPS RFSGSGSGTD FTLTISSLQP EDFATYYCQS YNDISTYNLA 100
FGGGTKVEIK RTVAAPSVFI FPPSDEQLKS GTASVVCLLN NFYPREAKVQ 150
WKVDNALQSG NSQESVTEQD SKDSTYSLSS TLTLSKADYE KHKVYACEVT 200
HQGLSSPVTK SFNRGEC                                     217
```

Post-translational modifications
Disulfide bridges location / Position des ponts disulfure / Posiciones de los puentes disulfuro
Intra-H (C23-C104) 22-95 147-203 264-324 370-428
22''-95'' 147''-203'' 264''-324'' 370''-428''
Intra-L (C23-C104) 23'-88' 137'-197'
23'''-88''' 137'''-197'''
Inter-H-L (h 5-CL 126) 223-217' 223''-217'''
Inter-H-H (h 11, h 14) 229-229'' 232-232''

N-glycosylation sites / Sites de N-glycosylation / Posiciones de N-glicosilación
H CH2 N84.4: 300, 300''
Fucosylated complex bi-antennary CHO-type glycans / glycanes de type CHO bi-antennaires complexes fucosylés / glicanos de tipo CHO biantenarios complejos fucosilados

C-terminal lysine clipping / Coupure de la lysine C-terminale / Recorte de lisina C-terminal
H CHS K2: 450, 450''

cupri histidinas

copper histidinate — di(L-histidinato)copper
copper supplement

histidinate de cuivre — di(L-histidinato)cuivre
supplément en cuivre

histidinato de cobre — di(L-histidinato)cobre
suplemento de cobre

$C_{12}H_{16}CuN_6O_4$ 13870-80-9

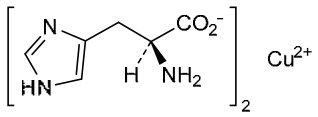

dabogratinibum

dabogratinib — [6-(5-{5-[(1*R*)-1-(3,5-dichloropyridin-4-yl)ethoxy]-1*H*-indazol-3-yl}pyridin-2-yl)-2,6-diazaspiro[3.3]heptan-2-yl](methyl)-λ^6-sulfanedione
fibroblast growth factor receptor inhibitor, antineoplastic

dabogratinib — [6-(5-{5-[(1*R*)-1-(3,5-dichloropyridin-4-yl)éthoxy]-1*H*-indazol-3-yl}pyridin-2-yl)-2,6-diazaspiro[3.3]heptan-2-yl](méthyl)- λ^6-sulfanedione
inhibiteur du récepteur du facteur de croissance des fibroblastes, antinéoplasique

dabogratinib — [6-(5-{5-[(1*R*)-1-(3,5-dicloropiridin-4-il)etoxi]-1*H*-indazol-3-il}piridin-2-il)-2,6-diazaespiro[3.3]heptan-2-il](metil)-λ^6-sulfanodiona
inhibidor del receptor del factor de crecimiento de fibroblastos, antineoplásico

$C_{25}H_{24}Cl_2N_6O_3S$ 2800223-30-5

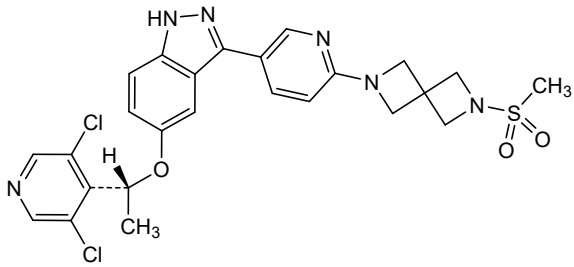

dalidnetugum #

dalidnetug — immunoglobulin G1-kappa, anti-[*Homo sapiens* APP (amyloid beta, A4 precursor protein) Abeta], humanized monoclonal antibody;

	H-gamma1 heavy chain humanized (1-449) [VH (*Homo sapiens* IGHV3-23*03 (87.8%) -(IGHD) - IGHJ4*01 (100%), CDR-IMGT [8.8.12] (26-33.51-58.97-108)) (1-119) -*Homo sapiens* IGHG1*03v (100%) G1m3>G1m17, nG1m1 CH1 K120, CH3 E12, M14 (CH1 R120>K (216) (120-217), hinge 1-15 (218-232), CH2 (233-342), CH3 E12 (358), M14 (360) (343-447), CHS (448-449)) (120-449)], (222-219')-disulfide with L-kappa light chain humanized (1'-219') [V-KAPPA (*Homo sapiens* IGKV2-30*02 (85.0%) - IGKJ1*01 (90.9%), CDR-IMGT [11.3.9] (27'-37'.55'-57'.94'-102')) (1'-112') -*Homo sapiens* IGKC*01 (100%) Km3 A45.1, V101 (C-KAPPA A45.1 (158'), V101 (196')) (113'-219')]; dimer (228-228'':231-231'')-bisdisulfide, produced in Chinese hamster ovary (CHO) cells, cell line CHO-S, glycoform alfa *clearance of amyloid beta, Alzheimer's disease*
dalidnetug	immunoglobuline G1-kappa, anti-[*Homo sapiens* APP (amyloïde bêta, protéine précurseur A4) Abêta]; anticorps monoclonal humanisé; chaîne lourde H-gamma1 humanisée (1-449) [VH (*Homo sapiens* IGHV3-23*03 (87.8%) -(IGHD) - IGHJ4*01 (100%), CDR-IMGT [8.8.12] (26-33.51-58.97-108)) (1-119) -*Homo sapiens* IGHG1*03v (100%) G1m3>G1m17, nG1m1 CH1 K120, CH3 E12, M14 (CH1 R120>K (216) (120-217), charnière 1-15 (218-232), CH2 (233-342), CH3 E12 (358), M14 (360) (343-447), CHS (448-449)) (120-449)], (222-219')-disulfure avec la chaîne légère L-kappa humanisée (1'-219') [V-KAPPA (*Homo sapiens* IGKV2-30*02 (85.0%) -IGKJ1*01 (90.9%), CDR-IMGT [11.3.9] (27'-37'.55'-57'.94'-102')) (1'-112') -*Homo sapiens* IGKC*01 (100%) Km3 A45.1, V101 (C-KAPPA A45.1 (158'), V101 (196')) (113'-219')]; dimère (228-228'':231-231'')-bisdisulfure, produit dans des cellules ovariennes de hamster chinois (CHO), lignée cellulaire CHO-S, glycoforme alfa *clairance d'amyloïde bêta, maladie d'Alzheimer*
dalidnetug	inmunoglobulina G1-kappa, anti-[*Homo sapiens* APP (amieloide beta, proteína precursor A4) Abeta]; anticuerpo monoclonal humanizado; cadena pesada H-gamma1 humanizada (1-449) [VH (*Homo sapiens* IGHV3-23*03 (87.8%) -(IGHD) - IGHJ4*01 (100%), CDR-IMGT [8.8.12] (26-33.51-58.97-108)) (1-119) -*Homo sapiens* IGHG1*03v (100%) G1m3>G1m17, nG1m1 CH1 K120, CH3 E12, M14(CH1 R120>K (216) (120-217), bisagra 1-15 (218-232), CH2 (233-342), CH3 E12 (358), M14 (360) (343-447), CHS (448-449)) (120-449)], (222-219')-disulfuro con la cadena ligera L-kappa humanizada (1'-219') [V-KAPPA (*Homo sapiens* IGKV2-30*02 (85.0%) - IGKJ1*01 (90.9%), CDR-IMGT [11.3.9] (27'-37'.55'-57'.94'-102')) (1'-112') -*Homo sapiens* IGKC*01 (100%) Km3 A45.1, V101 (C-KAPPA A45.1 (158'), V101 (196')) (113'-219')]; dímero (228-228'':231-231'')-bisdisulfuro, producido en las células ováricas de hámster chino (CHO), línea celular CHO-S, forma glicosilada alfa *eliminación de beta amiloide, enfermedad de Alzheimer*

2991369-43-6

Heavy chain / Chaîne lourde / Cadena pesada

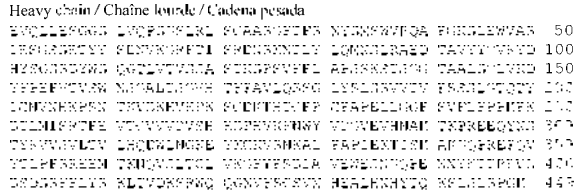

Light chain / Chaîne légère / Cadena ligera

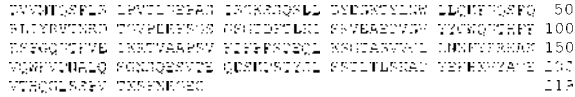

Post-translational modifications

Disulfide bridges location / Position des ponts disulfure / Posiciones de los puentes disulfuro

Intra-H (C23-C104) 22-96 146-202 263-323 369-427
22"-96" 146"-202" 263"-323" 369"-427"

Intra-L (C23-C104) 23'-93' 139'-199'
23'"-93'" 139'"-199'"

Inter-H-L (h 5-CL 126) 222-219' 222"-219'"

Inter-H-H (h 11, h 14) 228-228" 231-231"

N-glycosylation sites / Sites de N-glycosylation / Posiciones de N-glicosilación

H CH2 N84.4; 299, 299"

Fucosylated complex bi-antennary CHO-type glycans / glycanes de type CHO bi-antennaires complexes fucosylés / glicanos de tipo CHO biantenarios complejos fucosilados

C-terminal lysine clipping / Coupure de la lysine C-terminale / Recorte de lisina C-terminal

H CHS K2: 449, 449"

danifexorum

danifexor

1^2,1^6-dichloro-2^5-cyclopropyl-4,6-dioxa-7(2)-pyridina-2(3,4)-[1,2]oxazola-5(2,6)-naphthalena-1(1)-benzenaheptaphane-7^5-carboxylic acid
farnesoid X receptor agonist

danifexor

acide 1^2,1^6-dichloro-2^5-cyclopropyl-4,6-dioxa-7(2)-pyridina-2(3,4)-[1,2]oxazola-5(2,6)-naphtaléna-1(1)-benzénaheptaphane-7^5-carboxylique
agoniste du récepteur farnésoïde X

danifexor

ácido 2^5-ciclopropil-1^2,1^6-dicloro-4,6-dioxa-7(2)-piridina-2(3,4)-[1,2]oxazola-5(2,6)-naftalena-1(1)-bencenaheptafano-7^5-carboxílico
agonista del receptor de farnesoide X

$C_{29}H_{20}Cl_2N_2O_5$ 2648738-68-3

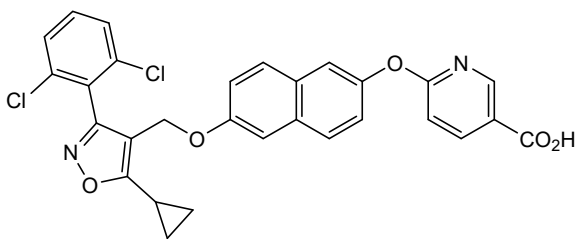

daraxonrasibum

daraxonrasib (1*S*,2*S*)-*N*-[(1^{2}*M*,4*S*,6^{3}*S*)-1^{1}-ethyl-1^{2}-{2-[(1*S*)-1-methoxyethyl]-5-(4-methylpiperazin-1-yl)pyridin-3-yl}-10,10-dimethyl-5,7-dioxo-1^{1}*H*-8-oxa-1(5,3)-indola-6(1,3)-[1,2]diazinana-2(4,2)-[1,3]thiazolacycloundecaphan-4-yl]-2-methylcyclopropane-1-carboxamide
Kirsten rat sarcoma viral oncogene homolog inhibitor, antineoplastic

daraxonrasib (1*S*,2*S*)-*N*-[(1^{2}*M*,4*S*,6^{3}*S*)-1^{1}-éthyl-1^{2}-{2-[(1*S*)-1-méthoxyéthyl]-5-(4-méthylpipérazin-1-yl)pyridin-3-yl}-10,10-diméthyl-5,7-dioxo-1^{1}*H*-8-oxa-1(5,3)-indola-6(1,3)-[1,2]diazinana-2(4,2)-[1,3]thiazolacycloundécaphan-4-yl]-2-méthylcyclopropane-1-carboxamide
inhibiteur d'homologue d'oncogène viral du sarcome de rat de Kirsten, antinéoplasique

daraxonrasib (1*S*,2*S*)-*N*-[(1^{2}*M*,4*S*,6^{6}*S*)-1^{1}-etil-10,10-dimetil-1^{2}-{5-(4-metilpiperazin-1-il)-2-[(1*S*)-1-metoxietil]piridin-3-il}-5,7-dioxo-1^{1}*H*-8-oxa-1(5,3)-indola-6(2,6)-[1,2]diazinana-2(4,2)-[1,3]tiazolaciclоundecafan-4-il]-2-metilciclopropano-1-carboxamida
inhibidor del homólogo del oncogen vírico del sarcoma de rata Kirsten, antineoplásico

$C_{44}H_{58}N_8O_5S$ 2765081-21-6

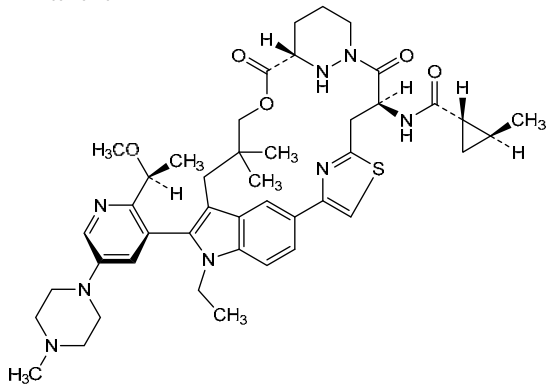

daretabartum #

daretabart immunoglobulin G1-kappa, anti-[*Homo sapiens* GD2 (disialoganglioside GD2)], monoclonal antibody;
H-gamma1 heavy chain (1-443) [VH Musmus/Homsap (*Mus musculus* IGHV1-42*04 (86.5%) -(IGHD) -IGHJ4*01 (71.4%) Q120>T (105), G121>Q (106), T122>G (107) /*Homo sapiens* IGHV1-46*01 (71.9%) -(IGHD) -IGHJ5*01 (75.0%) Q120>T (105), G121>Q (106), T122>G (107), L123>S (108), CDR-IMGT [8.8.6] (26-33.51-58.97-102)) (1-113) -*Homo sapiens* IGHG1*03, G1m3, nG1m1 CH1 R120, CH3 E12, M14, 5-G1v20 CH2 A105 (CH1 R120 (210) (114-211), hinge 1-15 (212-226), CH2 K105>A (318) (227-336), CH3 E12 (352), M14 (354) (337-441), CHS (442-443)) (114-443)], (216-220')-disulfide with L-kappa light chain (1'-220') [V-KAPPA Musmus/Homsap (*Mus musculus* IGKV1-110*01 (94.0%) -IGKJ5*01 (100%)/*Homo sapiens* IGKV2D-29*02 (82.0%) -IGKJ2*01 (81.8%) Q120>A (106'), I126>L (112'), CDR-IMGT [11.3.10] (27'-37'.55'-57'.94'-103')) (1'-113') -*Homo sapiens* IGKC*01 (100%) Km3 A45.1, V101 (C-KAPPA A45.1 (159'), V101 (197')) (114'-220')]; dimer (222-222":225-225")-bisdisulfide, produced in YB2/0 cell line, glycoform alfa
antineoplastic

darétabart immunoglobuline G1-kappa, anti-[*Homo sapiens* GD2 (disialoganglioside GD2)]; anticorps monoclonal;
chaîne lourde H-gamma1 (1-443) [VH Musmus/Homsap (*Mus musculus* IGHV1-42*04 (86.5%) -(IGHD) -IGHJ4*01 (71.4%) Q120>T (105), G121>Q (106), T122>G (107) /*Homo sapiens* IGHV1-46*01 (71.9%) -(IGHD) -IGHJ5*01 (75.0%) Q120>T (105), G121>Q (106), T122>G (107), L123>S (108), CDR-IMGT [8.8.6] (26-33.51-58.97-102)) (1-113) -*Homo sapiens* IGHG1*03, G1m3, nG1m1 CH1 R120, CH3 E12, M14, 5-G1v20 CH2 A105 (CH1 R120 (210) (114-211), charnière 1-15 (212-226), CH2 K105>A (318) (227-336), CH3 E12 (352), M14 (354) (337-441), CHS (442-443)) (114-443)], (216-220')-disulfure avec la chaîne légère L-kappa (1'-220') [V-KAPPA Musmus/Homsap (*Mus musculus* IGKV1-110*01 (94.0%) -IGKJ5*01 (100%)/*Homo sapiens* IGKV2D-29*02 (82.0%) -IGKJ2*01 (81.8%) Q120>A (106'), I126>L (112'), CDR-IMGT [11.3.10] (27'-37'.55'-57'.94'-103')) (1'-113') -*Homo sapiens* IGKC*01 (100%) Km3 A45.1, V101 (C-KAPPA A45.1 (159'), V101 (197')) (114'-220')]; dimère (222-222":225-225")-bisdisulfure, produit dans la lignée cellulaire YB2/0, glycoforme alfa
antinéoplasique

daretabart inmunoglobulina G1-kappa, anti-[*Homo sapiens* GD2 (disialoganglliósido GD2)]; anticuerpo monoclonal;
cadena pesada H-gamma1 (1-443) [VH Musmus/Homsap (*Mus musculus* IGHV1-42*04 (86.5%) -(IGHD) -IGHJ4*01 (71.4%) Q120>T (105), G121>Q (106), T122>G (107) /*Homo sapiens* IGHV1-46*01 (71.9%) -(IGHD) -IGHJ5*01 (75.0%) Q120>T (105), G121>Q (106), T122>G (107), L123>S (108), CDR-IMGT [8.8.6] (26-33.51-58.97-102)) (1-113) -*Homo sapiens* IGHG1*03, G1m3, nG1m1 CH1 R120, CH3 E12, M14, 5-G1v20 CH2 A105 (CH1 R120 (210) (114-211), bisagra 1-15 (212-226), CH2 K105>A (318) (227-336), CH3 E12 (352), M14 (354) (337-441), CHS (442-443)) (114-443)], (216-220')-disulfuro con la cadena ligera L-kappa (1'-220') [V-KAPPA Musmus/Homsap (*Mus musculus* IGKV1-110*01 (94.0%) -IGKJ5*01 (100%)/*Homo sapiens* IGKV2D-29*02 (82.0%) -IGKJ2*01 (81.8%) Q120>A (106'), I126>L (112'), CDR-IMGT [11.3.10] (27'-37'.55'-57'.94'-103')) (1'-113') -*Homo sapiens* IGKC*01 (100%) Km3 A45.1, V101 (C-KAPPA A45.1 (159'), V101 (197')) (114'-220')]; dímero (222-222":225-225")-bisdisulfuro, producido en la línea celular YB2/0, forma glicosilada alfa
antineoplásico

3011830-62-6

Heavy chain / Chaîne lourde / Cadena pesada

```
EVQLVQSGAE VEKPGASVKI SCKASGSSFT GYNMNWVRQN IGKSLEWIGA  50
IDPYYGGTSY NQKFKGRATL TVDKSTSTAY MHLKSLRSED TAVYYCVSGM 100
EYWGTQGSVT VSSASTKGPS VFPLAPSSKS TSGGTAALGC LVKDYFPEPV 150
TVSWNSGALT SGVHTFPAVL QSSGLYSLSS VVTVPSSSLG TQTYICNVNH 200
KPSNTKVDKR VEPKSCDKTH TCPPCPAPEL LGGPSVFLFP PKPKDTLMIS 250
RTPEVTCVVV DVSHEDPEVK FNWYVDGVEV HNAKTKPREE QYNSTYRVVS 300
VLTVLHQDWL NGKEYKCAVS NKALPAPIEK TISKAKGQPR EPQVYTLPPS 350
REEMTKNQVS LTCLVKGFYP SDIAVEWESN GQPENNYKTT PPVLDSDGSF 400
FLYSKLTVDK SRWQQGNVFS CSVMHEALHN HYTQKSLSLS PGK        443
```

Light chain / Chaîne légère / Cadena ligera

```
DVVMTQTPLS LPVTPGEPAS ISCRSSQSLV HRNGNTYLHW YLQKPGQSPK  50
LLIHKVSNRF SGVPDRFSGS GSGTDFTLKI SRVEAEDLGV YFCSQSTHVP 100
PLTFGAGTKL ELKRTVAAPS VFIFPPSDEQ LKSGTASVVC LLNNFYPREA 150
KVQWKVDNAL QSGNSQESVT EQDSKDSTYS LSSTLTLSKA DYEKHKVYAC 200
EVTHQGLSSP VTKSFNRGEC                                   220
```

Post-translational modifications
Disulfide bridges location / Position des ponts disulfure / Posiciones de los puentes disulfuro
Intra-H (C23-C104) 22-96 140-196 257-317 363-421
22"-96" 140"-196" 257"-317" 363"-421"
Intra-L (C23-C104) 23'-93' 140'-200'
23'"-93'" 140'"-200'"
Inter-H-L (h 5-CL 126) 216-220' 216"-220'"
Inter-H-H (h 11, h 14) 222-222" 225-225"

N-glycosylation sites / Sites de N-glycosylation / Posiciones de N-glicosilación
H CH2 N84.4: 293, 293"
Mainly (>40%) afucosylated complex bi-antennary YB2/0-type glycans / glycanes de type YB2/0 bi-antennaires complexes principalement (>40%) afucosylés / glicanos de tipo YB2/0 biantenarios complejos principalmente (>40%) afucosilados

C-terminal lysine clipping / Coupure de la lysine C-terminale / Recorte de lisina C-terminal
H CHS K2: 443, 443"

darlifarnibum

darlifarnib — (3*S*)-3-amino-3-(1-methyl-1*H*-imidazol-5-yl)-6-oxa-2(4,6)-quinolina-1,4(1,3)-dibenzenacyclohexaphane-2^2,4^4-dicarbonitrile
farnesyl transferase inhibitor, antineoplastic

darlifarnib — (3*S*)-3-amino-3-(1-méthyl-1*H*-imidazol-5-yl)-6-oxa-2(4,6)-quinoléina-1,4(1,3)-dibenzénacyclohexaphane-2^2,4^4-dicarbonitrile
inhibiteur de farnésyl transférase, antinéoplasique

darlifarnib — (3*S*)-3-amino-3-(1-metil-1*H*-imidazol-5-il)-6-oxa-2(4,6)-quinoleína-1,4(1,3)-dibencenaciclohexafano-2^2,4^4-dicarbonitrilo
inhibidor de la farnesil transferasa, antineoplásico

$C_{29}H_{20}N_6O$ 2939824-30-1

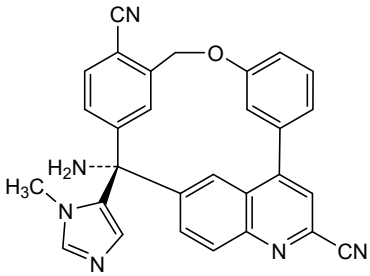

delocamtenum

delocamten — (6*S*,7*S*)-6-fluoro-7-(2-fluoro-5-methylphenyl)-3-(oxan-4-yl)-5,6,7,8-tetrahydropyrido[2,3-*d*]pyrimidine-2,4(1*H*,3*H*)-dione
cardiac myosin inhibitor

délocamten — (6*S*,7*S*)-6-fluoro-7-(2-fluoro-5-méthylphényl)-3-(oxan-4-yl)-5,6,7,8-tétrahydropyrido[2,3-*d*]pyrimidine-2,4(1*H*,3*H*)-dione
inhibiteur de myosine cardiaque

delocamtén — (6*S*,7*S*)-6-fluoro-7-(2-fluoro-5-metilfenil)-3-(oxan-4-il)-5,6,7,8-tetrahidropirido[2,3-*d*]pirimidina-2,4(1*H*,3*H*)-diona
inhibidor de la miosina cardíaca

$C_{19}H_{21}F_2N_3O_3$ 2417411-02-8

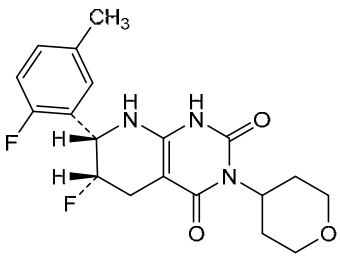

dencatistatum

dencatistat — 4-[2-(cyclopropanesulfonamido)pyrimidin-4-yl]-*N*-[5-(6-ethoxypyrazin-2-yl)pyridin-2-yl]oxane-4-carboxamide
CTP synthase 1 inhibitor, antineoplastic

dencatistat

4-[2-(cyclopropanesulfonamido)pyrimidin-4-yl]-*N*-[5-(6-éthoxypyrazin-2-yl)pyridin-2-yl]oxane-4-carboxamide
inhibiteur de la CTP synthase 1, antinéoplasique

dencatistat

4-[2-(ciclopropanosulfonamido)pirimidin-4-il]-*N*-[5-(6-etoxipirazin-2-il)piridin-2-il]oxano-4-carboxamida
inhibidor de la sintasa 1 de CTP, antineoplásico

$C_{24}H_{27}N_7O_5S$ 2377000-84-3

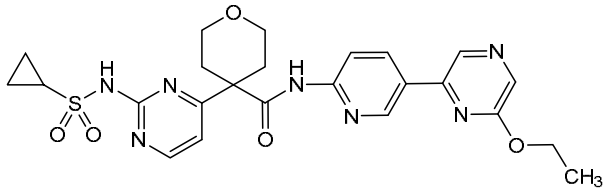

deulumateperonum

deulumateperone

1-(4-fluorophenyl)-4-[(6b*R*,10a*S*)-3-methyl-2,3,6b,9,10,10a-(2-^{2}H)hexahydro(2-^{2}H)-1*H*-pyrido[3',4':4,5]pyrrolo[1,2,3-*de*]quinoxalin-8(7*H*)-yl]butan-1-one
antipsychotic

deulumatépérone

1-(4-fluorophényl)-4-[(6b*R*,10a*S*)-3-méthyl-2,3,6b,9,10,10a-(2-^{2}H)hexahydro(2-^{2}H)-1*H*-pyrido[3',4':4,5]pyrrolo[1,2,3-*de*]quinoxalin-8(7*H*)-yl]butan-1-one
antipsychotique

deulumateperona

1-(4-fluorofenil)-4-[(6b*R*,10a*S*)-3-metil-2,3,6b,9,10,10a-(2-^{2}H)hexahidro(2-^{2}H)-1*H*-pirido[3',4':4,5]pirrolo[1,2,3-*de*]quinoxalin-8(7*H*)-il]butan-1-ona
antipsicótico

$C_{24}H_{26}{}^2H_2FN_3O$ 2102683-75-8

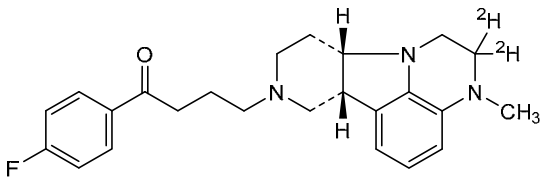

diranersenum

diranersen

all-P-ambo-2'-*O*-(2-methoxyethyl)-5-methyl-*P*-thiocytidylyl-(3'→5')-2'-*O*-(2-methoxyethyl)-5-methylcytidylyl-(3'→5')-2'-*O*-(2-methoxyethyl)-*P*-thioguanylyl-(3'→5')-2'-*O*-(2-methoxyethyl)-5-methyl-*P*-thiouridylyl-(3'→5')-2'-*O*-(2-methoxyethyl)-5-methyl-*P*-thiouridylyl-(3'→5')-*P*-thiothymidylyl-(3'→5')-*P*-thiothymidylyl-(3'→5')-2'-deoxy-5-methyl-*P*-thiocytidylyl-(3'→5')-*P*-thiothymidylyl-(3'→5')-*P*-thiothymidylyl-(3'→5')-2'-deoxy-*P*-thioadenylyl-(3'→5')-2'-deoxy-5-methyl-*P*-thiocytidylyl-(3'→5')-2'-deoxy-5-methyl-*P*-thiocytidylyl-(3'→5')-2'-*O*-(2-methoxyethyl)-*P*-thioadenylyl-(3'→5')-2'-*O*-(2-methoxyethyl)-5-methylcytidylyl-(3'→5')-2'-*O*-(2-methoxyethyl)-5-methyl-*P*-thiocytidylyl-(3'→5')-2'-*O*-(2-methoxyethyl)-5-methyl-*P*-thiocytidylyl-(3'→5')-2'-*O*-(2-methoxyethyl)-5-methyluridine
microtubule-associated protein tau synthesis reducer, Alzheimer's disease

diranersen

tout-P-ambo-2'-*O*-(2-méthoxyéthyl)-5-méthyl-*P*-thiocytidylyl-(3'→5')-2'-*O*-(2-méthoxyéthyl)-5-méthylcytidylyl-(3'→5')-2'-*O*-(2-méthoxyéthyl)-*P*-thioguanylyl-(3'→5')-2'-*O*-(2-méthoxyéthyl)-5-méthyl-*P*-thiouridylyl-(3'→5')-2'-*O*-(2-méthoxyéthyl)-5-méthyl-*P*-thiouridylyl-(3'→5')-*P*-thiothymidylyl-(3'→5')-*P*-thiothymidylyl-(3'→5')-2'-désoxy-5-méthyl-*P*-thiocytidylyl-(3'→5')-*P*-thiothymidylyl-(3'→5')-*P*-thiothymidylyl-(3'→5')-2'-désoxy-*P*-thioadénylyl-(3'→5')-2'-désoxy-5-méthyl-*P*-thiocytidylyl-(3'→5')-2'-désoxy-5-méthyl-*P*-thiocytidylyl-(3'→5')-2'-*O*-(2-méthoxyéthyl)-*P*-thioadénylyl-(3'→5')-2'-*O*-(2-méthoxyéthyl)-5-méthylcytidylyl-(3'→5')-2'-*O*-(2-méthoxyéthyl)-5-méthyl-*P*-thiocytidylyl-(3'→5')-2'-*O*-(2-méthoxyéthyl)-5-méthyl-*P*-thiocytidylyl-(3'→5')-2'-*O*-(2-méthoxyéthyl)-5-méthyluridine
réducteur de la synthèse de la protéine tau associée aux microtubules, maladie d'Alzheimer

diranersén

todo-P-ambo-5-metil-2'-*O*-(2-metoxietil)-*P*-tiocitidilil-(3'→5')-5-metil-2'-*O*-(2-metoxietil)citidilil-(3'→5')-2'-*O*-(2-metoxietil)-*P*-tioguanilil-(3'→5')-5-metil-2'-*O*-(2-metoxietil)-*P*-tiouridilil-(3'→5')-5-metil-2'-*O*-(2-metoxietil)-*P*-tiouridilil-(3'→5')-*P*-tiotimidilil-(3'→5')-*P*-tiotimidilil-(3'→5')-2'-desoxi-5-metil-*P*-tiocitidilil-(3'→5')-*P*-tiotimidilil-(3'→5')-*P*-tiotimidilil-(3'→5')-2'-desoxi-*P*-tioadenilil-(3'→5')-2'-desoxi-5-metil-*P*-tiocitidilil-(3'→5')-2'-desoxi-5-metil-*P*-tiocitidilil-(3'→5')-2'-*O*-(2-metoxietil)-*P*-tioadenilil-(3'→5')-5-metil-2'-*O*-(2-metoxietil)citidilil-(3'→5')-5-metil-2'-*O*-(2-metoxietil)-*P*-tiocitidilil-(3'→5')-5-metil-2'-*O*-(2-metoxietil)-*P*-tiocitidilil-(3'→5')-5-metil-2'-*O*-(2-metoxietil)uridina
reductor de la síntesis de la proteína tau asociada al microtúbulo, enfermedad de Alzheimer

$C_{210}H_{300}N_{53}O_{116}P_{17}S_{15}$ 2304711-06-4

(3'-5')C=C–G=U=U=dT=dT=dC=dT=dT=dA=dC=dC=A=C–C=C=U

N : nucleoside / nucléoside / nucleósido
dN : 2'-deoxy-N / 2'-désoxy-N / 2'-desoxi-N
N : 5-methyl-N / 5-méthyl-N / 5-metil-N
N : 2'-*O*-(2-methoxyethyl)-N / 2'-*O*-(2-méthoxyéthyl)-N / 2'-*O*-(metoxietil)-N
– : –PO(OH)– = : –PO(SH)–

dirozalkibum

dirozalkib

5-chloro-N^2-[7-methyl-8-(piperidin-4-yl)-2,3-dihydro-1,4-benzodioxin-5-yl]-N^4-[2-(propane-2-sulfonyl)phenyl]pyrimidine-2,4-diamine
anaplastic lymphoma kinase (ALK) inhibitor, antineoplastic

dirozalkib

5-chloro-N^2-[7-méthyl-8-(pipéridin-4-yl)-2,3-dihydro-1,4-benzodioxin-5-yl]-N^4-[2-(propane-2-sulfonyl)phényl]pyrimidine-2,4-diamine
inhibiteur de la kinase du lymphome anaplasique (ALK), antinéoplasique

dirozalkib

5-cloro-N^2-[7-metil-8-(piperidin-4-il)-2,3-dihidro-1,4-benzodioxin-5-il]-N^4-[2-(propano-2-sulfonil)fenil]pirimidina-2,4-diamina
inhibidor de la kinasa de linfoma anaplásico (ALK), antineoplásico

$C_{27}H_{32}ClN_5O_4S$ 1893419-37-8

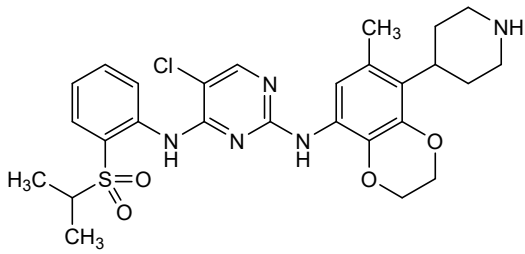

efclarofuspum alfa #

efclarofusp alfa

human vascular endothelial growth factor receptor 1 (VEGFR1, vascular permeability factor receptor, Fms-like tyrosine kinase 1, FLT1, tyrosine-protein kinase receptor FLT, tyrosine-protein kinase FRT, EC:2.7.10.1), fragment 103-206 (containing the Ig-like C2-type domain 2) (1-104), fused to human vascular endothelial growth factor receptor 2 (VEGFR2, fetal liver kinase 1, FLK1, protein-tyrosine kinase receptor flk-1, kinase insert domain receptor, KDR, CD309, EC:2.7.10.1), fragment 208-308 (containing the Ig-like C2-type domain 3) (105-205), fused to an immunoglobulin G1 (IgG1) Fc fragment (h-CH2-CH3-CHS domains) (206-431) [*Homo sapiens* IGHG1*01 (hinge (206-215), CH2 (216-325), CH3 (326-430), CHS K^{432}>del (431-431))] fused via the peptide linker $(G_4S)_3$ (432-446) to disintegrin rhodostomin [*Calloselasma rhodostoma* (Malayan pit viper, *Agkistrodon rhodostoma*)] (447-514), [S^{39}>K^{485}, R^{40}>K^{486}, G^{42}>R^{488}, K^{43}>T^{489}, R^{46}>A^{492}, I^{47}>R^{493}, P^{48}>G^{494}, M^{52}>N^{498}]-variant; dimer (211-211':214-214')-bisdisulfide; produced in Chinese hamster ovary (CHO) cells, cell line CHO-K1; glycoform alfa
angiogenesis inhibitor

efclarofusp alfa

récepteur 1 du facteur de croissance endothélial vasculaire humain (VEGFR1, récepteur du facteur de perméabilité vasculaire, tyrosine kinase 1 de type Fms, FLT1, récepteur tyrosine-protéine kinase FLT, tyrosine-protéine kinase FRT, EC:2.7.10.1), fragment 103-206 (contenant le domaine 2 de type Ig de type C2) (1-104), fusionné au récepteur 2 du facteur de croissance endothélial vasculaire humain (VEGFR2, kinase hépatique 1 fœtale, FLK1, récepteur protéine-tyrosine kinase flk-1, récepteur du domaine d'insertion de kinase, KDR, CD309, EC:2.7.10.1), fragment 208-308 (contenant le domaine 3 de type C2 de type Ig) (105-205), fusionné à un fragment Fc d'immunoglobuline G1 (IgG1) (domaines h-CH2-CH3-CHS) (206-431) [*Homo sapiens* IGHG1*01 (charnière (206-215), CH2 (216-325), CH3 (326-430), CHS K^{432}>del (431-431))] fusionné via le coupleur peptidique $(G_4S)_3$ (432-446) à la désintégrine rhodostomine [*Calloselasma rhodostoma* (vipère malaise, *Agkistrodon rhodostoma*)] (447-514), variant [S^{39}>K^{485}, R^{40}>K^{486}, G^{42}>R^{488}, K^{43}>T^{489}, R^{46}>A^{492}, I^{47}>R^{493}, P^{48}>G^{494}, M^{52}>N^{498}]; dimère (211-211':214-214')-bisdisulfure; produit dans des cellules d'ovaire de hamster chinois (CHO), lignée cellulaire CHO-K1; glycoforme alfa
inhibiteur de l'angiogenèse

efclarofusp alfa

receptor 1 del factor de crecimiento endotelial vascular humano (VEGFR1, receptor del factor de permeabilidad vascular, tirosina quinasa 1 similar a Fms, FLT1, receptor de tirosina-proteína quinasa FLT, tirosina-proteína quinasa FRT, EC:2.7.10.1), fragmento 103-206 (que contiene el dominio 2 tipo C2 similar a Ig) (1-104), fusionado al receptor 2 del factor de crecimiento endotelial vascular humano (VEGFR2, quinasa 1 de hígado fetal, FLK1, receptor de proteína tirosina quinasa flk-1, receptor de dominio de inserción de quinasa, KDR, CD309, EC:2.7.10.1), fragmento 208-308 (que contiene el dominio 3 tipo C2 similar a Ig) (105-205), fusionado a un fragmento Fc de inmunoglobulina G1 (IgG1) (dominios h-CH2-CH3-CHS) (206-431) [*Homo sapiens* IGHG1*01 (bisagra (206-215), CH2 (216-325), CH3 (326-430), CHS K^{432}>del (431-431))] fusionado mediante el enlazador peptídico $(G_4S)_3$ (432-446) a la desintegrina rodostomina [*Calloselasma rhodostoma* (víbora malaya, *Agkistrodon rhodostoma*)] (447-514), variante [S^{39}>K^{485}, R^{40}>K^{486}, G^{42}>R^{488}, K^{43}>T^{489}, R^{46}>A^{492}, I^{47}>R^{493}, P^{48}>G^{494}, M^{52}>N^{498}]; dímero (211-211':214-214')-bisdisulfuro; producido en células ováricas de hámster chino (CHO), línea celular CHO-K1; forma glicosilada alfa
inhibidor de la angiogénesis

3053638-35-7

Sequence / Séquence / Secuencia

```
SDTGRPFVEM YSEIPEIIHM TEGRELVIPC RVTSPNITVT LKKFPLDTLI   50
PDGKRIIWDS RKGFIISNAT YKEIGLLTCE ATVNGHLYKT NYLTHRQTNT  100
IIDVVLSPSH [illegible] [illegible] [illegible] [illegible]  150
[illegible] [illegible] [illegible] [illegible] [illegible]  200
[illegible] [illegible] [illegible] [illegible] [illegible]  [illegible]
[illegible] [illegible] [illegible] [illegible] [illegible]  300
[illegible] [illegible] [illegible] [illegible] [illegible]  350
[illegible] [illegible] [illegible] [illegible] [illegible]  400
[illegible] [illegible] [illegible] [illegible] [illegible]  [illegible]
[illegible] [illegible] [illegible] QCKFKKARTI CARGRGDNPD  500
[illegible] [illegible]                                      514
```

Mutations / Mutations / Mutaciónes
disintegrin: S^{39}>**K**^{485}, R^{40}>**K**^{486}, G^{42}>**R**^{488}, K^{43}>**T**^{489}, R^{46}>**A**^{492}, I^{47}>**R**^{493}, P^{48}>**G**^{494}, M^{52}>**N**^{498}

Peptide linker / Peptide liant / Peptido de unión
^{432}*GGGGSGGGGS GGGGS*^{446}

Post-translational modifications
Disulfide bridges location / Position des ponts disulfure / Posiciones de los puentes disulfuro
VEGFR1 IgC2 domain 2: 30-79 30'-79'
VEGFR2 IgC2 domain 3: 124-185 124'-185'
IgG1 Fc: 246-306 352-410 246'-306' 352'-410'
inter-IgG1 Fc: 211-211' 214-214'
disintegrin: 450-465 452-460 459-482 473-479 478-503 491-510 450'-465' 452'-460' 459'-482' 473'-479' 478'-503' 491'-510'

N-glycosylation sites / Sites de N-glycosylation / Posiciones de N-glicosilación
VEGFR1 IgC2 domain 2: N36, N68, N36', N68'
VEGFR2 IgC2 domain 3: N123, N196, N123', N196'; IgG1 Fc: N282, N282'

efitazanamivirum alfa #

efitazanamivir alfa

Fc fragment of human immunoglobulin G1 (1-247) [*Homo sapiens* IGHG1*01(CH1 final 15 residues (1-15), hinge (16-30), CH2 M^{52}>Y, S^{54}>T, T^{56}>E (31-140), CH3 (141-245), CHS (246-247))], dimer (26-26':29-29')-bisdisulfide, produced in Chinese hamster ovary (CHO) cells, cell line CHO-K1, glycoform alfa; substituted on an average of 4 to 5 L-lysine residues at N^6 with radical group 1-{4-[(23*R*,24*R*)-23-[(2*R*,3*R*,4*S*)-3-acetamido-4-(carbamimidoylamino)-6-carboxy-3,4-dihydro-2*H*-pyran-2-yl]-14-(2-{2-[({(1*R*,2*R*)-1-[(2*R*,3*R*,4*S*)-3-acetamido-4-(carbamimidoylamino)-6-carboxy-3,4-dihydro-2*H*-pyran-2-yl]-2,3-dihydroxypropoxy}carbonyl)(methyl)amino]ethoxy}ethyl)-24,25-dihydroxy-20-methyl-21-oxo-2,5,8,11,17,22-hexaoxa-14,20-diazapentacosan-1-yl]-1*H*-1,2,3-triazol-1-yl}-3,6,9,12-tetraoxapentadecan-15-oyl
neuraminidase inhibitor, antiviral

éfitazanamivir alfa	fragment Fc d'immunoglobuline humaine G1 (1-247) [*Homo sapiens* IGHG1*01(15 résidus finaux CH1 (1-15), charnière (16-30), CH2 M^{52}>Y, S^{54}>T, T^{56}>E (31-140), CH3 (141-245), CHS (246-247))], dimère (26-26':29-29')-bisdisulfure, produit dans des cellules ovariennes de hamster chinois (CHO), lignée cellulaire CHO-K1, glycoforme alfa; substitué en *N*^{6} de 4 à 5 résidus L-lysine en moyenne avec le groupe 1-(4-{(23*R*,24*R*)-14-(2-{2-[({(1*R*,2*R*)-1-[(2*R*,3*R*,4*S*)-3-acétamido-4-carbamimidamido-6-carboxy-3,4-dihydro-2*H*-pyran-2-yl]-2,3-dihydroxypropoxy}carbonyl)(méthyl)amino]éthoxy}éthyl)-23-[(2*R*,3*R*,4*S*)-3-acétamido-4-(carbamimidoylamino)-6-carboxy-3,4-dihydro-2*H*-pyran-2-yl]-24,25-dihydroxy-20-méthyl-21-oxo-2,5,8,11,17,22-hexaoxa-14,20-diazapentacosan-1-yl}-1*H*-1,2,3-triazol-1-yl)-15-oxo-3,6,9,12-tétraoxapentadécan-15-yle *inhibiteur de la neuraminidase, antiviral*
efitazanamivir alfa	fragmento Fc de inmunoglobulina humana G1 (1-247) [*Homo sapiens* IGHG1*01(15 residuos finales CH1 (1-15), bisagra (16-30), CH2 M^{52}>Y, S^{54}>T, T^{56}>E (31-140), CH3 (141-245), CHS (246-247))], dímero (26-26':29-29')-bisdisulfuro, producido en las células ováricas de hámster chino (CHO), línea celular CHO-K1, forma glicosilada alfa; sustituido en *N*^{6} de 4 a 5 residuos L-lisina por término medio con el grupo 1-(4-{(23*R*,24*R*)-14-(2-{2-[({(1*R*,2*R*)-1-[(2*R*,3*R*,4*S*)-3-acetamido-4-carbamimidamido-6-carboxi-3,4-dihidro-2*H*-piran-2-il]-2,3-dihidroxipropoxi}carbonil)(metil)amino]etoxi}etil)-23-[(2*R*,3*R*,4*S*)-3-acetamido-4-(carbamimidoilamino)-6-carboxi-3,4-dihidro-2*H*-piran-2-il]-24,25-dihidroxi-20-metil-21-oxo-2,5,8,11,17,22-hexaoxa-14,20-diazapentacosan-1-il}-1*H*-1,2,3-triazol-1-il)-15-oxo-3,6,9,12-tetraoxapentadecan-15-ilo *inhibidor de la neuraminidasa, antiviral*

2781830-14-4

Monomer sequence / Séquence du monomère / Secuencia del monómero

```
NVNHKPSNTK  VDKKVEPKSS  DKTHTCPPCP  APELLGGPSV  FLFPPKPKDT 50
LYITREPEVT  CVVVDVSHED  PEVKFNWYVD  GVEVHNAKTK  PREEQYNSTY 100
RVVSVLTVLH  QDWLNGKEYK  CKVSNKALPA  PIEKTISKAK  GQPREPQVYT 150
LPPSRDELTK  NQVSLTCLVK  GFYPSDIAVE  WESNGQPENN  YKTTPPVLDS 200
DGSFFLYSKL  TVDKSRWQQG  NVFSCSVMHE  ALHNHYTQKS  LSLSPGK    247
```

Post-translational modifications

Disulfide bridges location / Position des ponts disulfure / Posiciones de los puentes disulfuro

Intra	61-121	167-225
	61'-121'	167'-225'
Inter	26-26'	29-29'

N-glycosylation sites / Sites de N-glycosylation / Posiciones de N-glicosilación
97, 97'

C-terminal lysine clipping / Coupure de la lysine C-terminale / Recorte de lisina C-terminal
H CHS: 247, 247''

Potential modified residues / résidus modifiés potentiels / restos modificados potenciales*
K
*(*zanamivir*:protein ~ 9:1)

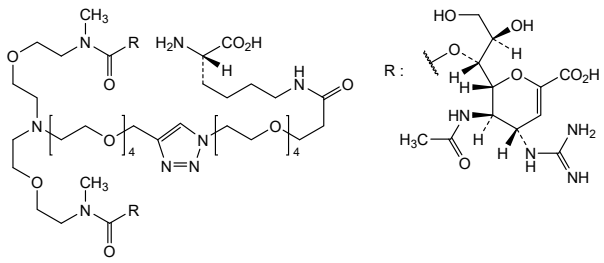

efranarelaxinum alfa #

efranarelaxin alfa

human immunoglobulin G1 (IgG1) Fc fragment (h-CH2-CH3-CHS domains) (1-226) [*Homo sapiens* IGHG1*03 (hinge (1-10), CH2 L^{14}>F, L^{15}>E, P^{111}>S (11-120), CH3 S^{134}>C, T^{146}>W (121-225), CHS K^{227}>del (226))] fused via peptide linker $(G_4S)_3G_5S$ (227-247) to the chain A of human relaxin H2 (RLN2) (1-24, 248-271 in the actual sequence), heterodimer (6-6':9-9':134-129':258-257':271-269')-pentakisdisulfide with human immunoglobulin G1 (IgG1) Fc fragment (h-CH2-CH3-CHS domains) (1'-226') [*Homo sapiens* IGHG1*03 (hinge (1'-10'), CH2 $L^{14'}$>F, $L^{15'}$>E, $P^{111'}$>S (11'-120'), CH3 $T^{146'}$>S, $L^{148'}$>A, $Y^{187'}$>V (121'-225'), CHS $K^{227'}$>del (226'))] fused via peptide linker $(G_4S)_3G_5S$ (227'-247') to the des-Asp^1-chain B of human relaxin H2 (RLN2) (2-29, 248'-275' in the actual sequence), produced in Chinese hamster ovary (CHO) cells, cell line CHO-K1, glycoform alfa
relaxin analogue

efranarélaxine alfa

fragment Fc de l'immunoglobuline G1 humaine (1-226) [*Homo sapiens* IGHG1*03 (charnière (1-10), CH2 L^{14}>F, L^{15}>E, P^{111}>S (11-120), CH3 S^{134}>C, T^{146}>W (121-225), CHS K^{227}>del (226))] fusionné via un coupleur peptidique $(G_4S)_3G_5S$ (227-247) à la chaîne A de la relaxine H2 (RLN2) humaine (1-24, 248-271 dans la sequence actuelle), hétérodimère (6-6':9-9':134-129':258-257':271-269')-pentakisdisulfure avec fragment Fc de l'immunoglobuline G1 humaine (1'-226') [*Homo sapiens* IGHG1*03 (charnière (1'-10'), CH2 $L^{14'}$>F, $L^{15'}$>E, $P^{111'}$>S (11'-120'), CH3 $T^{146'}$>S, $L^{148'}$>A, $Y^{187'}$>V (121'-225'), CHS $K^{227'}$>del (226'))] fusionné via un coupleur peptidique $(G_4S)_3G_5S$ (227'-247') à la dés-Asp^1-chaîne B de la relaxine H2 (RLN2) humaine (2-29, 248'-275' dans la sequence actuelle), produit dans des cellules ovariennes de hamster chinois (CHO), lignée cellulaire CHO-K1, glycoforme alfa
analogue de la relaxine

efranarelaxina alfa

fragmento Fc de la inmunoglobulina G1 humana (1-226) [*Homo sapiens* IGHG1*03 (bisagra (1-10), CH2 L^{14}>F, L^{15}>E, P^{111}>S (11-120), CH3 S^{134}>C, T^{146}>W (121-225), CHS K^{227}>del (226))] fusionado mediante el enlazador peptídico $(G_4S)_3G_5S$ (227-247) a la cadena A de la relaxina H2 (RLN2) humana (1-24, 248-271 en la secuencia actual), heterodímero (6-6':9-9':134-129':258-257':271-269')-pentakisdisulfuro con fragmento Fc de la inmunoglobulina G1 humana (1'-226') [*Homo sapiens* IGHG1*03 (bisagra (1'-10'), CH2 $L^{14'}$>F, $L^{15'}$>E, $P^{111'}$>S (11'-120'), CH3 $T^{146'}$>S, $L^{148'}$>A, $Y^{187'}$>V (121'-225'), CHS $K^{227'}$>del (226'))] fusionado mediante el enlazador peptídico $(G_4S)_3G_5S$ (227'-247') a la des-Asp^1-cadena B de la relaxina H2 (RLN2) humana (2-29, 248'-275' en la secuencia actual), producido en las células ováricas de hámster chino (CHO), línea celular CHO-K1, glicoforma alfa
análogo de la relaxina

2969217-22-7

Sequences / Séquences / Secuencias

Fc-$(G_4S)_3G_5$S-RLN2 A

```
DKTHTCPPCP APEFEGGPSV FLFPPKPKDT LMISRTPEVT CVVVDVSHED   50
PEVKFNWYVD GVEVHNAKTK PREEQYNSTY RVVSVLTVLH QDWLNGKEYK  100
CKVSNKALPA SIEKTISKAK GQPREPQVYT LPPCREEMTK NQVSLWCLVK  150
GFYPSDIAVE WESNGQPENN YKTTPPVLDS DGSFFLYSKL TVDKSRWQQG  200
NVFSCSVMHE ALHNHYTQKS LSLSPGGGGG SGGGGSGGGG SGGGGGSQLY  250
SALANKCCHV GCTKRSLARF C                                 271
```

Fc-$(G_4S)_3G_5$S-RLN2 B

```
DKTHTCPPCP APEFEGGPSV FLFPPKPKDT LMISRTPEVT CVVVDVSHED   50
PEVKFNWYVD GVEVHNAKTK PREEQYNSTY RVVSVLTVLH QDWLNGKEYK  100
CKVSNKALPA SIEKTISKAK GQPREPQVCT LPPSREEMTK NQVSLSCAVK  150
GFYPSDIAVE WESNGQPENN YKTTPPVLDS DGSFFLVSKL TVDKSRWQQG  200
NVFSCSVMHE ALHNHYTQKS LSLSPGGGGG SGGGGSGGGG SGGGGGSSWM  250
EEVIKLCGRE LVRAQIAICG MSTWS                              275
```

Mutations / Mutations / Mutaciónes

L^{14}>F, L^{15}>E, P^{111}>S, S^{134}>C, T146>W;
$L14'^{}$>F, $L15'^{}$>E, $P^{111'}$>S, $Y^{129'}$>C, $T^{146'}$>S, $L^{148'}$>A, $Y^{187'}$>V

Peptide linkers / Peptides liants / Péptidos de unión

^{227}GGGGSGGGGS GGGGSGGGGG S^{247} (1-21);
$^{227'}$GGGGSGGGGS GGGGSGGGGG $S^{247'}$ (1-21)

Post-translational modifications

Disulfide bridges location / Position des ponts disulfure / Posiciones de los puentes disulfuro

intra-Fc: 41-101 147-205 intra-RLN2 A: 257-261
41'-101' 147'-205'
inter-Fc-Fc': 6-6' 9-9' 134-129' inter-RLN2 A-B: 258-257' 271-269'

N-glycosylation sites / Sites de N-glycosylation / Posiciones de N-glicosilación

N77, N77'

egalognastatum

egalognastat — *N*-(5-{4-[(1*S*)-1-(2*H*-1,3-benzodioxol-5-yl)ethyl]piperazin-1-yl}-1,3,4-thiadiazol-2-yl)acetamide
O-GlcNAcase enzyme inhibitor

égalognastat — *N*-(5-{4-[(1*S*)-1-(2*H*-1,3-benzodioxol-5-yl)éthyl]pipérazin-1-yl}-1,3,4-thiadiazol-2-yl)acétamide
inhibiteur de l'enzyme O-GlcNAcase

egalognastat — *N*-(5-{4-[(1*S*)-1-(2*H*-1,3-benzodioxol-5-il)etil]piperazin-1-il}-1,3,4-tiadiazol-2-il)acetamida
inhibidor del enzima O-GlcNAcasa

$C_{17}H_{21}N_5O_3S$ 1884154-02-2

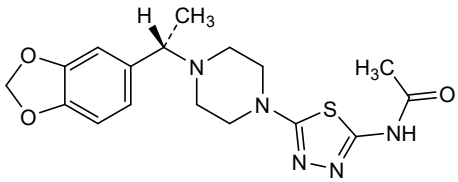

elecoglipronum

elecoglipron (3^4*S*)-3^2-(3-cyclopropyl-4-fluorophenyl)-5^7-[(4*S*)-2,2-dimethyloxan-4-yl]-1^4-fluoro-1^1,3^4-dimethyl-3^2,3^4,3^6,3^7-tetrahydro-1^1*H*,2^2*H*-3(3,5)-pyrazolo[4,3-*c*]pyridina-1(5)-indazola-5(2,3)-indolizina-7(3)-[1,2,4]oxadiazola-2(1,3)-imidazola-6(1,1)-ciclopropanaheptaphane-2^2,4,7^5(7^2*H*)-trione
glucagon-like peptide 1 (GLP-1) receptor agonist

élécoglipron (3^4*S*)-3^2-(3-cyclopropyl-4-fluorophényl)-5^7-[(4*S*)-2,2-diméthyloxan-4-yl]-1^4-fluoro-1^1,3^4-diméthyl-3^2,3^4,3^6,3^7-tétrahydro-1^1*H*,2^2*H*-3(3,5)-pyrazolo[4,3-c]pyridina-1(5)-indazola-5(2,3)-indolizina-7(3)-[1,2,4]oxadiazola-2(1,3)-imidazola-6(1,1)-ciclopropanaheptaphane-2^2,4,7^5(7^2*H*)-trione
agoniste du récepteur du peptide 1 de type glucagon (GLP-1)

elecogliprón (3^4*S*)-3^2-(3-ciclopropil-4-fluorofenil)-5^7-[(4*S*)-2,2-dimetiloxan-4-il]-1^4-fluoro-1^1,3^4-dimetil-3^2,3^4,3^6,3^7-tetrahidro-1^1*H*,2^2*H*-3(3,5)-pirazolo[4,3-c]piridina-1(5)-indazola-5(2,3)-indolizina-7(3)-[1,2,4]oxadiazola-2(1,3)-imidazola-6(1,1)-ciclopropanaheptafano-2^2,4,7^5(7^2*H*)-triona
agonista del receptor del péptido 1 similar al glucagón (GLP-1)

$C_{48}H_{46}F_2N_{10}O_5$ 3011682-49-5

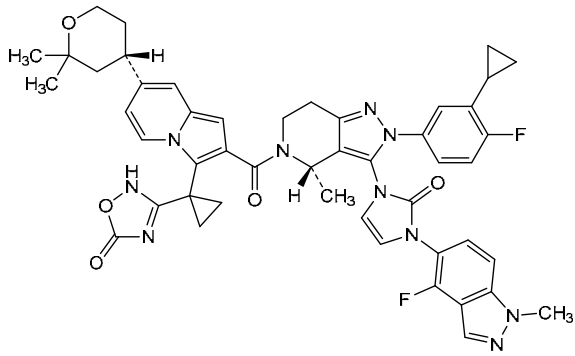

elegrobartum #

elegrobart immunoglobulin G1-kappa, anti-[*Homo sapiens* IGF1R (insulin-like growth factor 1 receptor, IGF1-R, IGF-1R, CD221)], monoclonal antibody;
H-gamma1 heavy chain (1-453) [VH Musmus/Homsap (*Mus musculus* IGHV1-69-5*01 (92.9%) -(IGHD) -IGHJ1*01 (93.8%) A120>Q (116)/*Homo sapiens* IGHV1-46*01 (77.6%) C104>F (96) -(IGHD) -IGHJ6*01 (100%), CDR-IMGT [8.8.17] (26-33.51-58.97-113)) (1-124) -*Homo sapiens* IGHG1*01, G1m17,1 CH1 K120, CH3 D12, L14, 9-G1v21 CH2 Y15.1, T16, E18 (CH1 K120 (221) (125-222), hinge 1-15 (223-237), CH2 M15.1>Y (259), S16>T (261), T18>E (263) (238-347), CH3 D12 (363), L14 (365) (348-452), CHS K2>del (453)) (125-453)], (227-219')-disulfide with L-kappa light chain (1'-219') [V-KAPPA Musmus/Homsap (*Mus musculus* IGKV1-117*01 (93.0%) -IGKJ1*02 (100%)/*Homo sapiens* IGKV2-30*02 (81.0%) -IGKJ4*01 (90.9%) V124>L (109'), CDR-IMGT [11.3.9] (27'-37'.55'-57'.94'-102')) (1'-112') -*Homo sapiens* IGKC*01 (100%) Km3 A45.1, V101 (C-KAPPA A45.1 (158'), V101 (196')) (113'-219')]; dimer (233-233'':236-236'')-bisdisulfide, produced in a cell line from Chinese hamster ovary (CHO) cells, derived from the cell line CHO-K1, glycoform alfa
thyroid eye disease

élégrobart immunoglobuline G1-kappa, anti-[*Homo sapiens* IGF1R (récepteur du facteur de croissance insuline-like 1, IGF1-R, IGF-1R, CD221)], anticorps monoclonal ;
chaîne lourde H-gamma1 (1-453) [VH Musmus/Homsap (*Mus musculus*

IGHV1-69-5*01 (92.9%) -(IGHD) -IGHJ1*01 (93.8%) A120>Q (116)/*Homo sapiens* IGHV1-46*01 (77.6%) C104>F (96) -(IGHD) -IGHJ5*04 (100%), CDR-IMGT [8.8.17] (26-33.51-58.97-113)) (1-124) -*Homo sapiens* IGHG1*01, G1m17,1 CH1 K120, CH3 D12, L14, 9-G1v21 CH2 Y15.1, T16, E18 (CH1 K120 (221) (125-222), charnière 1-15 (223-237), CH2 M15.1>Y (259), S16>T (261), T18>E (263) (238-347), CH3 D12 (363), L14 (365) (348-452), CHS K2>del (453)) (125-453)], (227-219')-disulfure avec la chaîne légère L-kappa (1'-219') [V-KAPPA Musmus/Homsap (*Mus musculus* IGKV1-117*01 (93.0%) -IGKJ1*02 (100%)/*Homo sapiens* IGKV2-30*02 (81.0%) -IGKJ4*01 (90.9%) V124>L (109'), CDR-IMGT [11.3.9] (27'-37'.55'-57'.94'-102')) (1'-112') -*Homo sapiens* IGKC*01 (100%) Km3 A45.1, V101 (C-KAPPA A45.1 (158'), V101 (196')) (113'-219')]; dimère (233-233'':236-236'')-bisdisulfure, produit dans une lignée cellulaire des cellules ovariennes de hamster chinois (CHO), dérivant de la lignée cellulaire CHO-K1, glycoforme alfa
maladie ophtalmologique liée à la thyroïde

elegrobart inmunoglobulina G1-kappa, anti-[*Homo sapiens* IGF1R (receptor 1 del factor de crecimiento similar a la insulina, IGF1-R, IGF-1R, CD221)], anticuerpo monoclonal;
cadena pesada H-gamma1 (1-453) [VH Musmus/Homsap (*Mus musculus* IGHV1-69-5*01 (92.9%) -(IGHD) -IGHJ1*01 (93.8%) A120>Q (116)/*Homo sapiens* IGHV1-46*01 (77.6%) C104>F (96) -(IGHD) -IGHJ5*04 (100%), CDR-IMGT [8.8.17] (26-33.51-58.97-113)) (1-124) -*Homo sapiens* IGHG1*01, G1m17,1 CH1 K120, CH3 D12, L14, 9-G1v21 CH2 Y15.1, T16, E18 (CH1 K120 (221) (125-222), bisagra 1-15 (223-237), CH2 M15.1>Y (259), S16>T (261), T18>E (263) (238-347), CH3 D12 (363), L14 (365) (348-452), CHS K2>del (453)) (125-453)], (227-219')-disulfuro con la cadena ligera L-kappa (1'-219') [V-KAPPA Musmus/Homsap (*Mus musculus* IGKV1-117*01 (93.0%) -IGKJ1*02 (100%)/*Homo sapiens* IGKV2-30*02 (81.0%) -IGKJ4*01 (90.9%) V124>L (109'), CDR-IMGT [11.3.9] (27'-37'.55'-57'.94'-102')) (1'-112') -*Homo sapiens* IGKC*01 (100%) Km3 A45.1, V101 (C-KAPPA A45.1 (158'), V101 (196')) (113'-219')]; dímero (233-233'':236-236'')-bisdisulfuro, producido en una línea celular de las células ováricas de hámster chino (CHO), línea celular derivada de CHO-K1, forma glicosilada alfa
enfermedad ocular tiroidea

2832924-76-0

Heavy chain / Chaîne lourde / Cadena pesada
[illegible] 50
[illegible] 100
[illegible] 150
[illegible] 200
[illegible] 250
[illegible] 300
[illegible] 350
[illegible] 400
[illegible] 450
SPG 453

Light chain / Chaîne légère / Cadena ligera
[illegible] 50
[illegible] 100
[illegible] 150
[illegible] 200
[illegible] 219

Post-translational modifications
Disulfide bridges location / Position des ponts disulfure / Posiciones de los puentes disulfuro
Intra-H (C23-C104) 22 * 151-207 268-328 374-432
22'' * 151''-207'' 268''-328'' 374''-432''
Intra-L (C23-C104) 23'-93' 139'-199'
23'''-93''' 139'''-199'''
Inter-H-L (h 5-CL 126) 227-219' 227''-219'''
Inter-H-H (h 11, h 14) 233-233'' 236-236''
* Free sulfhydryl owing to the amino acid change C104>F (96, 96'').

N-terminal glutaminyl cyclization / Cyclisation du glutaminyle N-terminal / Ciclación del glutaminilo N-terminal
Q > pyroglutamyl (pE, 5-oxoprolyl) / pyroglutamyle (pE, 5-oxoprolyle) / piroglutamilo (pE, 5-oxoprolilo)
H VH Q1: 1, 1''

N-glycosylation sites / Sites de N-glycosylation / Posiciones de N-glicosilación
H CH2 N84.4: 304, 304''
Fucosylated complex bi-antennary CHO-type glycans / glycanes de type CHO bi-antennaires complexes fucosylés / glicanos de tipo CHO biantenarios complejos fucosilados

elironrasibum

elironrasib

1-[4-(dimethylamino)-4-methylpent-2-ynoyl]-*N*-[(2*S*)-1-{[(1^2*M*,2^2*S*,4*S*,6^3*S*)-1^1-ethyl-1^2-{2-[(1*S*)-1-methoxyethyl]pyridin-3-yl}-10,10-dimethyl-5,7-dioxo-1^1*H*-8-oxa-1(5,3)-indola-2(4,2)-morpholina-6(1,3)-[1,2]diazinanacycloundecaphan-4-yl]amino}-3-methyl-1-oxobutan-2-yl]-4-fluoro-*N*-methylpiperidine-4-carboxamide
Kirsten rat sarcoma viral oncogene homolog inhibitor, antineoplastic

éliconrasib

1-[4-(diméthylamino)-4-méthylpent-2-ynoyl]-*N*-[(2*S*)-1-{[(1^2*M*,2^2*S*,4*S*,6^3*S*)-1^1-éthyl-1^2-{2-[(1*S*)-1-méthoxyéthyl]pyridin-3-yl}-10,10-diméthyl-5,7-dioxo-1^1*H*-8-oxa-1(5,3)-indola-2(4,2)-morpholina-6(1,3)-[1,2]diazinanacycloundécaphan-4-yl]amino}-3-méthyl-1-oxobutan-2-yl]-4-fluoro-*N*-méthylpipéridine-4-carboxamide
inhibiteur d'homologue d'oncogène viral du sarcome de rat de Kirsten, antinéoplasique

elironrasib

1-[4-(dimetilamino)-4-metilpent-2-inoil]-*N*-[(2*S*)-1-{[(1^2*M*,2^2*S*,4*S*,6^6*S*)-1^1-etil-10,10-dimetil-1^2-{2-[(1*S*)-1-metoxietil]piridin-3-il}-5,7-dioxo-1^1*H*-8-oxa-1(5,3)-indola-2(4,2)-morfolina-6(2,6)-[1,2]diazinanacicloundecafan-4-il]amino}-3-metil-1-oxobutan-2-il]-4-fluoro-*N*-metilpiperidina-4-carboxamida
inhibidor del homólogo del oncogen vírico del sarcoma de rata Kirsten, antineoplásico

$C_{55}H_{78}FN_9O_8$ 2641998-63-0

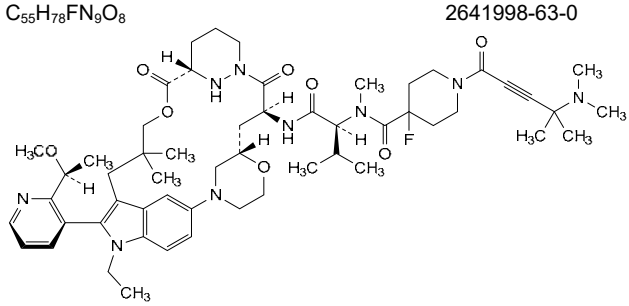

elisrasibum

elisrasib

[(2*S*)-4-[(7*S*)-7-[3-amino-2-fluoro-5-methyl-6-(trifluoromethyl)phenyl]-2-{[(2*R*,7a*S*)-2-fluorotetrahydro-1*H*-pyrrolizin-7a(5*H*)-yl]methoxy}-7,8-dihydro-5*H*-pyrano[4,3-*d*]pyrimidin-4-yl]-1-(2-fluoroprop-2-enoyl)piperazin-2-yl]acetonitrile
Kirsten rat sarcoma viral oncogene homolog inhibitor, antineoplastic

élisrasib

[(2*S*)-4-[(7*S*)-7-[3-amino-2-fluoro-5-méthyl-6-(trifluorométhyl)phényl]-2-{[(2*R*,7a*S*)-2-fluorotétrahydro-1*H*-pyrrolizin-7a(5*H*)-yl]méthoxy}-7,8-dihydro-5*H*-pyrano[4,3-*d*]pyrimidin-4-yl]-1-(2-fluoroprop-2-énoyl)pipérazin-2-yl]acétonitrile
inhibiteur d'homologue d'oncogène viral du sarcome de rat de Kirsten, antinéoplasique

elisrasib

[(2*S*)-4-[(7*S*)-7-[3-amino-2-fluoro-5-metil-6-(trifluorometil)fenil]-2-{[(2*R*,7a*S*)-2-fluorotetrahidro-1*H*-pirrolizin-7a(5*H*)-il]metoxi}-7,8-dihidro-5*H*-pirano[4,3-*d*]pirimidin-4-il]-1-(2-fluoroprop-2-enoil)piperazin-2-il]acetonitrilo
inhibidor del homólogo del oncogen vírico del sarcoma de rata Kirsten, antineoplásico

$C_{32}H_{35}F_6N_7O_3$ 2914919-85-8

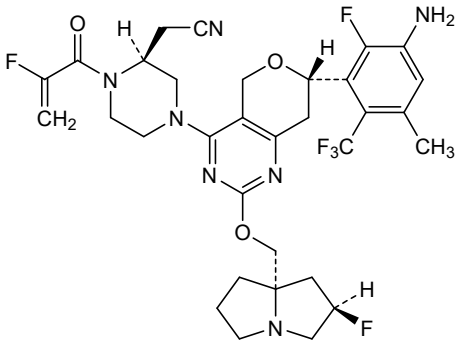

elsovaptanum

elsovaptan

[(3*S*)-7-chloro-3-methyl-2,3-dihydro-4*H*-1,4-benzoxazin-4-yl][6-(pyrimidin-2-yl)-2,6-diazaspiro[3.3]heptan-2-yl]methanone
vasopressin receptor antagonist, Alzheimer disease

elsovaptan

[(3*S*)-7-chloro-3-méthyl-2,3-dihydro-4*H*-1,4-benzoxazin-4-yl][6-(pyrimidin-2-yl)-2,6-diazaspiro[3.3]heptan-2-yl]méthanone
antagoniste du récepteur de la vasopressine, maladie d'Alzheimer

elsovaptán

[(3*S*)-7-cloro-3-metil-2,3-dihidro-4*H*-1,4-benzoxazin-4-il][6-(pirimidin-2-il)-2,6-diazaespiro[3.3]heptan-2-il]metanona
antagonista del receptor de vasopresina, enfermedad de Alzheimer

$C_{19}H_{20}ClN_5O_2$ 2296801-25-5

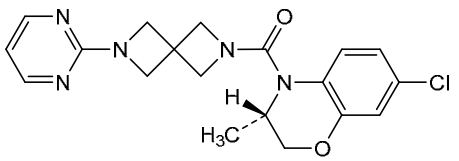

elunetiromum

elunetirom

2-(3,5-dichloro-4-{[4-hydroxy-3-(propan-2-yl)phenyl]methyl}phenoxy)-*N*-methylacetamide
thyroid hormone beta receptor agonist

élunétirom

2-(3,5-dichloro-4-{[4-hydroxy-3-(propan-2-yl)phényl]méthyl}phénoxy)-*N*-méthylacétamide
agoniste des récepteurs bêta de l'hormone thyroïdienne

elunetirom

2-(3,5-dicloro-4-{[4-hidroxi-3-(propan-2-il)fenil]metil}fenoxi)-*N*-metilacetamida
agonista del receptor beta de la hormona tiroidea

$C_{19}H_{21}Cl_2NO_3$ 2156649-32-8

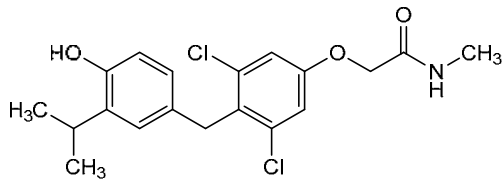

emupertinibum

emupertinib

N-{4-[4-amino-6-ethynyl-5-(quinolin-3-yl)-7*H*-pyrrolo[2,3-*d*]pyrimidin-7-yl]bicyclo[2.2.1]heptan-1-yl}-5-methylpyrazine-2-carboxamide
epidermal growth factor receptor tyrosine kinase inhibitor, antineoplastic

émupertinib

N-{4-[4-amino-6-éthynyl-5-(quinoléin-3-yl)-7*H*-pyrrolo[2,3-*d*]pyrimidin-7-yl]bicyclo[2.2.1]heptan-1-yl}-5-méthylpyrazine-2-carboxamide
inhibiteur de la tyrosine kinase du récepteur du facteur de croissance épidermique, antinéoplasique

emupertinib

N-{4-[4-amino-6-etinil-5-(quinolein-3-il)-7*H*-pirrolo[2,3-*d*]pirimidin-7-il]biciclo[2.2.1]heptan-1-il}-5-metilpirazina-2-carboxamida
inhibidor de la tirosina kinasa del receptor del factor de crecimiento epidérmico, antineoplásico

$C_{30}H_{26}N_8O$ 2472802-77-8

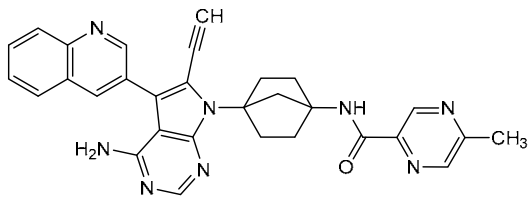

encofosbuvirum

encofosbuvir

propan-2-yl *N*-[(*P*$^{5'}$*S*,2'*R*)-2'-deoxy-2'-fluoro-3-({[*N*-(methoxycarbonyl)-L-methionyl]oxy}methyl)-2'-methyl-*O*^{P}-phenyl-5'-uridylyl]-L-alaninate
antiviral

encofosbuvir

N-[(*P*$^{5'}$*S*,2'*R*)-2'-désoxy-2'-fluoro-3-({[*N*-(méthoxycarbonyl)-L-méthionyl]oxy}méthyl)-2'-méthyl-*O*^{P}-phényl-5'-uridylyl]-L-alaninate de propan-2-yle
antiviral

encofosbuvir

N-[(*P*$^{5'}$*S*,2'*R*)-2'-desoxi-*O*^{P}-fenil-2'-fluoro-2'-metil-3-({[*N*-(metoxicarbonil)-L-metionil]oxi}metil)-5'-uridilil]-L-alaninato de propan-2-ilo
antiviral

$C_{30}H_{42}FN_4O_{13}PS$ 2232134-77-7

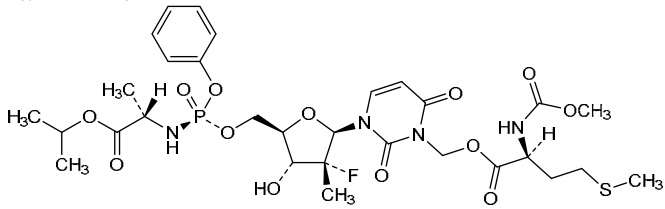

engasertibum

engasertib — 6-{4-[(1*S*,3*S*)-1-amino-3-hydroxycyclobutyl]phenyl}-1-ethyl-7-phenyl-1*H*-pyrido[2,3-*b*][1,4]oxazin-2(3*H*)-one
serine/threonine kinase inhibitor

engasertib — 6-{4-[(1*S*,3*S*)-1-amino-3-hydroxycyclobutyl]phényl}-1-éthyl-7-phényl-1*H*-pyrido[2,3-*b*][1,4]oxazin-2(3*H*)-one
inhibiteur de sérine/thréonine kinases

engasertib — 6-{4-[(1*S*,3*S*)-1-amino-3-hidroxiciclobutil]fenil}-1-etil-7-fenil-1*H*-pirido[2,3-*b*][1,4]oxazin-2(3*H*)-ona
inhibidor de la serina/treonina kinasa

$C_{25}H_{25}N_3O_3$ 1313439-71-2

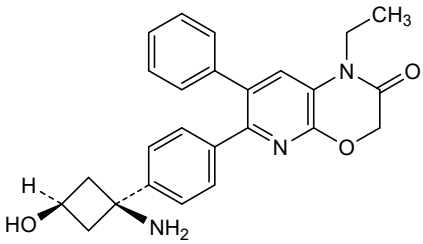

enozertinibum

enozertinib — *N*-[(7^3*R*)-8^3,8^5-difluoro-4^5-methoxy-5-aza-6(4,6)-pyrimidina-2(1,4)-piperazina-3(4,1)-piperidina-7(2,3)-[1,2]oxazolidina-4(1,4),8(1)-dibenzena-1(1)-ciclopropanaoctaphan-4^2-yl]prop-2-enamide
epidermal growth factor receptor tyrosine kinase inhibitor, antineoplastic

énozertinib — *N*-[(7^3*R*)-8^3,8^5-difluoro-4^5-méthoxy-5-aza-6(4,6)-pyrimidina-2(1,4)-pipérazina-3(4,1)-pipéridina-7(2,3)-[1,2]oxazolidina-4(1,4),8(1)-dibenzéna-1(1)-cyclopropanaoctaphan-4^2-yl]prop-2-énamide
inhibiteur de la tyrosine kinase du récepteur du facteur de croissance épidermique, antinéoplasique

enozertinib — *N*-[(7^3*R*)-8^3,8^5-difluoro-4^5-metoxi-5-aza-6(4,6)-pirimidina-2(1,4)-piperazina-3(4,1)-piperidina-7(2,3)-[1,2]oxazolidina-4(1,4),8(1)-dibencena-1(1)-ciclopropanaoctafan-4^2-il]prop-2-enamida
inhibidor de la tirosina kinasa del receptor del factor de crecimiento epidérmico, antineoplásico

$C_{35}H_{42}F_2N_8O_3$ 2489185-38-6

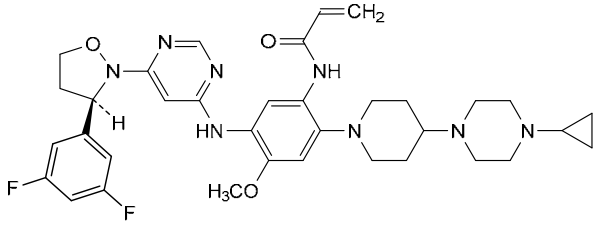

enzelkitugum #

enzelkitug

immunoglobulin G1-kappa, anti-[*Homo sapiens* CCR8 (C-C motif chemokine receptor 8, CKR-L1, CDw198) N-terminus], humanized monoclonal antibody;
H-gamma1 heavy chain humanized (1-449) [VH (*Homo sapiens* IGHV3-23*01 (81.6%) -(IGHD) -IGHJ3*02 (91.7%) M123>T (114), CDR-IMGT [8.7.13] (26-33.51-57.96-108)) (1-119) -*Homo sapiens* IGHG1*03v (100%) G1m3>G1m17, nG1m1 CH1 K120, CH3 E12, M14 (CH1 R120>K (216) (120-217), hinge 1-15 (218-232), CH2 (233-342), CH3 E12 (358), M14 (360) (343-447), CHS (448-449)) (120-449)], (222-218')-disulfide with L-kappa light chain humanized (1'-218') [V-KAPPA (*Homo sapiens* IGKV1-33*01 (87.8%) -IGKJ4*01 (100%), CDR-IMGT [6.3.13] (27'-32'.50'-52'.89'-101')) (1'-111') -*Homo sapiens* IGKC*01 (100%) Km3 A45.1, V101 (C-KAPPA A45.1 (157'), V101 (195')) (112'-218')]; dimer (228-228'':231-231'')-bisdisulfide, produced in Chinese hamster ovary (CHO) cells, cell line CHO-K1, glycoform alfa
antineoplastic

enzelkitug

immunoglobuline G1-kappa, anti-[*Homo sapiens* CCR8 (récepteur 8 de chimiokine C-C motif, CKR-L1, CDw198) N-terminus], anticorps monoclonal humanisé;
chaîne lourde H-gamma1 humanisée (1-449) [VH (*Homo sapiens* IGHV3-23*01 (81.6%) -(IGHD) -IGHJ3*02 (91.7%) M123>T (114), CDR-IMGT [8.7.13] (26-33.51-57.96-108)) (1-119) -*Homo sapiens* IGHG1*03v (100%) G1m3>G1m17, nG1m1 CH1 K120, CH3 E12, M14 (CH1 R120>K (216) (120-217), charnière 1-15 (218-232), CH2 (233-342), CH3 E12 (358), M14 (360) (343-447), CHS (448-449)) (120-449)], (222-218')-disulfure avec la chaîne légère L-kappa humanisée (1'-218') [V-KAPPA (*Homo sapiens* IGKV1-33*01 (87.8%) -IGKJ4*01 (100%), CDR-IMGT [6.3.13] (27'-32'.50'-52'.89'-101')) (1'-111') -*Homo sapiens* IGKC*01 (100%) Km3 A45.1, V101 (C-KAPPA A45.1 (157'), V101 (195')) (112'-218')]; dimère (228-228'':231-231'')-bisdisulfure, produit dans des cellules ovariennes de hamster chinois (CHO), lignée cellulaire CHO-K1, glycoforme alfa
antinéoplasique

enzelkitug

inmunoglobulina G1-kappa, anti-[*Homo sapiens* CCR8 (receptor 8 de quimiocina C-C motivo, CKR-L1, CDw198) N-terminus], anticuerpo monoclonal humanizado;

cadena pesada H-gamma1 humanizada (1-449) [VH (*Homo sapiens* IGHV3-23*01 (81.6%) -(IGHD) -IGHJ3*02 (91.7%) M123>T (114), CDR-IMGT [8.7.13] (26-33.51-57.96-108)) (1-119) -*Homo sapiens* IGHG1*03v (100%) G1m3>G1m17, nG1m1 CH1 K120, CH3 E12, M14 (CH1 R120>K (216) (120-217), bisagra 1-15 (218-232), CH2 (233-342), CH3 E12 (358), M14 (360) (343-447), CHS (448-449)) (120-449)], (222-218')-disulfuro con la cadena ligera L-kappa humanizada (1'-218') [V-KAPPA (*Homo sapiens* IGKV1-33*01 (87.8%) -IGKJ4*01 (100%), CDR-IMGT [6.3.13] (27'-32'.50'-52'.89'-101')) (1'-111') -*Homo sapiens* IGKC*01 (100%) Km3 A45.1, V101 (C-KAPPA A45.1 (157'), V101 (195')) (112'-218')]; dímero (228-228":231-231")-bisdisulfuro, producido en las células ováricas de hámster chino (CHO), línea celular CHO-K1, forma glicosilada alfa
antineoplásico

2999644-88-9

Heavy chain / Chaîne lourde / Cadena pesada

```
EVQLLESGGG LVQPGGSLRL SCAASGIDLS TYAMGWVRQA PGKGLEWVGL  50
IHRSGRTYYA TWAKGRFTIS KDSSKNTLYL QMNSLRAEDT AVYYCTRSYP 100
DYSATASIWG QGTTVTVSSA STKGPSVFPL APSSKSTSGG TAALGCLVKD 150
YFPEPVTVSW NSGALTSGVH TFPAVLQSSG LYSLSSVVTV PSSSLGTQTY 200
ICNVNHKPSN TKVDKKVEPK SCDKTHTCPP CPAPELLGGP SVFLFPPKPK 250
DTLMISRTPE VTCVVVDVSH EDPEVKFNWY VDGVEVHNAK TKPREEQYNS 300
TYRVVSVLTV LHQDWLNGKE YKCKVSNKAL PAPIEKTISK AKGQPREPQV 350
YTLPPSREEM TKNQVSLTCL VKGFYPSDIA VEWESNGQPE NNYKTTPPVL 400
DSDGSFFLYS KLTVDKSRWQ QGNVFSCSVM HEALHNHYTQ KSLSLSPGK  449
```

Light chain / Chaîne légère / Cadena ligera

```
DIQVTQSPSS LSASVGDRVT ITCQASENIA NALAWYQQKP GKPPKFLIYG  50
ASNLASGVPS RFSGSGSGTD FTFTISSLQP EDIATYYCQQ AYYGNSFVEG 100
TFGGGTKVEI KRTVAAPSVF IFPPSDEQLK SGTASVVCLL NNFYPREAKV 150
QWKVDNALQS GNSQESVTEQ DSKDSTYSLS STLTLSKADY EKHKVYACEV 200
THQGLSSPVT KSFNRGEC                                    218
```

Post-translational modifications

Disulfide bridges location / Position des ponts disulfure / Posiciones de los puentes disulfuro

Intra-H (C23-C104)	22-95	146-202	263-323	369-427
	22"-95"	146"-202"	263"-323"	369"-427"
Intra-L (C23-C104)	23'-88'	138'-198'		
	23'"-88'"	138'"-198'"		
Inter-H-L (h 5-CL 126)	222-218'	222"-218'"		
Inter-H-H (h 11, h 14)	228-228"	231-231"		

N-glycosylation sites / Sites de N-glycosylation / Posiciones de N-glicosilación
H CH2 N84.4: 299, 299"
Low fucosylated (<15%) complex bi-antennary CHO-type glycans / glycanes de type CHO bi-antennaires complexes faiblement fucosylés (<15%) / glicanos de tipo CHO biantenarios complejos bajo fucosilados (<15 %)

C-terminal lysine clipping / Coupure de la lysine C-terminale / Recorte de lisina C-terminal
H CHS K2: 449, 449"

epaldeudomidum

epaldeudomide — (1^3S)-5^2-fluoro($1^{3\text{-}2}$H)-3-oxa-2(2,4)-isoindola-7(4)-morpholina-1(3)-piperidina-5(1,4)-benzenaheptaphane-1^2,1^6,2^1(2^3H)-trione
immunomodulator, antineoplastic

épaldeudomide — (1^3S)-5^2-fluoro($1^{3\text{-}2}$H)-3-oxa-2(2,4)-isoindola-7(4)-morpholina-1(3)-pipéridina-5(1,4)-benzénaheptaphane-1^2,1^6,2^1(2^3H)-trione
immunomodulateur, antinéoplasique

epaldeudomida — (1^3S)-5^2-fluoro($1^{3\text{-}2}$H)-3-oxa-2(2,4)-isoindola-7(4)-morfolina-1(3)-piperidina-5(1,4)-bencenaheptafano-1^2,1^6,2^1(2^3H)-triona
inmunomodulador, antineoplásico

$C_{25}H_{25}{}^{2}HFN_3O_5$ 1918159-31-5

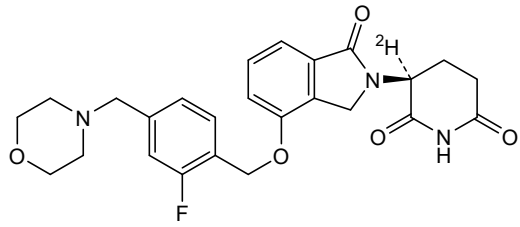

etuptamigum #

etuptamig — immunoglobulin L-kappa-H-gamma1_L-lambda-H-gamma1, anti-[*Homo sapiens* NCR3LG1 (natural killer cell cytotoxicity receptor 3 ligand 1, B7 homolog 6, B7-H6)] and anti-[*Homo sapiens* CD3E (CD3 epsilon, Leu-4)], monoclonal antibody, bispecific;
fused chain L-kappa-H-gamma1 anti-NCR3LG1 (1-698) (knob) [L-kappa anti-NCR3LG1 (1-214) [V-KAPPA (*Homo sapiens* IGKV1-16*01 (85.3%) -IGKJ2*01 (90.9%) Q120>A (100), CDR-IMGT [6.3.9] (27-32.50-52.89-97)) (1-107)-*Homo sapiens* IGKC*01 (100%) Km3 A45.1, V101 (C-KAPPA A45.1 (153'), V101 (191')) (108'-214')] -38-mer(tetraglycylseryl-bis(EGKSSGSGSESKST)-tetraglycylseryl) linker (215-252) -[H-gamma-1 heavy chain anti-NCR3LG1 (253-698) [VH (*Homo sapiens* IGHV1-46*01 (81.6%) -(IGHD) -IGHJ5*01 (92.3%), CDR-IMGT [8.8.10] (278-285.303-310.349-358)) (253-369)-*Homo sapiens* IGHG1*03, G1m3, nG1m1, CH1 R120, CH3 E12, M14,6-G1v14 CH2 A1.3, A1.2, 14-G1v32 CH3 W22 (knob) (CH1 R120 (466) (370-467), hinge 1-15 (468-482), CH2 L1.3>A (486), L1.2>A (487) (483-592), CH3 E12 (608), M14 (610), T22>W (618) (593-697), CHS K2>del (698)) (370-698)]];
fused chain L-lambda6-H-gamma1 anti-CD3E (1-707) (hole) [L-lambda6 anti-CD3E (1'-215') [V-LAMBDA Musmus/Homsap (*Mus musculus* IGLV1*01 (82.3%) -IGLJ1*01 (100%)/*Homo sapiens* IGLV7-46*01 (76.8%) -IGLJ3*02 (100%), CDR-IMGT [9.3.9] (26'-34'.52'-54'.91'-99')) (1'-109') -*Homo sapiens* IGLC6*01 (100%) (C-LAMBDA6) (110'-215')] -38-mer (tetraglycylseryl-bis(EGKSSGSGSESKST)-tetraglycylseryl) linker (216'-253') -[H-gamma-1 anti-CD3E (254'-707') [VH Musmus/Homsap (*Mus musculus* IGHV10-1*04 (93.0%) -(IGHD) -IGHJ3*01 (100%)/*Homo sapiens* IGHV3-73*01 (87.0%) -(IGHD) -IGHJ6*01 (81.8%) T123>L (373'), S128>A (378'), CDR-IMGT [8.10.16] (279'-286'.304'-313'.352'-367')) (254'-378')-*Homo sapiens* IGHG1*03, G1m3, nG1m1, CH1 R120, CH3 E12, M14, 6-G1v14 CH2 A1.3, A1.2,14-G1v33 CH3 S22, A24, V86 (hole), 10-G1v83 CH3 R115, F116 (CH1 R120 (475') (379'-476'), hinge 1-15 (477'-491'), CH2 L1.3>A (495'), L1.2>A (496') (492'-601'), CH3 E12 (617'), M14 (619'), T22>S (627'), L24>A (629'), Y86>V (668'), H115>R (696'), Y116>F (697') (602'-706'), CHS K2>del (707')) (379'-707')]]; dimer (478-487':481-490')-bisdisulfide, produced in Chinese hamster ovary (CHO) cells, cell line CHO-K1, glycoform alfa
antineoplastic

étuptamig — immunoglobuline L-kappa-H-gamma1_L-lambda-H-gamma1, anti-[*Homo sapiens* NCR3LG1 (ligand 1 du récepteur 3 de la cytotoxicité des cellules tueuses naturelles, B7 homologue 6, B7-H6)] et anti-[*Homo sapiens* CD3E (CD3 epsilon, Leu-4)], anticorps monoclonal, bispécifique;
chaîne fusionnée L-kappa-H-gamma1 anti-NCR3LG1 (1-698) (knob) [L-kappa anti-NCR3LG1 (1-214) [V-KAPPA (*Homo sapiens* IGKV1-16*01(85.3%) -IGKJ2*01 (90.9%) Q120>A (100), CDR-IMGT [6.3.9] (27-32.50-52.89-97)) (1-107)-*Homo sapiens* IGKC*01 (100%) Km3 A45.1,

V101 (C-KAPPA A45.1 (153'), V101 (191')) (108'-214')] -38-mer(GGGGS tétraglycylséryl-bis(EGKSSGSGSESKST)-tétraglycylséryl) linker (215-252) -[H-gamma1 anti-NCR3LG1 (253-698) [VH (*Homo sapiens* IGHV1-46*01 (81.6%) -(IGHD) -IGHJ5*01 (92.3%), CDR-IMGT [8.8.10] (278-285.303-310.349-358)) (253-369)-*Homo sapiens* IGHG1*03, G1m3, nG1m1, CH1 R120, CH3 E12, M14,6-G1v14 CH2 A1.3, A1.2, 14-G1v32 CH3 W22 (knob) (CH1 R120 (466) (370-467), charnière 1-15 (468-482), CH2 L1.3>A (486), L1.2>A (487) (483-592), CH3 E12 (608), M14 (610), T22>W (618) (593-697), CHS K2>del (698)) (370-698)]];
chaîne fusionnée L-lambda6-H-gamma1 anti-CD3E (1-707) (hole) [L-lambda6 anti-CD3E (1'-215') [V-LAMBDA Musmus/Homsap (*Mus musculus* IGLV1*01 (82.3%) -IGLJ1*01 (100%)/*Homo sapiens* IGLV7-46*01 (76.8%) -IGLJ3*02 (100%), CDR-IMGT [9.3.9] (26'-34'.52'-54'.91'-99')) (1'-109') -*Homo sapiens* IGLC6*01 (100%) (C-LAMBDA6) (110'-215')] -38-mer (GGGGS tétraglycylséryl-bis(EGKSSGSGSESKST)-tétraglycylséryl) linker (216'-253') -[H-gamma1 anti-CD3E (254'-707') [VH Musmus/Homsap (*Mus musculus* IGHV10-1*04 (93.0%) -(IGHD) -IGHJ3*01 (100%)/*Homo sapiens* IGHV3-73*01 (87.0%) -(IGHD) -IGHJ6*01 (81.8%) T123>L (373'), S128>A (378'), CDR-IMGT [8.10.16] (279'-286'.304'-313'.352'-367')) (254'-378')-*Homo sapiens* IGHG1*03, G1m3, nG1m1, CH1 R120, CH3 E12, M14, 6-G1v14 CH2 A1.3, A1.2,14-G1v33 CH3 S22, A24, V86 (hole), 10-G1v83 CH3 R115, F116 (CH1 R120 (475') (379'-476'), charnière 1-15 (477'-491'), CH2 L1.3>A (495'), L1.2>A (496') (492'-601'), CH3 E12 (617'), M14 (619'), T22>S (627'), L24>A (629'), Y86>V (668'), H115>R (696'), Y116>F (697') (602'-706'), CHS K2>del (707')) (379'-707')]]; dimère (478-487':481-490')-bisdisulfure, produit dans des cellules ovariennes de hamster chinois (CHO), lignée cellulaire CHO-K1, glycoforme alfa
antinéoplasique

etuptamig

inmunoglobulina L-kappa-H-gamma1_L-lambda-H-gamma1, anti-[*Homo sapiens* NCR3LG1 (ligando 1 del receptor 3 de la citotoxicidad de las células asesinas naturales, B7 homólogo 6, B7-H6)] y anti-[*Homo sapiens* CD3E (CD3 épsilon, Leu-4)], anticuerpo monoclonal, biespecífico;
cadena fusionada L-kappa-H-gamma1 anti-NCR3LG1 (1-698) (knob) [L-kappa anti-NCR3LG1 (1-214) [V-KAPPA (*Homo sapiens* IGKV1-16*01 (85.3%) -IGKJ2*01 (90.9%) Q120>A (100), CDR-IMGT [6.3.9] (27-32.50-52.89-97)) (1-107)-*Homo sapiens* IGKC*01 (100%) Km3 A45.1, V101 (C-KAPPA A45.1 (153'), V101 (191')) (108'-214')] -38-mer(GGGGS tetraglicilseril-bis(EGKSSGSGSESKST)-tetraglicilseril) enlace (215-252) -[H-gamma1 anti-NCR3LG1 (253-698) [VH (*Homo sapiens* IGHV1-46*01 (81.6%) -(IGHD) -IGHJ5*01 (92.3%), CDR-IMGT [8.8.10] (278-285.303-310.349-358)) (253-369)-*Homo sapiens* IGHG1*03, G1m3, nG1m1, CH1 R120, CH3 E12, M14,6-G1v14 CH2 A1.3, A1.2, 14-G1v32 CH3 W22 (knob) (CH1 R120 (466) (370-467), bisagra 1-15 (468-482), CH2 L1.3>A (486), L1.2>A (487) (483-592), CH3 E12 (608), M14 (610), T22>W (618) (593-697), CHS K2>del (698)) (370-698)]];
cadena fusionada L-lambda6-H-gamma1 anti-CD3E (1-707) (hole) [L-lambda6 anti-CD3E (1'-215') [V-LAMBDA Musmus/Homsap (*Mus musculus* IGLV1*01 (82.3%) -IGLJ1*01 (100%)/*Homo sapiens* IGLV7-46*01 (76.8%) -IGLJ3*02 (100%), CDR-IMGT [9.3.9] (26'-34'.52'-54'.91'-99')) (1'-109') -*Homo sapiens* IGLC6*01 (100%) (C-LAMBDA6) (110'-215')] -38-mer (GGGGS tetraglicilseril-bis(EGKSSGSGSESKST)-tetraglicilseril) enlace (216'-253') -[H-gamma1 anti-CD3E (254'-707') [VH Musmus/Homsap (*Mus musculus* IGHV10-1*04 (93.0%) -(IGHD) -IGHJ3*01 (100%)/*Homo sapiens* IGHV3-73*01 (87.0%) -(IGHD) -IGHJ6*01 (81.8%) T123>L (373'), S128>A (378'), CDR-IMGT [8.10.16] (279'-286'.304'-313'.352'-367')) (254'-378')-*Homo sapiens* IGHG1*03, G1m3, nG1m1, CH1 R120, CH3 E12, M14, 6-G1v14 CH2 A1.3, A1.2,14-G1v33 CH3 S22, A24, V86 (hole), 10-G1v83 CH3 R115, F116 (CH1 R120 (475') (379'-476'), bisagra 1-15 (477'-491'), CH2 L1.3>A (495'), L1.2>A (496') (492'-601'), CH3 E12 (617'), M14 (619'), T22>S (627'), L24>A (629'), Y86>V (668'), H115>R (696'), Y116>F (697') (602'-706'), CHS K2>del (707')) (379'-707')]];
dímero (478-487':481-490')-bisdisulfuro, producido en las células ováricas de hámster chino (CHO), línea celular CHO-K1, forma glicosilada alfa
antineoplásico

Fused chain / Chaîne fusionnée / Cadena fusionada:
L-kappa-H-gamma1 (L-H) anti-NCR3LG1 (knob)

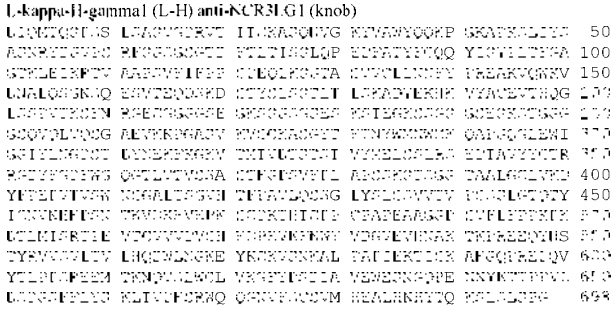

Fused chain / Chaîne fusionnée / Cadena fusionada:
L-lambda6-H-gamma1 (L'-H') anti-CD3E (hole)

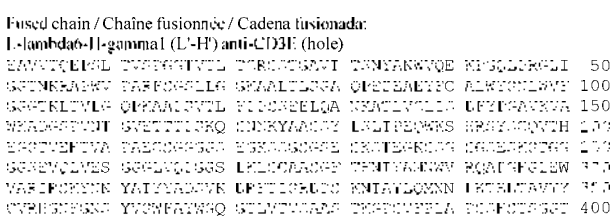

Post-translational modifications
Disulfide bridges location / Position des ponts disulfure / Posiciones de los puentes disulfuro

L-H	Intra-L (C23-C104)	23-88 134-194
(knob)	Intra-H (C23-C104)	274-348 396-452 513-573 619-677
	Intra-(L-H) (h 5-CL 126)	472-214
L'-H'	Intra-L' (C23-C104)	22'-90' 137'-196'
(hole)	Intra-H' (C23-C104)	275'-351' 405'-461' 522'-582' 628'-686'
	Intra-(L'-H') (h 5-CL 126)	481'-214'

Inter-(L-H)-(L'-H') (h 11, h 14) 478-487' 481-490'

N-glycosylation sites / Sites de N-glycosylation / Posiciones de N-glicosilación
H CH2 N84.4: 549, 558"
Fucosylated complex bi-antennary CHO-type glycans / glycanes de type CHO bi-antennaires complexes fucosylés / glicanos de tipo CHO biantenarios complejos fucosilados

exerenibartum #

exerenibart

immunoglobulin G4-kappa, anti-[*Homo sapiens* TMPRSS6 (transmembrane serine protease 6, matriptase-2, MT2)], *Homo sapiens* monoclonal antibody; H-gamma4 heavy chain *Homo sapiens* (1-451) [VH (*Homo sapiens* IGHV3-23*04 (95.9%) -(IGHD) -IGHJ1*01 (90.9%) L123>T (119), CDR-IMGT [8.8.17] (26-33.51-58.97-113)) (1-124) -*Homo sapiens* IGHG4*01, *nG4m(a)* CH2 L92, 12-G4v5 h P10 (CH1 (125-222), hinge 1-12 S10>P (232) (223-234), CH2 L92 (313) (235-344), CH3 (345-449), CHS (450-451)) (125-451)], (138-214')-disulfide with L-kappa light chain *Homo sapiens* (1'-214') [V-KAPPA (*Homo sapiens* IGKV1-12*01 (92.6%) -IGKJ3*01 (100%), CDR-IMGT [6.3.9] (27'-32'.50'-52'.89'-97')) (1'-107') -*Homo sapiens* IGKC*01 (100%) Km3 A45.1, V101 (C-KAPPA A45.1 (153'), V101 (191')) (108'-214')]; dimer (230-230":233-233")-bisdisulfide, produced in Chinese hamster ovary (CHO) cells, cell line CHO-K1, glycoform alfa
iron metabolism regulator

exérénibart

immunoglobuline G4-kappa, anti-[*Homo sapiens* TMPRSS6 (sérine protéase transmembranaire 6, matriptase-2, MT2)], anticorps monoclonal *Homo sapiens*;
chaîne lourde H-gamma4 *Homo sapiens* (1-451) [VH (*Homo sapiens* IGHV3-23*04 (95.9%) -(IGHD) -IGHJ1*01 (90.9%) L123>T (119), CDR-IMGT [8.8.17] (26-33.51-58.97-113)) (1-124) -*Homo sapiens* IGHG4*01, *nG4m(a)* CH2 L92, 12-G4v5 h P10(CH1 (125-222), charnière 1-12 S10>P (232) (223-234), CH2 L92 (313) (235-344), CH3 (345-449), CHS (450-451)) (125-451)], (138-214')-disulfure avec la chaîne légère L-kappa *Homo sapiens* (1'-214') [V-KAPPA (*Homo sapiens* IGKV1-12*01 (92.6%) -IGKJ3*01 (100%), CDR-IMGT [6.3.9] (27'-32'.50'-52'.89'-97')) (1'-107') -*Homo sapiens* IGKC*01 (100%) Km3 A45.1, V101 (C-KAPPA A45.1 (153'), V101 (191')) (108'-214')]; dimère (230-230":233-233")-bisdisulfure, produit dans des cellules ovariennes de hamster chinois (CHO), lignée cellulaire CHO-K1, glycoforme alfa
régulateur du métabolisme du fer

exerenibart

inmunoglobulina G4-kappa, anti-[*Homo sapiens* TMPRSS6 (serina proteasa transmembranaria 6, matriptasa-2, MT2)], anticuerpo monoclonal *Homo sapiens*;
cadena pesada H-gamma4 *Homo sapiens* (1-451) [VH (*Homo sapiens* IGHV3-23*04 (95.9%) -(IGHD) -IGHJ1*01 (90.9%) L123>T (119), CDR-IMGT [8.8.17] (26-33.51-58.97-113)) (1-124) -*Homo sapiens* IGHG4*01, *nG4m(a)* CH2 L92, 12-G4v5 h P10(CH1 (125-222), bisagra 1-12 S10>P (232) (223-234), CH2 L92 (313) (235-344), CH3 (345-449), CHS (450-451)) (125-451)], (138-214')-disulfuro con la cadena ligera L-kappa *Homo sapiens* (1'-214') [V-KAPPA (*Homo sapiens* IGKV1-12*01 (92.6%) -IGKJ3*01 (100%), CDR-IMGT [6.3.9] (27'-32'.50'-52'.89'-97')) (1'-107') -*Homo sapiens* IGKC*01 (100%) Km3 A45.1, V101 (C-KAPPA A45.1 (153'), V101 (191')) (108'-214')]; dímero (230-230":233-233")-bisdisulfuro, producido en las células ováricas de hámster chino (CHO), línea celular CHO-K1, forma glicosilada alfa
regulador del metabolismo del hierro

2996101-49-4

Heavy chain / Chaîne lourde / Cadena pesada

```
EVQLVPSGGG LVQPGGSLRL SCAASGFTFS SYAMTWVRQA PGKGLEWVSA  50
ISGSGGSTYY ADSVKGRFTI SRDNSKNTLY LQMNSLRAED TAVYYCAKDQ 100
PYLPGYYYGA MDVWGQGTTV TVSSASTKGP SVFPLAPSSK STSGGTAALG 150
CLVKDYFPEP VTVSWNSGAL TSGVHTFPAV LQSSGLYSLS SVVTVPSSSL 200
GTKTYTCNVD HKPSNTKVDK RVESKYGPPC PPCPAPEFLG GPSVFLFPPK 250
PKDTLMISRT PEVTCVVVDV SQEDPEVQFN WYVDGVEVHN AKTKPREEQF 300
NSTYRVVSVL TVLHQDWLNG KEYKCKVSNK GLPSSIEKTI SKAKGQPREP 350
QVYTLPPSQE EMTKNQVSLT CLVKGFYPSD IAVEWESNGQ PENNYKTTPP 400
VLDSDGSFFL YSRLTVDKSR WQEGNVFSCS VMHEALHNHY TQKSLSLSLG 450
K                                                       451
```

Light chain / Chaîne légère / Cadena ligera

```
EIVLTQSPGT LSLSPGERAT LSCRASQSVS SWLAWYQQKP GRAPRLLIYA  50
ASSRATGIPD RFSGSGSGTD FTLTISRLEP EDFAVYYCQQ YGSSPPTFGQ 100
GTKVEIKRTV AAPSVFIFPP SDEQLKSGTA SVVCLLNNFY PREAKVQWKV 150
DNALQSGNSQ ESVTEQDSKD STYSLSSTLT LSKADYEKHK VYACEVTHQG 200
LSSPVTKSFN RGEC                                         214
```

Post-translational modifications
Disulfide bridges location / Position des ponts disulfure / Posiciones de los puentes disulfuro
Intra-H (C23-C104) 22-96 151-207 265-325 371-429
22"-96" 151"-207" 265"-325" 371"-429"
Intra-L (C23-C104) 23'-88' 134'-194'
23'"-88"' 134'"-194'"
Inter-H-L (CH1 10-CL 126) 138-214' 138"-214'"
Inter-H-H (h 8, h 11) 230-230" 233-233"

N-glycosylation sites / Sites de **N**-glycosylation / Posiciones de **N**-glicosilación
H CH2 N84.4: 301, 301"
Fucosylated complex bi-antennary CHO-type glycans / glycanes de type CHO bi-antennaires complexes fucosylés / glicanos de tipo CHO biantenarios complejos fucosilados

C-terminal lysine clipping / Coupure de la lysine C-terminale / Recorte de lisina C-terminal
H CHS K2: 451, 451"

famlasertibum

famlasertib — 2-[4-({4-[3-(3-chlorophenyl)-1*H*-pyrrolo[2,3-*b*]pyridin-5-yl]phenyl}methyl)piperazin-1-yl]ethan-1-ol
serine/threonine kinase inhibitor, amyotrophic lateral sclerosis

famlasertib — 2-[4-({4-[3-(3-chlorophényl)-1*H*-pyrrolo[2,3-*b*]pyridin-5-yl]phényl}méthyl)pipérazin-1-yl]éthan-1-ol
inhibiteur de sérine/thréonine kinases, sclérose latérale amyotrophique

famlasertib — 2-[4-({4-[3-(3-clorofenil)-1*H*-pirrolo[2,3-*b*]piridin-5-il]fenil}metil)piperazin-1-il]etan-1-ol
inhibidor de la serina/treonina kinasa, esclarosis lateral amiotrófica

$C_{26}H_{27}ClN_4O$ 2375591-69-6

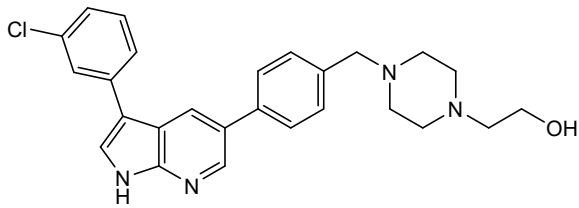

fexlamosum

fexlamose — 6-thio-α-D-glucopyranosyl 6-thio-α-D-glucopyranoside; 6,6'-dithiotrehalose
mucolytic

fexlamose — 6-thio-α-D-glucopyranoside de 6-thio-α-D-glucopyranosyle; 6,6'-dithiotréhalose
mucolytique

fexlamosa — 6-tio-α-D-glucopiranósido de 6-tio-α-D-glucopiranosilo; 6,6'-ditiotrehalosa
mucolítico

$C_{12}H_{22}O_9S_2$ 1285607-08-0

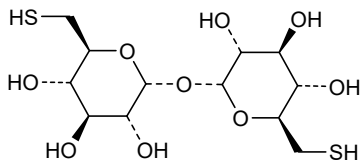

firsekibartum #

firsekibart — immunoglobulin G4-lambda2, anti-[*Homo sapiens* IL1B (interleukin 1 beta, IL-1B, 1L1F2)], *Homo sapiens* monoclonal antibody;
H-gamma4 heavy chain *Homo sapiens* (1-455) [VH (*Homo sapiens* IGHV3-49*05 (94.0%) -(IGHD) -IGHJ6*01 (94.4%), CDR-IMGT [8.10.19] (26-33.51-60.99-117)) (1-128) -*Homo sapiens* IGHG4*01, *nG4m(a)* CH2 L92, 12-G4v5 h P10(CH1 (129-226), hinge 1-12 S10>P (236) (227-238), CH2 L92 (317) (239-348), CH3 (349-453), CHS (454-455)) (129-455)], (142-211')-disulfide

with L-lambda2 light chain *Homo sapiens* (1'-212') [V-LAMBDA (*Homo sapiens* IGLV3-1*01 (96.8%) -IGLJ2*01 (100%), CDR-IMGT [6.3.9] (26'-31'.49'-51'.88'-96')) (1'-106') -*Homo sapiens* IGLC2*01 (100%) (C-LAMBDA2) (107'-212')]; dimer (234-234":237-237")-bisdisulfide, produced in Chinese hamster ovary (CHO) cells, cell line CHO-K1, glycoform alfa
anti-inflammatory

firsékibart immunoglobuline G4-lambda2, anti-[*Homo sapiens* IL1B (interleukine 1 bêta, IL-1B, 1L1F2)], anticorps monoclonal *Homo sapiens*;
chaîne lourde H-gamma4 *Homo sapiens* (1-455) [VH (*Homo sapiens* IGHV3-49*05 (94.0%) -(IGHD) -IGHJ6*01 (94.4%), CDR-IMGT [8.10.19] (26-33.51-60.99-117)) (1-128) -*Homo sapiens* IGHG4*01, *nG4m(a)* CH2 L92, 12-G4v5 h P10(CH1 (129-226), charnière 1-12 S10>P (236) (227-238), CH2 L92 (317) (239-348), CH3 (349-453), CHS (454-455)) (129-455)], (142-211')-disulfure avec la chaîne légère L-lambda2 *Homo sapiens* (1'-212') [V-LAMBDA (*Homo sapiens* IGLV3-1*01 (96.8%) -IGLJ2*01 (100%), CDR-IMGT [6.3.9] (26'-31'.49'-51'.88'-96')) (1'-106') -*Homo sapiens* IGLC2*01 (100%) (C-LAMBDA2) (107'-212')]; dimère (234-234":237-237")-bisdisulfure, produit dans des cellules ovariennes de hamster chinois (CHO), lignée cellulaire CHO-K1, glycoforme alfa
anti-inflammatoire

firsekibart inmunoglobulina G4-lambda2, anti-[*Homo sapiens* IL1B (interleukina 1 beta, IL-1B, 1L1F2)], anticuerpo monoclonal *Homo sapiens*;
cadena pesada H-gamma4 *Homo sapiens* (1-455) [VH (*Homo sapiens* IGHV3-49*05 (94.0%) -(IGHD) -IGHJ6*01 (94.4%), CDR-IMGT [8.10.19] (26-33.51-60.99-117)) (1-128) -*Homo sapiens* IGHG4*01, *nG4m(a)* CH2 L92, 12-G4v5 h P10(CH1 (129-226), bisagra 1-12 S10>P (236) (227-238), CH2 L92 (317) (239-348), CH3 (349-453), CHS (454-455)) (129-455)], (142-211')-disulfuro con la cadena ligera L-lambda2 *Homo sapiens* (1'-212') [V-LAMBDA (*Homo sapiens* IGLV3-1*01 (96.8%) -IGLJ2*01 (100%), CDR-IMGT [6.3.9] (26'-31'.49'-51'.88'-96')) (1'-106') -*Homo sapiens* IGLC2*01 (100%) (C-LAMBDA2) (107'-212')]; dímero (234-234":237-237")-bisdisulfuro, producido en las células ováricas de hámster chino (CHO), línea celular CHO-K1, forma glicosilada alfa
antiinflamatorio

2981430-39-9

Heavy chain / Chaîne lourde / Cadena pesada

```
EVQLVESGGG LVQPGRSLRL SCTASGFTFG DYAMSWFRQA PGKGLEWVGF   50
IRSKAYGGTT EYAASVKGRF TISRDDSKSI AYLQMNSLKT EDTAVYYCAR  100
EYSYGRSSEN YYYGMDVWGQ GTTVTVSSAS TKGPSVFPLA PSSKSTSGGT  150
AALGCLVKDY FPEPVTVSWN SGALTSGVHT FPAVLQSSGL YSLSSVVTVP  200
SSSLGTKTYT CNVDHKPSNT KVDKRVESKY GPPCPSCPAP EFLGGPSVFL  250
FPPKPKDTLM ISRTPEVTCV VVDVSQEDPE VQFNWYVDGV EVHNAKTKPR  300
EEQFNSTYRV VSVLTVLHQD WLNGKEYKCK VSNKGLPSSI EKTISKAKGQ  350
PREPQVYTLP PSQEEMTKNQ VSLTCLVKGF YPSDIAVEWE SNGQPENNYK  400
TTPPVLDSDG SFFLYSRLTV DKSRWQEGNV FSCSVMHEAL HNHYTQKSLS  450
LSLGK                                                   455
```

Light chain / Chaîne légère / Cadena ligera

```
SYVLTQPPSV SVSPGQTASI TCSGDKLGDK FACWFQQKPG QSPVLVIYQD   50
TERPSGIPER FSGSNSGNTA TLTISGTQAM DEADYYCQAW DSNTVVFGGG  100
TKLTVLGQPK AAPSVTLFPP SSEELQANKA TLVCLISDFY PGAVTVAWKA  150
DSSPVKAGVE TTTPSKQSNN KYAASSYLSL TPEQWKSHRS YSCQVTHEGS  200
TVEKTVAPTE CS                                           212
```

Post-translational modifications

Disulfide bridges location / Position des ponts disulfure / Posiciones de los puentes disulfuro

Intra-H (C23-C101)	22-98	105-112	155-211	269-329	375-433
	22"-98"	105"-112"	155"-211"	269"-329"	375"-433"
Intra-L (C23-C101)	22'-87'	134'-193'			
	22'"-87'"	134'"-193'"			
Inter-H-L (CH1 10-CL 126)	142-211'	142"-211'"			
Inter-H-H (h 8, h 11)	234-234"	237-237"			

N-glycosylation sites / Sites de N-glycosylation / Posiciones de N-glicosilación
H CH2 N84.4: 305, 305"
Fucosylated complex bi-antennary CHO-type glycans / glycanes de type CHO bi-antennaires complexes fucosylés / glicanos de tipo CHO biantenarios complejos fucosilados

C-terminal lysine clipping / Coupure de la lysine C-terminale / Recorte de lisina C-terminal
H CHS K2: 455, 455"

florcicaperum (^{18}F)

florcicaper (^{18}F) *rac*-{(1*R*,2*S*)-2-[(5*RS*)-5-(^{18}F)fluorotridecyl]cyclopropyl}acetic acid
imaging agent

florcicaper (^{18}F) acide *rac*-{(1*R*,2*S*)-2-[(5*RS*)-5-(^{18}F)fluorotridécyl]cyclopropyl}acétique
agent d'imagerie diagnostique

florcicapero (^{18}F) ácido *rac*-{(1*R*,2*S*)-2-[(5*RS*)-5-(^{18}F)fluorotridecil]ciclopropil}acético
agente de diagnóstico por imagen

$C_{18}H_{33}{}^{18}FO_2$ 855927-17-2

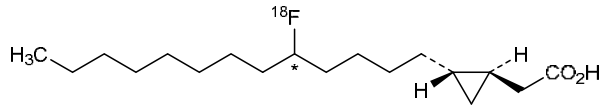

its epimer at C* and their enantiomers
son épimère en C* et leurs énantiomères
su epímero al C* y sus enantiómeros

florensocatibum

florensocatib (2*S*)-*N*-{(1*S*)-1-cyano-2-[2-fluoro-4-(3-methyl-2-oxo-2,3-dihydro-1,3-benzoxazol-5-yl)phenyl]ethyl}-1,4-oxazepane-2-carboxamide
cathepsin inhibitor

florensocatib (2*S*)-*N*-{(1*S*)-1-cyano-2-[2-fluoro-4-(3-méthyl-2-oxo-2,3-dihydro-1,3-benzoxazol-5-yl)phényl]éthyl}-1,4-oxazépane-2-carboxamide
inhibiteur de la cathepsine

florensocatib (2*S*)-*N*-{(1*S*)-1-ciano-2-[2-fluoro-4-(3-metil-2-oxo-2,3-dihidro-1,3-benzoxazol-5-il)fenil]etil}-1,4-oxazepano-2-carboxamida
inhibidor de la catepsina

$C_{23}H_{23}FN_4O_4$ 2762114-61-2

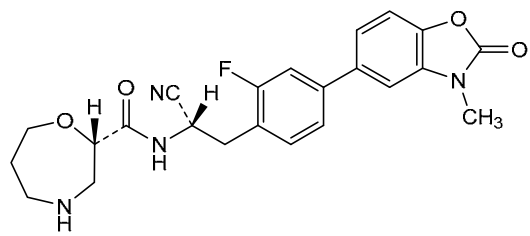

flormotridazum (^{18}F)

flormotridaz (^{18}F) 2-*tert*-butyl-4-chloro-5-[(3-{[4-({2-[2-(^{18}F)fluoroethoxy]ethoxy}methyl)-1*H*-1,2,3-triazol-1-yl]methyl}phenyl)methoxy]pyridazin-3(2*H*)-one
imaging agent

flormotridaz (^{18}F)

2-*tert*-butyl-4-chloro-5-[(3-{[4-({2-[2-(^{18}F)fluoroéthoxy]éthoxy}méthyl)-1*H*-1,2,3-triazol-1-yl]méthyl}phényl)méthoxy]pyridazin-3(2*H*)-one
agent d'imagerie diagnostique

flormotridaz (^{18}F)

2-*terc*-butil-4-cloro-5-[(3-{[4-({2-[2-(^{18}F)fluoroetoxi]etoxi}metil)-1*H*-1,2,3-triazol-1-il]metil}fenil)metoxi]piridazin-3(2*H*)-ona
agente de diagnóstico por imagen

$C_{23}H_{29}Cl^{18}FN_5O_4$ 2798832-03-6

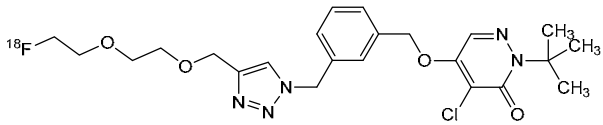

fosizensertibum

fosizensertib

(2*S*)-1-(5-{[1-(difluoromethyl)-1*H*-pyrazol-4-yl]ethynyl}-*N*-methylpyridine-3-carboxamido)-3-phenylpropan-2-yl dihydrogen phosphate
receptor-interacting serine/threonine protein (RIP-1) kinase inhibitor

fosizensertib

dihydrogénophosphate de (2*S*)-1-(5-{[1-(difluorométhyl)-1*H*-pyrazol-4-yl]éthynyl}-*N*-méthylpyridine-3-carboxamido)-3-phénylpropan-2-yle
inhibiteur de la protéine kinase 1 interagissant avec les récepteurs (RIP-1)

fosizensertib

dihidrógenofosfato de (2*S*)-1-(5-{[1-(difluorometil)-1*H*-pirazol-4-il]etinil}-*N*-metilpiridina-3-carboxamido)-3-fenilpropan-2-ilo
inhibidor del receptor que interactua con la proteína serina/treonina (RIP-1) kinasa

$C_{22}H_{21}F_2N_4O_5P$ 2905377-00-4

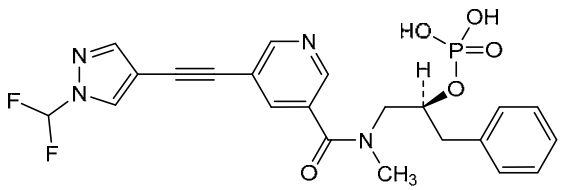

fosrugocrixanum

fosrugocrixan

(2*R*)-2-[(2-amino-5-{[(1*S*)-1-phenylethyl]sulfanyl}[1,3]thiazolo[4,5-*d*]pyrimidin-7-yl)amino]-4-methylpentyl dihydrogen phosphate
CX3C chemokine receptor 1 (CX3CR1) antagonist, anti-inflammatory

fosrugocrixan

dihydrogénophosphate de (2*R*)-2-[(2-amino-5-{[(1*S*)-1-phényléthyl]sulfanyl}[1,3]thiazolo[4,5-*d*]pyrimidin-7-yl)amino]-4-méthylpentyle
antagoniste du récepteur 1 de la chimioquine CX3C (CX3CR1), anti-inflammatoire

fosrugocrixán

dihidrogenofosfato de (2*R*)-2-[(2-amino-5-{[(1*S*)-1-feniletil]sulfanil}[1,3]tiazolo[4,5-*d*]pirimidin-7-il)amino]-4-metilpentilo
antagonista del receptor 1 de la quimioquina CX3C (CX3CR1), antiinflamatorio

$C_{19}H_{26}N_5O_4PS_2$ 2408145-38-8

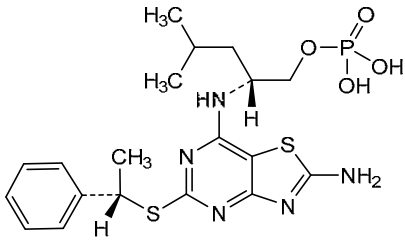

fudapirinum

fudapirine

(1*R*,2*S*)-1-[5-(4-chlorophenyl)-2-methoxypyridin-3-yl]-4-(dimethylamino)-2-(naphthalen-1-yl)-1-phenylbutan-2-ol
antibacterial

fudapirine

(1*R*,2*S*)-1-[5-(4-chlorophényl)-2-méthoxypyridin-3-yl]-4-(diméthylamino)-2-(naphtalén-1-yl)-1-phénylbutan-2-ol
antibactérien

fudapirina

(1*R*,2*S*)-1-[5-(4-clorofenil)-2-metoxipiridin-3-il]-4-(dimetilamino)-1-fenil-2-(naftalen-1-il)butan-2-ol
antibacteriano

$C_{34}H_{33}ClN_2O_2$ 1859978-72-5

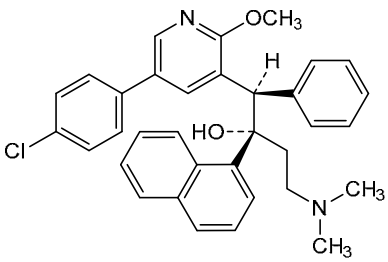

fulipiftidum

fulipiftide

pigment epithelium-derived factor *(Homo sapiens)* (PEDF, cell proliferation-inducing gene 35 protein, PIG-35, EPC-1, serpin F1), $N^{2.1}$-acetyl-(74-102)-peptide (1-29)-29-amide;
N-acetyl-L-seryl-L-leucylglycyl-L-alanyl-L-α-glutamyl-L-glutaminyl-L-arginyl-L-threonyl-L-α-glutamyl-L-seryl-L-isoleucyl-L-isoleucyl-L-histidyl-L-arginyl-L-alanyl-L-leucyl-L-tyrosyl-L-tyrosyl-L-α-aspartyl-L-leucyl-L-isoleucyl-L-seryl-L-seryl-L-prolyl-L-α-aspartyl-L-isoleucyl-L-histidylglycyl-L-threoninamide
anti-inflammatory

fulipiftide

facteur dérivé de l'épithélium pigmentaire *(Homo sapiens)* (PEDF, protéine du gène 35 induisant la prolifération cellulaire, PIG-35, EPC-1, serpine F1), $N^{2.1}$-acétyl-(74-102)-peptide (1-29)-29-amide;
N-acétyl-L-séryl-L-leucylglycyl-L-alanyl-L-α-glutamyl-L-glutaminyl-L-arginyl-L-thréonyl-L-α-glutamyl-L-séryl-L-isoleucyl-L-isoleucyl-L-histidyl-L-arginyl-L-alanyl-L-leucyl-L-tyrosyl-L-tyrosyl-L-α-aspartyl-L-leucyl-L-isoleucyl-L-séryl-L-séryl-L-prolyl-L-α-aspartyl-L-isoleucyl-L-histidylglycyl-L-thréoninamide
anti-inflammatoire

fulipiftida

factor derivado del epitelio pigmentario *(Homo sapiens)* (PEDF, proteína del gen 35 inductor de proliferación celular, PIG-35, EPC-1, serpina F1), $N^{2.1}$-acetil-(74-102)-péptido (1-29)-29-amida;
N-acetil-L-seril-L-leucilglicil-L-alanil-L-α-glutamil-L-glutaminil-L-arginil-L-treonil-L-α-glutamil-L-seril-L-isoleucil-L-isoleucil-L-histidil-L-arginil-L-alanil-L-leucil-L-tirosil-L-tirosil-L-α-aspartil-L-leucil-L-isoleucil-L-seril-L-seril-L-prolil-L-α-aspartil-L-isoleucil-L-histidilglicil-L-treoninamida
antiinflamatorio

$C_{144}H_{227}N_{41}O_{47}$ 2868985-56-0

SLGAEQRTES IIHRALYYDL ISSPDIHGT 29

Modified residues / Résidus modifiés / Restos modificados

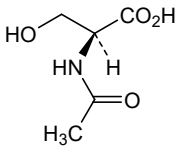

S (1)
N-Ac-L-Ser

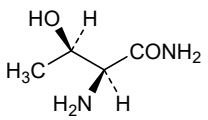

T (29)
L-Thr-NH_2

futermestotugum #

futermestotug

immunoglobulin G1-kappa, anti-[*Homo sapiens* CTLA4 (cytotoxic T-lymphocyte associated protein 4, CTLA-4, CD152)], humanized monoclonal antibody;
H-gamma1 heavy chain humanized (1-452) [VH (*Homo sapiens* IGHV3-23*04 (90.8%) -(IGHD) -IGHJ4*01 (80.0%) S128>A (122), CDR-IMGT [8.8.15] (26-33.51-58.97-111)) (1-122) - *Homo sapiens* IGHG1*03v (100%) G1m3>G1m17, nG1m1 CH1 K120, CH3 E12, M14 (CH1 R120>K (219) (123-220), hinge 1-15 (221-235), CH2 (236-345), CH3 E12 (361), M14 (363) (346-450), CHS (451-452)) (123-452)], (225-214')-disulfide with L-kappa light chain humanized (1'-214') [V-KAPPA (*Homo sapiens* IGKV1-9*01 (85.3%) -IGKJ4*01 (90.9%) V124>L (104'), CDR-IMGT [6.3.9] (27'-32'.50'-52'.89'-97')) (1'-107') - *Homo sapiens* IGKC*01 (100%) Km3 A45.1, V101 (C-KAPPA A45.1 (153'), V101 (191')) (108'-214')]; dimer (231-231":234-234")-bisdisulfide, produced in Chinese hamster ovary (CHO) cells, cell line CHO-K1, glycoform alfa
immunostimulant, antineoplastic

futermestotug

immunoglobuline G1-kappa, anti-[*Homo sapiens* CTLA4 (protéine 4 associée aux lymphocytes T cytotoxiques, CTLA-4, CD152)], anticorps monoclonal humanisé;

chaîne lourde H-gamma1 humanisée (1-452) [VH (*Homo sapiens* IGHV3-23*04 (90.8%) -(IGHD) -IGHJ4*01 (80.0%) S128>A (122), CDR-IMGT [8.8.15] (26-33.51-58.97-111)) (1-122) -*Homo sapiens* IGHG1*03v (100%) G1m3>G1m17, nG1m1 CH1 K120, CH3 E12, M14 (CH1 R120>K (219) (123-220), charnière 1-15 (221-235), CH2 (236-345), CH3 E12 (361), M14 (363) (346-450), CHS (451-452)) (123-452)], (225-214')-disulfure avec la chaîne légère L-kappa humanisée (1'-214') [V-KAPPA (*Homo sapiens* IGKV1-9*01 (85.3%) -IGKJ4*01 (90.9%) V124>L (104'), CDR-IMGT [6.3.9] (27'-32'.50'-52'.89'-97')) (1'-107') -*Homo sapiens* IGKC*01 (100%) Km3 A45.1, V101 (C-KAPPA A45.1 (153'), V101 (191')) (108'-214')]; dimère (231-231":234-234")-bisdisulfure, produit dans des cellules ovariennes de hamster chinois (CHO), lignée cellulaire CHO-K1, glycoforme alfa
immunostimulant, antinéoplasique

futermestotug

inmunoglobulina G1-kappa, anti-[*Homo sapiens* CTLA4 (proteína 4 asociada a los linfocitos T citotóxicos, CTLA-4, CD152)], anticuerpo monoclonal humanizado;
cadena pesada H-gamma1 humanizada (1-452) [VH (*Homo sapiens* IGHV3-23*04 (90.8%) -(IGHD) -IGHJ4*01 (80.0%) S128>A (122), CDR-IMGT [8.8.15] (26-33.51-58.97-111)) (1-122) -*Homo sapiens* IGHG1*03v (100%) G1m3>G1m17, nG1m1 CH1 K120, CH3 E12, M14 (CH1 R120>K (219) (123-220), bisagra 1-15 (221-235), CH2 (236-345), CH3 E12 (361), M14 (363) (346-450), CHS (451-452)) (123-452)], (225-214')-disulfuro con la cadena ligera L-kappa humanizada (1'-214') [V-KAPPA (*Homo sapiens* IGKV1-9*01 (85.3%) -IGKJ4*01 (90.9%) V124>L (104'), CDR-IMGT [6.3.9] (27'-32'.50'-52'.89'-97')) (1'-107') -*Homo sapiens* IGKC*01 (100%) Km3 A45.1, V101 (C-KAPPA A45.1 (153'), V101 (191')) (108'-214')]; dímero (231-231":234-234")-bisdisulfuro, producido en las células ováricas de hámster chino (CHO), línea celular CHO-K1, forma glicosilada alfa
inmunoestimulante, antineoplásico

3014361-57-7

Heavy chain / Chaîne lourde / Cadena pesada

```
EVQLVESGGG LVQPGGSLRL SCAASGFTFS SYTMSWVRQA PGKGLEWVAT  50
ISRGGGYTSY PDSVKGRFTI SRDNSKNTLY LQMNSLRAED TAVYYCARED 100
YGSSYVHWFA YWGQGTLVTV SAASTKGPSV FPLAPSSKST SGGTAALGCL 150
VKDYFPEPVT VSWNSGALTS GVHTFPAVLQ SSGLYSLSSV VTVPSSSLGT 200
QTYICNVNHK PSNTKVDKKV EPKSCDKTHT CPPCPAPELL GGPSVFLFPP 250
KPKDTLMISR TPEVTCVVVD VSHEDPEVKF NWYVDGVEVH NAKTKPREEQ 300
YNSTYRVVSV LTVLHQDWLN GKEYKCKVSN KALPAPIEKT ISKAKGQPRE 350
PQVYTLPPSR EEMTKNQVSL TCLVKGFYPS DIAVEWESNG QPENNYKTTP 400
PVLDSDGSFF LYSKLTVDKS RWQQGNVFSC SVMHEALHNH YTQKSLSLSP 450
GK                                                      452
```

Light chain / Chaîne légère / Cadena ligera

```
DIQMTQSPSF LSASVGDRVT ITCRAGENIY SYLAWYQQKP GKAPKLLIYN  50
ARTLAEGVPS RFSGSGSGTE FTLTISSLQP EDFATYYCQH HYGSPRTFGG 100
GTKLEIKRTV AAPSVFIFPP SDEQLKSGTA SVVCLLNNFY PREAKVQWKV 150
DNALQSGNSQ ESVTEQDSKD STYSLSSTLT LSKADYEKHK VYACEVTHQG 200
LSSPVTKSFN RGEC                                        214
```

Post-translational modifications
Disulfide bridges location / Position des ponts disulfure / Posiciones de los puentes disulfuro
Intra-H (C23-C104) 22-96 149-205 266-326 372-430
22"-96" 149"-205" 266"-326" 372"-430"
Intra-L (C23-C104) 23'-88' 134'-194'
23'"-88'" 134'"-194'"
Inter-H-L (h 5-CL 126) 225-214' 225"-214'"
Inter-H-H (h 11, h 14) 231-231" 234-234"

N-glycosylation sites / Sites de N-glycosylation / Posiciones de N-glicosilación
H CH2 N84.4: 302, 302"
Fucosylated complex bi-antennary CHO-type glycans / glycanes de type CHO bi-antennaires complexes fucosylés / glicanos de tipo CHO biantenarios complejos fucosilados

C-terminal lysine clipping / Coupure de la lysine C-terminale / Recorte de lisina C-terminal
H CHS K2: 452, 452"

gadosircoclamidum

gadosircoclamide

[2,2',2''-(10-{2-[(cyclohexylmethyl)amino]-2-oxo-κ*O*-ethyl}-1,4,7,10-tetraazacyclododecane-1,4,7-triyl-κ^4*N*^{1},*N*^{4},*N*^{7},*N*^{10})tri(acetato-κ*O*)]gadolinium
radiodiagnostic agent

gadosircoclamide

[2,2',2''-(10-{2-[(cyclohexylméthyl)amino]-2-oxo-κ*O*-éthyl}-1,4,7,10-tétraazacyclododécane-1,4,7-triyl-κ^4*N*^{1},*N*^{4},*N*^{7},*N*^{10})tri(acétato-κ*O*)]gadolinium
produit de radiodiagnostic

gadosircoclamida

[2,2',2''-(10-{2-[(ciclohexilmetil)amino]-2-oxo-κ*O*-etil}-1,4,7,10-tetraazaciclododecano-1,4,7-triil-κ^4*N*^{1},*N*^{4},*N*^{7},*N*^{10})tri(acetato-κ*O*)]gadolinio
agente de radiodiagnóstico

$C_{23}H_{38}GdN_5O_7$ 1801159-68-1

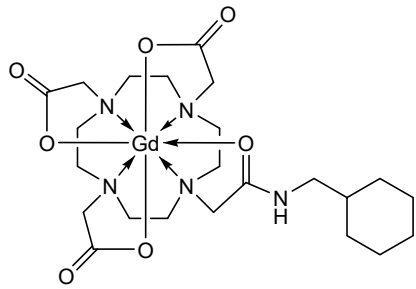

garetatugum #

garetatug

immunoglobulin G1-kappa, anti-[*Homo sapiens* CLDN18 (claudin 18, claudin-18, surfactant associated protein J, SFTPJ) isoform 2], humanized monoclonal antibody;
H-gamma1 heavy chain humanized (1-448) [VH (*Homo sapiens* IGHV1-3*01 (87.8%) -(IGHD) -IGHJ4*01 (92.9%) L123>T (113), CDR-IMGT [8.8.11] (26-33.51-58.97-107)) (1-118) -*Homo sapiens* IGHG1*01 (100%) G1m17,1 CH1 K120, CH3 D12, L14 (CH1 K120 (215) (119-216), hinge 1-15 (217-231), CH2 (232-341), CH3 D12 (357), L14 (359) (342-446), CHS (447-448)) (119-448)], (221-220')-disulfide with L-kappa light chain humanized (1'-220') [V-KAPPA (*Homo sapiens* IGKV4-1*01 (90.1%) -IGKJ2*02 (100%), CDR-IMGT [12.3.9] (27'-38'.56'-58'.95'-103')) (1'-113') -*Homo sapiens* IGKC*01 (100%) Km3 A45.1, V101 (C-KAPPA A45.1 (159'), V101 (197')) (114'-220')]; dimer (227-227'':230-230'')-bisdisulfide, produced in Chinese hamster ovary (CHO) cells, cell line CHO-K1, glycoform alfa
antineoplastic

garétatug

immunoglobuline G1-kappa, anti-[*Homo sapiens* CLDN18 (claudine 18, claudine-18, protéine J associée au surfactant, SFTPJ) isoforme 2], anticorps monoclonal humanisé;

chaîne lourde H-gamma1 humanisée (1-448) [VH (*Homo sapiens* IGHV1-3*01 (87.8%) -(IGHD) -IGHJ4*01 (92.9%) L123>T (113), CDR-IMGT [8.8.11] (26-33.51-58.97-107)) (1-118) -*Homo sapiens* IGHG1*01 (100%) G1m17,1 CH1 K120, CH3 D12, L14 (CH1 K120 (215) (119-216), charnière 1-15 (217-231), CH2 (232-341), CH3 D12 (357), L14 (359) (342-446), CHS (447-448)) (119-448)], (221-220')-disulfure avec la chaîne légère L-kappa humanisée (1'-220') [V-KAPPA (*Homo sapiens* IGKV4-1*01 (90.1%) -IGKJ2*02 (100%), CDR-IMGT [12.3.9] (27'-38'.56'-58'.95'-103')) (1'-113') -*Homo sapiens* IGKC*01 (100%) Km3 A45.1, V101 (C-KAPPA A45.1 (159'), V101 (197')) (114'-220')]; dimère (227-227'':230-230'')-bisdisulfure, produit dans des cellules ovariennes de hamster chinois (CHO), lignée cellulaire CHO-K1, glycoforme alfa

antinéoplasique

garetatug

inmunoglobulina G1-kappa, anti-[*Homo sapiens* CLDN18 (claudina 18, claudina-18, proteína J asociada al surfactante, SFTPJ) isoforma 2], anticuerpo monoclonal humanizado;
cadena pesada H-gamma1 humanizada (1-448) [VH (*Homo sapiens* IGHV1-3*01 (87.8%) -(IGHD) -IGHJ4*01 (92.9%) L123>T (113), CDR-IMGT [8.8.11] (26-33.51-58.97-107)) (1-118) -*Homo sapiens* IGHG1*01 (100%) G1m17,1 CH1 K120, CH3 D12, L14 (CH1 K120 (215) (119-216), bisagra 1-15 (217-231), CH2 (232-341), CH3 D12 (357), L14 (359) (342-446), CHS (447-448)) (119-448)], (221-220')-disulfuro con la cadena ligera L-kappa humanizada (1'-220') [V-KAPPA (*Homo sapiens* IGKV4-1*01 (90.1%) -IGKJ2*02 (100%), CDR-IMGT [12.3.9] (27'-38'.56'-58'.95'-103')) (1'-113') -*Homo sapiens* IGKC*01 (100%) Km3 A45.1, V101 (C-KAPPA A45.1 (159'), V101 (197')) (114'-220')]; dímero (227-227'':230-230'')-bisdisulfuro, producido en las células ováricas de hámster chino (CHO), línea celular CHO-K1, forma glicosilada alfa

antineoplásico

3023285-05-1

Heavy chain / Chaîne lourde / Cadena pesada

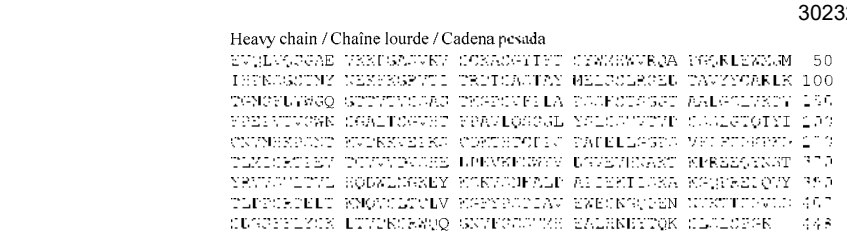

Light chain / Chaîne légère / Cadena ligera

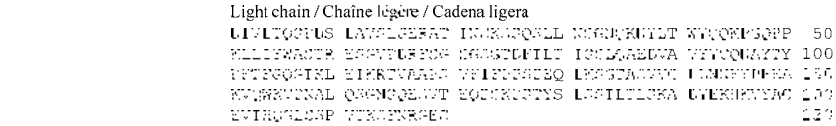

Post-translational modifications

Disulfide bridges location / Position des ponts disulfure / Posiciones de los puentes disulfuro

Intra-H (C 23-C 104) 22-96 145-201 262-322 368-426
22''-96'' 145''-201'' 262''-322'' 368''-426''
Intra-L (C 23-C 104) 23'-94' 140'-200'
23'''-94''' 140'''-200'''
Inter-H-L (h 5-CL 126) 221-220' 221''-220'''
Inter-H-H (h 11, h 14) 227-227'' 230-230''

N-glycosylation sites / Sites de N-glycosylation / Posiciones de N-glicosilación
H CH2 N84.4: 298, 298''
Fucosylated complex bi-antennary CHO-type glycans / glycanes de type CHO bi-antennaires complexes fucosylés / glicanos de tipo CHO biantenarios complejos fucosilados

C-terminal lysine clipping / Coupure de la lysine C-terminale / Recorte de lisina C-terminal
H CHS K2: 448, 448''

garetatugum rezetecanum #

garetatug rezetecan — immunoglobulin G1-kappa, anti-[*Homo sapiens* CLDN18 (claudin 18, claudin-18, surfactant associated protein J, SFTPJ) isoform 2], humanized monoclonal antibody; conjugated on an average of four cysteinyl residues to *rezetecan*, comprising a linker and a camptothecin derivative (*exatecan*);
H-gamma1 heavy chain humanized (1-448) [VH (*Homo sapiens* IGHV1-3*01 (87.8%) -(IGHD) -IGHJ4*01 (92.9%) L123>T (113), CDR-IMGT [8.8.11] (26-33.51-58.97-107)) (1-118) -*Homo sapiens* IGHG1*01 (100%) G1m17,1 CH1 K120, CH3 D12, L14 (CH1 K120 (215) (119-216), hinge 1-15 (217-231), CH2 (232-341), CH3 D12 (357), L14 (359) (342-446), CHS (447-448)) (119-448)], (221-220')-disulfide with L-kappa light chain humanized (1'-220') [V-KAPPA (*Homo sapiens* IGKV4-1*01 (90.1%) -IGKJ2*02 (100%), CDR-IMGT [12.3.9] (27'-38'.56'-58'.95'-103')) (1'-113') -*Homo sapiens* IGKC*01 (100%) Km3 A45.1, V101 (C-KAPPA A45.1 (159'), V101 (197')) (114'-220')]; dimer (227-227'':230-230'')-bisdisulfide, produced in Chinese hamster ovary (CHO) cells, cell line CHO-K1, glycoform alfa; substituted at the sulfur atoms of four L-cysteinyl residues on an average among 220', 220''', 221, 221'', 227, 227'', 230 and 230'' with (3*RS*)-1-[(2*R*,10*S*)-10-benzyl-2-cyclopropyl-1-{[(1*S*,9*S*)-9-ethyl-5-fluoro-9-hydroxy-4-methyl-10,13-dioxo-2,3,9,10,13,15-hexahydro-1*H*,12*H*-benzo[*de*]pyrano[3',4':6,7]indolizino[1,2-*b*]quinolin-1-yl]amino}-1,6,9,12,15,18-hexaoxo-3-oxa-5,8,11,14,17-pentaazatricosan-23-yl]-2,5-dioxopyrrolidin-3-yl (*rezetecan*) groups
antineoplastic

garétatug rézétecan — immunoglobuline G1-kappa, anti-[*Homo sapiens* CLDN18 (claudine 18, claudine-18, protéine J associée au surfactant, SFTPJ) isoforme 2], anticorps monoclonal humanisé, conjuguée par quatre résidus cystéinyles en moyenne au *rézétécan*, comprenant un linker et un dérivé de la camptothécine (*exatécan*);
chaîne lourde H-gamma1 humanisée (1-448) [VH (*Homo sapiens* IGHV1-3*01 (87.8%) -(IGHD) -IGHJ4*01 (92.9%) L123>T (113), CDR-IMGT [8.8.11] (26-33.51-58.97-107)) (1-118) -*Homo sapiens* IGHG1*01 (100%) G1m17,1 CH1 K120, CH3 D12, L14 (CH1 K120 (215) (119-216), charnière 1-15 (217-231), CH2 (232-341), CH3 D12 (357), L14 (359) (342-446), CHS (447-448)) (119-448)], (221-220')-disulfure avec la chaîne légère L-kappa humanisée (1'-220') [V-KAPPA (*Homo sapiens* IGKV4-1*01 (90.1%) -IGKJ2*02 (100%), CDR-IMGT [12.3.9] (27'-38'.56'-58'.95'-103')) (1'-113') -*Homo sapiens* IGKC*01 (100%) Km3 A45.1, V101 (C-KAPPA A45.1 (159'), V101 (197')) (114'-220')]; dimère (227-227'':230-230'')-bisdisulfure, produit dans des cellules ovariennes de hamster chinois (CHO), lignée cellulaire CHO-K1, glycoforme alfa; substitué, sur les atomes de soufre de quatre résidus L-cystéinyle en moyenne parmi 220', 220''', 221, 221'', 227, 227'', 230 et 230'', avec des groupes (3*RS*)-1-[(2*R*,10*S*)-10-benzyl-2-cyclopropyl-1-{[(1*S*,9*S*)-9-éthyl-5-fluoro-9-hydroxy-4-méthyl-10,13-dioxo-2,3,9,10,13,15-hexahydro-1*H*,12*H*-benzo[*de*]pyrano[3',4':6 ,7]indolizino[1,2-*b*]quinoléin-1-yl]amino}-1,6,9,12,15,18-hexaoxo-3-oxa-5,8,11,14,17-pentaazatricosan-23-yl]-2,5-dioxopyrrolidin-3-yle (*rézétécan*)
antinéoplasique

garetatug rezetecán — inmunoglobulina G1-kappa, anti-[*Homo sapiens* CLDN18 (claudina 18, claudina-18, proteína J asociada al surfactante, SFTPJ) isoforma 2], anticuerpo monoclonal humanizado, conjugado, por cuatro residuos de cisteinilo, por término medio a *rezetecán*, que comprende un enlace y un derivado de la camptotecina (*exatecán*);

cadena pesada H-gamma1 humanizada (1-448) [VH (*Homo sapiens* IGHV1-3*01 (87.8%) -(IGHD) -IGHJ4*01 (92.9%) L123>T (113), CDR-IMGT [8.8.11] (26-33.51-58.97-107)) (1-118) -*Homo sapiens* IGHG1*01 (100%) G1m17,1 CH1 K120, CH3 D12, L14 (CH1 K120 (215) (119-216), bisagra 1-15 (217-231), CH2 (232-341), CH3 D12 (357), L14 (359) (342-446), CHS (447-448)) (119-448)], (221-220')-disulfuro con la cadena ligera L-kappa humanizada (1'-220') [V-KAPPA (*Homo sapiens* IGKV4-1*01 (90.1%) -IGKJ2*02 (100%), CDR-IMGT [12.3.9] (27'-38'.56'-58'.95'-103')) (1'-113') -*Homo sapiens* IGKC*01 (100%) Km3 A45.1, V101 (C-KAPPA A45.1 (159'), V101 (197')) (114'-220')]; dímero (227-227'':230-230'')-bisdisulfuro, producido en las células ováricas de hámster chino (CHO), línea celular CHO-K1, forma glicosilada alfa; sustituido, en los átomos de azufre de cuatro residuos de L-cisteinilo en promedio de 220', 220''', 221, 221'', 227, 227'', 230 y 230'', con grupos (3*RS*)-1-[(2*R*,10*S*)-10-bencil-2-ciclopropil-1-{[(1*S*,9*S*)-9-etil-5-fluoro-9-hidroxi-4-metil-10,13-dioxo-2,3,9,10,13,15-hexahidro-1*H*,12*H*-benzo[*de*]pirano[3',4':6,7]indolizino[1,2-*b*]quinolein-1-il]amino}-1,6,9,12,15,18-hexaoxo-3-oxa-5,8,11,14,17-pentaazatricosan-23-il]-2,5-dioxopirrolidin-3-ilo (*rezetecán*)

antineoplásico

3023285-06-2

Heavy chain / Chaîne lourde / Cadena pesada (H, H'')

```
EVQLVQSGAE VKKPGASVKV SCKASGYTFT SYWMHWVRQA PGQGLEWMGN  50
INPSNGGTNY NEKFKSRVTI TRDTSATTAY MELSSLRSED TAVYYCARLK 100
DGNSFDYWGQ GTTVTVSSAS TKGPSVFPLA PSSKSTSGGT AALGCLVKDY 150
FPEPVTVSWN SGALTSGVHT FPAVLQSSGL YSLSSVVTVP SSSLGTQTYI 200
CNVNHKPSNT KVDKRVEPKS CDKTHTCPPC PAPELLGGPS VFLFPPKPKD 250
TLMISRTPEV TCVVVDVSHE DPEVKFNWYV DGVEVHNAKT KPREEQYNST 300
YRVVSVLTVL HQDWLNGKEY KCKVSNKALP APIEKTISKA KGQPREPQVY 350
TLPPSRDELT KNQVSLTCLV KGFYPSDIAV EWESNGQPEN NYKTTPPVLD 400
SDGSFFLYSK LTVDKSRWQQ GNVFSCSVMH EALHNHYTQK SLSLSPGK   448
```

Light chain / Chaîne légère / Cadena ligera (L', L'')

```
DIVLTQSPLS LAVSLGERAT INCKSSQSLL NSGNQKNYLT WYQQKPGQPP  50
KLLIYWASTR ESGVPDRFSG SGSGTDFTLT ISSLQAEDVA VYYCQNAYTY 100
PFTFGQGTKL EIKRTVAAPS VFIFPPSDEQ LKSGTASVVC LLNNFYPREA 150
KVQWKVDNAL QSGNSQESVT EQDSKDSTYS LSSTLTLSKA DYEKHKVYAC 200
EVTHQGLSSP VTKSFNRGEC                                  220
```

Post-translational modifications

Disulfide bridges location / Position des ponts disulfure / Posiciones de los puentes disulfuro

Intra-H (C 23-C 104) 22-96 145-201 262-322 368-426
22''-96'' 145''-201'' 262''-322'' 368''-426''

Intra-L (C 23-C 104) 23'-94' 140'-200'
23'''-94''' 140'''-200'''

Inter-H-L (h 5-CL 126)* 221-220'' 221''-220'''

Inter-H-H (h 11, h 14)* 227-227'' 230-230''

* Three or four of the four inter-chain disulfide bridges are not present, an average of 4 (3.5-4.5) cysteicyl being conjugated each via a thioether bond to a drug linker.

* Trois ou quatre des quatre ponts disulfures inter-chaînes ne sont pas présents, 4 (3.5-4.5) cystéicyl en moyenne étant chacun conjugué via une liaison thioéther à un linker-principe actif.

* Tres or cuatro de los cuatro puentes disulfuro inter-catenarios no estan presentes, una media de 4 (3.5-4.5) cisteinil está conjugada a conectores de principio activo

N-glycosylation sites / Sites de N-glycosylation / Posiciones de N-glicosilación

H (EU N84.4: 298, 298''

Fucosylated complex bi-antennary CHO-type glycans / glycanes de type CHO bi-antennaires complexes fucosylés / glicanos de tipo CHO biantenarios complejos fucosilados

C-terminal lysine clipping / Coupure de la lysine C-terminale / Recorte de lisina C-terminal

H (EU K2..448, 448''

Modified residues / Résidus modifiés / Restos modificados*

C (221, 227, 230, 230'', 221'', 227'', 230'', 220''')

*(*rezetec-mc*mAb ~ 4:1)

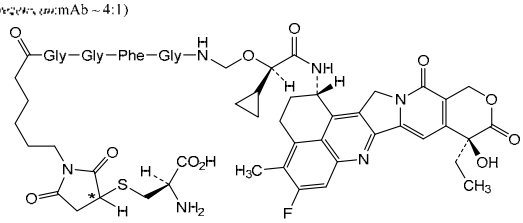

gatuzosiranum

gatuzosiran

all-P-ambo-[(2*R*,3*S*)-2-(hydroxymethyl)oxolan-3-yl] hydrogen 5'-*O*-({[(2*R*,3*S*)-3-({[(*cis*-4-{(3*S*,8*S*)-17-[(2-acetamido-2-deoxy-β-D-galactopyranosyl)oxy]-3,8-bis[(2-{2-[(2-acetamido-2-deoxy-β-D-galactopyranosyl)oxy]ethoxy}ethyl)carbamoyl]-6,11-dioxo-15-oxa-2,7,12-triazaheptadecan-1-oyl}cyclohexyl)oxy]hydroxyphosphorothioyl}oxy)oxolan-2-yl]methoxy}hydroxyphosphorothioyl)-2'-*O*-methylcytidylyl-(3'→5')-2'-*O*-methylguanylyl-(3'→5')-2'-*O*-methyluridylyl-(3'→5')-2'-*O*-methyladenylyl-(3'→5')-2'-*O*-methyladenylyl-(3'→5')-2'-*O*-methylguanylyl-(3'→5')-2'-*O*-methyladenylyl-(3'→5')-2'-*O*-methyladenylyl-(3'→5')-2'-deoxy-2'-fluoroguanylyl-(3'→5')-2'-*O*-methyluridylyl-(3'→5')-2'-deoxy-2'-fluorocytidylyl-(3'→5')-2'-*O*-methyluridylyl-(3'→5')-2'-deoxy-2'-fluoroguanylyl-(3'→5')-2'-*O*-methyladenylyl-(3'→5')-2'-*O*-methyluridylyl-(3'→5')-2'-*O*-methyladenylyl-(3'→5')-2'-*O*-methylguanylyl-(3'→5')-2'-*O*-methyladenylyl-(3'→5')-2'-*O*-methyluridylyl-(3'→5')-2'-*O*-methylguanylyl-(3'→5')-2'-*O*-methyl-*P*-thio-3'-adenylate

duplex with *all-P-ambo* 2'-*O*-methyl-*P*-thioguanylyl-(5'→3')-2'-deoxy-2'-fluorocytidylyl-(5'→3')-2'-*O*-methyladenylyl-(5'→3')-2'-deoxy-2'-fluorouridylyl-(5'→3')-2'-*O*-methyluridylyl-(5'→3')-2'-deoxy-2'-fluorocytidylyl-(5'→3')-2'-*O*-methyluridylyl-(5'→3')-2'-deoxy-2'-fluorouridylyl-(5'→3')-2'-*O*-methylcytidylyl-(5'→3')-2'-deoxy-2'-fluoroadenylyl-(5'→3')-2'-*O*-methylguanylyl-(5'→3')-2'-*O*-methyladenylyl-(5'→3')-2'-*O*-methylcytidylyl-(5'→3')-2'-*O*-methyluridylyl-(5'→3')-2'-*O*-methyladenylyl-(5'→3')-2'-deoxy-2'-fluorouridylyl-(5'→3')-2'-*O*-methylcytidylyl-(5'→3')-2'-deoxy-2'-fluoro-*P*-thiouridylyl-(5'→3')-2'-*O*-methyl-*P*-thioadenylyl-(5'→3')-2'-deoxy-2'-fluoro-*P*-thiocytidylyl-(5'→3')-2'-*O*-methyluridine

17-beta-hydroxysteroid dehydrogenase 13 synthesis reducer, fatty liver disease

gatuzosiran

tout-P-ambo-5'-*O*-({[(2*R*,3*S*)-3-({[(*cis*-4-{(3*S*,8*S*)-17-[(2-acétamido-2-désoxy-β-D-galactopyranosyl)oxy]-3,8-bis[(2-{2-[(2-acétamido-2-désoxy-β-D-galactopyranosyl)oxy]éthoxy}éthyl)carbamoyl]-6,11-dioxo-15-oxa-2,7,12-triazaheptadécan-1-oyl}cyclohexyl)oxy]hydroxyphosphorothioyl}oxy)oxolan-2-yl]méthoxy}hydroxyphosphorothioyl)-2'-*O*-méthylcytidylyl-(3'→5')-2'-*O*-méthylguanylyl-(3'→5')-2'-*O*-méthyluridylyl-(3'→5')-2'-*O*-méthyladénylyl-(3'→5')-2'-*O*-méthyladénylyl-(3'→5')-2'-*O*-méthylguanylyl-(3'→5')-2'-*O*-méthyladénylyl-(3'→5')-2'-*O*-méthyladénylyl-(3'→5')-2'-désoxy-2'-fluoroguanylyl-(3'→5')-2'-*O*-méthyluridylyl-(3'→5')-2'-désoxy-2'-fluorocytidylyl-(3'→5')-2'-*O*-méthyluridylyl-(3'→5')-2'-désoxy-2'-fluoroguanylyl-(3'→5')-2'-*O*-méthyladénylyl-(3'→5')-2'-*O*-méthyluridylyl-(3'→5')-2'-*O*-méthyladénylyl-(3'→5')-2'-*O*-méthylguanylyl-(3'→5')-2'-*O*-méthyladénylyl-(3'→5')-2'-*O*-méthyluridylyl-(3'→5')-2'-*O*-méthylguanylyl-(3'→5')-hydrogéno-2'-*O*-méthyl-*P*-thio-3'-adénylate de[(2*R*,3*S*)-2-(hydroxyméthyl)oxolan-3-yle]

duplex avec *tout-P-ambo*-2'-*O*-méthyl-*P*-thioguanylyl-(5'→3')-2'-désoxy-2'-fluorocytidylyl-(5'→3')-2'-*O*-méthyladénylyl-(5'→3')-2'-désoxy-2'-fluorouridylyl-(5'→3')-2'-*O*-méthyluridylyl-(5'→3')-2'-désoxy-2'-fluorocytidylyl-(5'→3')-2'-*O*-méthyluridylyl-(5'→3')-2'-désoxy-2'-fluorouridylyl-(5'→3')-2'-*O*-méthylcytidylyl-(5'→3')-2'-désoxy-2'-fluoroadénylyl-(5'→3')-2'-*O*-méthylguanylyl-(5'→3')-2'-*O*-méthyladénylyl-(5'→3')-2'-*O*-méthylcytidylyl-(5'→3')-2'-*O*-méthyluridylyl-(5'→3')-2'-*O*-méthyladénylyl-(5'→3')-2'-désoxy-2'-fluorouridylyl-(5'→3')-2'-*O*-méthylcytidylyl-(5'→3')-2'-désoxy-2'-fluoro-*P*-thiouridylyl-(5'→3')-2'-*O*-méthyl-*P*-thioadénylyl-(5'→3')-2'-désoxy-2'-fluoro-*P*-thiocytidylyl-(5'→3')-2'-*O*-méthyluridine

réducteur de synthèse de la 17-bêta-hydroxystéroïde déshydrogénase 13, stéatose hépatique

gatuzosirán

todo-P-ambo-5'-*O*-({[(2*R*,3*S*)-3-({[(*cis*-4-{(3*S*,8*S*)-17-[(2-acetamido-2-desoxi-β-D-galactopiranosil)oxi]-3,8-bis[(2-{2-[(2-acetamido-2-desoxi-β-D-galactopiranosil)oxi]etoxi}etil)carbamoil]-6,11-dioxo-15-oxa-2,7,12-triazaheptadecan-1-oil}ciclohexil)oxi]hidroxifosforotioil}oxi)oxolan-2-il]metoxi}hidroxifosforotioil)-2'-*O*-metilcitidilil-(3'→5')-2'-*O*-metilguanilil-(3'→5')-2'-*O*-metiluridilil-(3'→5')-2'-*O*-metiladenilil-(3'→5')-2'-*O*-metiladenilil-(3'→5')-2'-*O*-metilguanilil-(3'→5')-2'-*O*-metiladenilil-(3'→5')-2'-*O*-metiladenilil-(3'→5')-2'-desoxi-2'-fluoroguanilil-(3'→5')-2'-*O*-metiluridilil-(3'→5')-2'-desoxi-2'-fluorocitidilil-(3'→5')-2'-*O*-metiluridilil-(3'→5')-2'-desoxi-2'-fluoroguanilil-(3'→5')-2'-*O*-metiladenilil-(3'→5')-2'-*O*-metiluridilil-(3'→5')-2'-*O*-metiladenilil-(3'→5')-2'-*O*-metilguanilil-(3'→5')-2'-*O*-metiladenilil-(3'→5')-2'-*O*-metiluridilil-(3'→5')-2'-*O*-metilguanilil-(3'→5')-hidrógeno-2'-*O*-metil-*P*-tio-3'-adenilato de *O*-[(2*R*,3*S*)-2-(hidroximetil)oxolan-3-ilo]
dúplex con *todo-P-ambo*-2'-*O*-metil-*P*-tioguanilil-(5'→3')-2'-desoxi-2'-fluoroocitidilil-(5'→3')-2'-*O*-metiladenilil-(5'→3')-2'-desoxi-2'-fluorouridilil-(5'→3')-2'-*O*-metiluridilil-(5'→3')-2'-desoxi-2'-fluorocitidilil-(5'→3')-2'-*O*-metiluridilil-(5'→3')-2'-desoxi-2'-fluorouridilil-(5'→3')-2'-*O*-metilcitidilil-(5'→3')-2'-desoxi-2'-fluoroadenilil-(5'→3')-2'-*O*-metilguanilil-(5'→3')-2'-*O*-metiladenilil-(5'→3')-2'-*O*-metilcitidilil-(5'→3')-2'-*O*-metiluridilil-(5'→3')-2'-*O*-metiladenilil-(5'→3')-2'-desoxi-2'-fluorouridilil-(5'→3')-2'-*O*-metilcitidilil-(5'→3')-2'-desoxi-2'-fluoro-*P*-tiouridilil-(5'→3')-2'-*O*-metil-*P*-tioadenilil-(5'→3')-2'-desoxi-2'-fluoro-*P*-tiocitidilil-(5'→3')-2'-*O*-metiluridina
reductor dela síntesis de la 17-beta-hydroxiesteroide deshidrogenasa 13, enfermedad del hígado graso

$C_{493}H_{653}F_{11}N_{163}O_{311}P_{43}S_7$ 2409783-34-0

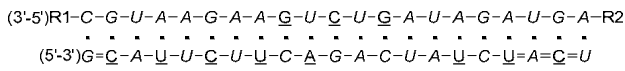

N : A,C,G,U
N : 2'-*O*-methyl-N / 2'-*O*-méthyl-N / 2'-*O*-metil-N
N : 2'-deoxy-2'-fluoro-N / 2'-désoxy-2'-fluoro-N / 2'-desoxi-2'-fluoro-N
– : –PO(OH)– = : –PO(SH)–

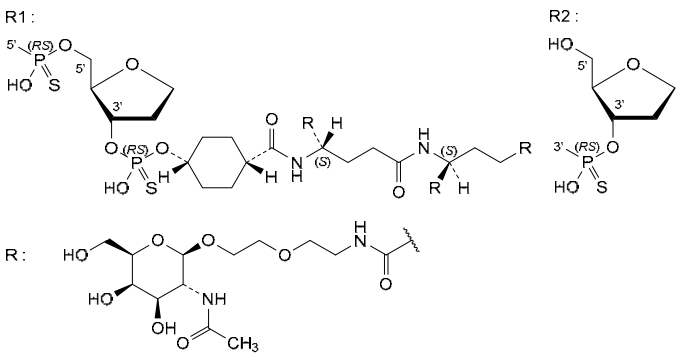

gintemetostatum

gintemetostat

(1*S*)-1-[(3*R*)-3-amino-4'-[(6-amino-9*H*-purin-9-yl)methyl]-6'-(2,5-difluoro-4-methoxyphenyl)-3,4,5,6-tetrahydro-2*H*-[1,3'-bipyridin]-3-yl]-2,2-difluoroethan-1-ol
antineoplastic

gintémétostat

(1*S*)-1-[(3*R*)-3-amino-4'-[(6-amino-9*H*-purin-9-yl)méthyl]-6'-(2,5-difluoro-4-méthoxyphényl)-3,4,5,6-tétrahydro-2*H*-[1,3'-bipyridin]-3-yl]-2,2-difluoroéthan-1-ol
antinéoplasique

gintemetostat (1*S*)-1-[(3*R*)-3-amino-4'-[(6-amino-9*H*-purin-9-il)metil]-6'-(2,5-difluoro-4-metoxifenil)-3,4,5,6-tetrahidro-2*H*-[1,3'-bipiridin]-3-il]-2,2-difluoroetan-1-ol
antineoplásico

$C_{25}H_{26}F_4N_8O_2$ 2604513-16-6

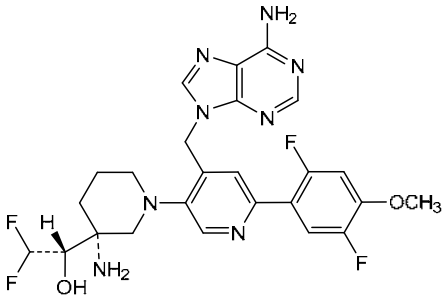

givopegsomatropinum #

givopegsomatropin human somatotropin (growth hormone, GH), conjugated to a two-arm polyethylene glycol carrier molecule; produced by *Escherichia coli*, mono-substituted at the N-terminus (F1) or at $N^{6.Lys}$ of either K38, K140, K145 or K158 with one N^2,N^6-bis{[α-methylpoly(oxyethylene)-ω-oxy]carbonyl}-L-lysyl group (~40 kDa)
growth hormone derivative

givopegsomatropine somatotropine humaine (hormone de croissance, GH), conjuguée à une molécule porteuse de polyéthylène glycol à deux bras; produite par *Escherichia coli*, mono-substituée à l'extrémité N-terminale (F1) ou en $N^{6.Lys}$ de K38, K140, K145 ou K158 par un groupe N^2,N^6-bis{[α-méthylpoly(oxyéthylène)-ω-oxy]carbonyl}-L-lysyle (~40 kDa)
dérivé de l'hormone de croissance

givopegsomatropina somatotropina humana (hormona de crecimiento, GH), conjugada con una molécula portadora con dos brazos de polietelenglicol; producida por *Escherichia coli*, mono-sustituida en el extremo N-terminal (F1) o en $N^{6.Lys}$ de K38, K140, K145 o K158 con un grupo N^2,N^6-bis{[α-metilpoli(oxietileno)-ω-oxi]carbonil}-L-lisilo (~40 kDa)
derivado de la hormona de crecimiento

3001334-30-8

Sequence / Séquence / Secuencia

```
FPTIPLSRLF DNAMLRAHRL HQLAFDTYQE FEEAYIPKEQ KYSFLQNPQT    50
SLCFSESIPT PSNREETQQK SNLELLRISL LLIQSWLEPV QFLRSVFANS   100
LVYGASDSNV YDLLKDLEEG IQTLMGRLED GSPRTGQIFK QTYSKFDTNS   150
HNDDALLKNY GLLYCFRKDM DKVETFLRIV QCRSVEGSCG F            191
```

Post-translational modifications
Disulfide bridges location / Position des ponts disulfure / Posiciones de los puentes disulfuro
53-165 182-189

N-glycosylation sites / Sites de N-glycosylation / Posiciones de N-glicosilación
none / aucun / ninguna

Potential modified residues / Résidus modifiés potentiels / restos modificados potenciales
F1, K38, K140, K145, or K158

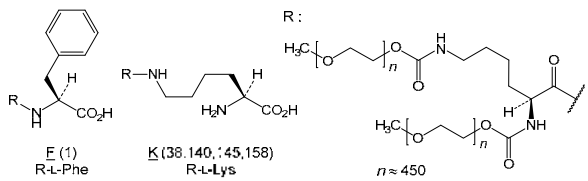

gozanertinibum

gozanertinib — (2*E*)-4-(dimethylamino)-*N*-[3-(4-{[(1*S*)-2-hydroxy-1-phenylethyl]amino}-6-phenylfuro[2,3-*d*]pyrimidin-5-yl)phenyl]but-2-enamide
epidermal growth factor receptor tyrosine kinase inhibitor, antineoplastic

gozanertinib — (2*E*)-4-(diméthylamino)-*N*-[3-(4-{[(1*S*)-2-hydroxy-1-phényléthyl]amino}-6-phénylfuro[2,3-*d*]pyrimidin-5-yl)phényl]but-2-énamide
inhibiteur de la tyrosine kinase du récepteur du facteur de croissance épidermique, antinéoplasique

gozanertinib — (2*E*)-4-(dimetilamino)-*N*-[3-(6-fenil-4-{[(1*S*)-1-fenil-2-hidroxietil]amino}furo[2,3-*d*]pirimidin-5-il)fenil]but-2-enamida
inhibidor del receptor de la tirosina kinasa del receptor del factor de crecimiento epidérmico, antineoplásico

$C_{32}H_{31}N_5O_3$ 1226549-49-0

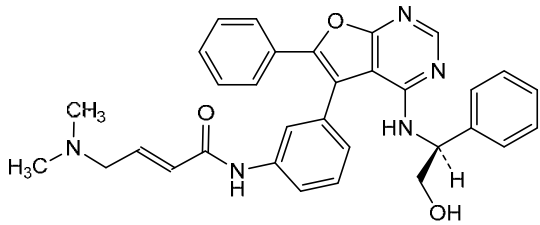

ifupinostatum

ifupinostat — *N*-hydroxy-2-[methyl({2-[6-(methylamino)pyridin-3-yl]-4-(morpholin-4-yl)thieno[3,2-*d*]pyrimidin-6-yl}methyl)amino]pyrimidine-5-carboxamide
histone deacetylase inhibitor, antineoplastic

ifupinostat — *N*-hydroxy-2-[méthyl({2-[6-(méthylamino)pyridin-3-yl]-4-(morpholin-4-yl)thiéno[3,2-*d*]pyrimidin-6-yl}méthyl)amino]pyrimidine-5-carboxamide
inhibiteur d'histone désacétylase, antinéoplasique

ifupinostat — *N*-hidroxi-2-[metil({2-[6-(metilamino)piridin-3-il]-4-(morfolin-4-il)tieno[3,2-*d*]pirimidin-6-il}metil)amino]pirimidina-5-carboxamida
inhibidor de la deacetilasa de la histona, antineoplásico

$C_{23}H_{25}N_9O_3S$ 1235449-52-1

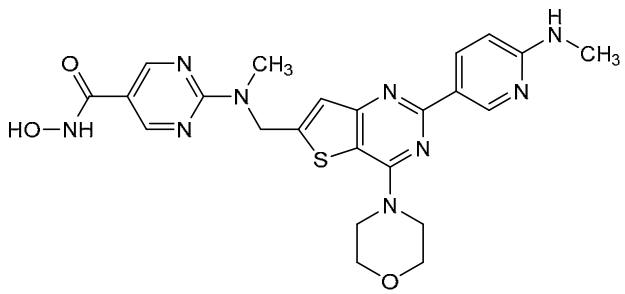

imapextidum

imapextide

glucagon-like peptide 1(15-35) [human GLP-1(15-35)] (1-21 in the real sequence), [G^{22}>E^{8}, A^{25}>V^{11}, K^{26}>R^{12}, K^{34}>R^{20}]-variant, fused to the C-terminal (30-39)-peptide of exendin-4 (*Heloderma suspectum*) (22-31), substituted at the N-atom of the L-α-aspartyl residue 1 with a 17-carboxyheptadecanoyl group;
N-(17-carboxyheptadecanoyl)-L-α-aspartyl-L-valyl-L-seryl-L-seryl-L-tyrosyl-L-leucyl-L-α-glutamyl-L-α-glutamyl-L-glutaminyl-L-alanyl-L-valyl-L-arginyl-L-α-glutamyl-L-phenylalanyl-L-isoleucyl-L-alanyl-L-tryptophyl-L-leucyl-L-valyl-L-arginylglycylglycyl-L-prolyl-L-seryl-L-serylglycyl-L-alanyl-L-prolyl-L-prolyl-L-prolyl-L-serine
glucagon-like peptide-1 (GLP-1) receptor antagonist, treatment of hypoglycemia

imapextide

peptide similaire au glucagon de type 1(15-35) [GLP-1(15-35) humain] (1-21 dans la séquence réelle), variante [G^{22}>E^{8}, A^{25}>V^{11}, K^{26}>R^{12}, K^{34}>R^{20}], fusionné au (30-39)-peptide C-terminal d'exendine-4 (*Heloderma suspectum*) (22-31), substitué en l'atome N du résidu L-α-aspartyle 1 par un groupe 17-carboxyheptadécanoyle;
N-(17-carboxyheptadécanoyl)-L-α-aspartyl-L-valyl-L-séryl-L-séryl-L-tyrosyl-L-leucyl-L-α-glutamyl-L-α-glutamyl-L-glutaminyl-L-alanyl-L-valyl-L-arginyl-L-α-glutamyl-L-phénylalanyl-L-isoleucyl-L-alanyl-L-tryptophyl-L-leucyl-L-valyl-L-arginylglycylglycyl-L-prolyl-L-séryl-L-sérylglycyl-L-alanyl-L-prolyl-L-prolyl-L-prolyl-L-sérine
antagoniste du récepteur du peptide-1 similaire au glucagon (GLP-1), traitement de l'hypoglycémie

imapextida

péptido similar al glucagón tipo 1(15-35) [GLP-1(15-35) humano] (1-21 en la secuencia real), variante [G^{22}>E^{8}, A^{25}>V^{11}, K^{26}>R^{12}, K^{34}>R^{20}], fusionado al (30-39)-péptido C-terminal de exendina-4 (*Heloderma suspectum*) (22-31), sustituido en el átomo de N del residuo L-α-aspartilo con un grupo 17-carboxiheptadecanoilo;
N-(17-carboxiheptadecanoil)-L-α-aspartil-L-valil-L-seril-L-seril-L-tyrosil-L-leucil-L-α-glutamil-L-α-glutamil-L-glutaminil-L-alanil-L-valil-L-arginil-L-α-glutamil-L-fenilalanil-L-isoleucil-L-alanil-L-triptofil-L-leucil-L-valil-L-arginilglicilglicil-L-prolil-L-seril-L-serilglicil-L-alanil-L-prolil-L-prolil-L-prolil-L-serina
antagonista del receptor del péptido 1 similar al glucagón (GLP-1), tratamiento de la hipoglucemia

$C_{166}H_{257}N_{39}O_{50}$ 3004569-93-8

DVSSYLEEQA VREFIAWLVR GGPSSGAPPP S 31

Modified residue / Résidu modifié / Resto modificado

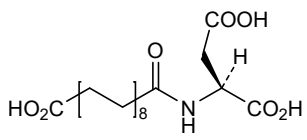

D (1)
N-(HO_2C-[CH_2]$_{16}$-CO)-L-Asp

imofinostatum

imofinostat (2*E*)-3-[1-(benzenesulfonyl)-2,3-dihydro-1*H*-indol-5-yl]-*N*-hydroxyprop-2-enamide
histone deacetylase inhibitor, antineoplastic

imofinostat (2*E*)-3-[1-(benzènesulfonyl)-2,3-dihydro-1*H*-indol-5-yl]-*N*-hydroxyprop-2-énamide
inhibiteur d'histone désacétylase, antinéoplasique

imofinostat (2*E*)-3-[1-(bencenosulfonil)-2,3-dihidro-1*H*-indol-5-il]-*N*-hidroxiprop-2-enamida
inhibidor de la deacetilasa de la histona, antineoplásico

$C_{17}H_{16}N_2O_4S$ 1338320-94-7

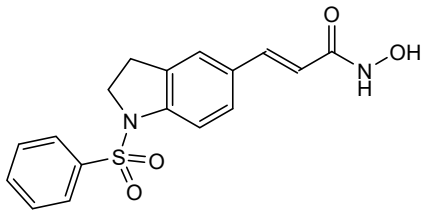

infliximabum beta #

infliximab beta immunoglobulin G1-kappa, anti-[*Homo sapiens* TNF (tumor necrosis factor, TNF superfamily member 2, TNFSF2, TNF-alpha, TNFA)], chimeric monoclonal antibody;
H-gamma1 heavy chain chimeric (1-450) [VH (*Mus musculus* IGHV6-6*02 (89.0%) -(IGHD) -IGHJ2*01 (92.9%), CDR-IMGT [8.10.11] (26-33.51-60.99-109)) (1-120) -*Homo sapiens* IGHG1*01 (100%) G1m17,1 CH1 K120, CH3 D12, L14 (CH1 K120 (217) (121-218), hinge 1-15 (219-233), CH2 (234-343), CH3 D12 (359), L14 (361) (344-448), CHS (449-450)) (121-450)], (223-214')-disulfide with L-kappa light chain chimeric (1'-214') [V-KAPPA (*Mus musculus* IGKV5-48*01 (93.7%) -IGKJ4*01 (83.3%) K123>N (103'), I126>V (106'), CDR-IMGT [6.3.9] (27'-32'.50'-52'.89'-97')) (1'-107') -*Homo sapiens* IGKC*01 (100%) Km3 A45.1, V101 (C-KAPPA A45.1 (153'), V101 (191')) (108'-214')]; dimer (229-229'':232-232'')-bisdisulfide, produced in Chinese hamster ovary (CHO) cells, cell line CHO-S, glycoform alfa
anti-inflammatory

infliximab bêta immunoglobuline G1-kappa, anti-[*Homo sapiens* TNF (facteur de nécrose tumorale, membre 2 de la superfamille du TNF, TNFSF2, TNF-alpha, TNFA)], anticorps monoclonal chimérique;
chaîne lourde H-gamma1 chimérique (1-450) [VH (*Mus musculus* IGHV6-6*02 (89.0%) -(IGHD) -IGHJ2*01 (92.9%), CDR-IMGT [8.10.11] (26-33.51-60.99-109)) (1-120) -*Homo sapiens* IGHG1*01 (100%) G1m17,1 CH1 K120, CH3 D12, L14 (CH1 K120 (217) (121-218), charnière 1-15 (219-233), CH2 (234-343), CH3 D12 (359), L14 (361) (344-448), CHS (449-450)) (121-450)], (223-214')-disulfure avec la chaîne légère L-kappa chimérique (1'-214') [V-KAPPA (*Mus musculus* IGKV5-48*01 (93.7%) -IGKJ4*01 (83.3%) K123>N (103'), I126>V (106'), CDR-IMGT [6.3.9] (27'-32'.50'-52'.89'-97')) (1'-107') -*Homo sapiens* IGKC*01 (100%) Km3 A45.1, V101 (C-KAPPA A45.1 (153'), V101 (191')) (108'-214')]; dimère (229-229'':232-232'')-bisdisulfure, produit dans des cellules ovariennes de hamster chinois (CHO), lignée cellulaire CHO-S, glycoforme alfa
anti-inflammatoire

infliximab beta

inmunoglobulina G1-kappa, anti-[*Homo sapiens* TNF (factor de necrosis tumoral, miembro 2 de la superfamilia del TNF, TNFSF2, TNF-alfa, TNFA)], anticuerpo monoclonal quimérico;
cadena pesada H-gamma1 quimérica (1-450) [VH (*Mus musculus* IGHV6-6*02 (89.0%) -(IGHD) -IGHJ2*01 (92.9%), CDR-IMGT [8.10.11] (26-33.51-60.99-109)) (1-120) -*Homo sapiens* IGHG1*01 (100%) G1m17,1 CH1 K120, CH3 D12, L14 (CH1 K120 (217) (121-218), bisagra 1-15 (219-233), CH2 (234-343), CH3 D12 (359), L14 (361) (344-448), CHS (449-450)) (121-450)], (223-214')-disulfuro con la cadena ligera L-kappa quimérica (1'-214') [V-KAPPA (*Mus musculus* IGKV5-48*01 (93.7%) -IGKJ4*01 (83.3%) K123>N (103'), I126>V (106'), CDR-IMGT [6.3.9] (27'-32'.50'-52'.89'-97')) (1'-107') -*Homo sapiens* IGKC*01 (100%) Km3 A45.1, V101 (C-KAPPA A45.1 (153'), V101 (191')) (108'-214')]; dímero (229-229":232-232")-bisdisulfuro, producido en las células ováricas de hámster chino (CHO), línea celular CHO-S, forma glicosilada alfa
antiinflamatorio

2639475-46-8

Heavy chain / Chaîne lourde / Cadena pesada

```
EVKLEESGGG LVQPGGSMKL SCVASGFIFS NHWMNWVRQS PEKGLEWVAE  50
IRSKSINSAT HYAESVKGRF TISRDDSKSA VYLQMTDLRT EDTGVYYCSR 100
NYYGSTYDYW GQGTTLTVSS ASTKGPSVFP LAPSSKSTSG GTAALGCLVK 150
DYFPEPVTVS WNSGALTSGV HTFPAVLQSS GLYSLSSVVT VPSSSLGTQT CIN 200
YICNVNHKPS NTKVDKKVEP KSCDKTHTCP PCPAPELLGG PSVFLFPPKP 250
KDTLMISRTP EVTCVVVDVS HEDPEVKFNW YVDGVEVHNA KTKPREEQYN 300
STYRVVSVLT VLHQDWLNGK EYKCKVSNKA LPAPIEKTIS KAKGQPREPQ 350
VYTLPPSREE LTKNQVSLTC LVKGFYPSDI AVEWESNGQP ENNYKTTPPV 400
LDSDGSFFLY SKLTVDKSRW QQGNVFSCSV MHEALHNHYT QKSLSLSPGK 450
```

Light chain / Chaîne légère / Cadena ligera

```
DIVMTQSPAI LSVSPGERVS FSCRASQFVG SSIHWYQQRT NGSPRLLIKY  50
ASESMSGIPS RFSGSGSGTD FTLSINTVES EDIADYYCQQ SHSWPFTFGS 100
GTNLEVKRTV AAPSVFIFPP SDRQLKSGTA SVVCLLNNFY PREAKVQWKV 150
DNALQSGNSQ ESVTEQDSKD STYSLSSTLT LSKADYEKHK VYACEVTHQG CIN
LSSPVTKSFN RGEC                                         214
```

Post-translational modifications
Disulfide bridges location / Position des ponts disulfure / Posiciones de los puentes disulfuro
Intra-H (C23-C104) 22-98 147-203 264-324 370-428
22"-98" 147"-203" 264"-324" 370"-428"
Intra-L (C23-C104) 23'-88' 134'-194'
23'"-88'" 134'"-194'"
Inter-H-L (h 5-CL 126) 223-214' 223"-214'"
Inter-H-H (h 11, h 14) 229-229" 232-232"

N-glycosylation sites / Sites de N-glycosylation / Posiciones de N-glicosilación
H CH2 N84.4: 300, 300"
Fucosylated complex bi-antennary CHO-type glycans / glycanes de type CHO bi-antennaires complexes fucosylés / glicanos de tipo CHO biantenarios complejos fucosilados

C-terminal lysine clipping / Coupure de la lysine C-terminale / Recorte de lisina C-terminal
H CHS K2: 450, 450"

inidascaminum

inidascamine

(2*R*,3*S*)-2-amino-3-hydroxy-3-(pyridin-4-yl)-1-(pyrrolidin-1-yl)propan-1-one
schizophrenia

inidascamine

(2*R*,3*S*)-2-amino-3-hydroxy-3-(pyridin-4-yl)-1-(pyrrolidin-1-yl)propan-1-one
schizophrénie

inidascamina (2*R*,3*S*)-2-amino-3-hidroxi-3-(piridin-4-il)-1-(pirrolidin-1-il)propan-1-ona
esquizofrenia

$C_{12}H_{17}N_3O_2$ 903884-71-9

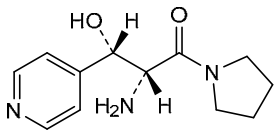

inlecitugum #

inlecitug immunoglobulin G1-kappa, anti-[*Homo sapiens* KDR (kinase insert domain receptor, vascular endothelial growth factor receptor 2, VEGFR2, VEGF-R2, FLK1, CD309)], chimeric monoclonal antibody;
H-gamma1 heavy chain chimeric (1-447) [VH (*Mus musculus* IGHV14-4*02 (91.8%) -(IGHD) -IGHJ4*01 (91.7%) S123>T (112), CDR-IMGT [8.8.10] (26-33.51-58.97-106)) (1-117) -*Homo sapiens* IGHG1*01 (100%) G1m17,1 CH1 K120, CH3 D12, L14 (CH1 K120 (214) (118-215), hinge 1-15 (216-230), CH2 (231-340), CH3 D12 (356), L14 (358) (341-445), CHS (446-447)) (118-447)], (220-213')-disulfide with L-kappa light chain chimeric (1'-213') [V-KAPPA (*Mus musculus* IGKV4-57*01 (98.9%) -IGKJ4*01 (100%), CDR-IMGT [5.3.9] (27'-31'.49'-51'.88'-96')) (1'-106') -*Homo sapiens* IGKC*01 (100%) Km3 A45.1, V101 (C-KAPPA A45.1 (152'), V101 (190')) (107'-213')]; dimer (226-226'':229-229'')-bisdisulfide, produced in Chinese hamster ovary (CHO) cells, cell line CHO-DG44, glycoform alfa
angiogenesis inhibitor, antineoplastic

inlécitug immunoglobuline G1-kappa, anti-[*Homo sapiens* KDR (récepteur à domaine insert kinase, récepteur 2 du facteur de croissance endothélial vasculaire, VEGFR2, VEGF-R2, FLK1, CD309)], anticorps monoclonal chimérique;
chaîne lourde H-gamma1 chimérique (1-447) [VH (*Mus musculus* IGHV14-4*02 (91.8%) -(IGHD) -IGHJ4*01 (91.7%) S123>T (112), CDR-IMGT [8.8.10] (26-33.51-58.97-106)) (1-117) -*Homo sapiens* IGHG1*01 (100%) G1m17,1 CH1 K120, CH3 D12, L14 (CH1 K120 (214) (118-215), charnière 1-15 (216-230), CH2 (231-340), CH3 D12 (356), L14 (358) (341-445), CHS (446-447)) (118-447)], (220-213')-disulfure avec la chaîne légère L-kappa chimérique (1'-213') [V-KAPPA (*Mus musculus* IGKV4-57*01 (98.9%) -IGKJ4*01 (100%), CDR-IMGT [5.3.9] (27'-31'.49'-51'.88'-96')) (1'-106') -*Homo sapiens* IGKC*01 (100%) Km3 A45.1, V101 (C-KAPPA A45.1 (152'), V101 (190')) (107'-213')]; dimère (226-226'':229-229'')-bisdisulfure, produit dans des cellules ovariennes de hamster chinois (CHO), lignée cellulaire CHO-DG44, glycoforme alfa
inhibiteur de l'angiogenèse, antinéoplasique

inlecitug inmunoglobulina G1-kappa, anti-[*Homo sapiens* KDR (receptor de dominio kinasa de inserción, receptor 2 del factor de crecimiento endotelial vascular, VEGFR2, VEGF-R2, FLK1, CD309)], anticuerpo monoclonal quimérico;
cadena pesada H-gamma1 quimérica (1-447) [VH (*Mus musculus* IGHV14-4*02 (91.8%) -(IGHD) -IGHJ4*01 (91.7%) S123>T (112), CDR-IMGT [8.8.10] (26-33.51-58.97-106)) (1-117) -*Homo sapiens* IGHG1*01 (100%) G1m17,1 CH1 K120, CH3 D12, L14 (CH1 K120 (214) (118-215), bisagra 1-15 (216-230), CH2 (231-340), CH3 D12 (356), L14 (358) (341-445), CHS (446-447)) (118-447)], (220-213')-disulfuro con la cadena ligera L-kappa quimérica (1'-213') [V-KAPPA (*Mus musculus* IGKV4-57*01 (98.9%) -IGKJ4*01 (100%), CDR-IMGT [5.3.9] (27'-31'.49'-51'.88'-96')) (1'-106') -*Homo sapiens* IGKC*01 (100%) Km3 A45.1, V101 (C-KAPPA A45.1 (152'), V101 (190')) (107'-213')]; dímero (226-226'':229-229'')-bisdisulfuro, producido en las células ováricas de hámster chino (CHO), línea celular CHO-DG44, forma glicosilada alfa
inhibidor de la angiogénesis, antineoplásico

2997627-68-4

Heavy chain / Chaîne lourde / Cadena pesada

```
QVKLQQSGAE LVGSGASVKL SCTTSGFNIK DYYMHWVKQR PEQGLEWIGW  50
IDPENGDSDY APKFQGKATM TADSSSNTAY LQLSSLTSED TAVYYCKAYY 100
GDYEGYWGQG TTVTVSSAST KGPSVFPLAP SSKSTSGGTA ALGCLVKDYF 150
PEPVTVSWNS GALTSGVHTF PAVLQSSGLY SLSSVVTVPS SSLGTQTYIC 200
NVNHKPSNTK VDKKVEPKSC DKTHTCPPCP APELLGGPSV FLFPPKPKDT 250
LMISRTPEVT CVVVDVSHED PEVKFNWYVD GVEVHNAKTK PREEQYNSTY 300
RVVSVLTVLH QDWLNGKEYK CKVSNKALPA PIEKTISKAK GQPREPQVYT 350
LPPSRDELTK NQVSLTCLVK GFYPSDIAVE WESNGQPENN YKTTPPVLDS 400
DGSFFLYSKL TVDKSRWQQG NVFSCSVMHE ALHNHYTQKS LSLSPGK    447
```

Light chain / Chaîne légère / Cadena ligera

```
DIELTQSPAI MSASPGEKVT ITCSASSSVS YMHWFQQKPG TSPKLWIYST  50
SNLASGVPAR FSGSGSGTSY SLTISRMEAE DAATYYCQQR SSYPFTFGSG 100
TKLEIKRTVA APSVFIFPPS DEQLKSGTAS VVCLLNNFYP REAKVQWKVD 150
NALQSGNSQE SVTEQDSKDS TYSLSSTLTL SKADYEKHKV YACEVTHQGL 200
SSPVTKSFNR GEC                                         213
```

Post-translational modifications

Disulfide bridges location / Position des ponts disulfure / Posiciones de los puentes disulfuro

Intra-H (C23-C104) 22-96 144-200 261-321 367-425
22"-96" 144"-200" 261"-321" 367"-425"
Intra-L (C23-C104) 23'-87' 133'-193'
23'"-87'" 133'"-193'"
Inter-H-L (h 5-CL 126) 220-213' 220"-213'"
Inter-H-H (h 11, h 14) 226-226" 229-229"

N-terminal glutaminyl cyclization / Cyclisation du glutaminyle N-terminal / Ciclación del glutaminilo N-terminal
Q > pyroglutamyl (pE, 5-oxoprolyl) / pyroglutamyle (pE, 5-oxoprolyle) / piroglutamilo (pE, 5-oxoprolilo)
H VH Q1: 1, 1"

N-glycosylation sites / Sites de N-glycosylation / Posiciones de N-glicosilación
H CH2 N84.4:
297, 297"
Fucosylated complex bi-antennary CHO-type glycans / glycanes de type CHO bi-antennaires complexes fucosylés / glicanos de tipo CHO biantenarios complejos fucosilados

C-terminal lysine clipping / Coupure de la lysine C-terminale / Recorte de lisina C-terminal
H CH3 K2: 447, 447"

ipanumeranum #

ipanumeran — messenger RNA (mRNA), 5'[1,2-[m^7G_m-(5'→5')-p-[P(R)]-s^p-p-G]]-capped, encoding codon-optimised human claudin-6 (CLDN6), flanked by 5' and 3' untranslated regions (UTRs), followed by a 3' polyadenylation (polyA) tail. The 5' UTR is derived from the human alpha-globin gene and contains an optimised Kozak sequence; the synthetic 3' UTR is a combination of two elements derived from the amino-terminal enhancer of split (AES) mRNA and the mitochondrial encoded 12S ribosomal RNA. The polyA tail consists of 30 adenosine residues followed by a 10-nucleotide linker sequence and another 70 adenosine residues
immunological agent for active immunization (antineoplastic)

ipanuméran — ARN messager (ARNm), coiffé en 5'[1,2-[m^7G_m-(5'→5')-p-[P(R)]-s^p-p-G]], codant, avec des codons optimisés, la claudine-6 humaine (CLDN6), flanqué des régions non traduites (UTRs) en 5' et en 3' et suivie d'une queue de polyadénylation (polyA) en 3'. La région UTR en 5' est dérivée du gène de l'alpha-globine humaine et contient une séquence Kozak optimisée; la région UTR en 3' synthétique est une combinaison de deux éléments dérivés de l'ARNm de l'amplificateur amino-terminal divisé (AES) et de l'ARN ribosomique 12S codé par les mitochondries. La queue polyA se compose de 30 résidus d'adénosine, suivis d'une séquence de liaison de 10 nucléotides et de 70 autres résidus d'adénosine
agent immunologique pour immunisation active (antinéoplasique)

ipanumerán ARN mensajero (ARNm), protegido con la caperuza 5'[1,2-[m^7G_m-(5'→5')-p-[P(R)]-s^p-p-G]], que codifica, con codones optimizados, claudina-6 (CLDN6) humana, flanqueado por regiones sin traducir (UTRs) 5' y 3' seguido de una cola de poliadenilación (poliA) en 3'. La 5' UTR deriva del gen de la alfa-globina humana y contiene una secuencia Kozak optimizada; la 3' UTR sintética es una combinación de dos elementos derivados del ARNm del potenciador amino-terminal de división (AES) y el ARN ribosómico 12S codificado en la mitocondria. El poliA consta de 30 residuos de adenosina seguidos de una secuencia enlazadora de 10 nucleótidos y otros 70 residuos de adenosina
agente inmunológico para inmunización activa (antineoplásico)

3026599-66-3

irodanoprostum

irodanoprost 7-[(2*R*)-2-{(1*E*,3*R*)-4,4-difluoro-3-[({4-[(4-hydroxy-4,4-diphosphonobutyl)carbamoyl]phenyl}acetyl)oxy]-4-phenylbut-1-en-1-yl}-5-oxopyrrolidin-1-yl]heptanoic acid
prostaglandin receptor agonist, osteogenesis-related diseases

irodanoprost acide 7-[(2*R*)-2-{(1*E*,3*R*)-4,4-difluoro-3-[({4-[(4-hydroxy-4,4-diphosphonobutyl)carbamoyl]phényl}acétyl)oxy]-4-phénylbut-1-én-1-yl}-5-oxopyrrolidin-1-yl]heptanoïque
agoniste des récepteurs des prostaglandines, maladies liées à l'ostéogenèse

irodanoprost ácido 7-[(2*R*)-2-{(1*E*,3*R*)-3-[({4-[(4,4-difosfono-4-hidroxibutil)carbamoil]fenil}acetil)oxi]-4-fenil-4,4-difluorobut-1-en-1-il}-5-oxopirrolidin-1-il]heptanoico
agonista del receptor de prostaglandinas, enfermedades relacionadas con la osteogénesis

$C_{34}H_{44}F_2N_2O_{13}P_2$ 2055490-48-5

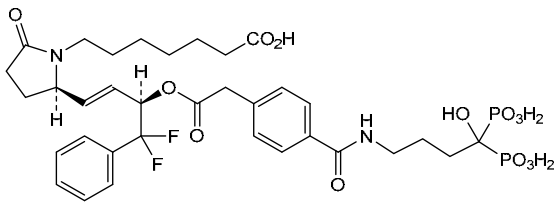

isuventatugum #

isuventatug immunoglobulin G1-kappa, anti-[*Homo sapiens* MICA (MIC-A, MH1-like A) and *Homo sapiens* MICB (MIC-B, MH1-like B)], monoclonal antibody; H-gamma1 heavy chain (1-450) [VH (*Homo sapiens* IGHV3-11*01 (93.8%) -(IGHD) -IGHJ4*01 (100%), CDR-IMGT [8.8.14] (26-33.51-58.97-110)) (1-121) -*Homo sapiens* IGHG1*03v (100%) G1m3>G1m17, nG1m1 CH1 K120, CH3 E12, M14 (CH1 R120>K (218) (122-219), hinge 1-15 (220-234), CH2 (235-344), CH3 E12 (360), M14 (362) (345-449), CHS K2>del (450)) (122-450)], (224-219')-disulfide with L-kappa light chain (1'-219') [V-KAPPA Musmus/Homsap (*Mus musculus* IGKV2-137*01 (90.0%) -IGKJ4*01 (91.7%) S120>P (105')/*Homo sapiens* IGKV2-28*01 (86.0%) -IGKJ2*02 (90.9%) Q120>P (105'), CDR-IMGT [11.3.9] (27'-37'.55'-57'.94-102')) (1'-112') -*Homo sapiens* IGKC*01 (100%) Km3 A45.1, V101 (C-KAPPA A45.1 (158'), V101 (196')) (113'-219')]; dimer (230-230'':233-233'')-bisdisulfide, produced in Chinese hamster ovary (CHO) cells, cell line CHO-DG44, glycoform alfa
antineoplastic

isuventatug

immunoglobuline G1-kappa, anti-[*Homo sapiens* MICA (MIC-A, MH1-like A) et *Homo sapiens* MICB (MIC-B, MH1-like B)], anticorps monoclonal; chaîne lourde H-gamma1 (1-450) [VH (*Homo sapiens* IGHV3-11*01 (93.8%) -(IGHD) -IGHJ4*01 (100%), CDR-IMGT [8.8.14] (26-33.51-58.97-110)) (1-121) -*Homo sapiens* IGHG1*03v (100%) G1m3>G1m17, nG1m1 CH1 K120, CH3 E12, M14 (CH1 R120>K (218) (122-219), charnière 1-15 (220-234), CH2 (235-344), CH3 E12 (360), M14 (362) (345-449), CHS K2>del (450)) (122-450)], (224-219')-disulfure avec la chaîne légère L-kappa (1'-219') [V-KAPPA Musmus/Homsap (*Mus musculus* IGKV2-137*01 (90.0%) -IGKJ4*01 (91.7%) S120>P (105')/*Homo sapiens* IGKV2-28*01 (86.0%) -IGKJ2*02 (90.9%) Q120>P (105'), CDR-IMGT [11.3.9] (27'-37'.55'-57'.94-102')) (1'-112') -*Homo sapiens* IGKC*01 (100%) Km3 A45.1, V101 (C-KAPPA A45.1 (158'), V101 (196')) (113'-219')]; dimère (230-230'':233-233'')-bisdisulfure, produit dans des cellules ovariennes de hamster chinois (CHO), lignée cellulaire CHO-DG44, glycoforme alfa

antinéoplasique

isuventatug

inmunoglobulina G1-kappa, anti-[*Homo sapiens* MICA (MIC-A, MH1-like A) y *Homo sapiens* MICB (MIC-B, MH1-like B)], anticuerpo monoclonal; cadena pesada H-gamma1 (1-450) [VH (*Homo sapiens* IGHV3-11*01 (93.8%) -(IGHD) -IGHJ4*01 (100%), CDR-IMGT [8.8.14] (26-33.51-58.97-110)) (1-121) -*Homo sapiens* IGHG1*03v (100%) G1m3>G1m17, nG1m1 CH1 K120, CH3 E12, M14 (CH1 R120>K (218) (122-219), bisagra 1-15 (220-234), CH2 (235-344), CH3 E12 (360), M14 (362) (345-449), CHS K2>del (450)) (122-450)], (224-219')-disulfuro con la cadena ligera L-kappa (1'-219') [V-KAPPA Musmus/Homsap (*Mus musculus* IGKV2-137*01 (90.0%) -IGKJ4*01 (91.7%) S120>P (105')/*Homo sapiens* IGKV2-28*01 (86.0%) -IGKJ2*02 (90.9%) Q120>P (105'), CDR-IMGT [11.3.9] (27'-37'.55'-57'.94-102')) (1'-112') -*Homo sapiens* IGKC*01 (100%) Km3 A45.1, V101 (C-KAPPA A45.1 (158'), V101 (196')) (113'-219')]; dímero (230-230'':233-233'')-bisdisulfuro, producido en las células ováricas de hámster chino (CHO), línea celular CHO-DG44, forma glicosilada alfa

antineoplásico

2986317-23-9

Heavy chain / Chaîne lourde / Cadena pesada

```
QVQLVESGGG LVKPGGSLRL SCAASGFTFS NYAMSWIRQA PGKGLEWVSY  50
ISPGGDYIYY ADSVKGRFTI SRDNAKNSLY LQMNSLRAED TAVYYCTTDR 100
RHYGSYAMDY WGQGTLVTVS SASTKGPSVF PLAPSSKSTS GGTAALGCLV 150
KDYFPEPVTV SWNSGALTSG VHTFPAVLQS SGLYSLSSVV TVPSSSLGTQ 200
TYICNVNHKP SNTKVDKKVE PKSCDKTHTC PPCPAPELLG GPSVFLFPPK 250
PKDTLMISRT PEVTCVVVDV SHEDPEVKFN WYVDGVEVHN AKTKPREEQY 300
NSTYRVVSVL TVLHQDWLNG KEYKCKVSNK ALPAPIEKTI SKAKGQPREP 350
QVYTLPPSRE EMTKNQVSLT CLVKGFYPSD IAVEWESNGQ PENNYKTTPP 400
VLDSDGSFFL YSKLTVDKSR WQQGNVFSCS VMHEALHNHY TQKSLSLSPG 450
```

Light chain / Chaîne légère / Cadena ligera

```
DIVMTQSPLS LPVTPGEPAS ISCRSSKSLL HSNLNTYLYW FLQKPGQSPQ  50
ILIYRMSNLA SGVPDRFSGS GSGTAFTLKI SRVEAEDVGV YYCMQHLEYP 100
FTFGPGTKLE IKRTVAAPSV FIFPPSDEQL KSGTASVVCL LNNFYPREAK 150
VQWKVDNALQ SGNSQESVTE QDSKDSTYSL SSTLTLSKAD YEKHKVYACE 200
VTHQGLSSPV TKSFNRGEC                                   219
```

Post-translational modifications

Disulfide bridges location / Position des ponts disulfure / Posiciones de los puentes disulfuro

Intra-H (C23-C104) 22-96 148-204 265-325 371-429
22"-96" 148"-204" 265"-325" 371"-429"
Intra-L (C23-C104) 23'-93' 139'-199'
23'"-93'" 139'"-199'"
Inter-H-L (h 5-CL 126) 224-219' 224"-219'"
Inter-H-H (h 11, h 14) 230-230" 233-233"

N-terminal glutaminyl cyclization / Cyclisation du glutaminyle N-terminal / Ciclación del glutaminilo N-terminal
Q > pyroglutamyl (pE, 5-oxoprolyl) / pyroglutamyle (pE, 5-oxoprolyle) / piroglutamilo (pE, 5-oxoprolilo)
H VH Q1: 1, 1"

N-glycosylation sites / Sites de N-glycosylation / Posiciones de N-glicosilación
H CH2 N84.4: 301, 301"
Fucosylated complex bi-antennary CHO-type glycans / glycanes de type CHO bi-antennaires complexes fucosylés / glicanos de tipo CHO biantenarios complejos fucosilados

itareparibum

itareparib — 2-(1-cyclohexylpiperidin-4-yl)-6-fluoro-3-oxo-2,3-dihydro-1*H*-isoindole-4-carboxamide
poly (ADP-ribose) polymerase (PARP) inhibitor, antineoplastic

itaréparib — 2-(1-cyclohexylpipéridin-4-yl)-6-fluoro-3-oxo-2,3-dihydro-1*H*-isoindole-4-carboxamide
inhibiteur de la poly-ADP-ribose polymérase, antinéoplasique

itareparib — 2-(1-ciclohexilpiperidin-4-il)-6-fluoro-3-oxo-2,3-dihidro-1*H*-isoindol-4-carboxamida
inhibidor de poli-ADP-ribosa polimerasa, antineoplásico

$C_{20}H_{26}FN_3O_2$ 1606995-47-4

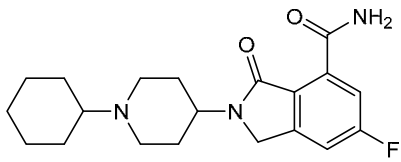

ixotatugum #

ixotatug — immunoglobulin G1-kappa, anti-[*Homo sapiens* CLDN6 (claudin 6, claudin-6)], monoclonal antibody;
H-gamma1 heavy chain (1-447) [VH Musmus/Homsap (*Mus musculus* IGHV6-3*01 (88.8%) -(IGHD) -IGHJ2*01 (90.9%) T123>L (112)/*Homo sapiens* IGHV3-23*03 (82.7%) -(IGHD) -IGHJ5*01 (91.7%) V124>L (113), CDR-IMGT [8.10.8] (26-33.51-60.99-106)) (1-117) -*Homo sapiens* IGHG1*01 (100%) G1m17,1 CH1 K120, CH3 D12, L14 (CH1 K120 (214) (118-215), hinge 1-15 (216-230), CH2 (231-340), CH3 D12 (356), L14 (358) (341-445), CHS (446-447)) (118-447)], (220-214')-disulfide with L-kappa light chain (1'-214') [V-KAPPA Musmus/Homsap (*Mus musculus* IGKV12-44*01 (83.2%) -IGKJ1*01 (91.7%) G120>Q (100')/*Homo sapiens* IGKV1-39*01 (83.2%) -IGKJ2*02 (100%), CDR-IMGT [6.3.9] (27'-32'.50'-52'.89'-97')) (1'-107') -*Homo sapiens* IGKC*01 (100%) Km3 A45.1, V101 (C-KAPPA A45.1 (153'), V101 (191')) (108'-214')]; dimer (226-226'':229-229'')-bisdisulfide, produced in a cell line from Chinese hamster ovary (CHO) cells, derived from the cell line CHO-S, glycoform alfa
antineoplastic

ixotatug — immunoglobuline G1-kappa, anti-[*Homo sapiens* CLDN6 (claudine 6, claudine-6)], anticorps monoclonal;
chaîne lourde H-gamma1 (1-447) [VH Musmus/Homsap (*Mus musculus* IGHV6-3*01 (88.8%) -(IGHD) -IGHJ2*01 (90.9%) T123>L (112)/*Homo sapiens* IGHV3-23*03 (82.7%) -(IGHD) -IGHJ5*01 (91.7%) V124>L (113), CDR-IMGT [8.10.8] (26-33.51-60.99-106)) (1-117) -*Homo sapiens* IGHG1*01 (100%) G1m17,1 CH1 K120, CH3 D12, L14 (CH1 K120 (214) (118-215), charnière 1-15 (216-230), CH2 (231-340), CH3 D12 (356), L14 (358) (341-445), CHS (446-447)) (118-447)], (220-214')-disulfure avec la chaîne légère L-kappa (1'-218') [V-KAPPA Musmus/Homsap (*Mus musculus* IGKV12-44*01 (83.2%) -IGKJ1*01 (91.7%) G120>Q (100')/*Homo sapiens* IGKV1-39*01 (83.2%) -IGKJ2*02 (100%), CDR-IMGT [6.3.9] (27'-32'.50'-52'.89'-97')) (1'-107') -*Homo sapiens* IGKC*01 (100%) Km3 A45.1, V101 (C-KAPPA A45.1 (153'), V101 (191')) (108'-214')]; dimère (226-226'':229-229'')-bisdisulfure, produit dans une lignée cellulaire des cellules ovariennes de hamster chinois (CHO), dérivant de la lignée cellulaire CHO-S, glycoforme alfa
antinéoplasique

ixotatug

inmunoglobulina G1-kappa, anti-[*Homo sapiens* CLDN6 (claudina 6, claudina-6)], anticuerpo monoclonal;
cadena pesada H-gamma1 (1-447) [VH Musmus/Homsap (*Mus musculus* IGHV6-3*01 (88.8%) -(IGHD) -IGHJ2*01 (90.9%) T123>L (112)/*Homo sapiens* IGHV3-23*03 (82.7%) -(IGHD) -IGHJ5*01 (91.7%) V124>L (113), CDR-IMGT [8.10.8] (26-33.51-60.99-106)) (1-117) -*Homo sapiens* IGHG1*01 (100%) G1m17,1 CH1 K120, CH3 D12, L14 (CH1 K120 (214) (118-215), bisagra 1-15 (216-230), CH2 (231-340), CH3 D12 (356), L14 (358) (341-445), CHS (446-447)) (118-447)], (220-214')-disulfuro con la cadena ligera L-kappa (1'-218') [V-KAPPA Musmus/Homsap (*Mus musculus* IGKV12-44*01 (83.2%) -IGKJ1*01 (91.7%) G120>Q (100')/*Homo sapiens* IGKV1-39*01 (83.2%) -IGKJ2*02 (100%), CDR-IMGT [6.3.9] (27'-32'.50'-52'.89'-97')) (1'-107') -*Homo sapiens* IGKC*01 (100%) Km3 A45.1, V101 (C-KAPPA A45.1 (153'), V101 (191')) (108'-214')]; dímero (226-226":229-229")-bisdisulfuro, producido en una línea celular de las células ováricas de hámster chino (CHO), línea celular derivada de CHO-S, forma glicosilada alfa
antineoplásico

3018936-99-4

Heavy chain / Chaîne lourde / Cadena pesada

```
EVQLQESGPG LVQPSQSMSL SCAVSGFTFS NYWMSWVRQA PGKGLEWVAQ  50
IRLKSDNYAT HYAESVKGRF TISRDDSKSI VYLQMNSLRA EDTGVYYCTG 100
GFLYAMDYWG QGTLVTVSAA STKGPSVFPL APSSKSTSGG TAALGCLVKD 150
YFPEPVTVSW NSGALTSGVH TFPAVLQSSG LYSLSSVVTV PSSSLGTQTY 200
VNHKPSNTKV DKRVEPKSCD KTHTCPPCPA PELLGGPSVF LFPPKPKDT 250
LMISRTPEVT CVVVDVSHED PEVKFNWYVD GVEVHNAKTK PREEQYNSTY 300
RVVSVLTVLH QDWLNGKEYK CKVSNKALPA PIEKTISKAK GQPREPQVYT 360
LPPSRDELTK NQVSLTCLVK GFYPSDIAVE WESNGQPENN YKTTPPVLDS 400
DGSFFLYSKL TVDKSRWQQG NVFSCSVMHE ALHNHYTQKS LSLSPGK    447
```

Light chain / Chaîne légère / Cadena ligera

```
DIQMTQSPSS LSASVGDRVT ITCRTSENIY SYLAWYQQKP GKAPKLLVYN  50
AKTLAEGVPS RFSGSGSGTD FTLTISSLQP EDFATYYCQH HYGTPFTFGQ 100
GTKLEIKRTV AAPSVFIFPP SDEQLKSGTA SVVCLLNNFY PREAKVQWKV 150
DNALQSGNSQ ESVTEQDSKD STYSLSSTLT LSKADYEKHK VYACEVTHQG 200
LSSPVTKSFN RGEC                                        214
```

Post-translational modifications
Disulfide bridges location / Position des ponts disulfure / Posiciones de los puentes disulfuro
Intra-H (C23-C 104) 22-98 144-200 261-321 367-425
22"-98" 144"-200" 261"-321" 367"-425"
Intra-L (C23-C 104) 23'-88' 134'-194'
23'"-88'" 134'"-194'"
Inter-H-L (h 5-CL 126) 220-214' 220"-214'"
Inter-H-H (h 11, h 14) 226-226" 229-229"

N-glycosylation sites / Sites de N-glycosylation / Posiciones de N-glicosilación
H CH2 N84.4: 297, 297"
Fucosylated complex bi-antennary CHO-type glycans / glycanes de type CHO bi-antennaires complexes fucosylés / glicanos de tipo CHO biantenarios complejos fucosilados

C-terminal lysine clipping / Coupure de la lysine C-terminale / Recorte de lisina C-terminal
H CHS K2: 447, 447"

ixotatugum vedotinum #
ixotatug vedotin

immunoglobulin G1-kappa, anti-[*Homo sapiens* CLDN6 (claudin 6, claudin-6)], monoclonal antibody, conjugated on an average of four cysteinyl residues to *vedotin*, comprising a cleavable linker and monomethylauristatin E (MMAE);

	H-gamma1 heavy chain (1-447) [VH Musmus/Homsap (*Mus musculus* IGHV6-3*01 (88.8%) -(IGHD) -IGHJ2*01 (90.9%) T123>L (112)/*Homo sapiens* IGHV3-23*03 (82.7%) -(IGHD) -IGHJ5*01 (91.7%) V124>L (113), CDR-IMGT [8.10.8] (26-33.51-60.99-106)) (1-117) -*Homo sapiens* IGHG1*01 (100%) G1m17,1 CH1 K120, CH3 D12, L14 (CH1 K120 (214) (118-215), hinge 1-15 (216-230), CH2 (231-340), CH3 D12 (356), L14 (358) (341-445), CHS (446-447)) (118-447)], (220-214')-disulfide with L-kappa light chain (1'-214') [V-KAPPA Musmus/Homsap (*Mus musculus* IGKV12-44*01 (83.2%) -IGKJ1*01 (91.7%) G120>Q (100')/*Homo sapiens* IGKV1-39*01 (83.2%) -IGKJ2*02 (100%), CDR-IMGT [6.3.9] (27'-32'.50'-52'.89'-97')) (1'-107') -*Homo sapiens* IGKC*01 (100%) Km3 A45.1, V101 (C-KAPPA A45.1 (153'), V101 (191')) (108'-214')]; dimer (226-226'':229-229'')-bisdisulfide, produced in a cell line from Chinese hamster ovary (CHO) cells, derived from the cell line CHO-S, glycoform alfa; substituted at the sulfur atoms of an average of four L-cysteinyl residues among 220, 226, 229, 214', 220'', 226'', 229'' and 214''' with (3*RS*)-1-(6-{[(2*S*)-1-{[(2*S*)-5-(carbamoylamino)-1-{4-[({[(2*S*)-1-{[(2*S*)-1-{[(3*R*,4*S*,5*S*)-1-{(2*S*)-2-[(1*R*,2*R*)-3-{[(1*S*,2*R*)-1-hydroxy-1-phenylpropan-2-yl]amino}-1-methoxy-2-methyl-3-oxopropyl]pyrrolidin-1-yl}-3-methoxy-5-methyl-1-oxoheptan-4-yl](methyl)amino}-3-methyl-1-oxobutan-2-yl]amino}-3-methyl-1-oxobutan-2-yl](methyl)carbamoyl}oxy)methyl]anilino}-1-oxopentan-2-yl]amino}-3-methyl-1-oxobutan-32-yl]amino}-6-oxohexyl)-2,5-dioxopyrrolidin-3-yl (*vedotin*) groups *antineoplastic*
ixotatug védotine	immunoglobuline G1-kappa, anti-[*Homo sapiens* CLDN6 (claudine 6, claudine-6)], anticorps monoclonal, conjugué par quatre résidus cystéinyle en moyenne à la *védotine*, comprenant un linker clivable et monométhylauristatine E (MMAE); chaîne lourde H-gamma1 (1-447) [VH Musmus/Homsap (*Mus musculus* IGHV6-3*01 (88.8%) -(IGHD) -IGHJ2*01 (90.9%) T123>L (112)/*Homo sapiens* IGHV3-23*03 (82.7%) -(IGHD) -IGHJ5*01 (91.7%) V124>L (113), CDR-IMGT [8.10.8] (26-33.51-60.99-106)) (1-117) -*Homo sapiens* IGHG1*01 (100%) G1m17,1 CH1 K120, CH3 D12, L14 (CH1 K120 (214) (118-215), charnière 1-15 (216-230), CH2 (231-340), CH3 D12 (356), L14 (358) (341-445), CHS (446-447)) (118-447)], (220-214')-disulfure avec la chaîne légère L-kappa (1'-218') [V-KAPPA Musmus/Homsap (*Mus musculus* IGKV12-44*01 (83.2%) -IGKJ1*01 (91.7%) G120>Q (100')/*Homo sapiens* IGKV1-39*01 (83.2%) -IGKJ2*02 (100%), CDR-IMGT [6.3.9] (27'-32'.50'-52'.89'-97')) (1'-107') -*Homo sapiens* IGKC*01 (100%) Km3 A45.1, V101 (C-KAPPA A45.1 (153'), V101 (191')) (108'-214')]; dimère (226-226'':229-229'')-bisdisulfure, produit dans une lignée cellulaire des cellules ovariennes de hamster chinois (CHO), dérivant de la lignée cellulaire CHO-S, glycoforme alfa;

	substitué sur l'atome de soufre de quatre résidus L-cystéinyle en moyenne parmi 220, 226, 229, 214', 220'', 226'', 229'' et 214''' avec des groupes (3*RS*)-1-(6-{[(2*S*)-1-{[(2*S*)-5-(carbamoylamino)-1-{4-[({[(2*S*)-1-{[(2*S*)-1-{[(3*R*,4*S*,5*S*)-1-{(2*S*)-2-[(1*R*,2*R*)-3-{[(1*S*,2*R*)-1-hydroxy-1-phénylpropan-2-yl]amino}-1-méthoxy-2-méthyl-3-oxopropyl]pyrrolidin-1-yl}-3-méthoxy-5-méthyl-1-oxoheptan-4-yl](méthyl)amino}-3-méthyl-1-oxobutan-2-yl]amino}-3-méthyl-1-oxobutan-2-yl](méthyl)carbamoyl}oxy)méthyl]anilino}-1-oxopentan-2-yl]amino}-3-méthyl-1-oxobutan-32-yl]amino}-6-oxohexyl)-2,5-dioxopyrrolidin-3-yle (*védotine*) *antinéoplasique*
ixotatug vedotina	inmunoglobulina G1-kappa, anti-[*Homo sapiens* CLDN6 (claudina 6, claudina-6)], anticuerpo monoclonal, conjugado en una media de cuatro residuos cisteinilo a la *vedotina*, que comprende un enlace escindible y monometilauristatina E (MMAE); cadena pesada H-gamma1 (1-447) [VH Musmus/Homsap (*Mus musculus* IGHV6-3*01 (88.8%) -(IGHD) -IGHJ2*01 (90.9%) T123>L (112)/*Homo sapiens* IGHV3-23*03 (82.7%) -(IGHD) -IGHJ5*01 (91.7%) V124>L (113), CDR-IMGT [8.10.8] (26-33.51-60.99-106)) (1-117) -*Homo sapiens* IGHG1*01 (100%) G1m17,1 CH1 K120, CH3 D12, L14 (CH1 K120 (214) (118-215), bisagra 1-15 (216-230), CH2 (231-340), CH3 D12 (356), L14 (358) (341-445), CHS (446-447)) (118-447)], (220-214')-disulfuro con la cadena ligera L-kappa (1'-218') [V-KAPPA Musmus/Homsap (*Mus musculus* IGKV12-44*01 (83.2%) -IGKJ1*01 (91.7%) G120>Q (100')/*Homo sapiens* IGKV1-39*01 (83.2%) -IGKJ2*02 (100%), CDR-IMGT [6.3.9] (27'-32'.50'-52'.89'-97')) (1'-107') -*Homo sapiens* IGKC*01 (100%) Km3 A45.1, V101 (C-KAPPA A45.1 (153'), V101 (191')) (108'-214')]; dímero (226-226'':229-229'')-bisdisulfuro, producido en una línea celular de las células ováricas de hámster chino (CHO), línea celular derivada de CHO-S, forma glicosilada alfa; sustituido en el átomo de azufre de cuatro residuos L-cisteinilo en promedio entre 220, 226, 229, 214', 220'', 226'', 229'' y 214''' con grupos (3*RS*)-1-(6-{[(2*S*)-1-{[(2*S*)-5-(carbamoilamino)-1-{4-[({[(2*S*)-1-{[(2*S*)-1-{[(3*R*,4*S*,5*S*)-1-{(2*S*)-2-[(1*R*,2*R*)-3-{[(1*S*,2*R*)-1-fenil-1-hidroxipropan-2-il]amino}-2-metil-1-metoxi-3-oxopropil]pirrolidin-1-il}-5-metil-3-metoxi-1-oxoheptan-4-il](metil)amino}-3-metil-1-oxobutan-2-il]amino}-3-metil-1-oxobutan-2-il](metil)carbamoil}oxi)metil]anilino}-1-oxopentan-2-il]amino}-3-metil-1-oxobutan-32-il]amino}-6-oxohexil)-2,5-dioxopirrolidin-3-ilo (*vedotina*) *antineoplásico*

3018937-00-0

Heavy chain / Chaîne lourde / Cadena pesada (H, H'')

```
EVQLVESGGG LVQPGGSMRL SCAASGFTFS NYWMSWVRQA PGKGLEWVAQ   50
IRLKSDNYAT HYAESVKGRF TISRDDSKSS VYLQMNSLRA EDTGVYYCTD  100
GPFSGSWGQG TLVTVSSAST KGPSVFPLAP SSKSTSGGTA ALGCLVKDYF  150
PEPVTVSWNS GALTSGVHTF PAVLQSSGLY SLSSVVTVPS SSLGTQTYIC  200
NVNHKPSNTK VDKKVEPKSC DKTHTCPPCP APELLGGPSV FLFPPKPKDT  250
LMISRTPEVT CVVVDVSHED PEVKFNWYVD GVEVHNAKTK PREEQYNSTY  300
RVVSVLTVLH QDWLNGKEYK CKVSNKALPA PIEKTISKAK GQPREPQVYT  350
LPPSREELTK NQVSLTCLVK GFYPSDIAVE WESNGQPENN YKTTPPVLDS  400
DGSFFLYSKL TVDKSRWQQG NVFSCSVMHE ALHNHYTQKS LSLSPGK     447
```

Light chain / Chaîne légère / Cadena ligera (L', L''')

```
DIQMTQSPSS LSASVGDRVT ITCRASENIY SYLAWYQQKP GKAPKLLIYN   50
AKTLAEGVPS RFSGSGSGTD FTLTISSLQP EDFATYYCQH HYTTPWTFGQ  100
GTKLEIKRTV AAPSVFIFPP SDEQLKSGTA SVVCLLNNFY PREAKVQWKV  150
DNALQSGNSQ ESVTEQDSKD STYSLSSTLT LSKADYEKHK VYACEVTHQG  200
LSSPVTKSFN RGEC                                         214
```

Post-translational modifications

Disulfide bridges location / Position des ponts disulfure / Posiciones de los puentes disulfuro

Intra-H (C23-C104) 22-98 144-200 261-321 367-425
22''-98'' 144''-200'' 261''-321'' 367''-425''

Intra-L (C23-C104) 23'-88' 134'-194'
23'''-88''' 134'''-194'''

Inter-H-L (h 5-CL 126)* 220-214' 220''-214'''

Inter-H-H (h 11, h 14)* 226-226'' 229-229''

*Two or three of the four inter-chain disulfide bridges are not present, an average of 4 cysteinyl being conjugated each via a thioether bond to a drug linker.

*Deux ou trois des quatre ponts disulfures inter-chaines ne sont pas présents, 4 cystéinyl en moyenne étant chacun conjugué via une liaison thioéther à un linker-principe actif.

*Dos o tres de los cuatro puentes disulfuro inter-catenarios no están presentes, una media de 4 cisteinil está conjugada a conectores de principio activo.

N-glycosylation sites / Sites de N-glycosylation / Posiciones de N-glicosilación

H CH2 N84.4: 297, 297''

Fucosylated complex bi-antennary CHO-type glycans / glycanes de type CHO bi-antennaires complexes fucosylés / glicanos de tipo CHO biantenarios complejos fucosilados

C-terminal lysine clipping / Coupure de la lysine C-terminale / Recorte de lisina C-terminal

H CH3 K2: 447, 447''

Potential modified residues / résidus modifiés potentiels / restos modificados potenciales*

C (220, 226, 229, 214', 220'', 226'', 229'', 214''')

*(*vedotin*:mAb ~ 4:1)

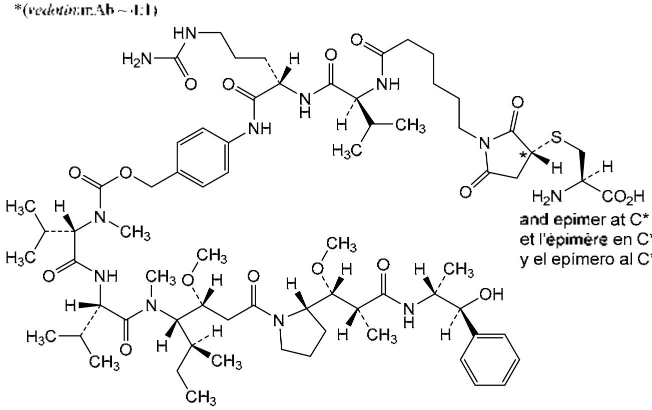

and epimer at C*
et l'épimère en C*
y el epímero al C*

lanisidenibum
lanisidenib

(3*S*)-*N*-{(1*S*)-1-(2-chlorophenyl)-2-[(3,3-difluorocyclobutyl)amino]-2-oxoethyl}-2-(4-cyanopyridin-2-yl)-*N*-(3-fluorophenyl)-1,1-dioxo-1λ[6],2-thiazolidine-3-carboxamide

isocitrate dehydrogenase inhibitor, antineoplastic

lanisidénib

(3*S*)-*N*-{(1*S*)-1-(2-chlorophenyl)-2-[(3,3-difluorocyclobutyl)amino]-2-oxoethyl}-2-(4-cyanopyridin-2-yl)-*N*-(3-fluorophenyl)-1,1-dioxo-1λ^6,2-thiazolidine-3-carboxamide
inhibiteur de l'isocitrate déshydrogénase, antinéoplasique

lanisidenib

(3*S*)-*N*-{(1*S*)-1-(2-chlorophenyl)-2-[(3,3-difluorocyclobutyl)amino]-2-oxoethyl}-2-(4-cyanopyridin-2-yl)-*N*-(3-fluorophenyl)-1,1-dioxo-1λ^6,2-thiazolidine-3-carboxamide
inhibidor de la isocitrato deshidrogenasa, antineoplásico

$C_{28}H_{23}ClF_3N_5O_4S$ 2135537-20-9

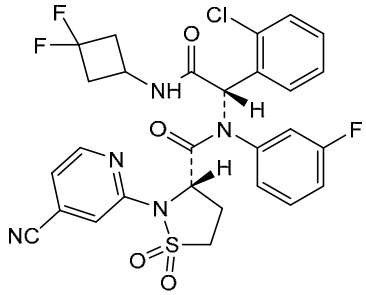

lanoracopanum

lanoracopan

4-{(2*S*,4*S*)-4-(cyclopropylmethoxy)-1-[(5-methoxy-7-methyl-1*H*-indol-4-yl)methyl]piperidin-2-yl}benzoic acid
complement factor B inhibitor

lanoracopan

acide 4-{(2*S*,4*S*)-4-(cyclopropylméthoxy)-1-[(5-méthoxy-7-méthyl-1*H*-indol-4-yl)méthyl]pipéridin-2-yl}benzoïque
inhibiteur du facteur B du complément

lanoracopán

ácido 4-{(2*S*,4*S*)-4-(ciclopropilmetoxi)-1-[(7-metil-5-metoxi-1*H*-indol-4-il)metil]piperidin-2-il}benzoico
inhibidor del factor B del complemento

$C_{27}H_{32}N_2O_4$ 2797066-85-2

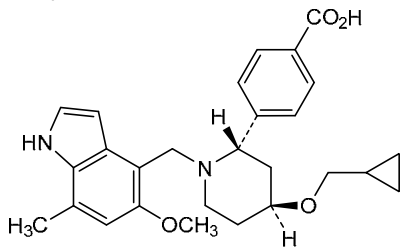

laporolimusum

laporolimus

(1*R*,2*R*,4*S*)-4-{(2*R*)-2-[(3*S*,6*R*,7*E*,9*R*,10*R*,12*R*,14*S*,15*E*,17*E*,19*E*,21*S*,23*S*,26*R*,27*R*,34a*S*)-9,27-dihydroxy-10,21-dimethoxy-6,8,12,14,20,26-hexamethyl-1,5,11,28,29-pentaoxo-1,4,5,6,9,10,11,12,13,14,21,22,23,24,25,26,27,28,29,31,32,33,34,34a-tetracosahydro-3*H*-23,27-epoxypyrido[2,1-*c*][1,4]oxazacyclohentriacontin-3-yl]propyl}-2-methoxycyclohexyl cyclohexanecarboxylate
immunosuppressant

laporolimus

cyclohexanecarboxylate de (1*R*,2*R*,4*S*)-4-{(2*R*)-2-[(3*S*,6*R*,7*E*,9*R*,10*R*,12*R*,14*S*,15*E*,17*E*,19*E*,21*S*,23*S*,26*R*,27*R*,34a*S*)-9,27-dihydroxy-10,21-diméthoxy-6,8,12,14,20,26-hexaméthyl-1,5,11,28,29-pentaoxo-1,4,5,6,9,10,11,12,13,14,21,22,23,24,25,26,27,28,29,31,32,33,34,34a-tétracosahydro-3*H*-23,27-époxypyrido[2,1-*c*][1,4]oxaazacyclohentriacontin-3-yl]propyl}-2-méthoxycyclohexyle
immunosuppresseur

laporólimus

ciclohexanocarboxilato de (1*R*,2*R*,4*S*)-4-{(2*R*)-2-[(3*S*,6*R*,7*E*,9*R*,10*R*,12*R*,14*S*,15*E*,17*E*,19*E*,21*S*,23*S*,26*R*,27*R*,34a*S*)-9,27-dihidroxi-6,8,12,14,20,26-hexametil-10,21-dimetoxi-1,5,11,28,29-pentaoxo-1,4,5,6,9,10,11,12,13,14,21,22,23,24,25,26,27,28,29,31,32,33,34,34a-tetracosahidro-3*H*-23,27-epoxipirido[2,1-*c*][1,4]oxaazaciclohentriacontin-3-il]propil}-2-metoxiciclohexilo
inmunosupresor

$C_{58}H_{89}NO_{14}$ 1504576-27-5

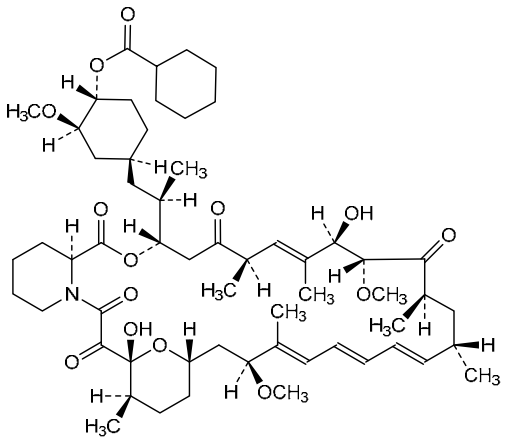

laromestrocelum

laromestrocel	allogeneic mesenchymal stromal cells (MSC) derived from bone marrow of healthy human donors. The cells are expanded in media containing fetal bovine serum. The cells are positive (≥95%) for the mesenchymal stromal cell surface markers CD73, CD90, CD105, and are negative (≤5%) for CD34 and negative (≤2%) for markers CD11b, CD19, CD45, and HLA class II histocompatibility antigen gamma chain (HLA-DR). The cells secrete immunomodulatory factors including the interleukin 1 receptor antagonist (IL-1RA), interleukin 4 (IL-4), IL-7, IL-8, IL- 10, IL-13, and granulocyte colony stimulating factor (G-CSF) upon stimulation. In absence of exogenous stimulation, the MSCs also secrete vascular endothelial growth factor A (VEGF-A) and tissue inhibitor of metalloproteinases 2 (TIMP-2). The secreted TIMP-2 is able to inhibit matrix metalloprotease-14 (MMP-14) activity in an *in vitro* assay *cell therapy (anti-inflammatory)*
laromestrocel	cellules stromales mésenchymateuses (CSM) allogéniques dérivées de la moelle osseuse de donneurs humains sains. Les cellules sont expansées dans un milieu contenant du sérum bovin fœtal. Les cellules sont positives (≥95%) pour les marqueurs de surface des cellules stromales mésenchymateuses CD73, CD90, CD105, et sont négatives (≤5%) pour CD34 et négatives (≤2%) pour les marqueurs CD11b, CD19, CD45 et la chaîne gamma de l'antigène d'histocompatibilité (HLA) de classe II (HLA-DR). Les cellules sécrètent des facteurs immunomodulateurs, notamment l'antagoniste du récepteur de l'interleukine 1 (IL-1RA), l'interleukine 4 (IL-4), l'IL-7, l'IL-8, l'IL-10, l'IL-13 et le facteur de stimulation des colonies de granulocytes (G-CSF), lors de la stimulation. En l'absence de stimulation exogène, les CSM sécrètent également le facteur de croissance endothélial vasculaire A (VEGF-A) et l'inhibiteur tissulaire des métalloprotéinases 2 (TIMP-2). Le TIMP-2 sécrété est capable d'inhiber l'activité de la métalloprotéase matricielle 14 (MMP-14) dans un essai *in vitro* *thérapie cellulaire (anti-inflammatoire)*
laromestrocel	células estromales mesenquimales (MSC) alogénicas derivadas de médula ósea de donantes sanos. Las células se expanden en medio que contiene suero bovino fetal. Las células son positivas (≥ 95%) para los marcadores de superficie de células estromales mesenquimales CD73, CD90, CD105 y son negativas (≤ 5%) para CD34 y negativas (≤2%) para los marcadores CD11b, CD19, CD45 y la cadena gamma del antígeno de histocompatibilidad HLA de clase II (HLA-DR). Las células secretan factores inmunomoduladores incluyendo el antagonista del receptor de interleuqina 1 (IL-1RA), interleuquina 4 (IL-4), IL-7, IL-8, IL-10, IL-13 y factor estimulador de colonias de granulocitos (G-CSF) tras estimulación. En ausencia de estimulación exógena, las MSC también secretan factor de crecimiento del endotelio vascular A (VEGF-A) e inhibidor tisular de metaloproteinasas 2 (TIMP-2). El TIMP-2 secretado es capaz de inhibir la actividad de la metaloproteinasa de matriz 14 (MMP-14) en un ensayo *in vitro* *terapia celular (antiinflamatorio)*

larubrilstatum

larubrilstat — (2-{[(5*R*)-6,7-dihydro-5*H*-cyclopenta[*b*]pyridin-5-yl]amino}pyrimidin-5-yl)(8-oxa-2-azaspiro[4.5]decan-2-yl)methanone
vascular non-inflammatory molecule-1 (VNN1) inhibitor

larubrilstat — (2-{[(5*R*)-6,7-dihydro-5*H*-cyclopenta[*b*]pyridin-5-yl]amino}pyrimidin-5-yl)(8-oxa-2-azaspiro[4.5]décan-2-yl)méthanone
inhibiteur de molécule-1 vasculaire non inflammatoire

larubrilstat — (2-{[(5*R*)-6,7-dihidro-5*H*-ciclopenta[*b*]piridin-5-il]amino}pirimidin-5-il)(8-oxa-2-azaespiro[4.5]decan-2-il)metanona
inhibidor de la molécula 1 vascular no inflamatoria

$C_{21}H_{25}N_5O_2$ 2765226-31-9

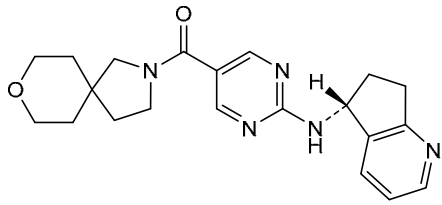

lasmotinibum

lasmotinib — 3-(carbamoylamino)-5-[(3-fluorophenyl)ethynyl]-*N*-[(3*S*)-piperidin-3-yl]thiophene-2-carboxamide
tyrosine kinase inhibitor, antineoplastic

lasmotinib — 3-(carbamoylamino)-5-[(3-fluorophényl)éthynyl]-*N*-[(3*S*)-pipéridin-3-yl]thiophène-2-carboxamide
inhibiteur de tyrosine kinase, antinéoplasique

lasmotinib — 3-(carbamoilamino)-5-[(3-fluorofenil)etinil]-*N*-[(3*S*)-piperidin-3-il]tiofeno-2-carboxamida
inhibidor de la tirosina kinasa, antineoplásico

$C_{19}H_{19}FN_4O_2S$ 2127107-15-5

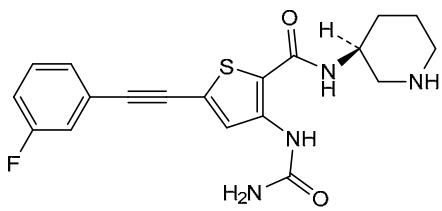

lasrekibartum #

lasrekibart	immunoglobulin G1-kappa, anti-[*Homo sapiens* IL5 (interleukin 5, IL-5)], humanized monoclonal antibody; H-gamma1 heavy chain humanized (1-448) [VH (*Homo sapiens* IGHV3-23*02 (88.7%) -(IGHD) -IGHJ4*01 (100%), CDR-IMGT [8.8.11] (26-33.51-58.97-107)) (1-118) -*Homo sapiens* IGHG1*01, G1m17,1 CH1 K120, CH3 D12, L14, 9-G1v21 CH2 Y15.1, T16, E18 (CH1 K120 (215) (119-216), hinge 1-15 (217-231), CH2 M15.1>Y (253), S16>T (255), T18>E (257) (232-341), CH3 D12 (357), L14 (359) (342-446), CHS (447-448)) (119-448)], (221-214')-disulfide with L-kappa light chain humanized (1'-214')[V-KAPPA (*Homo sapiens* IGKV1-6*01 (84.0%) -IGKJ4*01 (100%), CDR-IMGT [6.3.9] (27'-32'.50'-52'.89'-97')) (1'-107') -*Homo sapiens* IGKC*01 (100%) Km3 A45.1, V101 (C-KAPPA A45.1 (153'), V101 (191')) (108'-214')]; dimer (227-227'':230-230'')-bisdisulfide, produced in Chinese hamster ovary (CHO) cells, cell line CHO-K1, glycoform alfa *anti-inflammatory*
lasrékibart	immunoglobuline G1-kappa, anti-[*Homo sapiens* IL5 (interleukine 5, IL-5)], anticorps monoclonal humanisé; chaîne lourde H-gamma1 humanisée (1-448) [VH (*Homo sapiens* IGHV3-23*02 (88.7%) -(IGHD) -IGHJ4*01 (100%), CDR-IMGT [8.8.11] (26-33.51-58.97-107)) (1-118) -*Homo sapiens* IGHG1*01, G1m17,1 CH1 K120, CH3 D12, L14, 9-G1v21 CH2 Y15.1, T16, E18 (CH1 K120 (215) (119-216), charnière 1-15 (217-231), CH2 M15.1>Y (253), S16>T (255), T18>E (257) (232-341), CH3 D12 (357), L14 (359) (342-446), CHS (447-448)) (119-448)], (221-214')-disulfure avec la chaîne légère L-kappa humanisée (1'-214') [V-KAPPA (*Homo sapiens* IGKV1-6*01 (84.0%) -IGKJ4*01 (100%), CDR-IMGT [6.3.9] (27'-32'.50'-52'.89'-97')) (1'-107') -*Homo sapiens* IGKC*01 (100%) Km3 A45.1, V101 (C-KAPPA A45.1 (153'), V101 (191')) (108'-214')]; dimère (227-227'':230-230'')-bisdisulfure, produit dans des cellules ovariennes de hamster chinois (CHO), lignée cellulaire CHO-K1, glycoforme alfa *anti-inflammatoire*
lasrekibart	inmunoglobulina G1-kappa, anti-[*Homo sapiens* IL5 (interleukina 5, IL-5)], anticuerpo monoclonal humanizado; cadena pesada H-gamma1 humanizada (1-448) [VH (*Homo sapiens* IGHV3-23*02 (88.7%) -(IGHD) -IGHJ4*01 (100%), CDR-IMGT [8.8.11] (26-33.51-58.97-107)) (1-118) -*Homo sapiens* IGHG1*01, G1m17,1 CH1 K120, CH3 D12, L14, 9-G1v21 CH2 Y15.1, T16, E18 (CH1 K120 (215) (119-216), bisagra 1-15 (217-231), CH2 M15.1>Y (253), S16>T (255), T18>E (257) (232-341), CH3 D12 (357), L14 (359) (342-446), CHS (447-448)) (119-448)], (221-214')-disulfuro con la cadena ligera L-kappa humanizada (1'-214') [V-KAPPA (*Homo sapiens* IGKV1-6*01 (84.0%) -IGKJ4*01 (100%), CDR-IMGT [6.3.9] (27'-32'.50'-52'.89'-97')) (1'-107') -*Homo sapiens* IGKC*01 (100%) Km3 A45.1, V101 (C-KAPPA A45.1 (153'), V101 (191')) (108'-214')]; dímero (227-227'':230-230'')-bisdisulfuro, producido en las células ováricas de hámster chino (CHO), línea celular CHO-K1, forma glicosilada alfa *antiinflamatorio*

3021525-26-5

laventatugum tivedotinum #

laventatug tivedotin

immunoglobulin G1-kappa, anti-[*Homo sapiens* SLC39A6 (solute carrier family 39 member 6, solute carrier family 39 (metal ion transporter) member 6, solute carrier family 39 (zinc transporter) member 6, LIV-1, ZIP6)], humanized monoclonal antibody, conjugated on an average of four cysteinyl residues to *tivedotin*, comprising a cleavable monovalent linker and monomethylauristatin E (MMAE);
H-gamma1 heavy chain humanized (1-450) [VH (*Homo sapiens* IGHV1-69-2*01 (88.5%) -(IGHD) -IGHJ6*05 (81.8%) K120>Q (112), A127>S (119), CDR-IMGT [8.8.13] (26-33.51-58.97-109)) (1-120) -*Homo sapiens* IGHG1*01, G1m17,1 CH1 K120, CH3 D12, L14 (CH1 K120 (217) (121-218), hinge 1-15 (219-233), CH2 (234-343), CH3 D12 (359), L14 (361) (344-448), CHS (449-450)) (121-450)], (223-219')-disulfide with L-kappa light chain humanized (1'-219') [V-KAPPA (*Homo sapiens* IGKV2-29*02 (89.0%) -IGKJ2*01 (91.7%) Q120>G (105'), CDR-IMGT [11.3.9] (27'-37'.55'-57'.94'-102')) (1'-112') -*Homo sapiens* IGKC*01 (100%) Km3 A45.1, V101 (C-KAPPA A45.1 (158'), V101 (196')) (113'-219')]; dimer (229-229'':232-232'')-bisdisulfide, produced in Chinese hamster ovary (CHO) cells, cell line CHO-S, glycoform alfa; substituted at the sulfur atoms of an average of four L-cysteinyl residues among 223, 229, 232, 219', 223'', 229'', 232'' and 219''' with 2-oxo-2-({L-valyl-N^5-carbamoyl-L-ornithyl[(4-aminophenyl)methoxy]carbonyl-*N*-methyl-L-valyl-L-valyl-(3*R*,4*S*,5*S*)-3-methoxy-5-methyl-4-(methylamino)heptanoyl-(2*R*,3*R*)-*N*-[(1*S*,2*R*)-1-hydroxy-1-phenylpropan-2-yl]-3-methoxy-2-methyl-3-[(2*S*)-pyrrolidin-2-yl]propanamide}-$N^{2,1}$-yl)ethyl (*tivedotin*) groups
antineoplastic

laventatug tivédotine	immunoglobuline G1-kappa, anti-[*Homo sapiens* SLC39A6 (membre 6 de la famille 39 des transporteurs de solutés, membre 6 de la famille 39 (transporteur d'ion métal) des transporteurs de solutés, membre 6 de la famille 39 (transporteur du zinc) des transporteurs de solutés, LIV-1, ZIP6)], anticorps monoclonal humanisé; conjugué par quatre résidus cystéinyle en moyenne à la *tivédotine*, comprenant un linker monovalent clivable et monométhylauristatine E (MMAE); chaîne lourde H-gamma1 humanisée (1-450) [VH (*Homo sapiens* IGHV1-69-2*01 (88.5%) -(IGHD) -IGHJ6*05 (81.8%) K120>Q (112), A127>S (119), CDR-IMGT [8.8.13] (26-33.51-58.97-109)) (1-120) -*Homo sapiens* IGHG1*01, G1m17,1 CH1 K120, CH3 D12, L14 (CH1 K120 (217) (121-218), charnière 1-15 (219-233), CH2 (234-343), CH3 D12 (359), L14 (361) (344-448), CHS (449-450)) (121-450)], (223-219')-disulfure avec la chaîne légère L-kappa humanisée (1'-219') [V-KAPPA (*Homo sapiens* IGKV2-29*02 (89.0%) -IGKJ2*01 (91.7%) Q120>G (105'), CDR-IMGT [11.3.9] (27'-37'.55'-57'.94'-102')) (1'-112') -*Homo sapiens* IGKC*01 (100%) Km3 A45.1, V101 (C-KAPPA A45.1 (158'), V101 (196')) (113'-219')]; dimère (229-229'':232-232'')-bisdisulfure, produit dans des cellules ovariennes de hamster chinois (CHO), lignée cellulaire CHO-S, glycoforme alfa; substitué sur l'atome de soufre de quatre résidus L-cystéinyle en moyenne parmi 223, 229, 232, 219', 223'', 229'', 232'' et 219''' avec des groupes 2-oxo-2-({L-valyl-N^5-carbamoyl-L-ornithyl[(4-aminophényl)méthoxy]carbonyl-*N*-méthyl-L-valyl-L-valyl-(3*R*,4*S*,5*S*)-3-méthoxy-5-méthyl-4-(méthylamino)heptanoyl-(2*R*,3*R*)-*N*-[(1*S*,2*R*)-1-hydroxy-1-phénylpropan-2-yl]-3-méthoxy-2-méthyl-3-[(2*S*)-pyrrolidin-2-yl]propanamide}-$N^{2.1}$-yl)éthyle (*tivédotine*) *antinéoplasique*
laventatug tivedotina	inmunoglobulina G1-kappa, anti-[*Homo sapiens* SLC39A6 (miembro 6 de la familia 39 de los transportadores de solutos, miembro 6 de la familia 39 (transportador del ión metal) de los transportadores de los solutos, miembro 6 de la familia 39 (transportador del zinc) de los transportadores de solutos, LIV-1, ZIP6)], anticuerpo monoclonal humanizado, conjugado en una media de cuatro residuos cisteinilo a la *tivedotina*, que comprende un enlace monovalente escindible y monometilauristatina E (MMAE); cadena pesada H-gamma1 humanizada (1-450) [VH (*Homo sapiens* IGHV1-69-2*01 (88.5%) -(IGHD) -IGHJ6*05 (81.8%) K120>Q (112), A127>S (119), CDR-IMGT [8.8.13] (26-33.51-58.97-109)) (1-120) -*Homo sapiens* IGHG1*01 (100%) G1m17,1 CH1 K120, CH3 D12, L14 (CH1 K120 (217) (121-218), bisagra 1-15 (219-233), CH2 (234-343), CH3 D12 (359), L14 (361) (344-448), CHS (449-450)) (121-450)], (223-219')-disulfuro con la cadena ligera L-kappa humanizada (1'-219') [V-KAPPA (*Homo sapiens* IGKV2-29*02 (89.0%) -IGKJ2*01 (91.7%) Q120>G (105'), CDR-IMGT [11.3.9] (27'-37'.55'-57'.94'-102')) (1'-112') -*Homo sapiens* IGKC*01 (100%) Km3 A45.1, V101 (C-KAPPA A45.1 (158'), V101 (196')) (113'-219')]; dímero (229-229'':232-232'')-bisdisulfuro, producido en las células ováricas de hámster chino (CHO), línea celular CHO-S, forma glicosilada alfa, sustituido en el átomo de

azufre de 4 residuos L-cisteinilo en promedio entre 223, 229, 232, 219', 223", 229", 232" y 219"' con grupos 2-oxo-2-({L-valil-N^5-carbamoil-L-ornitil[(4-aminofenil)metoxi]carbonil-*N*-metil-L-valil-L-valil-(3*R*,4*S*,5*S*)-5-metil-4-(metilamino)-3-metoxiheptanoil-(2*R*,3*R*)-*N*-[(1*S*,2*R*)-1-fenil-1-hidroxipropan-2-il]-2-metil-3-metoxi-3-[(2*S*)-pirrolidin-2-il]propanamida}-$N^{2,1}$-il)etilo (*tivedotina*) *antineoplásico*

3009829-96-0

Heavy chain / Chaîne lourde / Cadena pesada (H, H")

```
EVQLVESGGGLVQPGGSLRLSCAASGFTFSSYAMSWVRQAPGKGLEWVSA 50
ISGSGGSTYYADSVKGRFTISRDNSKNTLYLQMNSLRAEDTAVYYCVRG 100
RFSGSWSFDY WGQGTLVTVSS ASTKGPSVFPLAPSSKSTSGGTAALGC 150
LVKDYFPEPV TVSWNSGALT SGVHTFPAVL QSSGLYSLSS VVTVPSSSLG 200
TQTYICNVNH KPSNTKVDKK VEPKSCDKTH TCPPCPAPEL LGGPSVFLFP 250
PKPKDTLMIS RTPEVTCVVV DVSHEDPEVK FNWYVDGVEV HNAKTKPREE 300
QYNSTYRVVS VLTVLHQDWL NGKEYKCKVS NKALPAPIEK TISKAKGQPR 350
EPQVYTLPPS QEEMTKNQVS LTCLVKGFYP SDIAVEWESN GQPENNYKTT 400
PPVLDSDGSF FLYSRLTVDK SRWQEGNVFS CSVMHEALHN HYTQKSLSLS 450
```

Light chain / Chaîne légère / Cadena ligera (L', L'")

```
DIVMTQTPLS LSVTPGQPAS ISCRSSQSLV HSDGNTYLEW YLQKPGQSPQ 50
LLIYEVSNRF SGVPDRFSGS GSGTDFTLKI SRVEAEDVGV YYCFQGSHVP 100
YTFGQGTKLE IKRTVAAPSV FIFPPSDEQL KSGTASVVCL LNNFYPREAK 150
VQWKVDNALQ SGNSQESVTE QDSKDSTYSL SSTLTLSKAD YEKHKVYACE 200
VTHQGLSSPV TKSFNRGEC 219
```

Post-translational modifications

Disulfide bridges location / Position des ponts disulfure / Posiciones de los puentes disulfuro

Intra-H (C23-C104) 22-96 147-203 264-324 370-428
22"-96" 147"-203" 264"-324" 370"-428"
Intra-L (C23-C104) 23'-93' 139'-199'
23'"-93'" 139'"-199'"
Inter-H-L (h5-CL 126)* 223-219' 223"-219'"
Inter-H-H (h11, h14)* 229-229" 232-232"

*Two or three of the four inter-chain disulfide bridges are not present, an average of 4 (3.8) cysteinyl being conjugated each via a thioether bond to a drug linker.
*Deux ou trois des quatre ponts disulfures inter-chaînes ne sont pas présents, 4 (3,8) cystéinyl en moyenne étant chacun conjugué via une liaison thioéther à un linker-principe actif.
*Dos o tres de los cuatro puentes disulfuro inter-catenarios no están presentes, una media de 4 (3.8) cisteinil está conjugada a conectores de principio activo.

N-glycosylation sites / Sites de N-glycosylation / Posiciones de N-glicosilación
H CH2 N84.4: 300, 300"
Fucosylated complex bi-antennary CHO-type glycans / glycanes de type CHO bi-antennaires complexes fucosylés / glicanos de tipo CHO biantenarios complejos fucosilados

C-terminal lysine clipping / Coupure de la lysine C-terminale / Recorte de lisina C-terminal
H CHS K2: 450, 450"

Potential modified residues / résidus modifiés potentiels / restos modificados potenciales*
C (223, 229, 232, 219', 223", 229", 232", 219"')
*(*inclusion*:mAb ~ 4:1)

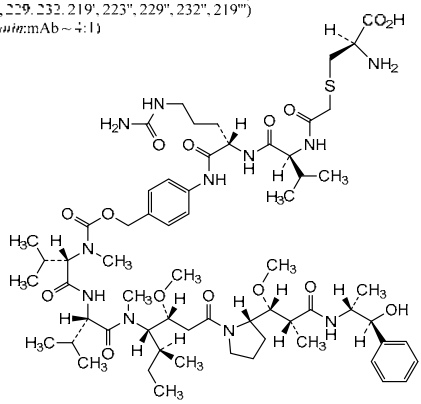

laventatugum #

laventatug — immunoglobulin G1-kappa, anti-[*Homo sapiens* SLC39A6 (solute carrier family 39 member 6, solute carrier family 39 (metal ion transporter) member 6, solute carrier family 39 (zinc transporter) member 6, LIV-1), ZIP6], humanized monoclonal antibody;
H-gamma1 heavy chain humanized (1-450) [VH (*Homo sapiens* IGHV1-69-2*01 (88.5%) -(IGHD) -IGHJ6*05 (81.8%) K120>Q (112), A127>S (119), CDR-IMGT [8.8.13] (26-33.51-58.97-109)) (1-120) -*Homo sapiens* IGHG1*01 (100%) G1m17,1 CH1 K120, CH3 D12, L14 (CH1 K120 (217) (121-218), hinge 1-15 (219-233), CH2 (234-343), CH3 D12 (359), L14 (361) (344-448), CHS (449-450)) (121-450)], (223-219')-disulfide with L-kappa light chain humanized (1'-219') [V-KAPPA (*Homo sapiens* IGKV2-29*02 (89.0%) -IGKJ2*01 (91.7%) Q120>G (105'), CDR-IMGT [11.3.9] (27'-37'.55'-57'.94'-102')) (1'-112') -*Homo sapiens* IGKC*01 (100%) Km3 A45.1, V101 (C-KAPPA A45.1 (158'), V101 (196')) (113'-219')]; dimer (229-229'':232-232'')-bisdisulfide, produced in Chinese hamster ovary (CHO) cells, cell line CHO-S, glycoform alfa
antineoplastic

laventatug — immunoglobuline G1-kappa, anti-[*Homo sapiens* SLC39A6 (membre 6 de la famille 39 des transporteurs de solutés, membre 6 de la famille 39 (transporteur d'ion métal) des transporteurs de solutés, membre 6 de la famille 39 (transporteur du zinc) des transporteurs de solutés, LIV-1, ZIP6)], anticorps monoclonal humanisé;
chaîne lourde H-gamma1 humanisée (1-450) [VH (*Homo sapiens* IGHV1-69-2*01 (88.5%) -(IGHD) -IGHJ6*05 (81.8%) K120>Q (112), A127>S (119), CDR-IMGT [8.8.13] (26-33.51-58.97-109)) (1-120) -*Homo sapiens* IGHG1*01 (100%) G1m17,1 CH1 K120, CH3 D12, L14 (CH1 K120 (217) (121-218), charnière 1-15 (219-233), CH2 (234-343), CH3 D12 (359), L14 (361) (344-448), CHS (449-450)) (121-450)], (223-219')-disulfure avec la chaîne légère L-kappa humanisée (1'-219') [V-KAPPA (*Homo sapiens* IGKV2-29*02 (89.0%) -IGKJ2*01 (91.7%) Q120>G (105'), CDR-IMGT [11.3.9] (27'-37'.55'-57'.94'-102')) (1'-112') -*Homo sapiens* IGKC*01 (100%) Km3 A45.1, V101 (C-KAPPA A45.1 (158'), V101 (196')) (113'-219')]; dimère (229-229'':232-232'')-bisdisulfure, produit dans des cellules ovariennes de hamster chinois (CHO), lignée cellulaire CHO-S, glycoforme alfa
antinéoplasique

laventatug — inmunoglobulina G1-kappa, anti-[*Homo sapiens* SLC39A6 (miembro 6 de la familia 39 de los transportadores de solutos, miembro 6 de la familia 39 (transportador del ión metal) de los transportadores de los solutos, miembro 6 de la familia 39 (transportador del zinc) de los transportadores de solutos, LIV-1, ZIP6)], anticuerpo monoclonal humanizado;
cadena pesada H-gamma1 humanizada (1-450) [VH (*Homo sapiens* IGHV1-69-2*01 (88.5%) -(IGHD) -IGHJ6*05 (81.8%) K120>Q (112), A127>S (119), CDR-IMGT [8.8.13] (26-33.51-58.97-109)) (1-120) -*Homo sapiens* IGHG1*01 (100%) G1m17,1 CH1 K120, CH3 D12, L14 (CH1 K120 (217) (121-218), bisagra 1-15 (219-233), CH2 (234-343), CH3 D12 (359), L14 (361) (344-448), CHS (449-450)) (121-450)], (223-219')-disulfuro con la cadena ligera L-kappa humanizada (1'-219') [V-KAPPA (*Homo sapiens* IGKV2-29*02 (89.0%) -IGKJ2*01 (91.7%) Q120>G (105'), CDR-IMGT [11.3.9] (27'-37'.55'-57'.94'-102')) (1'-112') -*Homo sapiens* IGKC*01 (100%) Km3 A45.1, V101 (C-KAPPA A45.1 (158'), V101 (196')) (113'-219')]; dímero (229-229'':232-232'')-bisdisulfuro, producido en las células ováricas de hámster chino (CHO), línea celular CHO-S, forma glicosilada alfa
antineoplásico

3009829-91-5

Heavy chain / Chaîne lourde / Cadena pesada

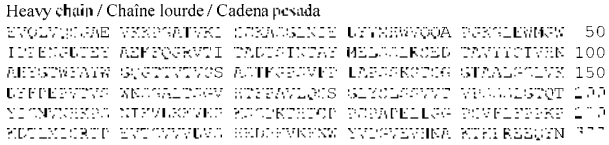

Light chain / Chaîne légère / Cadena ligera

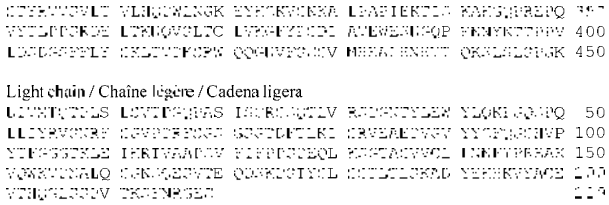

Post-translational modifications

Disulfide bridges location / Position des ponts disulfure / Posiciones de los puentes disulfuro

Intra-H (C23-C104) 22-96 147-203 264-324 370-428
22"-96" 147"-203" 264"-324" 370"-428"
Intra-L (C23-C104) 23'-93' 139'-199'
23'''-93''' 139'''-199'''
Inter-H-L (h 5-CL 126) 223-219' 223"-219'''
Inter-H-H (h 11, h 14) 229-229" 232-232"

N-glycosylation sites / Sites de N-glycosylation / Posiciones de N-glicosilación

H CH2 N84.4: 300, 300"

Fucosylated complex bi-antennary CHO-type glycans / glycanes de type CHO bi-antennaires complexes fucosylés / glicanos de tipo CHO biantenarios complejos fucosilados

C-terminal lysine clipping / Coupure de la lysine C-terminale / Recorte de lisina C-terminal

H CHS K2: 450, 450"

lecankitugum #

lecankitug	immunoglobulin G1-kappa, anti-[*Homo sapiens* IL17A (interleukin 17A, IL-17A) and IL17F (interleukin 17F, IL-17F)], humanized monoclonal antibody; H-gamma1 heavy chain humanized (1-448) [VH (*Homo sapiens* IGHV1-46*01 (83.7%) -(IGHD) -IGHJ4*01 (100%), CDR-IMGT [8.8.11] (26-33.51-58.97-107)) (1-118) -*Homo sapiens* IGHG1*01 (100%) G1m17,1 CH1 K120, CH3 D12, L14 (CH1 K120 (215) (119-216), hinge 1-15 (217-231), CH2 (232-341), CH3 D12 (357), L14 (359) (342-446), CHS (447-448)) (119-448)], (221-219')-disulfide with L-kappa light chain humanized (1'-219') [V-KAPPA (*Homo sapiens* IGKV2D-29*01 (89.0%) -IGKJ2*01 (100%), CDR-IMGT [11.3.9] (27'-37'.55'-57'.94'-102')) (1'-112') -*Homo sapiens* IGKC*01 (100%) Km3 A45.1, V101 (C-KAPPA A45.1 (158'), V101 (196')) (113'-219')]; dimer (227-227":230-230")-bisdisulfide, produced in a cell line from Chinese hamster ovary (CHO) cells, derived from the cell line CHO-K1, glycoform alfa *anti-inflammatory*
lécankitug	immunoglobuline G1-kappa, anti-[*Homo sapiens* IL17A (interleukine 17A, IL-17A) et IL17F (interleukine 17F, IL-17F)]; anticorps monoclonal humanisé;

chaîne lourde H-gamma1 humanisée (1-448) [VH (*Homo sapiens* IGHV1-46*01 (83.7%) -(IGHD) -IGHJ4*01 (100%), CDR-IMGT [8.8.11] (26-33.51-58.97-107)) (1-118) -*Homo sapiens* IGHG1*01 (100%) G1m17,1 CH1 K120, CH3 D12, L14 (CH1 K120 (215) (119-216), charnière 1-15 (217-231), CH2 (232-341), CH3 D12 (357), L14 (359) (342-446), CHS (447-448)) (119-448)], (221-219')-disulfure avec la chaîne légère L-kappa humanisée (1'-219') [V-KAPPA (*Homo sapiens* IGKV2D-29*01 (89.0%) -IGKJ2*01 (100%), CDR-IMGT [11.3.9] (27'-37'.55'-57'.94'-102')) (1'-112') -*Homo sapiens* IGKC*01 (100%) Km3 A45.1, V101 (C-KAPPA A45.1 (158'), V101 (196')) (113'-219')]; dimère (227-227'':230-230'')-bisdisulfure, produit dans une lignée cellulaire des cellules ovariennes de hamster chinois (CHO), dérivant de la lignée cellulaire CHO-K1, glycoforme alfa
anti-inflammatoire

lecankitug

inmunoglobulina G1-kappa, anti-[*Homo sapiens* IL17A (interleukina 17A, IL-17A) y IL17F (interleukina 17F, IL-17F)]; anticuerpo monoclonal humanizado;
cadena pesada H-gamma1 humanizada (1-448) [VH (*Homo sapiens* IGHV1-46*01 (83.7%) -(IGHD) -IGHJ4*01 (100%), CDR-IMGT [8.8.11] (26-33.51-58.97-107)) (1-118) -*Homo sapiens* IGHG1*01 (100%) G1m17,1 CH1 K120, CH3 D12, L14 (CH1 K120 (215) (119-216), bisagra 1-15 (217-231), CH2 (232-341), CH3 D12 (357), L14 (359) (342-446), CHS (447-448)) (119-448)], (221-219')-disulfuro con la cadena ligera L-kappa humanizada (1'-219') [V-KAPPA (*Homo sapiens* IGKV2D-29*01 (89.0%) -IGKJ2*01 (100%), CDR-IMGT [11.3.9] (27'-37'.55'-57'.94'-102')) (1'-112') -*Homo sapiens* IGKC*01 (100%) Km3 A45.1, V101 (C-KAPPA A45.1 (158'), V101 (196')) (113'-219')]; dímero (227-227'':230-230'')-bisdisulfuro, producido en una línea celular de las células ováricas de hámster chino (CHO), línea celular derivada de CHO-K1, forma glicosilada alfa
antiinflamatorio

2923284-76-6

Heavy chain / Chaîne lourde / Cadena pesada

```
QFQLVQSGAE VKKPGASVKV SCKASGYTFT DYNLNWVRQA PGKGLEWMGV  50
IHPDYGTTSY NQKFKDRVTM TVDTSTSTVY MELSSLRSED TAVYYCVRYD 100
YGDAMDYWGQ GTLVTVSSAS TKGPSVFPLA PSSKSTSGGT AALGCLVKDY 150
FPEPVTVSWN SGALTSGVHT FPAVLQSSGL YSLSSVVTVP SSSLGTQTYI 200
CNVNHKPSNT KVDKKVEPKS CDKTHTCPPC PAPELLGGPS VFLFPPKPKD 250
TLMISRTPEV TCVVVDVSHE DPEVKFNWYV DGVEVHNAKT KPREEQYNST 300
YRVVSVLTVL HQDWLNGKEY KCKVSNKALP APIEKTISKA KGQPREPQVY 350
TLPPSRDELT KNQVSLTCLV KGFYPSDIAV EWESNGQPEN NYKTTPPVLD 400
SDGSFFLYSK LTVDKSRWQQ GNVFSCSVMH EALHNHYTQK SLSLSPGK   448
```

Light chain / Chaîne légère / Cadena ligera

```
DIVMTQSPLS LSVTPGQPAS ISCRSSQSLV HSNGNTYLHW YLQKPGQPPQ  50
LLIYKVSNRF SGVPDRFSGS GSGTDFTLKI SRVEAEDVGV YYCSQSTHVP 100
LTFGQGTKLE IKRTVAAPSV FIFPPSDEQL KSGTASVVCL LNNFYPREAK 150
VQWKVDNALQ SGNSQESVTE QDSKDSTYSL SSTLTLSKAD YEKHKVYACE 200
VTHQGLSSPV TKSFNRGEC                                   219
```

Post-translational modifications

Disulfide bridges location / Position des ponts disulfure / Posiciones de los puentes disulfuro
Intra-H (C23-C104) 22-96 145-201 262-322 368-426
22"-96" 145"-201" 262"-322" 368"-426"
Intra-L (C23-C104) 23'-93' 139'-199'
23'"-93'" 139'"-199'"
Inter-H-L (h 5-CL 126) 221-219' 221"-219'"
Inter-H-H (h 11, h 14) 227-227" 230-230"

N-terminal glutaminyl cyclization / Cyclisation du glutaminyle N-terminal / Ciclación del glutaminilo N-terminal
Q > pyroglutamyl (pE, 5-oxoprolyl) / pyroglutamyle (pE, 5-oxoprolyle) / piroglutamilo (pE, 5-oxoprolilo)
H VH Q1: 1, 1"

N-glycosylation sites / Sites de N-glycosylation / Posiciones de N-glicosilación
H CH2 N84.4: 298, 298"
Fucosylated complex bi-antennary CHO-type glycans / glycanes de type CHO bi-antennaires complexes fucosylés / glicanos de tipo CHO biantenarios complejos fucosilados

C-terminal lysine clipping / Coupure de la lysine C-terminale / Recorte de lisina C-terminal
H CHS K2: 448, 448"

ledostomigum #

ledostomig immunoglobulin (H-gamma1-scFvhk_L-kappa) dimer, anti-[*Homo sapiens* NT5E (5'-nucleotidase ecto, 5'-nucleotidase, NT5, eN, eNT, NTE, CALJA, CD73)] and anti-[*Homo sapiens* PDCD1 (programmed cell death 1, PD-1, PD1, CD279)], monoclonal antibody, bispecific, tetravalent;
H-gamma1 heavy chain anti-NT5E fused to a scFvhk anti-PDCD1 (1-717) [H-gamma1 heavy chain anti-NT5E (1-451) [VH Musmus/Homsap (*Mus musculus* IGHV1-42-1*01 (82.7%) -(IGHD) -IGHJ2*01 (100%)/*Homo sapiens* IGHV1-46*01 (81.6%) -(IGHD) -IGHJ4*01 (86.7%) L123>T (116), V124>L (117), CDR-IMGT [8.8.14] (26-33.51-58.97-110)) (1-121)-*Homo sapiens* IGHG1*01, G1m17,1 CH1 K120, CH3 D12, L14, 6-G1v14-1 CH2 A1.3, A1.2, A1(CH1 K120 (218) (122-219), hinge 1-15 (220-234), CH2 L1.3>A (238), L1.2>A (239), G1>A (241) (235-344), CH3 D12 (360), L14 (362) (345-449), CHS (450-451)) (122-451)] -20-mer tetrakis(tetraglycyl-seryl) linker (452-471) -scFvhk anti-PDCD1 (472-717) [VH (*Homo sapiens* IGHV3-23*04 (88.7%) -(IGHD) -IGHJ6*01 (90.9%) T123>L (584), CDR-IMGT [8.8.11] (497-504.522-529.568-578)) (472-589) -20-mer tetrakis(tetraglycyl-seryl) linker (590-609) -V-KAPPA Musmus/Homsap (*Mus musculus* IGKV14-111*01 (86.3%) -IGKJ5*01 (100%)/*Homo sapiens* IGKV1-16*01 (80.0%) -IGKJ2*01 (81.8%) Q120>A (709), I126>L (715), CDR-IMGT [6.3.9] (636-641.659-661.698-706)) (610-717)]]; (224-220')-disulfide with L-kappa light chain anti-NT5E humanized (1'-220') [V-KAPPA (*Homo sapiens* IGKV4-1*01 (89.1%) -IGKJ2*01 (91.7%) Q120>G (106'), CDR-IMGT [12.3.9] (27'-38'.56'-58'.95'-103')) (1'-113') -*Homo sapiens* IGKC*01 (100%) Km3 A45.1, V101 (C-KAPPA A45.1 (159'), V101 (197')) (114'-220')]; dimer (230-230":233-233")-bisdisulfide, produced in Chinese hamster ovary (CHO) cells, glycoform alfa
immunostimulant, antineoplastic

lédostomig immunoglobuline (H-gamma1-scFvhk_L-kappa) dimère, anti-[*Homo sapiens* NT5E (5'-nucléotidase ecto, 5'-nucléotidase, NT5, eN, eNT, NTE, CALJA, CD73)] et anti-[*Homo sapiens* PDCD1 (protéine 1 de mort cellulaire programmée, PD-1, PD1, CD279)], anticorps monoclonal, bispécifique, tétravalent;
chaîne lourde H-gamma1 anti-NT5E fusionnée à un scFvhk anti-PDCD1 (1-717) [chaîne lourde H-gamma1 anti-NT5E (1-451) [VH Musmus/Homsap (*Mus musculus* IGHV1-42-1*01 (82.7%) -(IGHD) -IGHJ2*01 (100%)/*Homo sapiens* IGHV1-46*01 (81.6%) -(IGHD) -IGHJ4*01 (86.7%) L123>T (116), V124>L (117), CDR-IMGT [8.8.14] (26-33.51-58.97-110)) (1-121)-*Homo sapiens* IGHG1*01 G1m17,1 CH1 K120, CH3 D12, L14, 6-G1v14-1 CH2 A1.3, A1.2, A1(CH1 K120 (218) (122-219), charnière 1-15 (220-234), CH2 L1.3>A (238), L1.2>A (239), G1>A (241) (235-344), CH3 D12 (360), L14 (362) (345-449), CHS (450-451)) (122-451)] -20-mer tétrakis(tétraglycyl-séryl) linker (452-471) -scFvhk anti-PDCD1 (472-717) [VH (*Homo sapiens* IGHV3-23*04 (88.7%) -(IGHD) -IGHJ6*01 (90.9%) T123>L (584), CDR-IMGT [8.8.11] (497-504.522-529.568-578)) (472-589) -20-mer tétrakis(tétraglycyl-séryl) linker (590-609) -V-KAPPA Musmus/Homsap (*Mus musculus* IGKV14-111*01 (86.3%) -IGKJ5*01 (100%)/*Homo sapiens* IGKV1-16*01 (80.0%) -IGKJ2*01 (81.8%) Q120>A (709), I126>L (715), CDR-IMGT [6.3.9] (636-641.659-661.698-706)) (610-717)]]; (224-220')-disulfure avec la chaîne légère L-kappa anti-NT5E humanisée (1'-220') [V-KAPPA (*Homo sapiens* IGKV4-1*01 (89.1%) -IGKJ2*01 (91.7%) Q120>G (106'), CDR-IMGT [12.3.9] (27'-38'.56'-58'.95'-103')) (1'-113') -*Homo sapiens* IGKC*01 (100%) Km3 A45.1, V101 (C-KAPPA A45.1 (159'), V101 (197')) (114'-220')]; dimère (230-230":233-233")-bisdisulfure, produit dans des cellules ovariennes de hamster chinois (CHO), glycoforme alfa
immunostimulant, antinéoplasique

ledostomig inmunoglobulina (H-gamma1-scFvhk_L-kappa) dímero, anti-[*Homo sapiens* NT5E (5'-nucleotidasa ecto, 5'-nucleotidasa, NT5, eN, eNT, NTE, CALJA, CD73)] y anti-[*Homo sapiens* PDCD1 (proteína 1 de muerte celular programada, PD-1, PD1, CD279)], anticuerpo monoclonal, biespecífico, tetravalente;

cadena pesada H-gamma1 anti-NT5E fusionada con un scFvhk anti-PDCD1 (1-717) [cadena pesada H-gamma1 anti-NT5E (1-451) [VH Musmus/Homsap (*Mus musculus* IGHV1-42-1*01 (82.7%) -(IGHD) -IGHJ2*01 (100%)/*Homo sapiens* IGHV1-46*01 (81.6%) -(IGHD) -IGHJ4*01 (86.7%) L123>T (116), V124>L (117), CDR-IMGT [8.8.14] (26-33.51-58.97-110)) (1-121)-*Homo sapiens* IGHG1*01 G1m17,1 CH1 K120, CH3 D12, L14, 6-G1v14-1 CH2 A1.3, A1.2, A1(CH1 K120 (218) (122-219), bisagra 1-15 (220-234), CH2 L1.3>A (238), L1.2>A (239), G1>A (241) (235-344), CH3 D12 (360), L14 (362) (345-449), CHS (450-451)) (122-451)] -20-mer tetrakis(tetraglicil-seril) enlace (452-471) -scFvhk anti-PDCD1 (472-717) [VH (*Homo sapiens* IGHV3-23*04 (88.7%) -(IGHD) -IGHJ6*01 (90.9%) T123>L (584), CDR-IMGT [8.8.11] (497-504.522-529.568-578)) (472-589) -20-mer tetrakis(tetraglicil-seril) enlace (590-609) -V-KAPPA Musmus/Homsap (*Mus musculus* IGKV14-111*01 (86.3%) -IGKJ5*01 (100%)/*Homo sapiens* IGKV1-16*01 (80.0%) -IGKJ2*01 (81.8%) Q120>A (709), I126>L (715), CDR-IMGT [6.3.9] (636-641.659-661.698-706)) (610-717)]]; (224-220')-disulfuro com la cadena ligera L-kappa anti-NT5E humanizada (1'-220') [V-KAPPA (*Homo sapiens* IGKV4-1*01 (89.1%) -IGKJ2*01 (91.7%) Q120>G (106'), CDR-IMGT [12.3.9] (27'-38'.56'-58'.95'-103')) (1'-113') -*Homo sapiens* IGKC*01 (100%) Km3 A45.1, V101 (C-KAPPA A45.1 (159'), V101 (197')) (114'-220')]; dímero (230-230'':233-233'')-bisdisulfuro, producido en las células ováricas de hámster chino (CHO), forma glicosilada alfa

inmunoestimulante, antineoplásico

2769743-01-1

Heavy chain / Chaîne lourde / Cadena pesada: fused H-gamma1 anti-NT5E -scFvhk anti-PDCD1 (H, H'')

```
QVQLVQSGAE VVKPGASVKV SCKASGYSFT GYTMNWVRQA PGQNLEWIGL  50
INPYNAGTSY NQKFQGKVTL TVDKSTSTAY MELSSLRSED TAVYYCARSE 100
YRYGGDYFDY WGQGTTLTVS SASTKGPSVF PLAPSSKSTS GGTAALGCLV 150
KDYFPEPVTV SWNSGALTSG VHTFPAVLQS SGLYSLSSVV TVPSSSLGTQ 200
TYICNVNHKP SNTKVDKKVE PKSCDKTHTC PPCPAPEAAG APSVFLFPPK 250
PKDTLMISRT PEVTCVVVDV SHEDPEVKFN WYVDGVEVHN AKTKPREEQY 300
NSTYRVVSVL TVLHQDWLNG KEYKCKVSNK ALPAPIEKTI SKAKGQPREP 350
QVYTLPPSRD ELTKNQVSLT CLVKGFYPSD IAVEWESNGQ PENNYKTTPP 400
VLDSDGSFFL YSKLTVDKSR WQQGNVFSCS VMHEALHNHY TQKSLSLSPG 450
KGGGGSGGGG SGGGGSGGGG SEVQLVESGG GLVQPGGSLR LSCAASGFAF 500
SSYDMSWVRQ APGKGLDWVA TISGGGRYTY YPDSVKGRFT ISRDNSKNNL 550
YLQMNSLRAE DTALYYCANR YGEAWFAYWG QGTLVTVSSG GGGSGGGGSG 600
GGGSGGGGSD IQMTQSPSSM SASVGDRVTF TCRASQDINT YLSWFQQKPG 650
KSPKTLIYRA NRLVSGVPSR FSGSGSGQDY TLTISSLQPE DMATYYCLQY 700
DEFPLTFGAG TKLELKR                                    717
```

Light chain / Chaîne légère / Cadena ligera: L-kappa anti-NT5E (L', L'")

```
DIVMTQSPSS LAVSVGERVT ISCKSSQSLL NSSNQKNYLA WYQQKPGQAP  50
KLLIYFASTR ESGVPDRFSG SGSGTDFTLT ISSLQAEDVA VYYCQQHYDT 100
PYTFGGGTKL EIKRTVAAPS VFIFPPSDEQ LKSGTASVVC LLNNFYPREA 150
KVQWKVDNAL QSGNSQESVT EQDSKDSTYS LSSTLTLSKA DYEKHKVYAC 200
EVTHQGLSSP VTKSFNRGEC                                 220
```

Post-translational modifications

Disulfide bridges location / Position des ponts disulfure / Posiciones de los puentes disulfuro

Intra-H (C23-C104) 22-96 148-204 265-325 371-429
22"-96" 148"-204" 265"-325" 371"-429"
493-567 632-697
493"-567' 632"-697"

Intra-L (C23-C104) 23'-94' 140'-200'
23'"-94'" 140'"-200'"

Intra-H-L (h 5-CL 126) 224-220' 224"-220'"

Inter-H-H (h 11, h 14) 230-230" 233-233"

N-terminal glutaminyl cyclization / Cyclisation du glutaminyle N-terminal / Ciclación del glutaminilo N-terminal

Q > pyroglutamyl (pE, 5-oxoprolyl) / pyroglutamyle (pE, 5-oxoprolyle) / piroglutamilo (pE, 5-oxoprolilo)

H VH Q1: 1, 1"

N-glycosylation sites / Sites de N-glycosylation / Posiciones de N-glicosilación

H CH2 N84.4: 301, 301"

Fucosylated complex bi-antennary CHO-type glycans / glycanes de type CHO bi-antennaires complexes fucosylés / glicanos de tipo CHO biantenarios complejos fucosilados.

lerepmeranum #

lerepmeran	messenger RNA (mRNA), 5'(m^7G-(5'→5')-ppp-Gm)-capped, encoding codon-optimised human propionyl-CoA carboxylase subunit alpha (PCCA), flanked by 5' and 3' untranslated regions (UTRs), followed by a 3' polyadenylation (polyA) tail and concluded by a 5-nucleotide *Xba*I scar. The 3' UTR contains three microRNA-142 (miR-142) binding sites. Contains N^1-methylpseudouridine instead of uridine (*all*-U>$m^1\Psi$) *enzyme replacement therapy (propionic acidemia)*
lérepméran	ARN messager (ARNm), coiffé en 5'(m^7G-(5'→5')-ppp-Gm), codant, avec des codons optimisés, la sous-unité alpha de la propionyl-CoA carboxylase humaine (PCCA), flanqué des régions non traduites (UTRs) en 5' et 3', suivie d'une queue de polyadénylation (polyA) en 3' et conclue par une cicatrice *Xba*I de 5 nucléotides. Le 3' UTR contient trois sites de liaison du microARN-142 (miR-142). Contient de la N^1-méthylpseudouridine au lieu de l'uridine (*tout*-U>$m^1\Psi$) *thérapie enzymatique substitutive (acidémie propionique)*
lerepmerán	ARN mensajero (ARNm), protegido con la caperuza 5'(m^7G-(5'→5')-ppp-Gm), que codifica, con codones optimizados, la subunidad alfa de la propionil-CoA carboxilasa (PCCA), flanqueado por regiones sin traducir (UTRs) 5' y 3', seguido de una cola de poliadenilación (poliA) en 3' y concluido con una cicatriz *Xbal* de 5 nucleótidos. La 3' UTR contiene tres sitios de unión del microARN-142 (miR-142). Contiene N^1-metilpseudouridina en lugar de uridina (*todo*-U>$m^1\Psi$) *tratamiento enzimático de sustitución (acidemia propiónica)*

2924731-63-3

linvemastatum

linvemastat	*rac*-(1^4*R*)-7^2-methyl-5-oxa-3-thia-7(4)-pyridina-1(4)-imidazolidina-2(2,3)-furana-4(1,4)-benzenaheptaphane-1^2,1^5-dione *matrix metalloproteinase-12 inhibitor, lung diseases*
linvémastat	*rac*-(1^4*R*)-7^2-méthyl-5-oxa-3-thia-7(4)-pyridina-1(4)-imidazolidina-2(2,3)-furana-4(1,4)-benzénaheptaphane-1^2,1^5-dione *inhibiteur de la métalloprotéinase matricielle-12, maladies pulmonaires*
linvemastat	*rac*-(1^4*R*)-7^2-metil-5-oxa-3-tia-7(4)-piridina-1(4)-imidazolidina-2(2,3)-furana-4(1,4)-bencenaheptafano-1^2,1^5-diona *inhibidor de la metaloproteinasa 12 de la matrix, enfermedades pulmonares*

$C_{20}H_{17}N_3O_4S$ 2389060-50-6

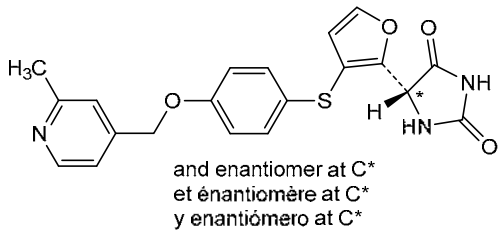

and enantiomer at C*
et énantiomère at C*
y enantiómero at C*

liraltagenum autoleucelum #

liraltagene autoleucel

autologous CD4+/CD8+ enriched T lymphocytes derived from leukapheresis material, transduced with a non-replicating murine stem cell virus (MSCV)-derived gamma retroviral vector, encoding codon-optimised follicle-stimulating hormone (FSH) (subunits FSHβ and CGα, linked by a glycine/serine spacer), preceded by the FSHβ signal peptide, and fused to a CD8α hinge and transmembrane domain, a 4-1BB co-stimulatory domain and a CD3ζ signalling domain, under control of the Moloney murine leukemia virus (MMLV) LTR promoter. The vector also has long terminal repeats (LTRs) derived from MSCV and an extended packaging signal (Ψ+) derived from MMLV and has a splice acceptor sequence immediately upstream of the start codon. A Kozak sequence precedes the transgene.
The leukapheresis material is enriched for the lymphocyte fraction prior to activation with anti-CD3 and interleukin 2 (IL-2). The cells are then transduced with the retroviral vector and expanded in growth media containing anti-CD3 and IL-2. The cell suspension consists of T lymphocytes (≥90% CD3+; ≤0.5% CD14+, ≤0.08% CD19+, ≤5% CD3-CD56+, ≤0.55% CD3-CD33+), with ≥10% of the T lymphocytes expressing the transgene. The transduced T lymphocytes demonstrate cytotoxicity against follicle-stimulating hormone receptor (FSHR)-expressing cells
cell-based gene therapy (antineoplastic)

liraltagène autoleucel

lymphocytes T autologues enrichis en CD4+/CD8+, dérivés de matériel de leucaphérèse, transduits avec un vecteur rétroviral gamma dérivé du virus des cellules souches murines (MSCV), non réplicatif, codant l'hormone folliculo-stimulante (FSH) à codons optimisés (sous-unités FSHβ et CGα, liées par un espaceur glycine/sérine), précédé du peptide signal FSHβ, et fusionné à un domaine charnière et un domaine transmembranaire CD8α, un domaine co-stimulateur 4-1BB et un domaine de signalisation CD3ζ, sous le contrôle du promoteur LTR du virus de la leucémie murine Moloney (MMLV). Le vecteur possède de répétitions terminales longues (LTRs) dérivées du MSCV et un signal d'encapsidation (Ψ+) dérivé du MMLV et possède une séquence accepteur d'épissage immédiatement en amont du codon d'initiation. Une séquence Kozak précède le transgène.

	Le matériel de leucaphérèse est enrichi en fraction lymphocytaire avant l'activation avec de l'anti-CD3 et de l'interleukine 2 (IL-2). Les cellules sont ensuite transduites avec le vecteur rétroviral et expansées dans un milieu de croissance contenant de l'anti-CD3 et de l'IL-2. La suspension cellulaire est constituée de lymphocytes T (≥90% CD3+; ≤0,5% CD14+, ≤0,08% CD19+, ≤5% CD3-CD56+, ≤0,55% CD3-CD33+), avec ≥10% des lymphocytes T exprimant le transgène. Les lymphocytes T transduits démontrent une cytotoxicité contre les cellules exprimant le récepteur de l'hormone folliculo-stimulante (FSHR) *thérapie génique à base de cellules (antinéoplasique)*
liraltagén autoleucel	linfocitos T CD4+/CD8+ enriquecidos autólogos derivados de material de leucoaféresis, transducidos con un vector gamma retroviral derivado del virus de células madre murino (MSCV), no replicativo, que codifica, con codones optimizados, la hormona estimuladora del folículo (FSH) (subunidades FSHβ an CGα, unidas mediante un espaciador glicina/serina), precedido por el péptido señal de FSHβ y fusionado a un dominio bisagra y transmembrana de CD8α, un dominio coestimulador de 4-1BB y un dominio de señalización de CD3ζ, bajo el control del promotor LTR del virus de la leucemia murina de Moloney (MMLV). El vector tiene repeticiónes terminales largas (LTRs) derivadas del MSCV y una señal empaquetadora (Ψ+) derivada del MMLV y tiene una secuencia aceptora del procesamiento inmediatamente antes del codón de iniciación. Una secuencia Kozack precede al transgén. El material de leucoaféresis se enriquece para la fracción de linfocitos antes de la activación con anti-CD3 e interleuquina 2 (IL-2). Las células después se transducen con el vector retroviral y se expanden en medio que contiene anti-CD3 e IL-2. La suspensión celular consiste en linfocitos T (≥90% CD3+; ≤0.5% CD14+, ≤0.08% CD19+, ≤5% CD3-CD56+, ≤0.55% CD3-CD33+), con ≥10% de los linfocitos T que expresan el transgén. Los linfocitos T transducidos muestran actividad citotóxica frente a células que expresan el receptor de la hormona estimuladora del folículo (FSHR) *terapia génica basada en células (antineoplásico)*
lirucitinibum lirucitinib	(*R*)-ethyl(imino)({*trans*-4-[methyl(7*H*-pyrrolo[2,3-*d*]pyrimidin-4-yl)amino]cyclohexyl}methyl)-λ^6-sulfanone *Janus tyrosine kinase inhibitor, anti-inflammatory*
lirucitinib	(*R*)-éthyl(imino)({*trans*-4-[méthyl(7*H*-pyrrolo[2,3-*d*]pyrimidin-4-yl)amino]cyclohexyl}méthyl)-λ^6-sulfanone *inhibiteur de la tyrosine kinase Janus, anti-inflammatoire*

lirucitinib

(*R*)-etil(imino)({*trans*-4-[metil(7*H*-pirrolo[2,3-*d*]pirimidin-4-il)amino]ciclohexil}metil)-λ^6-sulfanona
inhibidor de la tirosina kinasa Janus, antiinflamatorio

$C_{16}H_{25}N_5OS$ 2458115-78-9

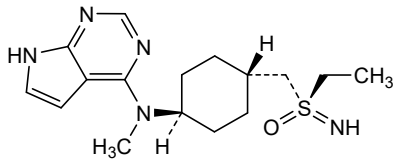

lixosiconum

lixosicone

3β-[(4-methoxyphenyl)methoxy]pregn-5-en-20-one
cannabinoid CB1 receptor signalling inhibitor

lixosicone

3β-[(4-méthoxyphényl)méthoxy]prégn-5-én-20-one
inhibiteur de signalisation du récepteur cannabinoïde CB1

lixosicona

3β-[(4-metoxifenil)metoxi]pregn-5-en-20-ona
inhibidor de la señalización del receptor cannabinoide CB1

$C_{29}H_{40}O_3$ 1610878-71-1

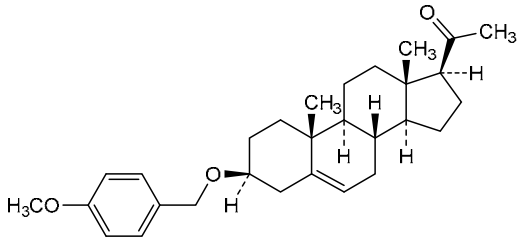

lomonitinibum

lomonitinib

3-(3,4-dimethoxyphenyl)-1-(1,2,3,4-tetrahydroisoquinolin-7-yl)-1*H*-pyrazolo[4,3-*c*]quinoline
tyrosine kinase inhibitor, antineoplastic

lomonitinib

3-(3,4-diméthoxyphényl)-1-(1,2,3,4-tétrahydroisoquinoléin-7-yl)-1*H*-pyrazolo[4,3-*c*]quinoléine
inhibiteur de tyrosine kinase, antinéoplasique

lomonitinib

3-(3,4-dimetoxifenil)-1-(1,2,3,4-tetrahidroisoquinolein-7-il)-1*H*-pirazolo[4,3-*c*]quinoleína
inhibidor de la tirosina kinasa, antineoplásico

$C_{27}H_{24}N_4O_2$ 2923221-56-9

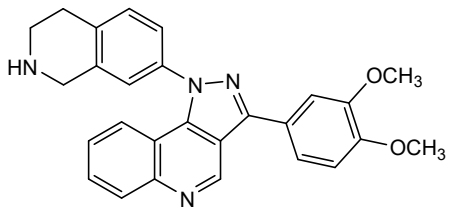

lonitoclaxum

lonitoclax — 5-(5-chloro-2-{(3*S*)-3-[(morpholin-4-yl)methyl]-3,4-dihydroisoquinoline-2(1*H*)-carbonyl}phenyl)-*N*-(4-hydroxyphenyl)-*N*-[(3-methoxy-2-methylphenyl)methyl]-1,2-dimethyl-1*H*-pyrrole-3-carboxamide
B-cell lymphoma 2 (Bcl-2) inhibitor, antineoplastic

lonitoclax — 5-(5-chloro-2-{(3*S*)-3-[(morpholin-4-yl)méthyl]-3,4-dihydroisoquinoléine-2(1*H*)-carbonyl}phényl)-*N*-(4-hydroxyphényl)-*N*-[(3-méthoxy-2-méthylphényl)méthyl]-1,2-diméthyl-1*H*-pyrrole-3-carboxamide
inhibiteur du lymphome à cellules B 2 (Bcl-2), antinéoplasique

lonitoclax — 5-(5-cloro-2-{(3*S*)-3-[(morfolin-4-il)metil]-3,4-dihidroisoquinoleína-2(1*H*)-carbonil}fenil)-*N*-(4-hidroxifenil)-1,2-dimetil-*N*-[(2-metil-3-metoxifenil)metil]-1*H*-pirrol-3-carboxamida
inhibidor del linfoma de células B 2 (Bcl-2), antineoplásico

$C_{43}H_{45}ClN_4O_5$ 2952589-57-8

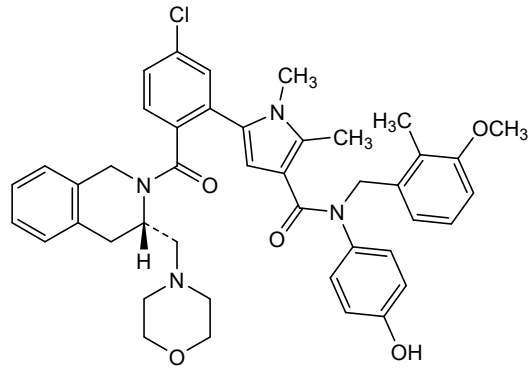

lumekefamidum

lumekefamide — L-tyrosyl-D-arginyl-L-phenylalanylglycinamide
μ-opioid receptor agonist, analgesic

lumékéfamide — L-tyrosyl-D-arginyl-L-phénylalanylglycinamide
agoniste du récepteur opioïde μ, analgésique

lumekefamida — L-tirosil-D-arginil-L-fenilalanilglicinamida
agonista del receptor opioide μ, analgésico

$C_{26}H_{36}N_8O_5$ 100304-60-7

H—Tyr—D-Arg—Phe—Gly—NH_2

lunsotogenum parvecum #

lunsotogene parvec	two recombinant, non-replicating adeno-associated virus serotype 1 (rAAV1) vectors containing the 5' and 3' portions, respectively, of the wild-type human otoferlin (OTOF) isoform 5 gene. The 5' vector contains exons 1-20 of the OTOF gene under expression control of the hair cell-specific myosin 15 (Myo15) promoter, followed by a splice donor and alkaline phosphatase homology region 3' to the transgene. The 3' vector contains the alkaline phosphatase homology region and a splice acceptor, followed by exons 21-45, and 47 of the OTOF gene and is terminated by a bovine somatotropin growth hormone polyadenylation sequence. Both vectors are flanked by AAV2 inverted terminal repeats *gene therapy (otoferlin-related auditory neuropathy)*
lunsotogène parvec	deux vecteurs recombinants de virus adéno-associés de sérotype 1 (rAAV1), non réplicatifs, contenant les parties 5' et 3', respectivement, de l'isoforme 5 du gène de l'otoferline humaine sauvage (OTOF). Le vecteur 5' contient les exons 1 à 20 du gène OTOF sous le contrôle de l'expression du promoteur de la myosine 15 (Myo15) spécifique des cellules ciliées, suivis d'un donneur d'épissage et d'une région d'homologie de la phosphatase alcaline 3' du transgène. Le vecteur 3' contient la région d'homologie de la phosphatase alcaline et un accepteur d'épissage, suivi des exons 21-45 et 47 du gène OTOF et se termine par une séquence de polyadénylation de l'hormone de croissance somatotropine bovine. Les deux vecteurs sont flanqués des répétitions terminales inversées de l'AAV2 *thérapie génique (neuropathie auditive liée à l'otoferline)*
lunsotogén parvec	dos vectores de virus adenoasociado del serotipo 1, recombinantes (rAAV1), no replicativos, que contienen las porciones 5' y 3', respectivamente, del tipo silvestre de la isoforma 5 del gen de la otoferlina (OTOF) humana. El vector 5' contiene los exones 1-20 del gen de OTOF bajo el control de expresión del promotor de la miosina 15 (Myio15) específica de células ciliadas, seguido de un dador del procesamiento y una región de homología de la fosfatasa alcalina 3' del transgén. El vector 3' contiene la región de homología de la fosfatasa alcalina y un aceptor de procesamiento, seguido de los exones 21-45 y 47 del gen de OTOF y se termina por una secuencia de poliadenilación de la hormona de crecimiento somatotropina bovina. Ambos vectores están flanqueados por las repeticiones terminales invertidas del AAV2 *terapia génica (neuropatía auditiva relacionada con otoferlín)*

2907748-12-1

macupatidum

macupatide

L-tyrosyl-2-methylalanyl-L-α-glutamylglycyl-L-threonyl-L-phenylalanyl-L-isoleucyl-L-seryl-L-α-aspartyl-L-tyrosyl-L-seryl-L-isoleucyl-2-methyl-L-leucyl-L-leucyl-L-α-aspartyl-L-lysyl-*N*^{6}-(17-{[*N*-(19-carboxynonadecanoyl)- L-γ-glutamyl]amino}-10-oxo-3,6,12,15-tetraoxa-9-azaheptadecan-1-oyl)-L-lysyl-L-histidyl-L-glutaminyl-2-methylalanyl-L-α-aspartyl-L-phenylalanyl-L-valyl-L-α-glutamyl-3-(pyridine-4-yl)-L-alanyl-L-leucyl-L-leucyl-L-α-glutamyl-L-alanylglycyl-L-prolyl-L-seryl-L-serylglycyl-L-alanyl-L-prolyl-L-prolyl-L-prolyl- L-serinamide

gastric inhibitory polypeptide (GIP) receptor agonist, antidiabetic

macupatide

L-tyrosyl-2-méthylalanyl-L-α-glutamylglycyl-L-thréonyl-L-phénylalanyl-L-isoleucyl-L-séryl-L-α-aspartyl-L-tyrosyl-L-séryl-L-isoleucyl-2-méthyl-L-leucyl-L-leucyl-L-α-aspartyl-L-lysyl-*N*^{6}-(17-{[*N*-(19-carboxynonadécanoyl)- L-γ-glutamyl]amino}-10-oxo-3,6,12,15-tétraoxa-9-azaheptadécan-1-oyl)-L-lysyl-L-histidyl-L-glutaminyl-2-méthylalanyl-L-α-aspartyl-L-phénylalanyl-L-valyl-L-α-glutamyl-3-(pyridine-4-yl)-L-alanyl-L-leucyl-L-leucyl-L-α-glutamyl-L-alanylglycyl-L-prolyl-L-séryl-L-sérylglycyl-L-alanyl-L-prolyl-L-prolyl-L-prolyl- L-sérinamide

agoniste des récepteurs polypeptidiques inhibiteurs gastriques, antidiabétique

macupatida

L-tirosil-2-metilalanil-L-α-glutamlglicil-L-treonil-L-fenilalanil-L-isoleucil-L-seril-L-α-aspartil-L-tirosil-L-seril-L-isoleucil-2-metil-L-leucil-L-leucil-L-α-aspartil-L-lisil-*N*^{6}-(17-{[*N*-(19-carboxinonadecanoil)- L-γ-glutamil]amino}-10-oxo-3,6,12,15-tetraoxa-9-azaheptadecan-1-oil)-L-lisil-L-histidil-L-glutaminil-2-metilalanil-L-α-aspartil-L-fenilalanil-L-valil-L-α-glutamil-3-(piridina-4-il)-L-alanil-L-leucil-L-leucil-L-α-glutamil-L-alanilglicil-L-prolil-L-seril-L-serilglicil-L-alanil-L-prolil-L-prolil-L-prolil- L-serinamida

agonista del receptor del polipéptido inhibidor gástrico, antidiabético

$C_{232}H_{357}N_{49}O_{72}$ 2923558-68-1

YAEGTFISDY SILLDKKHQA DFVEXLLEAG PSSGAPPPS 39

Modified residues / Résidus modifiés / Restos modificados

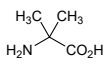

A (2, 20)
2-Me-L-Ala

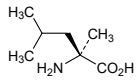

L (13)
2-Me-L-Leu

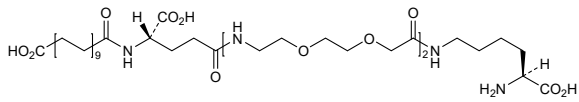

K (17)
N^6-(HO$_2$C-[CH$_2$]$_{18}$-CO-L-Glu-[NH-CH$_2$-CH$_2$-O-CH$_2$-CH$_2$-O-CH$_2$-CO]$_2$)-L-Lys

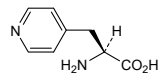

X (25)
pyridin-4-yl-L-Ala

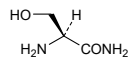

S (39)
L-Ser-NH$_2$

marpinersenum

marpinersen	*all-P-ambo*-2'-*O*-(2-methoxyethyl)-5-methyl-*P*-thiouridylyl-(3'→5')-2'-*O*-(2-methoxyethyl)guanylyl-(3'→5')-2'-*O*-(2-methoxyethyl)guanylyl-(3'→5')-2'-*O*-(2-methoxyethyl)adenylyl-(3'→5')-2'-*O*-(2-methoxyethyl)-5-methyluridylyl-(3'→5')-2'-*O*-(2-methoxyethyl)-5-methyluridylyl-(3'→5')-2'-deoxy-5-methyl-*P*-thiocytidylyl-(3'→5')-*P*-thiothymidylyl-(3'→5')-2'-deoxy-*P*-thioguanylyl-(3'→5')-*P*-thiothymidylyl-(3'→5')-2'-deoxy-*P*-thioadenylyl-(3'→5')-2'-deoxy-5-methyl-*P*-thiocytidylyl-(3'→5')-*P*-thiothymidylyl-(3'→5')-*P*-thiothymidylyl-(3'→5')-*P*-thiothymidylyl-(3'→5')-*P*-thiothymidylyl-(3'→5')-2'-*O*-(2-methoxyethyl)-5-methylcytidylyl-(3'→5')-2'-*O*-(2-methoxyethyl)-5-methyl-*P*-thiouridylyl-(3'→5')-2'-*O*-(2-methoxyethyl)-5-methyl-*P*-thiocytidylyl-(3'→5')-2'-*O*-(2-methoxyethyl)adenosine *ataxin-2 synthesis reducer, amyotrophic lateral sclerosis*
marpinersen	*tout-P-ambo*-2'-*O*-(2-méthoxyéthyl)-5-méthyl-*P*-thiouridylyl-(3'→5')-2'-*O*-(2-méthoxyéthyl)guanylyl-(3'→5')-2'-*O*-(2-méthoxyéthyl)guanylyl-(3'→5')-2'-*O*-(2-méthoxyéthyl)adénylyl-(3'→5')-2'-*O*-(2-méthoxyéthyl)-5-méthyluridylyl-(3'→5')-2'-*O*-(2-méthoxyéthyl)-5-méthyluridylyl-(3'→5')-2'-désoxy-5-méthyl-*P*-thiocytidylyl-(3'→5')-*P*-thiothymidylyl-(3'→5')-2'-désoxy-*P*-thioguanylyl-(3'→5')-*P*-thiothymidylyl-(3'→5')-2'-désoxy-*P*-thioadénylyl-(3'→5')-2'-désoxy-5-méthyl-*P*-thiocytidylyl-(3'→5')-*P*-thiothymidylyl-(3'→5')-*P*-thiothymidylyl-(3'→5')-*P*-thiothymidylyl-(3'→5')-2'-*O*-(2-méthoxyéthyl)-5-méthylcytidylyl-(3'→5')-2'-*O*-(2-méthoxyéthyl)-5-méthyl-*P*-thiouridylyl-(3'→5')-2'-*O*-(2-méthoxyéthyl)-5-méthyl-*P*-thiocytidylyl-(3'→5')-2'-*O*-(2-méthoxyéthyl)adénosine *réducteur de synthèse d'ataxine-2, sclérose latérale amyotrophique*
marpinersén	*todo-P-ambo*-5-metil-2'-*O*-(2-metoxietil)-*P*-tiouridilil-(3'→5')-2'-*O*-(2-metoxietil)guanilil-(3'→5')-2'-*O*-(2-metoxietil)guanilil-(3'→5')-2'-*O*-(2-metoxietil)adenilil-(3'→5')-5-metil-2'-*O*-(2-metoxietil)uridilil-(3'→5')-5-metil-2'-*O*-(2-metoxietil)uridilil-(3'→5')-2'-desoxi-5-metil-*P*-tiocitidilil-(3'→5')-*P*-tiotimidilil-(3'→5')-2'-desoxi-*P*-tioguanilil-(3'→5')-*P*-tiotimidilil-(3'→5')-2'-desoxi-*P*-tioadenilil-(3'→5')-2'-desoxi-5-metil-*P*-tiocitidilil-(3'→5')-*P*-tiotimidilil-(3'→5')-*P*-tiotimidilil-(3'→5')-*P*-tiotimidilil-(3'→5')-5-metil-2'-*O*-(2-metoxietil)citidilil-(3'→5')-5-metil-2'-*O*-(2-metoxietil)-*P*-tiouridilil-(3'→5')-5-metil-2'-*O*-(2-metoxietil)-*P*-tiocitidilil-(3'→5')-2'-*O*-(2-metoxietil)adenosina *reductor de la síntesis de ataxina 2, esclerosis lateral amiotrófica*

$C_{230}H_{319}N_{62}O_{132}P_{19}S_{13}$ 2757908-12-4

(3'-5')*U*=G-G-A-*U*-*U*-d*C*=dT=dG=dT=dA=d*C*=dT=dT=dT=dT=*C*-*U*=*C*=A

N : nucleoside / nucléoside / nucleósido
dN : 2'-deoxy-N / 2'-désoxy-N / 2'-desoxi-N
N : 5-methyl-N / 5-méthyl-N / 5-metil-N
N : 2'-*O*-(2-methoxyethyl)-N / 2'-*O*-(2-méthoxyéthyl)-N / 2'-*O*-(metoxietil)-N
– : –PO(OH)– =: –PO(SH)–

mazisotinum

mazisotine (1*R*,5*S*,6*r*)-*N*-{2-methyl-1-[(3-methylpyridin-2-yl)oxy]propan-2-yl}-3-azabicyclo[3.1.0]hexane-6-carboxamide
somatostatin receptor receptor agonist

mazisotine (1*R*,5*S*,6*r*)-*N*-{2-méthyl-1-[(3-méthylpyridin-2-yl)oxy]propan-2-yl}-3-azabicyclo[3.1.0]hexane-6-carboxamide
agoniste des récepteurs de la somatostatine

mazisotina (1*R*,5*S*,6*r*)-*N*-{2-metil-1-[(3-metilpiridin-2-il)oxi]propan-2-il}-3-azabiciclo[3.1.0]hexano-6-carboxamida
agonista del receptor de somatostatina

$C_{16}H_{23}N_3O_2$ 1638588-92-7

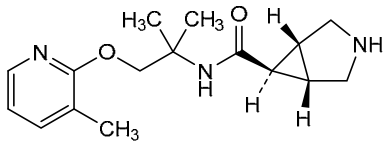

milpecitinibum

milpecitinib *N*-(3-{4-[5-(pyrrolidine-1-carbonyl)-1*H*-pyrrol-3-yl]-1,3-thiazol-2-yl}phenyl)acetamide
Janus tyrosine kinase inhibitor, anti-inflammatory (veterinary use)

milpécitinib *N*-(3-{4-[5-(pyrrolidine-1-carbonyl)-1*H*-pyrrol-3-yl]-1,3-thiazol-2-yl}phényl)acétamide
inhibiteur de tyrosine kinase Janus, anti-inflammatoire (usage vétérinaire)

milpecitinib *N*-(3-{4-[5-(pirrolidina-1-carbonil)-1*H*-pirrol-3-il]-1,3-tiazol-2-il}fenil)acetamida
inhibidor de la tirosina kinasa Janus, antiinflamatorio (uso veterinario)

$C_{20}H_{20}N_4O_2S$ 1415819-54-3

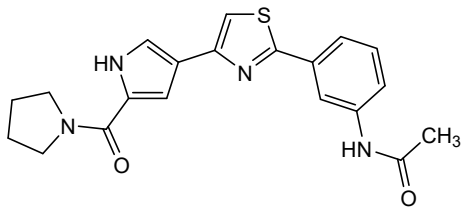

mirivadelgatum

mirivadelgat — {2-[4-(cyclopropylmethoxy)-3-{[(3-fluoro-4-methoxyphenyl)methyl]carbamoyl}phenyl]pyridin-3-yl}methyl L-valinate
aldehyde dehydrogenase 2 activator, antianaemic

mirivadelgat — L-valinate de {2-[4-(cyclopropylméthoxy)-3-{[(3-fluoro-4-méthoxyphényl)méthyl]carbamoyl}phényl]pyridin-3-yl}méthyle
activateur de l'aldéhyde déshydrogénase-2, antianémique

mirivadelgat — L-valinato de {2-[4-(ciclopropilmetoxi)-3-{[(3-fluoro-4-metoxifenil)metil]carbamoil}fenil]piridin-3-il}metilo
activador de la aldehido deshidrogenasa 2, antianémico

$C_{30}H_{34}FN_3O_5$ 1804941-96-5

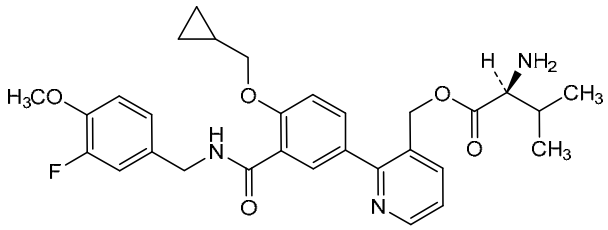

mivocabtagenum autoleucelum #

mivocabtagene autoleucel — autologous CD4+/CD8+ enriched T lymphocytes derived from leukapheresis material, transduced with a self-inactivating, non-replicating lentiviral vector encoding a CD19 targeting chimeric antigen receptor (CAR) comprising a CD8 alpha (CD8α) signal peptide, a single-chain variable fragment (scFv) derived from the human anti-CD19 monoclonal antibody clone 47G4, a CD8α hinge and transmembrane domain, a CD28 cytoplasmic co-stimulatory domain, and a CD3-zeta (CD3ζ) signaling domain, under control of the murine stem cell virus promoter.
The construct is flanked by 5' and 3' long terminal repeats (LTRs) and also contains a Ψ packaging signal, a Rev response element (RRE), a central polypurine tract (cPPT) sequence /central termination sequence (CTS) and an optimised Woodchuck hepatitis virus posttranscriptional regulatory element. The vector is pseudotyped with vesicular stomatitis virus (VSV) G glycoprotein.
The leukapheresis material is enriched for CD4+ and CD8+ T lymphocytes by positive immunoselection prior to activation with CD3 and CD28 agonists in growth media containing human serum, interleukin 7 (IL-7) and interleukin 5 (IL-5). The cells are then transduced with the lentiviral vector and expanded in growth media containing interleukin 7 (IL-7) and interleukin 5 (IL-5). The cell suspension consists of T lymphocytes (>80%), with greater than 10% of the T lymphocytes expressing the CAR-CD19 transgene. The transduced T lymphocytes demonstrate cytotoxicity against CD19-expressing cells and secrete interferon gamma (IFN-γ) and interleukin 2 (IL-2)
cell-based gene therapy (antineoplastic)

mivocabtagène autoleucel	lymphocytes T autologues enrichis en CD4+/CD8+ dérivés de matériel obtenu par leucaphérèse, transduits avec un vecteur lentiviral auto-inactivant et non réplicatif codant un récepteur antigénique chimérique (RAC) ciblant CD19, comprenant un peptide signal CD8 alpha (CD8α), un fragment variable à chaîne unique (scFv) dérivé du clone 47G4 d'anticorps monoclonal anti-CD19 humain, un domaine charnière et transmembranaire CD8α, un domaine co-stimulateur cytoplasmique CD28 et un domaine de signalisation CD3-zêta (CD3ζ), sous le contrôle du promoteur du virus des cellules souches murines. La construction est flanquée de répétitions terminales longues (LTRs) en 5' et en 3' et contient également un signal d'empaquetage Ψ, un élément de réponse Rev (RRE), une séquence de tractus polypurine central (cPPT)/séquence de terminaison centrale (CTS) et et un élément de régulation post-transcriptionnel optimisé du virus de l'hépatite de la marmotte. Le vecteur est pseudotypé avec la glycoprotéine G du virus de la stomatite vésiculaire (VSV). Le matériel de leucaphérèse est enrichi en lymphocytes T CD4+ et CD8+ par immunosélection positive avant activation avec des agonistes CD3 et CD28 dans un milieu de croissance contenant du sérum humain, de l'interleukine 7 (IL-7) et de l'interleukine 5 (IL-5). Les cellules sont ensuite transduites avec le vecteur lentiviral et expansées dans un milieu de croissance contenant de l'interleukine 7 (IL-7) et de l'interleukine 5 (IL-5). La suspension cellulaire est constituée de lymphocytes T (>80%), avec plus de 10% des lymphocytes T exprimant le transgène CAR-CD19. Les lymphocytes T transduits démontrent une cytotoxicité contre les cellules exprimant CD19 et sécrètent de l'interféron gamma (IFN-γ) et de l'interleukine 2 (IL-2) *thérapie génique à base de cellules (antinéoplasique)*
mivocabtagén autoleucel	linfocitos T CD4+/CD8+ autólogos enriquecidos, derivados de material de leucoaféresis, transducidos con un vector lentiviral auto inactivante, no replicativo, que codifica un receptor de antígenos quimérico (CAR) dirigido a CD19, que consta de un péptido señal de CD8 alfa (CD8α), un fragmento variable de cadena sencilla (scFv) derivado del anticuerpo monoclonal anti-CD19 clon 47G4, un dominio bisagra y transmembrana de CD8α, un dominio coestimulador citoplásmico de CD28 y un dominio de señalización de CD3-zeta (CD3ζ), bajo el control del promotor del virus de células madre murino. El constructo está flanqueado por repeticiones terminales largas (LTRs) en 5' y 3' y también contiene una señal de empaquetamiento ψ, un elemento de respuesta Rev (RRE), una secuencia de tracto de poli-purina (cPPT) central/terminación central (CTS) y un elemento regulador post-transcripcional del virus de la hepatitis de la marmota (WPRE) optimizado. El vector está seudotipado con la glicoproteína G del virus de la estomatitis vesicular (VSV).

El material de leucoaféresis se enriquece en linfocitos T CD4+ y CD8+ mediante inmunoselección positiva antes de la activación con agonistas de CD3 y CD28 en medio de crecimiento que contiene suero humano, interleuquina 7 (IL-7) e interleuquina 5 (IL-5). Las células se transducen a continuación con el vector lentiviral y se expanden en medio de crecimiento que contiene interleuquina 7 (IL-7) e interleuquina 5 (IL-5). La suspensión celular consiste en linfocitos T (≥80%) con más del 10% de los linfocitos T que expresan el transgén del CAR-CD19. Los linfocitos T transducidos muestran citotoxicidad frente a células que expresan CD19 y secretan interferón gamma (IFN-γ) e interleuquina 2 (IL-2)
terapia génica basada en células (antineoplásico)

moflerafuspum alfa #

moflerafusp alfa

human signal regulatory protein alpha (SIRPα) variant V2 D1 domain, (SIRPα V2D1) fragment 30-154 (1-125 in the actual sequence, comprising the first two extracellular loops of the D1 domain) variant (N^{110}>A^{80}) fused via peptide linker ^{126}GGGGSGGGGSGGGGS^{140} to the gamma 1 heavy chain of anti-(human programmed cell death 1 ligand 1 (PD-L1, programmed death ligand 1, PDCD1 ligand 1, B7 homolog 1, B7-H1, CD274)) (141-591) [VH (*Homo sapiens* IGHV1-46*01 -(IGHD) -IGHJ4*01, CDR-Kabat [5.17.12] (171-175.190-206.239-250)) (141-261) -*Homo sapiens* IGHG1*03 (CH1 (262-359), hinge (360-374), CH2 S^{442}>A, E^{477}>A, K^{478}>A (375-484), CH3 (485-589), CHS (590-591)) (262-591)], (364-214')-disulfide with kappa light chain anti-(human programmed cell death 1 ligand 1 (PD-L1, programmed death ligand 1, PDCD1 ligand 1, B7 homolog 1, B7-H1, CD274)) (1'-214') [V-KAPPA (*Homo sapiens* IGKV1-33*01 - IGKJ1*01, CDR-Kabat [11.7.9] (24'-34'.50'-56'.89'-97')) (1'-107') - *Homo sapiens* IGKC*01 (108'-214')]; dimer (370-370'':373-373'')-bisdisulfide, produced in Chinese hamster ovary (CHO) cells, cell line CHO-K1, glycoform alfa
antineoplastic

moflérafusp alfa

protéine régulatrice de signal alpha (SIRPα) humaine variant V2 domaine D1 (SIRPα V2D1) fragment 30-154 (1-125 dans la séquence réelle, comprenant les deux premières boucles extracellulaires du domaine D1), variant (N^{110}>A^{80}) fusionné, via un coupleur peptidique ^{126}GGGGSGGGGSGGGGS^{140}, à la chaîne lourde gamma 1 de l'anti-(ligand 1 de mort cellulaire programmée 1 humaine (PD-L1, ligand de mort programmée 1, ligand 1 PDCD1, homologue 1 B7, B7-H1, CD274)) (141-591) [VH (*Homo sapiens* IGHV1-46*01 -(IGHD) -IGHJ4*01, CDR-Kabat [5.17.12] (171-175.190-206.239-250)) (141-261) -*Homo sapiens* IGHG1*03 (CH1 (262-359), charnière (360-374), CH2 S^{442}>A, E^{477}>A, K^{478}>A (375-484), CH3 (485-589), CHS (590-591)) (262-591)], (364-214')-disulfure avec chaîne légère kappa anti-(ligand 1 de mort cellulaire programmée 1 humaine (PD-L1, ligand de mort programmée 1, ligand 1 PDCD1, homologue B7 1, B7-H1, CD274)) (1'-214') [V-KAPPA (*Homo sapiens* IGKV1-33*01 - IGKJ1*01, CDR-Kabat [11.7.9] (24'-34'.50'-56'.89'-97')) (1'- 107') - *Homo sapiens* IGKC*01 (108'-214')]; dimère (370-370'':373-373'')-bisdisulfure, produit dans les cellules d'ovaire de hamster chinois (CHO), lignée cellulaire CHO-K1, glycoforme alfa
antinéoplasique

moflerafusp alfa

proteína reguladora de señales alfa humana (SIRPα) variante V2 dominio D1 (SIRPα V2D1) fragmento 30-154 (1-125 en la secuencia real, que comprende los dos primeros bucles extracelulares del dominio D1) variante (N110>A80) fusionado mediante un enlazador peptídico ^{126}GGGGSGGGGSGGGGS^{140} a la cadena pesada gamma 1 de anti-(ligando 1 de muerte celular programada 1 humana (PD-L1, ligando 1 de muerte programada, ligando 1 de PDCD1, homólogo 1 de B7, B7-H1, CD274)) (141-591) [VH (*Homo sapiens* IGHV1-46*01 -(IGHD) - IGHJ4*01, CDR-Kabat [5.17.12] (171-175.190-206.239-250)) (141-261) - *Homo sapiens* IGHG1*03 (CH1 (262-359)), bisagra (360-374), CH2 S^{442}>A, E^{477}>A, K^{478}>A (375-484), CH3 (485-589), CHS (590-591)) (262-591)], (364 -214')-disulfuro con cadena ligera kappa anti-(ligando 1 de muerte celular programada 1 humana (PD-L1, ligando 1 de muerte programada, ligando 1 de PDCD1, homólogo 1 de B7, B7-H1, CD274)) (1'-214') [V-KAPPA (*Homo sapiens* IGKV1-33*01 -IGKJ1*01, CDR-Kabat [11.7.9] (24'-34'.50'-56'.89'-97')) (1'- 107') -*Homo sapiens* IGKC*01 (108'-214')]; dímero (370-370'':373-373'')-bisdisulfuro, producido en células de ovario de hámster chino (CHO), línea celular CHO-K1, glicoforma alfa

antineoplásico

2983848-20-8

Sequence / Séquence / Secuencia

SIRPα - IgG1 heavy chain

```
EEELQVIQPD KSVSVAAGES AILHCTVTSL IPVGPIQWFR GAGPARELIY   50
NQKEGHFPRV TTVSESTKRE NMDFSISISA ITPADAGTYY CVKFRKGSPD  100
TEFKSGAGTE LSVRAKPSAP VVSGPGGGGS GGGGSGGGGS QVQLVQSGAE  150
VKKPGASVKV SCKASGYTFT SNWMHWVRQA PGQGLEWMGM IHPNSGSSNY  200
NEKFKSRVTM TRDTSTSTVY MELSSLRSED TAVYYCARSY YGSSPYYFDY  250
WGQGTLVTVS SASTKGPSVF PLAPSSKSTS GGTAALGCLV KDYFPEPVTV  300
SWNSGALTSG VHTFPAVLQS SGLYSLSSVV TVPSSSLGTQ TYICNVNHKP  350
SNTKVDKRVE PKSCDKTHTC PPCPAPELLG GPSVFLFPPK PKDTLMISRT  400
PEVTCVVVDV SHEDPEVKFN WYVDGVEVHN AKTKPREEQY NATYRVVSVL  450
TVLHQDWLNG KEYKCKVSNK ALPAPIAATI SKAKGQPREP QVYTLPPSRE  500
EMTKNQVSLT CLVKGFYPSD IAVEWESNGQ PENNYKTTPP VLDSDGSFFL  550
YSKLTVDKSR WQQGNVFSCS VMHEALHNHY TQKSLSLSPG K           591
```

IgG1 light chain

```
DIQMTQSPSS LSASVGDRVT ITCRASQDII NYLNWYQQKP GKAPKLLIYY   50
TSRLHSGVPS RFSGSGSGTD FTFTISSLQP EDIATYYCQQ GDTLPWTFGQ  100
GTKVEIKRTV AAPSVFIFPP SDEQLKSGTA SVVCLLNNFY PREAKVQWKV  150
DNALQSGNSQ ESVTEQDSKD STYSLSSTLT LSKADYEKHK VYACEVTHQG  200
LSSPVTKSFN RGEC                                         214
```

Mutations / Mutations / Mutaciónes

SIRPα - IgG1 heavy chain: N^{110}>A^{80}, S^{442}>A, E^{477}>A, K^{478}>A

Peptide linker / Coupleur peptidique / Enlazador peptídico

^{126}GGGGSGGGGSGGGGS^{140}

Post-translation modifications

Disulfide bridges location / Position des ponts disulfure / Posiciones de los puentes disulfuro

Intra SIRPα-IgG1 heavy chain: 25-91, 162-236, 288-344, 405-465, 511-569, 25"-91", 162"-236", 288"-344", 405"-465", 511"-569"

Intra IgG1 light chain: 23'-88', 134'-194', 23'"-88'", 134'"-194'"

Inter IgG1 light chain - SIRPα-IgG1 heavy chain: 214'-364, 214'"-364"

Inter SIRPα-IgG1 heavy chain: 370-370", 373-373"

N-glycosylation sites / Sites de N-glycosylation / Posiciones de N-glicosilación

SIRPα-IgG1 heavy chain: 441, 441"

C-terminal lysine clipping / Coupure de la lysine C-terminale / Recorte de lisina C-terminal

SIRPα-IgG1 heavy chain: K591, K591"

moxetomidatum

moxetomidate

2-methoxyethyl 1-[(1*R*)-1-phenylethyl]-1*H*-imidazole-5-carboxylate
$GABA_A$ receptor agonist, hypnotic

moxétomidate

1-[(1*R*)-1-phényléthyl]-1*H*-imidazole-5-carboxylate de 2-méthoxyéthyle
agoniste du récepteur $GABA_A$, hypnotique

moxetomidato

1-[(1*R*)-1-feniletil]-1*H*-imidazol-5-carboxilato de 2-metoxietilo
agonista de los receptores $GABA_A$, hipnótico

$C_{15}H_{18}N_2O_3$ 1567838-90-7

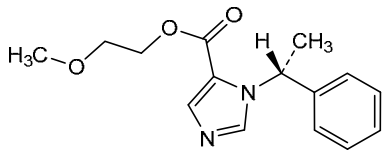

navlimetostatum

navlimetostat

(2*M*)-2-{4-[4-(aminomethyl)-1-oxo-1,2-dihydrophthalazin-6-yl]-1-methyl-1*H*-pyrazol-5-yl}-4-chloro-6-(cyclopropyloxy)-3-fluorobenzonitrile
antineoplastic

navlimétostat

(2*M*)-2-{4-[4-(aminométhyl)-1-oxo-1,2-dihydrophtalazin-6-yl]-1-méthyl-1*H*-pyrazol-5-yl}-4-chloro-6-(cyclopropyloxy)-3-fluorobenzonitrile
antinéoplasique

navlimetostat

(2*M*)-2-{4-[4-(aminometil)-1-oxo-1,2-dihidroftalazin-6-il]-1-metil-1*H*-pirazol-5-il}-4-cloro-6-(ciclopropiloxi)-3-fluorobenzonitrilo
antineoplásico

$C_{23}H_{18}ClFN_6O_2$ 2630904-45-7

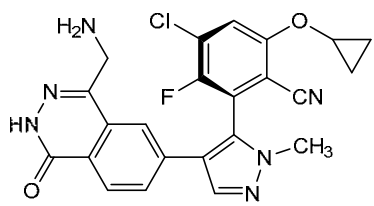

nedizantrepum

nedizantrep

1-({3-[(3*R*,5*R*)-5-(4-chlorophenyl)oxolan-3-yl]-1,2,4-oxadiazol-5-yl}methyl)-2,7-dimethyl-1,7-dihydro-6*H*-purin-6-one
transient receptor potential (TRP) ion channel antagonist

nédizantrep

1-({3-[(3*R*,5*R*)-5-(4-chlorophényl)oxolan-3-yl]-1,2,4-oxadiazol-5-yl}méthyl)-2,7-diméthyl-1,7-dihydro-6*H*-purin-6-one
antagoniste des canaux ioniques à potentiel de récepteur transitoire

nedizantrep

1-({3-[(3*R*,5*R*)-5-(4-clorofenil)oxolan-3-il]-1,2,4-oxadiazol-5-il}metil)-2,7-dimetil-1,7-dihidro-6*H*-purin-6-ona
antagonista del canal iónico del receptor de potencial transitorio

$C_{20}H_{19}ClN_6O_3$ 2376824-99-4

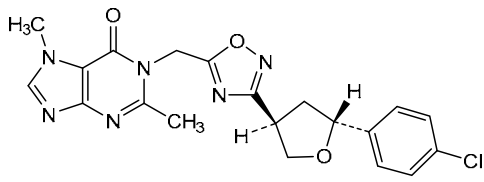

nelremagpranum

nelremagpran

3-{[2-chloro-4-(trifluoromethyl)phenoxy]methyl}-2-fluorobenzoic acid
Mas-related G protein-coupled receptor inverse agonist, anti-inflammatory

nelrémagpran

acide 3-{[2-chloro-4-(trifluorométhyl)phénoxy]méthyl}-2-fluorobenzoïque
agoniste inverse des récepteurs couplés aux protéines G liés à Mas, anti-inflammatoire

nelremagprán

ácido 3-{[2-cloro-4-(trifluorometil)fenoxi]metil}-2-fluorobenzoico
agonista inverso del receptor Mas acoplado a proteínas G, antiinflamatorio

$C_{15}H_9ClF_4O_3$ 2492595-24-9

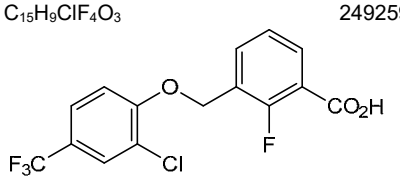

nesfrotamigum #

nesfrotamig

immunoglobulin (H-gamma1-scFvlh_L-kappa) dimer, anti-[*Homo sapiens* ERBB2 (receptor tyrosine-protein kinase erbB-2, epidermal growth factor receptor 2, EGFR2, HER2, HER-2, p185c-erbB2, NEU, CD340)] and anti-[*Homo sapiens* TNFRSF9 (TNF receptor superfamily member 9, 4-1BB, T cell antigen ILA, CD137)], humanized and *Homo sapiens* monoclonal antibody; bispecific, tetravalent;

H-gamma1 heavy chain anti-ERBB2 fused to a scFvlh anti-TNFRSF9 (1-719) [H-gamma1 heavy chain anti-ERBB2 humanized (1-450) [VH (*Homo sapiens* IGHV3-66*01 (81.6%) -(IGHD) -IGHJ4*01 (100%), CDR-IMGT [8.8.13] (26-33.51-58.97-109)) (1-120)-*Homo sapiens* IGHG1*03v (100%) G1m3>G1m17, nG1m1 CH1 K120, CH3 E12, M14 (CH1 R120>K (217) (121-218), hinge 1-15 (219-233), CH2 (234-343), CH3 E12 (359), M14 (361) (344-448), CHS (449-450)) (121-450)] -18-mer enneakis (glycyl-seryl) linker (451-468) -scFvlh anti-TNFRSF9 *Homo sapiens* (469-719), 11-scFv-v2 C120 (VL)-C49 (VH) [V-LAMBDA (*Homo sapiens* IGLV1-47*02 (91.8%) -IGLJ2*01 (90.9%) VL G120>C (571), CDR-IMGT [8.3.11] (493-501.519-521.558-568)) (469-578) -20-mer tetrakis(tetraglycyl-seryl) linker (579-598) -VH (*Homo sapiens* IGHV3-23*01 (93.9%) -IGHD -IGHJ4*01 (100%) VH G49>C (642), CDR-IMGT [8.8.14] (624-631.649-656.695-708)) (599-719)]]; (223-214')-disulfide with L-kappa light chain humanized (1'-214') [V-KAPPA (*Homo sapiens* IGKV1-39*01 (86.3%) -IGKJ1*01 (100%), CDR-IMGT [6.3.9] (27'-32'.50'-52'.89'-97')) (1'-107') -*Homo sapiens* IGKC*01 (100%) Km3 A45.1, V101 (C-KAPPA A45.1 (153'), V101 (191')) (108'-214')]; dimer (229-229'':232-232'')-bisdisulfide, produced in Chinese hamster ovary (CHO) cells, derived from the cell line CHO-K1, lacking the glutamine synthetase (GS-KO) gene, glycoform alfa
immunostimulant, antineoplastic

nesfrotamig

immunoglobuline (H-gamma1-scFvlh_L-kappa) dimère, anti-[*Homo sapiens* ERBB2 (récepteur tyrosine-protéine kinase erbB-2, récepteur 2 du facteur de croissance épidermique, EGFR2, HER2, HER-2, p185c-erbB2, NEU, CD340)] et anti-[*Homo sapiens* TNFRSF9 (membre 9 de la superfamille des récepteurs du TNF, 4-1BB, antigène ILA des cellules T, CD137)], anticorps monoclonal humanisé et *Homo sapiens*; bispécifique, tétravalent;
chaîne lourde H-gamma1 anti-ERBB2 fusionnée à un scFvlh anti-TNFRSF9 (1-719) [H-gamma1 chaîne lourde anti-ERBB2 humanisée (1-450) [VH (*Homo sapiens* IGHV3-66*01 (81.6%) -(IGHD) -IGHJ4*01 (100%), CDR-IMGT [8.8.13] (26-33.51-58.97-109)) (1-120) -*Homo sapiens* IGHG1*03v (100%) G1m3>G1m17, nG1m1 CH1 K120, CH3 E12, M14 (CH1 R120>K (217) (121-218), charnière 1-15 (219-233), CH2 (234-343), CH3 E12 (359), M14 (361) (344-448), CHS (449-450)) (121-450)] -18-mer énnéakis(glycyl-séryl) linker (451-468) -scFvlh anti-TNFRSF9 *Homo sapiens* (469-719), 11-scFv-v2 C120 (VL)-C49 (VH) [V-LAMBDA (*Homo sapiens* IGLV1-47*02 (91.8%) -IGLJ2*01 (90.9%) VL G120>C (571), CDR-IMGT [8.3.11] (493-501.519-521.558-568)) (469-578) -20-mer tétrakis(tétraglycyl-séryl) linker (579-598) -VH (*Homo sapiens* IGHV3-23*01 (93.9%) -IGHD -IGHJ4*01 (100%) VH G49>C (642), CDR-IMGT [8.8.14] (624-631.649-656.695-708)) (599-719)]]; (223-214')-disulfure avec la chaîne légère L-kappa humanisée (1'-214') [V-KAPPA (*Homo sapiens* IGKV1-39*01 (86.3%) -IGKJ1*01 (100%), CDR-IMGT [6.3.9] (27'-32'.50'-52'.89'-97')) (1'-107') -*Homo sapiens* IGKC*01 (100%) Km3 A45.1, V101 (C-KAPPA A45.1 (153'), V101 (191')) (108'-214')]; dimère (229-229'':232-232'')-bisdisulfure, produit dans des cellules ovariennes de hamster chinois (CHO), dérivant de la lignée cellulaire CHO-K1, ne présentant pas le gène de la glutamine synthétase (GS-KO), glycoforme alfa
immunostimulant, antinéoplasique

nesfrotamig

inmunoglobulina (H-gamma1-scFvlh_L-kappa) dímero, anti-[*Homo sapiens* ERBB2 (receptor tirosina-proteína kinasa erbB-2, receptor 2 del factor de crecimiento epidérmico, EGFR2, HER2, HER-2, p185c-erbB2, NEU, CD340)] y anti-[*Homo sapiens* TNFRSF9 (miembro 9 de la superfamilia de los receptores del TNF, 4-1BB, antígeno ILA de las células, CD137)],

anticuerpo monoclonal humanizado y *Homo sapiens*; biespecífico, tetravalente;
cadena pesada H-gamma1 anti-ERBB2 fusionada con un scFvlh anti-TNFRSF9 (1-719) [H-gamma1 cadena pesada anti-ERBB2 humanizada (1-450) [VH (*Homo sapiens* IGHV3-66*01 (81.6%) -(IGHD) -IGHJ4*01 (100%), CDR-IMGT [8.8.13] (26-33.51-58.97-109)) (1-120)-*Homo sapiens* IGHG1*03v (100%) G1m3>G1m17, nG1m1 CH1 K120, CH3 E12, M14 (CH1 R120>K (217) (121-218), bisagra 1-15 (219-233), CH2 (234-343), CH3 E12 (359), M14 (361) (344-448), CHS (449-450)) (121-450)] -18-mer eneakis(glicil-seril) enlace (451-468) -scFvlh anti-TNFRSF9 *Homo sapiens* (469-719), 11-scFv-v2 C120 (VL)-C49 (VH) [V-LAMBDA (*Homo sapiens* IGLV1-47*02 (91.8%) -IGLJ2*01 (90.9%) VL G120>C (571), CDR-IMGT [8.3.11] (493-501.519-521.558-568)) (469-578) -20-mer tetrakis(tetraglicil-seril) enlace(579-598) -VH (*Homo sapiens* IGHV3-23*01 (93.9%) -IGHD -IGHJ4*01 (100%) VH G49>C (642), CDR-IMGT [8.8.14] (624-631.649-656.695-708)) (599-719)]]; (223-214')-disulfuro con la cadena ligera L-kappa humanizada (1'-214') [V-KAPPA (*Homo sapiens* IGKV1-39*01 (86.3%) -IGKJ1*01 (100%), CDR-IMGT [6.3.9] (27'-32'.50'-52'.89'-97')) (1'-107') -*Homo sapiens* IGKC*01 (100%) Km3 A45.1, V101 (C-KAPPA A45.1 (153'), V101 (191')) (108'-214')]; dímero (229-229":232-232")-bisdisulfuro, producido en las células ováricas de hámster chino (CHO), línea celular derivada de CHO-K1, en ausencia del gen glutamina sintetasa (GS-KO), forma glicosilada alfa
inmunoestimulante, antineoplásico

2966936-23-0

Heavy chain / Chaîne lourde / Cadena pesada: fused H-gamma1 anti-ERBB2 -scFvlh anti-TNFRSF9 (H, H")

```
EVQLVESGGG LVQPGGSLRL SCAASGFNIK DTYIHWVRQA PGKGLEWVAR  50
IYPTNGYTRY ADSVKGRFTI SADTSKNTAY LQMNSLRAED TAVYYCSRWG 100
GDGFYAMDYW GQGTLVTVSS ASTKGPSVFP LAPSSKSTSG GTAALGCLVK 150
DYFPEPVTVS WNSGALTSGV HTFPAVLQSS GLYSLSSVVT VPSSSLGTQT 200
YICNVNHKPS NTKVDKRVEP KSCDKTHTCP PCPAPELLGG PSVFLFPPKP 250
KDTLMISRTP EVTCVVVDVS HEDPEVKFNW YVDGVEVHNA KTKPREEQYN 300
STYRVVSVLT VLHQDWLNGK EYKCKVSNKA LPAPIEKTIS KAKGQPREPQ 350
VYTLPPSREE MTKNQVSLTC LVKGFYPSDI AVEWESNGQP ENNYKTTPPV 400
LDSDGSFFLY SKLTVDKSRW QQGNVFSCSV MHEALHNHYT QKSLSLSPGK 450
GGSGGGGSGG GGSGGGGSQS VLTQPPSASG TPGQRVTISC SGSSSNIGSN 500
YVYWYQQLPG TAPKLLIYAN NQRPSGVPDR FSGSKSGTSA SLAISGLRSE 550
DEADYYCATW DDSLSGYVFG TGTKLTVLGT GTGSGTGSGT GSDVQLVESG 600
GGLVQPGGSL RLSCAASGFT FSSYAMSWVR QAPGKGLEWV SAISGSGGST 650
YYADSVKGRF TISRDNSKNT LYLQMNSLRA EDTAVYYCAK VTYFDAFDIW 700
GQGTMVTVSS                                            719
```

Light chain / Chaîne légère / Cadena ligera: L-kappa (L', L"')

```
DIQMTQSPSS LSASVGDRVT ITCRASQSVN TAVAWYQQKP GKAPKLLIYS  50
ASFLYSGVPS RFSGSRSGTE FTLTISSLQP EDFATYYCQQ HYTTPPTFGQ 100
GTKVEIKRTV AAPSVFIFPP SDEQLKSGTA SVVCLLNNFY PREAKVQWKV 150
DNALQSGNSQ ESVTEQDSKD STYSLSSTLT LSKADYEKHK VYACEVTHQG 200
LSSPVTKSFN RGEC                                       214
```

Post-translational modifications
Disulfide bridges location / Position des ponts disulfure / Posiciones de los puentes disulfuro
Intra-H (C23-C104) 22-96 147-203 264-324 370-428
22"-96" 147"-203" 264"-324" 370"-428"
490-557 620-694
490"-557" 620"-694"
Intra-H scFv C120 (VL)-C49 (VH)* 571-642
571"-642"
Intra-L (C23-C104) 23'-88' 134'-194'
23'"-88"' 134'"-194'"
Inter-H-L ((h 5-CL 126)) 223-214' 223"-214'"
Inter-H-H (h 11, h 14) 229-229" 232-232"
*engineered additional disulfide bond C120 (VL)-C49 (VH) to stabilize the scFv (variant 11-scFv-v2).

N-glycosylation sites / Sites de N-glycosylation / Posiciones de N-glicosilación
H CH2 N84.4: 300, 300"
Fucosylated complex bi-antennary CHO-type glycans / glycanes de type CHO bi-antennaires complexes fucosylés / glicanos de tipo CHO biantenarios complejos fucosilados.

netanasvirum

netanasvir

methyl {(2*S*)-1-[(1^2*S*,1^5*S*,5^2*S*,5^4*S*,7*R*)-7-[(methoxycarbonyl)amino]-5^4-(methoxymethyl)-1^5-methyl-6-oxo-3^2,3^3-dihydro-2^1*H*,3^1*H*,4^1*H*-2(2,7)-naphtho[1,2-*d*]imidazola-4(4,2)-imidazola-1(2),5(2,1)-dipyrrolidina-3(4,7)-indena-8(1)-benzenaoctaphan-1^1-yl]-3-methyl-1-oxobutan-2-yl}carbamate
antiviral

nétanasvir

{(2*S*)-1-[(1^2*S*,1^5*S*,5^2*S*,5^4*S*,7*R*)-7-[(méthoxycarbonyl)amino]-5^4-(méthoxyméthyl)-1^5-méthyl-6-oxo-3^2,3^3-dihydro-2^1*H*,3^1*H*,4^1*H*-2(2,7)-naphto[1,2-*d*]imidazola-4(4,2)-imidazola-1(2),5(2,1)-dipyrrolidina-3(4,7)-indéna-8(1)-benzénaoctaphan-1^1-yl]-3-méthyl-1-oxobutan-2-yl}carbamate de méthyle
antiviral

netanasvir

{(2*S*)-3-metil-1-[(1^2*S*,1^5*S*,5^2*S*,5^4*S*,7*R*)-1^5-metil-7-[(metoxicarbonil)amino]-5^4-(metoximetil)-6-oxo-3^2,3^3-dihidro-2^1*H*,3^1*H*,4^1*H*-2(2,7)-nafto[1,2-*d*]imidazola-4(4,2)-imidazola-1(2),5(2,1)-dipirrolidina-3(4,7)-indena-8(1)-bencenaoctafan-1^1-il]-1-oxobutan-2-il}carbamato de metilo
antiviral

$C_{51}H_{58}N_8O_7$ 2007900-70-9

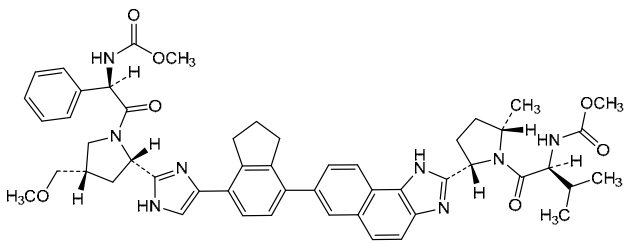

nivudirsenum

nivudirsen

all-P-ambo-5'-*O*-(1,10-dihydroxy-1-oxo-2,5,8-trioxa-1λ^5-phosphadecan-1-yl)-2'-*O*,4'-*C*-methylene-*P*-thioguanylyl-(3'→5')-2'-*O*,4'-*C*-methylene-*P*-thioguanylyl-(3'→5')-2'-*O*-methyl-*P*-thiouridylyl-(3'→5')-2'-*O*-methyl-*P*-thioadenylyl-(3'→5')-2'-*O*-methyl-*P*-thioadenylyl-(3'→5')-2'-*O*,4'-*C*-methylene-*P*-thioguanylyl-(3'→5')-2'-*O*-methyl-*P*-thiouridylyl-(3'→5')-2'-*O*-methyl-*P*-thiouridylyl-(3'→5')-2'-*O*,5-dimethyl-*P*-thiocytidylyl-(3'→5')-2'-*O*-methyl-*P*-thiouridylyl-(3'→5')-2'-*O*-methyl-*P*-thioguanylyl-(3'→5')-2'-*O*-methyl-*P*-thiouridylyl-(3'→5')-2'-*O*,5-dimethyl-*P*-thiocytidylyl-(3'→5')-2'-*O*,5-dimethyl-*P*-thiocytidylyl-(3'→5')-2'-*O*-methyl-*P*-thioadenylyl-(3'→5')-2'-*O*-methyl-*P*-thioadenylyl-(3'→5')-2'-*O*-methyl-*P*-thioguanylyl-(3'→5')-5-methyl-2'-*O*,4'-*C*-methylenecytidine
promotion of functional dystrophin synthesis

nivudirsen

tout-P-ambo-5'-*O*-(1,10-dihydroxy-1-oxo-2,5,8-trioxa-1λ^5-phosphadécan-1-yl)-2'-*O*,4'-*C*-méthylène-*P*-thioguanylyl-(3'→5')-2'-*O*,4'-*C*-méthylène-*P*-thioguanylyl-(3'→5')-2'-*O*-méthyl-*P*-thiouridylyl-(3'→5')-2'-*O*-méthyl-*P*-thioadénylyl-(3'→5')-2'-*O*-méthyl-*P*-thioadénylyl-(3'→5')-2'-*O*,4'-*C*-méthylène-*P*-thioguanylyl-(3'→5')-2'-*O*-méthyl-*P*-thiouridylyl-(3'→5')-2'-*O*-méthyl-*P*-thiouridylyl-(3'→5')-2'-*O*,5-diméthyl-*P*-thiocytidylyl-(3'→5')-2'-*O*-méthyl-*P*-thiouridylyl-(3'→5')-2'-*O*-méthyl-*P*-thioguanylyl-(3'→5')-2'-*O*-méthyl-*P*-thiouridylyl-(3'→5')-2'-*O*,5-diméthyl-*P*-thiocytidylyl

-(3'→5')-2'-*O*,5-diméthyl-*P*-thiocytidylyl-(3'→5')-2'-*O*-méthyl-*P*-thioadénylyl-(3'→5')-2'-*O*-méthyl-*P*-thioadénylyl-(3'→5')-2'-*O*-méthyl-*P*-thioguanylyl-(3'→5')-5-méthyl-2'-*O*,4'-*C*-méthylènecytidine
stimulation de la synthèse de dystrophine fonctionnelle

nivudirsén

todo-P-ambo-5'-*O*-(1,10-dihidroxi-1-oxo-2,5,8-trioxa-1λ^5-fosfadecan-1-il)-2'-*O*,4'-*C*-metileno-*P*-tioguanilil-(3'→5')-2'-*O*,4'-*C*-metileno-*P*-tioguanilil-(3'→5')-2'-*O*-metil-*P*-tiouridilil-(3'→5')-2'-*O*-metil-*P*-tioadenilil-(3'→5')-2'-*O*-metil-*P*-tioadenilil-(3'→5')-2'-*O*,4'-*C*-metileno-*P*-tioguanilil-(3'→5')-2'-*O*-metil-*P*-tiouridilil-(3'→5')-2'-*O*-metil-*P*-tiouridilil-(3'→5')-2'-*O*,5-dimetil-*P*-tiocitidilil-(3'→5')-2'-*O*-metil-*P*-tiouridilil-(3'→5')-2'-*O*-metil-*P*-tioguanilil-(3'→5')-2'-*O*-metil-*P*-tiouridilil-(3'→5')-2'-*O*,5-dimetil-*P*-tiocitidilil-(3'→5')-2'-*O*,5-dimetil-*P*-tiocitidilil-(3'→5')-2'-*O*-metil-*P*-tioadenilil-(3'→5')-2'-*O*-metil-*P*-tioadenilil-(3'→5')-2'-*O*-metil-*P*-tioguanilil-(3'→5')-5-metil-2'-*O*,4'-*C*-metilenocitidina
estimulación de la síntesis de distrofina funcional

$C_{199}H_{261}N_{67}O_{114}P_{18}S_{17}$ 3053113-45-1

R-G=G=U=A=A=G=U=U=m^{5}C=U=G=U=m^{5}C=m^{5}C=A=A=G=C

N: 2'-*O*-methyl-N / 2'-*O*-méthyl-N / 2'-*O*-metil-N
m^{5}N : 5-methyl-N / 5-méthyl-N / 5-metil-N
– : –PO(OH)– = : –PO(SH)–

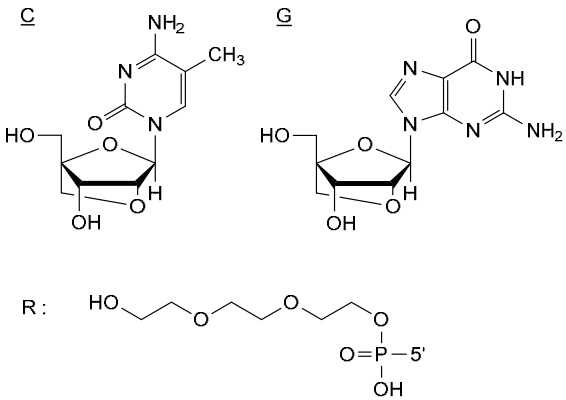

nufaleucelum
nufaleucel

human culture expanded activated autologous tumour-infiltrating lymphocytes (TIL), isolated from non-small cell lung cancer. The cells are mechanically isolated from resected tumour biopsies and culture-expanded using a two-step protocol consisting of a pre rapid expansion phase (Pre-REP) and a rapid expansion phase (REP) in serum-free media containing interleukin 2 (IL-2). During the REP, the cells are activated and expanded by culture on colloidal polymeric nanomatrix conjugated to humanized CD3 and CD28 agonists in media containing IL-2 in the absence of allogeneic irradiated feeder cells. The T lymphocytes (>80%) are a heterogeneous mixture of CD4+ and CD8+ T lymphocytes, predominantly with effector memory, central memory and effector cell subsets, and a low level of CD45+CD3-CD56+ natural killer (NK) cells (<10%). The T-lymphocytes demonstrate IFN-γ release (>1.0 fg/cell) after CD3/CD28 bead stimulation
cell therapy (antineoplastic)

nufaleucel

lymphocytes infiltrant la tumeur (LIT) autologues humains, activés et expansés en culture, isolés à partir du cancer du poumon non à petites cellules. Les cellules sont isolées mécaniquement à partir de biopsies tumorales réséquées et expansées en culture à l'aide d'un protocole en deux étapes comprenant une phase de pré-expansion rapide (Pre-REP) et une phase d'expansion rapide (REP) dans un milieu sans sérum contenant de l'interleukine 2 (IL-2). Au cours du REP, les cellules sont activées et expansées par culture sur nanomatrice polymère colloïdale conjuguée à des agonistes CD3 et CD28 humanisés, dans un milieu contenant de l'IL-2, en l'absence de cellules nourricières allogéniques irradiées. Les lymphocytes T (>80%) sont un mélange hétérogène de lymphocytes T CD4+ et CD8+, avec principalement des sous-types de cellules effectrices à mémoire, de mémoire centrale et de cellules effectrices, et d'un faible niveau de cellules tueuses naturelles (NK) CD45+CD3-CD56+ (<10%). Les lymphocytes T démontrent une libération d'IFN-γ (>1.0 fg/cellule) après stimulation par billes CD3/CD28
thérapie cellulaire (antinéoplasique)

nufaleucel

linfocitos infiltrantes de tumor (TIL) humanos autólogos activados y expandidos en cultivo, aislados de cáncer de pulmón de células no microcíticas. Las células se aíslan mecánicamente de biopsias de tumor resecado y se expanden en cultivo usando un protocolo de dos etapas que consiste en una pre fase de expansión rápida (Pre-REP) y una fase de expansión rápida (REP) en medio sin suero que contiene interleuquina 2 (IL-2). Durante la REP, las células se activan y expanden mediante cultivo en una nanomatriz polimérica coloidal conjugada con agonistas humanizados de CD3 y CD28 en medio que contiene IL-2 en ausencia de células alimentadoras irradiadas alogénicas. Los linfocitos T (>80%) son una mezcla heterogénea de linfocitos T CD4+ y CD8+, predominantemente con subtipos de células de memoria efectora, memoria central y efectoras, y un bajo nivel (<10%) de células natural killer (NK) CD45+CD3-CD56+. Los linfocitos T muestran liberación de IFN-γ (>1.0 fg/célula) tras la estimulación con bolas CD3/CD28
terapia celular (antineoplásico)

nuzefatidum

nuzefatide

$S^{3.4}$,$S^{3.11}$,$S^{3.18}$-[(1,3,5-triazinane-1,3,5-triyl)tris(3-oxopropane-3,1-diyl)][L-alanyl-N^6-carbamimidoyl-L-lysyl-L-α-aspartyl-L-cysteinyl-(4*R*)-4-hydroxy-L-prolyl-L-leucyl-L-valyl-L-asparaginyl-L-prolyl-L-leucyl-L-cysteinyl-L-leucyl-L-histidyl-L-prolyl-D-α-aspartyl-L-tryptophyl-N^6-carbamimidoyl-L-lysyl-L-cysteinamide]
ephrin receptor binding peptide

nuzéfatide

$S^{3.4}$,$S^{3.11}$,$S^{3.18}$-[(1,3,5-triazinane-1,3,5-triyl)tris(3-oxopropane-3,1-diyl)][L-alanyl-N^6-carbamimidoyl-L-lysyl-L-α-aspartyl-L-cystéinyl-(4*R*)-4-hydroxy-L-prolyl-L-leucyl-L-valyl-L-asparaginyl-L-prolyl-L-leucyl-L-cystéinyl-L-leucyl-L-histidyl-L-prolyl-D-α-aspartyl-L-tryptophyl-N^6-carbamimidoyl-L-lysyl-L-cystéinamide]
peptide de liaison au récepteur de l'éphrine

nuzefatida

$S^{3.4}$,$S^{3.11}$,$S^{3.18}$-[(1,3,5-triazinano-1,3,5-triil)tris(3-oxopropano-3,1-diil)][L-alanil-N^6-carbamimidoil-L-lisil-L-α-aspartil-L-cysteinil-(4*R*)-4-hidroxi-L-prolil-L-leucil-L-valil-L-asparaginil-L-prolil-L-leucil-L-cisteinil-L-leucil-L-histidil-L-prolil-D-α-aspartil-L-triptofil-N^6-carbamimidoil-L-lisil-L-cisteinamida]
péptido de unión al receptor efrin

$C_{105}H_{162}N_{32}O_{27}S_3$ 2598213-64-8

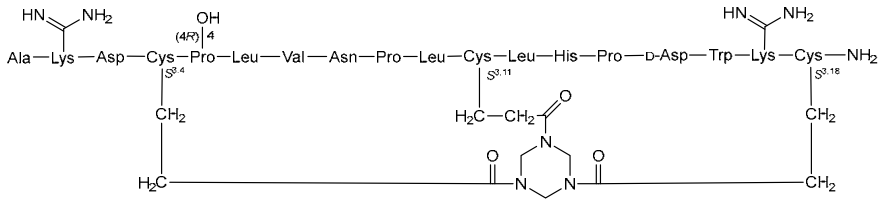

nuzefatidum pevedotinum

nuzefatide pevedotin

S$^{3.15}$,*S*$^{3.22}$,*S*$^{3.29}$-[(1,3,5-triazinane-1,3,5-triyl)tris(3-oxopropane-3,1-diyl)]{*N*-[5-oxo-5-({L-valyl-*N*^{5}-carbamoyl-L-ornithyl[(4-aminophenyl)methoxy]carbonyl-*N*-methyl-L-valyl-L-valyl-(3*R*,4*S*,5*S*)-3-methoxy-5-methyl-4-(methylamino)heptanoyl-(2*R*,3*R*)-*N*-[(1*S*,2*R*)-1-hydroxy-1-phenylpropan-2-yl]-3-methoxy-2-methyl-3-[(2*S*)-pyrrolidin-2-yl]propanamide}-*N*$^{2.1}$-yl)pentanoyl]-β-alanyldecakis(*N*-methylglycyl)-L-alanyl-*N*^{6}-carbamimidoyl-L-lysyl-L-α-aspartyl-L-cysteinyl-(4*R*)-4-hydroxy-L-prolyl-L-leucyl-L-valyl-L-asparaginyl-L-prolyl-L-leucyl-L-cysteinyl-L-leucyl-L-histidyl-L-prolyl-D-α-aspartyl-L-tryptophyl-*N*^{6}-carbamimidoyl-L-lysyl-L-cysteinamide}

ephrin receptor binding peptide, antineoplastic

nuzéfatide pévédotine

S$^{3.15}$,*S*$^{3.22}$,*S*$^{3.29}$-[(1,3,5-triazinane-1,3,5-triyl)tris(3-oxopropane-3,1-diyl)]{*N*-[5-oxo-5-({L-valyl-*N*^{5}-carbamoyl-L-ornithyl[(4-aminophényl)méthoxy]carbonyl-*N*-méthyl-L-valyl-L-valyl-(3*R*,4*S*,5*S*)-3-méthoxy-5-méthyl-4-(méthylamino)heptanoyl-(2*R*,3*R*)-*N*-[(1*S*,2*R*)-1-hydroxy-1-phénylpropan-2-yl]-3-méthoxy-2-méthyl-3-[(2*S*)-pyrrolidin-2-yl]propanamide}-*N*$^{2.1}$-yl)pentanoyl]-β-alanyldécakis(*N*-méthylglycyl)-L-alanyl-*N*^{6}-carbamimidoyl-L-lysyl-L-α-aspartyl-L-cystéinyl-(4*R*)-4-hydroxy-L-prolyl-L-leucyl-L-valyl-L-asparaginyl-L-prolyl-L-leucyl-L-cystéinyl-L-leucyl-L-histidyl-L-prolyl-D-α-aspartyl-L-tryptophyl-*N*^{6}-carbamimidoyl-L-lysyl-L-cystéinamide}

peptide de liaison au récepteur de l'éphrine, antinéoplasique

nuzefatida pevedotina

S$^{3.15}$,*S*$^{3.22}$,*S*$^{3.29}$-[(1,3,5-triazinane-1,3,5-triil)tris(3-oxopropane-3,1-diil)]{*N*-[5-oxo-5-({L-valil-*N*^{5}-carbamoil-L-ornitil[(4-aminofenil)metoxi]carbonil-*N*-metil-L-valil-L-valil-(3*R*,4*S*,5*S*)-5-metil-4-(metilamino)-3-metoxiheptanoil-(2*R*,3*R*)-*N*-[(1*S*,2*R*)-1-fenil-1-hidroxipropan-2-il]-2-metil-3-metoxi-3-[(2*S*)-pirrolidin-2-il]propanamida}-*N*$^{2.1}$-il)pentanoil]-β-alanildecakis(*N*-metilglicil)-L-alanil-*N*^{6}-carbamimidoil-L-lisil-L-α-aspartil-L-cisteinil-(4*R*)-4-hidroxi-L-prolil-L-leucil-L-valil-L-asparaginil-L-prolil-L-leucil-L-cisteinil-L-leucil-L-histidil-L-prolil-D-α-aspartil-L-triptofil-*N*^{6}-carbamimidoil-L-lisil-L-cisteinamida}

péptido de unión al receptor efrin, antineoplásico

$C_{201}H_{315}N_{53}O_{52}S_3$ 2648849-70-9

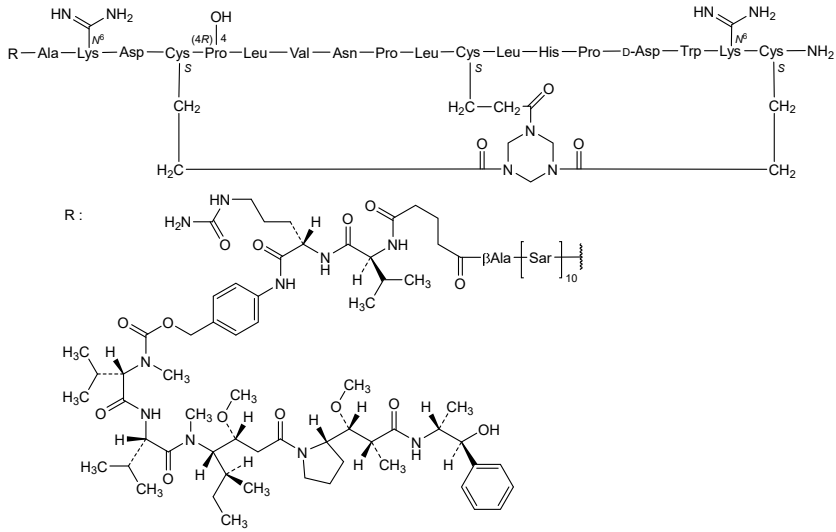

obudanersenum

obudanersen

all-P-ambo-2'-*O*-(2-methoxyethyl)-*P*-thioadenylyl-(3'→5')-2'-*O*-(2-methoxyethyl)-5-methylcytidylyl-(3'→5')-2'-*O*-(2-methoxyethyl)-5-methylcytidylyl-(3'→5')-2'-*O*-(2-methoxyethyl)adenylyl-(3'→5')-2'-*O*-(2-methoxyethyl)-5-methyluridylyl-(3'→5')-*P*-thiothymidylyl-(3'→5')-*P*-thiothymidylyl-(3'→5')-*P*-thiothymidylyl-(3'→5')-2'-deoxy-*P*-thioguanylyl-(3'→5')-2'-deoxy-*P*-thioadenylyl-(3'→5')-2'-deoxy-5-methyl-*P*-thiocytidylyl-(3'→5')-2'-deoxy-5-methyl-*P*-thiocytidylyl-(3'→5')-*P*-thiothymidylyl-(3'→5')-*P*-thiothymidylyl-(3'→5')-2'-deoxy-5-methyl-*P*-thiocytidylyl-(3'→5')-2'-*O*-(2-methoxyethyl)-5-methyluridylyl-(3'→5')-2'-*O*-(2-methoxyethyl)-5-methyluridylyl-(3'→5')-2'-*O*-(2-methoxyethyl)-*P*-thioadenylyl-(3'→5')-2'-*O*-(2-methoxyethyl)-*P*-thioguanylyl-(3'→5')-2'-*O*-(2-methoxyethyl)-5-methylcytidine

ubiquitin protein ligase E3A-antisense transcript reducer (Angelman Syndrome)

obudanersen

tout-P-ambo-2'-*O*-(2-méthoxyéthyl)-*P*-thioadénylyl-(3'→5')-2'-*O*-(2-méthoxyéthyl)-5-méthylcytidylyl-(3'→5')-2'-*O*-(2-méthoxyéthyl)-5-méthylcytidylyl-(3'→5')-2'-*O*-(2-méthoxyéthyl)adénylyl-(3'→5')-2'-*O*-(2-méthoxyéthyl)-5-méthyluridylyl-(3'→5')-*P*-thiothymidylyl-(3'→5')-*P*-thiothymidylyl-(3'→5')-*P*-thiothymidylyl-(3'→5')-2'-désoxy-*P*-thioguanylyl-(3'→5')-2'-désoxy-*P*-thioadénylyl-(3'→5')-2'-désoxy-5-méthyl-*P*-thiocytidylyl-(3'→5')-2'-désoxy-5-méthyl-*P*-thiocytidylyl-(3'→5')-*P*-thiothymidylyl-(3'→5')-*P*-thiothymidylyl-(3'→5')-2'-désoxy-5-méthyl-*P*-thiocytidylyl-(3'→5')-2'-*O*-(2-méthoxyéthyl)-5-méthyluridylyl-(3'→5')-2'-*O*-(2-méthoxyéthyl)-5-méthyluridylyl-(3'→5')-2'-*O*-(2-méthoxyéthyl)-*P*-thioadénylyl-(3'→5')-2'-*O*-(2-méthoxyéthyl)-*P*-thioguanylyl-(3'→5')-2'-*O*-(2-méthoxyéthyl)-5-méthylcytidine

réducteur de transcription antisens de l'ubiquitine protéine ligase E3A (syndrome d'Angelman)

obudanersén

todo-P-ambo-2'-*O*-(2-metoxietil)-*P*-tioadenilil-(3'→5')-5-metil-2'-*O*-(2-metoxietil)citidilil-(3'→5')-5-metil-2'-*O*-(2-metoxietil)citidilil-(3'→5')-2'-*O*-(2-metoxietil)adenilil-(3'→5')-5-metil-2'-*O*-(2-metoxietil)uridilil-(3'→5')-*P*-tiotimidilil-(3'→5')-*P*-tiotimidilil-(3'→5')-*P*-tiotimidilil-(3'→5')-2'-desoxi-*P*-tioguanilil-(3'→5')-2'-desoxi-*P*-tioadenilil-(3'→5')-2'-desoxi-5-metil-*P*-tiocitidilil-(3'→5')-2'-desoxi-5-metil-*P*-tiocitidilil-(3'→5')-*P*-tiotimidilil-(3'→5')-*P*-tiotimidilil-(3'→5')-2'-desoxi-5-metil-*P*-tiocitidilil-(3'→5')-5-metil-2'-*O*-(2-metoxietil)uridilil-(3'→5')-5-metil-2'-*O*-(2-metoxietil)uridilil-(3'→5')-2'-*O*-(2-metoxietil)-*P*-tioadenilil-(3'→5')-2'-*O*-(2-metoxietil)-*P*-tioguanilil-(3'→5')-5-metil-2'-*O*-(2-metoxietil)citidina

reductor de la transcripción antisense de la ligasa E3A de la proteína ubiquitina (síndrome de Angelman)

$C_{230}H_{321}N_{64}O_{129}P_{19}S_{13}$ 2834724-31-9

(3'-5') A=C–C–A–U–dT=dT=dT=dG=dA=d*C*=dC=dT=dT=d*C*=U–U–A=G=C

N : nucleoside / nucléoside / nucleósido
dN : 2'-deoxy-N / 2'-désoxy-N / 2'-desoxi-N
N : 5-methyl-N / 5-méthyl-N / 5-metil-N
N : 2'-*O*-(2-methoxyethyl)-N / 2'-*O*-(2-méthoxyéthyl)-N / 2'-*O*-(metoxietil)-N
– : –PO(OH)– = : –PO(SH)–

olisutrigini bromidum

olisutrigine bromide

(2*R*)-2-{2-[*N*-(2,3-dihydro-1*H*-inden-2-yl)-2-methylanilino]ethyl}-1,1-dimethylpiperidin-1-ium bromide
sodium channel blocker, analgesic

bromure d'olisutrigine

bromure de (2*R*)-2-{2-[*N*-(2,3-dihydro-1*H*-indén-2-yl)-2-méthylanilino]éthyl}-1,1-diméthylpipéridin-1-ium
bloqueur des canaux sodiques, analgésique

bromuro de olisutrigina

bromuro de (2*R*)-2-{2-[*N*-(2,3-dihidro-1*H*-inden-2-il)-2-metilanilino]etil}-1,1-dimetilpiperidin-1-io
bloqueador del canal de sodio, analgésico

$C_{25}H_{35}BrN_2$ 1393836-45-7

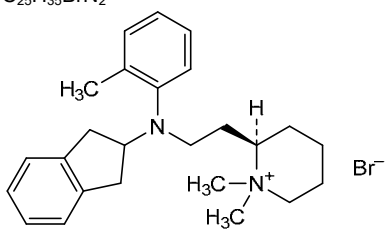

olmocabtagenum autoleucelum #

olmocabtagene autoleucel

autologous CD4+/CD8+ enriched T lymphocytes obtained by leukapheresis, transduced with a self-inactivating, non-replicating gamma Moloney murine leukemia virus (MMLV) vector encoding a chimeric antigen receptor (CAR) targeting claudin 6 (CLDN6), composed of a human IgG heavy chain signal peptide, a single chain variable fragment (scFv; IMAB206-C46S), a CD8 hinge and transmembrane domain, and a 4-1BB co-stimulatory and CD3ζ intracellular signalling

	domain, under control of the elongation factor 1 alpha short (EFS) promoter. The vector also contains an MMLV psi- region, an enlarged MMLV psi+ packaging region, a Kozak sequence, and a truncated version of the post-transcriptional regulatory element of the Woodchuck hepatitis virus (WPRE); flanked by 5' and 3' MMLV wildtype long terminal repeats (LTRs). The vector is pseudotyped with gibbon ape leukemia virus (GALV) envelope protein. The leukapheresis material is enriched for CD4+/CD8+ T lymphocytes by positive immunoselection, activated by CD3 and CD28 agonists and transduced with the retroviral vector. The cells are then expanded in media with interleukin 15 (IL-15) and interleukin 7 (IL-7). The T lymphocytes (≥80%; with ≤20% CD3- cells) are positive for the transgene (≥10% CAR positive) and secrete interferon gamma in response to CLDN6 expressing target cells *cell-based gene therapy (antineoplastic)*
olmocabtagène autoleucel	lymphocytes T autologues enrichis en CD4+/CD8+ obtenus par leucaphérèse, transduits avec un vecteur du virus de la leucémie murine gamma de Moloney (MMLV) auto-inactivant et non réplicatif codant pour un récepteur antigénique chimérique (RAC) ciblant claudine 6 (CLDN6) composé d'un peptide signal de chaîne lourde d'IgG humaine, d'un fragment variable à chaîne unique (scFv; IMAB206-C46S), d'un domaine charnière et transmembranaire CD8 et de domaines de co-stimulation 4-1BB et de signalisation intracellulaire CD3ζ, sous le contrôle du promoteur facteur d'élongation 1 alpha court (EFS). Le vecteur contient également une région ψ de MMLV, une région d'emballage ψ+ élargie de MMLV, une séquence Kozak et une version tronquée de l'élément régulateur post-transcriptionnel du virus de l'hépatite de la marmotte (WPRE); flanqué de répétitions terminales longues (LTRs) de MMLV de type sauvage en 5' et en 3'. Le vecteur est pseudotypé avec la protéine d'enveloppe du virus de la leucémie du singe gibbon (GALV). Le matériel de leucaphérèse est enrichi en lymphocytes T CD4+/CD8+ par immunosélection positive, activé par des agonistes CD3 et CD28 et transduit avec le vecteur rétroviral. Les cellules sont ensuite éxpansées dans un milieu contenant de l'interleukine 15 (IL-15) et de l'interleukine 7 (IL-7). Les lymphocytes T (≥80%; avec ≤20% de cellules CD3-) sont positifs pour le transgène (≥10% RAC positifs) et sécrètent de l'interféron gamma en réponse aux cellules cibles exprimant CLDN6 *thérapie génique à base de cellules (antinéoplasique)*
olmocabtagén autoleucel	linfocitos T CD4+/CD8+ autólogos enriquecidos, obtenidos por leucoaféresis, transducidos con un vector del virus gamma de la leucemia de Moloney murino (MMLV) auto-inactivante, no replicativo, que codifica un receptor de antígenos quimérico (CAR) anti-claudina 6 (CLDN6), compuesto por un péptido señal de la cadena pesada de la IgG humana, un fragmento variable de cadena sencilla (scFv; IMAB206-C46S), un dominio bisagra y transmembrana de CD8, y dominios intracelulares coestimulador de 4-1BB y señalización de CD3ζ, bajo

el control del promotor corto del factor de elongación 1 alfa (EFS). El vector también contiene una región psi de MMLV, una región alargada de empaquetamiento psi+ de MMLV, una secuencia Kozak y una versión truncada del elemento regulador post-transcripcionaldel virus de la hepatitis de la marmota (WPRE); flanqueado por repeticiones terminales largas (LTRs) de tipo salvaje del MMLV en 5' y 3'. El vector está seudotipado con la proteína de la envuelta del virus de la leucemia del Gibón (GALV).
El material de leucoaféresis se enriquece en linfocitos T CD4+/CD8+ mediante inmunoselección positiva, se activa con agonistas de CD3 y CD28 y se transduce con el vector retroviral. Las células se expanden después en medio con interleuquina 15 (IL-15) e interleuquina 7 (IL-7). Los linfocitos T (≥80%; con ≤20% de células CD3-) son positivos para el transgén (≥10% CAR positivos) y secretan interferón gamma en respuesta a células diana que expresan CLDN6
terapia génica basada en células (antineoplásico)

oloriglíflozinum

oloriglíflozin — 1-*C*-{4-chloro-3-[(4-ethoxyphenyl)methyl]phenyl}-1-*O*,5-*C*-methylene-D-*glycero*-α-D-*gluco*-heptopyranose
sodium glucose co-transporter inhibitor, antihyperglycaemic

oloriglíflozine — 1-*C*-{4-chloro-3-[(4-éthoxyphényl)méthyl]phényl}-1-*O*,5-*C*-méthylène-D-*glycéro*-α-D-*gluco*-heptopyranose
inhibiteur du co-transporteur de glucose et de sodium, antihyperglycémiant

oloriglíflozina — 1-*C*-{4-cloro-3-[(4-etoxifenil)metil]fenil}-1-*O*,5-*C*-metileno-D-*glicero*-α-D-*gluco*-heptopiranosa
inhibidor del cotransportador de sodio y glucosa, antihiperglucémico

$C_{23}H_{27}ClO_7$ 2035989-50-3

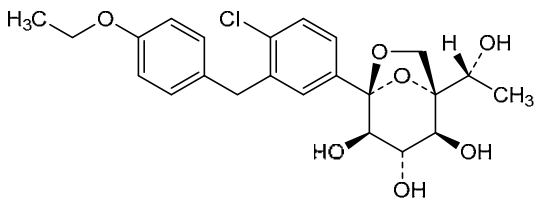

ompekimigum #

ompekimig — immunoglobulin (L-kappa-H-gamma1(_L-VH-G1(CH1-h))_L-kappa)_(H-gamma1_L-kappa), anti-[*Homo sapiens* IL4 (interleukin 4, IL-4)], anti-[*Homo sapiens* IL13 (interleukin 13, IL-13)] and anti-[*Homo sapiens* IL33 (interleukin 33, IL-33)], monoclonal antibody, trispecific, trivalent;
fused L-kappa-H-gamma1 chain anti-IL13 and anti-IL4 (1-674) [L-kappa anti-IL13 (1-218) [V-KAPPA (*Homo sapiens* IGKV1-39*01 (82.8%) -IGKJ4*01 (100%), CDR-IMGT [10.3.9] (27-36.54-56.93-101)) (1-111) -*Homo sapiens* IGKC*01 (100%) Km3 A45.1, V101 (C-KAPPA A45.1 (157), V101 (195)) (112-218)] -5-mer (tetraglycyl-seryl) linker (219-223) -H-gamma1 heavy chain anti-IL4 (224-674) [VH (*Homo*

sapiens IGHV2-5*08 (87.0%) -(IGHD) -IGHJ3*01 (92.9%) M123>T (339), CDR-IMGT [10.7.13] (249-258.276-282.321-333)) (224-344) -*Homo sapiens* IGHG1*03v, G1m3>G1m17, nG1m1, CH1 K120, CH3 E12, M14, 6-G1v14-1 CH2 A1.3, A1.2, A1, 9-G1v24 CH3 L107, S114, 14-G1v99-1 hinge E6, CH3 E24 (CH1 R120>K (441) (345-442), hinge 1-15 D6>E (448) (443-457), CH2 L1.3>A (461), L1.2>A (462), G1>A (464) (458-567), CH3 E12 (583), M14 (585), L24>E (595), M107>L (655), N114>S (661) (568-672), CHS (673-674)) (345-674)]]; (218-221')-disulfide with L-VH-G1(CH1-h) light chain anti-IL13 (1'-221')[VH (*Homo sapiens* IGHV3-21*07 (91.8%) -IGHD -IGHJ1*01 (100%), CDR-IMGT [8.7.12] (26'-33'.51'-57'.96'-107')) (1'-118') -*Homo sapiens* IGHG1*03v, G1m3>G1m17, nG1m1, CH1 K120 (CH1 R120>K (215') (119'-216'), hinge 1-5 (217'-221')) (119'-221')]; (447-218'")-disulfide with L-kappa light chain anti-IL4 (1'"-218'") [V-KAPPA (*Homo sapiens* IGKV1-39*01 (87.9%) -IGKJ4*01 (100%), CDR-IMGT [10.3.9] (27'"-36'".54'"-56'".93'"-101'")) (1'"-111'") -*Homo sapiens* IGKC*01 (100%) Km3 A45.1, V101 (C-KAPPA A45.1 (157'"), V101 (195'")) (112'"-218'")];
H-gamma1 heavy chain anti-IL33 (1"-451") [VH (*Homo sapiens* IGHV3-7*01 (89.9%) -(IGHD) -IGHJ4*01 (100%), CDR-IMGT [8.8.14] (26"-33".51"-58".97"-110")) (1"-121") -*Homo sapiens* IGHG1*03v, G1m3>G1m17, nG1m1 CH1 K120, CH3 E12, M14, 6-G1v14-1 CH2 A1.3, A1.2, A1, 9-G1v24 CH3 L107, S114, 14-G1v99-2 hinge R6, CH3 R88 (CH1 R120>K (218") (122"-219"), hinge 1-15 D6>R (225") (220"-234"), CH2 L1.3>A (238"), L1.2>A (239"), G1>A (241") (235"- 344"), CH3 E12 (360"), M14 (362"), K88>R (413"), M107>L (432"), N114>S (438") (345"-449"), CHS (450"-451")) (122"-451")], (224"-213"")-disulfide with L-kappa light chain anti-IL33 (1""-213"") [V-KAPPA (*Homo sapiens* IGKV1-6*01 (88.8%) -IGKJ4*01 (90.9%), CDR-IMGT [6.3.8] (27""-32"".50""-52"".89""-96"")) (1""-106"") -*Homo sapiens* IGKC*01 (100%) Km3 A45.1, V101 (C-KAPPA A45.1 (152""), V101 (190"")) (107""- 213"")]; dimer (453-230":456-233")-bisdisulfide, produced in Chinese hamster ovary (CHO) cells, cell line CHO-K1SV lacking the glutamine synthetase (GS-KO) gene, glycoform alfa
immunosuppressant, anti-inflammatory

ompékimig immunoglobuline (L-kappa-H-gamma1(_L-VH-G1(CH1-h))_L-kappa)_(H-gamma1_L-kappa), anti-[*Homo sapiens* IL4 (interleukine 4, IL-4)], anti-[*Homo sapiens* IL13 (interleukine 13, IL-13)] et anti-[*Homo sapiens* IL33 (interleukine 33, IL-33)], anticorps monoclonal, trispécifique, trivalent;
chaîne fusionnée L-kappa-H-gamma1 anti-IL13 et anti-IL4 (1-674) [L-kappa anti-IL13 (1-218) [V-KAPPA (*Homo sapiens* IGKV1-39*01 (82.8%) -IGKJ4*01 (100%), CDR-IMGT [10.3.9] (27-36.54-56.93-101)) (1-111) -*Homo sapiens* IGKC*01 (100%) Km3 A45.1, V101 (C-KAPPA A45.1 (157), V101 (195)) (112-218)] -5-mer (tétraglycyl-séryl) linker (219-223) -chaîne lourde H-gamma1 anti-IL4 (224-674) [VH (*Homo sapiens* IGHV2-5*08 (87.0%) -(IGHD) -IGHJ3*01 (92.9%) M123>T (339), CDR-IMGT [10.7.13] (249-258.276-282.321-333)) (224-344) -*Homo sapiens* IGHG1*03v, G1m3>G1m17, nG1m1, CH1 K120, CH3 E12, M14, 6-G1v14-1 CH2 A1.3, A1.2, A1, 9-G1v24 CH3 L107, S114, 14-G1v99-1 charnière E6, CH3 E24 (CH1 R120>K (441) (345-442), charnière 1-15 D6>E (448) (443-457), CH2 L1.3>A (461), L1.2>A (462), G1>A (464) (458-567), CH3 E12 (583), M14 (585), L24>E (595), M107>L (655), N114>S (661) (568-672), CHS (673-674)) (345-674)]]; (218-221')-disulfure avec la chaîne légère L-VH-G1(CH1-h) anti-IL13 (1'-221') [VH (*Homo sapiens* IGHV3-21*07 (91.8%) -IGHD -IGHJ1*01 (100%), CDR-IMGT [8.7.12] (26'-33'.51'-57'.96'-107')) (1'-118') -*Homo sapiens* IGHG1*03v, G1m3>G1m17, nG1m1, CH1 K120 (CH1 R120>K (215') (119'-216'), charnière 1-5 (217'-221')) (119'-221')]; (447-218'")-disulfure avec la chaîne légère L-kappa anti-IL4 (1'"-218'") [V-KAPPA (*Homo sapiens* IGKV1-39*01 (87.9%) -IGKJ4*01 (100%), CDR-IMGT [10.3.9] (27'"-36'".54'"-56'".93'"-101'")) (1'"-111'") -*Homo sapiens* IGKC*01 (100%) Km3 A45.1, V101 (C-KAPPA A45.1 (157'"), V101 (195'")) (112'"-218'")];

chaîne lourde H-gamma1 anti-IL33 (1''-451'') [VH (*Homo sapiens* IGHV3-7*01 (89.9%) -(IGHD) -IGHJ4*01 (100%), CDR-IMGT [8.8.14] (26''-33''.51''-58''.97''-110'')) (1''-121'') -*Homo sapiens* IGHG1*03v, G1m3>G1m17, nG1m1 CH1 K120, CH3 E12, M14, 6-G1v14-1 CH2 A1.3, A1.2, A1, 9-G1v24 CH3 L107, S114, 14-G1v99-2 charnière R6, CH3 R88(CH1 R120>K (218'') (122''-219''), charnière 1-15 D6>R (225'') (220''-234''), CH2 L1.3>A (238''), L1.2>A (239''), G1>A (241'') (235''- 344''), CH3 E12 (360''), M14 (362''), K88>R (413''), M107>L (432''), N114>S (438'') (345''-449''), CHS (450''-451'')) (122''-451'')], (224''-213'''')-disulfure avec la chaîne légère L-kappa anti-IL33 (1''''-213'''') [V-KAPPA (*Homo sapiens* IGKV1-6*01 (88.8%) -IGKJ4*01 (90.9%), CDR-IMGT [6.3.8] (27''''-32''''.50''''-52''''.89''''-96'''')) (1''''-106'''') -*Homo sapiens* IGKC*01 (100%) Km3 A45.1, V101 (C-KAPPA A45.1 (152''''), V101 (190'''')) (107''''- 213'''')]; dimère (453-230'':456-233'')-bisdisulfure, produit dans des cellules ovariennes de hamster chinois (CHO), lignée cellulaire CHO-K1SV ne présentant pas le gène de la glutamine synthétase (GS-KO), glycoforme alfa
immunosuppresseur, anti-inflammatoire

ompekimig inmunoglobulina (L-kappa-H-gamma1(_L-VH-G1(CH1-h))_L-kappa)_(H-gamma1_L-kappa), anti-[*Homo sapiens* IL4 (interleukina 4, IL-4)], anti-[*Homo sapiens* IL13 (interleukina 13, IL-13)] y anti-[*Homo sapiens* IL33 (interleukina 33, IL-33)], anticuerpo monoclonal, triespecífico, trivalente;
cadena fusionada L-kappa-H-gamma1 anti-IL13 y anti-IL4 (1-674) [L-kappa anti-IL13 (1-218) [V-KAPPA (*Homo sapiens* IGKV1-39*01 (82.8%) -IGKJ4*01 (100%), CDR-IMGT [10.3.9] (27-36.54-56.93-101)) (1-111) -*Homo sapiens* IGKC*01 (100%) Km3 A45.1, V101 (C-KAPPA A45.1 (157), V101 (195)) (112-218)] -5-mer (tetraglicil-seril) enlace (219-223) -cadena pesada H-gamma1 anti-IL4 (224-674) [VH (*Homo sapiens* IGHV2-5*08 (87.0%) -(IGHD) -IGHJ3*01 (92.9%) M123>T (339), CDR-IMGT [10.7.13] (249-258.276-282.321-333)) (224-344) -*Homo sapiens* IGHG1*03v, G1m3>G1m17, nG1m1, CH1 K120, CH3 E12, M14, 6-G1v14-1 CH2 A1.3, A1.2, A1, 9-G1v24 CH3 L107, S114, 14-G1v99-1 bisagra E6, CH3 E24 (CH1 R120>K (441) (345-442), bisagra 1-15 D6>E (448) (443-457), CH2 L1.3>A (461), L1.2>A (462), G1>A (464) (458-567), CH3 E12 (583), M14 (585), L24>E (595), M107>L (655), N114>S (661) (568-672), CHS (673-674)) (345-674)]]; (218-221')-disulfuro con la cadena ligera L-VH-G1(CH1-h) anti-IL13 (1'-221') [VH (*Homo sapiens* IGHV3-21*07 (91.8%) -IGHD -IGHJ1*01 (100%), CDR-IMGT [8.7.12] (26'-33'.51'-57'.96'-107')) (1'-118') -*Homo sapiens* IGHG1*03v, G1m3>G1m17, nG1m1, CH1 K120 (CH1 R120>K (215') (119'-216'), bisagra 1-5 (217'-221')) (119'-221')]; (447-218''')-disulfuro con la cadena ligera L-kappa anti-IL4 (1'''-218''') [V-KAPPA (*Homo sapiens* IGKV1-39*01 (87.9%) -IGKJ4*01 (100%), CDR-IMGT [10.3.9] (27'''-36'''.54'''-56'''.93'''-101''')) (1'''-111''') -*Homo sapiens* IGKC*01 (100%) Km3 A45.1, V101 (C-KAPPA A45.1 (157'''), V101 (195''')) (112'''-218''')];
cadena pesada H-gamma1 anti-IL33 (1''-451'') [VH (*Homo sapiens* IGHV3-7*01 (89.9%) -(IGHD) -IGHJ4*01 (100%), CDR-IMGT [8.8.14] (26''-33''.51''-58''.97''-110'')) (1''-121'') -*Homo sapiens* IGHG1*03v, G1m3>G1m17, nG1m1 CH1 K120, CH3 E12, M14, 6-G1v14-1 CH2 A1.3, A1.2, A1, 9-G1v24 CH3 L107, S114, 14-G1v99-2 bisagra R6, CH3 R88 (CH1 R120>K (218'') (122''-219''), bisagra 1-15 D6>R (225'') (220''-234''), CH2 L1.3>A (238''), L1.2>A (239''), G1>A (241'') (235''-344''), CH3 E12 (360''), M14 (362''), K88>R (413''), M107>L (432''), N114>S (438'') (345''-449''), CHS (450''-451'')) (122''-451'')], (224''-213'''')-disulfuro con la cadena ligera L-kappa anti-IL33 (1''''-213'''') [V-KAPPA (*Homo sapiens* IGKV1-6*01 (88.8%) -IGKJ4*01 (90.9%), CDR-IMGT [6.3.8] (27''''-32''''.50''''-52''''.89''''-96'''')) (1''''-106'''') -*Homo sapiens* IGKC*01 (100%) Km3 A45.1, V101 (C-KAPPA A45.1 (152''''), V101 (190'''')) (107''''- 213'''')]; dímero (453-230'':456-233'')-bisdisulfuro, producido en las células ováricas de hámster chino (CHO), línea celular CHO-K1SV en ausencia del gen de la glutamina sintetasa (GS-KO), forma glicosilada alfa
inmunosupresor, antiinflamatorio

2981477-39-6

Heavy chain / Chaîne lourde / Cadena pesada: fused L-kappa-H-gamma1 anti-IL13 and anti-IL4 (H)

```
DIQMTQSPSS LSASVGDRVT ITCKASESVD HFGWSLVHWY QQKPGKAPKL  50
LIYRASNLES GVPSRFSGSG SGTDFTLTIS SLQPEDFATY YCQQSNEDPW 100
TFGGGTKVEI KRTVAAPSVF IFPPSDEQLK SGTASVVCLL NNFYPREAKV 150
QWKVDNALQS GNSQESVTEQ DSKDSTYSLS STLTLSKADY EKHKVYACEV 200
THQGLSSPVT KSFNRGECGG GGSEVTLRES GPALVKPTQT LTLTCTFSGF 250
SLSNFGEGLS WIRQPPGKGL EWLAHIYWDD DKRYNPSLKS RLTISKDTSR 300
NQVVLTMTNM DPVDTATYYC ARRETVFYWY FDVWGQGTTV TVSSASTKGP 350
SVFPLAPSSK STSGGTAALG CLVKDYFPEP VTVSWNSGAL TSGVHTFPAV 400
LQSSGLYSLS SVVTVPSSSL GTQTYICNVN HKPSNTKVDK KVEPKSCEKT 450
HTCPPCPAPE AAGAPSVFLF PPKPKDTLMI SRTPEVTCVV VDVSHEDPEV 500
KFNWYVDGVE VHNAKTKPRE EQYNSTYRVV SVLTVLHQDW LNGKEYKCKV 550
SNKALPAPIE KTISKAKGQP REPQVYTLPP SREEMTKNQV SLTCEVKGFY 600
PSDIAVEWES NGQPENNYKT TPPVLDSDGS FFLYSKLTVD KSRWQQGNVF 650
SCSVLHEALH SHYTQKSLSL SPGK                              674
```

Light chain / Chaîne légère / Cadena ligera: L-VH-G1(CH1-h) anti-IL13 (L')

```
EVQLVESGGG LVQPGGSLRL SCAASGFTFS SYAMSWVRQA PGKGLEWVAS  50
ISSGDTTYYP DSVKGRFTIS RDNAKNSLYL QMNSLRAEDT AVYYCARNEG 100
YYFGLTLWGQ GTLVTVSSAS TKGPSVFPLA PSSKSTSGGT AALGCLVKDY 150
FPEPVTVSWN SGALTSGVHT FPAVLQSSGL YSLSSVVTVP SSSLGTQTYI 200
CNVNHKPSNT KVDKKVEPKS C                                221
```

Light chain / Chaîne légère / Cadena ligera: L-kappa anti-IL4 (L'")

```
DIQMTQSPSS LSASVGDRVT ITCRASQSVD EEGDSYMNWY QQKPGKAPKL  50
LIYAASNLES GVPSRFSGSG SGTDFTLTIS SLQPEDFATY YCQQSNKDPP 100
TFGGGTKVEI KRTVAAPSVF IFPPSDEQLK SGTASVVCLL NNFYPREAKV 150
QWKVDNALQS GNSQESVTEQ DSKDSTYSLS STLTLSKADY EKHKVYACEV 200
THQGLSSPVT KSFNRGEC                                    218
```

Heavy chain / Chaîne lourde / Cadena pesada: H-gamma1 anti-IL33 (H")

```
EVQLVESGGG LVQPGGSLRL SCAASGFTFS SYWMYWVRQA PGKGLEWVAA  50
ITPNAGEDYY PESVKGRFTI SRDNAKNSLY LQMNSLRAED TAVYYCARGQ 100
YYYTKYSLGY WGQGTLVTVS SASTKGPSVF PLAPSSKSTS GGTAALGCLV 150
KDYFPEPVTV SWNSGALTSG VHTFPAVLQS SGLYSLSSVV TVPSSSLGTQ 200
TYICNVNHKP SNTKVDKKVE PKSCRKTHTC PPCPAPEAAG APSVFLFPPK 250
PKDTLMISRT PEVTCVVVDV SHEDPEVKFN WYVDGVEVHN AKTKPREEQY 300
NSTYRVVSVL TVLHQDWLNG KEYKCKVSNK ALPAPIEKTI SKAKGQPREP 350
QVYTLPPSRE EMTKNQVSLT CLVKGFYPSD IAVEWESNGQ PENNYKTTPP 400
VLDSDGSFFL YSRLTVDKSR WQQGNVFSCS VLHEALHSHY TQKSLSLSPG 450
K                                                      451
```

Light chain / Chaîne légère / Cadena ligera: L-kappa anti-IL33 (L"")

```
DIQMTQSPSS LSASVGDRVT ITCRASQPIH NHLDWYQQKP GKAPKLLIYF  50
GKNLQEGVPS RFSGSGSGTD FTLTISSLQP EDFATYYCFQ YKKGWSFGGG 100
TKVEIKRTVA APSVFIFPPS DEQLKSGTAS VVCLLNNFYP REAKVQWKVD 150
NALQSGNSQE SVTEQDSKDS TYSLSSTLTL SKADYEKHKV YACEVTHQGL 200
SSPVTKSFNR GEC                                         213
```

Post-translational modifications

Disulfide bridges location / Position des ponts disulfure / Posiciones de los puentes disulfuro

Intra-H (C23-C104) 23-92 138-198 245-320 371-427 488-548 594-652
22"-96" 148"-204" 265"-325" 371"-429"

Intra-L (C23-C104) 22'-95' 145'-201'
23'"-92'" 138'"-198'"
23""-88"" 133""-193""

Inter-H-L' (CL 126-h 5)* 218-221'
Inter-H-L'" (h 5-CL 126) 447-218'" 224"-213""
Inter-H-H (h 11, h 14) 453-230" 456-233"
*crosslink / lien croisé / enlace cruzado

N-glycosylation sites / Sites de N-glycosylation / Posiciones de N-glicosilación
H CH2 N84.4: 524, 301"
Fucosylated complex bi-antennary CHO-type glycans / glycanes de type CHO bi-antennaires complexes fucosylés / glicanos de tipo CHO biantenarios complejos fucosilados

C-terminal lysine clipping / Coupure de la lysine C-terminale / Recorte de lisina C-terminal
H CHS K2: 674, 451"

ontunisertibum

ontunisertib — *N*-[(2,6-difluorophenyl)methyl]-2-[3-(6-methylpyridin-2-yl)-4-(quinolin-4-yl)-1*H*-pyrazol-1-yl]acetamide
serine/threonine kinase inhibitor

ontunisertib — *N*-[(2,6-difluorophényl)méthyl]-2-[3-(6-méthylpyridin-2-yl)-4-(quinoléin-4-yl)-1*H*-pyrazol-1-yl]acétamide
inhibiteur de sérine/thréonine kinases

ontunisertib — *N*-[(2,6-difluorofenil)metil]-2-[3-(6-metilpiridin-2-il)-4-(quinolein-4-il)-1*H*-pirazol-1-il]acetamida
inhibidor de la serina/treonina kinasa

$C_{27}H_{21}F_2N_5O$ 2647949-48-0

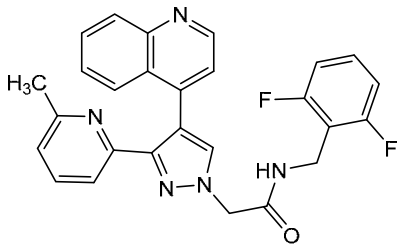

onvuzosiranum

onvuzosiran — *O*-[(2*R*,3*S*)-2-(hydroxymethyl)oxolan-3-yl] hydrogen *all-P-ambo*-3'-*O*-(2-{[(1-{17-[(2-acetamido-2-deoxy-β-D-galactopyranosyl)oxy]-3,6,9,12,15-pentaoxaheptadecan-1-yl}-1*H*-1,2,3-triazol-4-yl)methyl]amino}-2-oxoethyl)-2'-*O*-(2-{bis[(1-{17-[(2-acetamido-2-deoxy-β-D-galactopyranosyl)oxy]-3,6,9,12,15-pentaoxaheptadecan-1-yl}-1*H*-1,2,3-triazol-4-yl)methyl]amino}-2-oxoethyl)-*P*-thiocytidylyl-(5'→5')-2'-*O*-methyl-*P*-thiouridylyl-(3'→5')-2'-*O*-methylcytidylyl-(3'→5')-2'-*O*-methylcytidylyl-(3'→5')-2'-*O*-methyladenylyl-(3'→5')-2'-*O*-methylguanylyl-(3'→5')-2'-*O*-methylguanylyl-(3'→5')-2'-deoxy-2'-fluorocytidylyl-(3'→5')-2'-*O*-methyluridylyl-(3'→5')-2'-deoxy-2'-fluorocytidylyl-(3'→5')-2'-deoxy-2'-fluorocytidylyl-(3'→5')-2'-deoxy-2'-fluorouridylyl-(3'→5')-2'-deoxy-2'-fluorouridylyl-(3'→5')-2'-*O*-methyluridylyl-(3'→5')-2'-*O*-methylguanylyl-(3'→5')-2'-*O*-methyladenylyl-(3'→5')-2'-*O*-methyladenylyl-(3'→5')-2'-*O*-methyluridylyl-(3'→5')-2'-*O*-methyluridylyl-(3'→5')-2'-*O*-methyladenylyl-(3'→5')-2'-*O*-methyl-*P*-thiocytidylyl-(3'→5')-2'-*O*-methyl-*P*-thio-3'-adenylate
duplex with *all-P-ambo*-2'-*O*-methyl-*P*-thiouridylyl-(5'→3')-2'-*O*-methyl-*P*-thioguanylyl-(5'→3')-2'-*O*-methyladenylyl-(5'→3')-2'-deoxy-2'-fluoroguanylyl-(5'→3')-2'-*O*-methylguanylyl-(5'→3')-2'-deoxy-2'-fluorouridylyl-(5'→3')-2'-*O*-methylcytidylyl-(5'→3')-2'-deoxy-2'-fluorocytidylyl-(5'→3')-2'-*O*-methylguanylyl-(5'→3')-2'-deoxy-2'-fluoroadenylyl-(5'→3')-2'-*O*-methylguanylyl-(5'→3')-2'-deoxy-2'-fluoroguanylyl-(5'→3')-2'-*O*-methyladenylyl-(5'→3')-2'-deoxy-2'-fluoroadenylyl-(5'→3')-2'-*O*-methyladenylyl-(5'→3')-2'-deoxy-2'-fluorocytidylyl-(5'→3')-2'-*O*-methyluridylyl-(5'→3')-2'-deoxy-2'-fluorouridylyl-(5'→3')-2'-*O*-methyladenylyl-(5'→3')-2'-deoxy-2'-fluoroadenylyl-(5'→3')-2'-*O*-methyl-*P*-thiouridylyl-(5'→3')-2'-deoxy-2'-fluoro-*P*-thioguanylyl-(5'→3')-2'-*O*-methyluridine
prekallikrein synthesis reducer

onvuzosiran

tout-P-ambo-3'-*O*-(2-{[(1-{17-[(2-acétamido-2-désoxy-β-D-galactopyranosyl)oxy]-3,6,9,12,15-pentaoxaheptadécan-1-yl}-1*H*-1,2,3-triazol-4-yl)méthyl]amino}-2-oxoéthyl)-2'-*O*-(2-{bis[(1-{17-[(2-acétamido-2-désoxy-β-D-galactopyranosyl)oxy]-3,6,9,12,15-pentaoxaheptadécan-1-yl}-1*H*-1,2,3-triazol-4-yl)méthyl]amino}-2-oxoéthyl)-*P*-thiocytidylyl-(5'→5')-2'-*O*-méthyl-*P*-thiouridylyl-(3'→5')-2'-*O*-méthylcytidylyl-(3'→5')-2'-*O*-méthylcytidylyl-(3'→5')-2'-*O*-méthyladénylyl-(3'→5')-2'-*O*-méthylguanylyl-(3'→5')-2'-*O*-méthylguanylyl-(3'→5')-2'-désoxy-2'-fluorocytidylyl-(3'→5')-2'-*O*-méthyluridylyl-(3'→5')-2'-désoxy-2'-fluorocytidylyl-(3'→5')-2'-désoxy-2'-fluorocytidylyl-(3'→5')-2'-désoxy-2'-fluorouridylyl-(3'→5')-2'-désoxy-2'-fluorouridylyl-(3'→5')-2'-*O*-méthyluridylyl-(3'→5')-2'-*O*-méthylguanylyl-(3'→5')-2'-*O*-méthyladénylyl-(3'→5')-2'-*O*-méthyladénylyl-(3'→5')-2'-*O*-méthyluridylyl-(3'→5')-2'-*O*-méthyluridylyl-(3'→5')-2'-*O*-méthyladénylyl-(3'→5')-2'-*O*-méthyl-*P*-thiocytidylyl-(3'→5')-hydrogéno-2'-*O*-méthyl-*P*-thio-3'-adénylate de *O*-[(2*R*,3*S*)-2-(hydroxyméthyl)oxolan-3-yle]
duplex avec *tout-P-ambo*-2'-*O*-méthyl-*P*-thiouridylyl-(5'→3')-2'-*O*-méthyl-*P*-thioguanylyl-(5'→3')-2'-*O*-méthyladénylyl-(5'→3')-2'-désoxy-2'-fluoroguanylyl-(5'→3')-2'-*O*-méthylguanylyl-(5'→3')-2'-désoxy-2'-fluorouridylyl-(5'→3')-2'-*O*-méthylcytidylyl-(5'→3')-2'-désoxy-2'-fluorocytidylyl-(5'→3')-2'-*O*-méthylguanylyl-(5'→3')-2'-désoxy-2'-fluoroadénylyl-(5'→3')-2'-*O*-méthylguanylyl-(5'→3')-2'-désoxy-2'-fluoroguanylyl-(5'→3')-2'-*O*-méthyladénylyl-(5'→3')-2'-désoxy-2'-fluoroadénylyl-(5'→3')-2'-*O*-méthyladénylyl-(5'→3')-2'-désoxy-2'-fluorocytidylyl-(5'→3')-2'-*O*-méthyluridylyl-(5'→3')-2'-désoxy-2'-fluorouridylyl-(5'→3')-2'-*O*-méthyladénylyl-(5'→3')-2'-désoxy-2'-fluoroadénylyl-(5'→3')-2'-*O*-méthyl-*P*-thiouridylyl-(5'→3')-2'-désoxy-2'-fluoro-*P*-thioguanylyl-(5'→3')-2'-*O*-méthyluridine
réducteur de synthèse de prékallicréine

onvuzosirán

todo-P-ambo-3'-*O*-(2-{[(1-{17-[(2-acetamido-2-desoxi-β-D-galactopiranosil)oxi]-3,6,9,12,15-pentaoxaheptadecan-1-il}-1*H*-1,2,3-triazol-4-il)metil]amino}-2-oxoetil)-2'-*O*-(2-{bis[(1-{17-[(2-acetamido-2-desoxi-β-D-galactopiranosil)oxi]-3,6,9,12,15-pentaoxaheptadecan-1-il}-1*H*-1,2,3-triazol-4-il)metil]amino}-2-oxoetil)-*P*-tiocitidilil-(5'→5')-2'-*O*-metil-*P*-tiouridilil-(3'→5')-2'-*O*-metilcitidilil-(3'→5')-2'-*O*-metilcitidilil-(3'→5')-2'-*O*-metiladenilil-(3'→5')-2'-*O*-metilguanilil-(3'→5')-2'-*O*-metilguanilil-(3'→5')-2'-desoxi-2'-fluorocitidilil-(3'→5')-2'-*O*-metiluridilil-(3'→5')-2'-desoxi-2'-fluorocitidilil-(3'→5')-2'-desoxi-2'-fluorocitidilil-(3'→5')-2'-desoxi-2'-fluorouridilil-(3'→5')-2'-desoxi-2'-fluorouridilil-(3'→5')-2'-*O*-metiluridilil-(3'→5')-2'-*O*-metilguanilil-(3'→5')-2'-*O*-metiladenilil-(3'→5')-2'-*O*-metiladenilil-(3'→5')-2'-*O*-metiluridilil-(3'→5')-2'-*O*-metiluridilil-(3'→5')-2'-*O*-metiladenilil-(3'→5')-2'-*O*-metil-*P*-tiocitidilil-(3'→5')-hidrógeno-2'-*O*-metil-*P*-tio-3'-adenilato de *O*-[(2*R*,3*S*)-2-(hidroximetil)oxolan-3-ilo]
dúplex con *todo-P-ambo*-2'-*O*-metil-*P*-tiouridilil-(5'→3')-2'-*O*-metil-*P*-tioguanilil-(5'→3')-2'-*O*-metiladenilil-(5'→3')-2'-desoxi-2'-fluoroguanilil-(5'→3')-2'-*O*-metilguanilil-(5'→3')-2'-desoxi-2'-fluorouridilil-(5'→3')-2'-*O*-metilcitidilil-(5'→3')-2'-desoxi-2'-fluorocitidilil-(5'→3')-2'-*O*-metilguanilil-(5'→3')-2'-desoxi-2'-fluoroadenilil-(5'→3')-2'-*O*-metilguanilil-(5'→3')-2'-desoxi-2'-fluoroguanilil-(5'→3')-2'-*O*-metiladenilil-(5'→3')-2'-desoxi-2'-fluoroadenilil-(5'→3')-2'-*O*-metiladenilil-(5'→3')-2'-desoxi-2'-fluorocitidilil-(5'→3')-2'-*O*-metiluridilil-(5'→3')-2'-desoxi-2'-fluorouridilil-(5'→3')-2'-*O*-metiladenilil-(5'→3')-2'-desoxi-2'-fluoroadenilil-(5'→3')-2'-*O*-metil-*P*-tiouridilil-(5'→3')-2'-desoxi-2'-fluoro-*P*-tioguanilil-(5'→3')-2'-*O*-metiluridina
reductor de la síntesis de precalicreína

$C_{534}H_{707}F_{15}N_{180}O_{329}P_{44}S_8$ 2982817-49-0

(3'-5')**C**=*U*=*C*-*C*-*A*-*G*-*G*-C-*U*-C-C-U-U-*U*-*G*-*A*-*A*-*U*-*U*-*A*-*C*=*A*=R1
(5'-3')*U*=*G*=*A*-G-*G*-U-*C*-C-*G*-A-*G*-G-*A*-A-*A*-C-*U*-U-*A*-A-*U*=G=*U*

N : A,C,G,U
N : 2'-*O*-methyl-N / 2'-*O*-méthyl-N / 2'-*O*-metil-N
N : 2'-deoxy-2'-fluoro-N / 2'-désoxy-2'-fluoro-N / 2'-desoxi-2'-fluoro-N
– : –PO(OH)– = : –PO(SH)–

C= :

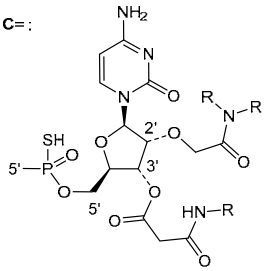

R :

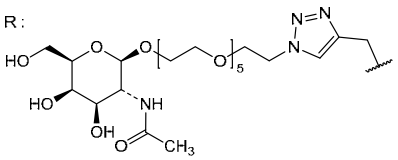

R1 :

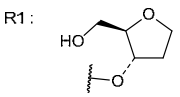

onzemipgenum parvecum #

onzemipgene parvec — recombinant non-replicating adeno-associated virus serotype 2 (rAAV2) vector, encoding a truncated soluble form of human CD59 (sCD59, membrane-independent human CD59) under control of the CAG promoter (cytomegalovirus (CMV) enhancer / chicken beta-actin (CBA) promoter / rabbit beta-globin acceptor containing chimeric intron) and a rabbit beta-globin polyadenylation signal
gene therapy (macular degeneration)

onzémipgène parvec — vecteur recombinant du virus adéno-associé non réplicatif de sérotype 2 (rAAV2) codant une forme tronquée soluble du CD59 humain (sCD59, CD59 humain indépendant de la membrane) sous le contrôle du promoteur CAG (amplificateur du cytomégalovirus (CMV) / promoteur de la bêta-actine de poulet (CBA) / intron chimérique contenant l'accepteur de la bêta-globine de lapin), et un signal de polyadénylation de bêta-globine de lapin
thérapie génique (dégénérescence maculaire)

onzemipgén parvec — vector de virus adenoasociado del serotipo 2, recombinante (rAAV2), no replicativo, que codifica una forma truncada soluble de CD59 humano (sCD59, CD59 humano independiente de membrana) bajo el control de un promotor CAG (potenciador de citomegalovirus (CMV) / promotor de beta actina de pollo (CBA) / intrón quimérico que contiene el aceptor de la beta globina de conejo) y una señal de poliadenilación de la beta globina de conejo
terapia génica (degeneración macular)

2269489-41-8

opakalimum

opakalim — *N*-(1-*tert*-butyl-6-cyano-4,7-difluoro-1*H*-1,3-benzimidazol-2-yl)-3,3-dimethylbutanamide
potassium channel activator, antiepileptic

opakalim — *N*-(1-*tert*-butyl-6-cyano-4,7-difluoro-1*H*-1,3-benzimidazol-2-yl)-3,3-diméthylbutanamide
activateur des canaux potassiques, antiépileptique

opakalim

N-(1-*terc*-butil-6-ciano-4,7-difluoro-1*H*-1,3-bencimidazol-2-il)-3,3-dimetilbutanamida
activador del canal de potasio, antiepiléptico

$C_{18}H_{22}F_2N_4O$ 2376397-93-0

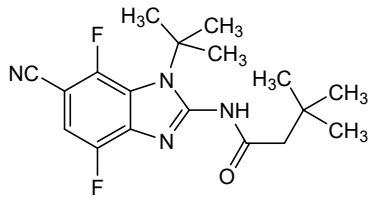

opamtistomigum

opamtistomig

immunoglobulin (H-gamma1-scFvhl_L-kappa) dimer, anti-[*Homo sapiens* CD274 (programmed cell death 1 ligand 1, PDL1, PD-L1, B7 homolog 1, B7H1, B7-H1, PDCD1LG1)] and anti-[*Homo sapiens* TNFRSF9 (TNF receptor superfamily member 9, 4-1BB, T cell antigen ILA, CD137)], humanized and *Homo sapiens* monoclonal antibody, tetravalent, bispecific;
H-gamma1 heavy chain anti-CD274 fused to a scFvhl anti-TNFRSF9 (1-714) [H-gamma1 heavy chain anti-CD274 humanized (1-449) [VH (*Homo sapiens* IGHV4-30-4*09 (87.8%) -(IGHD) -IGHJ4*01 (93.3%) L123>T (114), CDR-IMGT [8.7.13] (26-33.51-57.96-108)) (1-119)-*Homo sapiens* IGHG1*01, G1m17,1 CH1 K120, CH3 D12, L14, 6-G1v14-4 CH2 A1.3, A1.2, A114, 1-G1v66 CH2 A27 (CH1 K120 (216) (120-217), hinge 1-15 (218-232), CH2 L1.3>A (236), L1.2>A (237), D27>A (267), P114>A (331) (233-342), CH3 D12 (358), L14 (360) (343-447), CHS (448-449)) (120-449)] -15-mer tris(tetraglycyl-seryl) linker (450-464) -scFvhl anti-TNFRSF9 *Homo sapiens* (465-714), C49 (VH)-C120 (VL) 11-scFv-v1 [VH (*Homo sapiens* IGHV3-30*01 (92.9%) -IGHD -IGHJ6*03 (95.0%) G49>C (508), CDR-IMGT [8.8.17] (490-497.515-522.561-577)) (465-588) -15-mer tris(glycyl-tetraseryl) linker (589-603) -V-LAMBDA (*Homo sapiens* IGLV2-14*01 (91.9%) -IGLJ7*01 (90.9%) G120>C (707), CDR-IMGT [9.3.11] (629-637.655-657.694-704)) (604-714)]]; (222-214')-disulfide with L-kappa light chain anti-CD274 humanized (1'-214') [V-KAPPA (*Homo sapiens* IGKV1-16*01 (84.2%) -IGKJ2*01 (100%), CDR-IMGT [6.3.9] (27'-32'.50'-52'.89'-97')) (1'-107') -*Homo sapiens* IGKC*01 (100%), Km3 A45.1 (153'), V101 (191') (108'-214')]; dimer (228-228":231-231")-bisdisulfide, produced in Chinese hamster ovary (CHO) cells, cell line CHO-K1, glycoform alfa
immunostimulant, antineoplastic

opamtistomig

immunoglobuline (H-gamma1-scFvhl_L-kappa) dimère, anti-[*Homo sapiens* CD274 (ligand 1 de mort cellulaire programmée 1, PDL1, PD-L1, B7 homologue 1, B7H1, B7-H1, PDCD1LG1)] et anti-[*Homo sapiens* TNFRSF9 (membre 9 de la superfamille des récepteurs du TNF, 4-1BB, antigène ILA des cellules T, CD137)], anticorps monoclonal humanisé et *Homo sapiens*, tétravalent, bispécifique;

	chaîne lourde H-gamma1 anti-CD274 fusionnée à un scFvhl anti-TNFRSF9 (1-714) [chaîne lourde H-gamma1 anti-CD274 humanisée (1-449) [VH (*Homo sapiens* IGHV4-30-4*09 (87.8%) -(IGHD) -IGHJ4*01 (93.3%) L123>T (114), CDR-IMGT [8.7.13] (26-33.51-57.96-108)) (1-119)-*Homo sapiens* IGHG1*01, G1m17,1 CH1 K120, CH3 D12, L14, 6-G1v14-4 CH2 A1.3, A1.2, A114, 1-G1v66 CH2 A27 (CH1 K120 (216) (120-217), charnière 1-15 (218-232), CH2 L1.3>A (236), L1.2>A (237), D27>A (267), P114>A (331) (233-342), CH3 D12 (358), L14 (360) (343-447), CHS (448-449)) (120-449)] -15-mer tris(tétraglycyl-séryl) linker (450-464) -scFvhl anti-TNFRSF9 *Homo sapiens* (465-714), C49 (VH)-C120 (VL) 11-scFv-v1 [VH (*Homo sapiens* IGHV3-30*01 (92.9%) -IGHD -IGHJ6*03 (95.0%) G49>C (508), CDR-IMGT [8.8.17] (490-497.515-522.561-577)) (465-588) -15-mer tris(glycyl-tétraséryl) linker (589-603) -V-LAMBDA (*Homo sapiens* IGLV2-14*01 (91.9%) -IGLJ7*01 (90.9%) G120>C (707), CDR-IMGT [9.3.11] (629-637.655-657.694-704)) (604-714)]]; (222-214')-disulfure avec la chaîne légère L-kappa anti-CD274 humanisée (1'-214') [V-KAPPA (*Homo sapiens* IGKV1-16*01 (84.2%) -IGKJ2*01 (100%), CDR-IMGT [6.3.9] (27'-32'.50'-52'.89'-97')) (1'-107') -*Homo sapiens* IGKC*01 (100%), Km3 A45.1 (153'), V101 (191') (108'-214')]; dimère (228-228":231-231")-bisdisulfure, produit dans des cellules ovariennes de hamster chinois (CHO), lignée cellulaire CHO-K1, glycoforme alfa *immunostimulant, antinéoplasique*
opamtistomig	inmunoglobulina (H-gamma1-scFvhl_L-kappa) dímero, anti-[*Homo sapiens* CD274 (ligando 1 de muerte celular programada 1, PDL1, PD-L1, B7 homólogo 1, B7H1, B7-H1, PDCD1LG1)] y anti-[*Homo sapiens* TNFRSF9 (miembro 9 de la superfamilia de los receptores del TNF, 4-1BB, antígeno ILA de las células T, CD137)], anticuerpo monoclonal humanizado y *Homo sapiens*, tetravalente, biespecífico; cadena pesada H-gamma1 anti-CD274 fusionada con un scFvhl anti-TNFRSF9 (1-714) [cadena pesada H-gamma1 anti-CD274 humanizada (1-449) [VH (*Homo sapiens* IGHV4-30-4*09 (87.8%) -(IGHD) -IGHJ4*01 (93.3%) L123>T (114), CDR-IMGT [8.7.13] (26-33.51-57.96-108)) (1-119)-*Homo sapiens* IGHG1*01, G1m17,1 CH1 K120, CH3 D12, L14, 6-G1v14-4 CH2 A1.3, A1.2, A114, 1-G1v66 CH2 A27 (CH1 K120 (216) (120-217), bisagra 1-15 (218-232), CH2 L1.3>A (236), L1.2>A (237), D27>A (267), P114>A (331) (233-342), CH3 D12 (358), L14 (360) (343-447), CHS (448-449)) (120-449)] -15-mer tris(tetraglicil-seril) enlace (450-464) -scFvhl anti-TNFRSF9 *Homo sapiens* (465-714), C49 (VH)-C120 (VL) 11-scFv-v1 [VH (*Homo sapiens* IGHV3-30*01 (92.9%) -IGHD -IGHJ6*03 (95.0%) G49>C (508), CDR-IMGT [8.8.17] (490-497.515-522.561-577)) (465-588) -15-mer tris(glicil-tetraseril) enlace (589-603) -V-LAMBDA (*Homo sapiens* IGLV2-14*01 (91.9%) -IGLJ7*01 (90.9%) G120>C (707), CDR-IMGT [9.3.11] (629-637.655-657.694-704)) (604-714)]]; (222-214')-disulfuro con la cadena ligera L-kappa anti-CD274 humanizada (1'-214') [V-KAPPA (*Homo sapiens* IGKV1-16*01 (84.2%) -IGKJ2*01 (100%), CDR-IMGT [6.3.9] (27'-32'.50'-52'.89'-97')) (1'-107') -*Homo sapiens* IGKC*01 (100%), Km3 A45.1 (153'), V101 (191') (108'-214')]; dímero (228-228":231-231")-bisdisulfuro, producido en las células ováricas de hámster chino (CHO), línea celular CHO-K1, forma glicosilada alfa *inmunoestimulante, antineoplásico*

2923499-76-5

Heavy chain / Chaîne lourde / Cadena pesada: fused H-gamma4 anti-CD274 -scFvhl anti-TNFRSF9 (H, H'')

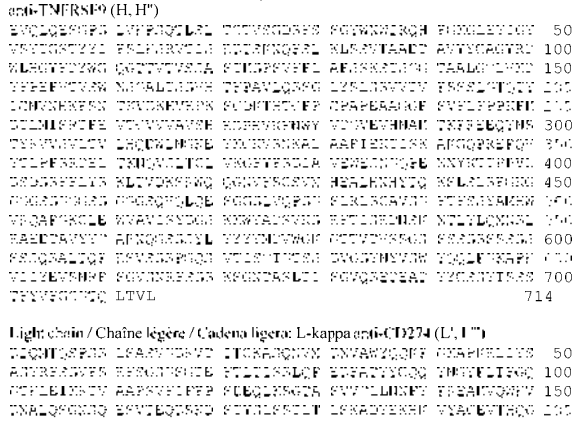

Light chain / Chaîne légère / Cadena ligera: L-kappa anti-CD274 (L', L'')

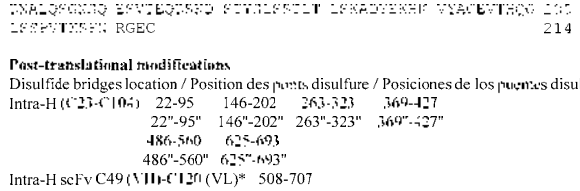

Post-translational modifications

Disulfide bridges location / Position des ponts disulfure / Posiciones de los puentes disulfuro

Intra-H (C23-C104) 22-95 146-202 263-323 369-427
22''-95'' 146''-202'' 263''-323'' 369''-427''
486-560 625-693
486''-560'' 625''-693''

Intra-H scFv C49 (VHh-CL20 (VL)* 508-707
508''-707''

Intra-L (C23-C104) 23'-88' 134'-194'
23'''-88''' 134'''-194'''

Inter-H-L (h 5-CL 126) 222-214' 222''-214'''

Inter-H-H (h 11, h 14) 228-228'' 231-231''

*engineered additional disulfide bond C49 (VHh-CL20 (VL) to stabilize the scFv (variant 1 [1-scFv-v1]).

N-glycosylation sites / Sites de N-glycosylation / Posiciones de N-glicosilación

H CH2 N84.4: 299, 299''

Fucosylated complex bi-antennary CHO-type glycans / glycanes de type CHO bi-antennaires complexes fucosylés / glicanos de tipo CHO biantenarios complejos fucosilados.

oturkibartum #

oturkibart	immunoglobulin G4-kappa, anti-[*Homo sapiens* IL4R (interleukin 4 receptor, IL4RA, IL-4RA, interleukin 13 receptor, CD124)], humanized monoclonal antibody; H-gamma4 heavy chain humanized (1-444) [VH (*Homo sapiens* IGHV3-66*01 (83.5%) -(IGHD) -IGHJ2*01 (85.7%) R120>Q (109), CDR-IMGT [8.7.11] (26-33.51-57.96-106)) (1-117) -*Homo sapiens* IGHG4*01, *nG4m(a)* CH2 L92, 12-G4v5 h P10 (CH1 (118-215), hinge 1-12 S10>P (225) (216-227), CH2 L92 (306) (228-337), CH3 (338-442), CHS (443-444)) (118-444)], (131-217')-disulfide with L-kappa light chain humanized (1'-217') [V-KAPPA (*Homo sapiens* IGKV1-27*01 (84.4%) -IGKJ2*02 (90.0%) L124>V (107'), CDR-IMGT [8.3.10] (27'-34'.52'-54'.91'-100')) (1'-110') -*Homo sapiens* IGKC*01 (100%) Km3 A45.1, V101 (C-KAPPA A45.1 (156'), V101 (194')) (111'-217')]; dimer (223-223'':226-226'')-bisdisulfide, produced in Chinese hamster ovary (CHO) cells, cell line CHO-S, glycoform alfa *anti-inflammatory*
oturkibart	immunoglobuline G4-kappa, anti-[*Homo sapiens* IL4R (récepteur de l'interleukine 4, IL4RA, IL-4RA, récepteur de l'interleukine 13, CD124)], anticorps monoclonal humanisé;

chaîne lourde H-gamma4 humanisée (1-444) [VH (*Homo sapiens* IGHV3-66*01 (83.5%) -(IGHD) -IGHJ2*01 (85.7%) R120>Q (109), CDR-IMGT [8.7.11] (26-33.51-57.96-106)) (1-117) -*Homo sapiens* IGHG4*01, *nG4m(a)* CH2 L92, 12-G4v5 h P10(CH1 (118-215), charnière 1-12 S10>P (225) (216-227), CH2 L92 (306) (228-337), CH3 (338-442), CHS (443-444)) (118-444)], (131-217')-disulfure avec la chaîne légère L-kappa humanisée (1'-217') [V-KAPPA (*Homo sapiens* IGKV1-27*01 (84.4%) -IGKJ2*02 (90.0%) L124>V (107'), CDR-IMGT [8.3.10] (27'-34'.52'-54'.91'-100')) (1'-110') -*Homo sapiens* IGKC*01 (100%) Km3 A45.1, V101 (C-KAPPA A45.1 (156'), V101 (194')) (111'-217')]; dimère (223-223":226-226")-bisdisulfure, produit dans des cellules ovariennes de hamster chinois (CHO), lignée cellulaire CHO-S, glycoforme alfa
anti-inflammatoire

oturkibart

inmunoglobulina G4-kappa, anti-[*Homo sapiens* IL4R (receptor de la interleukina, IL4RA, IL-4RA, receptor de la interleukina 13, CD124)], anticuerpo monoclonal humanizado*;*
cadena pesada H-gamma4 humanizada (1-444) [VH (*Homo sapiens* IGHV3-66*01 (83.5%) -(IGHD) -IGHJ2*01 (85.7%) R120>Q (109), CDR-IMGT [8.7.11] (26-33.51-57.96-106)) (1-117) -*Homo sapiens* IGHG4*01, *nG4m(a)* CH2 L92, 12-G4v5 h P10 (CH1 (118-215), bisagra 1-12 S10>P (225) (216-227), CH2 L92 (306) (228-337), CH3 (338-442), CHS (443-444)) (118-444)], (131-217')-disulfuro con la cadena ligera L-kappa humanizada *(*1'-217') [V-KAPPA (*Homo sapiens* IGKV1-27*01 (84.4%) -IGKJ2*02 (90.0%) L124>V (107'), CDR-IMGT [8.3.10] (27'-34'.52'-54'.91'-100')) (1'-110') -*Homo sapiens* IGKC*01 (100%) Km3 A45.1, V101 (C-KAPPA A45.1 (156'), V101 (194')) (111'-217')]; dímero (223-223":226-226")-bisdisulfuro, producido en las células ováricas de hámster chino (CHO), línea celular CHO-S, forma glicosilada alfa
antiinflamatorio

2956767-43-2

Heavy chain / Chaîne lourde / Cadena pesada

```
EVQLVESGGG LVQPGGSLRL SCAASGIDLR TNGXSNVRQA PGKGLEWVGI  50
IGSSGYMDYA SWAKGRFTIS RDNSKNTLYL QMNSLRAEDT AVYYCARIGD 100
SSSPALWGQG TLVTVSSAST KGPSVFPLAP SSKSTSGGTA ALGCLVKDYF 150
PEPVTVSWNS GALTSGVHTF PAVLQSSGLY SLSSVVTVPS SSLGTKTYTC 200
NVDHKPSNTK VDKRVESKYG PPCPPCPAPE FLGGPSVFLF PPKPKDTLMI 250
SRTPEVTCVV VDVSQEDPEV QFNWYVDGVE VHNAKTKPRE EQFNSTYRVV 300
SVLTVLHQDW LNGKEYKCKV SNKGLPSSIE KTISKAKGQP REPQVYTLPP 350
SQEEMTKNQV SLTCLVKGFY PSDIAVEWES NGQPENNYKT TPPVLDSDGS 400
FFLYSRLTVD KSRWQEGNVF SCSVMHEALH NHYTQKSLSL SLGK       444
```

Light chain / Chaîne légère / Cadena ligera

```
DIQMTQSPSS LSASVGDRVT ITCRASESVY KNNRLSWYQQ KPGKAPYLLI  50
YEASKVASGV PSRFSGSGSG TDFTLTISSL QPEDFATYYC AGAYPGNIYP 100
FGQGTKVEIK RTVAAPSVFI FPPSDEQLKS GTASVVCLLN NFYPREAKVQ 150
WKVDNALQSG NSQESVTEQD SKDSTYSLSS TLTLSKADYE KHKVYACEVT 200
HQGLSSPVTK SFNRGEC                                     217
```

Post-translational modifications
Disulfide bridges location / Position des ponts disulfure / Posiciones de los puentes disulfuro

Intra-H (C23-C104)	22-95	144-200	258-318	364-422	
	22"-95"	144"-200"	258"-318"	364"-422"	
Intra-L (C23-C104)	23'-90'	137'-197'			
	23'"-90'"	137'"-197'"			
Inter-H-L (CH1 10-CL 126)	131-217'	131"-217'"			
Inter-H-H (h 8, h 11)	223-223"	226-226"			

N-glycosylation sites / Sites de N-glycosylation / Posiciones de N-glicosilación
H CH2 N84.4: 294, 294"
Fucosylated complex bi-antennary CHO-type glycans / glycanes de type CHO bi-antennaires complexes fucosylés / glicanos de tipo CHO biantenarios complejos fucosilados

C-terminal lysine clipping / Coupure de la lysine C-terminale / Recorte de lisina C-terminal
H CHS K2: 444, 444"

ozisiranum

ozisiran

(2*RS*)-3-(1,23-bis[(2-acetamido-2-deoxy-β-D-galactopyranosyl)oxy]-14-{5-[(2-acetamido-2-deoxy-β-D-galactopyranosyl)oxy]pentanoyl}-5,19-dioxo-6,10,14,18-tetraazatricosan-10-yl)-2-hydroxy-3-oxopropyl hydrogen *all-P-ambo*-2'-*O*-methyl-*P*-thiocytidylyl-(3'→5')-2'-*O*-methyl-*P*-thiocytidylyl-(3'→5')-2'-*O*-methyluridylyl-(3'→5')-2'-*O*-methyluridylyl-(3'→5')-2'-*O*-methylguanylyl-(3'→5')-2'-*O*-methyladenylyl-(3'→5')-2'-deoxy-2'-fluoroguanylyl-(3'→5')-2'-deoxy-2'-fluoroguanylyl-(3'→5')-2'-deoxy-2'-fluorocytidylyl-(3'→5')-2'-*O*-methyladenylyl-(3'→5')-2'-*O*-methyluridylyl-(3'→5')-2'-*O*-methyladenylyl-(3'→5')-2'-*O*-methylcytidylyl-(3'→5')-2'-*O*-methyluridylyl-(3'→5')-2'-*O*-methyluridylyl-(3'→5')-2'-*O*-methylcytidylyl-(3'→5')-2'-*O*-methyladenylyl-(3'→5')-2'-*O*-methyladenylyl-(3'→5')-2'-*O*-methyl-3'-adenylate, duplex with *all-P-ambo*-2'-*O*-methyl-*P*-thiouridylyl-(5'→3')-2'-*O*-methyl-*P*-thiouridylyl-(5'→3')-2'-*O*-methylguanylyl-(5'→3')-2'-*O*-methylguanylyl-(5'→3')-2'-*O*-methyladenylyl-(5'→3')-2'-deoxy-2'-fluoroadenylyl-(5'→3')-2'-*O*-methylcytidylyl-(5'→3')-2'-deoxy-2'-fluorouridylyl-(5'→3')-2'-*O*-methylcytidylyl-(5'→3')-2'-*O*-methylcytidylyl-(5'→3')-2'-*O*-methylguanylyl-(5'→3')-2'-*O*-methyluridylyl-(5'→3')-2'-*O*-methyladenylyl-(5'→3')-2'-*O*-methyluridylyl-(5'→3')-2'-*O*-methylguanylyl-(5'→3')-2'-deoxy-2'-fluoroadenylyl-(5'→3')-2'-*O*-methyladenylyl-(5'→3')-2'-*O*-methylguanylyl-(5'→3')-2'-*O*-methyl-*P*-thiouridylyl-(5'→3')-2'-deoxy-2'-fluoro-*P*-thiouridylyl-(5'→3')-(5'*E*)-2'-*O*-methyl-5',$C^{5'}$-didehydro-$O^{5'}$-carba-5'-uridylic acid

hepatitis B virus (HBV) RNA transcript reducer, antiviral

ozisiran

tout-P-ambo-2'-*O*-méthyl-*P*-thiocytidylyl-(3'→5')-2'-*O*-méthyl-*P*-thiocytidylyl-(3'→5')-2'-*O*-méthyluridylyl-(3'→5')-2'-*O*-méthyluridylyl-(3'→5')-2'-*O*-méthylguanylyl-(3'→5')-2'-*O*-méthyladénylyl-(3'→5')-2'-désoxy-2'-fluoroguanylyl-(3'→5')-2'-désoxy-2'-fluoroguanylyl-(3'→5')-2'-désoxy-2'-fluorocytidylyl-(3'→5')-2'-*O*-méthyladénylyl-(3'→5')-2'-*O*-méthyluridylyl-(3'→5')-2'-*O*-méthyladénylyl-(3'→5')-2'-*O*-méthylcytidylyl-(3'→5')-2'-*O*-méthyluridylyl-(3'→5')-2'-*O*-méthyluridylyl-(3'→5')-2'-*O*-méthylcytidylyl-(3'→5')-2'-*O*-méthyladénylyl-(3'→5')-2'-*O*-méthyladénylyl-(3'→5')-hydrogéno-2'-*O*-méthyl-3'-adénylate de (2*RS*)-3-(1,23-bis[(2-acétamido-2-désoxy-β-D-galactopyranosyl)oxy]-14-{5-[(2-acétamido-2-désoxy-β-D-galactopyranosyl)oxy]pentanoyl}-5,19-dioxo-6,10,14,18-tétraazatricosan-10-yl)-2-hydroxy-3-oxopropyle, duplex avec acide *tout-P-ambo*-2'-*O*-méthyl-*P*-thiouridylyl-(5'→3')-2'-*O*-méthyl-*P*-thiouridylyl-(5'→3')-2'-*O*-méthylguanylyl-(5'→3')-2'-*O*-méthylguanylyl-(5'→3')-2'-*O*-méthyladénylyl-(5'→3')-2'-désoxy-2'-fluoroadénylyl-(5'→3')-2'-*O*-méthylcytidylyl-(5'→3')-2'-désoxy-2'-fluorouridylyl-(5'→3')-2'-*O*-méthylcytidylyl-(5'→3')-2'-*O*-méthylcytidylyl-(5'→3')-2'-*O*-méthylguanylyl-(5'→3')-2'-*O*-méthyluridylyl-(5'→3')-2'-*O*-méthyladénylyl-(5'→3')-2'-*O*-méthyluridylyl-(5'→3')-2'-*O*-méthylguanylyl-(5'→3')-2'-désoxy-2'-fluoroadénylyl-(5'→3')-2'-*O*-méthyladénylyl-(5'→3')-2'-*O*-méthylguanylyl-(5'→3')-2'-*O*-méthyl-*P*-thiouridylyl-(5'→3')-2'-désoxy-2'-fluoro-*P*-thiouridylyl-(5'→3')-(5'*E*)-2'-*O*-méthyl-5',$C^{5'}$-didéhydro-$O^{5'}$-carba-5'-uridylique

réducteur de transcription de l'ARN du virus de l'hépatite B (VHB), antiviral

ozisirán

todo-P-ambo-2'-*O*-metil-*P*-tiocitidilil-(3'→5')-2'-*O*-metil-*P*-tiocitidilil-(3'→5')-2'-*O*-metiluridilil-(3'→5')-2'-*O*-metiluridilil-(3'→5')-2'-*O*-metilguanilil-(3'→5')-2'-*O*-metiladenilil-(3'→5')-2'-desoxi-2'-fluoroguanilil-(3'→5')-2'-desoxi-2'-fluoroguanilil-(3'→5')-2'-desoxi-2'-fluorocitidilil-(3'→5')-2'-*O*-metiladenilil-(3'→5')-2'-*O*-metiluridilil-(3'→5')-2'-*O*-metiladenilil-(3'→5')-2'-*O*-metilcitidilil-(3'→5')-2'-*O*-metiluridilil-(3'→5')-2'-*O*-metiluridilil-(3'→5')-2'-*O*-metilcitidilil-(3'→5')-2'-*O*-metiladenilil-(3'→5')-2'-*O*-metiladenilil-(3'→5')-hidrógeno-2'-*O*-metil-3'-adenilato de (2*RS*)-3-(1,23-bis[(2-acetamido-2-desoxi-β-D-galactopiranosil)oxi]-14-{5-[(2-acetamido-2-desoxi-β-D-galactopiranosil)oxi]pentanoil}-5,19-dioxo-6,10,14,18-tetraazatricosan-10-il)-2-hidroxi-3-oxopropilo,
duplex con ácido *todo-P-ambo*-2'-*O*-metil-*P*-tiouridilil-(5'→3')-2'-*O*-metil-*P*-tiouridilil-(5'→3')-2'-*O*-metilguanilil-(5'→3')-2'-*O*-metilguanilil-(5'→3')-2'-*O*-metiladenilil-(5'→3')-2'-desoxi-2'-fluoroadenilil-(5'→3')-2'-*O*-metilcitidilil-(5'→3')-2'-desoxi-2'-fluorouridilil-(5'→3')-2'-*O*-metilcitidilil-(5'→3')-2'-*O*-metilcitidilil-(5'→3')-2'-*O*-metilguanilil-(5'→3')-2'-*O*-metiluridilil-(5'→3')-2'-*O*-metiladenilil-(5'→3')-2'-*O*-metiluridilil-(5'→3')-2'-*O*-metilguanilil-(5'→3')-2'-desoxi-2'-fluoroadenilil-(5'→3')-2'-*O*-metiladenilil-(5'→3')-2'-*O*-metilguanilil-(5'→3')-2'-*O*-metil-*P*-tiouridilil-(5'→3')-2'-desoxi-2'-fluoro-*P*-tiouridilil-(5'→3')-(5'*E*)-2'-*O*-metil-5',$C^{5'}$-didehidro-$O^{5'}$-carba-5'-uridílico
reductor de la transcripción de ARN del virus de la hepatitis B (HBV), antiviral

$C_{464}H_{619}F_7N_{152}O_{293}P_{40}S_6$ 3061406-96-7

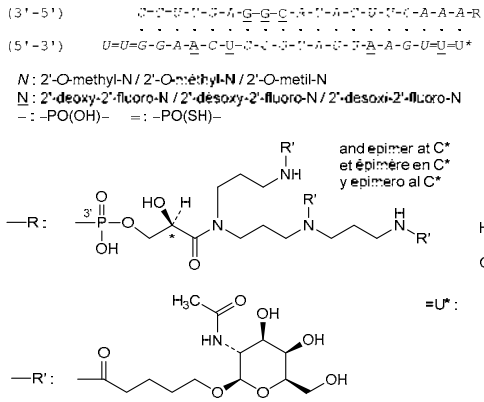

palacaparibum

palacaparib

6-fluoro-5-{4-[(5-fluoro-2-methyl-3-oxo-3,4-dihydroquinoxalin-6-yl)methyl]piperazin-1-yl}-*N*-methylpyridine-2-carboxamide
poly (ADP-ribose) polymerase (PARP) inhibitor, antineoplastic

palacaparib

6-fluoro-5-{4-[(5-fluoro-2-méthyl-3-oxo-3,4-dihydroquinoxalin-6-yl)méthyl]pipérazin-1-yl}-*N*-méthylpyridine-2-carboxamide
inhibiteur de la poly-ADP-ribose polymérase, antinéoplasique

palacaparib

6-fluoro-5-{4-[(5-fluoro-2-metil-3-oxo-3,4-dihidroquinoxalin-6-il)metil]piperazin-1-il}-*N*-metilpiridina-2-carboxamida
inhibidor de poli-ADP-ribosa polimerasa, antineoplásico

$C_{21}H_{22}F_2N_6O_2$ 2756333-39-6

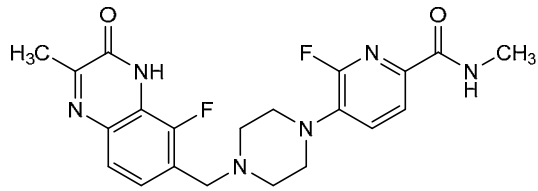

pariceractum

pariceract	5,7-dimethyl-*N*-[*trans*-4-(pentyloxy)cyclohexyl]pyrazolo[1,5-*a*]pyrimidine-3-carboxamide *beta-glucocerebrosidase activator, antiparkinsonian*
paricéract	5,7-diméthyl-*N*-[*trans*-4-(pentyloxy)cyclohexyl]pyrazolo[1,5-*a*]pyrimidine-3-carboxamide *activateur de bêta-glucocérébrosidase, antiparkinsonien*
pariceract	5,7-dimetil-*N*-[*trans*-4-(pentiloxi)ciclohexil]pirazolo[1,5-*a*]pirimidina-3-carboxamida *activador de la glucocerebrosidasa beta, antiparkinsoniano*

$C_{20}H_{30}N_4O_2$ 1919820-28-2

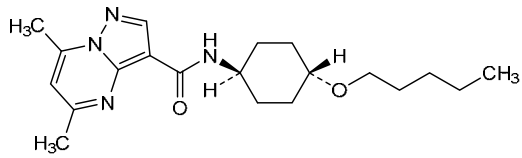

pasodacigibum

pasodacigib	6-fluoro-1-methyl-4-[4-(5-methyl-1,3-benzoxazol-2-yl)piperidin-1-yl]-2-oxo-1,2-dihydroquinoline-3-carboxamide *diacylglycerol kinase inhibitor, antineoplastic*
pasodacigib	6-fluoro-1-méthyl-4-[4-(5-méthyl-1,3-benzoxazol-2-yl)piperidin-1-yl]-2-oxo-1,2-dihydroquinoléine-3-carboxamide *inhibiteur de diacylglycérol kinase, antinéoplasique*
pasodacigib	6-fluoro-1-metil-4-[4-(5-metil-1,3-benzoxazol-2-il)piperidin-1-il]-2-oxo-1,2-dihidroquinoleina-3-carboxamida *inhibidor de la diacilglicerol kinasa, antineoplásico*

$C_{24}H_{23}FN_4O_3$ 2648721-77-9

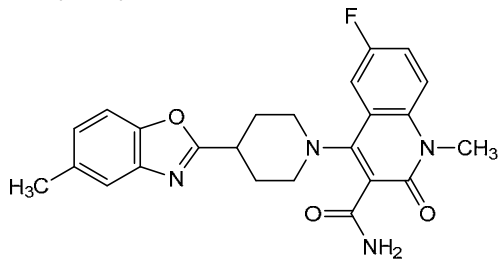

perzebertinibum

perzebertinib — 5-{[(4*R*)-3,3-difluoro-1-methylpiperidin-4-yl]oxy}-6-methoxy-*N*-{3-methyl-4-[([1,2,4]triazolo[1,5-*c*]pyrimidin-7-yl)oxy]phenyl}quinazolin-4-amine
epidermal growth factor receptor tyrosine kinase inhibitor, antineoplastic

perzébertinib — 5-{[(4*R*)-3,3-difluoro-1-méthylpipéridin-4-yl]oxy}-6-méthoxy-*N*-{3-méthyl-4-[([1,2,4]triazolo[1,5-*c*]pyrimidin-7-yl)oxy]phényl}quinazolin-4-amine
inhibiteur de la tyrosine kinase du récepteur du facteur de croissance épidermique, antinéoplasique

perzebertinib — 5-{[(4*R*)-3,3-difluoro-1-metilpiperidin-4-il]oxi}-*N*-{3-metil-4-[([1,2,4]triazolo[1,5-*c*]pirimidin-7-il)oxi]fenil}-6-metoxiquinazolin-4-amina
inhibidor de la tirosina kinasa del receptor del factor de crecimiento epidérmico, antineoplásico

$C_{27}H_{26}F_2N_8O_3$ 2414056-31-6

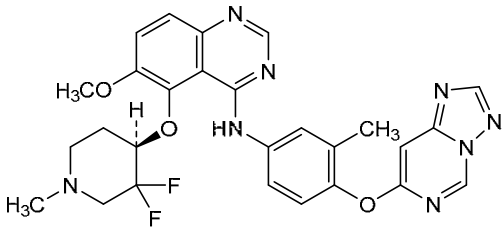

petadeferitrinum

petadeferitrin — (4*S*)-2-{2-hydroxy-4-[2-(2-methoxyethoxy)ethoxy]phenyl}-4-methyl-4,5-dihydro-1,3-thiazole-4-carboxylic acid
iron chelating agent

pétadéféritrine — acide (4*S*)-2-{2-hydroxy-4-[2-(2-méthoxyéthoxy)éthoxy]phényl}-4-méthyl-4,5-dihydro-1,3-thiazole-4-carboxylique
chélateur du fer

petadeferitrina — ácido (4*S*)-2-{2-hidroxi-4-[2-(2-metoxietoxi)etoxi]fenil}-4-metil-4,5-dihidro-1,3-tiazol-4-carboxílico
quelante del hierro

$C_{16}H_{21}NO_6S$ 911714-45-9

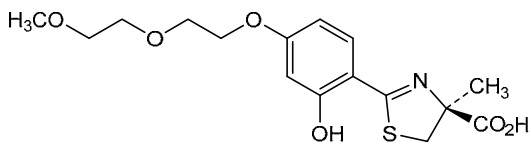

peturadolum

peturadol — 5-{[2-(6-amino-9*H*-purin-9-yl)ethyl]amino}pentan-1-ol
central analgesic

péturadol — 5-{[2-(6-amino-9*H*-purin-9-yl)éthyl]amino}pentan-1-ol
analgésique central

peturadol — 5-{[2-(6-amino-9*H*-purin-9-il)etil]amino}pentan-1-ol
analgésico central

$C_{12}H_{20}N_6O$ 686301-48-4

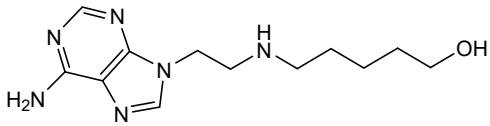

pezatresgenum leucelum #

pezatresgene leucel — allogeneic T lymphocytes derived from peripheral blood mononuclear cells (PBMCs) of a haploidentical hematopoietic cell transplantation (HCT) donor that is negative for the HA-1 genotype and/or negative for HLA A*02, engineered by transposon/transposase-mediated gene delivery to express a T cell receptor (TCR) that is specific for a 9-amino acid peptide (VLHDDLLEA) termed HA-1 derived from the Rho GTPase-activating protein 45 (ARHGAP45) and presented on HLA-A*02:01. The TCR comprises α and β subunits separated by a P2A self-cleaving peptide. The transgene also encodes a codon-optimised CD8 co-receptor consisting of α and β chains separated by a P2A self-cleaving peptide, with the CD8 co-receptor separated from the TCR by an additional P2A self-cleaving peptide. Each P2A sequence is preceded by a furin cleavage site. A 16 amino acid epitope encoding a portion of human CD34 is incorporated into the N-terminus of the CD8α chain. The transgene is under the control of a murine stem cell virus (MSCV) promoter, a Woodchuck hepatitis virus post-transcriptional response element and a simian virus 40 (SV40) polyadenylation (polyA) signal.
The transposase (Armyworm transposase) is introduced in form of an mRNA that comprises an anti-reverse cap analogue, a *Xenopus* globin 5' untranslated region (UTR), a Kozak sequence, the transposase open reading frame, and a *Xenopus* globin 3' UTR. The transgene is introduced via a nanoplasmid DNA vector and contains inverted terminal repeats (ITRs).
The leukapheresis material is electroporated with mRNA transposase as well as the nanoplasmid transposon followed by activation with CD2, CD3 and CD28 agonists. The cells are then grown in serum free media supplemented with interleukin 2 (IL-2), interleukin 7 (IL-7) and interleukin 15 (IL-15). The T lymphocytes (≥95%) are positive for the transgene (≥80% TCR+) and release interferon- gamma (IFN-γ) in response to co-culture with THP-1 cells that express the HA-1 target peptide
cell-based gene therapy (antineoplastic)

pézatresgène leucel — lymphocytes T allogéniques dérivés de cellules mononucléaires du sang périphérique (CMSP) d'un donneur haploidentiques de greffe de cellules hématopoïétiques (GCH) qui sont ngatifs pour le génotype HA-1 et/ou négatifs pour HLA A*02, modifiés par un système de délivrance de gènes par transposon/transposase pour exprimer un récepteur de lymphocytes T (TCR) spécifique d'un peptide de 9 acides aminés (VLHDDLLEA) appelé HA-1, dérivé de la protéine activatrice Rho GTPase 45 (ARHGAP45) et présenté sur HLA-A*02:01. Le TCR comprend des sous-unités α

et β, séparées par un peptide auto-clivant P2A. Le transgène code également avec des codons optimisés un co-récepteur CD8, constitué de chaînes α et β, séparées par un peptide auto-clivant P2A, le co-récepteur CD8 étant séparé du TCR par un autre peptide auto-clivant P2A.
Chaque séquence P2A est précédée d'un site de clivage de la furine. Un épitope de 16 acides aminés codant une partie du CD34 humain est incorporé à l'extrémité N-terminale de la chaîne CD8α. Le transgène est sous le contrôle d'un promoteur du virus des cellules souches murines (MSCV), d'un élément de réponse post-transcriptionnelle du virus de l'hépatite de la marmotte et d'un signal de polyadénylation (polyA) du virus simien 40 (SV40).
La transposase (transposase de la chenille légionnaire) est introduite sous la forme d'un ARNm qui comprend un analogue de la coiffe anti-inverse, une région 5' non traduite (UTR) de la globine de *Xenopus*, une séquence de Kozak, le cadre de lecture ouvert de la transposase et une région 3' UTR de la globine de *Xenopus*. Le transgène est introduit via l'ADN nanoplasmidique et contient des répétitions terminales inversées (RTI).
Le matériel de leucaphérèse est électroporé avec l'ARNm de la transposase ainsi que le transposon nanoplasmidique, suivie d'une activation avec des agonistes CD2, CD3 et CD28. Les cellules sont ensuite cultivées dans un milieu sans sérum, supplémenté en interleukine 2 (IL-2), d'interleukine 7 (IL-7) et d'interleukine 15 (IL-15). Les lymphocytes T (≥95%) sont positifs au transgène (≥80%+) et libèrent de l'interféron gamma (IFN-γ) en réponse à une co-culture avec des cellules THP-1 qui expriment le peptide cible HA-1
thérapie génique à base de cellules (antinéoplasique)

pezatresgén leucel

linfocitos T alogénicos derivados de células mononucleares de sangre periférica (PBMCs) de un donante de transplante de células hematopoyéticas (HCT) haploidéntico que es negativo para el genotipo HA-1 y/o negativo para HLA A*02, manipulados mediante un sistema de entrega genética mediado por transposón/transposasa para expresar el receptor de células T (TCR) que es específico para un péptido de 9 amino ácidos (VLHDDLLEA) llamado HA-1, derivado de la proteína activadora de GTPasa Rho 45 (ARHGAP45) y presentado en HLA-A*02:01. El TCR consta de subunidades α y β separadas por un péptido de auto-escisión P2A. El transgén también codifica, con codones optimizados, un correceptor CD8 que contiene cadenas α y β separadas por un péptido de auto-escisión P2A, con el correceptor CD8 separado del TCR por otro péptido de auto-escisión P2A. Cada secuencia P2A está precedida por un sitio de escisión de furina. En la zona N-terminal de la cadena CD8α se incorpora un epítopo de 16 amino ácidos que codifica una porción del CD34 humano. El transgén está bajo el control de un promotor del virus de células madre murino (MSCV), un elemento de respuesta post-transcripcional del virus de la hepatitis de la marmota (WPRE) y una señal de poliadenilación (poliA) del virus simio 40 (SV40).
La transposasa (transposasa de gusano soldado) se introduce en forma de un ARNm que contiene un análogo de caperuza anti-reverso, una región sin traducir (UTR) en 5' de la globina de *Xenopus*, una secuencia Kozak, el marco de lectura abierto de la transposasa, y una UTR en 3' de la globina de *Xenopus*. El transgén se introduce mediante un nanoplásmido de ADN y contiene repeticiones terminales invertidas (ITRs).

pivodisgenum parvecum #

pivodisgene parvec	recombinant, non-replicating adeno-associated virus serotype 8 (rAAV8) vector, encoding a codon-optimised miniaturised version of human dystrophin (microdystrophin variant ABD1-H1-R1-R2-R3-H3-R24-H4-CR-CT194), under control of a synthetic muscle-specific promoter (SPc5-12) and a small synthetic polyadenylation signal; flanked by AAV2 inverted terminal repeats. The expressed microdystrophin variant contains the actin-binding domain 1 (ABD1), four rod domains (R1-3, R24), three hinge domains (H1, H3, H4) and a cysteine rich (CR) domain; it also features the proximal portion of the C-terminal domain, amino acids 3361-3554 (CT194) *gene therapy (muscular dystrophy)*
pivodisgène parvec	vecteur recombinant de virus adéno-associé de sérotype 8 (rAAV8), non réplicatif, codant une version miniaturisée, optimisée en codons, de la dystrophine humaine (variante de microdystrophine ABD1-H1-R1-R2-R3-H3-R24-H4-CR-CT194), sous le contrôle d'un promoteur synthétique spécifique du muscle (SPc5-12) et d'un petit signal synthétique de polyadénylation; flanqué des répétitions terminales inversées AAV2. Le variant de microdystrophine exprimé contient le domaine de liaison à l'actine 1 (ABD1), quatre domaines en bâtonnets (R1-3, R24), trois domaines charnières (H1, H3, H4), et un domaine riche en cystéine (CR); il contient également la partie proximale du domaine C-terminal, acides aminés 3361-3554 (CT194) *thérapie génique (dystrophie musculaire)*
pivodisgén parvec	vector de virus adenoasociado del serotipo 8, recombinante (rAAV8), no replicativo, que codifica, con codones optimizados, una versión miniaturizada de la distrofina humana (microdistrofina variante ABD1-H1-R1-R2-R3-H3-R24-H4-CR-CT194), bajo el control de un promotor sintético específico de musculo (SPc5-12) y una pequeña señal de poliadenilación sintética; flanqueado por las repeticiones terminales invertidas del AAV2. La variante de microdistrofina expresada contiene el dominio 1 de unión a actina (ABD1), cuatro dominios rod (R1-3, R24), tres dominios bisagra (H1, H3, H4) y un dominio rico en cisteína (CR); también presenta la porción proximal del domino C-terminal, amino ácidos 3361-3554 (CT194) *terapia génica (distrofia muscular*

2648631-52-9

plencifgenum parvecum #

plencifgene parvec	recombinant, non-replicating adeno-associated virus (AAV) vector (with capsid variant A101) encoding codon-optimised human cystic fibrosis transmembrane conductance regulator (CFTR) with the regulatory domain deleted (CFTRΔR), under control of a 173bp cytomegalovirus (CMV173) minimal promoter and a short synthetic polyadenylation signal; flanked by AAV2 inverted terminal repeats. The variant A101 capsid is a chimera consisting primarily of serotype AAV1 but also including amino acids from serotypes AAV2, AAV4, AAV6 and AAV9 *gene therapy (cystic fibrosis)*

plencifgène parvec

vecteur de virus adéno-associé (AAV) recombinant, non réplicatif (avec variante de capside A101) codant un régulateur humain de conductance transmembranaire de la mucoviscidose (CFTR), optimisé en codons, avec le domaine régulateur supprimé (CFTRΔR), sous le contrôle d'un promoteur minimal de cytomégalovirus de 173 paires de bases (CMV173), et un court signal de polyadénylation synthétique; flanqué des répétitions terminales inversées AAV2. La capside variante A101 est une chimère, constituée principalement du sérotype AAV1, mais comprenant également des acides aminés des sérotypes AAV2, AAV4, AAV6 et AAV9
thérapie génique (mucoviscidose)

plencifgén parvec

vector de virus adenoasociado (AAV) recombinante, no replicativo (con la variante de cápside A101), que codifica, con codones optimizados, el regulador de la conductancia de transmembrana de la fibrosis quística (CFTR) humano con el domino regulador delecionado (CFTRΔR), bajo el control de un promotor mínimo de 173 bp del citomegalovirus (CMV173) y una señal sintética corta de poliadenilación; flanqueado por las repeticiones terminales invertidas de AAV2. La variante de cápside A101 es una quimera que consta primariamente del serotipo AAV1 pero también incluye amino ácidos de los serotipos AAV2, AAV4, AAV6 y AAV9
terapia génica (fibrosis quística)

2737363-32-3

plodicitinibum

plodicitinib

1-[(3*S*,4*R*)-3-({2-[(1-ethyl-1*H*-pyrazol-4-yl)amino]-7*H*-pyrrolo[2,3-*d*]pyrimidin-4-yl}oxy)-4-fluoropiperidin-1-yl]prop-2-en-1-one
Janus tyrosine kinase 3/TEC family kinase inhibitor, anti-inflammatory (veterinary use)

plodicitinib

1-[(3*S*,4*R*)-3-({2-[(1-éthyl-1*H*-pyrazol-4-yl)amino]-7*H*-pyrrolo[2,3-*d*]pyrimidin-4-yl}oxy)-4-fluoropipéridin-1-yl]prop-2-én-1-one
inhibiteur des kinases Janus 3 et de la famille TEC, anti-inflammatoire (usage vétérinaire)

plodicitinib

1-[(3*S*,4*R*)-3-({2-[(1-etil-1*H*-pirazol-4-il)amino]-7*H*-pirrolo[2,3-*d*]pirimidin-4-il}oxi)-4-fluoropiperidin-1-il]prop-2-en-1-ona
inhibidor de la familia de kinasas 3/TEC Janus, antiinflamatorio (uso veterinario)

$C_{19}H_{22}FN_7O_2$ 2360992-48-7

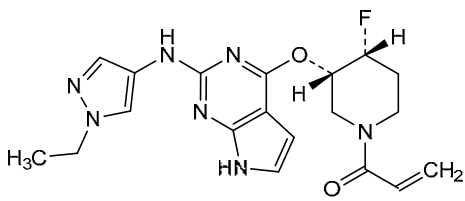

plozalizumabum plevistinagum #

plozalizumab plevistinag	immunoglobulin G1-kappa, anti-[*Homo sapiens* CCR2 (chemokine (C-C motif) receptor 2, C-C chemokine receptor 2, CC-CKR-2, CKR-2, monocyte chemoattractant protein 1 receptor, MCP-1-R, CD192)], humanized monoclonal antibody, conjugated, on an average of 3.8-4.4 cysteinyl residues, to *dazostinag* (a STING agonist) via a cleavable linker; H-gamma1 heavy chain humanized (1-447) [VH (*Homo sapiens* IGHV3-73*01 (86.9%) -(IGHD) -IGHJ1*01 (100%), CDR-IMGT [8.10.8] (26-33.51-60.99-106)) (1-117) -*Homo sapiens* IGHG1*01, G1m17,1 CH1 K120, CH3 D12, L14, 6-G1v3-1 A1.2, A1 (CH1 K120 (214) (118-215), hinge 1-15 (216-230), CH2 L1.2>A (235), G1>A (237) (231-340), CH3 D12 (356), L14 (358) (341-445), CHS (446-447)) (118-447)], (220-219')-disulfide with L-kappa light chain humanized (1'-219') [V-KAPPA (*Homo sapiens* IGKV2-30*02 (90.0%) -IGKJ5*01 (100%), CDR-IMGT [11.3.9] (27'-37'.55'-57'.94'-102')) (1'-112') -*Homo sapiens* IGKC*01 (100%) Km3 A45.1, V101 (C-KAPPA A45.1 (158'), V101 (196')) (113'-219')]; dimer (226-226'':229-229'')-bisdisulfide, produced in a cell line from Chinese hamster ovary (CHO) cells, derived from the cell line CHO-K1, glycoform alfa; substituted at the sulfur atoms of four L-cysteinyl residues on average among 220, 226, 229, 219', 220'', 226'', 229'' and 219''' with (3*RS*)-1-[(28*S*)-28-{[(2*S*)-1-{[(2*S*)-1-{4-[({[(2-{cyclo[($P^{3'}R$)-2'-deoxy-2'-fluoro-*P*-thioadenylyl-(3'→5')-($P^{2'}R$)-7-fluoro-7-carba-*P*-thioinosinylyl-(2'→5')]-$N^{6.1}$-carbonyl}phenyl)methyl](methyl) carbamoyl}oxy)methyl]anilino}-1-oxopropan-2-yl]amino}-3-methyl-1-oxobutan-2-yl]carbamoyl}-26-oxo-2,5,8,11,14,17,20,23-octaoxa-27-azadotriacontan-32-yl]-2,5-dioxopyrrolidin-3-yl (*plevistinag*) groups *antineoplastic*
plozalizumab plévistinag	immunoglobuline G1-kappa, anti-[*Homo sapiens* CCR2 (récepteur 2 de chimiokine (C-C motif), récepteur 2 de chimiokine C-C, CC-CKR-2, CKR-2, récepteur de la protéine 1 chimio-attractive du monocyte, MCP-1-R, CD192)], anticorps monoclonal humanisé; conjugué, sur 4,1 (3,8-4,4) cystéinyl en moyenne, via un linker maléimide-peg-val-ala-PAB clivable, à un agoniste synthétique de STING1 (stimulateur de la réponse à l'interféron cGAMP interacteur 1), conjugué sur une moyenne de 3,8 à 4,4 résidus cystéinyle au *dazostinag* (un agoniste du STING) via un linker clivable;

chaîne lourde H-gamma1 humanisée (1-447) [VH (*Homo sapiens* IGHV3-73*01 (86.9%) -(IGHD) -IGHJ1*01 (100%), CDR-IMGT [8.10.8] (26-33.51-60.99-106)) (1-117) -*Homo sapiens* IGHG1*01 G1m17,1 CH1 K120, CH3 D12, L14, 6-G1v3-1 A1.2, A1 (CH1 K120 (214) (118-215), charnière 1-15 (216-230), CH2 L1.2>A (235), G1>A (237) (231-340), CH3 D12 (356), L14 (358) (341-445), CHS (446-447)) (118-447)], (220-219')-disulfure avec la chaîne légère L-kappa humanisée (1'-219') [V-KAPPA (*Homo sapiens* IGKV2-30*02 (90.0%) -IGKJ5*01 (100%), CDR-IMGT [11.3.9] (27'-37'.55'-57'.94'-102')) (1'-112') -*Homo sapiens* IGKC*01 (100%) Km3 A45.1, V101 (C-KAPPA A45.1 (158'), V101 (196')) (113'-219')]; dimère (226-226'':229-229'')-bisdisulfure, produit dans une lignée cellulaire des cellules ovariennes de hamster chinois (CHO), dérivant de la lignée cellulaire CHO-K1, glycoforme alfa, substitué sur les atomes de soufre de 4 résidus L-cystéinyle en moyenne parmi 220, 226, 229, 219', 220'', 226'', 229'' et 219''' avec des groupes (3*RS*)-1-[(28*S*)-28-{[(2*S*)-1-{[(2*S*)-1-{4-[({[(2-{cyclo[(*P*$^{3'}$*R*)-2'-désoxy-2'-fluoro-*P*-thioadénylyl-(3'→5')-(*P*$^{2'}$*R*)-7-fluoro-7-carba-*P*-thioinosinylyl-(2'→5')]-*N*$^{6.1}$-carbonyl}phényl)méthyl](méthyl) carbamoyl}oxy)méthyl]anilino}-1-oxopropan-2-yl]amino}-3-méthyl-1-oxobutan-2-yl]carbamoyl}-26-oxo-2,5,8,11,14,17,20,23-octaoxa-27-azadotriacontan-32-yl]-2,5-dioxopyrrolidin-3-yle (*plévistinag*)
antinéoplasique

plozalizumab plevistinag

inmunoglobulina G1-kappa, anti-[*Homo sapiens* CCR2 (receptor 2 de quimiokina (C-C motif), receptor 2 de quimiokina C-C, CC-CKR-2, CKR-2, receptor de la proteína 1 quimioatrayente de monocitos, MCP-1-R, CD192)], anticuerpo monoclonal humanizado, conjugado, en un promedio de 3,8-4,4 residuos de cisteinilo, al *dazostinag* (un agonista del STING), a través de un enlace escindible; cadena pesada gamma1 humanizada (1-447) [VH (*Homo sapiens* IGHV3-73*01 (86.90%) -(IGHD)-IGHJ1*01 (100%), CDR-IMGT [8.10.8] (26-33.51-60.99-106)) (1-117) -*Homo sapiens* IGHG1*01, G1m17,1 CH1 K120, CH3 D12, L14, 6-G1v3-1 A1.2, A1 (CH1 K120 (214) (118-215), bisagra 1-15 (216-230), CH2 L1.2>A (235), G1>A (237) (231-340), CH3 D12 (356), L14 (358) (341-445), CHS (446-447)) (118-447)], (220-219')-disulfuro con la cadena ligera L-kappa humanizada (1'-219') [V-KAPPA (*Homo sapiens* IGKV2-30*02 (90.0%) -IGKJ5*01 (100%), CDR-IMGT [11.3.9] (27'-37'.55'-57'.94'-102')) (1'-112') -*Homo sapiens* IGKC*01 (100%) Km3 A45.1, V101 (C-KAPPA A45.1 (158'), V101 (196'))(113'-219')]; dímero (226-226'':229-229'')-bisdisulfuro, producido en una línea celular de las células ováricas de hámster chino (CHO), línea celular derivada de CHO-K1, forma glicosilada alfa, substituido en los átomo de azufre de 4 residuos L-cisteinilo por término medio entre 220, 226, 229, 219', 220'', 226'', 229'' y 219''' con grupos (3*RS*)-1-[(28*S*)-28-{[(2*S*)-1-{[(2*S*)-1-{4-[({[(2-{ciclo[(*P*$^{3'}$*R*)-2'-desoxi-2'-fluoro-*P*-tioadenilil-(3'→5')-(*P*$^{2'}$*R*)-7-fluoro-7-carba-*P*-tioinosinilil-(2'→5')]-*N*$^{6.1}$-carbonil}fenil)metil](metil)carbamoil} oxi)metil]anilino}-1-oxopropan-2-il]amino}-3-metil-1-oxobutan-2-il]carbamoil}-26-oxo-2,5,8,11,14,17,20,23-octaoxa-27-azadotriacontan-32-il]-2,5-dioxopirrolidin-3-ilo (*plevistinag*)
antineoplásico

2983832-01-3

Heavy chain / Chaîne lourde / Cadena pesada

```
EVQLVESGGG LVKPGGSLRL SCAASGFTFS AYAMNWVRQA PGKGLEWVGF   50
IRTKPAGYAT YYAASVKGRF TISRDDSKSI LYLQMNSLKT EDTAVYYCTT  100
PYGGSYRFDG FDVWGQGTMV TVSSASTKGP SVFPLAPSSK STSGGTAALG  150
CLVKDYFPEP VTVSWNSGAL TSGVHTFPAV LQSSGLYSLS SVVTVPSSSL  200
GTQTYICNVN HKPSNTKVDK KVEPKSCDKT HTCPPCPAPE LAGAPSVFLF  250
PPKPKDTLMI SRTPEVTCVV VDVSHEDPEV KFNWYVDGVE VHNAKTKPRE  300
EQYNSTYRVV SVLTVLHQDW LNGKEYKCKV SNKALPAPIE KTISKAKGQP  350
REPQVYTLPP SQEEMTKNQV SLTCLVKGFY PSDIAVEWES NGQPENNYKT  400
TPPVLDSDGS FFLYSRLTVD KSRWQEGNVF SCSVMHEALH NHYTQKSLSL  447
```

Light chain / Chaîne légère / Cadena ligera

```
DVVMTQSPLS LPVTLGQPAS ISCRSSQSLL DSDGKTFLNW FQQRPGQSPR   50
RLIYLVSKLD SGVPDRFSGS GSGTDFTLKI SRVEAEDVGV YYCWQGTHFP  100
QTFGQGTKVE IKRTVAAPSV FIFPPSDEQL KSGTASVVCL LNNFYPREAK  150
VQWKVDNALQ SGNSQESVTE QDSKDSTYSL SSTLTLSKAD YEKHKVYACE  200
VTHQGLSSPV TKSFNRGEC                                    219
```

Post-translational modifications

Disulfide bridges location / Position des ponts disulfure / Posiciones de los puentes disulfuro

Intra-H (C23-C104) 22-98 144-200 261-321 367-425
22''-98'' 144''-200'' 261''-321'' 367''-425''

Intra-L (C23-C104) 23'-93' 139'-199'
23'''-93''' 139'''-199'''

Inter-H-L (h 5-CL 126)* 220-219' 220''-219'''

Inter-H-H (h 11, h 14)* 226-226'' 229-229''

*The four inter-chain disulfide bridges are not present, an average of 4.1 (3.8-4.4) cysteinyl being conjugated, each via two (thioether bonds, to a drug linker.

*Il est quatre ponts disulfures inter-chaînes ne sont pas présents, de 4.1 (3.8-4.4) cysteinyl en moyenne étant chacune conjuguée, via deux liaisons (thioéther, à un linker-principe actif.

*Los cuatro puentes disulfuro inter-catenarios no estan presentes, una media de 4.1 (3.8-4.4) cisteinil está conjugada, a través de dos enlaces (tioéter, con un principio activo.

N-glycosylation sites / Sites de N-glycosylation / Posiciones de N-glicosilación

H CH2 N84.4: 297, 297''

Fucosylated complex bi-antennary CHO-type glycans / glycanes de type CHO bi-antennaires complexes fucosylés / glicanos de tipo CHO biantenarios complejos fucosilados

C-terminal lysine clipping / Coupure de la lysine C-terminale / Recorte de lisina C-terminal

H CH3 K2: 447, 447''

Potential modified residues / Résidus modifiés potentiels / Restos modificados potenciales*

C (220, 226, 229, 219', 220'', 226'', 229'', 219''')

*(*pfevarinag*mAb ~ 4:1)

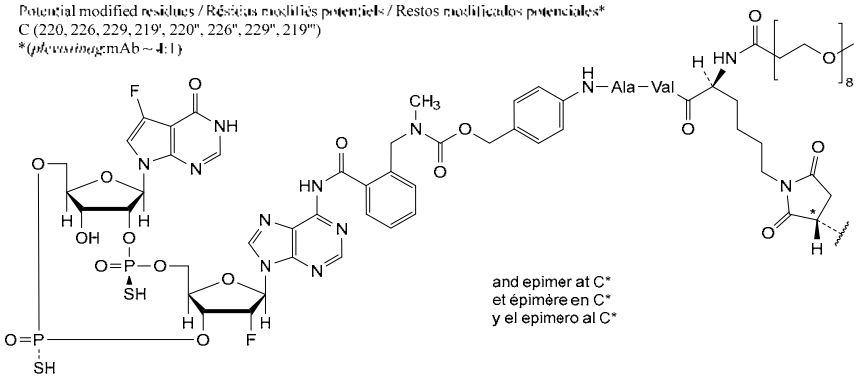

and epimer at C*
et épimère en C*
y el epimero al C*

potravitugum #

potravitug

immunoglobulin G1-kappa, anti-[BK polyomavirus (BKV) (betapolyomavirus hominis) major capsid protein VP1], *Homo sapiens* monoclonal antibody;
H-gamma1 heavy chain *Homo sapiens* (1-451) [VH (*Homo sapiens* IGHV4-34*01 (87.5%) -(IGHD) -IGHJ4*01 (100%), CDR-IMGT [8.7.15] (26-33.51-57.96-110)) (1-121) -*Homo sapiens* IGHG1*03v (100%) G1m3>G1m17, nG1m1 CH1 K120, CH3 E12, M14 (CH1 R120>K (218) (122-219), hinge 1-15 (220-234), CH2 (235- 344), CH3 E12 (360), M14 (362) (345-449), CHS (450-451)) (122-451)], (224-215')-

	disulfide with L-kappa light chain *Homo sapiens* (1'-215') [V-KAPPA (*Homo sapiens* IGKV3-20*01 (95.8%) -IGKJ3*01 (91.7%), CDR-IMGT [7.3.9] (27'-33'.51'-53'.90'-98')) (1'-108') -*Homo sapiens* IGKC*01 (100%) Km3 A45.1, V101 (C-KAPPA A45.1 (154'), V101 (192')) (109'- 215')]; dimer (230-230":233-233")-bisdisulfide, produced in Chinese hamster ovary (CHO) cells, derived from the cell line CHO-K1, lacking the glutamine synthetase (GS-KO) gene, glycoform alfa *antiviral*
potravitug	immunoglobuline G1-kappa, anti-[protéine majeure VP1 de la capside du polyomavirus BK (BKV) (betapolyomavirus hominis)], anticorps monoclonal *Homo sapiens*; chaîne lourde H-gamma1 *Homo sapiens* (1-451) [VH (*Homo sapiens* IGHV4-34*01 (87.5%) -(IGHD) -IGHJ4*01 (100%), CDR-IMGT [8.7.15] (26-33.51-57.96-110)) (1-121) -*Homo sapiens* IGHG1*03v (100%) G1m3>G1m17, nG1m1 CH1 K120, CH3 E12, M14 (CH1 R120>K (218) (122-219), charnière 1-15 (220-234), CH2 (235- 344), CH3 E12 (360), M14 (362) (345-449), CHS (450-451)) (122-451)], (224-215')-disulfure avec la chaîne légère L-kappa *Homo sapiens* (1'-215') [V-KAPPA (*Homo sapiens* IGKV3-20*01 (95.8%) -IGKJ3*01 (91.7%), CDR-IMGT [7.3.9] (27'-33'.51'-53'.90'-98')) (1'-108') -*Homo sapiens* IGKC*01 (100%) Km3 A45.1, V101 (C-KAPPA A45.1 (154'), V101 (192')) (109'-215')]; dimère (230-230":233-233")-bisdisulfure, produit dans des cellules ovariennes de hamster chinois (CHO), dérivant de la lignée cellulaire CHO-K1, ne présentant pas le gène de la glutamine synthétase (GS-KO), glycoforme alfa *antiviral*
potravitug	inmunoglobulina G1-kappa, anti-[proteína importante VP1 de la cápside del poliomavirus BK (BKV) (betapoliomavirus hominis)], anticuerpo monoclonal *Homo sapiens*; cadena pesada H-gamma1 *Homo sapiens* (1-451) [VH (*Homo sapiens* IGHV4-34*01 (87.5%) -(IGHD) -IGHJ4*01 (100%), CDR-IMGT [8.7.15] (26-33.51-57.96-110)) (1-121) -*Homo sapiens* IGHG1*03v (100%) G1m3>G1m17, nG1m1 CH1 K120, CH3 E12, M14 (CH1 R120>K (218) (122-219), bisagra 1-15 (220-234), CH2 (235- 344), CH3 E12 (360), M14 (362) (345-449), CHS (450-451)) (122-451)], (224-215')-disulfuro con la cadena ligera L-kappa *Homo sapiens* (1'-215') [V-KAPPA (*Homo sapiens* IGKV3-20*01 (95.8%) -IGKJ3*01 (91.7%), CDR-IMGT [7.3.9] (27'-33'.51'-53'.90'-98')) (1'-108') -*Homo sapiens* IGKC*01 (100%) Km3 A45.1, V101 (C-KAPPA A45.1 (154'), V101 (192')) (109'- 215')]; dímero (230-230":233-233")-bisdisulfuro, producido en las células ováricas de hámster chino (CHO), línea celular derivada de CHO-K1, en ausencia del gen glutamina sintetasa (GS-KO), forma glicosilada alfa *antiviral*

2923558-06-7

Heavy chain / Chaîne lourde / Cadena pesada

```
QVQLQQWGAG LLKPSETLSL TCAVYRGSFS AYYWTWFRQP PGKGLEWIGE  50
INHRGYTNYN PSLRGRVSIS VDTSKKQFSL KLRSVNAADT AVYYCATLRS 100
TSGWHDYFDY WGQGTLVTVS SASTKGPSVF PLAPSSKSTS GGTAALGCLV 150
KDYFPEPVTV SWNSGALTSG VHTFPAVLQS SGLYSLSSVV TVPSSSLGTQ 200
TYICNVNHKP SNTKVDKKVE PKSCDKTHTC PPCPAPELLG GPSVFLFPPK 250
PKDTLMISRT PEVTCVVVDV SHEDPEVKFN WYVDGVEVHN AKTKPREEQY 300
NSTYRVVSVL TVLHQDWLNG KEYKCKVSNK ALPAPIEKTI SKAKGQPREP 350
QVYTLPPSRE EMTKNQVSLT CLVKGFYPSD IAVEWESNGQ PENNYKTTPP 400
VLDSDGSFFL YSKLTVDKSR WQQGNVFSCS VMHEALHNHY TQKSLSLSPG 450
K                                                       451
```

Light chain / Chaîne légère / Cadena ligera

```
EIVLTQSPGT LSLSPGERAT LSCRASQSVS SSYLAWYQQT PGQAPRLLIY  50
GASSRATGIP DRFSGSGSGT DFTLTISRLE PEDFVVYFCL QYGSSPLTFG 100
PGTKVDIKRT VAAPSVFIFP PSDEQLKSGT ASVVCLLNNF YPREAKVQWK 150
VDNALQSGNS QESVTEQDSK DSTYSLSSTL TLSKADYEKH KVYACEVTHQ 200
GLSSPVTKSF NRGEC                                       215
```

Post-translational modifications

Disulfide bridges location / Position des ponts disulfure / Posiciones de los puentes disulfuro

Intra-H (C23-C104) 22-95 148-204 265-325 371-429
22"-95" 148"-204" 265"-325" 371"-429"
Intra-L (C23-C104) 23'-89' 135'-195'
23'"-89'" 135'"-195'"
Inter-H-L (h 5-CL 126) 224-215' 224"-215'"
Inter-H-H (h 11, h 14) 230-230" 233-233"

N-terminal glutaminyl cyclization / Cyclisation du glutaminyle N-terminal / Ciclación del glutaminilo N-terminal
Q > pyroglutamyl (pE, 5-oxoprolyl) / pyroglutamyle (pE, 5-oxoprolyle) / piroglutamilo (pE, 5-oxoprolilo)
H VH Q1: 1, 1"

N-glycosylation sites / Sites de N-glycosylation / Posiciones de N-glicosilación
H CH2 N84.4: 301, 301"
Fucosylated complex bi-antennary CHO-type glycans / glycanes de type CHO bi-antennaires complexes fucosylés / glicanos de tipo CHO biantenarios complejos fucosilados

C-terminal lysine clipping / Coupure de la lysine C-terminale / Recorte de lisina C-terminal
H CHS K2: 451, 451"

prifetrastatum

prifetrastat — 2-methoxy-*N*-{4-methoxy-6-[(1*H*-pyrazol-1-yl)methyl]-1,2-benzoxazol-3-yl}benzene-1-sulfonamide
antineoplastic

prifétrastat — 2-méthoxy-*N*-{4-méthoxy-6-[(1*H*-pyrazol-1-yl)méthyl]-1,2-benzoxazol-3-yl}benzène-1-sulfonamide
antinéoplasique

prifetrastat — 2-metoxi-*N*-{4-metoxi-6-[(1*H*-pirazol-1-il)metil]-1,2-benzoxazol-3-il}benceno-1-sulfonamida
antineoplásico

$C_{19}H_{18}N_4O_5S$ 2569008-99-5

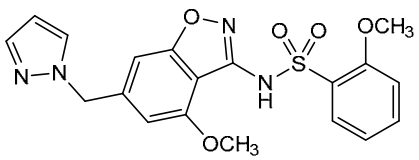

pruvonertinibum

pruvonertinib — *N*-(2-{[2-(dimethylamino)ethyl](methyl)amino}-4-methoxy-5-{[4-(8-methylimidazo[1,2-*a*]pyridin-3-yl)pyrimidin-2-yl]amino}phenyl)prop-2-enamide
epidermal growth factor receptor tyrosine kinase inhibitor, antineoplastic

pruvonertinib

N-(2-{[2-(diméthylamino)éthyl](méthyl)amino}-4-méthoxy-5-{[4-(8-méthylimidazo[1,2-*a*]pyridin-3-yl)pyrimidin-2-yl]amino}phényl)prop-2-énamide
inhibiteur de la tyrosine kinase du récepteur du facteur de croissance épidermique, antinéoplasique

pruvonertinib

N-(2-{[2-(dimetilamino)etil](metil)amino}-5-{[4-(8-metilimidazo[1,2-*a*]piridin-3-il)pirimidin-2-il]amino}-4-metoxifenil)prop-2-enamida
inhibidor del receptor del factor de crecimiento epidérmico, antineoplásico

$C_{27}H_{32}N_8O_2$ 2064269-82-3

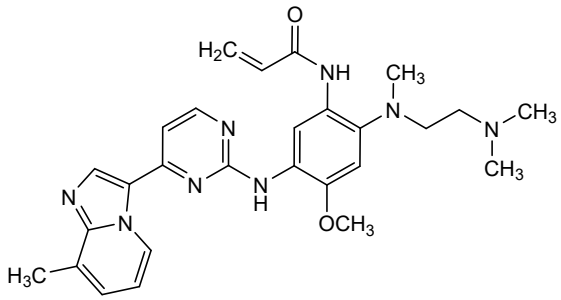

puliretgenum parvecum #

puliretgene parvec

recombinant non-replicating adeno-associated virus serotype 8 (rAAV8) vector encoding human cytochrome P450 family 4, subfamily V member 2 (CYP4V2) under control of a cytomegalovirus (CMV) immediate-early enhancer, chicken β-actin promoter and synthetic intron, and a bovine somatotropin polyadenylation signal; flanked by AAV2 inverted terminal repeats
gene therapy (Bietti's crystalline dystrophy)

puliretgène parvec

vecteur recombinant de virus adéno-associé non réplicatif de sérotype 8 (rAAV8) codant le membre 2 de la sous-famille V, famille 4 du cytochrome P450 humain (CYP4V2), sous le contrôle d'un amplificateur précoce immédiat du cytomégalovirus (CMV), d'un promoteur de la β-actine de poulet et d'un intron synthétique, ainsi que d'un signal de polyadénylation de la somatotropine bovine; flanqué des répétitions terminales inversées AAV2
thérapie génique (dystrophie cristalline de Bietti)

puliretgén parvec

vector de virus adenoasociado del serotipo 8, recombinante (rAAV8), no replicativo, que codifica el miembro 2 de la subfamilia V, familia 4 del citocromo P450 (CYP4V2) bajo el control de un potenciador inmediato-temprano de citomegalovirus (CMV), promotor de la β-actina de pollo y un intrón sintético, y una señal de poliadenilación de la somatotropina bovina; flanqueado por las repeticiones terminales invertidas del AAV2
terapia génica (distrofia cristalina de Bietti)

2923507-02-0

pumitamigum #

pumitamig — immunoglobulin (H-gamma1-VH_L-kappa) dimer, anti-[*Homo sapiens* VEGFA (vascular endothelial growth factor A, VEGF-A, VEGF)] and anti-[*Homo sapiens* CD274 (programmed cell death 1 ligand 1, PDL1, PD-L1, B7 homolog 1, B7H1, B7-H1, PDCD1LG1)], humanized monoclonal antibody, bispecific, tetravalent;
H-gamma1 heavy chain anti-VEGFA fused to a VH anti-CD274 (1-578) [H-gamma1 heavy chain anti-VEGFA humanized (1-452) [VH (*Homo sapiens* IGHV3-30*02 (76.8%) -(IGHD) -IGHJ4*01 (93.3%), CDR-IMGT [8.9.16] (26-33.51-59.97-112)) (1-123)-*Homo sapiens* IGHG1*01, G1m17,1 CH1 K120, CH3 D12, L14, 6-G1v14 CH2 A1.3, A1.2(CH1 K120 (220) (124-221), hinge 1-15 (222-236), CH2 L1.3>A (240), L1.2>A (241) (237-346), CH3 D12 (362), L14 (364) (347-451), CHS K2>del (452) (124-452)] -11-mer bis(tetraglycyl-seryl)-glycyl linker (453-463) -VH anti-CD274 humanized (*Homo sapiens* IGHV3-74*01 (88.8%) -(IGHD) -IGHJ3*01 (90.0%) W113>K (568), M118>Q (573), CDR-IMGT [8.8.8] (489-496.514-521.560-567)) (464-578)]; (226-214')-disulfide with L-kappa light chain humanized (1'-214') [V-KAPPA (*Homo sapiens* IGKV1-16*01 (88.4%) -IGKJ1*01 (100%), CDR-IMGT [6.3.9] (27'-32'.50'-52'.89'-97')) (1'-107') -*Homo sapiens* IGKC*01 (100%) Km3 A45.1, V101 (C-KAPPA A45.1 (153'), V101 (191')) (108'-214')]; dimer (232-232'':235-235'')-bisdisulfide, produced in Chinese hamster ovary (CHO) cells, cell line CHO-S, glycoform alfa
immunossupressant, antineoplastic

pumitamig — immunoglobuline (H-gamma1-VH_L-kappa) dimère, anti-[*Homo sapiens* VEGFA facteur de croissance A de l'endothélium vasculaire, VEGF-A, VEGF)] et anti-[*Homo sapiens* CD274 (ligand 1 de la protéine 1 de mort cellulaire programmée, PDL1, PD-L1, homologue B7.1, PDCD1LG1)], anticorps monoclonal humanisé, bispécifique, tétravalent;
chaîne lourde H-gamma1 anti-VEGFA fusionnée à un VH anti-CD274 (1-578) [chaine lourde H-gamma1 anti-VEGFA humanisée (1-452) [VH (*Homo sapiens* IGHV3-30*02 (76.8%) -(IGHD) -IGHJ4*01 (93.3%), CDR-IMGT [8.9.16] (26-33.51-59.97-112)) (1-123)-*Homo sapiens* IGHG1*01, G1m17,1 CH1 K120, CH3 D12, L14, 6-G1v14 CH2 A1.3, A1.2(CH1 K120 (220) (124-221), charnière 1-15 (222-236), CH2 L1.3>A (240), L1.2>A (241) (237-346), CH3 D12 (362), L14 (364) (347-451), CHS K2>del (452) (124-452)] -11-mer bis(tétraglycyl-séryl)-glycyl linker (453-463) -VH anti-CD274 humanisée (*Homo sapiens* IGHV3-74*01 (88.8%) -(IGHD) -IGHJ3*01 (90.0%) W113>K (568), M118>Q (573), CDR-IMGT [8.8.8] (489-496.514-521.560-567)) (464-578)]; (226-214')-disulfure avec la chaîne légère L-kappa humanisée (1'-214') [V-KAPPA (*Homo sapiens* IGKV1-16*01 (88.4%) -IGKJ1*01 (100%), CDR-IMGT [6.3.9] (27'-32'.50'-52'.89'-97')) (1'-107') -*Homo sapiens* IGKC*01 (100%) Km3 A45.1, V101 (C-KAPPA A45.1 (153'), V101 (191')) (108'-214')]; dimère (232-232'':235-235'')-bisdisulfure, produit dans des cellules ovariennes de hamster chinois (CHO), lignée cellulaire CHO-S, glycoforme alfa
immunosuppresseur, antinéoplasique

pumitamig — inmunoglobulina (H-gamma1-VH_L-kappa) dímero, anti-[*Homo sapiens* VEGFA factor de crecimiento A del endotelio vascular, VEGF-A, VEGF)] y anti-[*Homo sapiens* CD274 (ligando 1 de la proteína 1 de muerte celular programada, PDL1, PD-L1, homólogo B7.1, PDCD1LG1)], anticuerpo monoclonal humanizado, biespecífico, tetravalente;
cadena pesada H-gamma1 anti-VEGFA fusionada con un VH anti-CD274 (1-578) [cadena pesada H-gamma1 anti-VEGFA humanizada (1-452) [VH (*Homo sapiens* IGHV3-30*02 (76.8%) -(IGHD) -IGHJ4*01 (93.3%), CDR-IMGT [8.9.16] (26-33.51-59.97-112)) (1-123)-*Homo sapiens* IGHG1*01, G1m17,1 CH1 K120, CH3 D12, L14, 6-G1v14 CH2 A1.3, A1.2(CH1 K120 (220) (124-221), bisagra 1-15 (222-236), CH2 L1.3>A (240), L1.2>A (241) (237-346), CH3 D12 (362), L14 (364) (347-451), CHS K2>del (452) (124-452)] -11-mer bis(tetraglicil-seril)-glicil enlace (453-463) -VH anti-CD274 humanizada

(*Homo sapiens* IGHV3-74*01 (88.8%) -(IGHD) -IGHJ3*01 (90.0%) W113>K (568), M118>Q (573), CDR-IMGT [8.8.8] (489-496.514-521.560-567)) (464-578)]; (226-214')-disulfuro con la cadena ligera L-kappa humanizada (1'-214') [V-KAPPA (*Homo sapiens* IGKV1-16*01 (88.4%) -IGKJ1*01 (100%), CDR-IMGT [6.3.9] (27'-32'.50'-52'.89'-97')) (1'-107') -*Homo sapiens* IGKC*01 (100%) Km3 A45.1, V101 (C-KAPPA A45.1 (153'), V101 (191')) (108'-214')]; dímero (232-232":235-235")-bisdisulfuro, producido en las células ováricas de hámster chino (CHO), línea celular CHO-S, forma glicosilada alfa

2999726-97-3

Heavy chain / Chaîne lourde / Cadena pesada:
H-gamma1 anti-VEGFA fused to VH anti-CD274 (H, H")

```
EVQLVESGGG LVQPGGSLRL SCAASGYTFT NYGMNWVRQA PGKGLEWVGW  50
INTYTGEPTY AADFKRRFTF SLDTSKSTAY LQMNSLRAED TAVYYCAKYP 100
HYYGSSHWYF DVWGQGTLVT VSSASTKGPS VFPLAPSSKS TSGGTAALGC 150
LVKDYFPEPV TVSWNSGALT SGVHTFPAVL QSSGLYSLSS VVTVPSSSLG 200
TQTYICNVNH KPSNTKVDKK VEPKSCDKTH TCPPCPAPEA AGGPSVFLFP 250
PKPKDTLMIS RTPEVTCVVV DVSHEDPEVK FNWYVDGVEV HNAKTKPREE 300
QYNSTYRVVS VLTVLHQDWL NGKEYKCKVS NKALPAPIEK TISKAKGQPR 350
EPQVYTLPPS RDELTKNQVS LTCLVKGFYP SDIAVEWESN GQPENNYKTT 400
PPVLDSDGSF FLYSKLTVDK SRWQQGNVFS CSVMHEALHN HYTQKSLSLS 450
PGGGGGSGGG GSGEVQLQES GGGLVQPGGS LRLSCAASGF TFSSYWMYWL 500
RQAPGKGLEW VSSINSDSSS TYYRDSVKGR FTISRDNAKN TLYLQMNSLK 550
SEDTAVYYCA KDPGGYAKGQ GTQVTVSS                        578
```

Light chain / Chaîne légère / Cadena ligera: L-kappa : anti-VEGFA (L', L'")

```
DIQMTQSPSS LSASVGDRVT ITCSASQDIS NYLNWYQQKP GKAPKVLIYF  50
TSSLHSGVPS RFSGSGSGTD FTLTISSLQP EDFATYYCQQ YSTVPWTFGQ 100
GTKVEIKRTV AAPSVFIFPP SDEQLKSGTA SVVCLLNNFY PREAKVQWKV 150
DNALQSGNSQ ESVTEQDSKD STYSLSSTLT LSKADYEKHK VYACEVTHQG 200
LSSPVTKSFN RGEC                                      214
```

Post-translational modifications
Disulfide bridges location / Position des ponts disulfure / Posiciones de los puentes disulfuro
Intra-H (C23-C104) 22-96 150-206 267-327 373-431 485-559
22"-96" 150"-206" 267"-327" 373"-431" 485"-559"
Intra-L (C23-C104) 23'-88' 134'-194'
23'"-88'" 134'"-194'"
Intra-H-L (h 5-CL 126) 226-214' 226"-214'"
Inter-H-H (h 11, h 14) 232-232" 235-235"

N-glycosylation sites / Sites de N-glycosylation / Posiciones de N-glicosilación
H CH2 N84.4: 303, 303"
Fucosylated complex bi-antennary CHO-type glycans / glycanes de type CHO bi-antennaires complexes fucosylés / glicanos de tipo CHO biantenarios complejos fucosilados.

ralometostatum

ralometostat *N*-(6-amino-5-methylpyridin-3-yl)-2-[(2*R*,5*S*)-2-(1,3-benzothiazol -5-yl)-5-methylpiperidin-1-yl]-2-oxoacetamide
antineoplastic

ralométostat *N*-(6-amino-5-méthylpyridin-3-yl)-2-[(2*R*,5*S*)-2-(1,3-benzothiazol-5-yl)-5-methylpiperidin-1-yl]-2-oxoacetamide
antinéoplasique

ralometostat *N*-(6-amino-5-metilpiridin-3-il)-2-[(2*R*,5*S*)-2-(1,3-benzotiazol-5-il)-5-metilpiperidin-1-il]-2-oxoacetamida
antineoplásico

$C_{21}H_{23}N_5O_2S$ 2760481-53-4

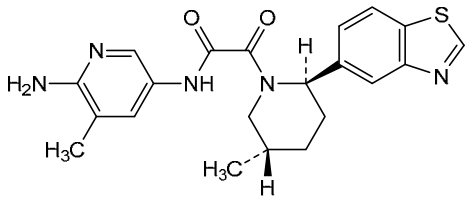

ramantamigum #

ramantamig immunoglobulin (H-gamma1-scFvkh_L-lambda2)_scFvkh-G1(h-CH2-CH3), anti-[*Homo sapiens* CD3E (CD3 epsilon, Leu-4)], anti-[*Homo sapiens* GPRC5D (G protein-coupled receptor class C group 5 member D)] and anti-[*Homo sapiens* TNFRSF17 (tumor necrosis factor (TNF) receptor superfamily member 17, B cell maturation antigen, BCMA, TNFRSF13A, CD269)], *Homo sapiens* monoclonal antibody; trispecific, trivalent;
H-gamma1 heavy chain anti-CD3E fused to a scFvkh anti-GPRC5D (1-721) [H-gamma1 heavy chain anti-CD3E *Homo sapiens* (1-450) [VH (*Homo sapiens* IGHV6-1*01 (88.1%) -(IGHD) -IGHJ4*01 (100%), CDR-IMGT [10.9.10] (26-35.53-61.100-109)) (1-120)-*Homo sapiens* IGHG1*03v, G1m3>G1m17, nG1m1 CH1 K120, CH3 E12, M14, 6-G1v14-67 CH2 A1.3, A1.2, S27, 14-G1v33 CH3 S22, A24, V86 (hole), 10-G1v83 CH3 R115, F116 (CH1 R120>K (217) (121-218), hinge 1-15 (219-233), CH2 L1.3>A (237), L1.2>A (238), D27>S (268) (234-343), CH3 E12 (359), M14 (361), T22>S (369), L24>A (371), Y86>V (410), H115>R (438), Y116>F (439) (344-448), CHS (449-450)) (121-450)] -20-mer tetrakis(tetraglycyl-seryl) linker (451-470) -scFvkh anti-GPRC5D *Homo sapiens* (471-721) [V-KAPPA (*Homo sapiens* IGKV2-24*01 (99.0%) -IGKJ2*02 (100%), CDR-IMGT [11.3.9] (497-507.525-527.564-572)) (471-582) -20-mer (GGSEGKSSGSGSESKSTGGS) linker (583-602) -VH (*Homo sapiens* IGHV2-26*04 (93.9%) -IGHD -IGHJ6*01 (100%), CDR-IMGT [10.7.11] (628-637.655-661.700-710)) (603-721)]]; (223-215')-disulfide with L-lambda2 light chain anti-CD3E *Homo sapiens* (1'-216') [V-LAMBDA (*Homo sapiens* IGLV2-23*02 (84.8%) -IGLJ2*01 (90.9%), CDR-IMGT [9.3.10] (26'-34'.52'-54'.91'-100')) (1'-110') -*Homo sapiens* IGLC2*01 (100%) (C-LAMBDA2) (111'-216')];
fused heavy chain scFvkh-G1(h-CH2-CH3) anti-TNFRSF17 *Homo sapiens* (1''-484'') [scFvkh anti-TNFRSF17 *Homo sapiens* (1''-252'') [V-KAPPA (*Homo sapiens* IGKV3-20*01 (94.8%) -IGKJ2*01 (100%), CDR-IMGT [7.3.10] (27''-33''.51''-53''.90''-99'')) (1''-109'') -20-mer (GGSEGKSSGSGSESKSTGGS) linker (110''-129'') -[VH (*Homo sapiens* IGHV3-23*01 (100%) -(IGHD) -IGHJ6*01 (94.4%), CDR-IMGT [8.8.16] (155''-162''.180''-187''.226''-241'')) (130''-252'')] -*Homo sapiens* IGHG1*03v h-CH2-CH3-CHS, nG1m1 CH3 E12, M14, 6-G1v14-67 CH2 A1.3, A1.2, S27, 14-G1v32 CH3 W22 (knob), 15-G1v37 hinge S5 [(hinge 1-15 C5>S(257'') (253''-267''), CH2 L1.3>A (271''), L1.2>A (272''), D27>S (302'') (268''-377''), CH3 E12 (393''), M14 (395''), T22>W (403'') (378''-482''), CHS (483''-484'')) (253''-484'')]]; dimer (229-263'': 232-266'')-bisdisulfide, produced in Chinese hamster ovary (CHO) cells, glycoform alfa
antineoplastic

ramantamig immunoglobuline (H-gamma1-scFvkh_L-lambda2)_ scFvkh-G1(h-CH2-CH3), anti-[*Homo sapiens* CD3E (CD3 epsilon, Leu-4)], anti-[*Homo sapiens* GPRC5D (membre D du groupe 5 de la classe C des récepteurs couplés aux protéines G)] and anti-[*Homo sapiens* TNFRSF17 (membre 17 de la superfamille des récepteurs du facteur de nécrose tumorale (TNF), antigène de maturation de cellule B, BCMA, TNFRSF13A, CD269)], anticorps monoclonal *Homo sapiens*; trispécifique, trivalent;
chaîne lourde H-gamma1 anti-CD3E fusionnée à un scFvkh anti-GPRC5D (1-721) [H-gamma1 heavy chain anti-CD3E *Homo sapiens* (1-450) [VH (*Homo sapiens* IGHV6-1*01 (88.1%) -(IGHD) -IGHJ4*01 (100%), CDR-IMGT [10.9.10] (26-35.53-61.100-109)) (1-120)-*Homo sapiens* IGHG1*03v, G1m3>G1m17, nG1m1 CH1 K120, CH3 E12, M14, 6-G1v14-67 CH2 A1.3, A1.2, S27, 14-G1v33 CH3 S22, A24, V86 (hole), 10-G1v83 CH3 R115, F116 (CH1 R120>K (217) (121-218), charnière 1-15 (219-233), CH2 L1.3>A (237), L1.2>A (238), D27>S (268) (234-343), CH3 E12 (359), M14 (361), T22>S (369), L24>A (371), Y86>V (410), H115>R (438), Y116>F (439) (344-448), CHS (449-450)) (121-450)] -20-mer tétrakis(tétraglycyl-séryl) linker (451-470) -scFvkh anti-GPRC5D *Homo sapiens* (471-721) [V-KAPPA (*Homo sapiens* IGKV2-24*01 (99.0%) -IGKJ2*02 (100%), CDR-IMGT [11.3.9] (497-507.525-527.564-572)) (471-582) -20-mer (GGSEGKSSGSGSESKSTGGS) linker (583-602) -VH (*Homo sapiens* IGHV2-26*04 (93.9%) -IGHD -IGHJ6*01 (100%), CDR-IMGT [10.7.11] (628-637.655-661.700-710)) (603-721)]]; (223-215')-disulfure avec la chaîne légère L-lambda2 anti-CD3E *Homo sapiens* (1'-216') [V-LAMBDA (*Homo sapiens* IGLV2-23*02 (84.8%) -IGLJ2*01 (90.9%), CDR-IMGT [9.3.10] (26'-34'.52'-54'.91'-100')) (1'-110') -*Homo sapiens* IGLC2*01 (100%) (C-LAMBDA2) (111'-216')];

chaîne lourde fusionnée scFvkh-G1(h-CH2-CH3) anti-TNFRSF17 *Homo sapiens* (1''-484'') [scFvkh anti-TNFRSF17 *Homo sapiens* (1''-252'') [V-KAPPA (*Homo sapiens* IGKV3-20*01 (94.8%) -IGKJ2*01 (100%), CDR-IMGT [7.3.10] (27''-33''.51''-53''.90''-99'')) (1''-109'') -20-mer (GGSEGKSSGSGSESKSTGGS) linker (110''-129'') -[VH (*Homo sapiens* IGHV3-23*01 (100%) -(IGHD) -IGHJ6*01 (94.4%), CDR-IMGT [8.8.16] (155''-162''.180''-187''.226''-241'')) (130''-252'')] -*Homo sapiens* IGHG1*03v h-CH2-CH3-CHS, nG1m1 CH3 E12, M14, 6-G1v14-67 CH2 A1.3, A1.2, S27, 14-G1v32 CH3 W22 (knob), 15-G1v37 charnière S5 [(charnière 1-15 C5>S(257'') (253''-267''), CH2 L1.3>A (271''), L1.2>A (272''), D27>S (302'') (268''-377''), CH3 E12 (393''), M14 (395''), T22>W (403'') (378''-482''), CHS (483''-484'')) (253''-484'')]]; dimère (229-263'': 232-266'')-bisdisulfure, produit dans des cellules ovariennes de hamster chinois (CHO), glycoforme alfa

antinéoplasique

ramantamig

inmunoglobulina (H-gamma1-scFvkh_L-lambda2)_ scFvkh-G1(h-CH2-CH3), anti-[*Homo sapiens* CD3E (CD3 épsilon, Leu-4)], anti-[*Homo sapiens* GPRC5D (miembro D del grupo 5 de la clase C de los receptores acoplados a proteínas G)] y anti-[*Homo sapiens* TNFRSF17 (miembro 17 de la superfamilia de los receptores del factor de necrosis tumoral (TNF), antígeno de maduración de célula B, BCMA, TNFRSF13A, CD269)], anticuerpo monoclonal *Homo sapiens*; triespecífico, trivalente;
cadena pesada H-gamma1 anti-CD3E fusionada con un scFvkh anti-GPRC5D (1-721) [H-gamma1 cadena pesada anti-CD3E *Homo sapiens* (1-450) [VH (*Homo sapiens* IGHV6-1*01 (88.1%) -(IGHD) -IGHJ4*01 (100%), CDR-IMGT [10.9.10] (26-35.53-61.100-109)) (1-120)-*Homo sapiens* IGHG1*03v, G1m3>G1m17, nG1m1 CH1 K120, CH3 E12, M14, 6-G1v14-67 CH2 A1.3, A1.2, S27, 14-G1v33 CH3 S22, A24, V86 (hole), 10-G1v83 CH3 R115, F116 (CH1 R120>K (217) (121-218), bisagra 1-15 (219-233), CH2 L1.3>A (237), L1.2>A (238), D27>S (268) (234-343), CH3 E12 (359), M14 (361), T22>S (369), L24>A (371), Y86>V (410), H115>R (438), Y116>F (439) (344-448), CHS (449-450)) (121-450)] -20-mer tetrakis(tetraglicil-seril) enlace (451-470) -scFvkh anti-GPRC5D *Homo sapiens* (471-721) [V-KAPPA (*Homo sapiens* IGKV2-24*01 (99.0%) -IGKJ2*02 (100%), CDR-IMGT [11.3.9] (497-507.525-527.564-572)) (471-582) -20-mer (GGSEGKSSGSGSESKSTGGS) enlace (583-602) -VH (*Homo sapiens* IGHV2-26*04 (93.9%) -IGHD -IGHJ6*01 (100%), CDR-IMGT [10.7.11] (628-637.655-661.700-710)) (603-721)]]; (223-215')-disulfuro con la cadena ligera L-lambda2 anti-CD3E *Homo sapiens* (1'-216') [V-LAMBDA (*Homo sapiens* IGLV2-23*02 (84.8%) -IGLJ2*01 (90.9%), CDR-IMGT [9.3.10] (26'-34'.52'-54'.91'-100')) (1'-110') -*Homo sapiens* IGLC2*01 (100%) (C-LAMBDA2) (111'-216')];
cadena pesada fusionada scFvkh-G1(h-CH2-CH3) anti-TNFRSF17 *Homo sapiens* (1''-484'') [scFvkh anti-TNFRSF17 *Homo sapiens* (1''-252'') [V-KAPPA (*Homo sapiens* IGKV3-20*01 (94.8%) -IGKJ2*01 (100%), CDR-IMGT [7.3.10] (27''-33''.51''-53''.90''-99'')) (1''-109'') -20-mer (GGSEGKSSGSGSESKSTGGS) enlace (110''-129'') -[VH (*Homo sapiens* IGHV3-23*01 (100%) -(IGHD) -IGHJ6*01 (94.4%), CDR-IMGT [8.8.16] (155''-162''.180''-187''.226''-241'')) (130''-252'')] -*Homo sapiens* IGHG1*03v h-CH2-CH3-CHS, nG1m1 CH3 E12, M14, 6-G1v14-67 CH2 A1.3, A1.2, S27, 14-G1v32 CH3 W22 (knob), 15-G1v37 bisagra S5 [(bisagra 1-15 C5>S(257'') (253''-267''), CH2 L1.3>A (271''), L1.2>A (272''), D27>S (302'') (268''-377''), CH3 E12 (393''), M14 (395''), T22>W (403'') (378''-482''), CHS (483''-484'')) (253''-484'')]]; dímero (229-263'': 232-266'')-bisdisulfuro, producido en las células ováricas de hámster chino (CHO), forma glicosilada alfa

antineoplásico

2988886-91-3

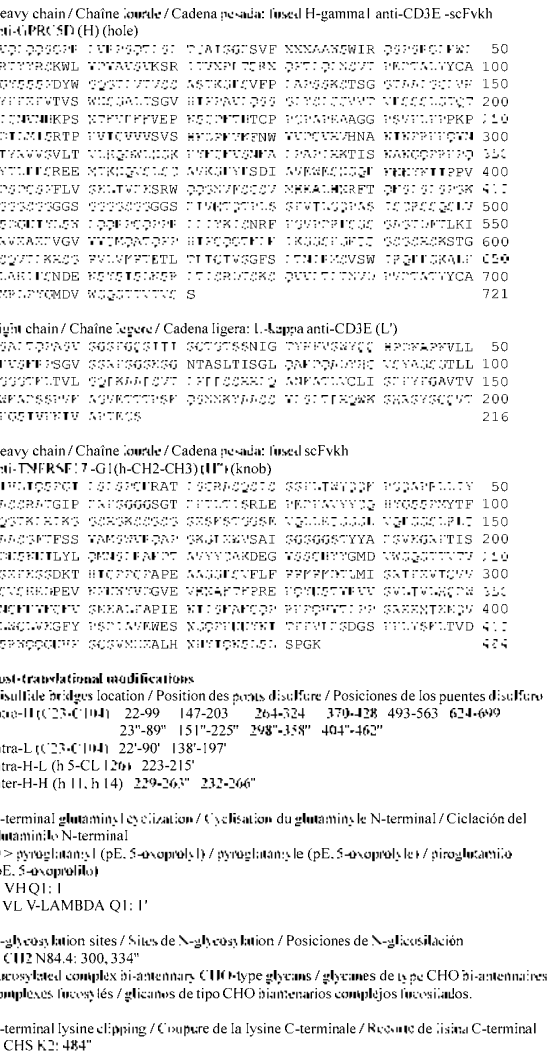

ranicabtagenum autoleucelum #

ranicabtagene autoleucel — autologous T lymphocytes obtained from peripheral blood mononuclear cells by leukapheresis, transduced with a non-replicating gamma-retroviral vector, encoding a chimeric antigen receptor targeting CD19, comprising a CD8α signal peptide, an anti-CD19 single chain variable fragment (scFv) (derived from clone FMC63), a CD8α hinge, a CD28 transmembrane region, an intracellular CD28 co-stimulatory and a CD3ζ signalling domain. The construct is flanked by 5' and 3' long terminal repeats (LTRs), derived from the myeloproliferative sarcoma virus (MPSV) and the murine embryonic stem cell virus (MESV), which contain a 5' LTR promoter and 3' LTR termination sequence. The vector also contains a psi packaging signal and is pseudotyped with gibbon ape leukemia virus (GALV) Env glycoprotein.

	The leukapheresis material is enriched for CD3+ T lymphocytes by positive immunoselection, prior to activation with CD3 and CD28 agonists. The cells are then transduced with the retroviral vector and expanded in media containing interleukin 2 (IL-2). The T lymphocytes (≥ 90%) are positive for the transgene (≥20% CAR positive), express CD107a (≥20%) and demonstrate cytotoxicity towards CD19 expressing cells *cell-based gene therapy (antineoplastic)*
ranicabtagène autoleucel	lymphocytes T autologues obtenus à partir de cellules mononucléaires du sang périphérique par leucaphérèse, transduits avec un vecteur gamma-rétroviral non réplicatif, codant un récepteur antigénique chimérique ciblant CD19, comprenant un peptide signal CD8α, un fragment variable à chaîne unique anti-CD19 (scFv) (dérivé du clone FMC63), une charnière CD8α, une région transmembranaire CD28, un domaine intracellulaire de co-stimulation CD28 et un domaine de signalisation CD3ζ. La construction est flanquée de répétitions terminales longues (LTRs) en 5' et en 3', dérivées du virus du sarcome myéloprolifératif (MPSV) et du virus des cellules souches embryonnaires murines (MESV), qui contiennent un promoteur LTR en 5', et une séquence de terminaison LTR en 3'. Le vecteur contient également un signal d'emballage ψ et est pseudotypé avec la glycoprotéine Env du virus de la leucémie du singe gibbon (GALV). Le matériel de leucaphérèse est enrichi en lymphocytes T CD3+ par immunosélection positive, avant activation avec des agonistes CD3 et CD28. Les cellules sont ensuite transduites avec le vecteur rétroviral et expansées dans un milieu contenant de l'interleukine 2 (IL-2). Les lymphocytes T (≥90%) sont positifs pour le transgène (≥20% RAC positifs), expriment CD107a (≥20%) et présentent une cytotoxicité envers les cellules exprimant CD19 *thérapie génique à base de cellules (antinéoplasique)*
ranicabtagén autoleucel	linfocitos T autólogos obtenidos de células mononucleares de sangre periférica por leucoaféresis, transducidos con un vector gamma retroviral, no replicativo, que codifica un receptor de antígenos quimérico dirigido a CD19, que consta de un péptido señal de CD8α, un fragmento variable de cadena sencilla (scFv) anti-CD19 (derivado del clon FMC63), una bisagra de CD8α, una región transmembrana de CD28, un dominio intracelular coestimulador de CD28 y un dominio de señalización de CD3ζ. El constructo está flanqueado por repeticiones terminales largas (LTRs) en 5' y 3', derivadas del virus del sarcoma mieloproliferativo (MPSV) y del virus de células madre embrionarias murino (MESV), que contienen un promotor 5' LTR y una secuencia de terminación 3' LTR. El vector también contiene una señal de empaquetamiento psi y está seudotipado con la glicoproteína Env del virus de la leucemia del Gibón (GALV). El material de leucoaféresis se enriquece en linfocitos T CD3+ mediante inmunoselección antes de la activación con agonistas de CD3 y CD28. Las células se transducen a continuación con el vector retroviral y se expanden en medio que contiene interleuquina 2 (IL-2). Los linfocitos T (≥90%) son positivos para el transgén (≥20% CAR positivos), expresan CD107a (≥20%) y muestran citotoxicidad frente células que expresan CD19 *terapia génica basada en células (antineoplásico)*

rapaprutugum #

rapaprutug	immunoglobulin G1-kappa, anti-[*Homo sapiens* KARS1 (lysyl-tRNA synthetase 1)], *Homo sapiens* monoclonal antibody; H-gamma1 heavy chain *Homo sapiens* (1-446) [VH (*Homo sapiens* IGHV3-23*01 (92.9%) -(IGHD) -IGHJ4*01 (100%), CDR-IMGT [8.8.9] (26-33.51-58.97-105)) (1-116) -*Homo sapiens* IGHG1*01 (100%) G1m17,1 CH1 K120, CH3 D12, L14 (CH1 K120 (213) (117-214), hinge 1-15 (215-229), CH2 (230-339), CH3 D12 (355), L14 (357) (340-444), CHS (445-446)) (117-446)], (219-217')-disulfide with V-lambda-C-kappa light chain *Homo sapiens* (1'-217') [V-LAMBDA (*Homo sapiens* IGLV1-47*02 (88.5%) -IGLJ2*01 (100%), CDR-IMGT [8.3.11] (26'-33'.51'-53'.90'-100')) (1'-110') -*Homo sapiens* IGKC*01 (100%) Km3 A45.1, V101 (C-KAPPA A45.1 (156'), V101 (194')) (111'-217')]; dimer (225-225'':228-228'')-bisdisulfide, produced in Chinese hamster ovary (CHO) cells, derived from the cell line CHO-K1, lacking the glutamine synthetase (GS-KO) gene, glycoform alfa *anti-inflammatory*
rapaprutug	immunoglobuline G1-kappa, anti-[*Homo sapiens* KARS1 (lysyl-ARNt synthétase 1)], anticorps monoclonal *Homo sapiens*; chaîne lourde H-gamma1 *Homo sapiens* (1-446) [VH (*Homo sapiens* IGHV3-23*01 (92.9%) -(IGHD) -IGHJ4*01 (100%), CDR-IMGT [8.8.9] (26-33.51-58.97-105)) (1-116) -*Homo sapiens* IGHG1*01 (100%) G1m17,1 CH1 K120, CH3 D12, L14 (CH1 K120 (213) (117-214), charnière 1-15 (215-229), CH2 (230-339), CH3 D12 (355), L14 (357) (340-444), CHS (445-446)) (117-446)], (219-217')-disulfure avec la chaîne légère V-lambda-C-kappa *Homo sapiens* (1'-217') [V-LAMBDA (*Homo sapiens* IGLV1-47*02 (88.5%) -IGLJ2*01 (100%), CDR-IMGT [8.3.11] (26'-33'.51'-53'.90'-100')) (1'-110') -*Homo sapiens* IGKC*01 (100%) Km3 A45.1, V101 (C-KAPPA A45.1 (156'), V101 (194')) (111'-217')]; dimère (225-225'':228-228'')-bisdisulfure, produit dans des cellules ovariennes de hamster chinois (CHO), dérivant de la lignée cellulaire CHO-K1, ne présentant pas le gène de la glutamine synthétase (GS-KO), glycoforme alfa *anti-inflammatoire*
rapaprutug	inmunoglobulina G1-kappa, anti-[*Homo sapiens* KARS1 (lisil-ARNt sintetasa 1)], anticuerpo monoclonal *Homo sapiens*; cadena pesada H-gamma1 *Homo sapiens* (1-446) [VH (*Homo sapiens* IGHV3-23*01 (92.9%) -(IGHD) -IGHJ4*01 (100%), CDR-IMGT [8.8.9] (26-33.51-58.97-105)) (1-116) -*Homo sapiens* IGHG1*01 (100%) G1m17,1 CH1 K120, CH3 D12, L14 (CH1 K120 (213) (117-214), bisagra 1-15 (215-229), CH2 (230-339), CH3 D12 (355), L14 (357) (340-444), CHS (445-446)) (117-446)], (219-217')-disulfuro con la cadena ligera V-lambda-C-kappa *Homo sapiens* (1'-217') [V-LAMBDA (*Homo sapiens* IGLV1-47*02 (88.5%) -IGLJ2*01 (100%), CDR-IMGT [8.3.11] (26'-33'.51'-53'.90'-100')) (1'-110') -*Homo sapiens* IGKC*01 (100%) Km3 A45.1, V101 (C-KAPPA A45.1 (156'), V101 (194')) (111'-217')]; dímero (225-225'':228-228'')-bisdisulfuro, producido en las células ováricas de hámster chino (CHO), línea celular derivada de CHO-K1, en ausencia del gen glutamina sintetasa (GS-KO), forma glicosilada alfa *antiinflamatorio*

2994192-38-8

Heavy chain / Chaîne lourde / Cadena pesada (H, H") Il-gammal

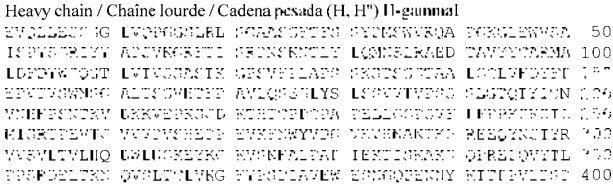

Light chain / Chaîne légère / Cadena ligera (L', L'") V-lambda-C-kappa

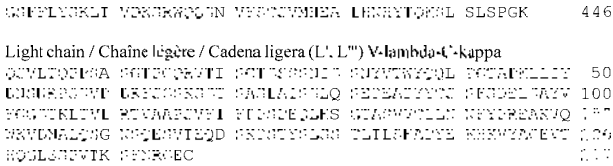

Post-translational modifications

Disulfide bridges location / Position des ponts disulfure / Posiciones de los puentes disulfuro

Intra-H (C23-C104) 22-96 143-199 260-320 366-424
22"-96" 143"-199" 260"-320" 366"-424"
Intra-L (C23-C104) 22'-89' 137'-197'
22'"-89'" 137'"-197'"
Inter-H-L (h 5-CL 126) 219-217' 219"-217'"
Inter-H-H (h 11, h 14) 225-225" 228-228"

N-terminal glutaminyl cyclization / Cyclisation du glutaminyle N-terminal / Ciclación del glutaminilo N-terminal
Q > pyroglutamyl (pE, 5-oxoprolyl) / pyroglutamyle (pE, 5-oxoprolyle) / piroglutamilo (pE, 5-oxoprolilo)
L VL V-LAMBDA Q1: 1', 1'"

N-glycosylation sites / Sites de N-glycosylation / Posiciones de N-glicosilación
H CH2 N84.4: 296, 296"
Fucosylated complex bi-antennary CHO-type glycans / glycanes de type CHO bi-antennaires complexes fucosylés / glicanos de tipo CHO biantenarios complejos fucosilados

C-terminal lysine clipping / Coupure de la lysine C-terminale / Recorte de lisina C-terminal
H CHS K2: 446, 446"

ratutrelvirum

ratutrelvir	(1*R*,2*S*,5*S*)-*N*-{(1*S*)-1-cyano-2-[(3*RS*)-2-oxo-2,3-dihydro-1*H*-indol-3-yl]ethyl}-3-[(2*S*)-3,3-dimethyl-2-(2,2,2-trifluoroacetamido)butanoyl]-6,6-dimethyl-3-azabicyclo[3.1.0]hexane-2-carboxamide *protease inhibitor, antiviral*
ratutrelvir	(1*R*,2*S*,5*S*)-*N*-{(1*S*)-1-cyano-2-[(3*RS*)-2-oxo-2,3-dihydro-1*H*-indol-3-yl])éthyl}-3-[(2*S*)-3,3-diméthyl-2-(2,2,2-trifluoroacétamido)butanoyl]-6,6-diméthyl-3-azabicyclo[3.1.0]hexane-2-carboxamide *inhibiteur de protéase, antiviral*
ratutrelvir	(1*R*,2*S*,5*S*)-*N*-{(1*S*)-1-ciano-2-[(3*RS*)-2-oxo-2,3-dihidro-1*H*-indol-3-il])etil}-3-[(2*S*)-3,3-dimetil-2-(2,2,2-trifluoroacetamido)butanoil]-6,6-dimetil-3-azabiciclo[3.1.0]hexano-2-carboxamida *inhibidor de la proteasa, antiviral*

$C_{27}H_{32}F_3N_5O_4$ 2929236-94-0

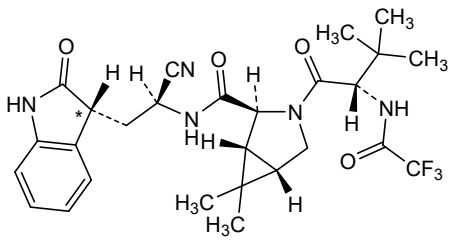

and epimer at C*
et l'épimère en C*
el epímero al C*

refisolonum

refisolone — 10-hydroxy-16α,17α-epoxyestr-4-en-3-one
$GABA_A$ receptor antagonist, migraine

réfisolone — 10-hydroxy-16α,17α-époxyestr-4-én-3-one
antagoniste des récepteurs $GABA_A$, migraine

refisolona — 10-hidroxi-16α,17α-epoxiestr-4-en-3-ona
antagonista de los receptores $GABA_A$, migraña

$C_{18}H_{24}O_3$ 202718-04-5

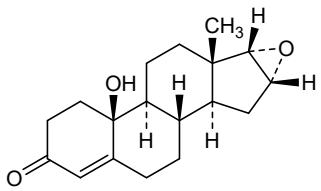

retavibartum #

retavibart — immunoglobulin G1-kappa, anti-[human respiratory syncytial virus (RSV) fusion glycoprotein F], *Homo sapiens* monoclonal antibody;
H-gamma1 heavy chain *Homo sapiens* (1-457) [VH (*Homo sapiens* IGHV5-51*01 (86.7%) -(IGHD) -IGHJ2*01 (93.8%), CDR-IMGT [8.8.20] (26-33.51-58.97-116)) (1-127) -*Homo sapiens* IGHG1*03, G1m3, nG1m1 CH1 R120, CH3 E12, M14, 9-G1v24 CH3 L107, S114 (CH1 R120 (224) (128-225), hinge 1-15 (226-240), CH2 (241-350), CH3 E12 (366), M14 (368), M107>L (438), N114>S (444) (351-455), CHS (456-457)) (128-457)], (230-215')-disulfide with L-kappa light chain *Homo sapiens* (1'-215') [V-KAPPA (*Homo sapiens* IGKV3-15*01 (92.6%) -IGKJ5*01 (91.7%) I126>N (107'), CDR-IMGT [6.3.10] (27'-32'.50'-52'.89'-98'))(1'-108') - *Homo sapiens* IGKC*01 (100%) Km3 A45.1, V101 (C-KAPPA A45.1 (154'), V101 (192')) (109'-215')]; dimer (236-236":239-239")-bisdisulfide, produced in Chinese hamster ovary (CHO) cells, cell line CHO-K1, glycoform alfa
antiviral

rétavibart — immunoglobuline G1-kappa, anti-[glycoprotéine de fusion F du virus respiratoire syncytial (VRS) humain], anticorps monoclonal *Homo sapiens*;
chaîne lourde H-gamma1 *Homo sapiens* (1-457) [VH (*Homo sapiens* IGHV5-51*01 (86.7%) -(IGHD) -IGHJ2*01 (93.8%), CDR-IMGT [8.8.20]

(26-33.51-58.97-116)) (1-127) -*Homo sapiens* IGHG1*03, G1m3, nG1m1 CH1 R120, CH3 E12, M14, 9-G1v24 CH3 L107, S114 (CH1 R120 (224) (128-225), charnière 1-15 (226-240), CH2 (241-350), CH3 E12 (366), M14 (368), M107>L (438), N114>S (444) (351-455), CHS (456-457)) (128-457)], (230-215')-disulfure avec la chaîne légère L-kappa *Homo sapiens* (1'-215') [V-KAPPA (*Homo sapiens* IGKV3-15*01 (92.6%) -IGKJ5*01 (91.7%) I126>N (107'), CDR-IMGT [6.3.10] (27'-32'.50'-52'.89'-98')) (1'-108') -*Homo sapiens* IGKC*01 (100%) Km3 A45.1, V101 (C-KAPPA A45.1 (154'), V101 (192')) (109'-215')]; dimère (236-236'':239-239'')-bisdisulfure, produit dans des cellules ovariennes de hamster chinois (CHO), lignée cellulaire CHO-K1, glycoforme alfa
antiviral

retavibart

inmunoglobulina G1-kappa, anti-[glicoproteína de fusión F del virus respiratorio sincitial (VRS) humano], anticuerpo monoclonal *Homo sapiens*;
cadena pesada H-gamma1 *Homo sapiens* (1-457) [VH (*Homo sapiens* IGHV5-51*01 (86.7%) -(IGHD) -IGHJ2*01 (93.8%), CDR-IMGT [8.8.20] (26-33.51-58.97-116)) (1-127) -*Homo sapiens* IGHG1*03, G1m3, nG1m1 CH1 R120, CH3 E12, M14, 9-G1v24 CH3 L107, S114 (CH1 R120 (224) (128-225), bisagra 1-15 (226-240), CH2 (241-350), CH3 E12 (366), M14 (368), M107>L (438), N114>S (444) (351-455), CHS (456-457)) (128-457)], (230-215')-disulfuro con la cadena ligera L-kappa *Homo sapiens* (1'-215') [V-KAPPA (*Homo sapiens* IGKV3-15*01 (92.6%) -IGKJ5*01 (91.7%) I126>N (107'), CDR-IMGT [6.3.10] (27'-32'.50'-52'.89'-98')) (1'-108') -*Homo sapiens* IGKC*01 (100%) Km3 A45.1, V101 (C-KAPPA A45.1 (154'), V101 (192')) (109'-215')]; dímero (236-236'':239-239'')-bisdisulfuro, producido en las células ováricas de hámster chino (CHO), línea celular CHO-K1, forma glicosilada alfa
antiviral

3023741-03-6

Heavy chain / Chaîne lourde / Cadena pesada

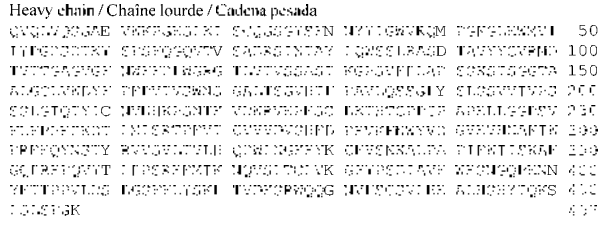

Light chain / Chaîne légère / Cadena ligera

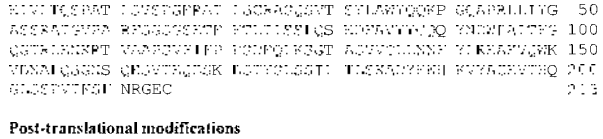

Post-translational modifications
Disulfide bridges location / Position des ponts disulfure / Posiciones de los puentes disulfuro
Intra-H (C23-C104) 22-96 154-210 271-331 377-435
22''-96'' 154''-210'' 271''-331'' 377''-435''
Intra-L (C23-C104) 23'-88' 135'-195'
23'''-88''' 135'''-195'''
Inter-H-L (h 5-CL 126) 230-215' 230''-215'''
Inter-H-H (h 11, h 14) 236-236'' 239-239''

N-terminal glutaminyl cyclization / Cyclisation du glutaminyle N-terminal / Ciclación del glutaminilo N-terminal
Q > pyroglutamyl (pE, 5-oxoprolyl) / pyroglutamyle (pE, 5-oxoprolyle) / piroglutamilo (pE, 5-oxoprolilo)
H VH Q1:1, 1''

N-glycosylation sites / Sites de N-glycosylation / Posiciones de N-glicosilación
H CH2 N84.4.307, 307''
Fucosylated complex bi-antennary CHO-type glycans / glycanes de type CHO bi-antennaires complexes fucosylés / glicanos de tipo CHO biantenarios complejos fucosilados

C-terminal lysine clipping / Coupure de la lysine C-terminale / Recorte de lisina C-terminal
H CHS K2:457, 457''

retogateinum #

retogatein — $N^{2.1}$-acetyl-[des-N-terminal methionyl]-glutamate decarboxylase 2 (*Homo sapiens*) (GAD2, 65 kDa glutamic acid decarboxylase, glutamate decarboxylase 65 kDa isoform, GAD65, EC:4.1.1.15), produced in *Spodoptera frugiperda* insect cells (cell line Sf9)
glutamate decarboxylase 2 (GAD2), immunomodulator

rétogatéine — $N^{2.1}$-acétyl-[des-méthionyle N-terminal]-glutamate décarboxylase 2 (*Homo sapiens*) (GAD2, 65 kDa acide glutamique décarboxylase, glutamate décarboxylase isoforme 65 kDa, GAD65, EC:4.1.1.15), produite par cellules d'insectes *Spodoptera frugiperda* (ligne cellulaire Sf9)
glutamate décarboxylase-2 (GAD2), immunomodulateur

retogateína — $N^{2.1}$-acetil-[des-metionilo N-terminal]-glutamato decarboxilasa 2 (*Homo sapiens*) (GAD2, 65 kDa ácido glutamico decarboxilasa, glutamato decarboxylasa isoforma 65 kDa, GAD65, EC:4.1.1.15), producido en células de insecto *Spodoptera frugiperda* (línea celular Sf9)
decarboxilasa 2 del glutamato (GAD2), inmunomodulador

2938906-46-6

Sequence / Séquence / Secuencia

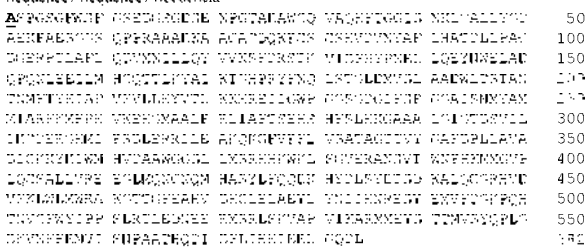

Post-translational modifications
Removal of N-terminal methionyl
M^{0}>del
Disulfide bridge location / Position du pont disulfure / Posición del puente disulfuro
162-303 (rarely 162-403 or 303-403)

N-Acetylation site / Site de N-acétylation / Posición de N-acetilación
A1 = *N*-acetyl-L-alanyl

N-glycosylation sites / Sites de N-glycosylation / Posiciones de N-glicosilación
none / aucun / ninguna

K^{395} = N^{6}-(pyridoxal phosphate)-Lys

rezosiconum

rezosicone — 3β-(benzyloxy)-17-methylpregn-5-en-20-one
cannabinoid CB1 receptor signalling inhibitor

rézosicone — 3β-(benzyloxy)-17-méthylprégn-5-én-20-one
inhibiteur de signalisation du récepteur cannabinoïde CB1

rezosicona — 3β-(benciloxi)-17-metilpregn-5-en-20-ona
inhibidor de la señalización del receptor cannabinoide CB1

$C_{29}H_{40}O_2$ 1414777-24-4

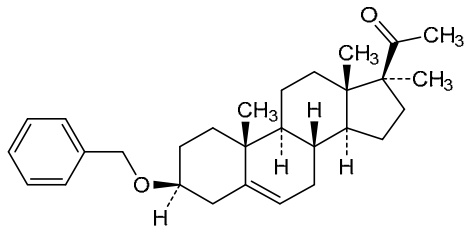

rezuforimodum

rezuforimod — *N*-[(4-bromophenyl)carbamoyl]-L-leucylglycine
N-formyl peptide receptor 1 and 2 agonist, anti-inflammatory

rézuforimod — *N*-[(4-bromophényl)carbamoyl]-L-leucylglycine
agoniste des récepteurs 1 et 2 du N-formyl peptide, anti-inflammatoire

rezuforimod — *N*-[(4-bromofenil)carbamoil]-L-leucilglicina
agonista de los receptores N-formil péptido 1 y 2, antiinflamatorio

$C_{15}H_{20}BrN_3O_4$ 1431754-15-2

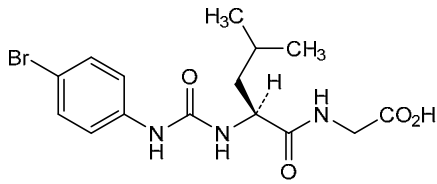

ricefidasum #

ricefidase — L-methionyl (1)-IgG endopeptidase (immunoglobulin G-degrading endopeptidase) of *Streptococcus equi* subsp. *zooepidemicus* strain H70 (ideE, ideZ), fragment 19-315 (2-298 in the actual sequence); produced by *Escherichia coli*; non-glycosylated *immunosuppressant*

ricéfidase — L-méthionyl (1)-IgG endopeptidase (endopeptidase qui dégrade l'immunoglobuline G, Ide) de *Streptococcus equi* subsp. *zooepidemicus* souche H70 (ideE, ideZ), fragment 19-315 (2-298 dans la séquence actuelle); produite par *Escherichia coli*; non-glycosylée *immunosuppresseur*

ricefidasa — L-metionil (1)-IgG endopeptidasa (endopeptidasa que degrada la inmunoglobulina G) de *Streptococcus equi* subsp. *zooepidemicus* cepa H70 (ideE, ideZ), fragmento 19-315 (2-298 en la secuencia actual); producida por *Escherichia coli*; no glicosilada *inmunosupresor*

3004804-10-5

Sequence / Séquence / Secuencia

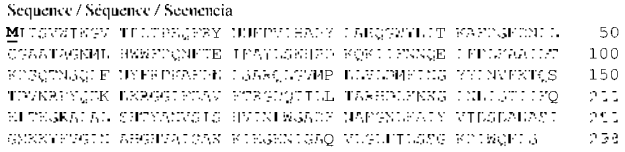

Mutation / Mutation / Mutación
Q^{18}>$\underline{M}^{1}$

Post-translational modifications
Disulfide bridges location / Position des ponts disulfure / Posiciones de los puentes disulfuro
none / aucune / ninguna

N-glycosylation sites / Sites de N-glycosylation / Posiciones de N-glicosilación
none / aucun / ninguna

rinvaterceptum #

rinvatercept

glycyl (1)-chimeric N-terminal (1-108)-peptide (2-109) combined from the sequences of the extracellular domains of the human activin type 2A and 2B receptors (ACTR-2A/B, ACVR2A/B, activin receptor type IIA/B, ACTR-IIA/B, EC:2.7.11.30), fused via a G_3 peptide linker (110-112) to an immunoglobulin G1 (IgG1) Fc fragment (h-CH2-CH3-CHS domains)(113-339) [*Homo sapiens* IGHG1*01 (hinge (113-122), CH2 (123-232), CH3 (233-337), CHS (338-339))], dimer (118-118':121-121')-bisdisulfide, produced in Chinese hamster ovary (CHO) cells; glycoform alfa
activin receptor type 2_A and 2_B ligand trap, neuromuscular diseases

rinvatercept

glycyl (1)-(1-108)-peptide N-terminal chimérique (2-109) combiné à partir des séquences des domaines extracellulaires des récepteurs d'activine de types 2A et 2B humains (ACTR-2A/B, ACVR2A/B, récepteur d'activine de type IIA/B, ACTR-IIA/B, EC:2.7.11.30), fusionné, via un coupleur peptidique G_3 (110-112), à un fragment Fc de l'immunoglobuline G1 (IgG1) (domaines h-CH2-CH3-CHS) (113-339) [*Homo sapiens* IGHG1*01 (charnière (113-122), CH2 (123-232), CH3 (233-337), CHS (338-339))], dimère (118-118',121-121')-bisdisulfure, produit dans des cellules ovariennes de hamster chinois (CHO); glycoforme alfa
piège à ligands des récepteurs d'activine de type 2_A et 2_B, maladies neuromusculaires

rinvatercept

glicil (1)-(1-108)-péptido N-terminal quimérico (2-109) combinado a partir de las secuencias de los dominios extracelulares de los receptores de activina de tipos 2A y 2B humanos (ACTR-2A/B, ACVR2A /B, receptor de activina tipo IIA/B, ACTR-IIA/B, EC:2.7.11.30), fusionado mediante un enlazador peptídico G_3 (110-112) a un fragmento Fc de la inmunoglobulina G1 (IgG1) (dominios h-CH2-CH3-CHS) (113-339) [*Homo sapiens* IGHG1*01 (bisagra (113-122), CH2 (123-232), CH3 (233-337), CHS (338-339))]; dímero (118-118',121-121')-bisdisulfuro, producido en las células ováricas de hámster chino (CHO); glicoforma alfa
trampa de ligando del receptor de activina de tipo 2_A y 2_B, enfermedades neuromusculares

2996105-98-5

Sequence / Séquence / Secuencia

GAILGRSETQ ECIYYNANWE LERTNQSGLE RCEGEQDKRL HCYASWRNSS 50
GT***IEIVKQGC WLDD***F***NCYDR TDCVEKKDSP*** Q***VYFCCCEGN MCNEKFSYFP*** 100
EMEVTQPTSG ***GG***DKTHTCPP CPAPELLGGP SVFLFPPKPK DTLMISRTPE 150
VTCVVVDVSH EDPEVKFNWY VDGVEVHNAK TKPREEQYNS TYRVVSVLTV 200
LHQDWLNGKE YKCKVSNKAL PAPIEKTISK AKGQPREPQV YTLPPSRDEL 250
TKNQVSLTCL VKGFYPSDIA VEWESNGQPE NNYKTTPPVL DSDGSFFLYS 300
KLTVDKSRWQ QGNVFSCSVM HEALHNHYTQ KSLSLSPGK 339

Chimeric peptide / Peptide chimérique / Péptido quimérico
ACTR-2A: ***1-10***, ***53-64***, ***66-80***, ***82-109***
ACTR-2B: 11-52, 65, 81

Peptide linker / Peptide liant / Péptido de unión
^{110}*GGG*^{112}

Post-translational modifications
Disulfide bridges location / Position des ponts disulfure / Posiciones de los puentes disulfuro
ActRIIA/B: 12-42 32-60 67-86 73-85 87-92 IgG1 Fc: 153-213 259-317
12'-42' 32'-60' 67'-86' 73'-85' 87'-92' 153'-213' 259'-317'
inter-IgG1 Fc: 118-118' 121-121'

N-glycosylation sites / Sites de N-glycosylation / Posiciones de N-glicosilación
ActRIIA/B: N25, N48, N25', N48'; IgG1 Fc: N189, N189'

O-glycosylation sites / Sites de O-glycosylation / Posiciones de O-glicosilación
IgG1 Fc: T115, S131, T115', S131'

C-terminal lysine clipping / Coupure de la lysine C-terminale / Recorte de lisina C-terminal
K339, K339'

ristoglogenum autogetemcelum #

ristoglogene autogetemcel

autologous CD34+ hematopoietic stem and progenitor cells (HSPCs) obtained from peripheral blood by leukapheresis, genetically modified *ex vivo* by electroporation of a guide RNA (gRNA) that targets the two γ-globin gene (*HBG1* and *HBG2*) promotors and a messenger RNA (mRNA) that encodes the adenine base editor 8.8 (ABE8.8). When introduced into CD34+ cells by electroporation the gRNA binds to the translated ABE8.8 protein, which targets the promoter regions of *HBG1* and *HBG2*, resulting in adenine to inosine modifications which subsequently leads to an A to G change.
The ABE8.8 mRNA is composed of three parts: (i) an impaired form of the *Streptococcus pyogenes* CRISPR-associated nuclease Cas9, referred to as Cas9 D10A nickase (nCas9-D10A), (ii) an *Escherichia coli* derived TadA deaminase that catalyses the adenosine to inosine conversion within a small activity window along the exposed, single-stranded DNA (ssDNA) formed within the R-loop, (iii) a C-terminal nuclear localization signal (NLS).
The cell suspension is enriched for CD34+ cells using magnetic bead separation. Following electroporation, the cells are cultured in media containing thrombopoietin, Fms-related tyrosine kinase 3 ligand (Flt3L), and stem cell factor (SCF). The substance consists of cells with ≥85% CD45+ and ≥75% CD34+ purity and ≥75% on-target editing.
cell-based gene therapy (hemoglobinopathy)

ristoglogène autogétemcel

cellules souches et progénitrices hématopoïétiques (CSPH) autologues CD34+, obtenues à partir de sang périphérique par leucaphérèse, génétiquement modifiées *ex vivo* par électroporation d'un ARN guide (ARNg) ciblant les deux

	promoteurs du gène de la γ-globine (*HBG1* et *HBG2*) et un ARN messager (ARNm) qui code l'éditeur de bases d'adénine 8.8 (ABE8.8). Lorsqu'il est introduit dans les cellules CD34+ par électroporation, l'ARNg se lie à la protéine ABE8.8 traduite, qui cible les régions promotrices de *HBG1* et *HBG2*, entraînant des modifications de l'adénine en inosine, qui conduisent ensuite à un changement A>G. L'ARNm ABE8.8 est composé de trois parties: (i) une forme altérée de la nucléase Cas9 associée à CRISPR de *Streptococcus pyogenes*, appelée Cas9 D10A nickase (nCas9-D10A); (ii) une désaminase TadA dérivée d'*Escherichia coli* qui catalyse la conversion de l'adénosine en inosine, dans une petite fenêtre d'activité le long de l'ADN simple brin (ADNsb) exposé formé dans la boucle R; (iii) un signal de localisation nucléaire C-terminal (SLN). La suspension cellulaire est enrichie en cellules CD34+ par séparation des billes magnétiques. Après l'électroporation, les cellules sont cultivées dans un milieu contenant de la thrombopoïétine, du ligand de la tyrosine kinase 3 lié au Fms (Flt3L) et du facteur de cellules souches (FCS). La substance est constituée de cellules avec une pureté ≥85% CD45+ et ≥75% CD34+ et une édition sur cible ≥75%. *thérapie génique à base de cellules (hémoglobinopathie)*
ristoglogén autogetemcel	células madre y progenitoras hematopoyéticas (HSPC) CD34+ autólogas, obtenidas de sangre periférica mediante leucoaféresis, modificadas genéticamente *ex vivo* mediante electroporación de un ARN guía (ARNg) dirigido a los promotores de los dos genes de la γ-globina (*HBG1* y *HBG2*) y un ARN mensajero (ARNm) que codifica el editor de bases de adenina 8.8 (ABE8.8). Cuando se introduce en las células CD34+ mediante electroporación, el ARNg se une a la proteína ABE8.8 traducida, la cual se dirige a las regiones promotoras de *HBG1* y *HBG2*, resultando en modificaciones de adenina a inosina que posteriormente conduce a un cambio de A a G. El ARNm de ABE8.8 está compuesto por tres partes: (i) una forma dañada de la nucleasa Cas9 asociada a CRISPR de *Streptococcus pyogenes*, referida como nicasa Cas9 D10A (nCas9-D10A), (ii) una deaminasa TadA derivada de *Escherichia coli* que cataliza la conversión de adenosina a inosina en una pequeña ventana de actividad a lo largo del ADN de cadena sencilla (ssADN) que se forma dentro del bucle R, (iii) una señal de localización nuclear (NLS) C-terminal. La suspensión celular se enriquece en células CD34+ mediante separación con bolas magnéticas. Tras la electroporación, las células se cultivan en medio que contiene trombopoyetina, ligando de tirosina quinasa 3 similar a Fms (Flt3L) y factor de células madre (SCF). La substancia consta de células con una pureza de ≥85% CD45+ y ≥75% CD34+ y ≥75% de edición en el sitio diana *terapia génica basada en células (hemoglobinopatía)*
rizavasertibum rizavasertib	(2*S*)-1-(1*H*-indol-3-yl)-3-{[5-(3-methyl-1*H*-indazol-5-yl)pyridin-3-yl]oxy}propan-2-amine *serine/threonine kinase inhibitor*

rizavasertib (2*S*)-1-(1*H*-indol-3-yl)-3-{[5-(3-méthyl-1*H*-indazol-5-yl)pyridin-3-yl]oxy}propan-2-amine
inhibiteur de sérine/thréonine kinases

rizavasertib (2*S*)-1-(1*H*-indol-3-il)-3-{[5-(3-metil-1*H*-indazol-5-il)piridin-3-il]oxi}propan-2-amina
inhibidor de la serina/treonina kinasa

$C_{24}H_{23}N_5O$ 552325-16-3

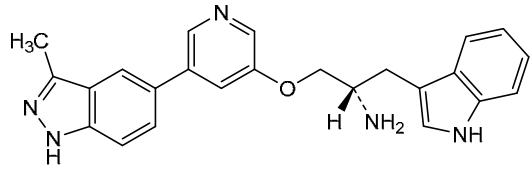

riztunitidum

riztunitide D-tyrosyl-D-valyl-D-α-aspartyl-D-lysyl-D-arginine
anti-inflammatory

riztunitide D-tyrosyl-D-valyl-D-α-aspartyl-D-lysyl-D-arginine
anti-inflammatoire

riztunitida D-tirosil-D-valil-D-α-aspartil-D-lisil-D-arginina
antiinflamatorio

$C_{30}H_{49}N_9O_9$ 2963586-07-2

D-Tyr—D-Val—D-Asp—D-Lys—D-Arg

rocavorexantum

rocavorexant *N*,6-dimethyl-3-(2*H*-1,2,3-triazol-2-yl)-*N*-[(2*S*)-1-{[5-(trifluoromethyl)pyrazin-2-yl]amino}propan-2-yl]pyridine-2-carboxamide
orexin-1 receptor antagonist

rocavorexant *N*,6-diméthyl-3-(2*H*-1,2,3-triazol-2-yl)-*N*-[(2*S*)-1-{[5-(trifluorométhyl)pyrazin-2-yl]amino}propan-2-yl]pyridine-2-carboxamide
antagoniste du récepteur de l'orexine 1

rocavorexant *N*,6-dimetil-3-(2*H*-1,2,3-triazol-2-il)-*N*-[(2*S*)-1-{[5-(trifluorometil)pirazin-2-il]amino}propan-2-il]piridina-2-carboxamida
antagonista del receptor de la orexina 1

$C_{18}H_{19}F_3N_8O$ 2115665-09-1

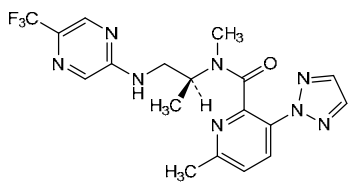

romaciclibum

romaciclib — 7,8-dibromo-9-methyl-2-(piperazin-1-yl)-5,6-dihydro-4*H*-imidazo[4,5,1-*ij*]quinoline
cyclin-dependent kinase inhibitor, antineoplastic

romaciclib — 7,8-dibromo-9-méthyl-2-(pipérazin-1-yl)-5,6-dihydro-4*H*-imidazo[4,5,1-*ij*]quinoléine
inhibiteur de la kinase cycline-dépendante, antinéoplasique

romaciclib — 7,8-dibromo-9-metil-2-(piperazin-1-il)-5,6-dihidro-4*H*-imidazo[4,5,1-*ij*]quinoleína
inhibidor de la kinasa dependiente de ciclinas, antineoplásico

$C_{15}H_{18}Br_2N_4$ 1609522-33-9

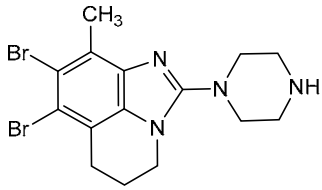

rondecabtagenum autoleucelum #

rondecabtagene autoleucel — autologous T lymphocytes obtained by leukapheresis enriched for the cell surface marker CD62L (also known as L-selectin) transduced with a self-inactivating non-replicating lentiviral vector encoding a tandem chimeric antigen receptor (CAR) targeting both CD20and CD19 [comprising a single chain variable fragment (scFvs) derived from the antibody clone Leu16 fused via flexible linkers to a scFvs derived from clone FMC63]. The transgene has a murine immunoglobulin kappa (mIgK) leader sequence and also comprises an IgG4 hinge, a CD28 transmembrane, and the intracellular 4-1BB co-stimulatory and CD3ζ signaling domains and is under control of the elongation factor 1 alpha (EF-1α) promoter and the Woodchuck hepatitis virus post-transcriptional regulatory element (WPRE) modified to eliminate the X-protein open reading frame. The vector genome also contains a human immunodeficiency virus (HIV) packaging signal, a Rev response element (RRE), central polypurine tract and central termination sequence (cPPT/CTS) and is flanked by 5' and 3' long terminal repeats (LTRs). The vector is pseudotyped with vesicular stomatitis virus (VSV) G glycoprotein.
The leukapheresis material is enriched for CD62L expressing T lymphocytes by positive immunoselection and cultured in media containing interleukin 2 (IL-2) and interleukin 15 (IL-15). The lymphocytes are activated by CD3 and CD28 agonists and transduced with the lentiviral vector followed by culture in media containing IL-2 and IL-15. The T lymphocytes (≥80%) are predominantly composed of naïve and central memory rich T lymphocyte subsets as measured by expression of CD62L and CD45RA surface markers, and positive for the transgene (≥10% CAR positive) with few (<5%) CD19 expressing B lymphocytes. The cells exhibit cytotoxicity and secrete interferon gamma in response to CD19 and CD20 expressing tumour cell lines
cell-based gene therapy (antineoplastic)

rondécabtagène autoleucel	lymphocytes T autologues obtenus par leucaphérèse, enrichis pour le marqueur de surface cellulaire CD62L (également connu sous le nom de L-sélectine) transduits avec un vecteur lentiviral non réplicatif auto-inactivant, codant un récepteur antigénique chimérique (RAC) en tandem ciblant à la fois CD20 et CD19 [comprenant un fragment variable à chaîne unique (scFvs) dérivé du clone d'anticorps Leu16 fusionné, via des coupleurs flexibles, à un scFvs dérivé du clone FMC63]. Le transgène possède une séquence de tête de l'immunoglobuline kappa murine (mIgK), et comprend également une charnière IgG4, un domain transmembranaire CD28 et les domaines intracellulaires de costimulation 4-1BB et de signalisation CD3ζ, et est sous le contrôle du promoteur du facteur d'élongation 1 alpha (EF-1α), et de l'élément régulateur post-transcriptionnel du virus de l'hépatite de la marmotte (WPRE), modifié pour éliminer le cadre de lecture ouvert de la protéine X. Le génome du vecteur contient également un signal d'empaquetage du virus de l'immunodéficience humaine (VIH), un élément de réponse Rev (RRE), une séquence de tractus polypurine central et de terminaison centrale (cPPT/CTS), et est flanqué de longues répétitions terminales (LTRs) en 5' et en 3'. Le vecteur est pseudotypé avec la glycoprotéine G du virus de la stomatite vésiculaire (VSV). Le matériel de leucaphérèse est enrichi en lymphocytes T exprimant CD62L, par immunosélection positive, et cultivé dans un milieu contenant de l'interleukine 2 (IL-2) et de l'interleukine 15 (IL-15). Les lymphocytes sont activés par les agonistes CD3 et CD28 et transduits avec le vecteur lentiviral suivi d'une culture dans un milieu contenant de l'IL-2 et de l'IL-15. Les lymphocytes T (≥80%) sont principalement composés de lymphocytes T riches en sous-types naïfs et mémoire centrale, mesurés par l'expression des marqueurs de surface CD62L et CD45RA, et positifs pour le transgène (≥10% RAC positifs) avec peu (<5%) de lymphocytes B exprimant CD19. Les cellules présentent une cytotoxicité et sécrètent de l'interféron gamma en réponse aux lignées de cellules tumorales exprimant CD19 et CD20 *thérapie génique à base de cellules (antinéoplasique)*
rondecabtagén autoleucel	linfocitos T autólogos obtenidos por leucoaféresis, enriquecidos para el marcador de superficie CD62L (también conocido como L-selectina), transducidos con un vector lentiviral auto inactivante, no replicativo, que codifica un tándem de receptores de antígenos quiméricos (CAR) dirigidos a CD20 y CD19 [consta de un fragmento variable de cadena sencilla (scFv) derivado del clon del anticuerpo Leu16 fusionado mediante enlaces flexibles a un scFv derivado del clon FMC63]. El transgén tiene una secuencia líder de la inmunoglobulina kappa murina (mIgK) y también consta de un dominio bisagra de IgG4, un dominio transmembrana de CD28, y los dominios intracelulares coestimulador de 4-1BB y de señalización de CD3ζ, y está bajo el control del promotor del factor de elongación 1 alfa (EF-1α) y el elemento regulador post-transcripcional del virus de la hepatitis de la marmota (WPRE) modificado para eliminar el marco de lectura abierto de la proteína X. El genoma del vector también contiene una señal de empaquetamiento del virus de la inmunodeficiencia humana (VIH), un elemento de respuesta Rev (RRE), una secuencia de tracto de poli-purina/terminación central (cPPT/CTS) y está flanqueado por repeticiones terminales largas (LTRs) en 5' y 3'. El vector está seudotipado con la

glicoproteína G del virus de la estomatitis vesicular (VSV). El material de leucoaféresis se enriquece en linfocitos T que expresan CD62L mediante inmunoselección positiva y se cultiva en medio que contiene interleuquina 2 (IL-2) e interleuquina 15 (IL-15). Los linfocitos se activan con agonistas de CD3 y CD28 y se transducen con el vector lentiviral seguido de cultivo en medio que contiene IL-2 e IL-15. Los linfocitos T (≥80%) están compuestos predominantemente por linfocitos T ricos en los subtipos naïve y memoria central, medido por la expresión de los marcadores de superficie CD62L y CD45RA, y positivos para el transgén (≥10% CAR positivos) con pocos (<5%) linfocitos B que expresan CD19. Las células muestran citotoxicidad y secretan interferón gamma en respuesta a líneas celulares tumorales que expresan CD19 y CD20
terapia génica basada en células (antineoplásico)

rugecitidum

rugecitide — neuregulin 4 (NRG4) (*Homo sapiens*), fragment 1-50, [^{1}MPTD4>^{1}GGGGSG^{6}, V^{25}>Q^{27}, E^{47}>K^{49}]-variant (1-52), not glycosylated
neuregulin analogue

rugécitide — neuréguline 4 (NRG4) (*Homo sapiens*), fragment 1-50, variant ^{1}MPTD^{4}>^{1}GGGGSG^{6}, V^{25}>Q^{27}, E^{47}>K^{49}] (1-52), non glycosylé
analogue de la neuréguline

rugecitida — neuregulina 4 (NRG4) (*Homo sapiens*), fragmento 1-50, variante [^{1}MPTD^{4}>^{1}GGGGSG^{6}, V^{25}>Q^{27}, E^{47}>K^{49}] (1-52), no glicosilado
análogo de la neurregulina

$C_{238}H_{355}N_{67}O_{72}S_6$ 2938226-27-6

Sequence / Séquence / Secuencia

```
GGGGSGHEEP CGPSHKSFCL XGGLCYQIPT IPSPFCRCVE XYIGARCEKV 50
FL                                                      52
```

Post-translational modifications
Disulfide bridges location / Position des ponts disulfure / Posiciones de los puentes disulfuro
11-25. 19-36. 38-47

rugocrixanum

rugocrixan — (2*R*)-2-[(2-amino-5-{[(1*S*)-1-phenylethyl]sulfanyl}[1,3]thiazolo[4,5-*d*]pyrimidin-7-yl)amino]-4-methylpentan-1-ol
CX3C chemokine receptor 1 (CX3CR1) antagonist, anti-inflammatory

rugocrixan — (2*R*)-2-[(2-amino-5-{[(1*S*)-1-phényléthyl]sulfanyl}[1,3]thiazolo[4,5-*d*]pyrimidin-7-yl)amino]-4-méthylpentan-1-ol
antagoniste du récepteur 1 de la chimioquine CX3C (CX3CR1), anti-inflammatoire

rugocrixán — (2*R*)-2-[(2-amino-5-{[(1*S*)-1-feniletil]sulfanil}[1,3]tiazolo[4,5-*d*]pirimidin-7-il)amino]-4-metilpentan-1-ol
antagonista del receptor 1 de la quimioquina CX3C (CX3CR1), antiinflamatorio

$C_{19}H_{25}N_5OS_2$ 911715-90-7

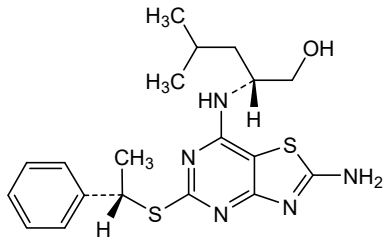

runitresgenum leucelum #

runitresgene leucel — allogeneic T lymphocytes derived from peripheral blood mononuclear cells (PBMCs) of a haploidentical hematopoietic cell transplantation (HCT) donor that is negative for the HA-2 genotype and/or negative for HLA A*02, engineered by transposon/transposase-mediated gene delivery to express a T cell receptor (TCR) that is specific for a 9-amino acid peptide (YIGEVLVSV) termed HA-2, derived from myosin 1G (MYO1G) and presented on HLA-A*02:01. The TCR comprises α and β subunits separated by a P2A self-cleaving peptide. The transgene also encodes a codon-optimised CD8 co-receptor consisting of α and β chains separated by a P2A self-cleaving peptide, with the CD8 co-receptor separated from the TCR by an additional P2A self-cleaving peptide. Each P2A sequence is preceded by a furin cleavage site. A 16 amino acid epitope encoding a portion of human CD34 is incorporated into the N-terminus of the CD8α chain. The transgene is under the control of a murine stem cell virus (MSCV) promoter, a Woodchuck hepatitis virus post-transcriptional response element and a simian virus 40 (SV40) polyadenylation (polyA) signal.
The transposase (Armyworm transposase) is introduced in form of an mRNA that comprises an anti-reverse cap analogue, a *Xenopus* globin 5' untranslated region (UTR), a Kozak sequence, the transposase open reading frame, and a *Xenopus* globin 3' UTR. The transgene is introduced via a nanoplasmid DNA and contains inverted terminal repeats (ITRs). The leukapheresis material is electroporated with mRNA transposase as well as the nanoplasmid transposon followed by activation with CD2, CD3 and CD28 agonists. The cells are grown in serum free media supplemented with interleukin 2 (IL-2), interleukin 7 (IL-7) and interleukin 15 (IL-15). The T lymphocytes (≥95%) are positive for the transgene (≥80% TCR+), and release interferon -gamma (IFN-γ) in response to co-culture with THP-1 cells that express the HA-2 target peptide
cell-based gene therapy (antineoplastic)

runitresgène leucel — lymphocytes T allogéniques dérivés de cellules mononucléaires du sang périphérique (CMSP) d'un donneur haploidentiques de greffe de cellules hématopoïétiques (GCH) qui sont négatifs pour le génotype HA-2 et/ou négatifs pour HLA A*02, modifiés par un système de délivrance de gènes par transposon/transposase, pour exprimer un récepteur de lymphocytes T (TCR) spécifique d'un peptide de 9 acides aminés (YIGEVLVSV) appelé HA-2, dérivé de la myosine 1G (MYO1G) et présenté sur HLA-A*02:01. Le TCR comprend des sous-unités α et β, séparées par un peptide auto-clivant P2A. Le transgène code également avec des codons optimisés un co-récepteur CD8 constitué de chaînes α et β séparées par un peptide auto-clivant P2A, le co-récepteur CD8 étant séparé du TCR par un autre peptide auto-clivant P2A. Chaque séquence P2A est précédée d'un site de clivage de la furine. Un épitope de 16 acides aminés codant pour une partie du CD34 humain est incorporé à l'extrémité N-terminale de la chaîne CD8α. Le transgène est sous le contrôle d'un promoteur du virus des cellules souches murines (MSCV),

d'un élément de réponse post-transcriptionnelle du virus de l'hépatite de la marmotte et d'un signal de polyadénylation (polyA) du virus simien 40 (SV40).
La transposase (transposase de la chenille légionnaire) est introduite sous la forme d'un ARNm qui comprend un analogue de la coiffe anti-inverse, une région 5' non traduite (UTR) de la globine de *Xenopus*, une séquence Kozak, le cadre de lecture ouvert de la transposase et une région 3' UTR de la globine de *Xenopus*. Le transgène est introduit via un vecteur d'ADN nanoplasmidique et contient des répétitions terminales inversées (RTI).
Le matériel de leucaphérèse est électroporé avec l'ARNm de la transposase ainsi que le transposon nanoplasmidique, suivi d'une activation avec des agonistes CD2, CD3 et CD28. Les cellules sont cultivées dans un milieu sans sérum supplémenté en interleukine 2 (IL-2), interleukine 7 (IL-7) et interleukine 15 (IL-15). Les lymphocytes T (≥95%) sont positifs pour le transgène (≥80% TCR+) et libèrent de l'interféron gamma (IFN-γ) en réponse à une co-culture avec des cellules THP-1 qui expriment le peptide cible HA-2
thérapie génique à base de cellules (antinéoplasique)

runitresgén leucel

linfocitos T alogénicos derivados de células mononucleares de sangre periférica (PBMCs) de un donante de transplante de células hematopoyéticas (HCT) haploidéntico que es negativo para el genotipo HA-2 y/o negativo para HLA A*02, manipulados mediante un sistema de entrega genética mediado por transposón/transposasa para expresar el receptor de células T (TCR) que es específico para un péptido de 9 amino ácidos (YIGEVLVSV) llamado HA-2, derivado de la miosina 1G (MYO1G) y presentado en HLA-A*02:01. El TCR consta de subunidades α y β separadas por un péptido de auto-escisión P2A. El transgén también codifica, con codones optimizados, un correceptor CD8 que contiene cadenas α y β separadas por un péptido de auto-escisión P2A, con el correceptor CD8 separado del TCR por un otro péptido de auto-escisión P2A. Cada secuencia P2A está precedida por un sitio de escisión de furina. En la zona N-terminal de la cadena CD8α se incorpora un epítopo de 16 amino ácidos que codifica una porción del CD34 humano. El transgén está bajo el control de un promotor del virus de células madre murino (MSCV), un elemento de respuesta post-transcripcional del virus de la hepatitis de la marmota (WPRE) y una señal de poliadenilación (poliA) del virus simio 40 (SV40).
La transposasa (transposasa de gusano soldado) se introduce en forma de un ARNm que contiene un análogo de caperuza anti-reverso, una región sin traducir (UTR) en 5' de la globina de *Xenopus*, una secuencia Kozak, el marco de lectura abierto de la transposasa, y una UTR en 3' de la globina de *Xenopus*. El transgén se introduce mediante un nanoplásmido de ADN y contiene repeticiones terminales invertidas (ITRs).
El material de leucoaféresis se electropora con el ARNm de la transposasa así como el nanoplásmido del transposón seguido de activación con agonistas de CD2, CD3 y CD28. Las células se crecen después en medio sin suero suplementado con interleuquina 2 (IL-2), interleuquina-7 (IL-7) e interleuquina 15 (IL-15). Los linfocitos T (≥95%) son positivos para el transgén (≥80%+) y liberan interferón gamma (IFN-γ) en respuesta al co-cultivo con células THP-1 que expresan el péptido diana HA-2
terapia génica basada en células (antineoplásico)

ruzaltatugum #

ruzaltatug	immunoglobulin G1-kappa, anti-[*Homo sapiens* ERBB3 (receptor tyrosine-protein kinase erbB-3, HER3)], *Homo sapiens* monoclonal antibody; H-gamma1 heavy chain *Homo sapiens* (1-447) [VH (*Homo sapiens* IGHV3-9*01 (97.0%) -(IGHD) -IGHJ4*01 (92.9%), CDR-IMGT [8.8.10] (26-33.51-58.97-106)) (1-117) -*Homo sapiens* IGHG1*01 (100%) G1m17,1 CH1 K120, CH3 D12, L14 (CH1 K120 (214) (118-215), hinge 1-15 (216-230), CH2 (231-340), CH3 D12 (356), L14 (358) (341-445), CHS (446-447)) (118-447)], (220-215')-disulfide with L-kappa light chain *Homo sapiens* (1'-215') [V-KAPPA (*Homo sapiens* IGKV1-39*01 (87.4%) -IGKJ2*04 (90.9%) L124>V (105'), CDR-IMGT [6.3.10] (27'-32'.50'-52'.89'-98')) (1'-108') -*Homo sapiens* IGKC*01 (100%) Km3 A45.1, V101 (C-KAPPA A45.1 (154'), V101 (192')) (109'-215')]; dimer (226-226'':229-229'')-bisdisulfide, produced in Chinese hamster ovary (CHO) cells, cell line CHO-K1, glycoform alfa *antineoplastic*
ruzaltatug	immunoglobuline G1-kappa, anti-[*Homo sapiens* ERBB3 (récepteur tyrosine-protéine kinase erbB-3, HER3)], anticorps monoclonal *Homo sapiens*; chaîne lourde H-gamma1 *Homo sapiens* (1-447) [VH (*Homo sapiens* IGHV3-9*01 (97.0%) -(IGHD) -IGHJ4*01 (92.9%), CDR-IMGT [8.8.10] (26-33.51-58.97-106)) (1-117) -*Homo sapiens* IGHG1*01 (100%) G1m17,1 CH1 K120, CH3 D12, L14 (CH1 K120 (214) (118-215), charnière 1-15 (216-230), CH2 (231-340), CH3 D12 (356), L14 (358) (341-445), CHS (446-447)) (118-447)], (220-215')-disulfure avec la chaîne légère L-kappa *Homo sapiens* (1'-215') [V-KAPPA (*Homo sapiens* IGKV1-39*01 (87.4%) -IGKJ2*04 (90.9%) L124>V (105'), CDR-IMGT [6.3.10] (27'-32'.50'-52'.89'-98')) (1'-108') -*Homo sapiens* IGKC*01 (100%) Km3 A45.1, V101 (C-KAPPA A45.1 (154'), V101 (192')) (109'-215')]; dimère (226-226'':229-229'')-bisdisulfure, produit dans des cellules ovariennes de hamster chinois (CHO), lignée cellulaire CHO-K1, glycoforme alfa *antinéoplasique*
ruzaltatug	inmunoglobulina G1-kappa, anti-[*Homo sapiens* ERBB3 (receptor tirosina-proteína kinasa erbB-3, HER3)], anticuerpo monoclonal *Homo sapiens*; cadena pesada H-gamma1 *Homo sapiens* (1-447) [VH (*Homo sapiens* IGHV3-9*01 (97.0%) -(IGHD) -IGHJ4*01 (92.9%), CDR-IMGT [8.8.10] (26-33.51-58.97-106)) (1-117) -*Homo sapiens* IGHG1*01 (100%) G1m17,1 CH1 K120, CH3 D12, L14 (CH1 K120 (214) (118-215), bisagra 1-15 (216-230), CH2 (231-340), CH3 D12 (356), L14 (358) (341-445), CHS (446-447)) (118-447)], (220-215')-disulfuro con la cadena ligera L-kappa *Homo sapiens* (1'-215') [V-KAPPA (*Homo sapiens* IGKV1-39*01 (87.4%) -IGKJ2*04 (90.9%) L124>V (105'), CDR-IMGT [6.3.10] (27'-32'.50'-52'.89'-98')) (1'-108') -*Homo sapiens* IGKC*01 (100%) Km3 A45.1, V101 (C-KAPPA A45.1 (154'), V101 (192')) (109'-215')]; dímero (226-226'':229-229'')-bisdisulfuro, producido en las células ováricas de hámster chino (CHO), línea celular CHO-K1, forma glicosilada alfa *antineoplásico*

2981438-63-3

Heavy chain / Chaîne lourde / Cadena pesada

```
QVQLVQSGGG LVQPGRSLRL SCAASGFTFD DYAMHWVRQA PGKGLEWVSG  50
ISWNSGSIGY ADSVKGRFTI SRDNAKNSLY LQMNSLRAED TALYYCAKEG 100
LPGLDYWGQG TLVTVSSAST KGPSVFPLAP SSKSTSGGTA ALGCLVKDYF 150
PEPVTVSWNS GALTSGVHTF PAVLQSSGLY SLSSVVTVPS SSLGTQTYIC 200
NVNHKPSNTK VDKKVEPKSC DKTHTCPPCP APELLGGPSV FLFPPKPKDT 250
LMISRTPEVT CVVVDVSHED PEVKFNWYVD GVEVHNAKTK PREEQYNSTY 300
RVVSVLTVLH QDWLNGKEYK CKVSNKALPA PIEKTISKAK GQPREPQVYT 350
LPPSRDELTK NQVSLTCLVK GFYPSDIAVE WESNGQPENN YKTTPPVLDS 400
DGSFFLYSKL TVDKSRWQQG NVFSCSVMHE ALHNHYTQKS LSLSPGK    447
```

Light chain / Chaîne légère / Cadena ligera

```
DIQMTQSPSS LSASIGDRAT ITCRASQHVG TYLNWYQQKP GKTPKLLISG  50
AANLQSGVPS RFSGSGSGTD FTLTISSLQP EDFATYYCQQ SYNTPPFSFG 100
QGTKVEIKRT VAAPSVFIFP PSDEQLKSGT ASVVCLLNNF YPREAKVQWK 150
VDNALQSGNS QESVTEQDSK DSTYSLSSTL TLSKADYEKH KVYACEVTHQ 200
GLSSPVTKSF NRGEC                                       215
```

Post-translational modifications

Disulfide bridges location / Position des ponts disulfure / Posiciones de los puentes disulfuro

Intra-H (C23-C104) 22-96 144-200 261-321 367-425
22"-96" 144"-200" 261"-321" 367"-425"
Intra-L (C23-C104) 23'-88' 135'-195'
23'"-88'" 135'"-195'"
Inter-H-L (h 5-CL 126) 220-215' 220"-215'"
Inter-H-H (h 11, h 14) 226-226" 229-229"

N-terminal glutaminyl cyclization / Cyclisation du glutaminyle N-terminal / Ciclación del glutaminilo N-terminal
Q > pyroglutamyl (pE, 5-oxoprolyl) / pyroglutamyle (pE, 5-oxoprolyle) / piroglutamilo (pE, 5-oxoprolilo)
H VH Q1: 1, 1"

N-glycosylation sites / Sites de N-glycosylation / Posiciones de N-glicosilación
H CH2 N84.4: 297, 297"
Fucosylated complex bi-antennary CHO-type glycans / glycanes de type CHO bi-antennaires complexes fucosylés / glicanos de tipo CHO biantenarios complejos fucosilados

C-terminal lysine clipping / Coupure de la lysine C-terminale / Recorte de lisina C-terminal
H CHS K2: 447, 447"

ruzaltatugum rezetecanum #

ruzaltatug rezetecan

immunoglobulin G1-kappa, anti-[*Homo sapiens* ERBB3 (receptor tyrosin-protein kinase erbB-3, HER3)], *Homo sapiens* monoclonal antibody,conjugated on an average of four cysteinyl residues to *rezetecan*, comprising a linker and a camptothecin derivative (*exatecan*);
H-gamma1 heavy chain *Homo sapiens* (1-447) [VH (*Homo sapiens* IGHV3-9*01 (97.0%) -(IGHD) -IGHJ4*01 (92.9%), CDR-IMGT [8.8.10] (26-33.51-58.97-106)) (1-117) -*Homo sapiens* IGHG1*01 (100%) G1m17,1 CH1 K120, CH3 D12, L14 (CH1 K120 (214) (118-215), hinge 1-15 (216-230), CH2 (231-340), CH3 D12 (356), L14 (358) (341-445), CHS (446-447)) (118-447)], (220-215')-disulfide with L-kappa light chain *Homo sapiens* (1'-215') [V-KAPPA (*Homo sapiens* IGKV1-39*01 (87.4%) -IGKJ2*04 (90.9%) L124>V (105'), CDR-IMGT [6.3.10] (27'-32'.50'-52'.89'-98')) (1'-108') -*Homo sapiens* IGKC*01 (100%) Km3 A45.1, V101 (C-KAPPA A45.1 (154'), V101 (192')) (109'-215')]; dimer (226-226":229-229")-bisdisulfide, produced in Chinese hamster ovary (CHO) cells, cell line CHO-K1, glycoform alfa; substituted at the sulfur atoms of four L-cysteinyl residues on an average among 215', 215'", 220, 220", 226, 226", 229 and 229" with (3*RS*)-1-[(2*R*,10*S*)-10-benzyl-2-cyclopropyl-1-{[(1*S*,9*S*)-9-ethyl-5-fluoro-9-hydroxy-4-methyl-10,13-dioxo-2,3,9,10,13,15-hexahydro-1*H*,12*H*-benzo[*de*]pyrano[3',4':6,7]indolizino[1,2-*b*]quinolin-1-yl]amino}-1,6,9,12,15,18-hexaoxo-3-oxa-5,8,11,14,17-pentaazatricosan-23-yl]-2,5-dioxopyrrolidin-3-yl (*rezetecan*) groups
antineoplastic

ruzaltatug rézétécan	immunoglobuline G1-kappa, anti-[*Homo sapiens* ERBB3 (récepteur tyrosine-protéine kinase erbB-3, HER3)], anticorps monoclonal *Homo sapiens*, conjuguée par quatre résidus cystéinyles en moyenne au *rézétécan*, comprenant un linker et un dérivé de la camptothécine (*exatécan*); chaîne lourde H-gamma1 *Homo sapiens* (1-447) [VH (*Homo sapiens* IGHV3-9*01 (97.0%) -(IGHD) -IGHJ4*01 (92.9%), CDR-IMGT [8.8.10] (26-33.51-58.97-106)) (1-117) -*Homo sapiens* IGHG1*01 (100%) G1m17,1 CH1 K120, CH3 D12, L14 (CH1 K120 (214) (118-215), charnière 1-15 (216-230), CH2 (231-340), CH3 D12 (356), L14 (358) (341-445), CHS (446-447)) (118-447)], (220-215')-disulfure avec la chaîne légère L-kappa *Homo sapiens* (1'-215') [V-KAPPA (*Homo sapiens* IGKV1-39*01 (87.4%) -IGKJ2*04 (90.9%) L124>V (105'), CDR-IMGT [6.3.10] (27'-32'.50'-52'.89'-98')) (1'-108') -*Homo sapiens* IGKC*01 (100%) Km3 A45.1, V101 (C-KAPPA A45.1 (154'), V101 (192')) (109'-215')]; dimère (226-226'':229-229'')-bisdisulfure, produit dans des cellules ovariennes de hamster chinois (CHO), lignée cellulaire CHO-K1, glycoforme alfa; substitué, sur les atomes de soufre de quatre résidus L-cystéinyle en moyenne parmi 215', 215''', 220, 220'', 226, 226'', 229 et 229'', avec des groupes (3*RS*)-1-[(2*R*,10*S*)-10-benzyl-2-cyclopropyl-1-{[(1*S*,9*S*)-9-éthyl-5-fluoro-9-hydroxy-4-méthyl-10,13-dioxo-2,3,9,10,13,15-hexahydro-1*H*,12*H*-benzo[*de*]pyrano[3',4':6 ,7]indolizino[1,2-*b*]quinoléin-1-yl]amino}-1,6,9,12,15,18-hexaoxo-3-oxa-5,8,11,14,17-pentaazatricosan-23-yl]-2,5-dioxopyrrolidin-3-yle (*rézétécan*) *antinéoplasique*
ruzaltatug rezetecán	inmunoglobulina G1-kappa, anti-[*Homo sapiens* ERBB3 (receptor tirosina-proteína kinasa erbB-3, HER3)], anticuerpo monoclonal *Homo sapiens*, conjugado, por cuatro residuos de cisteinilo, por término medio a *rezetecán*, que comprende un enlace y un derivado de la camptotecina (*exatecán*); cadena pesada H-gamma1 *Homo sapiens* (1-447) [VH (*Homo sapiens* IGHV3-9*01 (97.0%) -(IGHD) -IGHJ4*01 (92.9%), CDR-IMGT [8.8.10] (26-33.51-58.97-106)) (1-117) -*Homo sapiens* IGHG1*01 (100%) G1m17,1 CH1 K120, CH3 D12, L14 (CH1 K120 (214) (118-215), bisagra 1-15 (216-230), CH2 (231-340), CH3 D12 (356), L14 (358) (341-445), CHS (446-447)) (118-447)], (220-215')-disulfuro con la cadena ligera L-kappa *Homo sapiens* (1'-215') [V-KAPPA (*Homo sapiens* IGKV1-39*01 (87.4%) -IGKJ2*04 (90.9%) L124>V (105'), CDR-IMGT [6.3.10] (27'-32'.50'-52'.89'-98')) (1'-108') -*Homo sapiens* IGKC*01 (100%) Km3 A45.1, V101 (C-KAPPA A45.1 (154'), V101 (192')) (109'-215')]; dímero (226-226'':229-229'')-bisdisulfuro, producido en las células ováricas de hámster chino (CHO), línea celular CHO-K1, forma glicosilada alfa; sustituido, en los átomos de azufre de cuatro residuos de L-cisteinilo en promedio de 215', 215''', 220, 220'', 226, 226'', 229 y 229'', con grupos (3*RS*)-1-[(2*R*,10*S*)-10-bencil-2-ciclopropil-1-{[(1*S*,9*S*)-9-etil-5-fluoro-9-hidroxi-4-metil-10,13-dioxo-2,3,9,10,13,15-hexahidro-1*H*,12*H*-benzo[*de*]pirano[3',4':6,7]indolizino[1,2-*b*]quinolein-1-il]amino}-1,6,9,12,15,18-hexaoxo-3-oxa-5,8,11,14,17-pentaazatricosan-23-il]-2,5-dioxopirrolidin-3-ilo (*rezetecán*) *antineoplásico*

2981438-67-7

Heavy chain / Chaîne lourde / Cadena pesada (H, H'')

```
QV[illegible]LVQSG[illegible] LVQPGGSL[illegible]L SCAASGFTFD D[illegible]AM[illegible]WVR[illegible]A P[illegible]K[illegible]LEWVSG   50
[illegible]GY ADSVKGRFTI SRDNAKNSLY LQMNSLRAED TA[illegible]YY[illegible]AKEG 100
LP[illegible] TLVTVSSAST KGPSVFPLAP SSKSTSGGTA ALGCLVKDYF 150
PEPVTVSWNS GALTSGVHTF PAVLQSSGLY SLSSVVTVPS SSLGTQTYIC 200
NVNHKPSNTK VDKKVEPKSC DKTHTCPPCP APELLGGPSV FLFPPKPKDT 250
LMISRTPEVT CVVVDVSHED PEVKFNWYVD GVEVHNAKTK PREEQYNSTY 300
RVVSVLTVLH QDWLNGKEYK CKVSNKALPA PIEKTISKAK GQPREPQVYT 350
LPPSREELTK NQVSLTCLVK GFYPSDIAVE WESNGQPENN YKTTPPVLDS 400
DGSFFLYSKL TVDKSRWQQG NVFSCSVMHE ALHNHYTQKS LSLSPGK    447
```

Light chain / Chaîne légère / Cadena ligera (L', L''')

```
DIQMTQSPSS LSASVGDRAT ITCRASQSV[illegible] [illegible]LNWYQQKP GKTPKLLISG   50
AA[illegible]VPS RFSGSGSGTD FTLTISSLQP EDFATYYCQQ [illegible]FG 100
QGTKVEIKRT VAAPSVFIFP PSDEQLKSGT ASVVCLLNNF YPREAKVQWK 150
VDNALQSGNS QESVTEQDSK DSTYSLSSTL TLSKADYEKH KVYACEVTHQ 200
GLSSPVTKSF NRGEC                                       215
```

Post-translational modifications

Disulfide bridges location / Position des ponts disulfure / Posiciones de los puentes disulfuro

Intra-H (C23-C104) 22-96 144-200 261-321 367-425
22''-96'' 144''-200'' 261''-321'' 367''-425''

Intra-L (C23-C104) 23'-88' 135'-195'
23'''-88''' 135'''-195'''

Inter-H-L (h 5-CL 126)* 220-215' 220''-215'''

Inter-H-H (h 11, h 14)* 226-226'' 229-229''

*Two or three of the four inter-chain disulfide bridges are not present, an average of 4 cysteinyl being conjugated each via a thioether bond to a drug linker.

*Deux ou trois des quatre ponts disulfures inter-chaînes ne sont pas présents, 4 cystéinyl en moyenne étant chacun conjugué via une liaison thioether à un linker-principe actif.

*Dos o tres de los cuatro puentes disulfuro inter-catenarios no están presentes, una media de 4 cisteinil esta conjugada a conectores de principio activo.

N-terminal glutaminyl cyclization / Cyclisation du glutaminyle N-terminal / Ciclación del glutaminilo N-terminal

Q > pyroglutamyl (pE, 5-oxoprolyl) / pyroglutamyle (pE, 5-oxoprolyle) / piroglutamilo (pE, 5-oxoprolilo)

H VH Q1: 1, 1''

N-glycosylation sites / Sites de N-glycosylation / Posiciones de N-glicosilación

H CH2 N84.4: 297, 297''

Fucosylated complex bi-antennary CHO-type glycans / glycanes de type CHO bi-antennaires complexes fucosylés / glicanos de tipo CHO biantenarios complejos fucosilados

C-terminal lysine clipping / Coupure de la lysine C-terminale / Recorte de lisina C-terminal

H CHS K2: 447, 447''

Modified residues / Résidus modifiés / Restos modificados*

C (215', 215''', 220, 220'', 226, 226'', 229, 229'')

*(cysteinyl/mAb ~4:1)

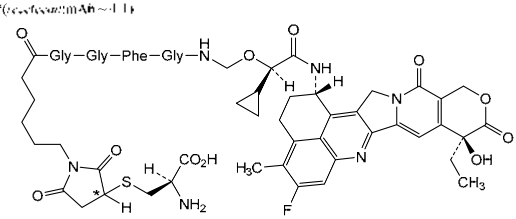

sasineprocelum
sasineprocel

autologous dopaminergic neuron precursor cells (DANPCs) derived from human induced pluripotent stem cells (iPSCs). The iPSCs are derived from patient skin fibroblasts that are expanded and reprogrammed by a non-integrating method with plasmid vectors expressing octamer-binding transcription factor 3/4 (OCT-3/4), SOX2, Krueppel-like factor 4 (KLF4), and L-Myc.
The cells are expanded on recombinant laminin and frozen as intermediates to be then thawed, expanded, dissociated with a proteolytic and collagenolytic enzyme mixture and initially seeded in medium supplemented with Rho-associated protein kinase (ROCK). Differentiation into dopaminergic precursor cells is then performed in neurobasal medium supplemented with serum

	replacement containing a transforming growth factor-β (TGFβ)/activin-Nodal signaling inhibitor, a bone morphogenetic protein (BMP) inhibitor, a glycogen synthase kinase (GSK) 3 inhibitor, a Sonic hedgehog (Shh) signaling activator and a γ-secretase inhibitor, as well as recombinant brain-derived neurotrophic factor (BDNF), glial cell-line-derived neurotrophic factor (GDNF), transforming growth factor β3 (TGFβ3) and Sonic hedgehog (Shh). The differentiated and mature DANPCs are then harvested, washed, and cryopreserved. The final cell population expresses forkhead box protein A2 (FoxA2; >80%) as characteristic factor of dopaminergic neurons, with a minor (<5%) cell population expressing paired box protein (PAX6). Uncommitted iPSCs are absent or present at low level (<0.1%; octamer-binding transcription factor 3/4 (OCT-3/4) and vertnin (VRTN)) *cell therapy (Parkinson's disease)*
sasinéprocel	cellules précurseures de neurones dopaminergiques autologues (DANPCs) dérivées de cellules souches pluripotentes induites humaines (CSPi). Les CSPi sont dérivées de fibroblastes cutanés de patients, qui sont expansés et reprogrammés par une méthode non intégrative avec des vecteurs plasmidiques exprimant le facteur de transcription 3/4 de liaison à l'octamère (OCT-3/4), SOX2, le facteur 4 de type Krueppel (KLF4), et L-Myc. Les cellules sont expansées sur de la laminine recombinante et congelées comme intermédiaires pour être ensuite décongelées, expansées, dissociées avec un mélange d'enzymes protéolytiques et collagénolytiques, et initialement ensemencées dans un milieu supplémenté en protéine kinase associée à Rho (ROCK). La différenciation en cellules précurseures dopaminergiques est ensuite réalisée dans un milieu neurobasal complété par un substitut de sérum contenant un inhibiteur de la signalisation du facteur de croissance transformant β (TGFβ)/activine-Nodal, un inhibiteur de la protéine morphogénétique osseuse (PMO), un inhibiteur de la glycogène synthase kinase (GSK) 3, un activateur de signalisation Sonic hedgehog (Shh) et un inhibiteur de la γ-sécrétase, ainsi que le facteur neurotrophique dérivé du cerveau (BDNF) recombinant, le facteur neurotrophe dérivé de la glie (GDNF), le facteur de croissance transformant β3 (TGFβ3) et Sonic hedgehog (Shh). Les DANPCs différenciées et matures sont ensuite récoltées, lavées et cryoconservées. La population cellulaire finale exprime la protéine A2 de la boîte forkhead (FoxA2; >80%) comme facteur caractéristique des neurones dopaminergiques, avec une population cellulaire mineure (<5%) exprimant la protéine paired box 6 (PAX6). Les CSPi non engagées sont absentes ou présentes à un faible niveau (<0,1%; facteur 3/4 de transcription de liaison à l'octamère (OCT-3/4) et la vertnine (VRTN)) *thérapie cellulaire (maladie de Parkinson)*

sasineprocel

células precursoras de neuronas dopaminérgicas (DANPCs) autólogas derivadas de células madre pluripotentes inducidas (iPSCs) humanas. Las iPSCs se derivan a partir de fibroblastos de la piel del paciente que son expandidos y reprogramados mediante un método no integrativo con vectores plasmídicos que expresan el factor 3/4 de trascripción de unión a octámero (OCT-3/4), SOX2, factor similar a Krueppel 4 (KLF4) y L-Myc.
Las células se expanden en laminina recombinante y se congelan como intermediarios para ser después descongeladas, expandidas, disociadas con una mezcla de enzimas proteolíticas y colagenolíticas y sembradas inicialmente en medio suplementado con proteína quinasa asociada a Rho (ROCK). La diferenciación a células precursoras dopaminérgicas se realiza en medio neurobasal suplementado con substituto de suero que contiene un inhibidor de la señalización del factor de crecimiento transformante β (TGFβ)/activina-Nodal, un inhibidor de la proteína morfogenética del hueso (BMP), un inhibidor de la glicogén sintasa quinasa (GSK) 3, un activador de señalización Sonic hedghog (Shh) y un inhibidor de la γ-secretasa, así como factor neurotrófico derivado de cerebro (BDNF) recombinante, factor neurotrófico derivado de línea celular de la glia (GDNF), factor de crecimiento transformante β3 (TGFβ3) y Sonic hedgehog (Shh). Las DANPCs diferenciadas y maduras se cosechan a continuación, se lavan y se criopreservan.
La población celular final expresa la proteína A2 de caja forkhead (FoxA2; >80%) como factor característico de neuronas dopaminérgicas, con una población celular menor (<5%) que expresa la proteína paired box 6 (PAX6). Las iPSCs sin diferenciar están ausentes o a bajo nivel (<0.1%; factor 3/4 de transcripción de unión a octámero (OCT-3/4) y vertnina (VRTN))
terapia celular (enfermedad de Parkinson)

secutrelvirum

secutrelvir

[5-(3-chloro-4-fluorophenyl)-3-(5-chloropyridin-3-yl)-6-(6,6-difluoro-2-azaspiro[3.3]heptan-2-yl)-2,4-dioxo-3,4-dihydropyrimidin-1(2*H*)-yl]acetonitrile
protease inhibitor, antiviral

sécutrelvir

[5-(3-chloro-4-fluorophényl)-3-(5-chloropyridin-3-yl)-6-(6,6-difluoro-2-azaspiro[3.3]heptan-2-yl)-2,4-dioxo-3,4-dihydropyrimidin-1(2*H*)-yl]acétonitrile
inhibiteur de protéase, antiviral

secutrelvir

[5-(3-cloro-4-fluorofenil)-3-(5-cloropiridin-3-il)-6-(6,6-difluoro-2-azaespiro[3.3]heptan-2-il)-2,4-dioxo-3,4-dihidropirimidin-1(2*H*)-il]acetonitrilo
inhibidor de la proteasa, antiviral

$C_{23}H_{16}Cl_2F_3N_5O_2$ 2996148-73-1

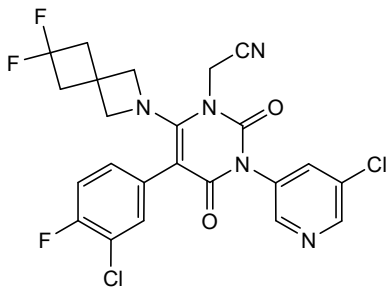

seldegamadlinum

seldegamadlin

(3'*R*,4'*S*,5'*R*)-6''-chloro-4'-(3-chloro-2-fluorophenyl)-*N*-[*trans*-4-(4-{1-[(3*RS*)-2,6-dioxopiperidin-3-yl]-3-methyl-2-oxo-2,3-dihydro-1*H*-1,3-benzimidazol-5-yl}piperidine-1-carbonyl)cyclohexyl]-2''-oxo-1'',2''-dihydrodispiro[cyclohexane-1,2'-pyrrolidine-3',3''-indole]-5'-carboxamide

E3 ubiquitin-protein ligase Mdm2 (Hdm2) degrader, antineoplastic

seldégamadline

(3'*R*,4'*S*,5'*R*)-6''-chloro-4'-(3-chloro-2-fluorophényl)-*N*-[*trans*-4-(4-{1-[(3*RS*)-2,6-dioxopipéridin-3-yl]-3-méthyl-2-oxo-2,3-dihydro-1*H*-1,3-benzimidazol-5-yl}pipéridine-1-carbonyl)cyclohexyl]-2''-oxo-1'',2''-dihydrodispiro[cyclohexane-1,2'-pyrrolidine-3',3''-indole]-5'-carboxamide

dégradeur de l'ubiquitine-protéine ligase E3 Mdm2, antinéoplasique

seldegamadlina

(3'*R*,4'*S*,5'*R*)-6''-cloro-4'-(3-cloro-2-fluorofenil)-*N*-[*trans*-4-(4-{1-[(3*RS*)-2,6-dioxopiperidin-3-il]-3-metil-2-oxo-2,3-dihidro-1*H*-1,3-benzimidazol-5-il}piperidina-1-carbonil)ciclohexil]-2''-oxo-1'',2''-dihidrodiespiro[ciclohexano-1,2'-pirrolidina-3',3''-indol]-5'-carboxamida

degrador de la ubiquitina-proteína ligasa E3 Mdm2, antineoplasico

$C_{48}H_{52}Cl_2FN_7O_6$ 2713618-08-5

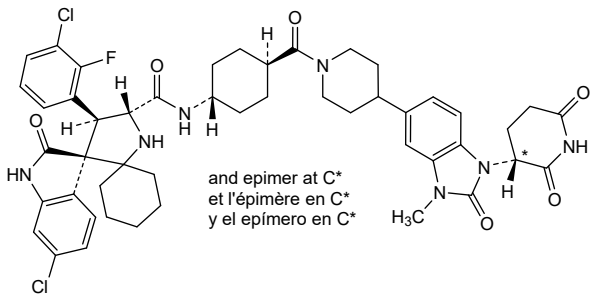

sersacabtagenum autoleucelum #

sersacabtagene autoleucel

autologous CD4+/CD8+ enriched T lymphocytes obtained from peripheral blood lymphocytes by leukapheresis, transduced with a self-inactivating lentiviral vector encoding a humanized chimeric antigen receptor (CAR) targeting CD20 that includes a CD8α signalling peptide, an anti-CD20 single chain variable fragment (scFv) derived from human monoclonal IgG1 kappa antibody *ofatumumab*, an IgG4 hinge region, CD8 transmembrane region, and an intracellular 4-1BB co-stimulatory and CD3ζ signalling domain under control of the elongation factor 1 alpha (EF-1α) promoter and a Woodchuck hepatitis virus posttranscriptional regulatory element (WPRE). The vector also contains an HIV-1 packaging signal (Ψ), *gag*, Rev response element (RRE), central polypurine tract and central termination sequence (cPPT/CTS), is flanked by 5' and 3' long terminal repeats (LTRs) and is pseudotyped by the vesicular stomatitis virus (VSV) G glycoprotein.

The leukapheresis material is enriched for CD4+/CD8+ T lymphocytes by positive immunoselection, activated by CD3 and CD28 agonists and transduced with the lentiviral vector. The cells are then expanded in media with serum replacement and interleukin 2 (IL-2). The T lymphocytes (≥90% CD3+; ≤1%

	CD19+ or CD20+) are positive for the transgene (≥10% CAR positive) and secrete interferon gamma in response to co-culture with CD20-expressing tumour cell lines. *cell-based gene therapy (antineoplastic)*
sersacabtagéne autoleucel	lymphocytes T autologues enrichis en CD4+/CD8+ obtenus à partir de lymphocytes du sang périphérique par leucaphérèse, transduits avec un vecteur lentiviral auto-inactivant codant un récepteur antigénique chimérique humanisé (RAC) ciblant CD20, qui comprend un peptide de signalisation CD8α, un fragment variable à chaîne unique anti-CD20 (scFv) dérivé de l'anticorps monoclonal IgG1 kappa humain *ofatumumab*, d'une région charnière IgG4, d'une région transmembranaire CD8 et d'un domaine intracellulaire de co-stimulation 4-1BB et de signalisation CD3ζ, sous le contrôle du promoteur du facteur d'élongation 1 alpha (EF-1α) et d'un élément régulateur post-transcriptionnel du virus de l'hépatite de la marmotte (WPRE). Le vecteur contient également un signal d'empaquetage du VIH-1 (Ψ), *gag*, un élément de réponse Rev (RRE), un tractus polypurine central et une séquence de terminaison centrale (cPPT/CTS), est flanqué de répétitions terminales longues (LTRs) en 5' et en 3' et est pseudotypé par la glycoprotéine G du virus de la stomatite vésiculaire (VSV). Le matériel de leucaphérèse est enrichi en lymphocytes T CD4+/CD8+ par immunosélection positive, activés par les agonistes CD3 et CD28 et transduits avec le vecteur lentiviral. Les cellules sont ensuite expansées dans un milieu avec remplacement de sérum et interleukine 2 (IL-2). Les lymphocytes T (≥90% CD3+; ≤1% CD19+ ou CD20+) sont positifs au transgène (≥10% RAC positif) et sécrètent de l'interféron gamma en réponse à une co-culture avec des lignées de cellules tumorales exprimant CD20 *thérapie génique à base de cellules (antinéoplasique)*
sersacabtagén autoleucel	linfocitos T CD4+/CD8+ autólogos enriquecidos obtenidos de linfocitos de sangre periférica por leucoaféresis, transducidos con un vector lentiviral auto inactivante, que codifica un receptor de antígenos quimérico (CAR) humanizado dirigido a CD20 que incluye un péptido señal de CD8α, un fragmento variable de cadena sencilla (scFv) anti-CD20 derivado del anticuerpo monoclonal humano IgG1 kappa *ofatumumab*, una región bisagra de IgG4, una región transmembrana de CD8, un dominio coestimulador de 4-1BB y un dominio de señalización de CD3ζ, bajo el control del promotor del factor de elongación 1 alfa (EF-1α) y un elemento regulador post-transcripcional del virus de la hepatitis de la marmota (WPRE). El vector también contiene una señal de empaquetamiento de HIV-1 (ψ), *gag*, un elemento de respuesta Rev (RRE), una secuencia de tracto de poli-purina/terminación central (cPPT/CTS), está flanqueado por repeticiones terminales largas (LTRs) en 5' y 3' y está seudotipado con la glicoproteína G del virus de la estomatitis vesicular (VSV). El material de leucoaféresis se enriquece en linfocitos T CD4+/CD8+ mediante inmunoselección positiva, se activa mediante agonistas de CD3 y CD28 y se transduce con el vector lentiviral. Las células se expanden después en medio con substituto de suero e interleuquina 2 (IL-2). Los linfocitos T (≥90% CD3+; ≤1% CD19+ o CD20+) son positivos para el transgén (≥10% positivos para el CAR) y secretan interferón gamma en respuesta al co-cultivo con líneas celulares tumorales que expresan CD20 *terapia génica basada en células (antineoplásico)*

setomagpranum

setomagpran — 3-chloro-*N*-[(1*R*,3*S*)-3-{[6-chloro-2-(trifluoromethyl)quinolin-4-yl]amino}cyclohexyl]-1-(2,2,2-trifluoroethyl)-1*H*-pyrazole-4-carboxamide
Mas-related G protein-coupled receptor antagonist, anti-inflammatory

sétomagpran — 3-chloro-*N*-[(1*R*,3*S*)-3-{[6-chloro-2-(trifluorométhyl)quinoléin-4-yl]amino}cyclohexyl]-1-(2,2,2-trifluoroéthyl)-1*H*-pyrazole-4-carboxamide
antagoniste des récepteurs couplés aux protéines G liés à Mas, anti-inflammatoire

setomagprán — 3-cloro-*N*-[(1*R*,3*S*)-3-{[6-cloro-2-(trifluorometil)quinolein-4-il]amino}ciclohexil]-1-(2,2,2-trifluoroetil)-1*H*-pirazol-4-carboxamida
antagonista del receptor Mas acoplado a proteínas G, intiinflamatorio

$C_{22}H_{19}Cl_2F_6N_5O$ 2991434-57-0

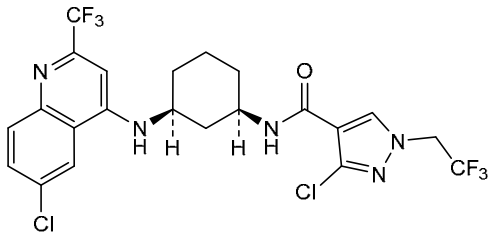

silevertinibum

silevertinib — (2*E*)-*N*-[4-(3-chloro-2-fluoroanilino)-7-{[(1*R*,5*S*)-3-methyl-3-azabicyclo[3.1.0]hexan-1-yl]ethynyl}quinazolin-6-yl]-4-(morpholin-4-yl)but-2-enamide
epidermal growth factor receptor tyrosine kinase inhibitor, antineoplastic

silévertinib — (2*E*)-*N*-[4-(3-chloro-2-fluoroanilino)-7-{[(1*R*,5*S*)-3-méthyl-3-azabicyclo[3.1.0]hexan-1-yl]éthynyl}quinazolin-6-yl]-4-(morpholin-4-yl)but-2-énamide
inhibiteur de la tyrosine kinase du récepteur du facteur de croissance épidermique, antinéoplasique

silevertinib — (2*E*)-*N*-[4-(3-cloro-2-fluoroanilino)-7-{[(1*R*,5*S*)-3-metil-3-azabiciclo[3.1.0]hexan-1-il]etinil}quinazolin-6-il]-4-(morfolin-4-il)but-2-enamida
inhibidor de la tirosina kinasa del receptor del factor de crecimiento epidérmico, antineoplásico

$C_{30}H_{30}ClFN_6O_2$ 2607829-38-7

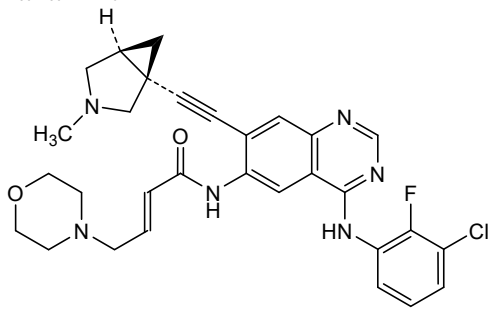

simedeutiromum

simedeutirom 2-(3,5-dichloro-4-{[(7*R*)-7-($^{2}H_3$)methyl-1-oxo-2,5,6,7-tetrahydro-1*H*-cyclopenta[*d*]pyridazin-4-yl]oxy}phenyl)-3,5-dioxo-2,3,4,5-tetrahydro-1,2,4-triazine-6-carbonitrile
thyroid hormone beta receptor agonist

simédeutirom 2-(3,5-dichloro-4-{[(7*R*)-7-($^{2}H_3$)méthyl-1-oxo-2,5,6,7-tétrahydro-1*H*-cyclopenta[*d*]pyridazin-4-yl]oxy}phényl)-3,5-dioxo-2,3,4,5-tétrahydro-1,2,4-triazine-6-carbonitrile
agoniste des récepteurs bêta de l'hormone thyroïdienne

simedeutirom 2-(3,5-dicloro-4-{[(7*R*)-7-($^{2}H_3$)metil-1-oxo-2,5,6,7-tetrahidro-1*H*-ciclopenta[*d*]piridazin-4-il]oxi}fenil)-3,5-dioxo-2,3,4,5-tetrahidro-1,2,4-triazina-6-carbonitrilo
agonista del receptor beta de la hormona tiroidea

$C_{18}H_9{}^{2}H_3Cl_2N_6O_4$ 2403721-24-2

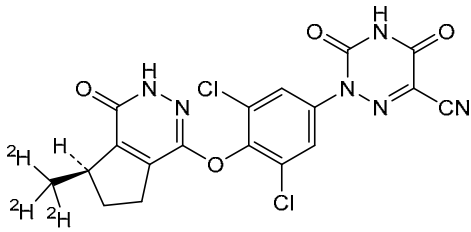

sitmutolimodum

sitmutolimod *all-P-ambo*-(3'→5')-*P*-thiothymidylyl-(3'→5')-2′-deoxy-*P*-thiocytidylyl-(3'→5')-2′-deoxy-*P*-thioguanylyl-(3'→5')-2′-deoxy-*P*-thiocytidylyl-(3'→5')-2′-deoxy-*P*-thioguanylyl-(3'→5')-2′-deoxy-*P*-thioadenylyl-(3'→5')-2′-deoxy-*P*-thioadenylyl-(3'→5')-2′-deoxy-*P*-thiocytidylyl-(3'→5')-2′-deoxy-*P*-thioguanylyl-(3'→5')-*P*-thiothymidylyl-(3'→5')-*P*-thiothymidylyl-(3'→5')-2′-deoxy-*P*-thiocytidylyl-(3'→5')-2′-deoxy-*P*-thioguanylyl-(3'→5')-2′-deoxy-*P*-thiocytidylyl-(3'→5')-2′-deoxy-*P*-thioguanylyl-(3'→5')-2′-deoxy-*P*-thiocytidylyl-(3'→5')-2′-deoxy-*P*-thioguanylyl-(3'→5')-*P*-thiothymidylyl-(3'→5')-2′-deoxy-*P*-thioadenylyl-(3'→5')-2′-deoxy-*P*-thiocytidylyl-(3'→5')-2′-deoxy-*P*-thioguanylyl-(3'→5')-*P*-thiothymidylyl-(3'→5')-2′-deoxy-*P*-thioadenylyl-(3'→5')-2′-deoxy-*P*-thiocytidylyl-(3'→5')-2′-deoxy-*P*-thioguanylyl-(3'→5')-2′-deoxy-*P*-thiocytidylyl-(3'→5')-2′-deoxy-*P*-thioguanylyl-(3'→5')-2′-deoxy-*P*-thioguanylyl
Toll-like receptor agonist, antineoplastic

sitmutolimod *tout-P-ambo*-(3'→5')-*P*-thiothymidylyl-(3'→5')-2′-désoxy-*P*-thiocytidylyl-(3'→5')-2′-désoxy-*P*-thioguanylyl-(3'→5')-2′-désoxy-*P*-thiocytidylyl-(3'→5')-2′-désoxy-*P*-thioguanylyl-(3'→5')-2′-désoxy-*P*-thioadénylyl-(3'→5')-2′-désoxy-*P*-thioadénylyl-(3'→5')-2′-désoxy-*P*-thiocytidylyl-(3'→5')-2′-désoxy-*P*-thioguanylyl-(3'→5')-*P*-thiothymidylyl-(3'→5')-*P*-thiothymidylyl-(3'→5')-2′-désoxy-*P*-thiocytidylyl-(3'→5')-2′-désoxy-*P*-thioguanylyl-(3'→5')-2′-désoxy-*P*-thiocytidylyl-(3'→5')-2′-désoxy-*P*-thiocytidylyl-(3'→5')-2′-désoxy-*P*-thioguanylyl-(3'→5')-2′-désoxy-*P*-thioguanylyl-(3'→5')-*P*-thiothymidylyl-(3'→5')-2′-désoxy-*P*-thioadénylyl-(3'→5')-2′-désoxy-*P*-thiocytidylyl-(3'→5')-2′-désoxy-*P*-thioguanylyl-(3'→5')-*P*-thiothymidylyl-(3'→5')-2′-désoxy-*P*-thioadénylyl-(3'→5')-2′-désoxy-*P*-thiocytidylyl-(3'→5')-2′-désoxy-*P*-thioguanylyl-(3'→5')-2′-désoxy-*P*-thiocytidylyl-(3'→5')-2′-désoxy-*P*-thioguanylyl-(3'→5')-2′-désoxy-*P*-thioguanylyl
agoniste des récepteurs de type Toll, antinéoplasique

sitmutolimod

todo-P-ambo-(3'→5')-*P*-tiotimidilil-(3'→5')-2′-desoxi-*P*-tiocitidilil-(3'→5')-2′-desoxi-*P*-tioguanilil-(3'→5')-2′-desoxi-*P*-tiocitidilil-(3'→5')-2′-desoxi-*P*-tioguanilil-(3'→5')-2′-desoxi-*P*-tioadenilil-(3'→5')-2′-desoxi-*P*-tioadenilil-(3'→5')-2′-desoxi-*P*-tiocitidilil-(3'→5')-2′-desoxi-*P*-tioguanilil-(3'→5')-*P*-tiotimidilil-(3'→5')-*P*-tiotimidilil-(3'→5')-2′-desoxi-*P*-tiocitidilil-(3'→5')-2′-desoxi-*P*-tioguanilil-(3'→5')-2′-desoxi-*P*-tiocitidilil-(3'→5')-2′-desoxi-*P*-tioguanilil-(3'→5')-2′-desoxi-*P*-tiocitidilil-(3'→5')-2′-desoxi-*P*-tioguanilil-(3'→5')-*P*-tiotimidilil-(3'→5')-2′-desoxi-*P*-tioadenilil-(3'→5')-2′-desoxi-*P*-tiocitidilil-(3'→5')-2′-desoxi-*P*-tioguanilil-(3'→5')-*P*-tiotimidilil-(3'→5')-2′-desoxi-*P*-tioadenilil-(3'→5')-2′-desoxi-*P*-tiocitidilil-(3'→5')-2′-desoxi-*P*-tioguanilil-(3'→5')-2′-desoxi-*P*-tiocitidilil-(3'→5')-2′-desoxi-*P*-tioguanilil-(3'→5')-2′-desoxi-*P*-tioguanilil
agonista del receptor de tipo Toll, antineoplásico

$C_{280}H_{354}N_{110}O_{145}P_{28}S_{28}$ 3002979-61-2

(3'-5') d(T=C=G=C=G=A=A=C=G=T=T=C=G=C=C=G=C=G=T=A=C=G=T=A=C=G=C=G=G)

N : nucleoside / nucléoside / nucleósido
dN : 2'-deoxy-N / 2'-désoxy-N / 2'-desoxi-N
= : -PO(SH)-

soclenicantum

soclenicant

6-[(2,3-dihydro-1*H*-inden-2-yl)amino]-1-ethyl-3-(morpholine-4-carbonyl)-1,8-naphthyridin-4(1*H*)-one
nicotinic acetylcholine receptor negative allosteric modulator, anxiolytic

soclénicant

6-[(2,3-dihydro-1*H*-indén-2-yl)amino]-1-éthyl-3-(morpholine-4-carbonyl)-1,8-naphtyridin-4(1*H*)-one
modulateur allostérique négatif des récepteurs nicotiniques de l'acétylcholine, anxiolytique

soclenicant

6-[(2,3-dihidro-1*H*-inden-2-il)amino]-1-etil-3-(morfolina-4-carbonil)-1,8-naftiridin-4(1*H*)-ona
modulador alostérico negativo del receptor nicotínico de la acetilcolina, ansiolítico

$C_{24}H_{26}N_4O_3$ 1020634-41-6

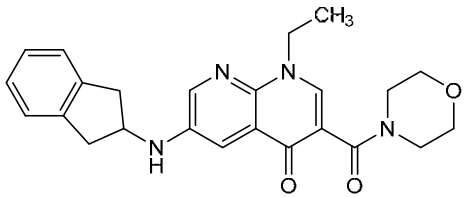

soficabtagenum geleucelum #

soficabtagene geleucel

allogeneic CD4+ and CD8+ T lymphocytes derived from leukapheresis material of healthy donors, genetically modified using CRISPR/Cas9 gene editing to knockout the expression of endogenous CD7 and TRAC using

	guide RNAs (gRNAs), followed by transduction with a self-inactivating, non-replicating lentivirus vector encoding an anti-CD7 chimeric antigen receptor (CAR) comprising a CD8 leader sequence, anti-CD7 single-chain variable fragment (scFv)(clone TH69), CD8 hinge, CD28 transmembrane domain, 4-1BB co-stimulatory domain and CD3ζ intracellular signalling domain, under control of the elongation factor 1 alpha (EF-1α) promoter. The transgene also encodes a truncated human CD34 extracellular domain separated from the CAR by a 2A peptide derived from porcine teschovirus-1. The CRISPR/Cas9 and gRNAs are introduced as a ribonucleoprotein (RNP) complex by electroporation. The lentivirus vector is flanked by 5' and 3' LTRs and also contains a viral packaging sequence ψ, partial gag, a Rev response element (RRE), a central polypurine tract/central termination sequence (cPPT/CTS) and a synthetic identification (ID) sequence. The vector is pseudotyped with VSV G envelope glycoprotein. The leukapheresis material is enriched for CD4+ and CD8+ T lymphocytes by positive immunoselection prior to activation with CD3 and CD28 agonists in growth media containing interleukin 7 (IL-7) and interleukin 15 (IL-15). The cells are gene-edited and then transduced with the lentiviral vector and expanded in growth media containing human AB serum, IL-7, and IL-15. The cell suspension consists of T lymphocytes (≥98.0% CD45+, ≤1.0% CD7+, ≤8.0% CD3+) with greater than 30% of the T lymphocytes expressing the CAR transgene and >70% (CD7) and >85% (TRAC) on-target gene editing. The transduced T lymphocytes demonstrate cytotoxicity against CD7+ T-lymphoblastic target cells *cell-based gene therapy (antineoplastic)*
soficabtagène géleucel	lymphocytes T allogéniques CD4+ et CD8+ dérivés de matériel de leucaphérèse de donneurs sains, génétiquement modifiés à l'aide de l'édition génique CRISPR/Cas9 pour éliminer l'expression endogènes de CD7 et TRAC à l'aide d'ARN guides (ARNg), suivis d'une transduction avec un vecteur lentiviral auto-inactivant et non réplicatif codant pour un récepteur antigénique chimérique (RAC) anti-CD7 comprenant une séquence de tête CD8, un fragment variable à chaîne unique (scFv) anti-CD7 (clone TH69), une charnière CD8, un domaine transmembranaire CD28, un domaine co-stimulateur 4-1BB et un domaine de signalisation intracellulaire CD3ζ, sous le contrôle du promoteur du facteur d'élongation 1 alpha (EF-1α). Le transgène code également pour un domaine extracellulaire tronqué du CD34 humain séparé du RAC par un peptide 2A dérivé du teschovirus-1 porcin. Le CRISPR/Cas9 et les ARNg sont introduits sous forme de complexe ribonucléoprotéique (RNP) par électroporation. Le vecteur lentiviral est flanqué de longues répétitions terminales en 5' et en 3' et contient également une séquence d'empaquetage virale ψ, une partie de gène *gag*, un élément de réponse Rev (RRE), une séquence centrale de tractus polypurine/terminaison centrale (cPPT/CTS) et une identification synthétique (ID). Le vecteur est pseudotypé avec la glycoprotéine G d'enveloppe du virus de la stomatite vésiculaire (VSV). Le matériel de leucaphérèse est enrichi en lymphocytes T CD4+ et CD8+ par immunosélection positive, avant activation avec des agonistes CD3 et CD28, dans un milieu de croissance contenant de l'interleukine 7 (IL-7) et de l'interleukine 15 (IL-15).

	Les cellules sont modifiées génétiquement, puis transduites avec le vecteur lentiviral et expansées dans un milieu de croissance contenant du sérum AB humain, de l'IL-7 et de l'IL-15. La suspension cellulaire est constituée de lymphocytes T (≥98.0% CD45+, ≤1.0% CD7+, ≤8.0% CD3+) avec plus de 30% de lymphocytes T exprimant le transgène RAC, et >70% (CD7) et >85% (TRAC) d'édition de gènes sur cible. Les lymphocytes T transduits démontrent une cytotoxicité contre les cellules cibles lymphoblastiques T CD7+
soficabtagén geleucel	linfocitos T CD4+ y CD8+ alogénicos derivados de material de leucoaféresis de donantes sanos, modificados genéticamente usando edición génica con CRISPR/Cas9 para eliminar la expresión de CD7 y TRAC endógenos usando ARNs guía (ARNg), seguido de transducción con un vector lentiviral auto-inactivante, no replicativo que codifica un receptor de antígenos quimérico (CAR) anti-CD7 que consta de una secuencia líder de CD8, un fragmento variable de cadena sencilla (scFv) anti-CD7 (clon TH69), bisagra de CD8, un dominio transmembrana de CD28, un dominio coestimulador de 4-1BB y un dominio de señalización intracelular de CD3ζ, bajo el control del promotor del factor de elongación 1 alfa (EF-1α). El transgén también codifica un dominio extracelular truncado de CD34 humano separado del CAR por un péptido 2A derivado del teschovirus porcino 1. El CRISP/Cas9 y los ARNg se introducen como un complejo de ribonucleoproteína (RNP) mediante electroporación. El vector lentiviral está flanqueado por repeticiones terminales largas (LTRs) en 5' y 3' y también contiene una secuencia de empaquetamiento viral ψ, un *gag* parcial, un elemento de respuesta Rev (RRE), una secuencia de tracto de poli-purina/terminación central (cPPT/CTS) y una secuencia de identificación (ID) sintética. El vector está seudotipado con la glicoproteína G de la envuelta de VSV. El material de leucoaféresis se enriquece en linfocitos T CD4+ y CD8+ mediante inmunoselección positiva antes de la activación con agonistas de CD3 y CD28 en medio de crecimiento que contiene interleuquina 7 (IL-7) e interleuquina 15 (IL-15). Las células se editan genéticamente y después se transducen con el vector lentiviral y se expanden en medio de crecimiento que contiene suero AB humano, IL-7 e IL-15. La suspensión celular consiste en linfocitos T (≥98.0% CD45+, ≤1.0% CD7+, ≤8.0% CD3+) con más del 30% de los linfocitos T que expresan el transgén del CAR y con ≥70% (CD7) y >85% (TRAC) de edición génica dirigida. Los linfocitos transducidos muestran citotoxicidad frente a células T linfoblásticas diana CD7+ *terapia génica basada en células (antineoplásico)*
solangeprasum	
solangepras	1-(2-[4-(2,4-difluorophenoxy)piperidin-1-yl]-3-{[(3*R*)-oxolan-3-yl]amino}-7,8-dihydropyrido[3,4-*b*]pyrazin-6(5*H*)-yl)ethan-1-one *G protein-coupled receptor 6 (GCPR6) inverse agonist, antiparkinsonian*
solangépras	1-(2-[4-(2,4-difluorophénoxy)pipéridin-1-yl]-3-{[(3*R*)-oxolan-3-yl]amino}-7,8-dihydropyrido[3,4-*b*]pyrazin-6(5*H*)-yl)éthan-1-one *agoniste inverse du récepteur 6 couplé aux protéines G (GCPR6), antiparkinsonien*
solangepras	1-(2-[4-(2,4-difluorofenoxi)piperidin-1-il]-3-{[(3*R*)-oxolan-3-il]amino}-7,8-dihidropiridо[3,4-*b*]pirazin-6(5*H*)-il)etan-1-ona *agonista inverso del receptor 6 (GCPR6) acoplado a proteínas G, antiparkinsoniano*

$C_{24}H_{29}F_2N_5O_3$ 2254706-21-1

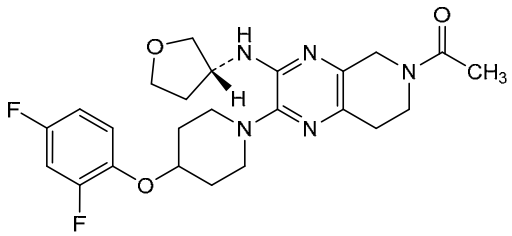

sonzivotidum filricianinum

sonzivotide filricianine 3-(3,3-dimethyl-2-{(Ξ)-2-[(3Ξ)-3-[(2Ξ)-2-{(3*RS*)-3-methyl-1-(3-sulfopropyl)-3-[(3*S*,7*S*,22*S*)-1,3,7,22-tetracarboxy-5,13,20,28-tetraoxo-4,6,12,21,27-pentaazahentriacontan-31-yl]-1,3-dihydro-2*H*-indol-2-ylidene}ethylidene]-2-(4-sulfophenoxy)cyclohex-1-en-1-yl]ethen-1-yl}-3*H*-indol-1-ium-1-yl)propane-1-sulfonate
diagnostic imaging agent

sonzivotide filricianine 3-(3,3-diméthyl-2-{(Ξ)-2-[(3Ξ)-3-[(2Ξ)-2-{(3*RS*)-3-méthyl-1-(3-sulfopropyl)-3-[(3*S*,7*S*,22*S*)-1,3,7,22-tétracarboxy-5,13,20,28-tétraoxo-4,6,12,21,27-pentaazahéntriacontan-31-yl]-1,3-dihydro-2*H*-indol-2-ylidène}éthylidène]-2-(4-sulfophénoxy)cyclohex-1-én-1-yl]éthén-1-yl}-3*H*-indol-1-ium-1-yl)propane-1-sulfonate
agent d'imagerie diagnostique

sonzivotida filricianina 3-(3,3-dimetil-2-{(Ξ)-2-[(3Ξ)-3-[(2Ξ)-2-{(3*RS*)-3-metil-1-(3-sulfopropil)-3-[(3*S*,7*S*,22*S*)-1,3,7,22-tetracarboxi-5,13,20,28-tetraoxo-4,6,12,21,27-pentaazahentriacontan-31-il]-1,3-dihidro-2*H*-indol-2-ilideno}etilideno]-2-(4-sulfofenoxi)ciclohex-1-en-1-il]eten-1-il}-3*H*-indol-1-io-1-il)propano-1-sulfonato
agente de diagnóstico por imagen

$C_{71}H_{95}N_7O_{22}S_3$ 2135637-99-7

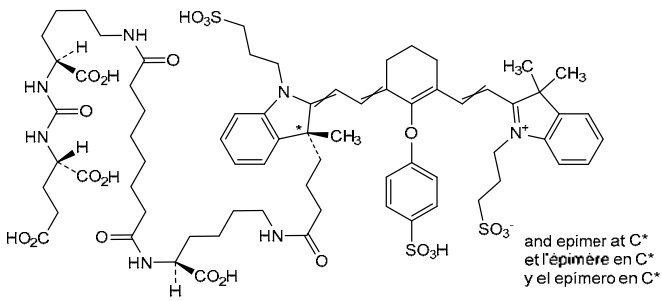

sosimerasibum

sosimerasib (2*R*,4a*R*,8*M*)-11-chloro-6-[2-(dimethylamino)ethyl]-10-(2-fluoro-6-hydroxyphenyl)-2-methyl-8-[4-methyl-2-(propan-2-yl)pyridin-3-yl]-3-(prop-2-enoyl)-2,3,4,4a,6,8-hexahydro-1*H*-pyrazino[1',2':4,5]pyrazino[2,3-*c*][1,8]naphthyridine-5,7-dione
Kirsten rat sarcoma viral oncogene homolog inhibitor, antineoplastic

sosimérasib (2*R*,4a*R*,8*M*)-11-chloro-6-[2-(diméthylamino)éthyl]-10-(2-fluoro-6-hydroxyphényl)-2-méthyl-8-[4-méthyl-2-(propan-2-yl)pyridin-3-yl]-3-(prop-2-énoyl)-2,3,4,4a,6,8-hexahydro-1*H*-pyrazino[1',2':4,5]pyrazino[2,3-*c*][1,8]naphtyridine-5,7-dione
inhibiteur d'homologue d'oncogène viral du sarcome de rat de Kirsten, antinéoplasique

sosimerasib (2*R*,4a*R*,8*M*)-11-cloro-6-[2-(dimetilamino)etil]-10-(2-fluoro-6-hidroxifenil)-2-metil-8-[4-metil-2-(propan-2-il)piridin-3-il]-3-(prop-2-enoil)-2,3,4,4a,6,8-hexahidro-1*H*-pirazino[1',2':4,5]pirazino[2,3-*c*][1,8]naftiridina-5,7-diona
inhibidor del homólogo del oncogen vírico del sarcoma de rata Kirsten, antineoplásico

$C_{36}H_{39}ClFN_7O_4$ 2839563-01-6

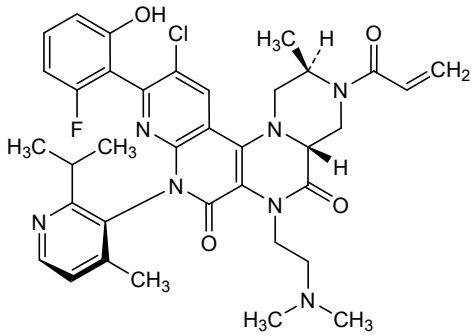

sumonerimodum

sumonerimod 3-(5-{[4-cyclopentyl-3-(trifluoromethyl)phenyl]methoxy}-3-methyl-1*H*-indol-2-yl)propanoic acid
sphingosine-1-phosphate receptor 1 agonist, immunomodulator

sumonérimod acide 3-(5-{[4-cyclopentyl-3-(trifluorométhyl)phényl]méthoxy}-3-méthyl-1*H*-indol-2-yl)propanoïque
agoniste du récepteur 1 du sphingosine-1-phosphate, immunomodulateur

sumonerimod ácido 3-(5-{[4-ciclopentil-3-(trifluorometil)fenil]metoxi}-3-metil-1*H*-indol-2-il)propanoico
agonista del receptor 1 de la esfingosina-1 fosfato, inmunomodulador

$C_{25}H_{26}F_3NO_3$ 2433782-42-2

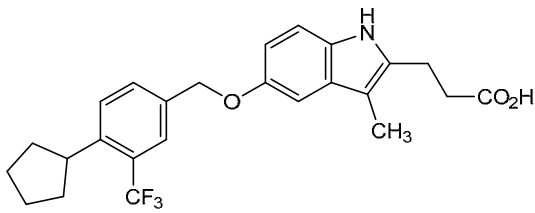

suraxavirum marboxilum

suraxavir marboxil ({(12'a*R*)-12'-[(11*S*)-7,8-difluoro-6,11-dihydrodibenzo[*b*,*e*]thiepin-11-yl]-6',8'-dioxo-6',8',12',12'a-tetrahydro-1'*H*,4'*H*-spiro[cyclopropane-1,3'-[1,4]oxazino[3,4-*c*]pyrido[2,1-*f*][1,2,4]triazin]-7'-yl}oxy)methyl methyl carbonate
antiviral

suraxavir marboxil

carbonate de ({(12'a*R*)-12'-[(11*S*)-7,8-difluoro-6,11-dihydrodibenzo[*b*,*e*]thiépin-11-yl]-6',8'-dioxo-6',8',12',12'a-tétrahydro-1'*H*,4'*H*-spiro[cyclopropane-1,3'-[1,4]oxazino[3,4-*c*]pyrido[2,1-*f*][1,2,4]triazin]-7'-yl}oxy)méthyle et de méthyle
antiviral

suraxavir marboxilo

carbonato de ({(12'a*R*)-12'-[(11*S*)-7,8-difluoro-6,11-dihidrodibenzo[*b*,*e*]tiepin-11-il]-6',8'-dioxo-6',8',12',12'a-tetrahidro-1'*H*,4'*H*-espiro[ciclopropano-1,3'-[1,4]oxazino[3,4-*c*]pirido[2,1-*f*][1,2,4]triazin]-7'-il}oxi)metilo y metilo
antiviral

$C_{29}H_{25}F_2N_3O_7S$ 2364589-86-4

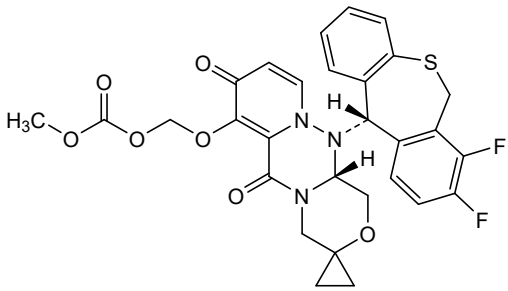

suvonstobartum #

suvonstobart

immunoglobulin G1-kappa, anti-[*Homo sapiens* CD24 (signal transducer CD24)], monoclonal antibody; H-gamma1 heavy chain (1-447) [VH Musmus/Homsap (*Mus musculus* IGHV3-1*02 (98.0%) -(IGHD) -IGHJ4*01 (87.5%) G121>R (110)/*Homo sapiens* IGHV4-30-4*09 (74.5%) -(IGHD) -IGHJ4*01 (78.6%) G121>R (110), L123>S (112), CDR-IMGT [9.7.10] (26-34.52-58.97-106)) (1-117) -*Homo sapiens* IGHG1*03,G1m3, nG1m1 CH1 R120, CH3 E12, M14, 2-G1v6 CH2 A85.4, A118, A119 (CH1 R120 (214) (118-215), hinge 1-15 (216-230), CH2 S85.4>A (298), E118>A (333), K119>A (334) (231-340), CH3 E12 (356), M14 (358) (341-445), CHS (446-447)) (118-447)], (220-220')-disulfide with L-kappa light chain (1'-220') [V-KAPPA (*Homo sapiens* IGKV1-27*01 (82.3%) -IGKJ4*01 (91.7%) I126>L (112'), CDR-IMGT [12.3.9] (27'-38'.56'-58'.95'-103')) (1'-113') -*Homo sapiens* IGKC*01 (100%) Km3 A45.1, V101 (C-KAPPA A45.1 (159'), V101 (197')) (114'-220')]; dimer (226-226'':229-229'')-bisdisulfide, produced in Chinese hamster ovary (CHO) cells, cell line CHO-K1, glycoform alfa
immunostimulant, antineoplastic

suvonstobart

immunoglobuline G1-kappa, anti-[*Homo sapiens* CD24 (transducteur de signal CD24)], anticorps monoclonal;

chaîne lourde H-gamma1 (1-447) [VH Musmus/Homsap (*Mus musculus* IGHV3-1*02 (98.0%) -(IGHD) -IGHJ4*01 (87.5%) G121>R (110)/*Homo sapiens* IGHV4-30-4*09 (74.5%) -(IGHD) -IGHJ4*01 (78.6%) G121>R (110), L123>S (112), CDR-IMGT [9.7.10] (26-34.52-58.97-106)) (1-117) -*Homo sapiens* IGHG1*03,G1m3, nG1m1 CH1 R120, CH3 E12, M14, 2-G1v6 CH2 A85.4, A118, A119 (CH1 R120 (214) (118-215), charnière 1-15 (216-230), CH2 S85.4>A (298), E118>A (333), K119>A (334) (231-340), CH3 E12 (356), M14 (358) (341-445), CHS (446-447)) (118-447)], (220-220')-disulfure avec la chaîne légère L-kappa (1'-220') [V-KAPPA (*Homo sapiens* IGKV1-27*01 (82.3%) -IGKJ4*01 (91.7%) I126>L (112'), CDR-IMGT [12.3.9] (27'-38'.56'-58'.95'-103')) (1'-113') -*Homo sapiens* IGKC*01 (100%) Km3 A45.1, V101 (C-KAPPA A45.1 (159'), V101 (197')) (114'-220')]; dimère (226-226'':229-229'')-bisdisulfure, produit dans des cellules ovariennes de hamster chinois (CHO), lignée cellulaire CHO-K1, glycoforme alfa
immunostimulant, antinéoplasique

suvonstobart

inmunoglobulina G1-kappa, anti-[*Homo sapiens* CD24 (transductor de señal CD24)], anticuerpo monoclonal;
cadena pesada H-gamma1 (1-447) [VH Musmus/Homsap (*Mus musculus* IGHV3-1*02 (98.0%) -(IGHD) -IGHJ4*01 (87.5%) G121>R (110)/*Homo sapiens* IGHV4-30-4*09 (74.5%) -(IGHD) -IGHJ4*01 (78.6%) G121>R (110), L123>S (112), CDR-IMGT [9.7.10] (26-34.52-58.97-106)) (1-117) -*Homo sapiens* IGHG1*03,G1m3, nG1m1 CH1 R120, CH3 E12, M14, 2-G1v6 CH2 A85.4, A118, A119 (CH1 R120 (214) (118-215), bisagra 1-15 (216-230), CH2 S85.4>A (298), E118>A (333), K119>A (334) (231-340), CH3 E12 (356), M14 (358) (341-445), CHS (446-447)) (118-447)], (220-220')-disulfuro con la cadena ligera L-kappa (1'-220') [V-KAPPA (*Homo sapiens* IGKV1-27*01 (82.3%) -IGKJ4*01 (91.7%) I126>L (112'), CDR-IMGT [12.3.9] (27'-38'.56'-58'.95'-103')) (1'-113') -*Homo sapiens* IGKC*01 (100%) Km3 A45.1, V101 (C-KAPPA A45.1 (159'), V101 (197')) (114'-220')]; dímero (226-226'':229-229'')-bisdisulfuro, producido en las células ováricas de hámster chino (CHO), línea celular CHO-K1, forma glicosilada alfa
inmunoestimulante, antineoplásico

2983834-87-1

Heavy chain / Chaîne lourde / Cadena pesada

```
EVQLQESGPD LVKPSQSLSL TCTVTGYSIT SDYAWHWIRQ FPGNKLEWMG  50
YISYSGSTSY NPSLKSRISI TRDTSKNQFF LQLNSVTTED TATYYCARGA 100
YGALDYWGQG TSVTVSSAST KGPSVFPLAP SSKSTSGGTA ALGCLVKDYF 150
PEPVTVSWNS GALTSGVHTF PAVLQSSGLY SLSSVVTVPS SSLGTQTYIC 200
NVNHKPSNTK VDKKVEPKSC DKTHTCPPCP APELLGGPSV FLFPPKPKDT 250
LMISRTPEVT CVVVDVSHED PEVKFNWYVD GVEVHNAKTK PREEQYNSTY 300
RVVSVLTVLH QDWLNGKEYK CKVSNKALPA PIAATISKAK GQPREPQVYT 350
LPPARDELTK NQVSLTCLVK GFYPSDIAVE WESNGQPENN YKTTPPVLDS 400
DGSFFLYSKL TVDKSRWQQG NVFSCSVMHE ALHNHYTQKS LSLSPGK    447
```

Light chain / Chaîne légère / Cadena ligera

```
DIQMTQSPSS LSASVGDRVT ITCKASQNIL YSSNQKNYLA WYQQKPGKAP  50
KLLIYWASTR ESGVPARFSG SGSGTDFTLT ISSLQPEDFA TYYCQQNFIY 100
FLTFGQGTKV EIKRTVAAPS VFIFPPSDEQ LKSGTASVVC LLNNFYPREA 150
KVQWKVDNAL QSGNSQESVT EQDSKDSTYS LSSTLTLSKA DYEKHKVYAC 200
EVTHQGLSSP VTKSFNRGEC                                   220
```

Post-translational modifications
Disulfide bridges location / Position des ponts disulfure / Posiciones de los puentes disulfuro
Intra-H (C23-C104) 22-96 144-200 261-321 367-425
22"-96" 144"-200" 261"-321" 367"-425"
Intra-L (C23-C104) 23'-94' 140'-200'
23'"-94'" 140'"-200'"
Inter-H-L (h 5-CL 126) 220-220' 220"-220'"
Inter-H-H (h 11, h 14) 226-226" 229-229"

N-glycosylation sites / Sites de N-glycosylation / Posiciones de N-glicosilación
H CH2 N84.4: 297, 297"
Fucosylated complex bi-antennary CHO-type glycans / glycanes de type CHO bi-antennaires complexes fucosylés / glicanos de tipo CHO biantenarios complejos fucosilados

C-terminal lysine clipping / Coupure de la lysine C-terminale / Recorte de lisina C-terminal
H CHS K2: 447, 447"

talicabtagene autoleucelum #

talicabtagene autoleucel — autologous peripheral blood mononuclear cells (PBMCs) obtained by leukapheresis enriched for CD3+ T lymphocytes, transduced with a self-inactivating non-replicating lentiviral vector encoding a chimeric antigen receptor (CAR) targeting CD19, comprising a CD8α leader sequence, a humanised anti-CD19 single chain variable fragment (scFv; derived from the FMC63 antibody), human CD8α hinge and transmembrane domain, human 4-1BB co-stimulatory domain and human CD3ζ signalling domain, under control of the elongation factor-1 alpha (EF-1α) promoter. The vector genome also contains an HIV-1 packaging signal (ψ), a Rev response element (RRE), a central polypurine tract (cPPT)/central termination sequence (CTS) and is flanked by 5' and 3' long terminal repeats (LTRs). The vector is pseudotyped with vesicular stomatitis virus (VSV) G glycoprotein. The leukapheresis material is enriched for CD3+ T lymphocytes by positive immunoselection, activated by CD3 and CD28 agonists and transduced with the lentiviral vector. The cells are then expanded in media supplemented with human AB serum and interleukin 2 (IL-2). The T lymphocytes (≥95%) are positive for the transgene (≥15% CAR positive) and are cytotoxic (≥50%) when co-cultured with CD19 expressing tumour cell lines
cell-based gene therapy (antineoplastic)

talicabtagène autoleucel — cellules mononucléaires du sang périphérique (PBMC) autologues, obtenues par leucaphérèse et enrichies en lymphocytes T CD3+, transduites avec un vecteur lentiviral non réplicatif auto-inactivant codant un récepteur antigénique chimérique (RAC) ciblant CD19, comprenant une séquence de tête CD8α, un fragment variable à chaîne unique anti-CD19 humanisé (scFv; dérivé de l'anticorps FMC63), un domaine charnière et un domain transmembranaire CD8α humain, un domaine co-stimulateur 4-1BB humain et un domaine de signalisation CD3ζ humain, sous le contrôle du promoteur du facteur d'élongation 1 alpha (EF-1α). Le génome du vecteur contient également un signal d'emballage du VIH-1 (ψ), un élément de réponse Rev (RRE), un tractus polypurine central (cPPT)/séquence de terminaison centrale (CTS), et est flanqué de répétitions terminales longues (LTRs) en 5' et en 3'. Le vecteur est pseudotypé avec la glycoprotéine G du virus de la stomatite vésiculaire (VSV).
Le matériel de leucaphérèse est enrichi en lymphocytes T CD3+ par immunosélection positive, activé par des agonistes CD3 et CD28 et transduit avec le vecteur lentiviral. Les cellules sont ensuite épansées dans un milieu supplémenté de sérum AB humain et d'interleukine 2 (IL-2). Les lymphocytes T (≥95%) sont positifs pour le transgène (≥15% RAC positifs), et sont cytotoxiques (≥50%) lorsqu'ils sont co-cultivés avec des lignées cellulaires tumorales exprimant CD19
thérapie génique à base de cellules (antinéoplasique)

talicabtagén autoleucel — células monucleares de sangre periférica (PBMCs) autólogas obtenidas por leucoaféresis, enriquecidas en linfocitos T CD3+, transducidas con un vector lentiviral auto-inactivante, no replicativo, que codifica un receptor de antígenos quimérico (CAR) dirigido a CD19, que consta de una secuencia líder de CD8α, un fragmento variable de cadena sencilla anti-CD19 humanizado (scFv; derivado del anticuerpo FMC63), un dominio bisagra y transmembrana de CD8α, un dominio coestimulador de 4-1BB humano y un dominio de señalización de CD3ζ humano, bajo el control del promotor del factor de elongación 1 alfa (EF-1α). El genoma del vector también contiene una señal de empaquetamiento del HIV-1 (ψ), un elemento de

respuesta Rev (RRE) y una secuencia de tracto de poli-purina central (cPPT)/terminación central (CTS), y está flanqueado por repeticiones terminales largas (LTRs) en 5' y 3'. El vector está seudotipado con la glicoproteína G del virus de la estomatitis vesicular (VSV).
El material de leucoaféresis se enriquece en linfocitos T CD3+ mediante inmunoselección positiva, se activa con agonistas de CD3 y CD28 y se transduce con el vector lentiviral. Las células se expanden después en medio suplementado con suero AB humano e interleuquina 2 (IL-2). Los linfocitos T (≥95%) son positivos para el transgén (≥15% CAR positivos) y son citotóxicos (≥50%) cuando se co-cultivan con líneas de células tumorales que expresan CD19
terapia génica basada en células (antineoplásico)

tanruprubartum

tanruprubart

immunoglobulin G4-kappa, anti-[*Homo sapiens* C1q (complement C1q)], monoclonal antibody;
H-gamma4 heavy chain (1-448) [VH Musmus/Homsap (*Mus musculus* IGHV1-64*01 (82.5%) -(IGHD) -IGHJ4*01 (92.9%) S123>T (116)/*Homo sapiens* IGHV1-46*01 (79.4%) -(IGHD) -IGHJ6*01 (92.9%), CDR-IMGT [8.8.14] (26-33.51-58.97-110)) (1-121) -*Homo sapiens* IGHG4*01, *nG4m(a)* CH2 L92, 12-G4v5 h P10, 6-G4v3 CH2 E1.2 (CH1 (122-219), hinge 1-12 S10>P (229) (220-231), CH2 L1.2>E (236), L92 (310) (232-341), CH3 (342-446), CHS (447-448)) (122-448)], (135-214')-disulfide with L-kappa light chain (1'-214') [V-KAPPA Musmus/Homsap (*Mus musculus* IGKV16-104*01 (89.5%) -IGKJ2*03 (90.9%) S120>Q (100')/*Homo sapiens* IGKV1-9*03 (80.9%) -IGKJ2*01 (100%), CDR-IMGT [6.3.9] (27'-32'.50'-52'.89'-97')) (1'-107') -*Homo sapiens* IGKC*01 (100%) Km3 A45.1, V101 (C-KAPPA A45.1 (153'), V101 (191')) (108'-214')]; dimer (227-227'':230-230'')-bisdisulfide, produced in Chinese hamster ovary (CHO) cells, derived from the cell line CHO-K1SV, lacking the glutamine synthetase (GS-KO) gene, glycoform alfa
immunosuppressant

tanruprubart

immunoglobuline G4-kappa, anti-[*Homo sapiens* C1q (complément C1q)], anticorps monoclonal;
chaîne lourde H-gamma4 (1-448) [VH Musmus/Homsap (*Mus musculus* IGHV1-64*01 (82.5%) -(IGHD) -IGHJ4*01 (92.9%) S123>T (116)/*Homo sapiens* IGHV1-46*01 (79.4%) -(IGHD) -IGHJ6*01 (92.9%), CDR-IMGT [8.8.14] (26-33.51-58.97-110)) (1-121) -*Homo sapiens* IGHG4*01, *nG4m(a)* CH2 L92, 12-G4v5 h P10, 6-G4v3 CH2 E1.2 (CH1 (122-219), charnière 1-12 S10>P (229) (220-231), CH2 L1.2>E (236), L92 (310) (232-341), CH3 (342-446), CHS (447-448)) (122-448)], (135-214')-disulfure avec la chaîne légère L-kappa (1'-214') [V-KAPPA Musmus/Homsap (*Mus musculus* IGKV16-104*01 (89.5%) -IGKJ2*03 (90.9%) S120>Q (100')/*Homo sapiens* IGKV1-9*03 (80.9%) -IGKJ2*01 (100%), CDR-IMGT [6.3.9] (27'-32'.50'-52'.89'-97')) (1'-107') -*Homo sapiens* IGKC*01 (100%) Km3 A45.1, V101 (C-KAPPA A45.1 (153'), V101 (191')) (108'-214')]; dimère (227-227'':230-230'')-bisdisulfure, produit dans des cellules ovariennes de hamster chinois (CHO), dérivant de la lignée cellulaire CHO-K1SV, ne présentant pas le gène de la glutamine synthétase (GS-KO), glycoforme alfa
immunosuppresseur

tanruprubart

inmunoglobulina G4-kappa, anti-[*Homo sapiens* C1q (complemento C1q)], anticuerpo monoclonal;
cadena pesada H-gamma4 (1-448) [VH Musmus/Homsap (*Mus musculus* IGHV1-64*01 (82.5%) -(IGHD) -IGHJ4*01 (92.9%) S123>T (116)/*Homo sapiens* IGHV1-46*01 (79.4%) -(IGHD) -IGHJ6*01 (92.9%), CDR-IMGT [8.8.14] (26-33.51-58.97-110)) (1-121) -*Homo sapiens* IGHG4*01, *nG4m(a)* CH2 L92, 12-G4v5 h P10, 6-G4v3 CH2 E1.2 (CH1 (122-219), bisagra 1-12 S10>P (229) (220-231), CH2 L1.2>E (236), L92 (310) (232-341), CH3 (342-446), CHS (447-448)) (122-448)], (135-214')-disulfuro con la cadena ligera L-kappa (1'-214') [V-KAPPA Musmus/Homsap (*Mus musculus* IGKV16-104*01 (89.5%) -IGKJ2*03 (90.9%) S120>Q (100')/*Homo sapiens* IGKV1-9*03 (80.9%) -IGKJ2*01 (100%), CDR-IMGT [6.3.9] (27'-32'.50'-52'.89'-97')) (1'-107') -*Homo sapiens* IGKC*01 (100%) Km3 A45.1, V101 (C-KAPPA A45.1 (153'), V101 (191')) (108'-214')]; dímero (227-227'':230-230'')-bisdisulfuro, producido en las células ováricas de hámster chino (CHO), línea celular derivada de CHO-K1SV, en ausencia del gen glutamina sintetasa (GS-KO), forma glicosilada alfa
inmunosupresor

2065212-40-8

Heavy chain / Chaîne lourde / Cadena pesada

```
QVQLVQSGAE LKKPGASVKV SCKSSGYHFT SYWMHWVKQA PGQGLEWIGV  50
IHPNSGSINY NEKFESRVTI TVDKSTSTAY MELSSLRSED TAVYYCAGER 100
DSTEVLPMDY WGQGTTVTVS SASTKGPSVF PLAPCSRSTS ESTAALGCLV 150
KDYFPEPVTV SWNSGALTSG VHTFPAVLQS SGLYSLSSVV TVPSSSLGTK 200
TYTCNVDHKP SNTKVDKRVE SKYGPPCPPC PAPEFEGGPS VFLFPPKPKD 250
TLMISRTPEV TCVVVDVSQE DPEVQFNWYV DGVEVHNAKT KPREEQFNST 300
YRVVSVLTVL HQDWLNGKEY KCKVSNKGLP SSIEKTISKA KGQPREPQVY 350
TLPPSQEEMT KNQVSLTCLV KGFYPSDIAV EWESNGQPEN NYKTTPPVLD 400
SDGSFFLYSR LTVDKSRWQE GNVFSCSVMH EALHNHYTQK SLSLSLGK   448
```

Light chain / Chaîne légère / Cadena ligera

```
DVQITQSPSS LSASLGERAT INCRASKSIN KYLAWYQQKP GKAPKLLIYS  50
GSTLQSGIPA RFSGSGSGTD FTLTISSLEP EDFAMYYCQQ HNEYPLTFGQ 100
GTKLEIKRTV AAPSVFIFPP SDEQLKSGTA SVVCLLNNFY PREAKVQWKV 150
DNALQSGNSQ ESVTEQDSKD STYSLSSTLT LSKADYEKHK VYACEVTHQG 200
LSSPVTKSFN RGEC                                        214
```

Post-translational modifications
Disulfide bridges location / Position des ponts disulfure / Posiciones de los puentes disulfuro
Intra-H (C23-C104) 22-96 148-204 262-322 368-426
22"-96" 148"-204" 262"-322" 368"-426"
Intra-L (C23-C104) 23'-88' 134'-194'
23'"-88'" 134'"-194'"
Inter-H-L (CH1 10-CL 126) 135-214' 135"-214'"
Inter-H-H (h 8, h 11) 227-227" 230-230"

N-terminal glutaminyl cyclization / Cyclisation du glutaminyle N-terminal / Ciclación del glutaminilo N-terminal
Q > pyroglutamyl (pE, 5-oxoprolyl) / pyroglutamyle (pE, 5-oxoprolyle) / piroglutamilo (pE, 5-oxoprolilo)
H VH Q1: 1, 1"

N-glycosylation sites / Sites de N-glycosylation / Posiciones de N-glicosilación
H CH2 N84.4: 298, 298"
Fucosylated complex bi-antennary CHO-type glycans / glycanes de type CHO bi-antennaires complexes fucosylés / glicanos de tipo CHO biantenarios complejos fucosilados

C-terminal lysine clipping / Coupure de la lysine C-terminale / Recorte de lisina C-terminal
H CHS K2: 448, 448"

tarvicopanum

tarvicopan

[2-({7-[2-(aminomethyl)pyridin-4-yl]-2-methyl-1-benzofuran-5-yl}methoxy)phenyl]acetic acid
complement factor D inhibitor

tarvicopan

acide [2-({7-[2-(aminométhyl)pyridin-4-yl]-2-méthyl-1-benzofuran-5-yl}méthoxy)phényl]acétique
inhibiteur du facteur D du complément

tarvicopán

ácido [2-({7-[2-(aminometil)piridin-4-il]-2-metil-1-benzofuran-5-il}metoxi)fenil]acético
inhibidor del factor D del complemento

$C_{24}H_{22}N_2O_4$ 2378381-06-5

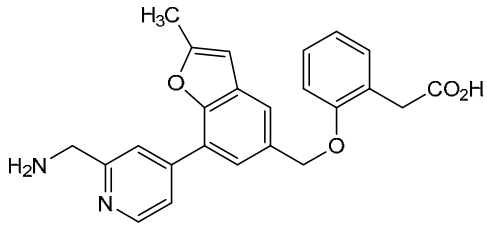

technetium (^{99m}Tc) gleceparinum sodium

technetium (^{99m}Tc) gleceparin sodium

sodium salt of heparin with degree of sulfatation about 2.7 per disaccharide unit, fractionated to a product containing ≥ 50 % of molecules with mass > 20 kDa, radiolabeled with (^{99m}Tc)technetium
imaging agent

technétium (^{99m}Tc) glécéparine sodique

sel de sodium d'héparine avec une degré de sulfatation d'environ 2,7 par unité disaccharidique, fractionné en un produit contenant ≥ 50 % de molécules de masse > 20 kDa, radiomarqué avec du (^{99m}Tc)technétium
agent d'imagerie diagnostique

tecnecio (^{99m}Tc) gleceparina sódica

sal sódica de heparina con un grado de sulfatación de aproximadamente 2,7 por unidad disacarídica, fraccionada hasta obtener un producto que contenga ≥ 50 % de moléculas con masa > 20 kDa, radiomarcado con (^{99m}Tc)tecnecio
agente de diagnóstico por imagen

3004691-95-3

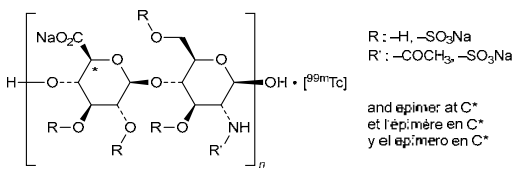

tersolisibum

tersolisib

N-(2-aminopyrimidin-5-yl)-*N'*-[(1*R*)-1-(5,7-difluoro-3-methyl-1-benzofuran-2-yl)-2,2,2-trifluoroethyl]urea
phosphatidylinositol 3-kinase inhibitor, antineoplastic

tersolisib

N-(2-aminopyrimidin-5-yl)-*N*'-[(1*R*)-1-(5,7-difluoro-3-méthyl-1-benzofuran-2-yl)-2,2,2-trifluoroéthyl]urée
inhibiteur de la phosphatidylinositol 3-kinase (PI3K), antinéoplasique

tersolisib

N-(2-aminopirimidin-5-il)-*N*'-[(1*R*)-1-(5,7-difluoro-3-metil-1-benzofuran-2-il)-2,2,2-trifluoroetil]urea
inhibidor de la kinasa-3 del fosfatidilinositol (PI3K), antineoplásico

$C_{16}H_{12}F_5N_5O_2$ 2883540-92-7

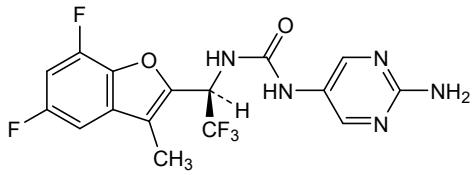

tetrandrinum

tetrandrine

(1^1*S*,3^1*S*)-1^6,3^6,3^7,5^4-tetramethoxy-1^2,3^2-dimethyl-1^1,1^2,1^3,1^4,3^1,3^2,3^3,3^4-octahydro-2,6-dioxa-1(7,1),3(8,1)-diisoquinolina-5(1,3),7(1,4)-dibenzenacyclooctaphane;
6,6',7,12-tetramethoxy-2,2'-dimethyl-1-*epi*-berbaman
multi-drug resistance (MDR) modulator, antineoplastic

tétrandrine

(1^1*S*,3^1*S*)-1^6,3^6,3^7,5^4-tétraméthoxy-1^2,3^2-diméthyl-1^1,1^2,1^3,1^4,3^1,3^2,3^3,3^4-octahydro-2,6-dioxa-1(7,1),3(8,1)-diisoquinoléina-5(1,3),7(1,4)-dibenzénacyclooctaphane;
6,6',7,12-tétraméthoxy-2,2'-diméthyl-1-*épi*-berbamane
modulateur de la multirésistance aux médicaments (MDR), antinéoplasique

tetrandrina

(1^1*S*,3^1*S*)-1^2,3^2-dimetil-1^6,3^6,3^7,5^4-tetrametoxi-1^1,1^2,1^3,1^4,3^1,3^2,3^3,3^4-octahidro-2,6-dioxa-1(7,1),3(8,1)-diisoquinoleina-5(1,3),7(1,4)-dibencenaciclooctafano;
2,2'-dimetil-6,6',7,12-tetrametoxi-1-*epi*-berbamano
modulador de resistencia a múltiples fármacos (MDR), antineoplásico

$C_{38}H_{42}N_2O_6$ 518-34-3

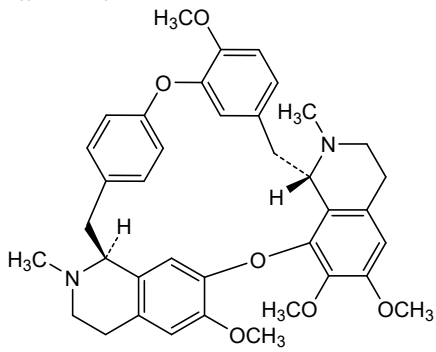

tezusomantum

tezusomant

N-(15-carboxypentadecanoyl)-L-γ-glutamyl-L-γ-glutamyl-N^{6}-{$N^{6.2}$,$C^{1.7}$-anhydro-$S^{N.1}$,$C^{3.13}$-cyclo[4-carboxy-*N*-(sulfanylacetyl)-L-phenylalanyl-N^{2}-methyl-L-lysyl-L-valyl-L-valyl-L-seryl-L-asparaginyl-1-(carboxymethyl)-L-tryptophyl-4-carboxy-L-phenylalanyl-L-lysyl-5-hydroxy-L-tryptophyl-2-methylalanyl-L-valyl-L-alanyl]}-L-lysinamide

growth hormone receptor antagonist, acromegaly

tézusomant

N-(15-carboxypentadécanoyl)-L-γ-glutamyl-L-γ-glutamyl-N^{6}-{$N^{6.2}$,$C^{1.7}$-anhydro-$S^{N.1}$,$C^{3.13}$-cyclo[4-carboxy-*N*-(sulfanylacétyl)-L-phénylalanyl-N^{2}-méthyl-L-lysyl-L-valyl-L-valyl-L-séryl-L-asparaginyl-1-(carboxyméthyl)-L-tryptophyl-4-carboxy-L-phénylalanyl-L-lysyl-5-hydroxy-L-tryptophyl-2-méthylalanyl-L-valyl-L-alanyl]}-L-lysinamide

antagoniste du récepteur de l'homone de croissance, acromégalie

tezusomant

N-(15-carboxipentadecanoil)-L-γ-glutamil-L-γ-glutamil-N^{6}-{$N^{6.2}$,$C^{1.7}$-anhidro-$S^{N.1}$,$C^{3.13}$-ciclo[4-carboxi-*N*-(sulfanilacetil)-L-fenilalanil-N^{2}-metil-L-lisil-L-valil-L-valil-L-seril-L-asparaginil-1-(carboximetil)-L-triptofil-4-carboxi-L-fenilalanil-L-lisil-5-hidroxi-L-triptofil-2-metilalanil-L-valil-L-alanil]}-L-lisinamida

antagonista del receptor de la hormona del crecimiento, acromegalia

$C_{120}H_{171}N_{23}O_{32}S$ 2802416-72-2

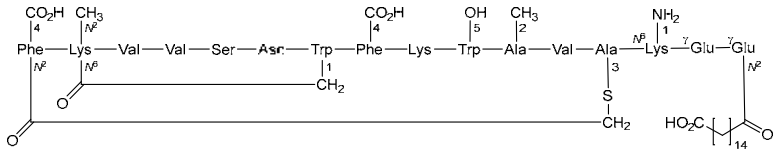

tilrekimigum #

tilrekimig

immunoglobulin (L-kappa-H-gamma1 (_L-VH-G1(CH1-h))_L-kappa)_(H-gamma1_L-lambda2), anti-[*Homo sapiens* IL4 (interleukin 4, IL-4)], anti-[*Homo sapiens* IL13 (interleukin 13, IL-13)] and anti-[*Homo sapiens* TSLP (thymic stromal lymphopoietin)], humanized and *Homo sapiens* monoclonal antibody, trispecific, trivalent;
fused L-kappa-H-gamma1 heavy chain anti-IL13 and anti-IL4 (1-674) [L-kappa anti-IL13 humanized (1-218) [V-KAPPA (*Homo sapiens* IGKV1-39*01 (82.8%) -IGKJ4*01 (100%), CDR-IMGT [10.3.9] (27-36.54-56.93-101)) (1-111) -*Homo sapiens* IGKC*01 (100%) Km3 A45.1, V101 (C-KAPPA A45.1 (157), V101 (195)) (112-218)]-5-mer (tetraglycyl-seryl) linker (219-223) -H-gamma1 heavy chain anti-IL4 *Homo sapiens* (224-674) [VH (*Homo sapiens* IGHV2-5*08 (87.0%) -(IGHD) -IGHJ3*01 (92.9%) M123>T (339), CDR-IMGT [10.7.13] (249-258.276-282.321-333)) (224-344) -*Homo sapiens* IGHG1*03v, G1m3>G1m17, nG1m1, CH1 K120, CH3 E12, M14, 6-G1v14-1 CH2 A1.3, A1.2, A1, 9-G1v24 CH3 L107, S114, 14-G1v99-1 hinge E6, CH3 E24 (CH1 R120>K (441) (345-442), hinge 1-15 D6>E (448) (443-457), CH2 L1.3>A (461), L1.2>A (462), G1>A (464) (458-567), CH3 E12 (583), M14 (585), L24>E (595), M107>L (655), N114>S (661) (568-672), CHS (673-674)) (345-674)]]; (218-221')-disulfide with L-VH-G1(CH1-h) light chain anti-IL13 humanized (1'-221') [VH (*Homo sapiens* IGHV3-21*07 (91.8%) -IGHD -IGHJ1*01 (100%), CDR-IMGT [8.7.12] (26'-33'.51'-57'.96'-107')) (1'-118') -*Homo*

sapiens IGHG1*03v, G1m3>G1m17, nG1m1, CH1 K120 (CH1 R120>K (215') (119'-216'), hinge 1-5 (217'-221')) (119'-221')]; (447-218'")-disulfide with L-kappa light chain *Homo sapiens* anti-IL4 *Homo sapiens* (1'"-218'") [V-KAPPA (*Homo sapiens* IGKV1-39*01 (87.9%) -IGKJ4*01 (100%), CDR-IMGT [10.3.9] (27'"-36'".54'"-56'".93'"-101'")) (1'"-111'") -*Homo sapiens* IGKC*01 (100%) Km3 A45.1, V101 (C-KAPPA A45.1 (157'"), V101 (195'")) (112'"-218'")]; H-gamma1 heavy chain anti-TSLP *Homo sapiens* (1"-452") [VH (*Homo sapiens* IGHV3-33*01 (95.9%) -(IGHD) -IGHJ3*02 (93.8%), CDR-IMGT [8.8.15] (26"-33".51"-58".97"-111")) (1"-122")-*Homo sapiens* IGHG1*03v, G1m3>G1m17, nG1m1 CH1 K120, CH3 E12, M14, 6-G1v14-1 CH2 A1.3, A1.2, A1, 9-G1v24 CH3 L107, S114, 14-G1v99-2 hinge R6, CH3 R88 (CH1 R120>K (219") (123"-220"), hinge 1-15 D6>R (226") (221"-235"), CH2 L1.3>A (239"), L1.2>A (240"), G1>A (242") (236"- 345"), CH3 E12 (361"), M14 (363"), K88>R (414"), M107>L (433"), N114>S (439") (346"-450"), CHS (451"-452")) (123"-452")], (225"-213'"")-disulfide with L-lambda2 light chain anti-TSLP *Homo sapiens* (1'""-214'"") [V-LAMBDA (*Homo sapiens* IGLV3-21*02 (94.8%) -IGLJ2*01 (100%), CDR-IMGT [6.3.11] (26'""-31'"".49'""-51'"".88'""-98'"")) (1'""-108'"") -*Homo sapiens* IGLC2*01 (100%) (C-LAMBDA2) (109'""-214'"")]; dimer (453-231":456-234")-bisdisulfide, produced in Chinese hamster ovary (CHO) cells, cell line CHO-K1SV lacking the glutamine synthetase (GS-KO) gene, glycoform alfa

immunosuppressant, anti-inflammatory

tilrékimig

immunoglobuline (L-kappa-H-gamma1 (_L-VH-G1(CH1-h))_L-kappa)_(H-gamma1_L-lambda2), anti-[*Homo sapiens* IL4 (interleukine 4, IL-4)], anti-[*Homo sapiens* IL13 (interleukine 13, IL-13)] et anti-[*Homo sapiens* TSLP (lymphopoïétine stromale thymique)], anticorps monoclonal humanisé et *Homo sapiens* trispécifique, trivalent;
chaîne fusionnée L-kappa-H-gamma1 anti-IL13 et anti-IL4 (1-674) [L-kappa anti-IL13 humanisée (1-218) [V-KAPPA (*Homo sapiens* IGKV1-39*01 (82.8%) -IGKJ4*01 (100%), CDR-IMGT [10.3.9] (27-36.54-56.93-101)) (1-111) -*Homo sapiens* IGKC*01 (100%) Km3 A45.1, V101 (C-KAPPA A45.1 (157), V101 (195)) (112-218)] -5-mer (tétraglycyl-séryl) linker (219-223) -chaîne lourde H-gamma1 anti-IL4 *Homo sapiens* (224-674) [VH (*Homo sapiens* IGHV2-5*08 (87.0%) -(IGHD) -IGHJ3*01 (92.9%) M123>T (339), CDR-IMGT [10.7.13] (249-258.276-282.321-333)) (224-344) -*Homo sapiens* IGHG1*03v, G1m3>G1m17, nG1m1, CH1 K120, CH3 E12, M14, 6-G1v14-1 CH2 A1.3, A1.2, A1, 9-G1v24 CH3 L107, S114, 14-G1v99-1 hinge E6, CH3 E24 (CH1 R120>K (441) (345-442), charnière 1-15 D6>E (448) (443-457), CH2 L1.3>A (461), L1.2>A (462), G1>A (464) (458-567), CH3 E12 (583), M14 (585), L24>E (595), M107>L (655), N114>S (661) (568-672), CHS (673-674)) (345-674)]]; (218-221')-disulfure avec la chaîne légère L-VH-G1(CH1-h) anti-IL13 humanisée (1'-221')[VH (*Homo sapiens* IGHV3-21*07 (91.8%) -IGHD -IGHJ1*01 (100%), CDR-IMGT [8.7.12] (26'-33'.51'-57'.96'-107')) (1'-118') -*Homo sapiens* IGHG1*03v, G1m3>G1m17, nG1m1, CH1 K120 (CH1 R120>K (215') (119'-216'), charnière 1-5 (217'-221')) (119'-221')]; (447-218'")-disulfure avec la chaîne légère L-kappa anti-IL4 *Homo sapiens* (1'"-218'") [V-KAPPA (*Homo sapiens* IGKV1-39*01 (87.9%) -IGKJ4*01 (100%), CDR-IMGT [10.3.9] (27'"-36'".54'"-56'".93'"-101'")) (1'"-111'") -*Homo sapiens* IGKC*01 (100%) Km3 A45.1, V101 (C-KAPPA A45.1 (157'"), V101 (195'")) (112'"-218'")]; chaîne lourde H-gamma1 anti-TSLP *Homo sapiens* (1"-452") [VH (*Homo sapiens* IGHV3-33*01 (95.9%) -(IGHD) -IGHJ3*02 (93.8%), CDR-IMGT [8.8.15] (26"-33".51"-58".97"-111")) (1"-122") -*Homo*

	sapiens IGHG1*03v, G1m3>G1m17, nG1m1 CH1 K120, CH3 E12, M14, 6-G1v14-1 CH2 A1.3, A1.2, A1, 9-G1v24 CH3 L107, S114, 14-G1v99-2 hinge R6, CH3 R88 (CH1 R120>K (219") (123"-220"), charnière 1-15 D6>R (226") (221"-235"), CH2 L1.3>A (239"), L1.2>A (240"), G1>A (242") (236"- 345"), CH3 E12 (361"), M14 (363"), K88>R (414"), M107>L (433"), N114>S (439") (346"-450"), CHS (451"-452")) (123"-452")], (225"-213"")-disulfure avec la chaîne légère L-lambda2 anti-TSLP *Homo sapiens* (1""-214"") [V-LAMBDA (*Homo sapiens* IGLV3-21*02 (94.8%) -IGLJ2*01 (100%), CDR-IMGT [6.3.11] (26""-31"".49""-51"".88""-98"")) (1""-108"") -*Homo sapiens* IGLC2*01 (100%) (C-LAMBDA2) (109""-214"")]; dimère (453-231":456-234")-bisdisulfure, produit dans des cellules ovariennes de hamster chinois (CHO), lignée cellulaire CHO-K1SV ne présentant pas le gène de la glutamine synthétase (GS-KO), glycoforme alfa *immunosuppresseur, anti-inflammatoire*
tilrekimig	inmunoglobulina (L-kappa-H-gamma1 (_L-VH-G1(CH1-h))_L-kappa)_(H-gamma1_L-lambda2), anti-[*Homo sapiens* IL4 (interleukina 4, IL-4)], anti-[*Homo sapiens* IL13 (interleukina 13, IL-13)] y anti-[*Homo sapiens* TSLP (linfopoyetina estromal tímica)], anticuerpo monoclonal humanizado y *Homo sapiens* triespecífico, trivalente; cadena fusionada L-kappa-H-gamma1 anti-IL13 anti-IL4 (1-674) [L-kappa anti-IL13 humanizada (1-218) [V-KAPPA (*Homo sapiens* IGKV1-39*01 (82.8%) -IGKJ4*01 (100%), CDR-IMGT [10.3.9] (27-36.54-56.93-101)) (1-111) -*Homo sapiens* IGKC*01 (100%) Km3 A45.1, V101 (C-KAPPA A45.1 (157), V101 (195)) (112-218)] -5-mer (tetraglicil-seril) enlace (219-223) -cadena pesada H-gamma1 anti-IL4 *Homo sapiens* (224-674) [VH (*Homo sapiens* IGHV2-5*08 (87.0%) -(IGHD) -IGHJ3*01 (92.9%) M123>T (339), CDR-IMGT [10.7.13] (249-258.276-282.321-333)) (224-344) -*Homo sapiens* IGHG1*03v, G1m3>G1m17, nG1m1, CH1 K120, CH3 E12, M14, 6-G1v14-1 CH2 A1.3, A1.2, A1, 9-G1v24 CH3 L107, S114, 14-G1v99-1 bisagra E6, CH3 E24 (CH1 R120>K (441) (345-442), bisagra 1-15 D6>E (448) (443-457), CH2 L1.3>A (461), L1.2>A (462), G1>A (464) (458-567), CH3 E12 (583), M14 (585), L24>E (595), M107>L (655), N114>S (661) (568-672), CHS (673-674)) (345-674)]]; (218-221')-disulfuro con la cadena ligera L-VH-G1(CH1-h) anti-IL13 humanizada (1'-221')[VH (*Homo sapiens* IGHV3-21*07 (91.8%) -IGHD -IGHJ1*01 (100%), CDR-IMGT [8.7.12] (26'-33'.51'-57'.96'-107')) (1'-118') -*Homo sapiens* IGHG1*03v, G1m3>G1m17, nG1m1, CH1 K120 (CH1 R120>K (215') (119'-216'), bisagra 1-5 (217'-221')) (119'-221')]; (447-218"')-disulfuro con la cadena ligera L-kappa anti-IL4 *Homo sapiens* (1"'-218"') [V-KAPPA (*Homo sapiens* IGKV1-39*01 (87.9%) -IGKJ4*01 (100%), CDR-IMGT [10.3.9] (27"'-36"'.54"'-56"'.93"'-101"')) (1"'-111"') -*Homo sapiens* IGKC*01 (100%) Km3 A45.1, V101 (C-KAPPA A45.1 (157"'), V101 (195"')) (112"'-218"')]; cadena pesada H-gamma1 anti-TSLP *Homo sapiens* (1"-452") [VH (*Homo sapiens* IGHV3-33*01 (95.9%) -(IGHD) -IGHJ3*02 (93.8%), CDR-IMGT [8.8.15] (26"-33".51"-58".97"-111")) (1"-122") -*Homo sapiens* IGHG1*03v, G1m3>G1m17, nG1m1 CH1 K120, CH3 E12, M14, 6-G1v14-1 CH2 A1.3, A1.2, A1, 9-G1v24 CH3 L107, S114, 14-G1v99-2 bisagra R6, CH3 R88 (CH1 R120>K (219") (123"-220"), bisagra 1-15 D6>R (226") (221"-235"), CH2 L1.3>A (239"), L1.2>A (240"), G1>A (242") (236"- 345"), CH3 E12 (361"), M14 (363"), K88>R (414"), M107>L (433"), N114>S (439") (346"-450"), CHS (451"-452")) (123"-452")], (225"-213"")-disulfuro con la cadena

ligera L-lambda2 anti-TSLP *Homo sapiens* (1""-214"") [V-LAMBDA (*Homo sapiens* IGLV3-21*02 (94.8%) -IGLJ2*01 (100%), CDR-IMGT [6.3.11] (26""-31"".49""-51"".88""-98"")) (1""-108"") -*Homo sapiens* IGLC2*01 (100%) (C-LAMBDA2) (109""-214"")]; dímero (453-231":456-234")-bisdisulfuro, producido en las células ováricas de hámster chino (CHO), línea celular CHO-K1SV en ausencia del gen de la glutamina sintetasa (GS-KO), forma glicosilada alfa *inmunosupresor, antiinflamatorio*

2981469-90-1

Heavy chain / Chaîne lourde / Cadena pesada: fused L-kappa-H-gamma1 anti-IL13 and anti-IL4 (H)

```
DIQMTQSPSS LSASVGDRVT ITCRASQSVD YDGDSFMNWY QQKPGKAPKL   50
LIYAASNLES GVPSRFSGSG SGTDFTLTIS SLQPEDFATY YCQQSNEDPW  100
TFGQGTKVEI KRTVAAPSVF IFPPSDEQLK SGTASVVCLL NNFYPREAKV  150
QWKVDNALQS GNSQESVTEQ DSKDSTYSLS STLTLSKADY EKHKVYACEV  200
THQGLSSPVT KSFNRGEC                                     218
```

Light chain / Chaîne légère / Cadena ligera: L-VH-G1(CH1-h) anti-IL13 (L')

```
EVQLVESGGG LVQPGGSLRL SCAASGFTFS SYAMSWVRQA PGKGLEWVAS   50
ISGSGGSTYY ADSVKGRFTI SRDNSKNTLY LQMNSLRAED TAVYYCAPNE  100
YYGNAFDYWG QGTLVTVSSA STKGPSVFPL APSSKSTSGG TAALGCLVKD  150
YFPEPVTVSW NSGALTSGVH TFPAVLQSSG LYSLSSVVTV PSSSLGTQTY  200
ICNVNHKPSN TKVDKRVEPK SC                                221
```

Light chain / Chaîne légère / Cadena ligera: L-kappa anti-IL4 (L"")

```
DIQMTQSPSS LSASVGDRVT ITCRASQSVD YDGDSFMNWY QQKPGKAPKL   50
LIYAASNLES GVPSRFSGSG SGTDFTLTIS SLQPEDFATY YCQQSNEDPT  100
TFGQGTKVEI KRTVAAPSVF IFPPSDEQLK SGTASVVCLL NNFYPREAKV  150
QWKVDNALQS GNSQESVTEQ DSKDSTYSLS STLTLSKADY EKHKVYACEV  200
THQGLSSPVT KSFNRGEC                                     218
```

Heavy chain / Chaîne lourde / Cadena pesada: H-gamma1 anti-TSLP (H")

```
QMQLVESGGG VVQPGRSLRL SCAASGFTFS DYSMHWVRQA PGKGLEWVAV   50
IWYDGSNKHY ADSVKGRFTI SRDNSKNTLY LQMNSLRAED TAVYYCARAP  100
QWELAPFDAF DIWGQGTMVT VSSASTKGPS VFPLAPSSKS TSGGTAALGC  150
LVKDYFPEPV TVSWNSGALT SGVHTFPAVL QSSGLYSLSS VVTVPSSSLG  200
TQTYICNVNH KPSNTKVDKR VEPKSCDKTH TCPPCPAPEA AGAPSVFLFP  250
PKPKDTLMIS RTPEVTCVVV DVSHEDPEVK FNWYVDGVEV HNAKTKPREQ  300
YNSTYRVVSV LTVLHQDWLN GKEYKCKVSN KALPAPIEKT ISKAKGQPRE  350
PQVYTLPPSR EEMTKNQVSL TCLVKGFYPS DIAVEWESNG QPENNYKTTP  400
PVLDSDGSFF LYSRLTVDKS RWQEGNVFSC SVMHEALHNH YTQKSLSLSP  450
GK                                                      452
```

Light chain / Chaîne légère / Cadena ligera: L-lambda2 anti-TSLP (L"")

```
QSVLTQPPSV SVAPGQTARI TCGGNNIGSK SVHWYQQKPG QAPVLVVYDD  50
RDRPSGIPER FSGSNSGNTA TLTISRVEAG DEADYYCQVW DSSSDHVVFG 100
GGTKLTVLGQ PKAAPSVTLF PPSSEELQAN KATLVCLISD FYPGAVTVAW 150
KADSSPVKAG VETTTPSKQS NNKYAASSYL SLTPEQWKSH RSYSCQVTHE 200
GSTVEKTVAP TECS                                         214
```

Post-translational modifications

Disulfide bridges location / Position des ponts disulfure / Posiciones de los puentes disulfuro

Intra-H (C23-C104) 23-92 138-198 245-320 371-427 488-518 594-652
22"-96" 149"-205" 266"-326" 372"-430"

Intra-L (C23-C104) 22'-95' 145'-201'
23'"-92'" 138'"-198'"
22""-87"" 136""-195""

Inter-H-L' (CL 126-h 5)* 218-221'

Inter-H-L" (h 5-CL 126) 447-218'" 225"-213'"

Inter-H-H (h 11- h 14) 453-231" 456-234"

*crosslink / lien croisé / enlace cruzado

N-terminal glutaminyl cyclization / Cyclisation du glutaminyle N-terminal / Ciclación del glutaminilo N-terminal

Q> pyroglutamyl (pE, 5-oxoprolyl) / pyroglutamyle (pE, 5-oxoprolyle) / pirroglutamilo (pE, 5-oxoprolilo)

H VH Q1: 1"

N-glycosylation sites / Sites de N-glycosylation / Posiciones de N-glicosilación

H CH2 N84.4: 524, 302"

Fucosylated complex bi-antennary CHO-type glycans / glycanes de type CHO bi-antennaires complexes fucosylés / glicanos de tipo CHO biantenarios complejos fucosilados

C-terminal lysine clipping / Coupure de la lysine C-terminale / Recorte de lisina C-terminal

H CHS K2: 674, 452'

tivinectidum

tivinectide

$N^{6.5}$,$N^{6.5'}$-({12-[2-(2-{2-[3-oxo-3-({$S^{3.1}$,$S^{3.5}$,$S^{3.15}$-[(1,3,5-triazinane-1,3,5-triyl)tris(3-oxopropane-3,1-diyl)][L-cysteinyl-L-prolyl-3-(naphthalen-1-yl)-L-alanyl-L-α-aspartyl-L-cysteinyl-L-methionyl-N^6-carbamimidoyl-L-lysyl-L-α-aspartyl-L-tryptophyl-L-seryl-L-threonyl-L-prolyl-(4*R*)-4-hydroxy-L-prolyl-L-tryptophyl-L-cysteinamide]}-$N^{2.1}$-yl)propoxy]ethoxy}ethoxy)ethyl]-3,6,9,15,18,21-hexaoxa-12-azatricosane-1,23-diyl}bis[1*H*-1,2,3-triazole-1,4-diyl(1-oxopropane-3,1-diyl)])bis{$S^{3.1}$,$S^{3.8}$,$S^{3.15}$-[(1,3,5-triazinane-1,3,5-triyl)tris(3-oxopropane-3,1-diyl)][*N*-acetyl-L-cysteinyl-4-methyl-L-leucyl-L-prolyl-L-α-glutamyl-L-lysyl-L-prolyl-L-tyrosyl-L-cysteinyl-L-phenylalanyl-L-alanyl-L-α-aspartyl-L-prolyl-L-tyrosyl-(2*S*)-2-aminohexanoyl-L-cysteinyl-L-alaninamide]}

immunostimulant, antineoplastic

tivinectide

$N^{6.5}$,$N^{6.5'}$-({12-[2-(2-{2-[3-oxo-3-({$S^{3.1}$,$S^{3.5}$,$S^{3.15}$-[(1,3,5-triazinane-1,3,5-triyl)tris(3-oxopropane-3,1-diyl)][-L-cystéinyl-L-prolyl-3-(naphtalén-1-yl)-L-alanyl-L-α-aspartyl-L-cystéinyl-L-méthionyl-N^6-carbamimidoyl-L-lysyl-L-α-aspartyl-L-tryptophyl-L-séryl-L-thréonyl-L-prolyl-(4*R*)-4-hydroxy-L-prolyl-L-tryptophyl-L-cystéinamide]}-$N^{2.1}$-yl)propoxy]éthoxy}éthoxy)éthyl]-3,6,9,15,18,21-hexaoxa-12-azatricosane-1,23-diyl}bis[1*H*-1,2,3-triazole-1,4-diyl(1-oxopropane-3,1-diyl)])bis{$S^{3.1}$,$S^{3.8}$,$S^{3.15}$-[(1,3,5-triazinane-1,3,5-triyl)tris(3-oxopropane-3,1-diyl)][*N*-acétyl-L-cystéinyl-4-méthyl-L-leucyl-L-prolyl-L-α-glutamyl-L-lysyl-L-prolyl-L-tyrosyl-L-cystéinyl-L-phénylalanyl-L-alanyl-L-α-aspartyl-L-prolyl-L-tyrosyl-(2*S*)-2-aminohexanoyl-L-cystéinyl-L-alaninamide]}

immunostimulant, antinéoplasique

tivinectida

$N^{6.5}$,$N^{6.5'}$-({12-[2-(2-{2-[3-oxo-3-({$S^{3.1}$,$S^{3.5}$,$S^{3.15}$-[(1,3,5-triazinano-1,3,5-triil)tris(3-oxopropano-3,1-diil)][-L-cisteinil-L-prolil-3-(naftalen-1-il)-L-alanil-L-α-aspartil-L-cisteinil-L-metionil-N^6-carbamimidoil-L-lisil-L-α-aspartil-L-triptofil-L-seril-L-treonil-L-prolil-(4*R*)-4-hidroxi-L-prolil-L-triptofil-L-cisteinamida]}-$N^{2.1}$-il)propoxi]etoxi}etoxi)etil]-3,6,9,15,18,21-hexaoxa-12-azatricosano-1,23-diil}bis[1*H*-1,2,3-triazolo-1,4-diil(1-oxopropano-3,1-diil)])bis{$S^{3.1}$,$S^{3.8}$,$S^{3.15}$-[(1,3,5-triazinano-1,3,5-triil)tris(3-oxopropano-3,1-diil)][*N*-acetil-L-cisteinil-4-metil-L-leucil-L-prolil-L-α-glutamil-L-lisil-L-prolil-L-tirosil-L-cisteinil-L-fenilalanil-L-alanil-L-α-aspartil-L-prolil-L-tirosil-(2*S*)-2-aminohexanoil-L-cisteinil-L-alaninamida]}

inmunoestimulante, antineoplásico

$C_{331}H_{467}N_{73}O_{89}S_{10}$ 2762739-36-4

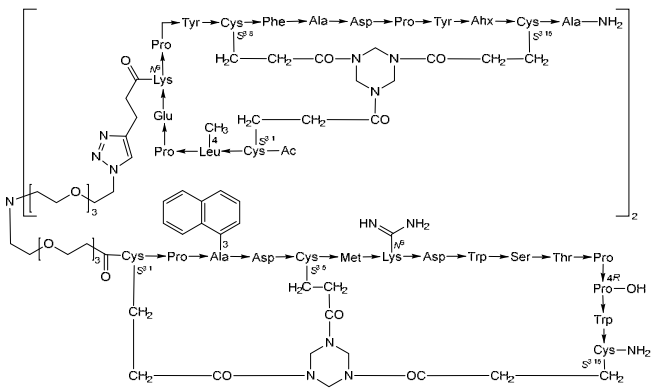

tivoxavirum marboxilum

tivoxavir marboxil

({(12a*R*)-12-[(10*S*)-6,7-difluoro-5,10-dihydrothieno[3,2-*c*][2]benzothiepin-10-yl]-6,8-dioxo-3,4,6,8,12,12a-hexahydro-1*H*-[1,4]oxazino[3,4-*c*]pyrido[2,1-*f*][1,2,4]triazin-7-yl}oxy)methyl methyl carbonate
antiviral

tivoxavir marboxil

carbonate de ({(12a*R*)-12-[(10*S*)-6,7-difluoro-5,10-dihydrothiéno[3,2-*c*][2]benzothiépin-10-yl]-6,8-dioxo-3,4,6,8,12,12a-hexahydro-1*H*-[1,4]oxazino[3,4-*c*]pyrido[2,1-*f*][1,2,4]triazin-7-yl}oxy)méthyle et de méthyle
antiviral

tivoxavir marboxilo

carbonato de ({(12a*R*)-12-[(10*S*)-6,7-difluoro-5,10-dihidrotieno[3,2-*c*][2]benzotiepin-10-il]-6,8-dioxo-3,4,6,8,12,12a-hexahidro-1*H*-[1,4]oxazino[3,4-*c*]pirido[2,1-*f*][1,2,4]triazin-7-il}oxi)metilo y metilo
antiviral

$C_{25}H_{21}F_2N_3O_7S_2$ 2417851-93-3

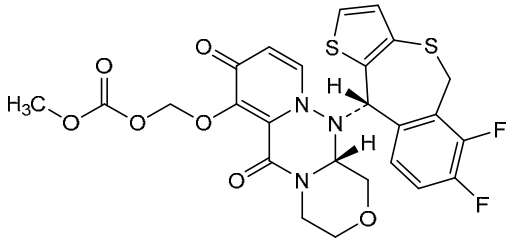

tixentamigum #

tixentamig

immunoglobulin (H-gamma1_L-kappa)_scFvhh-G1(h-CH2-CH3), anti-[*Homo sapiens* CD3E (CD3 epsilon, Leu-4)] and anti-[*Homo sapiens* CLDN18 (claudin 18, claudin-18, surfactant associated protein J, SFTPJ) isoform 2], monoclonal antibody, bispecific, trivalent;
H-gamma1 heavy chain anti-CD3E (1-455) [VH (*Homo sapiens* IGHV3-73*01 (92.0%) -(IGHD) -IGHJ6*01 (90.9%) T123>L (120), CDR-IMGT [8.10.16] (26-33.51-60.99-114))(1-125) -*Homo sapiens* IGHG1*03v, G1m3>G1m17, nG1m1 CH1 K120, CH3 E12, M14, 6-G1v14-1 CH2 A1.3, A1.2, A1, 14-G1v32 CH3 W22 (knob), 14-G1v74 CH3 C10 (CH1R120>K (222) (126-223), hinge 1-15 (224-238), CH2 L1.3>A (242), L1.2>A (243), G1>A (245) (239-348), CH3 S10>C (362), E12 (364), M14 (366), T22>W (374) (349-453), CHS (454-455)) (126-455)], (228-214')-disulfide with L-lambda2 light chain anti-CD3E (1'-215') [V-LAMBDA Musmus/Homsap (*Mus musculus* IGLV1*01 (81.2%) -IGLJ1*01 (100%)/*Homo sapiens* IGLV7-46*02 (80.0%) -IGLJ3*02 (100%), CDR-IMGT [9.3.9] (26'-34'.52'-54'.91'-99')) (1'-109') -*Homo sapiens* IGLC2*01 (100%) (C-LAMBDA2) (110'-215')];

	scFvhh-G1(h-CH2-CH3) heavy chain anti-CLDN18 (1"-491") [VH (*Homo sapiens* IGHV3-74*03 (94.9%) -(IGHD) -IGHJ1*01 (90.0%) W118>R (111"), L124>T (116"), CDR-IMGT [8.8.14] (26"-33".51"-58".97"-110")) (1"-121") -15-mer tris(tetraglycyl-seryl) linker (122"-136") -VH (*Homo sapiens* IGHV3-74*03 (94.9%) -IGHD -IGHJ1*01 (90.0%) W118>R (247"), L124>T (252"), CDR-IMGT [8.8.14] (162"-169".187"-194".233"-246")) (137"-257") -2-mer alanyl-seryl linker (258"-259") -*Homo sapiens* IGHG1*03v h-CH2-CH3-CHS, G1m3>G1m17, nG1m1 CH3 E12, M14, 15-G1v37 hinge S5, 6-G1v14-1 CH2 A1.3, A1.2, A1, 14-G1v33 CH3 S22, A24, V86 (hole), 14-G1v75 CH3 C5 (hinge 1-15 C5>S (264") (260"-274"), CH2 L1.3>A (278), L1.2>A (279), G1>A (281) (275"-384"), CH3 Y5>C (393"), E12 (400), M14 (402), T22>S (410"), L24>A (412"), Y86>V (451") (385"-489"), CHS (490"-491")) (260"-491")]; dimer (234-270":237-273")-bisdisulfide, produced in a cell line from Chinese hamster ovary (CHO) cells, derived from the cell line CHO-K1, glycoform alfa *antineoplastic*
tixentamig	immunoglobuline (H-gamma1_L-kappa)_scFvhh-G1(h-CH2-CH3), anti-[*Homo sapiens* CD3E (CD3 epsilon, Leu-4)] and anti-[*Homo sapiens* CLDN18 (claudine 18, claudine-18, protéine J associée au surfactant, SFTPJ) isoforme 2], anticorps monoclonal, bispécifique, trivalent; chaîne lourde H-gamma1 anti-CD3E (1-455) [VH (*Homo sapiens* IGHV3-73*01 (92.0%) -(IGHD) -IGHJ6*01 (90.9%) T123>L (120), CDR-IMGT [8.10.16] (26-33.51-60.99-114)) (1-125) -*Homo sapiens* IGHG1*03v, G1m3>G1m17, nG1m1 CH1 K120, CH3 E12, M14, 6-G1v14-1 CH2 A1.3, A1.2, A1, 14-G1v32 CH3 W22 (knob), 14-G1v74 CH3 C10 (CH1R120>K (222) (126-223), charnière 1-15 (224-238), CH2 L1.3>A (242), L1.2>A (243), G1>A (245) (239-348), CH3 S10>C (362), E12 (364), M14 (366), T22>W (374) (349-453), CHS (454-455)) (126-455)], (228-214')-bisdisulfure avec la chaine légère L-lambda2 anti-CD3E (1'-215') [V-LAMBDA Musmus/Homsap (*Mus musculus* IGLV1*01 (81.2%) -IGLJ1*01 (100%)/*Homo sapiens* IGLV7-46*02 (80.0%) -IGLJ3*02 (100%), CDR-IMGT [9.3.9] (26'-34'.52'-54'.91'-99')) (1'-109') -*Homo sapiens* IGLC2*01 (100%) (C-LAMBDA2) (110'-215')]; chaîne lourde scFvhh-G1(h-CH2-CH3) anti-CLDN18 (1"-491") [VH (*Homo sapiens* IGHV3-74*03 (94.9%) -(IGHD) -IGHJ1*01 (90.0%) W118>R (111"), L124>T (116"), CDR-IMGT [8.8.14] (26"-33".51"-58".97"-110")) (1"-121") -15-mer tris(tétraglycyl-séryl) linker (122"-136") -VH (*Homo*

	sapiens IGHV3-74*03 (94.9%) -IGHD -IGHJ1*01 (90.0%) W118>R (247"), L124>T (252"), CDR-IMGT [8.8.14] (162"-169".187"-194".233"-246")) (137"-257") -2-mer alanyl-séryl linker (258"-259") -*Homo sapiens* IGHG1*03v h-CH2-CH3-CHS, G1m3>G1m17, nG1m1 CH3 E12, M14, 15-G1v37 charnière S5, 6-G1v14-1 CH2 A1.3, A1.2, A1, 14-G1v33 CH3 S22, A24, V86 (hole), 14-G1v75 CH3 C5 (charnière 1-15 C5>S (264") (260"-274"), CH2 L1.3>A (278), L1.2>A (279), G1>A (281) (275"-384"), CH3 Y5>C (393"), E12 (400), M14 (402), T22>S (410"), L24>A (412"), Y86>V (451") (385"-489"), CHS (490"-491")) (260"-491")]; dimère (234-270":237-273")-bisdisulfure, produit dans une lignée cellulaire des cellules ovariennes de hamster chinois (CHO), dérivant de la lignée cellulaire CHO-K1, glycoforme alfa *antinéoplasique*
tixentamig	inmunoglobulina (H-gamma1_L-kappa)_scFvhh-G1(h-CH2-CH3), anti-[*Homo sapiens* CD3E (CD3 épsilon, Leu-4)] y anti-[*Homo sapiens* CLDN18 (claudina 18, claudina-18, proteína J asociada a los surfactantes, SFTPJ) isoforma 2], anticuerpo monoclonal, biespecífico, trivalente; cadena pesada H-gamma1 anti-CD3E (1-455) [VH (*Homo sapiens* IGHV3-73*01 (92.0%) -(IGHD) -IGHJ6*01 (90.9%) T123>L (120), CDR-IMGT [8.10.16] (26-33.51-60.99-114)) (1-125) -*Homo sapiens* IGHG1*03v, G1m3>G1m17, nG1m1 CH1 K120, CH3 E12, M14, 6-G1v14-1 CH2 A1.3, A1.2, A1, 14-G1v32 CH3 W22 (knob), 14-G1v74 CH3 C10 (CH1R120>K (222) (126-223), bisagra 1-15 (224-238), CH2 L1.3>A (242), L1.2>A (243), G1>A (245) (239-348), CH3 S10>C (362), E12 (364), M14 (366), T22>W (374) (349-453), CHS (454-455)) (126-455)], (228-214')-bisdisulfuro con la cadena ligera L-lambda2 anti-CD3E (1'-215') [V-LAMBDA Musmus/Homsap (*Mus musculus* IGLV1*01 (81.2%) -IGLJ1*01 (100%)/*Homo sapiens* IGLV7-46*02 (80.0%) -IGLJ3*02 (100%), CDR-IMGT [9.3.9] (26'-34'.52'-54'.91'-99')) (1'-109') -*Homo sapiens* IGLC2*01 (100%) (C-LAMBDA2) (110'-215')]; cadena pesada scFvhh-G1(h-CH2-CH3) anti-CLDN18 (1"-491") [VH (*Homo sapiens* IGHV3-74*03 (94.9%) -(IGHD) -IGHJ1*01 (90.0%) W118>R (111"), L124>T (116"), CDR-IMGT [8.8.14] (26"-33".51"-58".97"-110")) (1"-121") -15-mer tris(tetraglicil-seril) enlace (122"-136") -VH (*Homo sapiens* IGHV3-74*03 (94.9%) -IGHD -IGHJ1*01 (90.0%) W118>R (247"), L124>T (252"), CDR-IMGT [8.8.14] (162"-169".187"-194".233"-246")) (137"-257") -2-mer alanyl-séryl linker (258"-259") -*Homo sapiens* IGHG1*03v h-CH2-CH3-CHS, G1m3>G1m17, nG1m1 CH3 E12, M14, 15-G1v37 bisagra S5, 6-G1v14-1 CH2 A1.3, A1.2, A1, 14-G1v33 CH3 S22, A24, V86 (hole), 14-G1v75 CH3 C5 (bisagra 1-15 C5>S (264") (260"-274"), CH2 L1.3>A (278), L1.2>A (279), G1>A (281) (275"-384"), CH3 Y5>C (393"), E12 (400), M14 (402), T22>S (410"), L24>A (412"), Y86>V (451") (385"-489"), CHS (490"-491")) (260"-491")]; dímero (234-270":237-273")-bisdisulfuro, producido en una línea celular de las células ováricas de hámster chino (CHO), línea celular derivada de CHO-K1, forma glicosilada alfa *antineoplásico*

2969220-04-8

Heavy chain / Chaîne lourde / Cadena pesada : 11-gamma1 anti-CD3E (knob) (H)

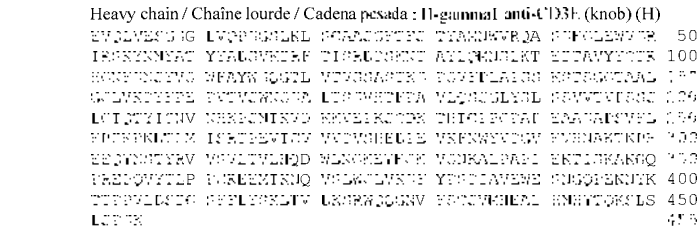

Light chain / Chaîne légère / Cadena ligera : L-lambda2 anti-CD3E (L')

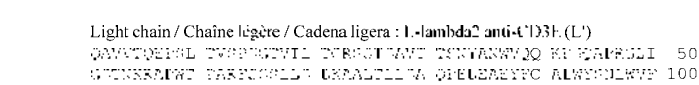

Heavy chain / Chaîne lourde / Cadena pesada : scFvhh-G1(h-CH2-CH3) anti-CLDN18 (hole) (H")

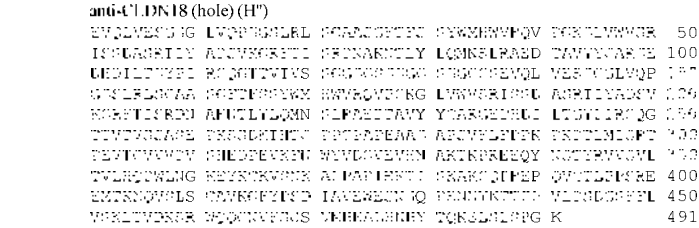

Post-translational modifications

Disulfide bridges location / Position des ponts disulfure / Posiciones de los puentes disulfuro

Intra-H (C23-C104) 22-98 152-208 269-329 375-433
22"-96" 158"-232" 305"-365" 411"-469"
Intra-L (C23-C104) 22'-90' 137'-196'
Inter-H-L (h 5-CL 126) 228-214'
Inter-H-H (h 11, h 14) 234-270" 237-273"
Inter-H-H (CH3 C10-C5)* 362-393"
*variants 14-G1v74 (H CH3 C10) and 14-G1v75 (H" CH3 C5) creating an additional inter-H-H disulfide bond.

N-terminal glutaminyl cyclization / Cyclisation du glutaminyle N-terminal / Ciclación del glutaminilo N-terminal
Q > pyroglutamyl (pE, 5-oxoprolyl) / pyroglutamyle (pE, 5-oxoprolyle) / piroglutamilo (pE, 5-oxoprolilo)
L VL V-LAMBDA Q1: 1'

N-glycosylation sites / Sites de N-glycosylation / Posiciones de N-glicosilación
H CH2 N84.4: 305, 341"
Fucosylated complex bi-antennary CHO-type glycans / glycanes de type CHO bi-antennaires complexes fucosylés / glicanos de tipo CHO biantenarios complejos fucosilados.

C-terminal lysine clipping / Coupure de la lysine C-terminale / Recorte de lisina C-terminal
H CHS K2: 455, 491"

tixestobartum #

tixestobart — immunoglobulin G1-lambda2, anti-[*Homo sapiens* CD27 (TNFRSF7, tumor necrosis factor receptor (TNFR) superfamily member 7)], *Homo sapiens* monoclonal antibody;

	H-gamma1 heavy chain *Homo sapiens* (1-445) [VH (*Homo sapiens* IGHV7-4-1*02 (91.8%) -(IGHD) - IGHJ4*01 (100%), CDR-IMGT [8.8.9] (26-33.51-58.97-105)) (1-116) -*Homo sapiens* IGHG1*03, G1m3, nG1m1 CH1 R120, CH3 E12, M14, 6-G1v4-2 CH2 R114, 10-G1v98 CH3 R1 (CH1 R120 (213) (117-214), hinge 1-15 (215-229), CH2 P114>R (328) (230-339), CH3 E1>R (344), E12 (355), M14 (357) (340-444), CHS K2>del (445)) (117-445)], (219-215')-disulfide with L-lambda2 light chain *Homo sapiens* (1'-216') [V-LAMBDA (*Homo sapiens* IGLV2-14*03 (94.7%) -IGLJ3*02 (100%), CDR-IMGT [9.3.10] (26'-34'.52'-54'.91'-100')) (1'-110') -*Homo sapiens* IGLC2*01 (100%) (C-LAMBDA2) (111'-216')]; dimer (225-225'':228-228'')-bisdisulfide, produced in Chinese hamster ovary (CHO) cells, glycoform alfa *immunostimulant, antineoplastic*
tixestobart	immunoglobuline G1-lambda2, anti-[*Homo sapiens* CD27 (TNFRSF7, membre 7 de la superfamille des récepteurs du facteur de nécrose tumorale (TNFR))], anticorps monoclonal *Homo sapiens*; chaîne lourde H-gamma1 *Homo sapiens* (1-445) [VH (*Homo sapiens* IGHV7-4-1*02 (91.8%) -(IGHD) - IGHJ4*01 (100%), CDR-IMGT [8.8.9] (26-33.51-58.97-105)) (1-116) -*Homo sapiens* IGHG1*03, G1m3, nG1m1 CH1 R120, CH3 E12, M14, 6-G1v4-2 CH2 R114, 10-G1v98 CH3 R1 (CH1 R120 (213) (117-214), charnière 1-15 (215-229), CH2 P114>R (328) (230-339), CH3 E1>R (344), E12 (355), M14 (357) (340-444), CHS K2>del (445)) (117-445)], (219-215')-disulfure avec la chaîne légère L-lambda2 *Homo sapiens* (1'-216') [V-LAMBDA (*Homo sapiens* IGLV2-14*03 (94.7%) -IGLJ3*02 (100%), CDR-IMGT [9.3.10] (26'-34'.52'-54'.91'-100')) (1'-110') -*Homo sapiens* IGLC2*01 (100%) (C-LAMBDA2) (111'-216')]; dimère (225-225'':228-228'')-bisdisulfure, produit dans des cellules ovariennes de hamster chinois (CHO), glycoforme alfa *immunostimulant, antinéoplasique*
tixestobart	inmunoglobulina G1-lambda2, anti-[*Homo sapiens* CD27 (TNFRSF7, miembro 7 de la superfamilia de los receptores del factor de necrosis tumoral (TNFR))], anticuerpo monoclonal *Homo sapiens*; cadena pesada H-gamma1 *Homo sapiens* (1-445) [VH (*Homo sapiens* IGHV7-4-1*02 (91.8%) -(IGHD) - IGHJ4*01 (100%), CDR-IMGT [8.8.9] (26-33.51-58.97-105)) (1-116) -*Homo sapiens* IGHG1*03, G1m3, nG1m1 CH1 R120, CH3 E12, M14, 6-G1v4-2 CH2 R114, 10-G1v98 CH3 R1 (CH1 R120 (213) (117-214), bisagra 1-15 (215-229), CH2 P114>R (328) (230-339), CH3 E1>R (344), E12 (355), M14 (357) (340-444), CHS K2>del (445)) (117-445)], (219-215')-disulfuro con la cadena ligera L-lambda2 *Homo sapiens* (1'-216') [V-LAMBDA (*Homo sapiens* IGLV2-14*03 (94.7%) -IGLJ3*02 (100%), CDR-IMGT [9.3.10] (26'-34'.52'-54'.91'-100')) (1'-110') -*Homo sapiens* IGLC2*01 (100%) (C-LAMBDA2) (111'-216')]; dímero (225-225'':228-228'')-bisdisulfuro, producido en las células ováricas de hámster chino (CHO), forma glicosilada alfa *inmunoestimulante, antineoplásico*

2733575-82-9

Heavy chain / Chaîne lourde / Cadena pesada

```
QVQLMQSGSE LKKPGASVKV SCRASGYTFT TYAMNWVRQA PGQGPEWMGW  50
INTNTGNPTY AQGFTGRFVF SLDTTVTTTY LQISSLKAED TAVYFCAREA 100
GSFDYWGQGT LVTVSSASTK GPSVFPLAPS SKSTSGGTAA LGCLVKDYFP 150
EPVTVSWNSG ALTSGVHTFP AVLQSSGLYS LSSVVTVPSS SLGTQTYICN 200
VNHKPSNTKV DKRVEPKSCD KTHTCPPCPA PELLGGPSVF LFPPKPKDTL 250
MISRTPEVTC VVVDVSHEDP EVKFNWYVDG VEVHNAKTKP REEQYNSTYR 300
VVSVLTVLHQ DWLNGKEYKC KVSNKALRAP IEKTISKAKG QPRRPQVYTL 350
PPSREEMTKN QVSLTCLVKG FYPSDIAVEW ESNGQPENNY KTTPPVLDSD 400
GSFFLYSKLT VDKSRWQQGN VFSCSVMHEA LHNHYTQKSL SLSPG      445
```

Light chain / Chaîne légère / Cadena ligera

```
QSALTQPASV SGSPGQSITI SCTGTSSDVY YYNYVSWYQQ HPGRAPKLVI  50
YDVSNRPSGV SNRFSGSKSG NTASLTISGL RAEDEADYYC SSYTVNRVWV 100
FGGGTKLTVL GQPKAAPSVT LFPPSSEELQ ANKATLVCLI SDFYPGAVTV 150
AWKADSSPVK AGVETTTPSK QSNNKYAASS YLSLTPEQWK SHRSYSCQVT 200
HEGSTVEKTV APTECS                                      216
```

Post-translational modifications

Disulfide bridges location / Position des ponts disulfure / Posiciones de los puentes disulfuro

Intra-H (C23-C104) 22-96 143-199 260-320 366-424
22"-96" 143"-199" 260"-320" 366"-424"
Intra-L (C23-C104) 22'-90' 138'-197'
22'"-90'" 138'"-197'"
Inter-H-L (h 5-CL 126) 219-215' 219"-215'"
Inter-H-H (h 11, h 14) 225-225" 228-228"

N-terminal glutaminyl cyclization / Cyclisation du glutaminyle N-terminal / Ciclación del glutaminilo N-terminal

Q > pyroglutamyl (pE, 5-oxoprolyl) / pyroglutamyle (pE, 5-oxoprolyle) / piroglutamilo (pE, 5-oxoprolilo)
H VH Q1: 1, 1"
L VL V-LAMBDA Q1: 1', 1'"

N-glycosylation sites / Sites de N-glycosylation / Posiciones de N-glicosilación

H CH2 N84.4: 296, 296"

Fucosylated complex bi-antennary CHO-type glycans / glycanes de type CHO bi-antennaires complexes fucosylés / glicanos de tipo CHO biantenarios complejos fucosilados

tofacitinibum etocomilum

tofacitinib etocomil — (4-{[(3*R*,4*R*)-1-(cyanoacetyl)-4-methylpiperidin-3-yl](methyl)amino}-7*H*-pyrrolo[2,3-*d*]pyrimidin-7-yl)methyl (4*RS*)-4-ethyloctanoate
Janus tyrosine kinase inhibitor, anti-inflammatory

tofacitinib étocomil — (4*RS*)-4-éthyloctanoate de (4-{[(3*R*,4*R*)-1-(cyanoacétyl)-4-méthylpipéridin-3-yl](méthyl)amino}-7*H*-pyrrolo[2,3-*d*]pyrimidin-7-yl)méthyle
inhibiteur de la tyrosine kinase Janus, anti-inflammatoire

tofacitinib etocomilo — (4*RS*)-4-etiloctanoato de (4-{[(3*R*,4*R*)-1-(cianoacetil)-4-metilpiperidin-3-il](metil)amino}-7*H*-pirrolo[2,3-*d*]pirimidin-7-il)metilo
inhibidor de la tirosina kinasa Janus, antiinflamatorio

$C_{27}H_{40}N_6O_3$ 2812383-82-5

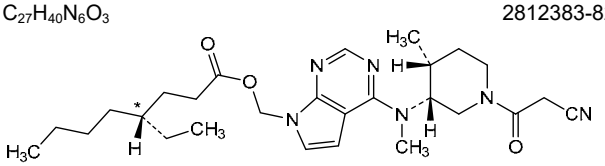

and epimer at C*
et l'épimère en C*
y el epímero en C*

torvutatugum #

torvutatug	immunoglobulin G1-kappa, anti-[*Homo sapiens* FOLR1 (folate receptor 1, folate receptor alpha, FR-alpha, adult folate-binding protein, FBP, ovarian tumor-associated antigen MOv18)], *Homo sapiens* monoclonal antibody; H-gamma1 heavy chain *Homo sapiens* (1-449) [VH (*Homo sapiens* IGHV6-1*01 (98.0%) -(IGHD) -IGHJ4*01 (100%), CDR-IMGT [10.9.9] (26-35.53-61.100-108)) (1-119) -*Homo sapiens* IGHG1*03 (100%) G1m3, nG1m1 CH1 R120, CH3 E12, M14 (CH1 R120 (216) (120-217), hinge 1-15 (218-232), CH2 (233-342), CH3 E12 (358), M14 (360) (343-447), CHS (448-449)) (120-449)], (222-215')-disulfide with L-kappa light chain *Homo sapiens* (1'-215') [V-KAPPA (*Homo sapiens* IGKV1-5*03 (98.9%) -IGKJ4*01 (100%), CDR-IMGT [6.3.10] (27'-32'.50'-52'.89'-98')) (1'-108') -*Homo sapiens* IGKC*01 (100%) Km3 A45.1, V101 (C-KAPPA A45.1 (154'), V101 (192')) (109'-215')]; dimer (228-228":231-231")-bisdisulfide, produced in a cell line from Chinese hamster ovary (CHO) cells, derived from the cell line CHO-K1, glycoform alfa *antineoplastic*
torvutatug	immunoglobuline G1-kappa, anti-[*Homo sapiens* FOLR1 (récepteur 1 du folate, récepteur alpha du folate, FR-alpha, protéine de l'adulte liant le folate, FBP, antigène MOv18 associé à des tumeurs ovariennes)], anticorps monoclonal *Homo sapiens*; chaîne lourde H-gamma1 *Homo sapiens* (1-449) [VH (*Homo sapiens* IGHV6-1*01 (98.0%) -(IGHD) -IGHJ4*01 (100%), CDR-IMGT [10.9.9] (26-35.53-61.100-108)) (1-119) -*Homo sapiens* IGHG1*03 (100%) G1m3, nG1m1 CH1 R120, CH3 E12, M14 (CH1 R120 (216) (120-217), charnière 1-15 (218-232), CH2 (233-342), CH3 E12 (358), M14 (360) (343-447), CHS (448-449)) (120-449)], (222-215')-disulfure avec la chaîne légère L-kappa *Homo sapiens* (1'-215') [V-KAPPA (*Homo sapiens* IGKV1-5*03 (98.9%) -IGKJ4*01 (100%), CDR-IMGT [6.3.10] (27'-32'.50'-52'.89'-98')) (1'-108') -*Homo sapiens* IGKC*01 (100%) Km3 A45.1, V101 (C-KAPPA A45.1 (154'), V101 (192')) (109'-215')]; dimère (228-228":231-231")-bisdisulfure, produit dans une lignée cellulaire des cellules ovariennes de hamster chinois (CHO), dérivant de la lignée cellulaire CHO-K1, glycoforme alfa *antinéoplasique*
torvutatug	inmunoglobulina G1-kappa, anti-[*Homo sapiens* FOLR1 (receptor 1 del folato, receptor alfa del folato, FR-alfa, proteína adulta fijadora de folato, FBP, antígeno MOv18 asociado a los tumores ováricos)], anticuerpo monoclonal *Homo sapiens*; cadena pesada H-gamma1 *Homo sapiens* (1-449) [VH (*Homo sapiens* IGHV6-1*01 (98.0%) -(IGHD) -IGHJ4*01 (100%), CDR-IMGT [10.9.9] (26-35.53-61.100-108)) (1-119) -*Homo sapiens* IGHG1*03 (100%) G1m3, nG1m1 CH1 R120, CH3 E12, M14 (CH1 R120 (216) (120-217), bisagra 1-15 (218-232), CH2 (233-342), CH3 E12 (358), M14 (360) (343-447), CHS (448-449)) (120-449)], (222-215')-disulfuro con la cadena ligera L-kappa *Homo sapiens* (1'-215') [V-KAPPA (*Homo sapiens* IGKV1-5*03 (98.9%) -IGKJ4*01 (100%), CDR-IMGT [6.3.10] (27'-32'.50'-52'.89'-98')) (1'-108') -*Homo sapiens* IGKC*01 (100%) Km3 A45.1, V101 (C-KAPPA A45.1 (154'), V101 (192')) (109'-215')]; dímero (228-228":231-231")-bisdisulfuro, producido en una línea celular de las células ováricas de hámster chino (CHO), línea celular derivada de CHO-K1, forma glicosilada alfa *antineoplásico*

2975630-15-8

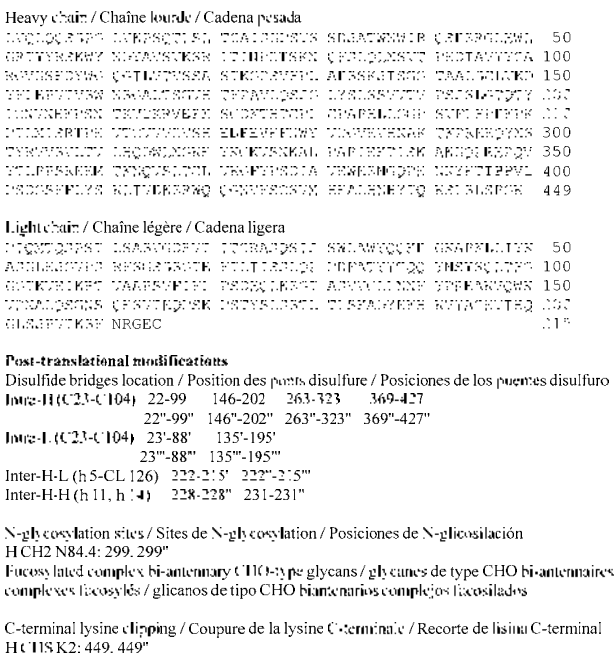

torvutatugum samrotecanum #

torvutatug samrotecan	immunoglobulin G1-kappa, anti-[*Homo sapiens* FOLR1 (folate receptor 1, folate receptor alpha, FR-alpha, adult folate-binding protein, FBP, ovarian tumor-associated antigen MOv18)], *Homo sapiens* monoclonal antibody; conjugated on eight cysteinyl residues to *samrotecan*, comprising a linker and a camptothecin derivative (*exatecan*); H-gamma1 heavy chain *Homo sapiens* (1-449) [VH (*Homo sapiens* IGHV6-1*01 (98.0%) -(IGHD) -IGHJ4*01 (100%), CDR-IMGT [10.9.9] (26-35.53-61.100-108)) (1-119) -*Homo sapiens* IGHG1*03 (100%) G1m3, nG1m1 CH1 R120, CH3 E12, M14 (CH1 R120 (216) (120-217), hinge 1-15 (218-232), CH2 (233-342), CH3 E12 (358), M14 (360) (343-447), CHS (448-449)) (120-449)], (222-215')-disulfide with L-kappa light chain *Homo sapiens* (1'-215') [V-KAPPA (*Homo sapiens* IGKV1-5*03 (98.9%) -IGKJ4*01 (100%), CDR-IMGT [6.3.10] (27'-32'.50'-52'.89'-98')) (1'-108') -*Homo sapiens* IGKC*01 (100%) Km3 A45.1, V101 (C-KAPPA A45.1 (154'), V101 (192')) (109'-215')]; dimer (228-228":231-231")-bisdisulfide, produced in a cell line from Chinese hamster ovary (CHO) cells, derived from the cell line CHO-K1, glycoform alfa; substituted at the eight sulfur atoms of L-cysteinyl residues 222, 228, 231, 215', 222", 228", 231" and 215'" with (3*RS*)-1-[(2*S*,5*S*)-1-{[(9*S*)-9-ethyl-9-hydroxy-10,13-dioxo-2,3,9,10,13,15-hexahydro-1*H*,12*H*-benzo[*de*]pyrano[3',4':6,7]indolizino[1,2-*b*]quinolin-4-yl]amino}-2-methyl-1,4,7,35-tetraoxo-5-(propan-2-yl)-10,13,16,19,22,25,28,31-octaoxa-3,6,34-triazaheptatriacontan-37-yl]-2,5-dioxopyrrolidin-3-yl (*samrotecan*) groups *antineoplastic*

torvutatug samrotécan	immunoglobuline G1-kappa, anti-[*Homo sapiens* FOLR1 (récepteur 1 du folate, récepteur alpha du folate, FR-alpha, protéine de l'adulte liant le folate, FBP, antigène MOv18 associé à des tumeurs ovariennes)], anticorps monoclonal *Homo sapiens*; conjugué par huit résidus cystéinyle au *samrotécan*, comprenant un linker et un dérivé de la camptothécine (*exatécan*); chaîne lourde H-gamma1 *Homo sapiens* (1-449) [VH (*Homo sapiens* IGHV6-1*01 (98.0%) -(IGHD) -IGHJ4*01 (100%), CDR-IMGT [10.9.9] (26-35.53-61.100-108)) (1-119) -*Homo sapiens* IGHG1*03 (100%) G1m3, nG1m1 CH1 R120, CH3 E12, M14 (CH1 R120 (216) (120-217), charnière 1-15 (218-232), CH2 (233-342), CH3 E12 (358), M14 (360) (343-447), CHS (448-449)) (120-449)], (222-215')-disulfure avec la chaîne légère L-kappa *Homo sapiens* (1'-215') [V-KAPPA (*Homo sapiens* IGKV1-5*03 (98.9%) -IGKJ4*01 (100%), CDR-IMGT [6.3.10] (27'-32'.50'-52'.89'-98')) (1'-108') -*Homo sapiens* IGKC*01 (100%) Km3 A45.1, V101 (C-KAPPA A45.1 (154'), V101 (192')) (109'-215')]; dimère (228-228'':231-231'')-bisdisulfure, produit dans une lignée cellulaire des cellules ovariennes de hamster chinois (CHO), dérivant de la lignée cellulaire CHO-K1, glycoforme alfa; substitué sur l'atome de soufre des résidus L-cystéinyle 222, 228, 231, 215', 222'', 228'', 231'' et 215''' avec des groupes (3*RS*)-1-[(2*S*,5*S*)-1-{[(9*S*)-9-éthyl-9-hydroxy-10,13-dioxo-2,3,9,10,13,15-hexahydro-1*H*,12*H*-benzo[*de*]pyrano[3',4':6,7]indolizino[1,2-*b*]quinoléin-4-yl]amino}-2-méthyl-1,4,7,35-tétraoxo-5-(propan-2-yl)-10,13,16,19,22,25,28,31-octaoxa-3,6,34-triazaheptatriacontan-37-yl]-2,5-dioxopyrrolidin-3-yle (*samrotécan*) *antinéoplasique*
torvutatug samrotecán	inmunoglobulina G1-kappa, anti-[*Homo sapiens* FOLR1 (receptor 1 del folato, receptor alfa del folato, FR-alfa, proteína adulta fijadora de folato, FBP, antígeno MOv18 asociado a los tumores ováricos)], anticuerpo monoclonal *Homo sapiens*, conjugué par ocho résidus cystéinyle au *samrotécan*, que comprende un enlace y un derivado de la camptotecina (*exatecán*); cadena pesada H-gamma1 *Homo sapiens* (1-449) [VH (*Homo sapiens* IGHV6-1*01 (98.0%) -(IGHD) -IGHJ4*01 (100%), CDR-IMGT [10.9.9] (26-35.53-61.100-108)) (1-119) -*Homo sapiens* IGHG1*03 (100%) G1m3, nG1m1 CH1 R120, CH3 E12, M14 (CH1 R120 (216) (120-217), bisagra 1-15 (218-232), CH2 (233-342), CH3 E12 (358), M14 (360) (343-447), CHS (448-449)) (120-449)], (222-215')-disulfuro con la cadena ligera L-kappa *Homo sapiens* (1'-215') [V-KAPPA (*Homo sapiens* IGKV1-5*03 (98.9%) -IGKJ4*01 (100%), CDR-IMGT [6.3.10] (27'-32'.50'-52'.89'-98')) (1'-108') -*Homo sapiens* IGKC*01 (100%) Km3 A45.1, V101 (C-KAPPA A45.1 (154'), V101 (192')) (109'-215')]; dímero (228-228'':231-231'')-bisdisulfuro, producido en una línea celular de las células ováricas de hámster chino (CHO), línea celular derivada de CHO-K1, forma glicosilada alfa; sustituido en el átomo de azufre de los residuos L-cisteinilo 222, 228, 231, 215', 222'', 228'', 231'' y 215'' con grupos (3*RS*)-1-[(2*S*,5*S*)-1-{[(9*S*)-9-etil-9-hidroxi-10,13-dioxo-2,3,9,10,13,15-hexahidro-1*H*,12*H*-benzo[*de*]pirano[3',4':6,7]indolizino[1,2-*b*]quinolein-4-il]amino}-2-metil-1,4,7,35-tetraoxo-5-(propan-2-il)-10,13,16,19,22,25,28,31-octaoxa-3,6,34-triazaheptatriacontan-37-il]-2,5-dioxopirrolidin-3-ilo (*samrotecán*) *antineoplásico*

2975630-26-1

Heavy chain / Chaîne lourde / Cadena pesada (H, H")

```
LVQLQQSGPG LVKPSQTLSL TCAISGDSVS SDSATWNWIR QSPSRGLEWL  50
GRTYYRSKWY NDYAVSVKSR ITINPDTSKN QFSLQLNSVT PEDTAVYYCA 100
RGVGSFDYWG QGTLVTVSSA STKGPSVFPL APSSKSTSGG TAALGCLVKD 150
YFPEPVTVSW NSGALTSGVH TFPAVLQSSG LYSLSSVVTV PSSSLGTQTY 200
ICNVNHKPSN TKVDKRVEPK SCDKTHTCPP CPAPELLGGP SVFLFPPKPK 250
DTLMISRTPE VTCVVVDVSH EDPEVKFNWY VDGVEVHNAK TKPREEQYNS 300
TYRVVSVLTV LHQDWLNGKE YKCKVSNKAL PAPIEKTISK AKGQPREPQV 350
YTLPPSREEM TKNQVSLTCL VKGFYPSDIA VEWESNGQPE NNYKTTPPVL 400
DSDGSFFLYS KLTVDKSRWQ QGNVFSCSVM HEALHNHYTQ KSLSLSPGK  449
```

Light chain / Chaîne légère / Cadena ligera (L', L'")

```
DIQMTQSPST LSASVGDRVT ITCRASQSIS SWLAWYQQKP GKAPKLLIYK  50
ASGLESGVPS RFSGSGSGTE FTLTISSLQP DDFATYYCQQ YNSYSQLTFG 100
GGTKVEIKRT VAAPSVFIFP PSDEQLKSGT ASVVCLLNNF YPREAKVQWK 150
VDNALQSGNS QESVTEQDSK DSTYSLSSTL TLSKADYEKH KVYACEVTHQ 200
GLSSPVTKSF NRGEC                                       215
```

Post-translational modifications

Disulfide bridges location / Position des ponts disulfure / Posiciones de los puentes disulfuro

Intra-H (C23-C104) 22-99 146-202 263-323 369-427
22"-99" 146"-202" 263"-323" 369"-427"
Intra-L (C23-C104) 23'-88' 135'-195'
23'"-88'" 135'"-195'"
Inter-H-L (h 5-CL 126)* 222-215' 222"-215'"
Inter-H-H (h 11, h 14)* 228-228" 231-231"

*The inter-chain disulfide bridges are not present, the 8 cysteinyl being conjugated each via a thioether bond to a drug linker.

*Les ponts disulfures inter-chaînes ne sont pas présents, les 8 cystéinyl étant chacun conjugué via une liaison thioéther à un linker-principe actif.

*Los puentes disulfuro entre cadenas no están presentes, cada uno de los 8 cisteinil está conjugada a través de un enlace tioéter a un linker-principio activo.

N-glycosylation sites / Sites de N-glycosylation / Posiciones de N-glicosilación
H CH2 N84.4: 299, 299"
Fucosylated complex bi-antennary CHO-type glycans / glycanes de type CHO bi-antennaires complexes fucosylés / glicanos de tipo CHO biantenarios complejos fucosilados

C-terminal lysine clipping / Coupure de la lysine C-terminale / Recorte de lisina C-terminal
H CHS K2: 449, 449"

Modified residues / Résidus modifiés / Restos modificados*
C (222, 228, 231, 215', 222", 228", 231", 215'")
*(*samrotecan*:mAb 8:1)

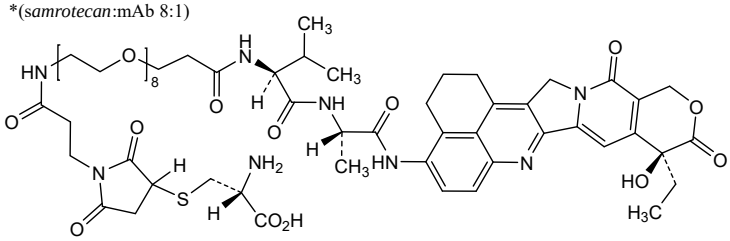

tosposertibum

tosposertib — 6-[2-(6-methylpyridin-2-yl)-5,6-dihydro-1*H*-imidazo[1,2-*a*]imidazol-3-yl][1,2,4]triazolo[1,5-*a*]pyridine

serine/threonine kinase inhibitor, antifibrotic

tosposertib

6-[2-(6-méthylpyridin-2-yl)-5,6-dihydro-1*H*-imidazo[1,2-a]imidazol-3-yl][1,2,4]triazolo[1,5-a]pyridine
inhibiteur de sérine/thréonine kinases, antifibrotique

tosposertib

6-[2-(6-metilpiridin-2-il)-5,6-dihidro-1*H*-imidazo[1,2-a]imidazol-3-il][1,2,4]triazolo[1,5-a]piridina
inhibidor de la serina/treonina kinasa, antifibrótico

$C_{17}H_{15}N_7$ 1418305-55-1

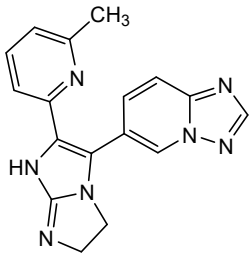

trovostobartum #

trovostobart

immunoglobulin G1-kappa, anti-[*Homo sapiens* VSIR (V-set immunoregulatory receptor, B7H5, B7-H5, PDCD1 homolog, PD-1H, stress induced secreted protein 1, SISP1, V-domain Ig suppressor of T cell activation, VISTA)], *Homo sapiens* monoclonal antibody;
H-gamma1 heavy chain *Homo sapiens* (1-447) [VH (*Homo sapiens* IGHV4-59*01 (99.0%) -(IGHD) -IGHJ3*02 (93.3%) T125>I (114), CDR-IMGT [8.7.11] (26-33.51-57.96-106)) (1-117) -*Homo sapiens* IGHG1*01, G1m17,1 CH1 K120, CH3 D12, L14, 9-G1v21 CH2 Y15.1, T16, E18 (CH1 K120 (214) (118-215), hinge 1-15 (216-230), CH2 M15.1>Y (252), S16>T (254), T18>E (256) (231-340), CH3 D12 (356), L14 (358) (341-445), CHS (446-447)) (118-447)], (220-214')-disulfide with L-kappa light chain *Homo sapiens* (1'-214') [V-KAPPA (*Homo sapiens* IGKV3-11*01 (96.8%) -IGKJ4*01 (100%), CDR-IMGT [6.3.9] (27'-32'.50'-52'.89'-97')) (1'-107') -*Homo sapiens* IGKC*01 (100%) Km3 A45.1, V101 (C-KAPPA A45.1 (153'), V101 (191')) (108'-214')]; dimer (226-226'':229-229'')-bisdisulfide, produced in a cell line derived from Chinese hamster ovary (CHO) cells, glycoform alfa
immunostimulant, antineoplastic

trovostobart

immunoglobuline G1-kappa, anti-[*Homo sapiens* VSIR (récepteur immunorégulateur du V-set, B7H5, B7-H5, homologue du PDCD1, PD-1H, protéine 1 secrétée induite par le stress, SISP1, suppresseur d'activation de cellule T du V-set Ig, VISTA)], anticorps monoclonal *Homo sapiens*;
chaîne lourde H-gamma1 *Homo sapiens* (1-447) [VH (*Homo sapiens* IGHV4-59*01 (99.0%) -(IGHD) -IGHJ3*02 (93.3%) T125>I (114), CDR-IMGT [8.7.11] (26-33.51-57.96-106)) (1-117) -*Homo sapiens* IGHG1*01, G1m17,1 CH1 K120, CH3 D12, L14, 9-G1v21 CH2 Y15.1, T16, E18 (CH1 K120 (214) (118-215), charnière 1-15 (216-230), CH2 M15.1>Y (252), S16>T (254), T18>E (256) (231-340), CH3 D12 (356), L14 (358) (341-445), CHS (446-447)) (118-447)], (220-214')-disulfure avec la chaîne

légère L-kappa *Homo sapiens* (1'-214') [V-KAPPA (*Homo sapiens* IGKV3-11*01 (96.8%) -IGKJ4*01 (100%), CDR-IMGT [6.3.9] (27'-32'.50'-52'.89'-97')) (1'-107') -*Homo sapiens* IGKC*01 (100%) Km3 A45.1, V101 (C-KAPPA A45.1 (153'), V101 (191')) (108'-214')]; dimère (226-226'':229-229'')-bisdisulfure, produit dans une lignée cellulaire dérivant des cellules ovariennes de hamster chinois (CHO), glycoforme alfa
immunostimulant, antinéoplasique

trovostobart

inmunoglobulina G1-kappa, anti-[*Homo sapiens* VSIR (receptor inmunoregulador del V-set, B7H5, B7-H5, homólogo del PDCD1, PD-1H, proteína 1 secretada inducida por el estrés, SISP1, supresor de activación de célula T del V-set Ig, VISTA)], anticuerpo monoclonal *Homo sapiens*;
cadena pesada H-gamma1 *Homo sapiens* (1-447) [VH (*Homo sapiens* IGHV4-59*01 (99.0%) -(IGHD) -IGHJ3*02 (93.3%) T125>I (114), CDR-IMGT [8.7.11] (26-33.51-57.96-106)) (1-117) -*Homo sapiens* IGHG1*01, G1m17,1 CH1 K120, CH3 D12, L14, 9-G1v21 CH2 Y15.1, T16, E18 (CH1 K120 (214) (118-215), bisagra 1-15 (216-230), CH2 M15.1>Y (252), S16>T (254), T18>E (256) (231-340), CH3 D12 (356), L14 (358) (341-445), CHS (446-447)) (118-447)], (220-214')-disulfuro con la cadena ligera L-kappa *Homo sapiens* (1'-214') [V-KAPPA (*Homo sapiens* IGKV3-11*01 (96.8%) -IGKJ4*01 (100%), CDR-IMGT [6.3.9] (27'-32'.50'-52'.89'-97')) (1'-107') -*Homo sapiens* IGKC*01 (100%) Km3 A45.1, V101 (C-KAPPA A45.1 (153'), V101 (191')) (108'-214')]; dímero (226-226'':229-229'')-bisdisulfuro, producido en una línea celular derivada de las células ováricas de hámster chino (CHO), forma glicosilada alfa
inmunoestimulante, antineoplásico

3006784-09-1

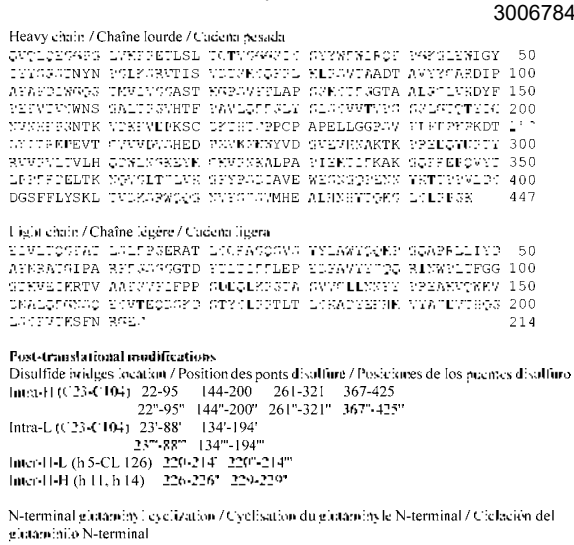

ubavitinibum

ubavitinib — *N*-(4-{[5-fluoro-7-(2-methoxyethoxy)quinazolin-4-yl]amino}phenyl)-2-[4-(propan-2-yl)-1*H*-1,2,3-triazol-1-yl]acetamide
tyrosine kinase inhibitor, antineoplastic

ubavitinib — *N*-(4-{[5-fluoro-7-(2-methoxyethoxy)quinazolin-4-yl]amino}phenyl)-2-[4-(propan-2-yl)-1*H*-1,2,3-triazol-1-yl]acetamide
inhibiteur de tyrosine kinase, antinéoplasique

ubavitinib — *N*-(4-{[5-fluoro-7-(2-metoxietoxi)quinazolin-4-il]amino}fenil)-2-[4-(propan-2-il)-1*H*-1,2,3-triazol-1-il]acetamida
inhibidor de la tirosina kinasa, antineoplásico

$C_{24}H_{26}FN_7O_3$ 2248003-60-1

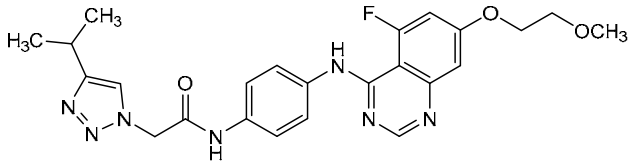

ubletamigum #

ubletamig — immunoglobulin (H-gamma4_L-kappa)_(H-gamma4_L-kappa), anti-[*Homo sapiens* MUC16 (mucin 16, MUC-16, cancer antigen 125, CA125)] and anti-[*Homo sapiens* CD28 (T cell specific surface glycoprotein CD28, TP44)], *Homo sapiens* monoclonal antibody, bispecific, bivalent;
H-gamma4 heavy chain anti-MUC16 *Homo sapiens* (1-455) [VH (*Homo sapiens* IGHV3-49*04 (93.9%) -(IGHD) -IGHJ6*04 (90.0%) K120>R (121), CDR-IMGT [8.10.20] (26-33.51-60.99-118)) (1-129)-*Homo sapiens* IGHG4*01 nG4m(a) CH2 L92, 12-G4v5 h P10, 6-G4v7 CH2 delE1.4, P1.3, V1.2, A1.1 (CH1 (130-227), hinge 1-12 S10>P (237) (228-239), CH2 E1.4>del, F1.3>P (242), L1.2>V (243), G1.1>A (244), L92 (318) (240-348), CH3 (349-453), CHS (454-455)) (130-455)], (143-215')-disulfide with common L-kappa light chain *Homo sapiens* (1'-215') [V-KAPPA (*Homo sapiens* IGKV3-20*01 (100%) -IGKJ1*01 (100%), CDR-IMGT [7.3.9] (27'-33'.51'-53'.90'-98')) (1'-108') -*Homo sapiens* IGKC*01 (100%) Km3 A45.1, V101 (C-KAPPA A45.1 (154'), V101 (192') (109'-215')];
H-gamma4 heavy chain anti-CD28 *Homo sapiens* (1"-448") [VH (*Homo sapiens* IGHV4-59*01 (96.9%) -(IGHD) -IGHJ6*01 (100%), CDR-IMGT [8.7.16] (26"-33".51"-57".96"-111")) (1"-122")-*Homo sapiens* IGHG4*01 nG4m(a) CH2 L92, 12-G4v5 h P10, 6-G4v7 CH2 delE1.4, P1.3, V1.2, A1.1, 10-G4v8 CH3 R115, F116, P125(CH1 (123"-220"), hinge 1-12 S10>P (230") (221"-232"), CH2 E1.4>del, F1.3>P (235"), L1.2>V (236"), G1.1>A (237"), L92 (311") (233"-341"), CH3 H115>R (436"), Y116>F (437"), L125>P (446") (342"-446"), CHS (447"-448")) (123"-448")], (136"-215"')-disulfide with common L-kappa light chain *Homo sapiens* (1"'-215"') [V-KAPPA (*Homo sapiens* IGKV3-20*01 (100%) -IGKJ1*01 (100%), CDR-IMGT [7.3.9] (27"'-33"'.51"'-53"'.90"'-98"')) (1"'-108"') -*Homo sapiens* IGKC*01 (100%) Km3 A45.1, V101 (C-KAPPA A45.1 (154"'), V101 (192"') (109"'-215"')]; dimer (235-228": 238-231")-bisdisulfide, produced in Chinese hamster ovary (CHO) cells, cell line CHO-K1, glycoform alfa
antineoplastic

ublétamig	immunoglobuline (H-gamma4_L-kappa)_(H-gamma4_L-kappa), anti-[*Homo sapiens* MUC16 (mucine 16, MUC-16, antigène de cancer 125, CA125)] et anti-[*Homo sapiens* CD28 (glycoprotéine de surface CD28 spécifique des cellules T, TP44)], anticorps monoclonal *Homo sapiens,* bispécifique, bivalent; chaîne lourde H-gamma4 anti-MUC16 *Homo sapiens* (1-455) [VH (*Homo sapiens* IGHV3-49*04 (93.9%) -(IGHD) -IGHJ6*04 (90.0%) K120>R (121), CDR-IMGT [8.10.20] (26-33.51-60.99-118)) (1-129)-*Homo sapiens* IGHG4*01 nG4m(a) CH2 L92, 12-G4v5 h P10, 6-G4v7 CH2 delE1.4, P1.3, V1.2, A1.1 (CH1 (130-227), charnière 1-12 S10>P (237) (228-239), CH2 E1.4>del, F1.3>P (242), L1.2>V (243), G1.1>A (244), L92 (318) (240-348), CH3 (349-453), CHS (454-455)) (130-455)], (143-215')-disulfure avec la chaîne légère L-kappa commune *Homo sapiens* (1'-215') [V-KAPPA (*Homo sapiens* IGKV3-20*01 (100%) -IGKJ1*01 (100%), CDR-IMGT [7.3.9] (27'-33'.51'-53'.90'-98')) (1'-108') -*Homo sapiens* IGKC*01 (100%) Km3 A45.1, V101 (C-KAPPA A45.1 (154'), V101 (192') (109'-215')]; chaîne lourde H-gamma4 anti-CD28 *Homo sapiens* (1''-448'') [VH (*Homo sapiens* IGHV4-59*01 (96.9%) -(IGHD) -IGHJ6*01 (100%), CDR-IMGT [8.7.16] (26''-33''.51''-57''.96''-111'')) (1''-122'')-*Homo sapiens* IGHG4*01 nG4m(a) CH2 L92, 12-G4v5 h P10, 6-G4v7 CH2 delE1.4, P1.3, V1.2, A1.1,10-G4v8 CH3 R115, F116, P125 (CH1 (123''-220''), charnière 1-12 S10>P (230'') (221''-232''), CH2 E1.4>del, F1.3>P (235''), L1.2>V (236''), G1.1>A (237''), L92 (311'') (233''-341''), CH3 H115>R (436''), Y116>F (437''), L125>P (446'') (342''-446''), CHS (447''-448'')) (123''-448'')], (136''-215''')-disulfure avec la chaîne légère L-kappa commune *Homo sapiens* (1'''-215''') [V-KAPPA (*Homo sapiens* IGKV3-20*01 (100%) -IGKJ1*01 (100%), CDR-IMGT [7.3.9] (27'''-33'''.51'''-53'''.90'''-98''')) (1'''-108''') -*Homo sapiens* IGKC*01 (100%) Km3 A45.1, V101 (C-KAPPA A45.1 (154'''), V101 (192''') (109'''-215''')]; dimère (235-228'': 238-231'')-bisdisulfure, produit dans des cellules ovariennes de hamster chinois (CHO), lignée cellulaire CHO-K1, glycoforme alfa *antinéoplasique*
ubletamig	inmunoglobulina (H-gamma4_L-kappa)_(H-gamma4_L-kappa), anti-[*Homo sapiens* MUC16 (mucina 16, MUC-16, antígeno de cáncer 125, CA125)] y anti-[*Homo sapiens* CD28 (glicoproteína de superficie CD28 específico de las células T, TP44)], anticuerpo monoclonal *Homo sapiens,* biespecífico, bivalente; cadena pesada H-gamma4 anti-MUC16 *Homo sapiens* (1-455) [VH (*Homo sapiens* IGHV3-49*04 (93.9%) -(IGHD) -IGHJ6*04 (90.0%) K120>R (121), CDR-IMGT [8.10.20] (26-33.51-60.99-118)) (1-129)-*Homo sapiens* IGHG4*01 nG4m(a) CH2 L92, 12-G4v5 h P10, 6-G4v7 CH2 delE1.4, P1.3, V1.2, A1.1 (CH1 (130-227), bisagra 1-12 S10>P (237) (228-239), CH2 E1.4>del, F1.3>P (242), L1.2>V (243), G1.1>A (244), L92 (318) (240-348), CH3 (349-453), CHS (454-455)) (130-455)], (143-215')-disulfuro con la cadena ligera L-kappa común *Homo sapiens* (1'-215') [V-KAPPA (*Homo sapiens* IGKV3-20*01 (100%) -IGKJ1*01 (100%), CDR-IMGT [7.3.9] (27'-33'.51'-53'.90'-98')) (1'-108') -*Homo sapiens* IGKC*01 (100%) Km3 A45.1, V101 (C-KAPPA A45.1 (154'), V101 (192') (109'-215')]; cadena pesada H-gamma4 anti-CD28 *Homo sapiens* (1''-448'') [VH (*Homo sapiens* IGHV4-59*01 (96.9%) -(IGHD) -IGHJ6*01 (100%), CDR-IMGT [8.7.16] (26''-33''.51''-57''.96''-111'')) (1''-122'')-*Homo sapiens* IGHG4*01 nG4m(a) CH2 L92, 12-G4v5 h P10, 6-G4v7 CH2 delE1.4, P1.3, V1.2, A1.1,10-G4v8 CH3 R115, F116, P125 (CH1 (123''-220''), bisagra 1-12 S10>P (230'') (221''-232''), CH2 E1.4>del, F1.3>P (235''), L1.2>V (236''), G1.1>A (237''), L92 (311'') (233''-341''), CH3 H115>R (436''), Y116>F (437''), L125>P (446'') (342''-446''), CHS (447''-448'')) (123''-448'')], (136''-215''')-disulfuro con la cadena

ligera L-kappa común *Homo sapiens* (1'"-215'") [V-KAPPA (*Homo sapiens* IGKV3-20*01 (100%) -IGKJ1*01 (100%), CDR-IMGT [7.3.9] (27'"-33'".51'"-53'".90'"-98'")) (1'"-108'") -*Homo sapiens* IGKC*01 (100%) Km3 A45.1, V101 (C-KAPPA A45.1 (154'"), V101 (192'") (109'"-215'")];dímero (235-228": 238-231")-bisdisulfuro, producido en las células ováricas de hámster chino (CHO), línea celular CHO-K1, forma glicosilada alfa

antineoplásico

3008247-27-3

Heavy chain / Chaîne lourde / Cadena pesada: H-gamma4 anti-MUC16 (H)

```
EVQLVESGGG LEQPGRSLRL SCTASGFAFG DHTMSWVRQA PGKGLEWVGF  50
IRSRAYGGTT EYAASVKGRF TISRDDSKSI AYLQMDSLKT EDTAVYYCTS 100
GGYDSSLHYY YYYHGMDVWG RGTTVTVSSA STKGPSVFPL APCSRSTSES 150
TAALGCLVKD YFPEPVTVSW NSGALTSGVH TFPAVLQSSG LYSLSSVVTV 200
PSSSLGTKTY TCNVDHKPSN TKVDKRVESK YGPPCPPCPA PPVAGPSVFL 250
FPPKPKDTLM ISRTPEVTCV VVDVSQEDPE VQFNWYVDGV EVHNAKTKPR 300
EEQFNSTYRV VSVLTVLHQD WLNGKEYKCK VSNKGLPSSI EKTISKAKGQ 350
PREPQVYTLP PSQEEMTKNQ VSLTCLVKGF YPSDIAVEWE SNGQPENNYK 400
TTPPVLDSDG SFFLYSRLTV DKSRWQEGNV FSCSVMHEAL HNHYTQKSLS 450
LSLGK                                                   455
```

Heavy chain / Chaîne lourde / Cadena pesada: H-gamma4 anti-CD28 (H")

```
QVQLQESGPG LVKPSETLSL TCTVSGGSIS SYYWSWIRQP PGKGLEWIGY  50
IYYSGITHYN PSLKSRVTIS VDTSKIQFSL KLSSVTAADT AVYYCARWGV 100
RRDYYYYGMD VWGQGTTVTV SSASTKGPSV FPLAPCSRST SESTAALGCL 150
VKDYFPEPVT VSWNSGALTS GVHTFPAVLQ SSGLYSLSSV VTVPSSSLGT 200
KTYTCNVDHK PSNTKVDKRV ESKYGPPCPP CPAPPVAGPS VFLFPPKPKD 250
TLMISRTPEV TCVVVDVSQE DPEVQFNWYV DGVEVHNAKT KPREEQFNST 300
YRVVSVLTVL HQDWLNGKEY KCKVSNKGLP SSIEKTISKA KGQPREPQVY 350
TLPPSQEEMT KNQVSLTCLV KGFYPSDIAV EWESNGQPEN NYKTTPPVLD 400
SDGSFFLYSR LTVDKSRWQE GNVFSCSVMH EALHNRFTQK SLSLSPGK   448
```

Light chain / Chaîne légère / Cadena ligera: L-kappa common (L', L'")

```
EIVLTQSPGT LSLSPGERAT LSCRASQSVS SSYLAWYQQK PGQAPRLLIY  50
GASSRATGIP DRFSGSGSGT DFTLTISRLE PEDFAVYYCQ QYGSSPWTFG 100
QGTKVEIKRT VAAPSVFIFP PSDEQLKSGT ASVVCLLNNF YPREAKVQWK 150
VDNALQSGNS QESVTEQDSK DSTYSLSSTL TLSKADYEKH KVYACEVTHQ 200
GLSSPVTKSF NRGEC                                        215
```

Post-translational modifications

Disulfide bridges location / Position des ponts disulfure / Posiciones de los puentes disulfuro

Intra-H (C23-C104) 22-98 156-212 269-329 375-433
22"-95" 149"-205" 262"-322" 368"-426"

Intra-L (C23-C104) 23'-89' 135'-195'
23'"-89'" 135'"-195'"

Inter-H-L (CH1 10-CL 126) 143-215' 136"-215'"

Inter-H-H (h 8, h 11) 235-228" 238-231"

N-terminal glutaminyl cyclization / Cyclisation du glutaminyle N-terminal / Ciclación del glutaminilo N-terminal

Q > pyroglutamyl (pE, 5-oxoprolyl) / pyroglutamyle (pE, 5-oxoprolyle) / piroglutamilo (pE, 5-oxoprolilo)

H VH Q1: 1"

N-glycosylation sites / Sites de N-glycosylation / Posiciones de N-glicosilación

H CH2 N84.4: 305, 298"

Fucosylated complex bi-antennary CHO-type glycans / glycanes de type CHO bi-antennaires complexes fucosylés / glicanos de tipo CHO biantenarios complejos fucosilados.

C-terminal lysine clipping / Coupure de la lysine C-terminale / Recorte de lisina C-terminal

H CHS K2: 455, 448"

utenpanii chloridum

utenpanium chloride — 5-(3,6-dibromo-9*H*-carbazol-9-yl)-*N*,*N*,*N*-trimethylpentan-1-aminium chloride
serine/threonine kinase inhibitor

chlorure d'utenpanium — chlorure de 5-(3,6-dibromo-9*H*-carbazol-9-yl)-*N*,*N*,*N*-triméthylpentan-1-aminium
inhibiteur de sérine/thréonine kinases

cloruro de utenpanio — cloruro de 5-(3,6-dibromo-9*H*-carbazol-9-il)-*N*,*N*,*N*-trimetilpentan-1-aminio
inhibidor de la serina/treonina kinasa

$C_{20}H_{25}Br_2ClN_2$ 1436920-57-8

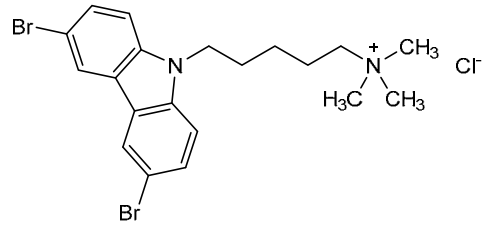

vecantoxatugum #

vecantoxatug — immunoglobulin G1-kappa, anti-[*Clostridium tetani* tetanus toxin (TeNT, neurotoxin)], humanized monoclonal antibody; H-gamma1 heavy chain humanized (1-445) [VH (*Homo sapiens* IGHV1-69*02 (81.4%) -(IGHD) -IGHJ4*01 (85.7%) L123>M (110), CDR-IMGT [8.8.8] (26-33.51-58.97-104)) (1-115) -*Homo sapiens* IGHG1*03 (100%) G1m3, nG1m1 CH1 R120, CH3 E12, M14 (CH1 R120 (212) (116-213), hinge 1-15 (214-228), CH2 (229-338), CH3 E12 (354), M14 (356) (339-443), CHS (444-445)) (116-445)], (218-214')-disulfide with L-kappa light chain humanized (1'-214') [V-KAPPA (*Homo sapiens* IGKV1-NL1*01 (86.3%) -IGKJ2*01 (100%), CDR-IMGT [6.3.9] (27'-32'.50'-52'.89'-97')) (1'-107') -*Homo sapiens* IGKC*01 (100%) Km3 A45.1, V101 (C-KAPPA A45.1 (153'), V101 (191')) (108'-214')]; dimer (224-224": 227-227")-bisdisulfide, produced in Chinese hamster ovary (CHO) cells, glycoform alfa
antitoxin, tetanus

vécantoxatug — immunoglobuline G1-kappa, anti-[*Clostridium tetani* toxine tétanique (TeNt, neurotoxine)], anticorps monoclonal humanisé; chaîne lourde H-gamma1 humanisée (1-445) [VH (*Homo sapiens* IGHV1-69*02 (81.4%) -(IGHD) -IGHJ4*01 (85.7%) L123>M (110), CDR-IMGT [8.8.8] (26-33.51-58.97-104)) (1-115) -*Homo sapiens* IGHG1*03 (100%) G1m3, nG1m1 CH1 R120, CH3 E12, M14 (CH1 R120 (212) (116-213), charnière 1-15 (214-228), CH2 (229-338), CH3 E12 (354), M14 (356) (339-443), CHS (444-445)) (116-445)], (218-214')-disulfure avec la chaîne légère L-kappa humanisée (1'-214') [V-KAPPA (*Homo sapiens* IGKV1-NL1*01 (86.3%) -IGKJ2*01 (100%), CDR-IMGT [6.3.9] (27'-32'.50'-52'.89'-97')) (1'-107') -*Homo sapiens* IGKC*01 (100%) Km3 A45.1, V101 (C-KAPPA A45.1 (153'), V101 (191')) (108'-214')]; dimère (224-224": 227-227")-bisdisulfure, produit

dans des cellules ovariennes de hamster chinois (CHO), glycoforme alfa
antitoxine, tétanos

vecantoxatug

inmunoglobulina G1-kappa, anti-[*Clostridium tetani* toxina tetánica (TeNt, neurotoxina)], anticuerpo monoclonal humanizado;
cadena pesada H-gamma1 humanizada (1-445) [VH (*Homo sapiens* IGHV1-69*02 (81.4%) -(IGHD) -IGHJ4*01 (85.7%) L123>M (110), CDR-IMGT [8.8.8] (26-33.51-58.97-104)) (1-115) -*Homo sapiens* IGHG1*03 (100%) G1m3, nG1m1 CH1 R120, CH3 E12, M14 (CH1 R120 (212) (116-213), bisagra 1-15 (214-228), CH2 (229-338), CH3 E12 (354), M14 (356) (339-443), CHS (444-445)) (116-445)], (218-214')-disulfuro con la cadena ligera L-kappa humanizada (1'-214') [V-KAPPA (*Homo sapiens* IGKV1-NL1*01 (86.3%) -IGKJ2*01 (100%), CDR-IMGT [6.3.9] (27'-32'.50'-52'.89'-97')) (1'-107') -*Homo sapiens* IGKC*01 (100%) Km3 A45.1, V101 (C-KAPPA A45.1 (153'), V101 (191')) (108'-214')]; dímero (224-224": 227-227")-bisdisulfuro, producido en las células ováricas de hámster chino (CHO), forma glicosilada alfa
antitoxina, tétanos

2956766-52-0

Heavy chain / Chaîne lourde / Cadena pesada

```
QVQLVQSGAE VKKPGSSVKV SCKASGYTFT SYWINWVRQA PGQGLEWMGE   50
INPSNGRTNY NEKFKSRVTL TVDKSTSTAY MELSSLRSED TAVYYCARSP  100
RDFPWFQGTM VTVSSASTKG PSVFPLAPSS KSTSGGTAAL GCLVKDYFPE  150
PVTVSWNSGA LTSGVHTFPA VLQSSGLYSL SSVVTVPSSS LGTQTYICNV  200
NHKPSNTKVD KRVEPKSCDK THTCPPCPAP ELLGGPSVFL FPPKPKDTLM  250
ISRTPEVTCV VVDVSHEDPE VKFNWYVDGV EVHNAKTKPR EEQYNSTYRV  300
VSVLTVLHQD WLNGKEYKCK VSNKALPAPI EKTISKAKGQ PREPQVYTLP  350
PSRDELTKNQ VSLTCLVKGF YPSDIAVEWE SNGQPENNYK TTPPVLDSDG  400
SFFLYSKLTV DKSRWQQGNV FSCSVMHEAL HNHYTQKSLS LSPGK       445
```

Light chain / Chaîne légère / Cadena ligera

```
DIQMTQSPSS LSASVGDRVT ITCRASQDIS SALVWYQQKP GKAPKRLIYA  50
TSSLDSGVPS RFSGSGSGTD YTLTISSLQP EDFATYYCLQ YASSPYTFGQ  100
GTKLEIKRTV AAPSVFIFPP SDEQLKSGTA SVVCLLNNFY PREAKVQWKV  150
DNALQSGNSQ ESVTEQDSKD STYSLSSTLT LSKADYEKHK VYACEVTHQG  200
LSSPVTKSFN RGEC                                         214
```

Post-translational modifications
Disulfide bridges location / Position des ponts disulfure / Posiciones de los puentes disulfuro
Intra-H (C23-C104) 22-96 142-198 259-319 365-423
22"-96" 142"-198" 259"-319" 365"-423"
Intra-L (C23-C104) 23'-88' 134'-194'
23'"-88'" 134'"-194'"
Inter-H-L (h 5-CL 126) 218-214' 218"-214'"
Inter-H-H (h 11, h 14) 224-224" 227-227"

N-terminal glutaminyl cyclization / Cyclisation du glutaminyle **N**-terminal / Ciclación del glutaminilo **N**-terminal
Q > pyroglutamyl (pE, 5-oxoprolyl) / pyroglutamyle (pE, 5-oxoprolyle) / piroglutamilo (pE, 5-oxoprolilo)
H VH Q1: 1, 1"

N-glycosylation sites / Sites de **N**-glycosylation / Posiciones de **N**-glicosilación
H CH2 N84.4: 295, 295"
Fucosylated complex bi-antennary CHO-type glycans / glycanes de type CHO bi-antennaires complexes fucosylés / glicanos de tipo CHO biantenarios complejos fucosilados.

C-terminal lysine clipping / Coupure de la lysine C-terminale / Recorte de lisina C-terminal
H CHS K2: 445, 445"

velaprumigum #

velaprumig

immunoglobulin scFvkh-L-VH-G1(CH1-h)_scFvkh-L-kappa, anti-[*Homo sapiens* CD40LG (CD40 ligand, CD40L, tumor necrosis factor ligand superfamily member 5, TNFSF5, tumor necrosis factor related activation protein, TRAP, CD154)] and anti-[*Homo sapiens* ALB (albumin, human serum albumin, HSA)], monoclonal antibody, bispecific, trivalent;
fused scFvkh-L-VH-G1(CH1-h) chain anti-CD40LG and anti-ALB (1-483) [scFvkh anti-CD40LG (1-245) [V-KAPPA Musmus/Homsap (*Mus musculus* IGKV3-7*01 (87.9%) -IGKJ1*02 (100%)/*Homo sapiens* IGKV3-11*01 (75.5%) -IGKJ4*01 (90.9%) V124>L (108), CDR-IMGT [10.3.9] (27-36.54-56.93-101)) (1-112) -15-mer tris(tetraglycyl-seryl) linker (113-127) -VH Musmus/Homsap (*Mus musculus* IGHV1-47-14*01 (88.8%) -(IGHD) -IGHJ3*01 (90.9%) A128>S (245)/*Homo sapiens* IGHV1-46*01 (76.5%) -IGHD -IGHJ1*01 (100%), CDR-IMGT [8.8.11] (153-160.178-185.224-234)) (128-245)] -15-mer tris(tetraglycyl-seryl) linker (246-260) -VH-G1(CH1-h) anti-ALB (261-483) [VH anti-ALB (*Homo sapiens* IGHV3-21*01 (90.8%) -IGHD -IGHJ4*01 (92.9%), CDR-IMGT [8.8.13] (286-293.311-318.357-369)) (261-380) -*Homo sapiens* IGHG1*01 CH1-h, G1m17,1CH1 K120, 10-G1v100-1 CH1 E16, 15-G1v37 h S5 (CH1 G16>E (400), K120 (477) (381-478), hinge 1-5 C5>S (483) (479-483)) (381-483)]];
fused scFvkh-L-KAPPA chain anti-CD40LG and anti-ALB (1'-478') [scFvkh anti-CD40LG (1'-245') [V-KAPPA Musmus/Homsap (*Mus musculus* IGKV3-7*01 (87.9%) -IGKJ1*02 (100%)/*Homo sapiens* IGKV3-11*01 (75.5%) -IGKJ4*01 (90.9%) V124>L (108'), CDR-IMGT [10.3.9] (27'-36'.54'-56'.93'-101')) (1'-112') -15-mer tris(tetraglycyl-seryl) linker (113'-127') -VH Musmus/Homsap (*Mus musculus* IGHV1-47-14*01 (88.8%) -(IGHD) -IGHJ3*01 (90.9%) A128>S (245')/*Homo sapiens* IGHV1-46*01 (76.5%) -IGHD -IGHJ1*01 (100%), CDR-IMGT [8.8.11] (153'-160'.178'-185'.224'-234')) (128'-245')]-18-mer (GSTSGSGKPGSGEGSTKG) linker (246'-263') -L-KAPPA anti-ALB (264'-478') [V-KAPPA anti-ALB (*Homo sapiens* IGKV3-15*01 (85.7%) -IGKJ2*01 (90.9%) K123>Q (367'), CDR-IMGT [6.3.10] (290'-295'.313'-315'.352'-361')) (264'-371') -*Homo sapiens* IGKC*01, Km3 A45.1, V101, 15-KCv36 S126 (C-KAPPA A45.1 (417'), V101 (455'), C226>S (478') (372'-478')]], produced in Chinese hamster ovary (CHO) cells, cell line CHO-DG44, non-glycosylated
immunosuppressant

vélaprumig

immunoglobuline scFvkh-L-VH-G1(CH1-h)_scFvkh-L-kappa, anti-[*Homo sapiens* CD40LG (CD40 ligand, CD40L, membre 5 de la superfamille des ligands facteurs de nécrose tumorale, TNFSF5, protéine d'activation apparentée au facteur de nécrose tumorale, TRAP, CD154)] et anti-[*Homo sapiens* ALB (albumine, sérum albumine humaine, SAH)], anticorps monoclonal, bispecific, trivalent;
chaîne fusionnée scFvkh-L-VH-G1(CH1-h) anti-CD40LG et anti-ALB (1-483) [scFvkh anti-CD40LG (1-245) [V-KAPPA Musmus/Homsap (*Mus musculus* IGKV3-7*01 (87.9%) -IGKJ1*02 (100%)/*Homo sapiens* IGKV3-11*01 (75.5%) -IGKJ4*01 (90.9%) V124>L (108), CDR-IMGT [10.3.9] (27-36.54-56.93-101)) (1-112) -15-mer tris(tétraglycyl-séryl) linker (113-127) -VH Musmus/Homsap (*Mus musculus* IGHV1-47-14*01 (88.8%) -(IGHD) -IGHJ3*01 (90.9%) A128>S (245)/*Homo sapiens* IGHV1-46*01 (76.5%) -IGHD -IGHJ1*01 (100%), CDR-IMGT [8.8.11] (153-160.178-185.224-234)) (128-245)] -15-mer tris(tétraglycyl-séryl) linker (246-260) -[VH-G1(CH1-h) anti-ALB (261-483) [VH anti-ALB (*Homo sapiens* IGHV3-21*01 (90.8%) -IGHD -IGHJ4*01 (92.9%), CDR-IMGT [8.8.13] (286-293.311-318.357-369)) (261-380)] -*Homo sapiens* IGHG1*01 CH1-h, G1m17,1CH1 K120, 10-G1v100-1 CH1 E16, 15-G1v37 h S5 [(CH1 G16>E (400), K120 (477) (381-478), hinge 1-5 C5>S (483) (479-483)) (381-483)]];

	chaîne fusionnée scFvkh-L-KAPPA anti-CD40LG et anti-ALB (1'-478') [scFvkh anti-CD40LG (1'-245') [V-KAPPA Musmus/Homsap (*Mus musculus* IGKV3-7*01 (87.9%) -IGKJ1*02 (100%)/*Homo sapiens* IGKV3-11*01 (75.5%) -IGKJ4*01 (90.9%) V124>L (108'), CDR-IMGT [10.3.9] (27'-36'.54'-56'.93'-101')) (1'-112') -15-mer tris(tétraglycyl-séryl) linker (113'-127') -VH Musmus/Homsap (*Mus musculus* IGHV1-47-14*01 (88.8%) -(IGHD) -IGHJ3*01 (90.9%) A128>S (245')/*Homo sapiens* IGHV1-46*01 (76.5%) -IGHD -IGHJ1*01 (100%), CDR-IMGT [8.8.11] (153'-160'.178'-185'.224'-234')) (128'-245')] -18-mer (GSTSGSGKPGSGEGSTKG) linker (246'-263') -L-KAPPA anti-ALB (264'-478') [V-KAPPA anti-ALB (*Homo sapiens* IGKV3-15*01 (85.7%) -IGKJ2*01 (90.9%) K123>Q (367'), CDR-IMGT [6.3.10] (290'-295'.313'-315'.352'-361')) (264'-371') -*Homo sapiens* IGKC*01, Km3 A45.1, V101, 15-KCv36 S126 (C-KAPPA A45.1 (417'), V101 (455'), C226>S (478')) (372'-478')]], produit dans des cellules ovariennes de hamster chinois (CHO), lignée cellulaire CHO-DG44, non-glycosylé *immunosuppresseur*
velaprumig	inmunoglobulina scFvkh-L-VH-G1(CH1-h) scFvkh-L-kappa, anti-[*Homo sapiens* CD40LG (CD40 ligando, CD40L, miembro 5 de la superfamilia de los ligandos factores de necrosis tumoral, TNFSF5, proteína de activación asociada al factor de necrosis tumoral, TRAP, CD154)] y anti-[*Homo sapiens* ALB (albúmina, albumina sérica humana, SAH)], anticuerpo monoclonal, bispecífico, trivalente; cadena fusionada scFvkh-L-VH-G1(CH1-h) anti-CD40LG y anti-ALB (1-483) [scFvkh anti-CD40LG (1-245) [V-KAPPA Musmus/Homsap (*Mus musculus* IGKV3-7*01 (87.9%) -IGKJ1*02 (100%)/*Homo sapiens* IGKV3-11*01 (75.5%) -IGKJ4*01 (90.9%) V124>L (108), CDR-IMGT [10.3.9] (27-36.54-56.93-101)) (1-112) -15-mer tris(tetraglicil-seril) enlace(113-127) -VH Musmus/Homsap (*Mus musculus* IGHV1-47-14*01 (88.8%) -(IGHD) -IGHJ3*01 (90.9%) A128>S (245)/*Homo sapiens* IGHV1-46*01 (76.5%) -IGHD -IGHJ1*01 (100%), CDR-IMGT [8.8.11] (153-160.178-185.224-234)) (128-245)] -15-mer tris(tetraglicil-seril) enlace (246-260) -[VH-G1(CH1-h) anti-ALB (261-483) [VH anti-ALB (*Homo sapiens* IGHV3-21*01 (90.8%) -IGHD -IGHJ4*01 (92.9%), CDR-IMGT [8.8.13] (286-293.311-318.357-369)) (261-380)] -*Homo sapiens* IGHG1*01 CH1-h, G1m17,1CH1 K120, 10-G1v100-1 CH1 E16, 15-G1v37 h S5 [(CH1 G16>E (400), K120 (477) (381-478), bisagra 1-5 C5>S (483) (479-483)) (381-483)]]; cadena fusionada scFvkh-L-KAPPA anti-CD40LG y anti-ALB (1'-478') [scFvkh anti-CD40LG (1'-245') [V-KAPPA Musmus/Homsap (*Mus musculus* IGKV3-7*01 (87.9%) -IGKJ1*02 (100%)/*Homo sapiens* IGKV3-11*01 (75.5%) -IGKJ4*01 (90.9%) V124>L (108'), CDR-IMGT [10.3.9] (27'-36'.54'-56'.93'-101')) (1'-112') -15-mer tris(tetraglicil-seril) enlace (113'-127') -VH Musmus/Homsap (*Mus musculus* IGHV1-47-14*01 (88.8%) -(IGHD) -IGHJ3*01 (90.9%) A128>S (245')/*Homo sapiens* IGHV1-46*01 (76.5%) -IGHD -IGHJ1*01 (100%), CDR-IMGT [8.8.11] (153'-160'.178'-185'.224'-234')) (128'-245')] -18-mer (GSTSGSGKPGSGEGSTKG) enlace (246'-263') -L-KAPPA anti-ALB (264'-478') [V-KAPPA anti-ALB (*Homo sapiens* IGKV3-15*01 (85.7%) -IGKJ2*01 (90.9%) K123>Q (367'), CDR-IMGT [6.3.10] (290'-295'.313'-315'.352'-361')) (264'-371') -*Homo sapiens* IGKC*01, Km3 A45.1, V101, 15-KCv36 S126 (C-KAPPA A45.1 (417'), V101 (455'), C226>S (478')) (372'-478')]], producido en las células ováricas de hámster chino (CHO), línea celular CHO-DG44, no glicosilado *inmunosupresor*

2988741-17-7

Heavy chain / Chaîne lourde / Cadena pesada: fused scFvkh
anti-CD40LG -L-VH-G1(CH1-h) anti-ALB (H)

```
DIVLTQSPAT LSVSPGERAT LSCRASQRVS SSTYSYMHWY QQKPGQAPRL  50
LIKYASQSLS GIPARFSGSG SGTDFTLTIS SVEPEDFAVY YCQHSWEIPP 100
TFGGGTKLEI KGGGGSGGGG SGGGGSQVQ LVQSGAEVKK PGASVKLSCK 150
ASGYTFTSYY MYWVRQAPGQ GLEWIGEINP SNGGTNFNEK FKSRATLTVD 200
KSASTAYMEL SSLRSEDTAV YYCTRRDYRK DMDSWGQGTL VTVSSGGGGS 250
GGGGSGGGGS QVQLVQSGPE VKKPGSSVKL SCKASGGPIF AYSNSWVRQA 300
PGKGLEWMGG ISSSGRYIEY AEKVKGRFTI SRDDAKNSLY LQMNSLKAED 350
TAVYYCARET VMAPFALDYW GQGTLVTVSS AGTKGPSVFP LAPSSKSTSG 400
GTAALGCLVK DYFPEPVTVS WNSGALTSGV HTFPAVLQSS GLYSLSSVVT 450
VPSSSLGTQT YICNVNHKPS NTKVDKKVEP KSC                   483
```

Heavy chain / Chaîne lourde / Cadena pesada: fused scFvkh
anti-CD40LG -L-kappa anti-ALB (H')

```
DIVLTQSPAT LSVSPGERAT LSCRASQRVS SSTYSYMHWY QQKPGQAPRL  50
LIKYASQSLS GIPARFSGSG SGTDFTLTIS SVEPEDFAVY YCQHSWEIPP 100
TFGGGTKLEI KGGGGSGGGG SGGGGSQVQ LVQSGAEVKK PGASVKLSCK 150
ASGYTFTSYY MYWVRQAPGQ GLEWIGEINP SNGGTNFNEK FKSRATLTVD 200
KSASTAYMEL SSLRSEDTAV YYCTRRDYRK DMDSWGQGTL VTVSSGGGGS 250
GGPSVFPLAP SSKSTSGGTA ALGCLVKDYF PEPVTVSWNS GALTSGVHTF 300
PAVLQSSGLY SLSSVVTVPS SSLGTQTYIC NVNHKPSNTK VDKKVEPKSC 350
DKTHTCPPCP APELLGGPSV FLFPPKPKDT LMISRTPEVT CVVVDVSHED 400
PEVKFNWYVD GVEVHNAKTK PREEQYNSTY RVVSVLTVLH QDWLNGKEYK 450
CKVSNKALPA PIEKTISKAK GQPREPQVYT LPPSRDELTK NQVSLTCLVK 500
GFYPSDIAVE WESNGQPENN YKTTPPVLDS DGSFFLYSKL TVDKSRWQQG 550
NVFSCSVMHE ALHNHYTQKS LSLSPGK                          577
```

Post-translational modifications
Disulfide bridges location / Position des ponts disulfure / Posiciones de los puentes disulfuro
Intra-H (C23-C104) 23-92 149-223 282-356 407-463
Intra-H' (C23-C104) 23'-92' 149'-223' 286'-351' 398'-458'

No **N**-glycosylation sites / pas de sites de **N**-glycosylation / ningún posición de **N**-glycosilación

veludacigibum

veludacigib — (2*R*)-2-{*N*-[4-amino-5-(4-methoxybenzoyl)-1,3-thiazol-2-yl]-4-fluoroanilino}propanamide
diacylglycerol kinase inhibitor, antineoplastic

véludacigib — (2*R*)-2-{*N*-[4-amino-5-(4-méthoxybenzoyl)-1,3-thiazol-2-yl]-4-fluoroanilino}propanamide
inhibiteur de diacylglycérol kinase, antinéoplasique

veludacigib — (2*R*)-2-{*N*-[4-amino-5-(4-metoxibenzoil)-1,3-tiazol-2-il]-4-fluoroanilino}propanamida
inhibidor de la diacilglicerol kinasa, antineoplásico

$C_{20}H_{19}FN_4O_3S$ 2732902-08-6

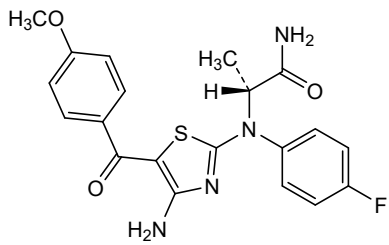

verducatibum

verducatib

(1*R*,3*S*,4*S*)-*N*-[(1*S*)-1-cyano-2-{2-fluoro-4-[1'-(oxetan-3-yl)-3*H*-spiro[[2]benzofuran-1,4'-piperidin]-6-yl]phenyl}ethyl]-2-azabicyclo[2.2.1]heptane-3-carboxamide
cathepsin inhibitor

verducatib

(1*R*,3*S*,4*S*)-*N*-[(1*S*)-1-cyano-2-{2-fluoro-4-[1'-(oxétan-3-yl)-3*H*-spiro[[2]benzofurane-1,4'-pipéridin]-6-yl]phényl}éthyl]-2-azabicyclo[2.2.1]heptane-3-carboxamide
inhibiteur de la cathepsine

verducatib

(1*R*,3*S*,4*S*)-*N*-[(1*S*)-1-ciano-2-{2-fluoro-4-[1'-(oxetan-3-il)-3*H*-espiro[[2]benzofurano-1,4'-piperidin]-6-il]fenil}etil]-2-azabiciclo[2.2.1]heptano-3-carboxamida
inhibidor de la catepsina

$C_{31}H_{35}FN_4O_3$ 1887236-33-0

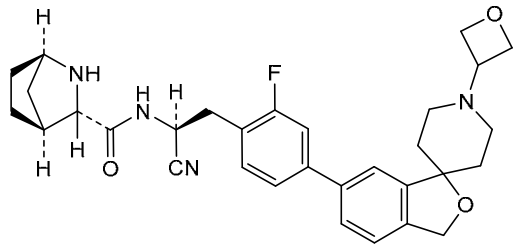

vilagletistatum

vilagletistat

methyl (2*E*,6*S*)-7-[(1-{2-[(2-ethylbutyl)amino]-2-oxoethyl}-2-oxo-1,2-dihydropyridin-3-yl)amino]-6-(1-methyl-1*H*-imidazole-5-carboxamido)-7-oxohept-2-enoate
transglutaminase 2 inhibitor, celiac disease

vilaglétistat

(2*E*,6*S*)-7-[(1-{2-[(2-éthylbutyl)amino]-2-oxoéthyl}-2-oxo-1,2-dihydropyridin-3-yl)amino]-6-(1-méthyl-1*H*-imidazole-5-carboxamido)-7-oxohept-2-énoate de méthyle
inhibiteur de la transglutaminase 2, maladie cœliaque

vilagletistat

(2*E*,6*S*)-7-[(1-{2-[(2-etilbutil)amino]-2-oxoetil}-2-oxo-1,2-dihidropiridin-3-il)amino]-6-(1-metil-1*H*-imidazol-5-carboxamido)-7-oxohept-2-enoato de metilo
inhibidor de la transglutaminasa 2, enfermedad celíaca

$C_{26}H_{36}N_6O_6$ 1542132-88-6

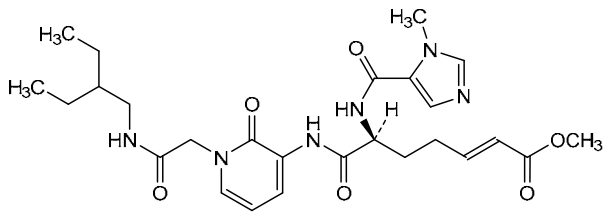

vopimetostatum

vopimetostat — *N*-(6-amino-5-ethylpyridin-3-yl)-2-{(2*R*,5*S*)-5-methyl-2-[2-(1-methylpiperidin-4-yl)-1,3-benzothiazol-5-yl]piperidin-1-yl}-2-oxoacetamide
antineoplastic

vopimétostat — *N*-(6-amino-5-éthylpyridin-3-yl)-2-{(2*R*,5*S*)-5-méthyl-2-[2-(1-méthylpipéridin-4-yl)-1,3-benzothiazol-5-yl]pipéridin-1-yl}-2-oxoacétamide
antinéoplasique

vopimetostat — *N*-(6-amino-5-etilpiridin-3-il)-2-{(2*R*,5*S*)-5-metil-2-[2-(1-metilpiperidin-4-il)-1,3-benzotiazol-5-il]piperidin-1-il}-2-oxoacetamida
antineoplásico

$C_{28}H_{36}N_6O_2S$ 2760483-96-1

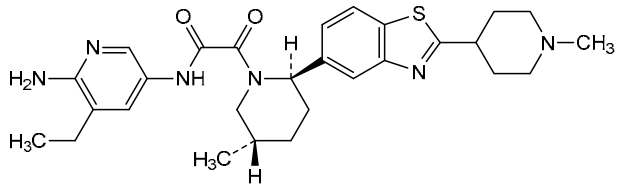

vortosiranum

vortosiran — (2*RS*)-3-(1,23-bis[(2-acetamido-2-deoxy-β-D-galactopyranosyl)oxy]-14-{5-[(2-acetamido-2-deoxy-β-D-galactopyranosyl)oxy]pentanoyl}-5,19-dioxo-6,10,14,18-tetraazatricosan-10-yl)-2-hydroxy-3-oxopropyl hydrogen *all-P-ambo*-2'-*O*-methyl-*P*-thioguanylyl-(3'→5')-2'-*O*-methyl-*P*-thiouridylyl-(3'→5')-2'-*O*-methyladenylyl-(3'→5')-2'-*O*-methylcytidylyl-(3'→5')-2'-*O*-methylguanylyl-(3'→5')-2'-*O*-methyluridylyl-(3'→5')-2'-deoxy-2'-fluoroguanylyl-(3'→5')-2'-deoxy-2'-fluoroguanylyl-(3'→5')-2'-deoxy-2'-fluoroadenylyl-(3'→5')-2'-*O*-methylcytidylyl-(3'→5')-2'-*O*-methyluridylyl-(3'→5')-2'-*O*-methylguanylyl-(3'→5')-2'-*O*-methylguanylyl-(3'→5')-2'-*O*-methyladenylyl-(3'→5')-2'-*O*-methyluridylyl-(3'→5')-2'-*O*-methyluridylyl-(3'→5')-2'-*O*-methylcytidylyl-(3'→5')-2'-*O*-methyluridylyl-(3'→5')-2'-*O*-methyl-3'-guanylate
duplex with *all-P-ambo*-2'-*O*-methyl-*P*-thiouridylyl-(5'→3')-2'-*O*-methyl-*P*-thiouridylyl-(5'→3')-2'-*O*-methylcytidylyl-(5'→3')-2'-*O*-methyladenylyl-(5'→3')-2'-*O*-methyluridylyl-(5'→3')-2'-deoxy-2'-fluoroguanylyl-(5'→3')-2'-*O*-methylcytidylyl-(5'→3')-2'-deoxy-2'-fluoroadenylyl-(5'→3')-2'-*O*-methylcytidylyl-(5'→3')-2'-*O*-methylcytidylyl-(5'→3')-2'-*O*-methyluridylyl-(5'→3')-2'-*O*-methylguanylyl-(5'→3')-2'-*O*-methyladenylyl-(5'→3')-2'-*O*-methylcytidylyl-(5'→3')-2'-*O*-methylcytidylyl-(5'→3')-2'-deoxy-2'-fluorouridylyl-(5'→3')-2'-*O*-methyladenylyl-(5'→3')-2'-*O*-methyladenylyl-(5'→3')-2'-*O*-methyl-*P*-thioguanylyl-(5'→3')-2'-deoxy-2'-fluoro-*P*-thioadenylyl-(5'→3')-cytidine
blood coagulation factor XI synthesis reducer, anticoagulant

vortosiran — (2*RS*)-3-(1,23-bis[(2-acétamido-2-désoxy-β-D-galactopyranosyl)oxy]-14-{5-[(2-acétamido-2-désoxy-β-D-galactopyranosyl)oxy]pentanoyl}-5,19-dioxo-6,10,14,18-tétraazatricosan-10-yl)-2-hydroxy-3-oxopropyl hydrogène *tout-P-ambo*-2'-*O*-méthyl-*P*-thioguanylyl-(3'→5')-2'-*O*-méthyl-*P*-thiouridylyl-(3'→5')-2'-*O*-méthyladénylyl-(3'→5')-2'-*O*-

méthylcytidylyl-(3'→5')-2'-*O*-méthylguanylyl-(3'→5')-2'-*O*-méthyluridylyl-(3'→5')-2'-désoxy-2'-fluoroguanylyl-(3'→5')-2'-désoxy-2'-fluoroguanylyl-(3'→5')-2'-désoxy-2'-fluoroadénylyl-(3'→5')-2'-*O*-méthylcytidylyl-(3'→5')-2'-*O*-méthyluridylyl-(3'→5')-2'-*O*-méthylguanylyl-(3'→5')-2'-*O*-méthylguanylyl-(3'→5')-2'-*O*-méthyladénylyl-(3'→5')-2'-*O*-méthyluridylyl-(3'→5')-2'-*O*-méthyluridylyl-(3'→5')-2'-*O*-méthylcytidylyl-(3'→5')-2'-*O*-méthyluridylyl-(3'→5')-2'-*O*-méthyl-3'-guanylate
duplex avec *tout-P-ambo*-2'-*O*-méthyl-*P*-thiouridylyl-(5'→3')-2'-*O*-méthyl-*P*-thiouridylyl-(5'→3')-2'-*O*-méthylcytidylyl-(5'→3')-2'-*O*-méthyladénylyl-(5'→3')-2'-*O*-méthyluridylyl-(5'→3')-2'-désoxy-2'-fluoroguanylyl-(5'→3')-2'-*O*-méthylcytidylyl-(5'→3')-2'-désoxy-2'-fluoroadénylyl-(5'→3')-2'-*O*-méthylcytidylyl-(5'→3')-2'-*O*-méthylcytidylyl-(5'→3')-2'-*O*-méhyluridylyl-(5'→3')-2'-*O*-méthylguanylyl-(5'→3')-2'-*O*-méthyladénylyl-(5'→3')-2'-*O*-méthylcytidylyl-(5'→3')-2'-*O*-méhylcytidylyl-(5'→3')-2'-désoxy-2'-fluorouridylyl-(5'→3')-2'-*O*-méthyladénylyl-(5'→3')-2'-*O*-méthyladénylyl-(5'→3')-2'-*O*-méthyl-*P*-thioguanylyl-(5'→3')-2'-désoxy-2'-fluoro-*P*-thioadénylyl-(5'→3')-cytidine
réducteur de la synthèse du facteur XI de la coagulation sanguine, anticoagulant

vortosirán

(2*RS*)-3-(1,23-bis[(2-acetamido-2-desoxi-β-D-galactopiranosil)oxi]-14-{5-[(2-acetamido-2-desoxi-β-D-galactopiranosil)oxi]pentanoil}-5,19-dioxo-6,10,14,18-tetraazatricosan-10-il)-2-hidroxi-3-oxopropil hidrógeno *todo-P-ambo*-2'-*O*-metil-*P*-tioguanilil-(3'→5')-2'-*O*-metil-*P*-tiouridilil-(3'→5')-2'-*O*-metiladenilil-(3'→5')-2'-*O*-metilcitidilil-(3'→5')-2'-*O*-metilguanilil-(3'→5')-2'-*O*-metiluridilil-(3'→5')-2'-desoxi-2'-fluoroguanilil-(3'→5')-2'-desoxi-2'-fluoroguanilil-(3'→5')-2'-desoxi-2'-fluoroadenilil-(3'→5')-2'-*O*-metilcitidilil-(3'→5')-2'-*O*-metiluridilil-(3'→5')-2'-*O*-metilguanilil-(3'→5')-2'-*O*-metilguanilil-(3'→5')-2'-*O*-metiladenilil-(3'→5')-2'-*O*-metiluridilil-(3'→5')-2'-*O*-metiluridilil-(3'→5')-2'-*O*-metilcitidilil-(3'→5')-2'-*O*-metiluridilil-(3'→5')-2'-*O*-metil-3'-guanilato
dúplex con *todo-P-ambo*-2'-*O*-metil-*P*-tiouridilil-(5'→3')-2'-*O*-metil-*P*-tiouridilil-(5'→3')-2'-*O*-metilcitidilil-(5'→3')-2'-*O*-metiladenilil-(5'→3')-2'-*O*-metiluridilil-(5'→3')-2'-desoxi-2'-fluoroguanilil-(5'→3')-2'-*O*-metilcitidilil-(5'→3')-2'-desoxi-2'-fluoroadenilil-(5'→3')-2'-*O*-metilcitidilil-(5'→3')-2'-*O*-metilcitidilil-(5'→3')-2'-*O*-metiluridilil-(5'→3')-2'-*O*-metilguanilil-(5'→3')-2'-*O*-metiladenilil-(5'→3')-2'-*O*-metilcitidilil-(5'→3')-2'-*O*-metilcitidilil-(5'→3')-2'-desoxi-2'-fluorouridyilil-(5'→3')-2'-*O*-metiladenilil-(5'→3')-2'-*O*-metiladenilil-(5'→3')-2'-*O*-metil-*P*-tioguanilil-(5'→3')-2'-desoxi-2'-fluoro-*P*-tioadenilil-(5'→3')-citidina
reductor de la síntesis del factor de coagulación sanguínea XI, anticoagulante

$C_{463}H_{620}F_7N_{154}O_{291}P_{39}S_6$ 3061406-99-0

(3'-5')*G=U=A-C-G-U-*G*-*G*-*A*-C-U-G-G-A-U-U-C-U-G-R*
(5'-3')*U=U=C-A-U-*G*-C-*A*-C-C-U-G-A-C-C-*U*-A-A-G=*A*=C*

N : A,C,G,U
N : 2'-*O*-methyl-N / 2'-*O*-méthyl-N / 2'-*O*-metil-N
N : 2'-deoxy-2'-fluoro-N / 2'-désoxy-2'-fluoro-N / 2'-desoxi-2'-fluoro-N
– : –PO(OH)– = : –PO(SH)–

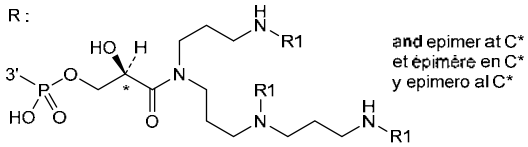

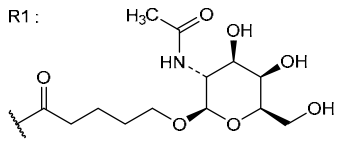

xeruborbactamum isoboxilum

xeruborbactam isoboxil

[(2-methylpropanoyl)oxy]methyl (1a*R*,7b*S*)-5-fluoro-2-hydroxy-1,1a,2,7b-tetrahydrocyclopropa[*c*][1,2]benzoxaborinine-4-carboxylate
beta-lactamase inhibitor

xéruborbactam isoboxil

(1a*R*,7b*S*)-5-fluoro-2-hydroxy-1,1a,2,7b-tétrahydrocyclopropa[*c*][1,2]benzoxaborinine-4-carboxylate de [(2-méthylpropanoyl)oxy]méthyle
inhibiteur de bêta-lactamase

xeruborbactam isoboxilo

(1a*R*,7b*S*)-5-fluoro-2-hidroxi-1,1a,2,7b-tetrahidrociclopropa[*c*][1,2]benzoxaborinina-4-carboxilato de [(2-metilpropanoil)oxi]metilo
inhibidor de la beta lactamasa

$C_{15}H_{16}BFO_6$ 2708983-65-5

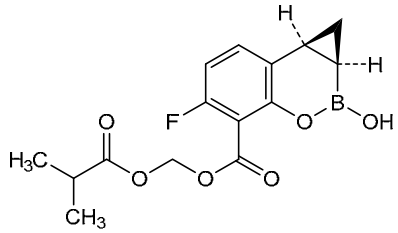

zaladenantum

zaladenant

{5-amino-8-[2-methyl-6-(trifluoromethyl)pyridin-4-yl]-7-phenyl[1,2,4]triazolo[1,5-*c*]pyrimidin-2-yl}methanol
adenosine receptor antagonist, antineoplastic

zaladénant

{5-amino-8-[2-méthyl-6-(trifluorométhyl)pyridin-4-yl]-7-phényl[1,2,4]triazolo[1,5-*c*]pyrimidin-2-yl}méthanol
antagoniste des récepteurs de l'adénosine, antinéoplasique

zaladenant

{5-amino-7-fenil-8-[2-metil-6-(trifluorometil)piridin-4-il][1,2,4]triazolo[1,5-*c*]pirimidin-2-il}metanol
antagonista del receptor de la adenosina, antineoplásico

$C_{19}H_{15}F_3N_6O$ 2246426-52-6

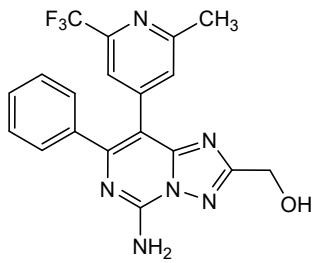

zalsupindolum

zalsupindole (2*R*)-1-(5-methoxy-1*H*-indol-1-yl)-*N*,*N*-dimethylpropan-2-amine
antidepressant

zalsupindole (2*R*)-1-(5-méthoxy-1*H*-indol-1-yl)-*N*,*N*-diméthylpropan-2-amine
antidépresseur

zalsupindol (2*R*)-*N*,*N*-dimetil-1-(5-metoxi-1*H*-indol-1-il)propan-2-amina
antidepresivo

$C_{14}H_{20}N_2O$ 2481740-94-5

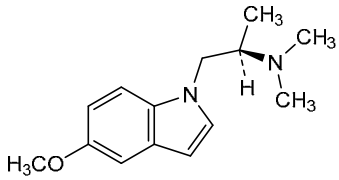

zedoresertibum

zedoresertib 3-(2,6-dichlorophenyl)-1-methyl-7-[3-methyl-4-(1-methylpiperidin-4-yl)anilino]-2,3-dihydropyrimido[4,5-*d*]pyrimidin-4(1*H*)-one
serine/threonine kinase inhibitor, antineoplastic

zédorésertib 3-(2,6-dichlorophényl)-1-méthyl-7-[3-méthyl-4-(1-méthylpipéridin-4-yl)anilino]-2,3-dihydropyrimido[4,5-*d*]pyrimidin-4(1*H*)-one
inhibiteur de sérine/thréonine kinases, antinéoplasique

zedoresertib 3-(2,6-diclorofenil)-1-metil-7-[3-metil-4-(1-metilpiperidin-4-il)anilino]-2,3-dihidropirimido[4,5-*d*]pirimidin-4(1*H*)-ona
inhibidor de la serina/treonina kinasa, antineoplásico

$C_{26}H_{28}Cl_2N_6O$ 2243882-74-6

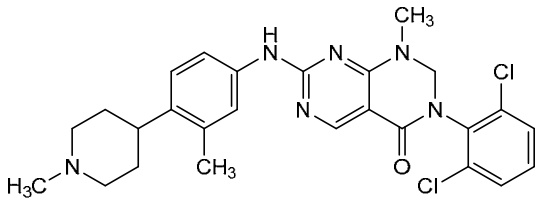

zeltociclibum

zeltociclib {3-[2-{[(2*S*)-1-hydroxypropan-2-yl]amino}-5-(trifluoromethyl)pyrimidin-4-yl]-1*H*-indol-7-yl}di(methyl)-λ^5-phosphanone
cyclin-dependent kinase inhibitor, antineoplastic

zeltociclib {3-[2-{[(2*S*)-1-hydroxypropan-2-yl]amino}-5-(trifluorométhyl)pyrimidin-4-yl]-1*H*-indol-7-yl}di(méthyl)-λ^5-phosphanone
inhibiteur de la kinase cycline-dépendante, antinéoplasique

zeltociclib

{3-[2-{[(2*S*)-1-hidroxipropan-2-il]amino}-5-(trifluorometil)pirimidin-4-il]-1*H*-indol-7-il}di(metil)-λ^5-fosfanona

inhibidor de la kinasa dependiente de ciclinas, antineoplásico

$C_{18}H_{20}F_3N_4O_2P$ 2789697-52-3

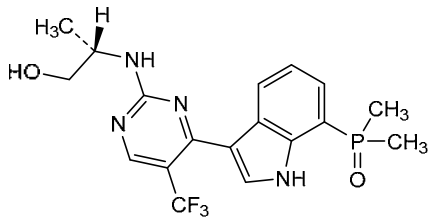

zemocimigum #

zemocimig

immunoglobulin (H-gamma4_L-kappa)_(H-gamma4_L-lambda2), anti-[*Homo sapiens* F9a (coagulation factor F9, coagulation factor IX, hemophilia B) activated] and anti-[*Homo sapiens* F10 (coagulation factor 10, coagulation factor X)], humanized and *Homo sapiens* monoclonal antibody, bispecific, bivalent;
H-gamma4 heavy chain anti-F9a humanized (1-447) [VH (*Homo sapiens* IGHV3-23*04 (87.8%) -(IGHD) -IGHJ4*01 (100%), CDR-IMGT [8.8.15] (26-33.51-58.97-111)) (1-122)-*Homo sapiens* IGHG4*01, nG4m(a) CH2 L92, 12-G4v5 h P10, 17-G4v57-1 CH1 K84.2, 18-G4v11 CH1 Q100, CH2 Y84.3, 14-G4v12-1 CH3 K12, 12-G4v6 CH3 K88, 9-G4v78 L107, A114, 10-G4v89 CH3 R118, E120 (CH1 Q84.2>K (180), K100>Q (201) (123-220), hinge 1-12 S10>P (230) (221-232), CH2 F84.3>Y (298), L92 (311) (233-342), CH3 E12>K (358), R88>K (411), M107>L (430), N114>A (436), Q118>R (440), S120>E (442) (343-447)) (123-447)], (136-214')-disulfide with L-kappa light chain anti-F9a *Homo sapiens* (1'-214') [V-KAPPA (*Homo sapiens* IGKV3D-11*02 (84.4%) -IGKJ4*01 (100%), CDR-IMGT [6.3.9] (27'-32'.50'-52'.89'-97')) (1'-107') -*Homo sapiens* IGKC*01 (98.1%) Km3 A45.1, V101 KCv57-1 E20, E90 (C-KAPPA S20>E (131'), A45.1 (153'), T90>E (180), V101 (191')) (108'-214')];
H-gamma4 heavy chain anti-F10 humanized (1''-444'') [VH (*Homo sapiens* IGHV1-2*06 (74.5%) -(IGHD) -IGHJ4*01 (80.0%) Q120>E (111''), CDR-IMGT [8.8.12] (26''-33''.51''-58''.97''-108'')) (1''-119'')-*Homo sapiens* IGHG4*01, nG4m(a) CH2 L92, 12-G4v5 h P10, 17-G4v57-2 CH1 E26, K84.2, 18-G4v11 CH1 Q100, CH2 Y84.3, 12-G4v6 CH3 K88, 9-G4v78 L107, A114, 10-G4v89 CH3 R118, E120, 14-G4v13 CH3 E119 (CH1 K26>E (149''), Q84.2>E (177''), K100>Q (198'') (120''-217''), hinge 1-12 S10>P (227'') (218''-229''), CH2 F84.3>Y (295''), L92 (308'') (230''-339''), CH3 R88>K (408''), M107>L (427''), N114>A (433''), Q118>R (437''), K119>E (438''), S120>E (439'') (340''-444'')) (120''-444'')], (133''-212''')-disulfide with L-lambda2 light chain anti-F10 *Homo sapiens* (1''-213''') [V-LAMBDA (*Homo sapiens* IGLV3-9*01 (78.7%) -IGLJ2*01 (81.8%) L124>V (104'''), L127>V (107'''), CDR-IMGT [6.3.10] (26'''-31'''.49'''-51'''.88'''-97''')) (1'''-107''') -*Homo sapiens* IGLC2*01 (98.1%) LC2v57-2 K20, K90 (C-LAMBDA2 T20>K (132'''), S90>K (180''')) (108'''-213''')]; dimer (228-225'':231-228'')-bisdisulfide, produced in Chinese hamster ovary (CHO) cells, cell line CHO-DXB11, glycoform alfa

antihaemophilic agent

zémocimig	immunoglobuline (H-gamma4_L-kappa)_(H-gamma4_L-lambda2), anti-[*Homo sapiens* F9a (facteur de coagulation F9, facteur de coagulation IX, hémophilie B) activé] et anti-[*Homo sapiens* F10 (facteur de coagulation 10, facteur de coagulation X)], anticorps monoclonal humanisé et *Homo sapiens,* bispécifique, bivalent; chaîne lourde H-gamma4 anti-F9a humanisée (1-447) [VH (*Homo sapiens* IGHV3-23*04 (87.8%) -(IGHD) -IGHJ4*01 (100%), CDR-IMGT [8.8.15] (26-33.51-58.97-111)) (1-122)-*Homo sapiens* IGHG4*01, nG4m(a) CH2 L92, 12-G4v5 h P10, 17-G4v57-1 CH1 K84.2, 18-G4v11 CH1 Q100, CH2 Y84.3, 14-G4v12-1 CH3 K12, 12-G4v6 CH3 K88, 9-G4v78 L107, A114, 10-G4v89 CH3 R118, E120 (CH1 Q84.2>K (180), K100>Q (201) (123-220), charnière 1-12 S10>P (230) (221-232), CH2 F84.3>Y (298), L92 (311) (233-342), CH3 E12>K (358), R88>K (411), M107>L (430), N114>A (436), Q118>R (440), S120>E (442) (343-447)) (123-447)], (136-214')-disulfure avec la chaîne légère L-kappa anti-F9a *Homo sapiens* (1'-214') [V-KAPPA (*Homo sapiens* IGKV3D-11*02 (84.4%) -IGKJ4*01 (100%), CDR-IMGT [6.3.9] (27'-32'.50'-52'.89'-97')) (1'-107') -*Homo sapiens* IGKC*01 (98.1%) Km3 A45.1, V101 KCv57-1 E20, E90 (C-KAPPA S20>E (131'), A45.1 (153'), T90>E (180), V101 (191')) (108'-214')]; chaîne lourde H-gamma4 anti-F10 humanisée (1''-444'') [VH (*Homo sapiens* IGHV1-2*06 (74.5%) -(IGHD) -IGHJ4*01 (80.0%) Q120>E (111''), CDR-IMGT [8.8.12] (26''-33''.51''-58''.97''-108'')) (1''-119'')-*Homo sapiens* IGHG4*01, nG4m(a) CH2 L92, 12-G4v5 h P10, 17-G4v57-2 CH1 E26, K84.2, 18-G4v11 CH1 Q100, CH2 Y84.3, 12-G4v6 CH3 K88, 9-G4v78 CH3 L107, A114, 10-G4v89 CH3 R118, E120, 14-G4v13 CH3 E119 (CH1 K26>E (149''), Q84.2>E (177''), K100>Q (198'') (120''-217''), charnière 1-12 S10>P (227'') (218''-229''), CH2 F84.3>Y (295''), L92 (308'') (230''-339''), CH3 R88>K (408''), M107>L (427''), N114>A (433''), Q118>R (437''), K119>E (438''), S120>E (439'') (340''-444'')) (120''-444'')], (133''-212''')-disulfure avec la chaîne légère L-lambda2 anti-F10 *Homo sapiens* (1''-213''') [V-LAMBDA (*Homo sapiens* IGLV3-9*01 (78.7%) -IGLJ2*01 (81.8%) L124>V (104'''), L127>V (107'''), CDR-IMGT [6.3.10] (26'''-31'''.49'''-51'''.88'''-97''')) (1'''-107''') -*Homo sapiens* IGLC2*01 (98.1%) LC2v57-2 K20, K90 (C-LAMBDA2 T20>K (132'''), S90>K (180''')) (108'''-213''')]; dimère (228-225'': 231-228'')-bisdisulfure, produit dans des cellules ovariennes de hamster chinois (CHO), lignée cellulaire CHO-DXB11, glycoforme alfa *agent antihémophilique*
zemocimig	inmunoglobulina (H-gamma4_L-kappa)_(H-gamma4_L-lambda2), anti-[*Homo sapiens* F9a (factor de coagulación F9, factor de coagulación IX, hemofilia B) activado] y anti-[*Homo sapiens* F10 (factor de coagulación 10, factor de coagulación X)], anticuerpo monoclonal humanizado y *Homo sapiens,* bispecífico, bivalente; cadena pesada H-gamma4 anti-F9a humanizada (1-447) [VH (*Homo sapiens* IGHV3-23*04 (87.8%) -(IGHD) -IGHJ4*01 (100%), CDR-IMGT [8.8.15] (26-33.51-58.97-111)) (1-122)-*Homo sapiens* IGHG4*01, nG4m(a) CH2 L92, 12-G4v5 h P10, 17-G4v57-1 CH1 K84.2, 18-G4v11 CH1 Q100, CH2 Y84.3, 14-G4v12-1 CH3 K12, 12-G4v6 CH3 K88, 9-G4v78 L107, A114, 10-G4v89 CH3 R118, E120 (CH1 Q84.2>K (180), K100>Q (201) (123-220), bisagra 1-12 S10>P (230) (221-232), CH2 F84.3>Y (298), L92 (311) (233-342), CH3 E12>K (358), R88>K (411), M107>L (430), N114>A (436), Q118>R (440), S120>E (442) (343-447)) (123-447)], (136-214')-disulfuro con la cadena ligera L-kappa anti-F9a *Homo sapiens* (1'-214') [V-KAPPA (*Homo sapiens* IGKV3D-11*02 (84.4%) -IGKJ4*01 (100%), CDR-IMGT [6.3.9] (27'-32'.50'-52'.89'-97')) (1'-107') -*Homo sapiens* IGKC*01 (98.1%) Km3 A45.1, V101 KCv57-1 E20, E90 (C-KAPPA S20>E (131'), A45.1 (153'), T90>E (180), V101 (191')) (108'-214')];

cadena pesada H-gamma4 anti-F10 humanizada (1"-444") [VH (*Homo sapiens* IGHV1-2*06 (74.5%) -(IGHD) -IGHJ4*01 (80.0%) Q120>E (111"), CDR-IMGT [8.8.12] (26"-33".51"-58".97"-108")) (1"-119")-*Homo sapiens* IGHG4*01, nG4m(a) CH2 L92, 12-G4v5 h P10, 17-G4v57-2 CH1 E26, K84.2, 18-G4v11 CH1 Q100, CH2 Y84.3, 12-G4v6 CH3 K88, 9-G4v78 CH3 L107, A114, 10-G4v89 CH3 R118, E120, 14-G4v13 CH3 E119 (CH1 K26>E (149"), Q84.2>E (177"), K100>Q (198") (120"-217"), bisagra 1-12 S10>P (227") (218"-229"), CH2 F84.3>Y (295"), L92 (308") (230"-339"), CH3 R88>K (408"), M107>L (427"), N114>A (433"), Q118>R (437"), K119>E (438"), S120>E (439") (340"-444")) (120"-444")], (133"-212"')-disulfuro con la cadena ligera L-lambda2 anti-F10 *Homo sapiens* (1"-213"') [V-LAMBDA (*Homo sapiens* IGLV3-9*01 (78.7%) -IGLJ2*01 (81.8%) L124>V (104"'), L127>V (107"'), CDR-IMGT [6.3.10] (26"'-31"'.49"'-51"'.88"'-97"')) (1"'-107"') -*Homo sapiens* IGLC2*01 (98.1%) LC2v57-2 K20, K90 (C-LAMBDA2 T20>K (132"'), S90>K (180"')) (108"'-213"')]; dímero (228-225": 231-228")-bisdisulfuro, producido en las células ováricas de hámster chino (CHO), línea celular CHO-DXB11, forma glicosilada alfa

agente antihemofílico

2955620-21-8

Heavy chain / Chaîne lourde / Cadena pesada: H-gamma4 anti-F9a (H)

```
QVQLVQSGAE VKKPGASVKL SCKASGYTFT TYDINWVRQA PGQGLEWMGW    50
ISTYSGNTNY AQKFQGRVTM TTDTSTSTAY MELRSLRSDD TAVYYCARDI   100
GRESSSWIFD YWGQGTLVTV SSASTKGPSV FPLAPCSRST SESTAALGCL   150
VKDYFPEPVT VSWNSGALTS GVHTFPAVLK QSSGLYSLSS VVTVPSSSLG   200
TQTYICNVNH KPSNTKVDKR VEPKSCDKPP CPAPEFLGGP SVFLFPPKPK   250
DTLMISRTPE VTCVVVDVSQ EDPEVQFNWY VDGVEVHNAK TKPREEQFNS   300
TYRVVSVLTV LHQDWLNGKE YKCKVSNKGL PSSIEKTISK AKGQPREPQV   350
YTLPPSQEEM TKNQVSLTCL VKGFYPSDIA VEWESNGQPE NNYKTTPPVL   400
DSDGSFFLYS RLTVDKSRWQ EGNVFSCSVM HEALHNHYTQ KSLSLSLG    447

Light chain / Chaîne légère / Cadena ligera: L-kappa anti-F9a (L')

DIVLTQSPAT LSVTPGERAT LSCRASRSVR RLAWYQQKPG QAPRLLIYG    50
ASTRETGIPA RFSGSGSGTD FTLTINPLEA EDAATYYCQQ YRDPPGTFGG   100
GTKVEIERTV AAPSVFIFPP SDEQLKSGTA SVVCLLNNFY PREAKVQWKV   150
DNALQSGNSQ ESVTEQDSKD STYSLSSTLT LSKADYEKHK VYACEVTHQG   200
LSSPVTKSFN RGEC                                          214
```

Heavy chain / Chaîne lourde / Cadena pesada: H-gamma4 anti-F10 (H")

```
QVQLVQSGAE LKKPGASVKV SCKASGYTFT DYYMHWVRQA PGQGLEWMGV    50
INPNSGGTIY NEKFQDRLTM TRDKSTSTAY MELSSLRSED TATYYCARRR   100
GYGTYLDVWG EGTLVTVSSA STKGPSVFPL APSSKSTSGG TAALGCLVED   150
YFPEPVTVSW NSGALTSGVH TFPAVLESSG LYSLSSVVTV PSSSLGTQTY   200
ICNVNHKPSN TKVDKRVESK YGPPCPSCPA PEFLGGPSVF LFPPKPKDTL   250
MISRTPEVTC VVVDVSQEDP EVQFNWYVDG VEVHNAKTKP REEQFNSTYR   300
VVSVLTVLHQ DWLNGKEYKC KVSNKGLPSS IEKTISKAKG QPREPQVYTL   350
PPSQEEMTKN QVSLTCLVKG FYPSDIAVEW ESNGQPENNY KTTPPVLDSD   400
GSFFLYSRLT VDKSRWQEGN VFSCSVMHEA LHNHYTQEEL SLSP         444
```

Light chain / Chaîne légère / Cadena ligera: L-lambda anti-F10 (L"')

```
SYVLTQPPSV SVAPGQTATI TCGGNNIGSK SVHWYQQKPG QAPVLVVHDS    50
ARPSGIPERF SGSNSGNTAT LTISRVEAGD EADYYCQVWD SSSDHVVFGG   100
GTKVTVLGQP KAAPSVTLFP PSSEELQANK ATLVCLISDF YPGAVTVAWK   150
ADSSPVKAGV ETTTPSKQSN NKYAASSYLS LTPEQWKSHR SYSCQVTHEG   200
STVEKTVAPT ECS                                           213
```

Post-translational modifications

Disulfide bridges location / Position des ponts disulfure / Posiciones de los puentes disulfuro

Intra-H (C23-C104) 22-96 149-205 263-323 369-427
227"-96" 146"-202" 260"-320" 366"-424"

Intra-L (C23-C104) 23'-88' 134'-194'
22"'-87"' 135"'-194"'

Inter-H-L (CH1 10-CL 126) 136-214' 133"-212"'

Inter-H-H (h 8, h 11) 228-225" 231-228"

N-terminal glutaminyl cyclization / Cyclisation du glutaminyle N-terminal / Ciclación del glutaminilo N-terminal

Q > pyroglutamyl (pE, 5-oxoprolyl) / pyroglutamyle (pE, 5-oxoprolyle) / piroglutamilo (pE, 5-oxoprolilo)

H VH Q1: 1, 1"

N-glycosylation sites / Sites de N-glycosylation / Posiciones de N-glicosilación

H CH2 N84.4: 299, 296"

Fucosylated complex bi-antennary CHO-type glycans / glycanes de type CHO bi-antennaires complexes fucosylés / glicanos de tipo CHO biantenarios complejos fucosilados.

zilvetriginum

zilvetrigine — 2-(4-*tert*-butyl-5-chloro-2-methylphenyl)-4-oxo-1,4-dihydro-1,6-naphthyridine-5-carboxamide
sodium channel blocker, analgesic

zilvétrigine — 2-(4-*tert*-butyl-5-chloro-2-méthylphényl)-4-oxo-1,4-dihydro-1,6-naphtyridine-5-carboxamide
bloqueur des canaux sodiques, analgésique

zilvetrigina — 2-(4-*terc*-butil-5-cloro-2-metilfenil)-4-oxo-1,4-dihidro-1,6-naftiridina-5-carboxamida
bloqueador del canal de sodio, analgésico

$C_{20}H_{20}ClN_3O_2$ 3002072-52-5

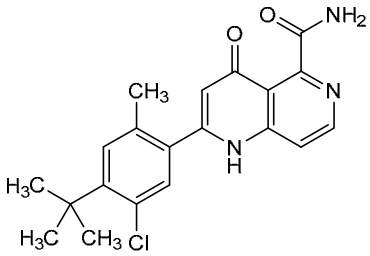

zolacabtagenum autoleucelum #

zolacabtagene autoleucel — autologous CD4+ and CD8+ T lymphocytes obtained by leukapheresis and transduced with a self-inactivating, non-replicating lentiviral vector encoding (i) a CD19 specific chimeric antigen receptor (CAR) and (ii) truncated human epidermal growth factor receptor (EGFRt) separated from the CAR by a T2A self-cleaving peptide, under control of a chimeric promoter composed of the elongation factor 1 alpha (EF-1α) promoter/R region of the human T cell leukaemia virus 1 (HTLV-1 R) and a Woodchuck hepatitis virus posttranscriptional regulatory element (WPRE). The CD19-specific CAR transgene consists of a single-chain variable fragment (scFv) derived from a CD19-specific monoclonal antibody (FMC63), an IgG4 hinge region, a CD28 transmembrane domain, and the intracellular CD137 (4-1BB) co-stimulatory and CD3ζ signalling domains. Both transgenes, the CD19-specific CAR and the EGFRt, are preceded by human granulocyte-macrophage colony-stimulating factor receptor alpha (GMCSFR-alpha) signal peptide sequence. The vector genome also contains a psi packaging signal, a splice donor, partial *gag*, Rev response element (RRE), a DNA FLAP, and a splice acceptor. The vector is flanked by 5' and 3' long terminal repeats (LTRs) and is pseudotyped by vesicular stomatitis virus (VSV) G glycoprotein. The leukapheresis material is sorted to co-select the CD4+ and CD8+ T lymphocytes by positive immunoselection prior to activation with CD3 and CD28 agonists in growth media containing interleukin 2 (IL-2), interleukin 7 (IL-7) and interleukin 15 (IL-15). The mixed CD4+/CD8+ cells are then transduced with the lentiviral vector and minimally expanded in growth media containing IL-2, IL-7 and IL-15. The cell suspension consists of CD4+ and CD8+ lymphocytes that are ≥80% CD3+ and contain ≥10% CD3+CAR+ cells. The transduced T lymphocytes release interferon gamma (IFN-γ) by co-culture with target cells *in vitro*
cell-based gene therapy (antineoplastic)

zolacabtagène autoleucel	lymphocytes T autologues CD4+ et CD8+ obtenus par leucaphérèse et transduits avec un vecteur lentiviral auto-inactivant et non réplicatif codant (i) un récepteur antigénique chimérique (RAC) spécifique de CD19 et (ii) un récepteur du facteur de croissance épidermique humain tronqué (EGFRt) séparé du RAC par un peptide auto-clivant T2A, sous le contrôle d'un promoteur chimérique composé du facteur d'élongation 1-alpha (EF1-α) promoteur/région R du virus T-lymphotrope humain 1 (HTLV-1 R) et d'un élément régulateur post-transcriptionnel du virus de l'hépatite Woodchuck (WPRE). Le transgène RAC spécifique de CD19 est constitué d'un fragment variable à chaîne unique (scFv) dérivé d'un anticorps monoclonal spécifique de CD19 (FMC63), d'une région charnière IgG4, d'un domaine transmembranaire CD28 et les domaines intracellulaires de co-stimulation CD137 (4-1BB), et de signalisation CD3ζ. Les deux transgènes, le RAC spécifiques de CD19 et le EGFRt, sont précédés d'une séquence de peptide signal du récepteur alpha du facteur de stimulation des colonies de granulocytes-macrophages humains (GMCSFR-alpha). Le génome du vecteur contient également un signal d'empaquetage psi, un donneur d'épissage, une partie du gène *gag*, un élément de réponse Rev (RRE), un volet d'ADN, et un accepteur d'épissage. Le vecteur est flanqué de répétitions terminales longues (LTRs) en 5' et 3' et est pseudotypé par la glycoprotéine G du virus de la stomatite vésiculaire (VSV). Le matériel de leucaphérèse est trié pour co-sélectionner les lymphocytes T CD4+ et CD8+ par immunosélection positive avant activation avec les agonistes CD3 et CD28 dans un milieu de croissance contenant de l'interleukine 2 (IL-2), de l'interleukine 7 (IL-7) et de l'interleukine 15 (IL -15). Le mélange de cellules CD4+/CD8+ est ensuite transduit avec le vecteur lentiviral et expansées de façon minimale dans un milieu de croissance contenant de l'IL-2, de l'IL-7 et de l'IL-15. La suspension cellulaire est constituée de lymphocytes CD4+ et CD8+ qui sont ≥80% CD3+ et contiennent ≥10% de cellules CD3+RAC+. Les lymphocytes T transduits libèrent de l'interféron gamma (IFN-γ) par co-culture avec des cellules cibles *in vitro* *thérapie génique à base de cellules (antinéoplasique)*
zolacabtagén autoleucel	linfocitos T CD4+ y CD8+ autólogos obtenidos por leucoaféresis y transducidos con un vector lentiviral auto inactivante, no replicativo que codifica (i) un receptor de antígenos quimérico (CAR) específico de CD19 y (ii) un receptor truncado del factor de crecimiento epidérmico (EGFRt) humano separado del CAR por un péptido de auto-escisión T2A, bajo el control de un promotor quimérico compuesto del factor de elongación 1-alfa (EF1-α) promotor/región R del virus linfotrópico T humano 1 (HTLV-1 R) y un elemento regulador post-transcripcional del virus de la hepatitis de la marmota (WPRE). El transgén CAR específico de CD19 consiste en un fragmento variable de cadena sencilla (scFv) derivado de un anticuerpo monoclonal específico de CD19 (FMC63), una región bisagra de IgG4, un domino transmembrana de CD28 y los dominios intracelulares coestimulador de CD137 (4-1BB) y de señalización de CD3ζ. Ambos transgenes, el CAR específico de CD19 y el EGFRt, están precedidos por una secuencia de péptido señal del receptor alfa del factor estimulador de colonias de granulocitos-macrófagos (GMCSFR-alfa) humano. El genoma del vector también contiene una secuencia de empaquetamiento psi, un donante de procesamiento, un *gag* parcial, un elemento de respuesta Rev (RRE), una solapa de ADN, y un aceptor de procesamiento.El vector está

flanqueado por repeticiones terminales largas (LTRs) en 5' y 3' y está seudotipado con la glicoproteína G del virus de la estomatitis vesicular (VSV).
El material de leucoaféresis es clasificado para la co-selección de linfocitos T CD4+ y CD8+ mediante inmunoselección positiva antes de la activación con agonistas de CD3 y CD28 en medio de crecimiento que contiene interleuquina 2 (IL-2), interleuquina 7 (IL-7) e interleuquina 15 (IL-15). La mezcla de células CD4+/CD8+ después se transducen con el vector lentiviral y se expanden mínimamente en medio de crecimiento que contiene IL-2, IL-7 e IL-15. La suspensión celular consiste en linfocitos T CD4+ y CD8+ que son ≥80% CD3+ y contien ≥10% de células CD3+CAR+. Los linfocitos T transducidos liberan interferón gamma (IFN-γ) mediante co-cultivo con células diana *in vitro terapia génica basada en células (antineoplásico)*

zoldonrasibum

zoldonrasib (2*S*)-2-cyclopentyl-2-{(5*S*)-7-[(2*R*,3*R*)-3-cyclopropyl-1-methylaziridine-2-carbonyl]-2,7-diazaspiro[4.4]nonan-2-yl}-*N*-[(1^2*M*,2^2*S*,4*S*,6^3*S*)-1^2-{5-(4-cyclopropylpiperazin-1-yl)-2-[(1*S*)-1-methoxyethyl]pyridin-3-yl}-10,10-dimethyl-5,7-dioxo-1^1-(2,2,2-trifluoroethyl)-1^1*H*-8-oxa-1(5,3)-indola-2(4,2)-morpholina-6(1,3)-[1,2]diazinanacycloundecaphan-4-yl]acetamide
Kirsten rat sarcoma viral oncogene homolog inhibitor, antineoplastic

zoldonrasib (2*S*)-2-cyclopentyl-2-{(5*S*)-7-[(2*R*,3*R*)-3-cyclopropyl-1-méthylaziridine-2-carbonyl]-2,7-diazaspiro[4.4]nonan-2-yl}-*N*-[(1^2*M*,2^2*S*,4*S*,6^3*S*)-1^2-{5-(4-cyclopropylpipérazin-1-yl)-2-[(1*S*)-1-méthoxyéthyl]pyridin-3-yl}-10,10-diméthyl-5,7-dioxo-1^1-(2,2,2-trifluoroéthyl)-1^1*H*-8-oxa-1(5,3)-indola-2(4,2)-morpholina-6(1,3)-[1,2]diazinanacycloundécaphan-4-yl]acétamide
inhibiteur d'homologue d'oncogène viral du sarcome de rat de Kirsten, antinéoplasique

zoldonrasib (2*S*)-2-ciclopentil-2-{(5*S*)-7-[(2*R*,3*R*)-3-ciclopropil-1-metilaziridina-2-carbonil]-2,7-diazaspiro[4.4]nonan-2-il}-*N*-[(1^2*M*,2^2*S*,4*S*,6^3*S*)-1^2-{5-(4-ciclopropilpiperazin-1-il)-2-[(1*S*)-1-metoxietil]piridin-3-il}-10,10-dimetil-5,7-dioxo-1^1-(2,2,2-trifluoroetil)-1^1*H*-8-oxa-1(5,3)-indola-2(4,2)-morfolina-6(1,3)-[1,2]diazinanaciclоundecafan-4-il]acetamida
inhibidor del homólogo del oncogen vírico del sarcoma de rata Kirsten, antineoplásico

$C_{63}H_{88}F_3N_{11}O_7$ 3034802-05-3

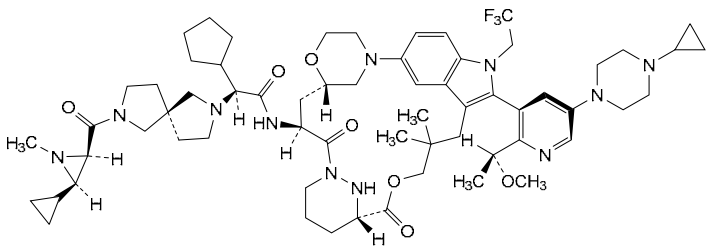

zoninterferonum alfa-2b #

zoninterferon alfa-2b immunoglobulin single-chain VH domain (1-115), anti-(human albumin (ALB, human serum albumin, HSA)) [*Homo sapiens* IGHV3-23*04 - (IGHD) -IGHJ1*01, (CDR-Kabat [5.17.6] (31-35.50-66.99-104))],

fused via the protease-cleavable peptide linker SGGPALFKSSFPPGS (116-130) with human interferon α-2 (IFN-α-2, interferon α-A, LeIF A, IFNA2, IFNA2A, IFNA2B) (131-295) and via the same linker (296-310) with another identical immunoglobulin single chain VH domain (311-425), anti-(human albumin (ALB, human serum albumin, HSA)) [*Homo sapiens* IGHV3-23*04 -(IGHD) -IGHJ1*01, (CDR-Kabat [5.17.6] (341-345.360-376.409-414))], produced by a cell line derived from human embryonic kidney (HEK293) cells; glycoform alfa
immunomodulator, antineoplastic

zoninterféron alfa-2b

domaine VH monocaténaire d'immunoglobuline (1-115), anti-(albumine humaine (ALB, sérum-albumine humaine, SAH)) [*Homo sapiens* IGHV3-23*04 -(IGHD) -IGHJ1*01, (CDR-Kabat [5.17.6] (31-35.50-66.99-104))], fusionné via le coupleur peptidique SGGPALFKSSFPPGS clivable par les protéases (116-130) avec l'interféron α-2 humain (IFN-α-2, interféron α-A, LeIF A, IFNA2, IFNA2A, IFNA2B) (131-295) et via le même coupleur peptidique (296-310) avec un autre domaine VH monocaténaire d'immunoglobuline identique (311-425), anti-(albumine humaine (ALB, sérum albumine humaine, SAH)) [*Homo sapiens* IGHV3-23*04 -(IGHD) -IGHJ1*01, (CDR-Kabat [5.17.6] (341-345.360-376.409-414))], produite par une lignée cellulaire dérivée de cellules rénales embryonnaires humaines (HEK293); glycoforme alfa
immunomodulateur, antinéoplasique

zoninterferón alfa-2b

dominio VH monocatenario de inmunoglobulina (1-115), anti-[albúmina humana (ALB, albúmina sérica humana, ASH)] [*Homo sapiens* IGHV3-23*04 -(IGHD) -IGHJ1*01, (CDR-Kabat [5.17.6] (31-35.50-66.99-104))], fusionado mediante el conector peptídico SGGPALFKSSFPPGS escindible por proteasa (116-130) con interferón α-2 humano (IFN-α-2, interferón α-A, LeIF A, IFNA2, IFNA2A, IFNA2B) (131-295) y a través del mismo conector (296-310) con otro dominio VH monocatenario de inmunoglobulina idéntico (311-425), anti-(albúmina humana (ALB, albúmina sérica humana, ASH) [*Homo sapiens* IGHV3-23*04 -(IGHD) -IGHJ1*01, (CDR-Kabat [5.17.6] (341-345.360-376.409-414))], producido por una línea celular derivada de células renales embrionarias humanas (HEK293); glicoforma alfa
inmunomodulador, antineoplásico

2999644-80-1

Sequence / Séquence / Secuencia

```
EVQLVESGGG LVQPGGSLRL SCAASGFTFS SYAMSWVRQA PGKGLEWVSS   50
ISGSGGSTLY ADSVKGRFTI SRDNSKNTLY LQMNSLRAED TAVYYCTIGG  100
SLSRSSQGTL VTVSSGGGGS LAFKSSFPLA CDLPQTHSLG SRRTLMLLAQ  150
MRRISLFSCL KDRHDFGFPQ EEFGNQFQKA ETIPVLHEMI QQIFNLFSTK  200
DSSAAWDETL LDKFYTELYQ QLNDLEACVI QGVGVTETPL MKEDSILAVR  250
KYFQRITLYL KEKKYSPCAW EVVRAEIMRS FSLSTNLQES LRSKEGGGPA  300
LFKSSFPPGS EVQLVESGGG LVQPGGSLRL SCAASGFTFS SYAMSWVRQA  350
PGKGLEWVSS ISGSGGSTLY ADSVKGRFTI SRDNSKNTLY LQMNSLRAED  400
TAVYYCTIGG SLSRSSQGTL VTVSS                              425
```

Peptide linkers / Coupleurs peptidiques / Enlazadores peptídicos
^{116}SGGPALFKSS FPPGS^{130} (1-15)
^{296}SGGPALFKSS FPPGS^{310} (1-21)

Post-translational modifications
Disulfide bridges location / Position des ponts disulfure / Posiciones de los puentes disulfuro
intra-VH 1: 22-96
intra-IFNA2: 131-228, 159-268
intra-VH 2: 332-406

O-Glycosylation site / Site de O-glycosylation / Posición de O-glicosilación
T236

zovaglutidum

zovaglutide glucagon-like peptide 1(7-37) [human GLP-1(7-37)] (1-31), (A^8>2-MeAla^2, G^{22}>E^{16}, K^{34}>R^{28}, R^{36}>G^{30})-variant, fused to the artificial 40-peptide (GAQP)9GQKP (32-71), substituted at *N*^{6} of each of the two lysyl residues 20 and 70 with a (22*S*)-22,40-dicarboxy-10,19,24-trioxo-3,6,12,15-tetraoxa-9,18,23-triazatetracontan-1-oyl group
glucagon-like peptide 1 (GLP-1) receptor agonist, antidiabetic

zovaglutide peptide similaire au glucagon de type 1(7-37) [GLP-1(7-37) humain] (1-31), variant (A^8>2-MeAla^2, G22>E16, K^{34}>R^{28}, R^{36}>G^{30}), fusionné au 40-peptide artificiel (GAQP)9GQKP (32-71), substitué en *N*^{6} de chacun des deux résidus lysyles 20 et 70 par un groupe (22*S*)-22,40-dicarboxy-10,19,24-trioxo-3,6,12,15-tétraoxa-9,18,23-triazatétracontan-1-oyle
agoniste du récepteur du peptide-1 similaire au glucagon (GLP-1), antidiabétique

zovaglutida péptido similar al glucagón tipo 1(7-37) [GLP-1(7-37) humano] (1-31), variante (A^8>2-MeAla^2, G^{22}>E^{16}, K^{34}>R^{28}, R^{36}>G^{30}), fusionado a un 40-péptido artificial (32-71), sustituido en *N*^{6} de cada uno de los dos residuos lisilo 20 y 70 con un grupo (22*S*)-22,40-dicarboxi-10,19,24-trioxo-3,6,12,15-tetraoxa-9,18,23-triazatetracontan-1-oilo
agonista del receptor del péptido 1 similar al glucagón (GLP-1), antidiabético

$C_{374}H_{584}N_{96}O_{123}$ 3013543-64-8

```
HXEGTFTSDV SSYLEEQAAK EFIAWLVRGG GGAQPGAQPG AQPGAQPGAQ 50
PGAQPGAQPG AQPGAQPGQK P                                 71
```

Modified residues / Résidus modifiés / Restos modificados

X (2)

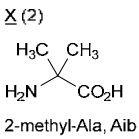

2-methyl-Ala, Aib

K (20, 70)

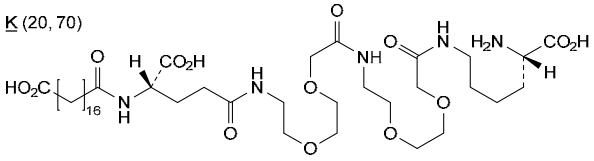

Electronic structure available on MedNet: https://extranet.who.int/soinn/
Structure électronique disponible sur MedNet: https://extranet.who.int/soinn/
Estructura electrónica disponible en MedNet: https://extranet.who.int/soinn/

Proposed International Nonproprietary Names: List 132 –COVID-19 (special edition)
Comments on, or formal objections to, the proposed names may be forwarded by any person to the INN Programme of the World Health Organization within four months of the date of their publication in *WHO Drug Information*, i.e., for **List 132 of Proposed INN not later than 13 June 2025. Publication date:** 14.02.2025

Dénominations communes internationales proposées: Liste 132 - COVID-19 (édition spéciale)
Des observations ou des objections formelles à l'égard des dénominations proposées peuvent être adressées par toute personne au Programme des Dénominations communes internationales de l'Organisation mondiale de la Santé dans un délai de quatre mois à compter de la date de leur publication dans *WHO Drug Information*, c'est à dire pour la **Liste 132 de DCI Proposées le 13 juin 2025 au plus tard. Date de publication :** 14.02.2025

Denominaciones Comunes Internacionales Propuestas: Lista 132 - COVID-19 (edición especial)
Cualquier persona puede dirigir observaciones u objeciones respecto de las denominaciones propuestas, al Programa de Comunes Internacionales de la Organización Mundial de la Salud, en un plazo de cuatro meses, contados desde la fecha de su publicación en *WHO Drug Information*, es decir, para **la Lista 132 de DCI Propuestas el 13 de Junio de 2025 a más tardar.**
Fecha de publicación: 14.02.2025

Proposed INN (Latin, English, French, Spanish)	*Chemical name or description: Action and use: Molecular formula, Chemical Abstracts Service (CAS) registry number: Graphic formula*
DCI Proposée	*Nom chimique ou description: Propriétés et indications: Formule brute, Numéro dans le registre du CAS: Formule développée*
DCI Propuesta	*Nombre químico o descripción: Acción y uso: Fórmula molecular, Número de registro del CAS: Fórmula desarrollada*

cemivameranum #

cemivameran	messenger RNA (mRNA), 5'-capped, encoding a full-length, codon-optimised pre-fusion stabilised conformation variant (K982P and V983P) of the SARS-CoV-2 (severe acute respiratory syndrome coronavirus 2) spike (S) glycoprotein (Omicron KP.2 variant; GISAID: EPI_ISL_18912216), flanked by 5' and 3' untranslated regions and a 3' polyadenylation (polyA) tail; contains N^1-methylpseudouridine instead of uridine (*all*-U>$m^1\Psi$) *immunological agent for active immunization (anti-SARS-CoV-2)*
cémivaméran	ARN messager (ARNm), coiffé en 5', codant une variante de conformation stabilisée de préfusion, de longueur complète, optimisée par codon (K982P et V983P) de la glycoprotéine du spicule (S) du SRAS-CoV-2 (coronavirus 2 du syndrome respiratoire aigu sévère) (variant Omicron KP.2; GISAID: EPI_ISL_18912216), flanqué en 5' et 3' de régions non traduites et d'une queue de polyadénylation (polyA) en 3'; contient de la N^1-méthylpseudouridine en lieu de l'uridine (*tout*-U>$m^1\Psi$) *agent immunologique pour immunisation active (anti-SRAS-CoV-2)*

cemivamerán	ARN mensajero (ARNm), protegido en 5', que codifica, con codones optimizados, para la secuencia completa de una variante estabilizada en conformación pre-fusión (K982P y V983P) de la glicoproteína de la espícula (S) del SRAS-Cov-2 (coronavirus 2 del síndrome respiratorio agudo severo) (variante Omicron KP.2; GISAID: EPI_ISL_18912216), flanqueada por regiones sin traducir 5' y 3' y una cola de poliadenilación (poliA) en 3'; contiene *N*^{1}-metilpseudouridina en lugar de uridina (*todo*-U>m$^{1}\Psi$) *agente inmunológico para inmunización activa (anti-SRAS-CoV-2)* 3036385-75-5

girocovateinum #

girocovatein	severe acute respiratory syndrome coronavirus 2 (SARS-CoV-2), omicron lineage JN.1 (Gisaid: EPI_ISL_18872762) spike (S) glycoprotein receptor binding domain (RBD) fragment (303-520, 1-218 in the current sequence), variant (K^{520}>G^{218}) fused to severe acute respiratory syndrome coronavirus 2 (SARS-CoV-2), omicron lineage JN.1 spike (S) glycoprotein receptor binding domain (RBD) fragment (303-520, 219-436 in the current sequence, K^{436}>del), single chain homodimer, produced in Chinese hamster ovary (CHO) cells, cell line CHO-K1, glycoform alfa *immunological agent for active immunization (anti-SARS-CoV-2)*
girocovatéine	fragment du domaine de liaison au récepteur (RBD) de la glycoprotéine du spicule (S) du coronavirus 2 du syndrome respiratoire aigu sévère (SRAS-CoV-2), lignée omicron JN.1 (Gisaid: EPI_ISL_18872762) (303-520, 1-218 dans la séquence en cours), variant (K^{520}>G^{218}), fusionné au fragment du domaine de liaison au récepteur de la glycoprotéine du spicule (S) du coronavirus 2 du syndrome respiratoire aigu sévère (SRAS-CoV-2), lignée omicron JN.1 (303-520, 220-438 dans la séquence en cours), homodimère monocaténaire, produit dans des cellules ovariennes de hamster chinois (CHO), lignée cellulaire CHO-K1 glycoforme alfa *agent immunologique pour immunisation active (anti-SRAS-CoV-2)*
girocovateína	fragmento del dominio de unión al receptor (RBD) de la glicoproteína de espícula (S) del coronavirus 2 del síndrome respiratorio agudo severo (SRAS-CoV-2), linaje ómicron JN.1 (Gisaid: EPI_ISL_18872762) (303-520, 1-218 en la secuencia actual), variante (K^{520}>G^{218}), fusionado al fragmento del dominio de unión al receptor (RBD) de la glicoproteína de espícula (S) del coronavirus 2 del síndrome respiratorio agudo severo (SRAS-CoV-2), linaje ómicron JN.1 (303-520, 220-438 en la secuencia actual), homodímero de cadena única, producido en células ováricas de hámster Chino (CHO), línea celular CHO-K1, glicoforma alfa *agente inmunológico para inmunización activa (anti-SRAS-CoV-2)*

3038651-03-2

Sequence / Séquence / Secuencia

```
RVQPTESIVR FPNVTNLCPF HEVFNATRFA SVYAWNRTRI SNCVADYSVL  50
YNFAPFFAFK CYGVSPTKLN DLCFTNVYAD SFVIKGNEVS QIAPGQTGNI 100
ADYNYKLPDD FTGCVIAWNS NKLDSKHSGN YDYWYRSFRK SKLKPFERDI 150
STEIYQAGNK PCKGKGPNCY FPLQSYGFRP TYGVGHQPYR VVVLSFELLH 200
APATVCGPKK STNLVKNGRV QPTESIVRFP NVTNLCPFHE VFNATRFASV 250
YAWNRTRISN CVADYSVLYN SAPFFAFKCY GVSPTKLNDL CFTNVYADSF 300
VIKGNEVSQI APGQTGNIAD YNYKLPDDFT GCVIAWNSNK LDSKHSGNYD 350
YWYRSFRKSK LKPFERDIST EIYQAGNKPC KGKGPNCYFP LQSYGFRPTY 400
GVGHQPYRVV VLSFELLHAP ATVCGPKKST NLVKNK                436
```

Mutation / Mutation / Mutación
$K^{520}>\underline{G}^{218}$

Post-translational modifications
Disulfide bridges location / Position des ponts disulfure / Posiciones de los puentes disulfuro
Intra-chain: 18-43, 61-114, 73-206, 162-169, 236-261, 279-332, 291-424, 380-387

N-glycosylation sites / Sites de N-glycosylation / Posiciones de N-glicosilación
N13, N25; N231, N243

O-glycosylation sites / Sites de O-glycosylation / Posiciones de O-glicosilación
T5, T223

C-terminal lysine clipping / Coupure de la lysine C-terminale / Recorte de lisina C-terminal
436

ibramvibartum #

ibramvibart	immunoglobulin G1-kappa, anti-[severe acute respiratory syndrome coronavirus 2 (SARS-CoV-2) spike (S) protein, receptor binding domain (RBD)], *Homo sapiens* monoclonal antibody; H-gamma1 heavy chain *Homo sapiens* (1-454) [VH (*Homo sapiens* IGHV3-21*07 (88.8%) -(IGHD) -IGHJ4*01 (92.9%), CDR-IMGT [8.8.17] (26-33.51-58.97-113)) (1-124) -*Homo sapiens* IGHG1*03, G1m3, nG1m1 CH1 R120, CH3 E12, M14, 9-G1v78 CH3 L107 A114 (CH1 R120 (221) (125-222), hinge 1-15 (223-237), CH2 (238-347), CH3 E12 (363), M14 (365), M107>L (435), N114>A (441) (348-452), CHS (453-454)) (125-454)], (227-217')-disulfide with L-lambda2 light chain *Homo sapiens* (1'-218') [V-LAMBDA (*Homo sapiens* IGLV1-40*01 (92.8%) -IGLJ1*01 (91.7%), CDR-IMGT [9.3.12] (26'-34'.52'-54'.91'-102')) (1'-112') -*Homo sapiens* IGLC2*01 (100%) (C-LAMBDA2) (113'-218')]; dimer (233-233'':236-236'')-bisdisulfide, produced in Chinese hamster ovary (CHO) cells, cell line CHO-K1, glycoform alfa *antiviral*
ibramvibart	immunoglobuline G1-kappa, anti-[domaine de liaison au récepteur (RBD) de la glycoprotéine spike (S) du coronavirus 2 du syndrome respiratoire aigu sévère (SRAS-CoV-2)], anticorps monoclonal *Homo sapiens*; chaîne lourde H-gamma1 *Homo sapiens* (1-454) [VH (*Homo sapiens* IGHV3-21*07 (88.8%) -(IGHD) -IGHJ4*01 (92.9%), CDR-IMGT [8.8.17] (26-33.51-58.97-113)) (1-124) -*Homo sapiens* IGHG1*03, G1m3, nG1m1 CH1 R120, CH3 E12, M14, 9-G1v78 CH3 L107 A114 (CH1 R120 (221) (125-222), charnière 1-15 (223-237), CH2 (238-347), CH3 E12 (363), M14 (365), M107>L (435), N114>A (441) (348-452), CHS (453-454)) (125-454)], (227-217')-disulfure avec la chaîne légère L-lambda2 *Homo sapiens* (1'-218') [V-LAMBDA (*Homo sapiens* IGLV1-40*01 (92.8%) -IGLJ1*01 (91.7%), CDR-IMGT [9.3.12] (26'-34'.52'-54'.91'-102')) (1'-112') -*Homo sapiens* IGLC2*01 (100%) (C-LAMBDA2) (113'-218')];

dimère (233-233'':236-236'')-bisdisulfure, produit dans des cellules ovariennes de hamster chinois (CHO), lignée cellulaire CHO-K1, glycoforme alfa
antiviral

ibramvibart

immunoglobulina G1-kappa, anti-[dominio de unión al receptor (RBD) de la glicoproteína spike (S) del coronavirus 2 (humano) del síndrome respiratorio agudo severo (SRAS-CoV-2)], anticuerpo monoclonal *Homo sapiens*;
cadena pesada H-gamma1 *Homo sapiens* (1-454) [VH (*Homo sapiens* IGHV3-21*07 (88.8%) -(IGHD) -IGHJ4*01 (92.9%), CDR-IMGT [8.8.17] (26-33.51-58.97-113)) (1-124) -*Homo sapiens* IGHG1*03, G1m3, nG1m1 CH1 R120, CH3 E12, M14, 9-G1v78 CH3 L107 A114 (CH1 R120 (221) (125-222), bisagra 1-15 (223-237), CH2 (238-347), CH3 E12 (363), M14 (365), M107>L (435), N114>A (441) (348-452), CHS (453-454)) (125-454)], (227-217')-disulfuro con la cadena ligera L-lambda2 *Homo sapiens* (1'-218') [V-LAMBDA (*Homo sapiens* IGLV1-40*01 (92.8%) -IGLJ1*01 (91.7%), CDR-IMGT [9.3.12] (26'-34'.52'-54'.91'-102')) (1'-112') -*Homo sapiens* IGLC2*01 (100%) (C-LAMBDA2) (113'-218')]; dímero (233-233'':236-236'')-bisdisulfuro, producido en las células ováricas de hámster chino (CHO), línea celular CHO-K1, forma glicosilada alfa
antiviral

3031270-42-2

Heavy chain / Chaîne lourde / Cadena pesada

```
EVQLVESGGG LVKPGGSLRL SCAASGFEFG SYEMNWVRQA PGKGLEWVSS  50
ISEDGYTTYY PDSLKGRFTI SRDSAKNSLY LQMNSLRADD TAVYYCARDF 100
GGDTNWAGTG FTYWGQGTLV TVSSASTKGP SVFPLAPSSK STSGGTAALG 150
CLVKDYFPEP VTVSWNSGAL TSGVHTFPAV LQSSGLYSLS SVVTVPSSSL 200
GTQTYICNVN HKPSNTKVDK RVEPKSCDKT HTCPPCPAPE LLGGPSVFLF 250
PPKPKDTLMI SRTPEVTCVV VDVSHEDPEV KFNWYVDGVE VHNAKTKPRE 300
EQYNSTYRVV SVLTVLHQDW LNGKEYKCKV SNKALPAPIE KTISKAKGQP 350
REPQVYTLPP SREEMTKNQV SLTCLVKGFY PSDIAVEWES NGQPENNYKT 400
TPPVLDSDGS FFLYSKLTVD KSRWQQGNVF SCSVLHEALH AHYTQKSLSL 450
SPGK                                                    454
```

Light chain / Chaîne légère / Cadena ligera

```
QSVLTQPPSV SGAPGQRITI SCEGSSSNIG AGYDVHWYQQ LPGTAPKLLI  50
YGSSVRNYGV PDRFSGSKSG TSASLAITGL QAEDEADYYC QSYDSDLGIL 100
YTFGTGTKVT VLGQPKAAPS VTLFPPSSEE LQANKATLVC LISDFYPGAV 150
TVAWKADSSP VKAGVETTTP SKQSNNKYAA SSYLSLTPEQ WKSHRSYSCQ 200
VTHEGSTVEK TVAPTECS                                    218
```

Post-translational modifications
Disulfide bridges location / Position des ponts disulfure / Posiciones de los puentes disulfuro
Intra-H (C23-C104) 22-96 151-207 268-328 374-432
22"-96" 151"-207" 268"-328" 374"-432"
Intra-L (C23-C104) 22'-90' 140'-199'
22'"-90'" 140'"-199'"
Inter-H-L (h 5-CL 126) 227-217' 227"-217'"
Inter-H-H (h 11, h 14) 233-233" 236-236"

N-terminal glutaminyl cyclization / Cyclisation du glutaminyle N-terminal / Ciclación del glutaminilo N-terminal
Q > pyroglutamyl (pE, 5-oxoprolyl) / pyroglutamyle (pE, 5-oxoprolyle) / piroglutamilo (pE, 5-oxoprolilo)
L VL V-LAMBDA Q1: 1', 1'"

N-glycosylation sites / Sites de N-glycosylation / Posiciones de N-glicosilación
H CH2 N84.4: 304, 304"
Fucosylated complex bi-antennary CHO-type glycans / glycanes de type CHO bi-antennaires complexes fucosylés / glicanos de tipo CHO biantenarios complejos fucosilados

C-terminal lysine clipping / Coupure de la lysine C-terminale / Recorte de lisina C-terminal
H CHS K2: 454, 454"

rubravameranum #

rubravameran — self-amplifying messenger RNA (mRNA), 5'-capped, encoding Venezuelan equine encephalitis virus (VEEV; strain TC-83) RNA-dependent RNA polymerase complex (VEEV non-structural proteins 1-4 [nsP1, nsP2, nsP3 and nsP4]) and a codon-optimised receptor binding domain (RBD) of the SARS-CoV-2 (severe acute respiratory syndrome coronavirus 2) spike (S) glycoprotein (Omicron XBB.1.5 variant derived from GenBank ID: OQ054680.1; amino acids 323-527), preceded by the SARS-CoV-2 signal peptide and fused to an H1N1 influenza virus hemagglutinin transmembrane domain and a universal (pan) HLA DR-binding epitope (PADRE), flanked by VEEV 5' and 3' untranslated regions (UTRs) and terminated with a 3' polyadenylation (polyA) tail; contains 5-methylcytosine instead of cytosine (*all*-C>5mC). Generation of the SARS-CoV-2 RBD mRNA is under control of the VEEV subgenomic promoter
immunological agent for active immunization (anti-SARS-CoV-2)

rubravaméran — ARN messager auto-amplifiant (ARNm), avec une coiffe en 5', codant pour le complexe d'ARN polymérase ARN-dépendante (protéines non structurales 1-4 [nsP1, nsP2, nsP3 et nsP4]) du virus de l'encéphalite équine vénézuélienne (VEEV; souche TC-83) et un domaine de liaison au récepteur (RBD), optimisé pour les codons, de la glycoprotéine du spicule (S) (variante Omicron XBB.1.5 dérivée de GenBank ID: OQ054680.1; acides aminés 323 à 527), du SRAS-CoV-2 (coronavirus 2 du syndrome respiratoire aigu sévère), précédée du peptide signal du SRAS-CoV-2 et fusionnée à un domaine transmembranaire d'hémagglutinine du virus de la grippe H1N1, et à un épitope universel (pan) de liaison au HLA DR (PADRE), flanqué des régions non traduites de VEEV (UTRs) en 3' et 5' et terminées par une queue de polyadénylation (polyA) en 3'; contient de la 5-méthylcytosine au lieu de la cytosine (*tout*-C>5mC). La génération de l'ARNm du SRAS-CoV-2 RBD est sous le contrôle du promoteur subgénomique du VEEV
agent immunologique pour immunisation active (anti-SRAS-CoV-2)

rubravamerán — ARN mensajero (ARNm) auto amplificante, protegido mediante caperuza en 5', que codifica el complejo de ARN polimerasa dependiente de ARN (proteínas no estructurales 1-4 de VEEV [nsP1, nsP2, nsP3 y nsP4]) del virus de la encefalitis equina venezolana (VEEV; cepa TC-83) y un dominio de unión al receptor con codones optimizados (RBD) de la glicoproteína de la espícula (S) (variante Omicron XBB.1.5 derivada de GenBank ID: OQ054680.1; aminoácidos 323-527) del SRAS-CoV-2 (coronavirus 2 del síndrome respiratorio agudo severo), precedido por el péptido señal del SRAS-CoV-2 y fusionado a un dominio transmembrana de la hemaglutinina del virus de la gripe H1N1 y un epítopo universal (pan) de unión a HLA DR (PADRE), flanqueado por regiones no traducidas (UTRs) 5' y 3' de VEEV y terminado con una cola de poliadenilación 3' (poliA); contiene 5-metilcitosina en lugar de citosina (*todos*-C>5 mC). La generación del ARNm de RBD del SRAS-CoV-2 está bajo el control del promotor subgenómico de VEEV
agente inmunológico para inmunización activa (anti-SRAS-CoV-2)

3004804-43-4

tagovameranum #

tagovameran — self-amplifying messenger RNA (mRNA), 5'-capped, encoding codon-optimised Venezuelan equine encephalitis virus (VEEV) RNA-dependent RNA polymerase complex (VEEV proteins nsP1, nsP2, nsP3 and nsP4) and a full-length codon-optimised pre-fusion stabilised conformation variant (K981P and V982P) of the SARS-CoV-2 (severe acute respiratory

	syndrome coronavirus 2) spike (S) glycoprotein BA.4/BA.5 variant (derived from GenBank ID: UVX18152) containing furin cleavage-inactivating mutations (R677G, R678S and R680S), flanked by 5' and 3' untranslated regions and a 3' polyadenylation (poly(A) tail; generation of capped S glycoprotein mRNA is under control of a VEEV subgenomic promoter *immunological agent for active immunization (anti-SARS-CoV-2)*
tagovaméran	ARN messager (ARNm) auto-amplifiant, avec une coiffe en 5', codant l'ARN polymérase dépendante de l'ARN du virus de l'encéphalite équine vénézuélienne (VEEV) optimisé par codon (protéines nsP1, nsP2, nsP3 et nsP4 de VEEV) et une variante de conformation stabilisée de préfusion (K981P et V982P), de séquence complète, optimisée par codon, de la glycoprotéine du spicule (S) du SRAS-CoV-2 (coronavirus 2 du syndrome respiratoire aigu sévère) variant BA.4/BA.5 (dérivé de la base de données GenBank ID: UVX18152), contenant des mutations inactivant le clivage par la furine (R677G, R678S et R680S), flanqué en 5' et 3' par des régions non traduites et une queue de polyadénylation (polyA) en 3'; la génération de l'ARNm de la glycoprotéine S coiffée est sous le contrôle du promoteur subgénomique de VEEV *agent immunologique pour immunisation active (anti-SRAS-CoV-2)*
tagovamerán	ARN mensajero (ARNm) auto amplificante, protegido en 5', que codifica, con codones optimizados, para una ARN polimerasa dependiente de ARN del virus de la encefalitis equina venezolana (VEEV) (proteínas nsP1, nsP2, nsP3 y nsP4 de VEEV) y para una secuencia completa, con codones optimizados, de una variante estabilizada en conformación pre-fusión (K981P y V982P) de la glicoproteína de la espícula (S) del SRAS-CoV-2 (coronavirus 2 del síndrome respiratorio agudo severo) variante BA.4/BA.5 (derivada de GenBank ID: UVX18152) que contiene mutaciones inactivantes de la rotura por furina (R677G, R678S y R680S), flanqueado por regiones sin traducir 5' y 3' y una cola de poliadenilación (poliA) en 3'; la generación del ARNm protegido de la glicoproteína S está bajo el control del promotor subgenómico de VEEV *agente inmunológico para inmunización activa (anti-SRAS-CoV-2)*
	2923496-70-0

Names for chemical modifications of INN (substituent groups, counterions, adduct partners, etc.):

Many pharmaceutical substances for which an International Nonproprietary Name (INN) has been established are used as modified derivatives (salts, esters, protein-drug conjugates, solvates, etc.). The chemical modification (including counterions) involved may be of complex nature and it is then inconvenient to use its systematic chemical name. Consequently, shorter nonproprietary names for such modifications have been devised, and these are recommended for creating modified International Nonproprietary Names (INNM).

Dénominations applicables aux modifications chimiques des DCI (groupes substituants, contre-ions, adduits, etc.) :

Certaines substances pour lesquelles une dénomination commune internationale proposée a été établie sont parfois utilisées comme dérivés modifiés (sels, esters, médicaments conjugués à des protéines, produits de solvatation, etc.). Les modifications chimiques (incluant les contre-ions) sont alors quelques fois si complexes qu'il est malcommode de les désigner conformément à la nomenclature chimique systématique. Des dénominations communes abrégées ont donc été formées ou choisies pour certaines d'entre elles et il est suggéré de les employer pour créer les dénominations communes internationales modifiées (DCIM).

Denominaciones aplicables a modificaciones químicas de las DCI (grupos sustituyentes, contraiones, aductos, etc.):

Muchas sustancias farmacéuticas para las cuales hay establecidas una denominación común internacional (DCI) pueden usarse como derivados modificados (sales, ésteres, medicamentos conjugados con proteínas, solvatos, etc.). Las modificaciones químicas (incluidos los contraiones) implicadas pueden ser de naturaleza compleja y por tanto es inapropiado utilizar su nombre químico sistemático. Como consecuencia, se han diseñado denominaciones abreviadas para estas modificaciones y se recomiendan para la creación de Denominaciones Comunes Internacionales modificadas (DCIM).

etocomilum

etocomil	{[(4*RS*)-4-ethyloctanoyl]oxy}methyl
étocomil	{[(4*RS*)-4-éthyloctanoyl]oxy}méthyle
etocomilo	{[(4*RS*)-4-etiloctanoil]oxi}metilo

-$C_{11}H_{21}O_3$

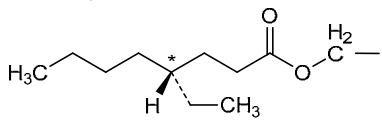

and epimer at C*
et l'épimère en C*
y el epímero en C*

filricianinum

filricianine	4-[(2Ξ,3*RS*)-2-{(2Ξ)-2-[3-{(1Ξ)-2-[3,3-dimethyl-1-(3-sulfonatopropyl)-3*H*-indol-1-ium-2-yl]ethen-1-yl}-2-(4-sulfophenoxy)cyclohex-2-en-1-ylidene]ethylidene}-3-methyl-1-(3-sulfopropyl)-2,3-dihydro-1*H*-indol-3-yl]butanoyl
filricianine	4-[(2Ξ,3*RS*)-2-{(2Ξ)-2-[3-{(1Ξ)-2-[3,3-diméthyl-1-(3-sulfonatopropyl)-3*H*-indol-1-ium-2-yl]éthén-1-yl}-2-(4-sulfophénoxy)cyclohex-2-én-1-ylidène]éthylidène}-3-méthyl-1-(3-sulfopropyl)-2,3-dihydro-1*H*-indol-3-yl]butanoyle
filricianina	4-[(2Ξ,3*RS*)-2-{(2Ξ)-2-[3-{(1Ξ)-2-[3,3-dimetil-1-(3-sulfonatopropil)-3*H*-indol-1-ium-2-il]eten-1-il}-2-(4-sulfofenoxi)ciclohex-2-en-1-ilidene]etilidene}-3-metil-1-(3-sulfopropil)-2,3-dihidro-1*H*-indol-3-il]butanoilo

$C_{71}H_{95}N_7O_{22}S_3$

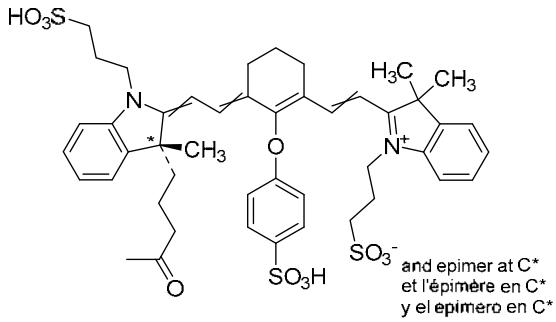

guraxetanum

guraxetan	(4*R*)-4-carboxy-4-[4,7,10-tris(carboxymethyl)-1,4,7,10-tetraazacyclododecan-1-yl]butanoyl
guraxétan	(4*R*)-4-carboxy-4-[4,7,10-tris(carboxyméthyl)-1,4,7,10-tétraazacyclododécan-1-yl]butanoyle
guraxetán	(4*R*)-4-carboxi-4-[4,7,10-tris(carboximetil)-1,4,7,10-tetraazaciclododecan-1-il]butanoilo

$C_{19}H_{31}N_4O_9$

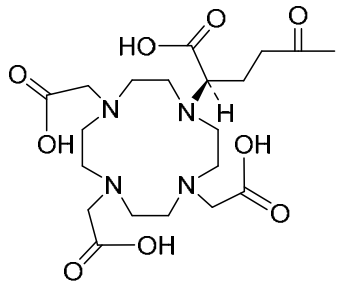

histidinas

histidinate	L-histidinate
histidinate	L-histidinate
histidinato	L-histidinato

$C_6H_8N_3O_2^-$

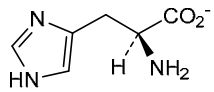

isoboxilum

isoboxil	[(2-methylpropanoyl)oxy]methyl
isoboxil	[(2-méthylpropanoyl)oxy]méthyle
isoboxilo	[(2-metilpropanoil)oxi]metilo

$C_5H_9O_2$

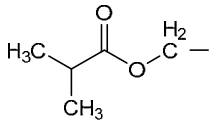

miristatum

miristate	tetradecanoate (ester or salt)
miristate	tétradécanoate (ester ou sel)
miristato	tetradecanoato (éster o sal)

$C_{14}H_{27}O_2$ or / ou / o $C_{14}H_{27}O_2^-$

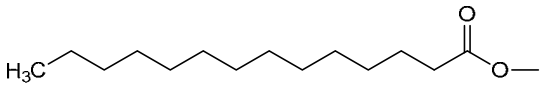

plevistinagum

plevistinag (3*RS*)-1-[(28*S*)-28-{[(2*S*)-1-{[(2*S*)-1-{4-[({[(2-{cyclo[(*P*$^{3'}$*R*)-2'-deoxy-2'-fluoro-*P*-thioadenylyl-(3'→5')-(*P*$^{2'}$*R*)-7-fluoro-7-carba-*P*-thioinosinylyl-(2'→5')]-*N*$^{6.1}$-carbonyl}phenyl)methyl](methyl)carbamoyl}oxy)methyl]anilino}-1-oxopropan-2-yl]amino}-3-methyl-1-oxobutan-2-yl]carbamoyl}-26-oxo-2,5,8,11,14,17,20,23-octaoxa-27-azadotriacontan-32-yl]-2,5-dioxopyrrolidin-3-yl

plévistinag (3*RS*)-1-[(28*S*)-28-{[(2*S*)-1-{[(2*S*)-1-{4-[({[(2-{cyclo[(*P*$^{3'}$*R*)-2'-désoxy-2'-fluoro-*P*-thioadénylyl-(3'→5')-(*P*$^{2'}$*R*)-7-fluoro-7-carba-*P*-thioinosinylyl-(2'→5')]-*N*$^{6.1}$-carbonyl}phényl)méthyl](méthyl)carbamoyl}oxy)méthyl]anilino}-1-oxopropan-2-yl]amino}-3-méthyl-1-oxobutan-2-yl]carbamoyl}-26-oxo-2,5,8,11,14,17,20,23-octaoxa-27-azadotriacontan-32-yl]-2,5-dioxopyrrolidin-3-yle

plevistinag (3*RS*)-1-[(28*S*)-28-{[(2*S*)-1-{[(2*S*)-1-{4-[({[(2-{ciclo[(*P*$^{3'}$*R*)-2'-desoxi-2'-fluoro-*P*-tioadenilil-(3'→5')-(*P*$^{2'}$*R*)-7-fluoro-7-carba-*P*-tioinosinilil-(2'→5')]-*N*$^{6.1}$-carbonil}fenil)metil](metil)carbamoil}oxi)metil]anilino}-1-oxopropan-2-il]amino}-3-metil-1-oxobutan-2-il]carbamoil}-26-oxo-2,5,8,11,14,17,20,23-octaoxa-27-azadotriacontan-32-il]-2,5-dioxopirrolidin-3-ilo

$C_{74}H_{99}F_2N_{14}O_{27}P_2S_2$

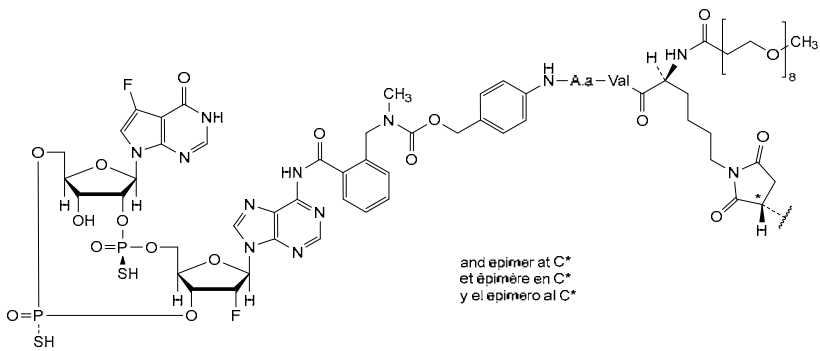

repodatecanum

repodatecan 2-(2-{8-[(10*S*)-10-benzyl-1-{[(1*S*,9*S*)-9-ethyl-5-fluoro-9-hydroxy-4-methyl-10,13-dioxo-2,3,9,10,13,15-hexahydro-1*H*,12*H*-benzo[*de*]pyrano[3',4':6,7]indolizino[1,2-*b*]quinolin-1-yl]amino}-1,6,9,12,15,18,34-heptaoxo-3,21,24,27,30-pentaoxa-5,8,11,14,17,33-hexaazaheptatriacontan-37-oyl]-8,9-dihydro-1(*or* 3)*H*-dibenzo[*b*,*f*][1,2,3]triazolo[4,5-*d*]azocin-1(*or* 3)-yl}acetamido)-2-deoxy-β-D-galactopyranosyl

répodatécan

2-(2-{8-[(10*S*)-10-benzyl-1-{[(1*S*,9*S*)-9-éthyl-5-fluoro-9-hydroxy-4-méthyl-10,13-dioxo-2,3,9,10,13,15-hexahydro-1*H*,12*H*-benzo[*de*]pyrano[3',4':6,7]indolizino[1,2-b]quinoléin-1-yl]amino}-1,6,9,12,15,18,34-heptaoxo-3,21,24,27,30-pentaoxa-5,8,11,14,17,33-hexaazaheptatriacontan-37-oyl]-8,9-dihydro-1(*ou* 3)*H*-dibenzo[*b*,*f*][1,2,3]triazolo[4,5-*d*]azocin-1(*ou* 3)-yl}acétamido)-2-désoxy-β-D-galactopyranosyle

repodatecán

2-(2-{8-[(10*S*)-10-bencil-1-{[(1*S*,9*S*)-9-etil-5-fluoro-9-hidroxi-4-metil-10,13-dioxo-2,3,9,10,13,15-hexahidro-1*H*,12*H*-benzo[*de*]pirano[3',4':6,7]indolizino[1,2-*b*]quinolein-1-il]amino}-1,6,9,12,15,18,34-heptaoxo-3,21,24,27,30-pentaoxa-5,8,11,14,17,33-hexaazaheptatriacontan-37-oil]-8,9-dihidro-1(*o* 3)*H*-dibenzo[*b*,*f*][1,2,3]triazolo[4,5-*d*]azocin-1(*o* 3)-il}acetamido)-2-desoxi-β-D-galactopiranosilo

$C_{80}H_{92}N_{13}O_{22}$

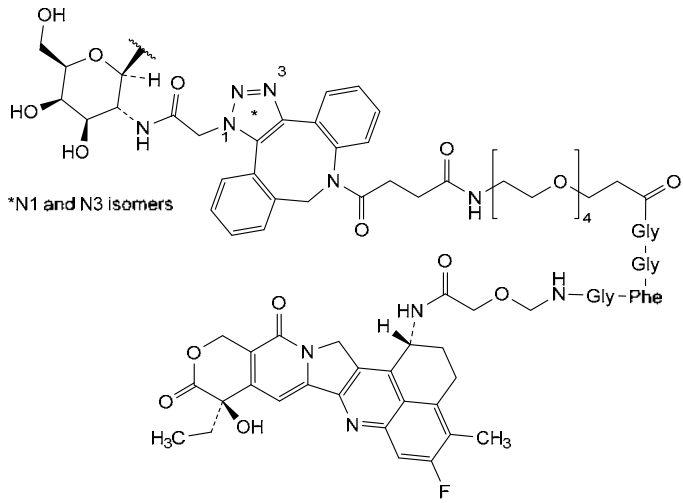

tivedotinum

tivedotin

2-{[(2*S*)-1-{[(2*S*)-1-{4-[(5*S*,8*S*,11*S*,12*R*)-11-[(2*S*)-butan-2-yl]-12-(2-{(2*S*)-2-[(1*R*,2*R*)-3-{[(1*S*,2*R*)-1-hydroxy-1-phenylpropan-2-yl]amino}-1-methoxy-2-methyl-3-oxopropyl]pyrrolidin-1-yl}-2-oxoethyl)-4,10-dimethyl-3,6,9-trioxo-5,8-di(propan-2-yl)-2,13-dioxa-4,7,10-triazatetradecan-1-yl]anilino}-5-(carbamoylamino)-1-oxopentan-2-yl]amino}-3-methyl-1-oxobutan-2-yl]amino}-2-oxoethyl;
2-oxo-2-({L-valyl-N^5-carbamoyl-L-ornithyl[(4-aminophenyl)methoxy]carbonyl-*N*-methyl-L-valyl-L-valyl-(3*R*,4*S*,5*S*)-3-methoxy-5-methyl-4-(methylamino)heptanoyl-(2*R*,3*R*)-*N*-[(1*S*,2*R*)-1-hydroxy-1-phenylpropan-2-yl]-3-methoxy-2-methyl-3-[(2*S*)-pyrrolidin-2-yl]propanamide}-$N^{2.1}$-yl)ethyl

tivédotine

2-{[(2*S*)-1-{[(2*S*)-1-{4-[(5*S*,8*S*,11*S*,12*R*)-11-[(2*S*)-butan-2-yl]-12-(2-{(2*S*)-2-[(1*R*,2*R*)-3-{[(1*S*,2*R*)-1-hydroxy-1-phénylpropan-2-yl]amino}-1-méthoxy-2-méthyl-3-oxopropyl]pyrrolidin-1-yl}-2-oxoéthyl)-4,10-diméthyl-3,6,9-trioxo-5,8-di(propan-2-yl)-2,13-dioxa-4,7,10-triazatétradécan-1-yl]anilino}-5-(carbamoylamino)-1-oxopentan-2-yl]amino}-3-méthyl-1-oxobutan-2-yl]amino}-2-oxoéthyle;
2-oxo-2-({L-valyl-N^5-carbamoyl-L-ornithyl[(4-aminophényl)méthoxy]carbonyl-*N*-méthyl-L-valyl-L-valyl-(3*R*,4*S*,5*S*)-3-méthoxy-5-méthyl-4-(méthylamino)heptanoyl-(2*R*,3*R*)-*N*-[(1*S*,2*R*)-1-hydroxy-1-phénylpropan-2-yl]-3-méthoxy-2-méthyl-3-[(2*S*)-pyrrolidin-2-yl]propanamide}-$N^{2.1}$-yl)éthyle

tivedotina

2-{[(2*S*)-1-{[(2*S*)-1-{4-[(5*S*,8*S*,11*S*,12*R*)-11-[(2*S*)-butan-2-il]-12-(2-{(2*S*)-2-[(1*R*,2*R*)-3-{[(1*S*,2*R*)-1-fenil-1-hidroxopropan-2-il]amino}-1-metoxi-2-metil-3-oxopropil]pirrolidin-1-il}-2-oxoetil)-4,10-dimetil-3,6,9-trioxo-5,8-di(propan-2-il)-2,13-dioxa-4,7,10-triazatetradecan-1-il]anilino}-5-(carbamoilamino)-1-oxopentan-2-il]amino}-3-metil-1-oxobutan-2-il]amino}-2-oxoetilo;
2-oxo-2-({L-valil-N^5-carbamoil-L-ornitil[(4-aminofenil)metoxi]carbonil-*N*-metil-L-valil-L-valil-(3*R*,4*S*,5*S*)-5-metil-4-(metilamino)-3-metoxiheptanoil-(2*R*,3*R*)-*N*-[(1*S*,2*R*)-1-fenil-1-hidroxipropan-2-il]-2-metil-3-metoxi-3-[(2*S*)-pirrolidin-2-il]propanamida}-$N^{2.1}$-il)etilo

$C_{60}H_{95}N_{10}O_{13}$

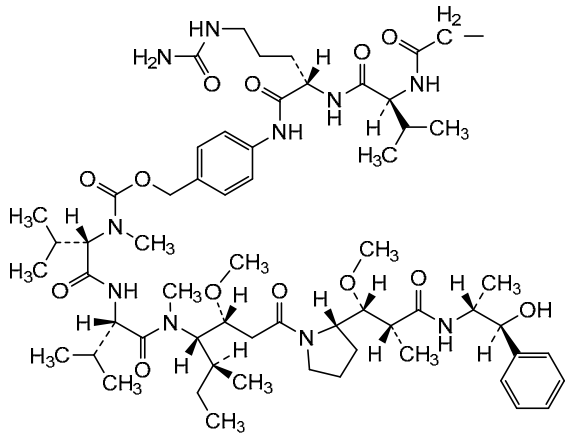

AMENDMENTS TO PREVIOUS LISTS
MODIFICATIONS APPORTÉES AUX LISTES ANTÉRIEURES
MODIFICACIONES A LAS LISTAS ANTERIORES

Proposed International Nonproprietary Names (Prop. INN): List 118
Dénominations communes internationales proposées (DCI Prop.): Liste 118
Denominaciones Comunes Internacionales Propuestas (DCI Prop.): Lista 118
(WHO Drug Information, Vol. 31, No. 4, 2017)

p.702-703 **rebisufligenum etisparvovecum #**

rebisufligene etisparvovec
rébisufligène étisparvovec
rebisufligén etisparvovec

Please note that the MedNet file has been updated
Veuillez noter que le fichier MedNet a été mis à jour
Tenga en cuenta que se ha actualizado el archivo MedNet

Proposed International Nonproprietary Names (Prop. INN): List 120
Dénominations communes internationales proposées (DCI Prop.): Liste 120
Denominaciones Comunes Internacionales Propuestas (DCI Prop.): Lista 120
(WHO Drug Information, Vol. 32, No. 4, 2018)

p.510-512 **teclistamabum #**
teclistamab

replace the chemical name by the following one

immunoglobulin G4-lambda, anti-[*Homo sapiens* TNFRSF17 (TNF receptor superfamily member 17, tumor necrosis factor receptor superfamily, member 17, B cell maturation antigen, BCMA, BCM, TNFRSF13A, CD269)] and anti-[*Homo sapiens* CD3 epsilon (CD3E, Leu-4)], monoclonal antibody, bispecific; gamma4 heavy chain anti-TNFRSF17 (1-448) [VH (*Homo sapiens* IGHV4-39*01 (97.0%) -(IGHD) -IGHJ4*01 (100%)) [10.7.13] (1-121) -*Homo sapiens* IGHG4*01, nG4m(a) CH2 L92, G4v5 h P10, G4v4 CH2 A1.3, A1.2 (CH1 (122-219), hinge S10>P (229) (220-231), CH2 L92 (310), F1.3>A (235), L1.2>A (236) (232-341), CH3 (342-446), CHS (447-448)) (122-448)], (135-213')-disulfide with lambda light chain anti-TNFRSF17 (1'-214') [V-LAMBDA (*Homo sapiens* IGLV3-21*02 (96.9%) -IGLJ2*01 (100.0%)) [6.3.11] (1'-108') -*Homo sapiens* IGLC2*01 (99.1%) A43>G (152) (109'-214')];
gamma4 heavy chain anti-CD3E (1"-452") [VH (*Mus musculus* IGHV10-1*02 (89.8%) -(IGHD) -IGHJ3*01 (93.3%)/*Homo sapiens* IGHV3-72*01 (88.0%) -(IGHD) -IGHJ6*01 (90.9%)) [8.10.16] (1"-125") -*Homo sapiens* IGHG4*01, nG4m(a) CH2 L92, G4v5 h P10, G4v4 CH2 A1.3, A1.2, G4v10 CH3 F85.1, K88 (CH1 (126-223), hinge S10>P (233) (224-235), CH2 L92 (314), F1.3>A (239), L1.2>A (240) (236-345), CH3 F85.1>L (410), R88>K (414) (346-450), CHS (451-452)) (126"-452")], (139"-214"')-disulfide with lambda light chain anti-CD3 (1"'-215"') [V-LAMBDA (*Homo sapiens* IGLV7-43*01 (81.9%) -IGLJ3*02 (100%)) [9.3.9] (1"'-109"') -*Homo sapiens* IGLC2*01 (100%) (110"'-215"')]; dimer (**227-231":230-234"**)-bisdisulfide

Proposed International Nonproprietary Names (Prop. INN): List 129
Dénominations communes internationales proposées (DCI Prop.): Liste 129
Denominaciones Comunes Internacionales Propuestas (DCI Prop.): Lista 129
(WHO Drug Information, Vol. 37, No. 2, 2023)

p.340-341 **cemacabtagenum ansegedleucelum #**

cemacabtagene ansegedleucel	*replace the chemical name by the following one*
cémacabtagène anségedleucel	*remplacer le nom chimique par le suivant*
cemacabtagén ansegedleucel	*sustitúyase el nombre químico por el siguiente*

EN, lines 12-18	The expressed transgene comprises a mouse kappa light chain leader sequence, an anti-CD19 single chain variable fragment (scFv) derived from clone 4G7, a CD8α hinge and transmembrane domain, **and a 4-1BB (CD137) co-stimulatory and CD3ζ (TCRζ) intracellular signalling domain,** under control of the human elongation factor 1 alpha (EF1α) short (EFS) promoter.
EN, lines 29-31	At the end of expansion, TCR- cells **are enriched by negative selection with residual TCR+ cells depleted** using magnetic bead purification.
FR, lignes 14-20	Le transgène exprimé comprend une séquence de tête de chaîne légère kappa de souris, un fragment variable à chaîne unique (scFv) anti-CD19 dérivé du clone 4G7, un domaine charnière et transmembranaire CD8α, **ainsi que un domaine de co-stimulation 4-1BB (CD137) et un domaine de signalisation intracellulaire CD3ζ (TCRζ),** sous le contrôle du promoteur court (EFS) du facteur d'élongation 1 alpha (EF1α) humain.
FR, lignes 33-37	À la fin de l'expansion, les cellules TCR- **sont enrichies par sélection négative et les cellules TCR+ résiduelles sont éliminées** à l'aide d'une technologie de purification magnétique.
ES, líneas 13-19	El transgén expresado contiene una secuencia líder de la cadena ligera kappa de ratón, un fragmento variable de cadena sencilla (scFv) anti-CD19 derivado del clon 4G7, un dominio bisagra y transmembrana de CD8α, **un dominio co-estimulador de 4-1BB (CD137) y un dominio de señalización intracelulares de CD3ζ (TCRζ),** bajo el control del promotor corto del factor de elongación 1 alfa (EF1α) humano.
ES, líneas 32-34	Al final de la expansión, las células TCR- **se enriquecen mediante selección negativa y las células TCR+ residuales se eliminan** usando tecnología de purificación magnética.

p.408-409 **migaldendranibum**

migaldendranib	*replace the chemical name and structure by the following ones*
migaldendranib	*remplacer le nom chimique et la structure par les suivants*
migaldendranib	*sustitúyase el nombre químico y la estructura por los siguientes*

2-{[1-(1-{5-[(***Z***)-(5-fluoro-2-oxo-1,2-dihydro-3*H*-indol-3-ylidene)methyl]-2,4-dimethyl-1*H*-pyrrol-3-yl}-1,6-dioxo-9,12,15-trioxa-2,5-diazaheptadecan-17-yl)-1*H*-1,2,3-triazol-4-yl]methoxy}ethyl ether with about 11% of hydroxy groups of a regular dendrimer α,α',α'',α'''-(ethylenedinitrilo)tetrakis(ω-hexadecakis{3-[(2-hydroxyethyl)amino]-3-oxopropyl}-*dendro*^{G4}-[(3-oxopropane-1,3-diyl)azanediylethylenenitrilo])

éther 2-{[1-(1-{5-[(***Z***)-(5-fluoro-2-oxo-1,2-dihydro-3*H*-indol-3-ylidène)méthyl]-2,4-diméthyl-1*H*-pyrrol-3-yl}-1,6-dioxo-9,12,15-trioxa-2,5-diazaheptadécan-17-yl)-1*H*-1,2,3-triazol-4-yl]méthoxy}éthylique avec approximativement 11% de groupes terminaux hydroxy d'un dendrimère régulier α,α',α'',α'''-(éthylènedinitrilo)tétrakis(ω-hexadécakis{3-[(2-hydroxyéthyl)amino]-3-oxopropyl}-*dendro*^{G4}-[(3-oxopropane-1,3-diyl)azanediyléthylènenitrilo])

éter 2-{[1-(1-{5-[(***Z***)-(5-fluoro-2-oxo-1,2-dihidro-3*H*-indol-3-ilideno)metil]-2,4-dimetil-1*H*-pirrol-3-il}-1,6-dioxo-9,12,15-trioxa-2,5-diazaheptadecan-17-il)-1*H*-1,2,3-triazol-4-il]metoxi}etílico con aproximadamente 11% de grupos terminales hidroxi de un dendrímero regular α,α',α'',α'''-(etilenodinitrilo)tetrakis(ω-hexadecakis{3-[(2-hidroxietil)amino]-3-oxopropil}-*dendro*^{G4}-[(3-oxopropano-1,3-diil)azanediiletilenonitrilo])

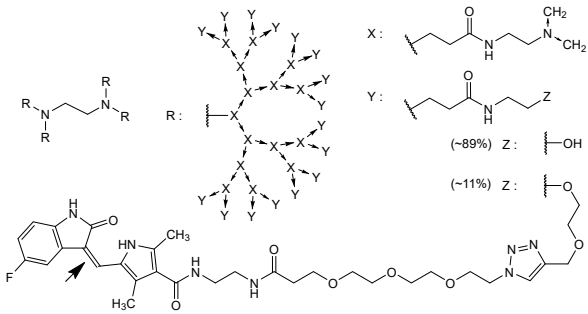

p.438	*delete/supprimer/suprimáse*	*insert/insérer/insertese*
	pobrolitidum	**getacatetidum**
	pobrolitide	getacatetide
	pobrolitide	gétacatétide
	pobrolitida	getacatetida

Proposed International Nonproprietary Names (Prop. INN): List 130
Dénominations communes internationales proposées (DCI Prop.): Liste 130
Denominaciones Comunes Internacionales Propuestas (DCI Prop.): Lista 130
(WHO Drug Information, Vol. 37, No. 4, 2023)

p.979-981 **atigotatugum #**

atigotatug *replace the chemical name and structure by the following ones*
atigotatug *remplacer le nom chimique et la structure par les suivants*
atigotatug *sustitúyase el nombre químico y la estructura por los siguientes*

immunoglobulin G1-kappa, anti-[Fucosyl-GM1 (fucosylated monosialoganglioside 1)], *Homo sapiens* monoclonal antibody; H-gamma1 heavy chain *Homo sapiens* (1-**451**) [VH (*Homo sapiens* IGHV3-48*02 (90.7%) -(IGHD) -IGHJ3*01 (92.3%) M123>T (117), CDR-IMGT [8.8.15] (26-33.51-58.97-111)) (1-122) -*Homo sapiens* IGHG1*03 (100%), G1m3, nG1m1 CH1 R120, CH3 E12, M14 (CH1 R120 (219) (123-220), hinge 1-15 (221-235), CH2 (236-345), CH3 E12 (361), M14 (363) (346-450), CHS **K2>del** (**451**) (123-**451**)], (225-214')-disulfide with L-kappa light chain *Homo sapiens* (1'-214') [V-

KAPPA (*Homo sapiens* IGKV1D-16*01 (100%) -IGKJ4*01 (100%), CDR-IMGT [6.3.9] (27'-32'.50'-52'.89'-97')) (1'-107') -*Homo sapiens* IGKC*01 (100%), Km3 A45.1 (153'), V101 (191') (108'-214')]; dimer (231-231":234-234")-bisdisulfide, produced in Chinese hamster ovary (CHO) cells, cell line **CHO-K1**, lacking the enzyme alpha-(1,6)-fucosyltransferase (FUT8), glycoform alfa

immunoglobuline G1-kappa, anti-[Fucosyl-GM1 (monosialoganglioside 1 fucosylé)], anticorps monoclonal *Homo sapiens*;
chaîne lourde H-gamma1 *Homo sapiens* (1-**451**) [VH (*Homo sapiens* IGHV3-48*02 (90.7%) -(IGHD) -IGHJ3*01 (92.3%) M123>T (117), CDR-IMGT [8.8.15] (26-33.51-58.97-111)) (1-122) -*Homo sapiens* IGHG1*03 (100%), G1m3, nG1m1 CH1 R120, CH3 E12, M14 (CH1 R120 (219) (123-220), charnière 1-15 (221-235), CH2 (236-345), CH3 E12 (361), M14 (363) (346-450), CHS **K2>del** (**451**)) (123-**451**)], (225-214')-disulfure avec la chaîne légère L-kappa *Homo sapiens* (1'-214') [V-KAPPA (*Homo sapiens* IGKV1D-16*01 (100%) -IGKJ4*01 (100%), CDR-IMGT [6.3.9] (27'-32'.50'-52'.89'-97')) (1'-107') -*Homo sapiens* IGKC*01 (100%), Km3 A45.1 (153'), V101 (191') (108'-214')]; dimère (231-231":234-234")-bisdisulfure, produit dans des cellules ovariennes de hamster chinois (CHO), lignée cellulaire **CHO-K1**, ne présentant pas l'enzyme alpha-(1,6)-fucosyltransférase (FUT8), glycoforme alfa

inmunoglobulina G1-kappa, anti-[Fucosil-GM1 (monosialogangliósido 1 fucosilado)], anticuerpo monoclonal *Homo sapiens*;
cadena pesada H-gamma1 *Homo sapiens* (1-**451**) [VH (*Homo sapiens* IGHV3-48*02 (90.7%) -(IGHD) -IGHJ3*01 (92.3%) M123>T (117), CDR-IMGT [8.8.15] (26-33.51-58.97-111)) (1-122) -*Homo sapiens* IGHG1*03 (100%), G1m3, nG1m1 CH1 R120, CH3 E12, M14 (CH1 R120 (219) (123-220), bisagra 1-15 (221-235), CH2 (236-345), CH3 E12 (361), M14 (363) (346-450), CHS **K2>del** (**451**)) (123-**451**)], (225-214')-disulfuro con la cadena ligera L-kappa *Homo sapiens* (1'-214') [V-KAPPA (*Homo sapiens* IGKV1D-16*01 (100%) -IGKJ4*01 (100%), CDR-IMGT [6.3.9] (27'-32'.50'-52'.89'-97')) (1'-107') -*Homo sapiens* IGKC*01 (100%), Km3 A45.1 (153'), V101 (191') (108'-214')]; dímero (231-231":234-234")-bisdisulfuro, producido en las células ováricas de hámster chino (CHO), línea celular **CHO-K1**, en ausencia de la enzima alfa-1,6-fucosiltransferasa (FUT8), forma glicosilada alfa

Heavy chain / Chaîne lourde / Cadena pesada

```
EVQLVESGGG SVQPGESLRL SCVASGFTFS RYKMNWVRQA PGKGLEWVSY  50
ISRSGRDIYY ADSVKGRFTI SRDNAKNSLY LQMNSLRDED TAVYYCAGTV 100
TTYYYDFGMD VWGQGTTVTV SSASTKGPSV FPLAPSSKST SGGTAALGCL 150
VKDYFPEPVT VSWNSGALTS GVHTFPAVLQ SSGLYSLSSV VTVPSSSLGT 200
QTYICNVNHK PSNTKVDKRV EPKSCDKTHT CPPCPAPELL GGPSVFLFPP 250
KPKDTLMISR TPEVTCVVVD VSHEDPEVKF NWYVDGVEVH NAKTKPREEQ 300
YNSTYRVVSV LTVLHQDWLN GKEYKCKVSN KALPAPIEKT ISKAKGQPRE 350
PQVYTLPPSR EEMTKNQVSL TCLVKGFYPS DIAVEWESNG QPENNYKTTP 400
PVLDSDGSFF LYSKLTVDKS RWQQGNVFSC SVMHEALHNH YTQKSLSLSP 450
G                                                       451
```

Light chain / Chaîne légère / Cadena ligera

```
DIQMTQSPSS LSASVGDRVT ITCRASQGIS SWLAWYQQKP EKAPKSLIYA  50
ASSLQSGVPS RFSGSGSGTD FTLTISSLQP EDFATYYCQQ YNSYPPTFGG 100
GTKVEIKRTV AAPSVFIFPP SDEQLKSGTA SVVCLLNNFY PREAKVQWKV 150
DNALQSGNSQ ESVTEQDSKD STYSLSSTLT LSKADYEKHK VYACEVTHQG 200
LSSPVTKSFN RGEC                                        214
```

Post-translational modifications
Disulfide bridges location / Position des ponts disulfure / Posiciones de los puentes disulfuro
Intra-H (C23-C104) 22-96 149-205 266-326 372-430
22"-96" 149"-205" 266"-326" 372"-430"
Intra-L (C23-C104) 23'-88' 134'-194'
23'"-88'" 134'"-194'"
Inter-H-L (h 5-CL 126) 225-214' 225"-214'"
Inter-H-H (h 11, h 14) 231-231" 234-234"

N-glycosylation sites / Sites de N-glycosylation / Posiciones de N-glicosilación
H CH2 N84.4: 302, 302"
Afucosylated complex bi-antennary CHO-type glycans / glycanes de type CHO bi-antennaires complexes afucosylés / glicanos de tipo CHO biantenarios complejos afucosilados

p.998-1000 **calotatugum ginistinagum #**

calotatug ginistinag *replace the chemical name, the CAS RN and structure by the following ones*

calotatug ginistinag *remplacer le nom chimique, le numéro de registre du CAS et la structure par les suivants*

calotatug ginistinag *sustitúyase el nombre químico, el número del CAS y la estructura por los siguientes*

immunoglobulin G1-kappa, anti-[*Homo sapiens* ERBB2 (receptor tyrosine-protein kinase erbB-2, epidermal growth factor receptor 2, EGFR2, HER2, HER-2, p185c-erbB2, NEU, CD340)], *Homo sapiens* monoclonal antibody, conjugated on 8 cysteinyl residues to a STING agonist, with a ratio of 1 to 8;
H-gamma1 heavy chain *Homo sapiens* (1-446) [VH (*Homo sapiens* IGHV3-48*01 (100%) -(IGHD) -IGHJ2*01 (100%), CDR-IMGT [8.8.10] (26-33.51-58.97-106)) (1-117) -*Homo sapiens* IGHG1*01 (100%), G1m17,1 CH1 K120, CH3 D12, L14 (CH1 K120 (214) (118-215), hinge 1-15 (216-230), CH2 (231-340), CH3 D12 (356), L14 (358) (341-445), CHS K2>del (446)) (118-446)], (220-215')-disulfide with L-kappa light chain *Homo sapiens* (1'-215') [V-KAPPA (*Homo sapiens* IGKV3-20*01 (97.9%) -IGKJ4*01 (100%), CDR-IMGT [7.3.9] (27'-33'.51'-53'.90'-98')) (1'-108') -*Homo sapiens* IGKC*01 (100%), Km3 A45.1 (154'), V101 (192') (109'-215')]; dimer (226-226":229-229")-bisdisulfide, produced in Chinese hamster ovary (CHO) cells, cell line CHO-K1SV, glycoform alfa; substituted at the sulfur atom of eight l-cysteinyl residues at position 220, 226, 229, 215', 220", 226", 229" and 215'" with (3*RS*)-1-[(4*S*,47*S*,53*S*,54*R*,55*R*,56*R*)-4-[(15***R****S*)-20-{[(6*E*)-4^{6},9^{5}-dicarbamoyl-1^{4},12^{4}-diethyl-1^{2},12^{2}-dimethyl-2,11-dioxo-3,10-diaza-4(2,3)-imidazo[4,5-*b*]pyridina-9(1,2)-[1,3]benzimidazola-1,12(5)-bis[1,3]oxazoladodecaphan-6-en-9^{7}-yl]oxy}-15-methyl-3,13,16-trioxo-7,10,17-trioxa-4,14-diazaicosan-1-yl]-53,54,55,56,57-pentahydroxy-2,5,8,11,14,17,45,50-octaoxo-47-{[(2*S*,3*R*,4*R*,5*R*)-2,3,4,5,6-pentahydroxyhexyl]carbamoyl}-21,24,27,30,33,36,39,42-octaoxa-3,6,9,12,15,18,46,51-octaazaheptapentacontan-1-yl]-2,5-dioxopyrrolidin-3-yl (*ginistinag*) groups

immunoglobuline G1-kappa, anti-[*Homo sapiens* ERBB2 (récepteur tyrosine-protéine kinase erbB-2, récepteur 2 du facteur de croissance épidermique, EGFR2, HER2, HER-2, p185c-erbB2, NEU, CD340)], anticorps monoclonal *Homo sapiens*, conjugué par 8 résidus cystéinyle à un agoniste STING avec un rapport de 1 à 8; chaîne lourde H-gamma1 *Homo sapiens* (1-446) [VH (*Homo sapiens* IGHV3-48*01 (100%) -(IGHD) -IGHJ2*01 (100%), CDR-IMGT [8.8.10] (26-33.51-58.97-106)) (1-117) -*Homo sapiens* IGHG1*01 (100%), G1m17,1 CH1 K120, CH3 D12, L14 (CH1 K120 (214) (118-215), charnière 1-15 (216-230), CH2 (231-340), CH3 D12 (356), L14 (358) (341-445), CHS K2>del (446)) (118-446)], (220-215')-disulfure avec la chaîne légère L-kappa *Homo sapiens* (1'-215') [V-KAPPA (*Homo sapiens* IGKV3-20*01 (97.9%) -IGKJ4*01 (100%), CDR-IMGT [7.3.9] (27'-33'.51'-53'.90'-98')) (1'-108') -*Homo sapiens* IGKC*01

(100%), Km3 A45.1 (154'), V101 (192') (109'-215')]; dimère (226-226'':229-229'')-bisdisulfure, produit dans des cellules ovariennes de hamster chinois (CHO), lignée cellulaire CHO-K1SV, glycoforme alfa; substitué sur l'atome de soufre de 8 résidus l-cystéinyle en position 220, 226, 229, 215', 220'', 226'', 229'' et 215''' avec le groupement (3*RS*)-1-[(4*S*,47*S*,53*S*,54*R*,55*R*,56*R*)-4-[(15***R****S*)-20-{[(6*E*)-4^{6},9^{5}-dicarbamoyl-1^{4},12^{4}-diéthyl-1^{2},12^{2}-diméthyl-2,11-dioxo-3,10-diaza-4(2,3)-imidazo[4,5-*b*]pyridina-9(1,2)-[1,3]benzimidazola-1,12(5)-bis[1,3]oxazoladodécaphan-6-én-9^{7}-yl]oxy}-15-méthyl-3,13,16-trioxo-7,10,17-trioxa-4,14-diazaicosan-1-yl]-53,54,55,56,57-pentahydroxy-2,5,8,11,14,17,45,50-octaoxo-47-{[(2*S*,3*R*,4*R*,5*R*)-2,3,4,5,6-pentahydroxyhexyl]carbamoyl}-21,24,27,30,33,36,39,42-octaoxa-3,6,9,12,15,18,46,51-octaazaheptapentacontan-1-yl]-2,5-dioxopyrrolidin-3-yle (*ginistinag*)

inmunoglobulina G1-kappa, anti-[*Homo sapiens* ERBB2 (receptor tirosina-proteína kinasa erbB-2, receptor 2 del factor de crecimiento epidérmico, EGFR2, HER2, HER-2, p185c-erbB2, NEU, CD340)], anticuerpo monoclonal *Homo sapiens*, conjugado por 8 residuos cisteinilo a un agonista STING con un ratio de 1 a 8; cadena pesada H-gamma1 *Homo sapiens* (1-446) [VH (*Homo sapiens* IGHV3-48*01 (100%) -(IGHD) -IGHJ2*01 (100%), CDR-IMGT [8.8.10] (26-33.51-58.97-106)) (1-117) -*Homo sapiens* IGHG1*01 (100%), G1m17,1 CH1 K120, CH3 D12, L14 (CH1 K120 (214) (118-215), bisagra 1-15 (216-230), CH2 (231-340), CH3 D12 (356), L14 (358) (341-445), CHS K2>del (446)) (118-446)], (220-215')-disulfuro con la cadena ligera L-kappa *Homo sapiens* (1'-215') [V-KAPPA (*Homo sapiens* IGKV3-20*01 (97.9%) -IGKJ4*01 (100%), CDR-IMGT [7.3.9] (27'-33'.51'-53'.90'-98')) (1'-108') -*Homo sapiens* IGKC*01 (100%), Km3 A45.1 (154'), V101 (192') (109'-215')]; dímero (226-226'':229-229'')-bisdisulfuro, producido en las células ováricas de hámster chino (CHO), línea celular CHO-K1SV, forma glicosilada alfa; substituido sobre el átomo de azufre de 8 residuos l-cisteinilo en posición 220, 226, 229, 215', 220'', 226'', 229'' y 215''' con el grupo (3*RS*)-1-[(4*S*,47*S*,53*S*,54*R*,55*R*,56*R*)-4-[(15***R****S*)-20-{[(6*E*)-4^{6},9^{5}-dicarbamoil-1^{4},12^{4}-dietil-1^{2},12^{2}-dimetil-2,11-dioxo-3,10-diaza-4(2,3)-imidazo[4,5-*b*]piridina-9(1,2)-[1,3]benzimidazola-1,12(5)-bis[1,3]oxazoladodecafan-6-en-9^{7}-il]oxi}-15-metil-3,13,16-trioxo-7,10,17-trioxa-4,14-diazaicosan-1-il]-53,54,55,56,57-pentahidroxi-2,5,8,11,14,17,45,50-octaoxo-47-{[(2*S*,3*R*,4*R*,5*R*)-2,3,4,5,6-pentahidroxihexil]carbamoil}-21,24,27,30,33,36,39,42-octaoxa-3,6,9,12,15,18,46,51-octaazaheptapentacontan-1-il]-2,5-dioxopirrolidin-3-ilo (*ginistinag*)

3032312-00-5

Heavy chain / Chaîne lourde / Cadena pesada

```
EVQLVESGGG LVQPGGSLRL SCAASGFTFS SYSMNWVRQA PGKGLEWVSY  50
ISSSSSTIYY ADSVKGRFTI SRDNAKNSLY LQMNSLRAED TAVYYCARGG 100
HGYFDLWGRG TLVTVSSAST KGPSVFPLAP SSKSTSGGTA ALGCLVKDYF 150
PEPVTVSWNS GALTSGVHTF PAVLQSSGLY SLSSVVTVPS SSLGTQTYIC 200
NVNHKPSNTK VDKKVEPKSC DKTHTCPPCP APELLGGPSV FLFPPKPKDT 250
LMISRTPEVT CVVVDVSHED PEVKFNWYVD GVEVHNAKTK PREEQYNSTY 300
RVVSVLTVLH QDWLNGKEYK CKVSNKALPA PIEKTISKAK GQPREPQVYT 350
LPPSRDELTK NQVSLTCLVK GFYPSDIAVE WESNGQPENN YKTTPPVLDS 400
DGSFFLYSKL TVDKSRWQQG NVFSCSVMHE ALHNHYTQKS LSLSPG     446
```

Light chain / Chaîne légère / Cadena ligera

```
EIVLTQSPGT LSLSPGERAT LSCRASQSVS SSYLAWYQQK PGQAPRLLIY  50
GASSRATGIP DRFSGSGSGT DFTLTISRLE PEDFAVYYCQ QYHHSPLTFG 100
GGTKVEIKRT VAAPSVFIFP PSDEQLKSGT ASVVCLLNNF YPREAKVQWK 150
VDNALQSGNS QESVTEQDSK DSTYSLSSTL TLSKADYEKH KVYACEVTHQ 200
GLSSPVTKSF NRGEC                                      215
```

Post-translational modifications

Disulfide bridges location / Position des ponts disulfure / Posiciones de los puentes disulfuro

Intra-H (C23-C104) 22-96 144-200 261-321 367-425
22"-96" 144"-200" 261"-321" 367"-425"

Intra-L (C23-C104) 23'-89' 135'-195'
23'"-89'" 135'"-195'"

Inter-H-L* (h 5-CL 126) 220-215' 220"-215'"

Inter-H-H* (h 11, h 14) 226-226" 229-229"

* The four inter-chain disulfide bridges are not present, an average of 8 cysteinyl being conjugated each via a thioether bond to a drug linker.

* Les quatre ponts disulfures inter-chaînes ne sont pas présents, 8 cystéinyl en moyenne étant chacun conjugué via une liaison thioéther à un linker-principe actif.

* Los cuatro puentes disulfuro inter-catenarios no estan presentes, una media de 8 cisteinil está conjugada a conectores de principio activo.

N-glycosylation sites / Sites de N-glycosylation / Posiciones de N-glicosilación

H CH2 N84.4: 297, 297"

Fucosylated complex bi-antennary CHO-type glycans / glycanes de type CHO bi-antennaires complexes fucosylés / glicanos de tipo CHO biantenarios complejos fucosilados

Potential modified residues / résidus modifiés potentiels / restos modificados potenciales*

C (220, 226, 229, 215', 220", 226", 229", 215'")

*(*ginistinag*:mAb ~ 8:1)

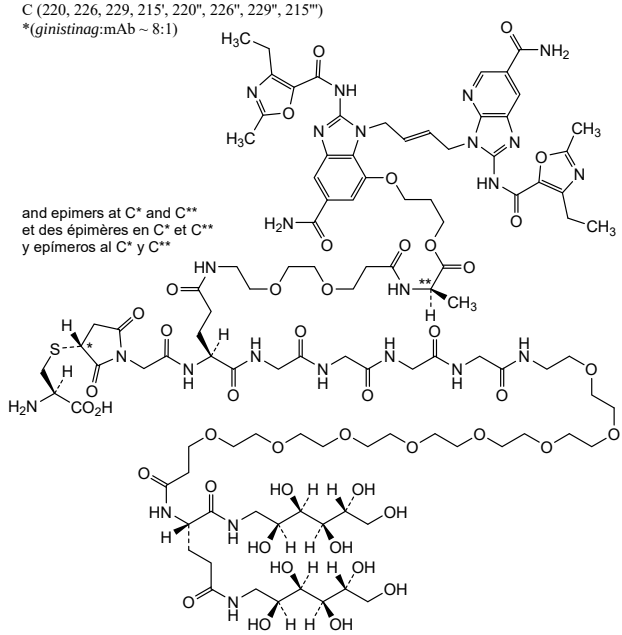

	delete/supprimer/suprimáse	*insert/insérer/insertese*
p.1011 -1012	**dalmitamigum**	**marlotamigum**
	dalmitamig	marlotamig
	dalmitamig	marlotamig
	dalmitamig	marlotamig

p.1071 **lonvoguranum**

lonvoguran *replace the chemical name by the following one*

all-P-ambo-2'-*O*-methyl-*P*-thioguanylyl-(3'→5')-2'-*O*-methyl-*P*-thioguanylyl-(3'→5')-2'-*O*-methyl-*P*-thioadenylyl-(3'→5')-uridylyl-(3'→5')-uridylyl-(3'→5')-guanylyl-(3'→5')-cytidylyl-(3'→5')-guanylyl-(3'→5')-uridylyl-(3'→5')-adenylyl-(3'→5')-uridylyl-(3'→5')-guanylyl-(3'→5')-guanylyl-(3'→5')-guanylyl-(3'→5')-adenylyl-(3'→5')-cytidylyl-(3'→5')-adenylyl-(3'→5')-cytidylyl-(3'→5')-adenylyl-(3'→5')-guanylyl-(3'→5')-uridylyl-(3'→5')-uridylyl-(3'→5')-uridylyl-(3'→5')-uridylyl-(3'→5')-adenylyl-(3'→5')-guanylyl-(3'→5')-adenylyl-(3'→5')-2'-*O*-methylguanylyl-(3'→5')-2'-*O*-methylcytidylyl-(3'→5')-2'-*O*-methyluridylyl-(3'→5')-2'-*O*-methyladenylyl-(3'→5')-2'-*O*-methylguanylyl-(3'→5')-2'-*O*-methyladenylyl-(3'→5')-2'-*O*-methyladenylyl-(3'→5')-2'-*O*-methyladenylyl-(3'→5')-2'-*O*-methyluridylyl-(3'→5')-2'-*O*-methyladenylyl-(3'→5')-2'-*O*-methylguanylyl-(3'→5')-2'-*O*-methylcytidylyl-(3'→5')-adenylyl-(3'→5')-adenylyl-(3'→5')-guanylyl-(3'→5')-uridylyl-(3'→5')-uridylyl-(3'→5')-adenylyl-(3'→5')-adenylyl-(3'→5')-adenylyl-(3'→5')-adenylyl-(3'→5')-uridylyl-(3'→5')-adenylyl-(3'→5')-adenylyl-(3'→5')-guanylyl-(3'→5')-guanylyl-(3'→5')-cytidylyl-(3'→5')-uridylyl-(3'→5')-adenylyl-(3'→5')-guanylyl-(3'→5')-uridylyl-(3'→5')-cytidylyl-(3'→5')-cytidylyl-(3'→5')-guanylyl-(3'→5')-uridylyl-(3'→5')-uridylyl-(3'→5')-adenylyl-(3'→5')-uridylyl-(3'→5')-cytidylyl-(3'→5')-adenylyl-**(3'→5')-2'-*O*-methyladenylyl**-(3'→5')-2'-*O*-methylcytidylyl-(3'→5')-2'-*O*-methyluridylyl-(3'→5')-2'-*O*-methyluridylyl-(3'→5')-2'-*O*-methylguanylyl-(3'→5')-2'-*O*-methyladenylyl-(3'→5')-2'-*O*-methyladenylyl-(3'→5')-2'-*O*-methyladenylyl-(3'→5')-2'-*O*-methyladenylyl-(3'→5')-2'-*O*-methyluridylyl-(3'→5')-2'-*O*-methylguanylyl-(3'→5')-2'-*O*-methylguanylyl-(3'→5')-2'-*O*-methylcytidylyl-(3'→5')-2'-*O*-methyladenylyl-(3'→5')-2'-*O*-methylcytidylyl-(3'→5')-2'-*O*-methylcytidylyl-(3'→5')-2'-*O*-methyladenylyl-(3'→5')-2'-*O*-methylguanylyl-(3'→5')-2'-*O*-methyluridylyl-(3'→5')-2'-*O*-methylcytidylyl-(3'→5')-2'-*O*-methylguanylyl-(3'→5')-2'-*O*-methyluridylyl-(3'→5')-2'-*O*-methylguanylyl-(3'→5')-2'-*O*-methylcytidylyl-(3'→5')-2'-*O*-methyl-*P*-thiouridylyl-(3'→5')-2'-*O*-methyl-*P*-thiouridylyl-(3'→5')-2'-*O*-methyl-*P*-thiouridylyl-(3'→5')-2'-*O*-methyluridine

	delete/supprimer/suprimáse	*insert/insérer/insertese*
p.1155 -1156	**segigratinibum**	**ratangratinibum**
	segigratinib	ratangratinib
	ségigratinib	ratangratinib
	segigratinib	ratangratinib

p.1179-1182 **tilatamigum samrotecanum #**

tilatamig samrotecan
tilatamig samrotécan
tilatamig samrotecán

replace the chemical name and structure by the following ones
remplacer le nom chimique et la structure par les suivants
sustitúyase el nombre químico y la estructura por los siguientes

immunoglobulin G1-kappa/G1-lambda, anti-[*Homo sapiens* MET (met proto-oncogene, hepatocyte growth factor (HGF) receptor, HGFR, scatter factor (SF) receptor, HGF/SF receptor, receptor tyrosine-protein kinase c-met, papillary renal cell carcinoma 2, RCCP2)] and anti-[*Homo sapiens* EGFR (epidermal growth factor receptor, receptor tyrosine-protein kinase erbB-1, ERBB1, HER1, HER-1, ERBB)], *Homo sapiens* monoclonal antibody, bispecific, conjugated on 6 cysteinyl residues to *samrotecan*;
H-gamma1 heavy chain anti-MET *Homo sapiens* (1-446) [VH (*Homo sapiens* IGHV1-8*01 (95.9%) -(IGHD) -IGHJ3*01 (100%), CDR-IMGT [8.8.9] (26-33.51-58.97-105)) (1-116)-*Homo sapiens* IGHG1*03, G1m3, nG1m1 CH1 R120, CH3 E12, M14, G1v39 CH2 F1.3, E1.2, S116, G1v33 CH3 S22, A24, V86 (hole), G1v75 CH3 C5 (CH1 R120 (213) (117-214), hinge 1-15 (215-229), CH2 L1.3>F (233), L1.2>E (234), P116>S (330) (230-339), CH3 Y5>C (348), E12 (355), M14 (357) T22>S (365), L24>A (367), Y86>V (406) (hole) (340-444), CHS (445-446)) (117-446)], (219-214')-disulfide with L-kappa light chain anti-MET *Homo sapiens* (1'-214') [V-KAPPA (*Homo sapiens* IGKV1-5*03 (92.6%) -IGKJ4*01 (90.9%) V124>L (104'), CDR-IMGT [6.3.9] (27'-32'.50'-52'.89'-97')) (1'-107') -*Homo sapiens* IGKC*01 (100%), Km3 A45.1 (153'), V101 (191') (108'-214')];
H-gamma1 heavy chain anti-EGFR *Homo sapiens* (1''-454'') [VH (*Homo sapiens* IGHV1-69*06 (83.7%) -(IGHD) -IGHJ1*01 (100%), CDR-IMGT [8.8.17] (26''-33''.51''-58''.97''-113'')) (1''-124'') -*Homo sapiens* IGHG1*03, G1m3, nG1m1 CH1 R120, CH3 E12, M14, G1v39 CH2 F1.3, E1.2, S116, G1v32 CH3 W22 (knob), G1v74 CH3 C10, G1v58 CH1 C5, h V5 (CH1 F5>C (133''), R120 (221'') (125''-222''), hinge 1-15 C5>V (227'') (223''-237''), CH2 L1.3>F (241''), L1.2>E (242''), P116>S (338'') (238''-347''), CH3 S10>C (361''), E12 (363''), M14 (365''), T22>W (373'') (348''-452''), CHS (453''-454'')) (125''-454'')], (133''-126''')-disulfide with L-lambda2 light chain anti-EGFR *Homo sapiens* (1'''-217''') [V-LAMBDA (*Homo sapiens* IGLV2-14*05 (94.9%) -IGLJ2*01 (90.9%), CDR-IMGT [9.3.11] (26'''-34'''.52'''-54'''.91'''-101''')) (1'''-111''') -*Homo sapiens* IGLC2*01 (98.1%), LC2v58 C10, V126, S10>C (126'''), C126>V (216''') (112'''-217''')]; dimer (225-233'':228-236'')-bisdisulfide, produced in a cell line from Chinese hamster ovary (CHO) cells, derived from the cell line CHO-K1, glycoform alfa; substituted at the sulfur atoms of L-cysteinyl residues **219, 225, 228, 214', 233'' and 236''** with **(3*RS*)-**1-[(2*S*,5*S*)-1-{[(9*S*)-9-ethyl-9-hydroxy-10,13-dioxo-2,3,9,10,13,15-hexahydro-1*H*,12*H*-benzo[*de*]pyrano[3',4':6,7]indolizino[1,2-*b*]quinolin-4-yl]amino}-2-methyl-1,4,7,35-tetraoxo-5-(propan-2-yl)-10,13,16,19,22,25,28,31-octaoxa-3,6,34-triazaheptatriacontan-37-yl]-2,5-dioxopyrrolidin-3-yl (*samrotecan*) groups

immunoglobuline G1-kappa/G1-lambda, anti-[*Homo sapiens* MET (proto-oncogène met, récepteur du facteur de croissance hépatocytaire, HGFR, récepteur du facteur de dispersion (SF), récepteur de l'HGF/SF, récepteur protéine-tyrosine kinase c-met, carcinome papillaire à cellules rénales 2, RCCP2)] et anti-[*Homo sapiens* EGFR (récepteur du facteur de croissance épidermique, récepteur tyrosine-protéine kinase erbB-1, ERBB1, HER1, HER-1, ERBB)], anticorps monoclonal *Homo sapiens*, bispécifique, conjugué par 6 résidus cystéinyle au *samrotécan*;
chaîne lourde H-gamma1 anti-MET *Homo sapiens* (1-446) [VH (*Homo sapiens* IGHV1-8*01 (95.9%) -(IGHD) -IGHJ3*01 (100%), CDR-IMGT [8.8.9] (26-33.51-58.97-105)) (1-116)-*Homo sapiens* IGHG1*03, G1m3, nG1m1 CH1 R120, CH3 E12, M14, G1v39 CH2 F1.3, E1.2, S116, G1v33 CH3 S22, A24, V86 (hole), G1v75 CH3 C5 (CH1 R120 (213) (117-214), charnière 1-15 (215-229), CH2 L1.3>F (233), L1.2>E (234), P116>S (330) (230-339), CH3 Y5>C (348), E12 (355), M14 (357), T22>S (365), L24>A (367), Y86>V (406) (hole) (340-444), CHS (445-446)) (117-446)], (219-214')-disulfure avec la chaîne légère L-kappa

anti-MET *Homo sapiens* (1'-214') [V-KAPPA (*Homo sapiens* IGKV1-5*03 (92.6%) -IGKJ4*01 (90.9%) V124>L (104), CDR-IMGT [6.3.9] (27'-32'.50'-52'.89'-97')) (1'-107') -*Homo sapiens* IGKC*01 (100%), Km3 A45.1 (153'), V101 (191') (108'-214')];
chaîne lourde H-gamma1 anti-EGFR *Homo sapiens* 1''-454'') [VH (*Homo sapiens* IGHV1-69*06 (83.7%) -(IGHD) -IGHJ1*01 (100%), CDR-IMGT [8.8.17] (26''-33''.51''-58''.97''-113'')) (1''-124'') -*Homo sapiens* IGHG1*03, G1m3, nG1m1 CH1 R120, CH3 E12, M14, G1v39 CH2 F1.3, E1.2, S116, G1v32 CH3 W22 (knob), G1v74 CH3 C10, G1v58 CH1 C5, h V5 (CH1 F5>C (133''), R120 (221'') (125''-222''), charnière 1-15 C5>V (227'') (223''-237''), CH2 L1.3>F (241''), L1.2>E (242''), P116>S (338'') (238''-347''), CH3 S10>C (361''), E12 (363''), M14 (365''), T22>W (373'') (348''-452''), CHS (453''-454'')) (125''-454'')], (133''-126''')-disulfure avec la chaîne légère L-lambda2 anti-EGFR *Homo sapiens* (1'''-217''') [V-LAMBDA (*Homo sapiens* IGLV2-14*05 (94.9%) -IGLJ2*01 (90.9%), CDR-IMGT [9.3.11] (26'''-34'''.52'''-54'''.91'''-101''')) (1'''-111''') -*Homo sapiens* IGLC2*01 (98.1%), LC2v58 C10, V126, S10>C (126'''), C126>V (216''') (112'''-217''')]; dimère (225-233'':228-236'')-bisdisulfure, produit dans une lignée cellulaire des cellules ovariennes de hamster chinois (CHO), dérivant de la lignée cellulaire CHO-K1, glycoforme alfa; substitué sur l'atome de soufre des résidus L-cystéinyle **219, 225, 228, 214', 233'' et 236''** avec des groupes **(3*RS*)-**1-[(2*S*,5*S*)-1-{[(9*S*)-9-éthyl-9-hydroxy-10,13-dioxo-2,3,9,10,13,15-hexahydro-1*H*,12*H*-benzo[*de*]pyrano[3',4':6,7]indolizino[1,2-*b*]quinoléin-4-yl]amino}-2-méthyl-1,4,7,35-tétraoxo-5-(propan-2-yl)-10,13,16,19,22,25,28,31-octaoxa-3,6,34-triazaheptatriacontan-37-yl]-2,5-dioxopyrrolidin-3-yle (*samrotécan*)

inmunoglobulina G1-kappa/G1-lambda, anti-[*Homo sapiens* MET (proto-oncogén met, receptor del factor de crecimiento hepatocitario, HGFR, receptor del factor de dispersión (SF), receptor del HGF/SF, receptor proteína-tirosina kinasa c-met, carcinoma papilar con células renales 2, RCCP2)] y anti-[*Homo sapiens* EGFR (receptor del factor de crecimiento epidérmico, receptor tirosina-proteína kinasa erbB-1, ERBB1, HER1, HER-1, ERBB)], anticuerpo monoclonal *Homo sapiens*, biespecífico, conjugué par 6 résidus cystéinyle au *samrotécan*; cadena pesada H-gamma1 anti-MET *Homo sapiens* (1-446) [VH (*Homo sapiens* IGHV1-8*01 (95.9%) -(IGHD) -IGHJ3*01 (100%), CDR-IMGT [8.8.9] (26-33.51-58.97-105)) (1-116)-*Homo sapiens* IGHG1*03, G1m3, nG1m1 CH1 R120, CH3 E12, M14, G1v39 CH2 F1.3, E1.2, S116, G1v33 CH3 S22, A24, V86 (hole), G1v75 CH3 C5 (CH1 R120 (213) (117-214), bisagra 1-15 (215-229), CH2 L1.3>F (233), L1.2>E (234), P116>S (330) (230-339), CH3 Y5>C (348), E12 (355), M14 (357), T22>S (365), L24>A (367), Y86>V (406) (hole) (340-444), CHS (445-446)) (117-446)], (219-214')-disulfuro con la cadena ligera L-kappa anti-MET *Homo sapiens* (1'-214') [V-KAPPA (*Homo sapiens* IGKV1-5*03 (92.6%) -IGKJ4*01 (90.9%) V124>L (104), CDR-IMGT [6.3.9] (27'-32'.50'-52'.89'-97')) (1'-107') -*Homo sapiens* IGKC*01 (100%), Km3 A45.1 (153'), V101 (191') (108'-214')];
cadena pesada H-gamma1 anti-EGFR *Homo sapiens* 1''-454'') [VH (*Homo sapiens* IGHV1-69*06 (83.7%) -(IGHD) -IGHJ1*01 (100%), CDR-IMGT [8.8.17] (26''-33''.51''-58''.97''-113'')) (1''-124'') -*Homo sapiens* IGHG1*03, G1m3, nG1m1 CH1 R120, CH3 E12, M14, G1v39 CH2 F1.3, E1.2, S116, G1v32 CH3 W22 (knob), G1v74 CH3 C10, G1v58 CH1 C5, h V5 (CH1 F5>C (133''), R120 (221'') (125''-222''), bisagra 1-15 C5>V (227'') (223''-237''), CH2 L1.3>F (241''), L1.2>E (242''), P116>S (338'') (238''-347''), CH3 S10>C (361''), E12 (363''), M14 (365''), T22>W (373'') (348''-452''), CHS (453''-454'')) (125''-454'')], (133''-126''')-disulfuro con la cadena ligera L-lambda2 anti-EGFR *Homo sapiens* (1'''-217''') [V-LAMBDA (*Homo sapiens* IGLV2-14*05 (94.9%) -IGLJ2*01 (90.9%), CDR-IMGT [9.3.11] (26'''-34'''.52'''-54'''.91'''-101''')) (1'''-111''') -*Homo sapiens* IGLC2*01 (98.1%), LC2v58 C10, V126, S10>C (126'''), C126>V (216''') (112'''-217''')]; dímero (225-233'':228-236'')-bisdisulfuro, producido en una línea celular de las células ováricas de hámster chino (CHO), línea celular derivada de CHO-K1, forma glicosilada alfa; sustituido en el átomo de azufre de los residuos L-cisteinilo **219, 225, 228, 214', 233'' y 236''** con grupos **(3*RS*)-**1-[(2*S*,5*S*)-1-{[(9*S*)-9-etil-9-hidroxi-10,13-dioxo-2,3,9,10,13,15-hexahidro-1*H*,12*H*-

benzo[*de*]pirano[3',4':6,7]indolizino [1,2-*b*]quinolin-4-il]amino}-2-metil-1,4,7,35-tetraoxo-5-(propan-2-il)-10,13,16,19, 22, 25,28,31-octaoxa-3,6,34-triazaheptatriacontan-37-il]-2,5-dioxopirrolidin-3-ilo (*samrotecán*)

Heavy chain / Chaîne lourde / Cadena pesada anti-MET (hole) (H)

```
QVQLVQSGAE VKKPGASVKV SCKASGYTFT DYYIHWVRQA PGQGLEWMGW  50
INPNSGGTGY AQKFQGRVTM TRDTSISTAY MELSRLRSED TAVYYCARRQ 100
GYDWYFDVWG QGTTVTVSSA STKGPSVFPL APSSKSTSGG TAALGCLVKD 150
YFPEPVTVSW NSGALTSGVH TFPAVLQSSG LYSLSSVVTV PSSSLGTQTY 200
VCNVNHKPSN TKVDKKVEPK SCDKTHTCPP CPAPELLGGP SVFLFPPKPK 250
DTLMISRTPE VTCVVVDVSH EDPEVKFNWY VDGVEVHNAK TKPREEQYNS 300
TYRVVSVLTV LHQDWLNGKE YKCKVSNKAL PAPIEKTISK AKGQPREPQV 350
YTLPPSREEM TKNQVSLTCL VKGFYPSDIA VEWESNGQPE NNYKTTPPVL 400
DSDGSFFLYS KLTVDKSRWQ QGNVFSCSVM HEALHNHYTQ KSLSLSPGK  446
```

Light chain / Chaîne légère / Cadena ligera anti-MET (L')

```
DIQMTQSPSS LSASVGDRVT ITCRASQTIY HWLAWYQQIP EKAPKLLIYK  50
ASSLASGVPS RFSGSGSGTE FTLTISSLQP DDFATYYCQQ YNSYPFTFGG 100
GTKLEIKRTV AAPSVFIFPP SDEQLKSGTA SVVCLLNNFY PREAKVQWKV 150
DNALQSGNSQ ESVTEQDSKD STYSLSSTLT LSKADYEKHK VYACEVTHQG 200
LSSPVTKSFN RGEC                                        214
```

Heavy chain / Chaîne lourde / Cadena pesada anti-EGFR (knob) (H")

```
QVQLVQSGAE VKKPGASVKV SCKASGYTFS DYEMHWVRQA PGQGLEWMGA  50
IVAVSGETEY AQKFQGRVTI TADESTSTAY MELSSLRSED TAVYYCARRL 100
MIAIIGPGAP DLSWFQDFLV TVSSASTKGP SVFPLAPSSK STSGGTAALG 150
CLVKDYFPEP VTVSWNSGAL TSGVHTFPAV LQSSGLYSLS SVVTVPSSSL 200
GTQTYICNVN HKPSNTKVDK KVEPKSCDKT HTCPPCPAPE LLGGPSVFLF 250
PPKPKDTLMI SRTPEVTCVV VDVSHEDPEV KFNWYVDGVE VHNAKTKPRE 300
EQYNSTYRVV SVLTVLHQDW LNGKEYKCKV SNKALPAPIE KTISKAKGQP 350
REPQVYTLPP SRDELTKNQV SLSCAVKGFY PSDIAVEWES NGQPENNYKT 400
TPPVLDSDGS FFLYSKLTVD KSRWQQGNVF SCSVMHEALH NHYTQKSLSL 450
SPGK                                                   454
```

Light chain / Chaîne légère / Cadena ligera anti-EGFR (L")

```
QMALTQPPSV SVAPGQTART SCTGDSIGVG KYYVQWYQQV PGQAPVLVMI  50
YDSDRPSGIP ERFSGSKSGN TATLTISRGL QAEDEADYYC GSYDSSSVLE 100
GGGTKLTVLG QPKAAPSVTL FPPSSEELQA NKATLVCLIS DFYPGAVTVA 150
WKADSSPVKA GVETTTPSKQ SNNKYAASSY LSLTPEQWKS HRSYSCQVTH 200
EGSTVEKTVA PTECS                                       215
```

Post-translational modifications

Disulfide bridges location / Position des ponts disulfure / Posiciones de los puentes disulfuro

Intra-H (C 23-C 104) 22-96 143-199 260-320 366-424
22"-96" 151"-207" 268"-328" 374"-432"
Intra-L (C 23-C 104) 23'-88' 134'-194'
22"'-90"' 139"'-198"'
Inter-H-L (h 5-CL 126)* 219-214' 133"-126"
Inter-H-H (h 11, h 14)* 225-233" 228-236"
Inter-H-H (C-HC5-C10)** 348-361"

*At least three inter-chain disulfide bridges are not present, an average of 6 cysteinyl being conjugated each via a thioether bond to a drug linker.
*Au moins trois ponts disulfures inter-chaînes ne sont pas présents, 6 cystéinyl en moyenne étant chacun conjugué via une liaison thioéther à un linker-principe actif
*Al menos tres puentes disulfuro inter-cadenarios no están presentes, una media de 6 cisteinil está conjugada a conectores de principio activo
**variants G1v75 (C HC5) and G1v74 (C HC10) creating an additional inter-H-H disulfide bond.
**variantes G1v75 (C HC5) et G1v74 (C HC10) créant une liaison disulfure inter-H-H supplémentaire.
**variantes G1v75 (C HC5) y G1v74 (C HC10) que crean un enlace disulfuro inter-H-H adicional

N-terminal glutaminyl cyclization / Cyclisation du glutaminyle N-terminal / Ciclación del glutaminilo N-terminal
Q > pyroglutamyl (pE, 5-oxoprolyl) / pyroglutamyle (pE, 5-oxoprolyle) / piroglutamilo (pE, 5-oxoprolilo)
H VH Q1: 1, 1"
L VL Q1: 1"'

N-glycosylation sites / Sites de N-glycosylation / Posiciones de N-glicosilación
H CH2 N84.4: 296, 304"
Fucosylated complex bi-antennary CHO-type glycans / glycanes de type CHO bi-antennaires complexes fucosylés / glicanos de tipo CHO biantenarios complejos fucosilados.

C-terminal lysine clipping / Coupure de la lysine C-terminale / Recorte de lisina C-terminal
H CHS K2: 446, 454"

Modified residues / résidus modifiés / restos modificados*
C (219, 225, 228, 214', 233", 236")
*(*anticorps*: mAb ~ 6:1)

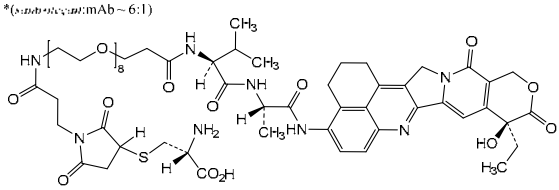

p.1185-1186 **trosunilimabum #**
trosunilimab
trosunilimab
trosunilimab

replace the chemical name by the following one
remplacer le nom chimique par le suivante
sustitúyase el nombre químico por lo siguiente

immunoglobulin G1-kappa, anti-[*Homo sapiens* integrin ITGA4_ITGB7 (integrin alpha4 (CD49d)_beta7, integrin α4β7, lymphocyte Peyer's patch adhesion molecule 1, LPAM-1)]; gamma1 heavy chain (1-442) [VH (*Homo sapiens* IGHV1-69*11 (**79.2%**) -(IGHD) -IGHJ3*01 (92.3%) M123>T (107), CDR-IMGT [8.8.5] (26-33.51-58.97-101)) (1-112) -*Homo sapiens* IGHG1*03v, G1m3>G1m17, nG1m1 (CH1 R120>K (209) (113-210), hinge 1-15 (211-225), CH2 (226-335), CH3 E12 (351), M14 (353) (336-440), CHS (441-442)) (113-442)], (215-214')-disulfide with kappa light chain (1'-214') [V-KAPPA Musmus/Homsap (*Mus musculus* IGKV14-100*01 (85.3%) -IGKJ1*01 (91.7%) L124>V (104)/*Homo sapiens* IGKV1-33*01 (80.0%) -IGKJ4*01 (100%), CDR-IMGT [6.3.9] (27-32.50-52.89-97)) (1'-107') -*Homo sapiens* IGKC*01 (100%), Km3 A45.1 (153), V101 (191) (108'-214')]; dimer (221-221":224-224")-bisdisulfide, produced in Chinese hamster ovary (CHO) cells, glycoform alfa

immunoglobuline G1-kappa, anti-[*Homo sapiens* intégrine ITGA4_ITGB7 (intégrine alpha4 (CD49d)_bêta7, intégrine α4β7, récepteur d'adressage spécifique des plaques de Peyer, LPAM-1)];
chaîne lourde gamma1 (1-442) [VH (*Homo sapiens* IGHV1-69*11 (**79.2%**) -(IGHD) -IGHJ3*01 (92.3%) M123>T (107), CDR-IMGT [8.8.5] (26-33.51-58.97-101)) (1-112) -*Homo sapiens* IGHG1*03v, G1m3>G1m17, nG1m1 (CH1 R120>K (209) (113-210), charnière 1-15 (211-225), CH2 (226-335), CH3 E12 (351), M14 (353) (336-440), CHS (441-442)) (113-442)], (215-214')-disulfure avec la chaîne légère kappa (1'-214') [V-KAPPA Musmus/Homsap (*Mus musculus* IGKV14-100*01 (85.3%) -IGKJ1*01 (91.7%) L124>V (104)/*Homo sapiens* IGKV1-33*01 (80.0%) -IGKJ4*01 (100%), CDR-IMGT [6.3.9] (27-32.50-52.89-97)) (1'-107') -*Homo sapiens* IGKC*01 (100%), Km3 A45.1 (153), V101 (191) (108'-214')]; dimère (221-221":224-224")-bisdisulfure, produit dans des cellules ovariennes de hamster chinois (CHO), glycoforme alfa

inmunoglobulina G1-kappa, anti-[*Homo sapiens* integrina ITGA4_ITGB7 (integrina alfa4 (CD49d)_beta7, integrina α4β7, receptor específico de las placas de Peyer, LPAM-1)];
cadena pesada gamma1 (1-442) [VH (*Homo sapiens* IGHV1-69*11 (**79.2%**) -(IGHD) -IGHJ3*01 (92.3%) M123>T (107), CDR-IMGT [8.8.5] (26-33.51-58.97-101)) (1-112) -*Homo sapiens* IGHG1*03v, G1m3>G1m17, nG1m1 (CH1 R120>K (209) (113-210), bisagra 1-15 (211-225), CH2 (226-335), CH3 E12 (351), M14 (353) (336-440), CHS (441-442)) (113-442)], (215-214')-disulfure con la cadena ligera kappa (1'-214') [V-KAPPA Musmus/Homsap (*Mus musculus* IGKV14-100*01 (85.3%) -IGKJ1*01 (91.7%) L124>V (104)/*Homo sapiens* IGKV1-33*01 (80.0%) -IGKJ4*01 (100%), CDR-IMGT [6.3.9] (27-32.50-52.89-97)) (1'-107') -*Homo sapiens* IGKC*01 (100%), Km3 A45.1 (153), V101 (191) (108'-214')]; dímero (221-221":224-224")-bisdisulfuro, producido en las células ováricas de hámster chino (CHO), forma glicosilada alfa

Proposed International Nonproprietary Names (Prop. INN): List 131
Dénominations communes internationales proposées (DCI Prop.): Liste 131
Denominaciones Comunes Internacionales Propuestas (DCI Prop.): Lista 131
(WHO Drug Information, Vol. 38, No. 2, 2024)

p.237-239

actinium (^{225}Ac) alpitatugum satetraxetanum #

actinium (^{225}Ac) alpitatug satetraxetan
actinium (^{225}Ac) alpitatug satétraxétan
actinio (^{225}Ac) alpitatug satetraxetán

replace the chemical name and structure by the following ones
remplacer le nom chimique et la structure par les suivants
sustitúyase el nombre químico y la estructura por los siguientes

immunoglobulin G1-kappa, anti-[*Homo sapiens* KLK2 (kallikrein-2, kallikrein peptidase 2, kallikrein 2 prostatic)], humanized monoclonal antibody, conjugated to *satetraxetan* (DOTA derivative) and radiolabelled with actinium-225;
H-gamma1 heavy chain humanized (1-447) [VH (*Homo sapiens* IGHV4-28*01 (90.7%) -(IGHD) -IGHJ1*01 (100%), CDR-IMGT [9.7.10] (26-34.52-58.97-106)) (1-117) -*Homo sapiens* IGHG1*03v (100%) G1m3>G1m17, nG1m1 CH1 K120, CH3 E12, M14 (CH1 R120>K (214) (118-215), hinge 1-15 (216-230), CH2 (231-340), CH3 E12 (356), M14 (358) (341-445), CHS (446-447)) (118-447)], (220-218')-disulfide with L-kappa light chain humanized (1'-218') [V-KAPPA (*Homo sapiens* IGKV4-1*01 (81.2%) -IGKJ2*01 (100%), CDR-IMGT [10.3.9] (27'-36'.54'-56'.93'-101')) (1'-111') -*Homo sapiens* IGKC*01 (100%) Km3 A45.1, V101 (C-KAPPA A45.1 (157'), V101 (195')) (112'-218')]; dimer (226-226'':229-229'')-bisdisulfide, produced in Chinese hamster ovary (CHO) cells, glycoform alfa; conjugated via the side chain nitrogen of an average of 3 lysine residues to **(^{225}Ac)actinium** radiolabeled *rac*-(4-{[(2*R*)-1,4,7,10-tetrakis(carboxymethyl)-1,4,7,10-tetraazacyclododecan-2-yl]methyl}phenyl)carbamothioyl (*satetraxetan*)

immunoglobuline G1-kappa, anti-[*Homo sapiens* KLK2 (kallikréine-2, kallikréine peptidase 2, kallikréine prostatique)], anticorps monoclonal humanisé; conjugué au *satétraxétan* (dérivé DOTA) et radiomarqué à l'actinium-225;
chaîne lourde H-gamma1 humanisée (1-447) [VH (*Homo sapiens* IGHV4-28*01 (90.7%) -(IGHD) -IGHJ1*01 (100%), CDR-IMGT [9.7.10] (26-34.52-58.97-106)) (1-117) -*Homo sapiens* IGHG1*03v (100%) G1m3>G1m17, nG1m1 CH1 K120, CH3 E12, M14 (CH1 R120>K (214) (118-215), charnière 1-15 (216-230), CH2 (231-340), CH3 E12 (356), M14 (358) (341-445), CHS (446-447)) (118-447)], (220-218')-disulfure avec la chaîne légère L-kappa humanisée (1'-218') [V-KAPPA (*Homo sapiens* IGKV4-1*01 (81.2%) -IGKJ2*01 (100%), CDR-IMGT [10.3.9] (27'-36'.54'-56'.93'-101')) (1'-111') -*Homo sapiens* IGKC*01 (100%) Km3 A45.1, V101 (C-KAPPA A45.1 (157'), V101 (195')) (112'-218')]; dimère (226-226'':229-229'')-bisdisulfure, produit dans des cellules ovariennes de hamster chinois (CHO), glycoforme alfa; conjugué par l'azote de la chaîne latérale de 3 résidus lysine en moyenne au *rac*-(4-{[(2*R*)-1,4,7,10-tétrakis(carboxyméthyl)-1,4,7,10-tétraazacyclododécan-2-yl]méthyl}phényl)carbamothioyle (*satétraxétan*) et radiomarqué au **(^{225}Ac)actinium**

inmunoglobulina G1-kappa, anti-[*Homo sapiens* KLK2

(kalikreína-2, kalikreína peptidasa 2, kalikreína prostática)], anticuerpo monoclonal humanizado; conjugado con *satetraxetán* (derivado DOTA) y radiomarcado con el actinio-225; cadena pesada H-gamma1 humanizada (1-447) [VH (*Homo sapiens* IGHV4-28*01 (90.7%) -(IGHD) -IGHJ1*01 (100%), CDR-IMGT [9.7.10] (26-34.52-58.97-106)) (1-117) -*Homo sapiens* IGHG1*03v (100%) G1m3>G1m17, nG1m1 CH1 K120, CH3 E12, M14 (CH1 R120>K (214) (118-215), bisagra 1-15 (216-230), CH2 (231-340), CH3 E12 (356), M14 (358) (341-445), CHS (446-447)) (118-447)], (220-218')-disulfuro con la cadena ligera L-kappa humanizada (1'-218') [V-KAPPA (*Homo sapiens* IGKV4-1*01 (81.2%) -IGKJ2*01 (100%), CDR-IMGT [10.3.9] (27'-36'.54'-56'.93'-101')) (1'-111') -*Homo sapiens* IGKC*01 (100%) Km3 A45.1, V101 (C-KAPPA A45.1 (157'), V101 (195')) (112'-218')]; dímero (226-226":229-229")-bisdisulfuro, producido en las células ováricas de hámster chino (CHO), forma glicosilada alfa; conjugado por el nitrógeno de la cadena lateral de 3 residuos de lisina en promedio al *rac*-(4-{[(2*R*)-1,4,7,10-tetrakis(carboximetil)-1,4,7,10-tetraazaciclododecan-2-il]metil}fenil)carbamotioilo (*satetraxetán*) y radiomarcado con el **(^{225}Ac)actinio**

Heavy chain / Chaîne lourde / Cadena pesada

```
QVQLQESGPG LVKPSETLSL TCAVSGNSIT SGYYWNWIRQ PPGKGLEWIG  50
YIYYSGSTTY NPSLKSRVTM SVDTSKNQFS LKLSSVTAAD TAVYYCATGY 100
YVGYSWAFDI WGQGTMVTVS SASTKGPSVF PLAPSSKSTS GGTAALGCLV 150
KDYFPEPVTV SWNSGALTSG VHTFPAVLQS SGLYSLSSVV TVPSSSLGTK 200
TYTCNVDHKP SNTKVDKRVE SKYGPPCPPC PAPEFLGGPS VFLFPPKPKD 250
TLMISRTPEV TCVVVDVSQE DPEVQFNWYV DGVEVHNAKT KPREEQFNST 300
YRVVSVLTVL HQDWLNGKEY KCKVSNKGLP SSIEKTISKA KGQPREPQVY 350
TLPPSQEEMT KNQVSLTCLV KGFYPSDIAV EWESNGQPEN NYKTTPPVLD 400
SDGSFFLYSK LTVDKSRWQE GNVFSCSVMH EALHNHYTQK SLSLSPGK    447
```

Light chain / Chaîne légère / Cadena ligera

```
DIVMTQSPDT LAVSLGERAT INCKASQSVT YFGTSLMHWY QQKPGQPPKL  50
LIYAASNPES GVPDRFSGSG SGTDFTLTIS SLQAEDVAVY YCQQSREFPT 100
TFGQGTKVEI KRTVAAPSVF IFPPSDEQLK SGTASVVCLL NNFYPREAKV 150
QWKVDNALQS GNSQESVTEQ DSKDSTYSLS STLTLSKADY EKHKVYACEV 200
THQGLSSPVT KSFNRGEC                                    218
```

Post-translational modifications

Disulfide bridges location / Position des ponts disulfure / Posiciones de los puentes disulfuro

Intra-H (C23-C104)	22-96	144-200	261-321	367-425
	22"-96"	144"-200"	261"-321"	367"-425"
Intra-L (C23-C104)	23'-92'	138'-198'		
	23'"-92'"	138'"-198'"		
Inter-H-L (h 5-CL 126)	220-218'	220"-218"		
Inter-H-H (h 11, h 14)	226-226"	229-229"		

N-terminal glutaminyl cyclization / Cyclisation du glutamique N-terminal / Ciclación del glutamilo N-terminal

Q > pyroglutamyl (pE, 5-oxoprolyl) / pyroglutamyle (pE, 5-oxoprolyle) / piroglutamilo (pE, 5-oxoprolilo)

H VH Q1: 1, 1"

N-glycosylation sites / Sites de N-glycosylation / Posiciones de N-glicosilación

H CH2 N84.4: 297, 297"

Fucosylated complex bi-antennary CHO-type glycans / glycanes de type CHO bi-antennaires complexes fucosylés / glicanos de tipo CHO biantenarios complejos fucosilados

C-terminal lysine clipping / Coupure de la lysine C-terminale / Recorte de lisina C-terminal

H CHS K2: 447, 447"

Potential modified residues / résidus modifiés potentiels / restos modificados potenciales*

K (65, **222**, 246, 248, 392, 49', 130', 211', 65", **222"**, 246", 248", 392", 49'", 130'", 211'") *(sites réactifs/zamAb ~ 3:1)

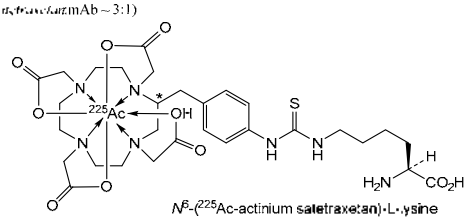

N^{ε}-(225Ac-actinium satetraxetan)-L-lysine

p.276 **cadapersenum**
-277 cadapersen *replace the molecular formula by the following one*
cadapersen *remplacer la formule moléculaire brute par la suivante*
cadapersén *sustitúyase el nombre químico y la fórmula molecular por los siguientes*

5'-[hidrogenofosfato de (17*S*,20*S*)-1-[(2-acetamido-2-desoxi-β-D-galactopiranosil)oxi]-17-{2-[2-(2-{2-[(2-acetamido-2-desoxi-β-D-galactopiranosil)oxi]etoxi}eto**x**i)etoxi]acetamido}-20-{1-[(2-acetamido-2-desoxi-β-D-galactopiranosil)oxi]-11-oxo-3,6,9-trioxa-12-azahexadecan-16-il}-11,18,21-trioxo-3,6,9-trioxa-12,19,22-triazaoctacosan-28-ilo] de *todo-P-ambo*-2'-desoxicitidilil-(3'→5')-2'-desoxiadenilil-(3'→5')-5-metil-2'-*O*,4'-*C*-metileno-*P*-tiocitidilil-(3'→5')-5-metil-2'-*O*,4'-*C*-metileno-*P*-tiocitidilil-(3'→5')-*P*-tiotimidilil-(3'→5')-2'-desoxi-*P*-tioadenilil-(3'→5')-*P*-tiotimidilil-(3'→5')-*P*-tiotimidilil-(3'→5')-2'-desoxi-*P*-tioadenilil-(3'→5')-2'-desoxi-*P*-tioadenilil-(3'→5')-2'-desoxi-*P*-tiocitidilil-(3'→5')-2'-desoxi-*P*-tioadenilil-(3'→5')-*P*-tiotimidilil-(3'→5')-2'-desoxi-*P*-tiocitidilil-(3'→5')-2'-*O*,4'-*C*-metileno-*P*-tioadenilil-(3'→5')-2'-*O*,4'-*C*-metileno-*P*-tioguanilil-(3'→5')-2'-*O*,4'-*C*-metileno-*P*-tioadenilil-(3'→5')-5-metil-2'-*O*,4'-*C*-metilen**o**citidina

$C_{259}H_{\mathbf{378}}N_{76}O_{135}P_{19}S_{16}$

p.356 **isomiosaminum**
isomiosamine *replace the chemical name by the following one*
isomiosamine *remplacer le nom chimique par le suivant*
isomiosamina *sustitúyase el nombre químico por el siguiente*

rac-**3**-[(**2*R***)-3,4-dihydro-2*H*-pyrrol-2-**yl]py**ridine
rac-**3**-[(**2*R***)-3,4-dihydro-2*H*-pyrrol-2-**yl]py**ridine
rac-**3**-[(**2*R***)-3,4-dihidro-2*H*-pirrol-2-**il]pi**ridina

p.400-401 **pangumestrocelum**
pangumestrocel *replace the chemical name by the following one*
pangumestrocel *remplacer le nom chimique par le suivant*
pangumestrocel *sustitúyase el nombre químico por el siguiente*

EN, lines 10-12 The final cells express CD73, CD90, and CD105 (**≥95%)** and are negative for CD34, CD45, CD11b, CD19 and HLA-DR (**≤2%**).

FR, lignes 11-13 Au final, les cellules expriment CD73, CD90 et CD 105 (**≥95%**) et sont négatives pour CD34, CD45, CD11b, CD19 et HLA-DR (**≤2%**).

ES, líneas 10-12 Las células finales expresan CD73, CD90 y CD105 (**≥95%**) y son negativas para CD34, CD45, CD11b, CD19 y HLA-DR (**≤2%**).

p.410-411 **pivicasiranum**
pivicasiran *replace the chemical name by the following one*
pivicasiran *remplacer le nom chimique par le suivant*
pivicasirán *sustitúyase el nombre químico por el siguiente*

[(2*S*,4*R*)-1-{1-[(2-acetamido-2-deoxy-β-D-galactopyranosyl)oxy]-16,16-bis({3-[(3-{5-[(2-acetamido-2-deoxy-β-D-galactopyranosyl)oxy]pentanamido}propyl)amino]-3-oxopro**poxy**}methyl)-5,11,18-trioxo-14-oxa-6,10,17-

triazanonacosan-29-oyl}-4-hydroxypyrrolidin-2-yl]methyl hydrogen *all-P-ambo*-2'-*O*-methyl-*P*-thiocytidylyl-(3'→5')-2'-*O*-methyl-*P*-thioadenylyl-(3'→5')-2'-*O*-methyluridylyl-(3'→5')-2'-*O*-methyluridylyl-(3'→5')-2'-*O*-methyladenylyl-(3'→5')-2'-*O*-methylguanylyl-(3'→5')-2'-deoxy-2'-fluoroguanylyl-(3'→5')-2'-*O*-methyladenylyl-(3'→5')-2'-deoxy-2'-fluorouridylyl-(3'→5')-2'-deoxy-2'-fluoroadenylyl-(3'→5')-2'-deoxy-2'-fluoroadenylyl-(3'→5')-2'-*O*-methyluridylyl-(3'→5')-2'-*O*-methylguanylyl-(3'→5')-2'-*O*-methyluridylyl-(3'→5')-2'-*O*-methylcytidylyl-(3'→5')-2'-*O*-methyluridylyl-(3'→5')-2'-*O*-methyluridylyl-(3'→5')-2'-*O*-methyladenylyl-(3'→5')-2'-*O*-methyluridylyl-(3'→5')-2'-*O*-methylguanylyl-(3'→5')-2'-*O*-methyl-**3'-**uridylate duplex with *all-P-ambo*-2'-*O*-methyl-*P*-thioguanylyl-(5'→3')-2'-*O*-methyl-*P*-thioguanylyl-(5'→3')-2'-*O*-methylguanylyl-(5'→3')-2'-*O*-methyluridylyl-(5'→3')-2'-*O*-methyladenylyl-(5'→3')-2'-*O*-methyladenylyl-(5'→3')-2'-*O*-methyluridylyl-(5'→3')-2'-deoxy-2'-fluorocytidylyl-(5'→3')-2'-*O*-methylcytidylyl-(5'→3')-2'-deoxy-2'-fluorouridylyl-(5'→3')-2'-*O*-methyladenylyl-(5'→3')-2'-*O*-methyluridylyl-(5'→3')-2'-*O*-methyluridylyl-(5'→3')-2'-*O*-methyladenylyl-(5'→3')-2'-deoxy-2'-fluorocytidylyl-(5'→3')-2'-deoxy-2'-fluoroadenylyl-(5'→3')-2'-*O*-methylguanylyl-(5'→3')-2'-deoxy-2'-fluoroadenylyl-(5'→3')-2'-*O*-methyladenylyl-(5'→3')-2'-*O*-methyluridylyl-(5'→3')-2'-*O*-methyl-*P*-thioadenylyl-(5'→3')-2'-deoxy-2'-fluoro-*P*-thiocytidylyl-(5'→3')-2'-*O*-methyladenosine

tout-P-ambo-2'-*O*-méthyl-*P*-thiocytidylyl-(3'→5')-2'-*O*-méthyl-*P*-thioadénylyl-(3'→5')-2'-*O*-méthyluridylyl-(3'→5')-2'-*O*-méthyluridylyl-(3'→5')-2'-*O*-méthyladénylyl-(3'→5')-2'-*O*-méthylguanylyl-(3'→5')-2'-désoxy-2'-fluoroguanylyl-(3'→5')-2'-*O*-méthyladénylyl-(3'→5')-2'-désoxy-2'-fluorouridylyl-(3'→5')-2'-désoxy-2'-fluoroadénylyl-(3'→5')-2'-désoxy-2'-fluoroadénylyl-(3'→5')-2'-*O*-méthyluridylyl-(3'→5')-2'-*O*-méthylguanylyl-(3'→5')-2'-*O*-méthyluridylyl-(3'→5')-2'-*O*-méthylcytidylyl-(3'→5')-2'-*O*-méthyluridylyl-(3'→5')-2'-*O*-méthyluridylyl-(3'→5')-2'-*O*-méthyladénylyl-(3'→5')-2'-*O*-méthyluridylyl-(3'→5')-2'-*O*-méthylguanylyl-(3'→5')-hydrogéno-2'-*O*-méthyl-**3'**-uridylate de [(2*S*,4*R*)-1-{1-[(2-acétamido-2-désoxy-β-D-galactopyranosyl)oxy]-16,16-bis({3-[(3-{5-[(2-acétamido-2-désoxy-β-D-galactopyranosyl)oxy]pentanamido}propyl)amino]-3-oxopro**poxy**}méthyl)-5,11,18-trioxo-14-oxa-6,10,17-triazanonacosan-29-oyl}-4-hydroxypyrrolidin-2-yl]méthyle duplex avec *tout-P-ambo*-2'-*O*-méthyl-*P*-thioguanylyl-(5'→3')-2'-*O*-méthyl-*P*-thioguanylyl-(5'→3')-2'-*O*-méthylguanylyl-(5'→3')-2'-*O*-méthyluridylyl-(5'→3')-2'-*O*-méthyladénylyl-(5'→3')-2'-*O*-méthyladénylyl-(5'→3')-2'-*O*-méthyluridylyl-(5'→3')-2'-désoxy-2'-fluorocytidylyl-(5'→3')-2'-*O*-méthylcytidylyl-(5'→3')-2'-désoxy-2'-fluorouridylyl-(5'→3')-2'-*O*-méthyladénylyl-(5'→3')-2'-*O*-méthyluridylyl-(5'→3')-2'-*O*-méthyluridylyl-(5'→3')-2'-*O*-méthyladénylyl-(5'→3')-2'-désoxy-2'-fluorocytidylyl-(5'→3')-2'-désoxy-2'-fluoroadénylyl-(5'→3')-2'-*O*-méthylguanylyl-(5'→3')-2'-désoxy-2'-fluoroadénylyl-(5'→3')-2'-*O*-méthyladénylyl-(5'→3')-2'-*O*-méthyluridylyl-(5'→3')-2'-*O*-méthyl-*P*-thioadénylyl-(5'→3')-2'-désoxy-2'-fluoro-*P*-thiocytidylyl-(5'→3')-2'-*O*-méthyladénosine

todo-P-ambo-2'-*O*-metil-*P*-tiocitidilil-(3'→5')-2'-*O*-metil-*P*-tioadenilil-(3'→5')-2'-*O*-metiluridilil-(3'→5')-2'-*O*-metiluridilil-(3'→5')-2'-*O*-metiladenilil-(3'→5')-2'-*O*-metilguanilil-(3'→5')-2'-desoxi-2'-fluoroguanilil-(3'→5')-2'-*O*-metiladenilil-(3'→5')-2'-

desoxi-2'-fluorouridilil-(3'→5')-2'-desoxi-2'-fluoroadenilil-(3'→5')-2'-desoxi-2'-fluoroadenilil-(3'→5')-2'-*O*-metiluridilil-(3'→5')-2'-*O*-metilguanilil-(3'→5')-2'-*O*-metiluridilil-(3'→5')-2'-*O*-metilcitidilil-(3'→5')-2'-*O*-metiluridilil-(3'→5')-2'-*O*-metiluridilil-(3'→5')-2'-*O*-metiladenilil-(3'→5')-2'-*O*-metiluridilil-(3'→5')-2'-*O*-metilguanilil-(3'→5')-hidrógeno-2'-*O*-metil-**3'**-uridilato de [(2*S*,4*R*)-1-(1-[(2-acetamido-2-desoxi-β-D-galactopiranosil)oxi]-16,16-bis({3-[(3-{5-[(2-acetamido-2-desoxi-β-D-galactopiranosil)oxi]pentanamido}propil)amino]-3-oxoprop**oxi**}metil)-5,11,18-trioxo-14-oxa-6,10,17-triazanonacosan-29-oil)-4-hidroxipirrolidin-2-il]metilo dúplex con *todo-P-ambo*-2'-*O*-metil-*P*-tioguanilil-(5'→3')-2'-*O*-metil-*P*-tioguanilil-(5'→3')-2'-*O*-metilguanilil-(5'→3')-2'-*O*-metiluridilil-(5'→3')-2'-*O*-metiladenilil-(5'→3')-2'-*O*-metiladenilil-(5'→3')-2'-*O*-metiluridilil-(5'→3')-2'-desoxi-2'-fluorocitidilil-(5'→3')-2'-*O*-metilcitidilil-(5'→3')-2'-desoxi-2'-fluorouridilil-(5'→3')-2'-*O*-metiladenilil-(5'→3')-2'-*O*-metiluridilil-(5'→3')-2'-*O*-metiluridilil-(5'→3')-2'-*O*-metiladenilil-(5'→3')-2'-desoxi-2'-fluorocitidilil-(5'→3')-2'-desoxi-2'-fluoroadenilil-(5'→3')-2'-*O*-metilguanilil-(5'→3')-2'-desoxi-2'-fluoroadenilil-(5'→3')-2'-*O*-metiladenilil-(5'→3')-2'-*O*-metiluridilil-(5'→3')-2'-*O*-metil-*P*-tioadenilil-(5'→3')-2'-desoxi-2'-fluoro-*P*-tiocitidilil-(5'→3')-2'-*O*-metiladenosina

p.414

plumbum (^{212}Pb) lapemelanotidum zapixetanum

lead (^{212}Pb) lapemelanotide zapixetan	*replace the molecular formula by the following one*
plomb (^{212}Pb) lapémélanotide zapixétan	*remplacer la formule moléculaire brute par la suivante*
plomo (^{212}Pb) lapemelanotida zapixetán	*sustitúyase la fórmula molecular por la siguiente*

$C_{79}H_{117}N_{25}O_{18}$**^{212}Pb**

p.437-438 **senvesiranum**

senvesiran	*replace the chemical name by the following one*
senvésiran	*remplacer le nom chimique par le suivant*
senvesirán	*sustitúyase el nombre químico por el siguiente*

[(2*S*,4*R*)-1-{1-[(2-acetamido-2-deoxy-β-D-galactopyranosyl)oxy]-16,16-bis({3-[(3-{5-[(2-acetamido-2-deoxy-β-D-galactopyranosyl)oxy]pentanamido}propyl)amino]-3-oxoprop**oxy**}methyl)-5,11,18-trioxo-14-oxa-6,10,17-triazanonacosan-29-oyl}-4-hydroxypyrrolidin-2-yl]methyl hydrogen *all-P-ambo*-2'-*O*-methyl-*P*-thioguanylyl-(3'→5')-2'-*O*-methyl-*P*-thiocytidylyl-(3'→5')-2'-*O*-methyladenylyl-(3'→5')-2'-*O*-methylguanylyl-(3'→5')-2'-*O*-methylguanylyl-(3'→5')-2'-*O*-methyladenylyl-(3'→5')-2'-*O*-methyladenylyl-(3'→5')-2'-*O*-methylguanylyl-(3'→5')-2'-deoxy-2'-fluorocytidylyl-(3'→5')-2'-deoxy-2'-fluoroadenylyl-(3'→5')-2'-deoxy-2'-fluorocytidylyl-(3'→5')-2'-*O*-methyluridylyl-(3'→5')-2'-*O*-methylguanylyl-(3'→5')-2'-*O*-methyladenylyl-(3'→5')-2'-*O*-methylguanylyl-(3'→5')-2'-*O*-methyladenylyl-(3'→5')-2'-*O*-methyluridylyl-(3'→5')-2'-*O*-methyluridylyl-(3'→5')-2'-*O*-methylcytidylyl-(3'→5')-2'-*O*-methylguanylyl-(3'→5')-2'-*O*-methyl-**3'**-uridylate duplex with *all-P-ambo*-2'-*O*-methyl-*P*-thiocytidylyl-(5'→3')-2'-*O*-methyl-*P*-thioadenylyl-(5'→3')-2'-*O*-methylcytidylyl-(5'→3')-2'-*O*-methylguanylyl-(5'→3')-2'-*O*-methyluridylyl-(5'→3')-2'-*O*-

methylcytidylyl-(5'→3')-2'-*O*-methylcytidylyl-(5'→3')-2'-*O*-methyluridylyl-(5'→3')-2'-*O*-methyluridylyl-(5'→3')-2'-deoxy-2'-fluorocytidylyl-(5'→3')-2'-*O*-methylguanylyl-(5'→3')-thymidylyl-(5'→3')-2'-*O*-methylguanylyl-(5'→3')-2'-*O*-methyladenylyl-(5'→3')-2'-*O*-methylcytidylyl-(5'→3')-2'-*O*-methyluridylyl-(5'→3')-2'-deoxycytidylyl-(5'→3')-2'-*O*-methyluridylyl-(5'→3')-2'-deoxyadenylyl-(5'→3')-2'-*O*-methyladenylyl-(5'→3')-2'-*O*-methyl-*P*-thioguanylyl-(5'→3')-2'-deoxy-*P*-thiocytidylyl-(5'→3')-2'-*O*-methyladenosine

tout-P-ambo-2'-*O*-méthyl-*P*-thioguanylyl-(3'→5')-2'-*O*-méthyl-*P*-thiocytidylyl-(3'→5')-2'-*O*-méthyladénylyl-(3'→5')-2'-*O*-méthylguanylyl-(3'→5')-2'-*O*-méthylguanylyl-(3'→5')-2'-*O*-méthyladénylyl-(3'→5')-2'-*O*-méthyladénylyl-(3'→5')-2'-*O*-méthylguanylyl-(3'→5')-2'-désoxy-2'-fluorocytidylyl-(3'→5')-2'-désoxy-2'-fluoroadénylyl-(3'→5')-2'-désoxy-2'-fluorocytidylyl-(3'→5')-2'-*O*-méthyluridylyl-(3'→5')-2'-*O*-méthylguanylyl-(3'→5')-2'-*O*-méthyladénylyl-(3'→5')-2'-*O*-méthylguanylyl-(3'→5')-2'-*O*-méthyladénylyl-(3'→5')-2'-*O*-méthyluridylyl-(3'→5')-2'-*O*-méthyluridylyl-(3'→5')-2'-*O*-méthylcytidylyl-(3'→5')-2'-*O*-méthylguanylyl-(3'→5')-hydrogéno-2'-*O*-méthyl-**3'**-uridylate de [(2*S*,4*R*)-1-{1-[(2-acétamido-2-désoxy-β-D-galactopyranosyl)oxy]-16,16-bis({3-[(3-{5-[(2-acétamido-2-désoxy-β-D-galactopyranosyl)oxy]pentanamido}propyl)amino]-3-oxoprop**oxy**}méthyl)-5,11,18-trioxo-14-oxa-6,10,17-triazanonacosan-29-oyl}-4-hydroxypyrrolidin-2-yl]méthyle duplex avec *tout-P-ambo*-2'-*O*-méthyl-*P*-thiocytidylyl-(5'→3')-2'-*O*-méthyl-*P*-thioadénylyl-(5'→3')-2'-*O*-méthylcytidylyl-(5'→3')-2'-*O*-méthylguanylyl-(5'→3')-2'-*O*-méthyluridylyl-(5'→3')-2'-*O*-méthylcytidylyl-(5'→3')-2'-*O*-méthylcytidylyl-(5'→3')-2'-*O*-méthyluridylyl-(5'→3')-2'-*O*-méthyluridylyl-(5'→3')-2'-désoxy-2'-fluorocytidylyl-(5'→3')-2'-*O*-méthylguanylyl-(5'→3')-thymidylyl-(5'→3')-2'-*O*-méthylguanylyl-(5'→3')-2'-*O*-méthyladénylyl-(5'→3')-2'-*O*-méthylcytidylyl-(5'→3')-2'-*O*-méthyluridylyl-(5'→3')-2'-désoxycytidylyl-(5'→3')-2'-*O*-méthyluridylyl-(5'→3')-2'-désoxyadénylyl-(5'→3')-2'-*O*-méthyladénylyl-(5'→3')-2'-*O*-méthyl-*P*-thioguanylyl-(5'→3')-2'-désoxy-*P*-thiocytidylyl-(5'→3')-2'-*O*-méthyladénosine

todo-P-ambo-2'-*O*-metil-*P*-tioguanilil-(3'→5')-2'-*O*-metil-*P*-tiocitidilil-(3'→5')-2'-*O*-metiladenilil-(3'→5')-2'-*O*-metilguanilil-(3'→5')-2'-*O*-metilguanilil-(3'→5')-2'-*O*-metiladenilil-(3'→5')-2'-*O*-metiladenilil-(3'→5')-2'-*O*-metilguanilil-(3'→5')-2'-desoxi-2'-fluorocitidilil-(3'→5')-2'-desoxi-2'-fluoroadenilil-(3'→5')-2'-desoxi-2'-fluorocitidilil-(3'→5')-2'-*O*-metiluridilil-(3'→5')-2'-*O*-metilguanilil-(3'→5')-2'-*O*-metiladenilil-(3'→5')-2'-*O*-metilguanilil-(3'→5')-2'-*O*-metiladenilil-(3'→5')-2'-*O*-metiluridilil-(3'→5')-2'-*O*-metiluridilil-(3'→5')-2'-*O*-metilcitidilil-(3'→5')-2'-*O*-metilguanilil-(3'→5')-hidrógeno-2'-*O*-metil-**3'**-uridilato de [(2S,4R)-1-(1-[(2-acetamido-2-desoxi-β-D-galactopiranosil)oxi]-16,16-bis({3-[(3-{5-[(2-acetamido-2-desoxi-β-D-galactopiranosil)oxi]pentanamido}propil)amino]-3-oxoprop**oxi**}metil)-5,11,18-trioxo-14-oxa-6,10,17-triazanonacosan-29-oil)-4-hidroxipirrolidin-2-il]metilo dúplex con *todo-P-ambo*-2'-*O*-metil-*P*-tiocitidilil-(5'→3')-2'-*O*-metil-*P*-tioadenilil-(5'→3')-2'-*O*-metilcitidilil-(5'→3')-2'-*O*-metilguanilil-(5'→3')-2'-*O*-metiluridilil-(5'→3')-2'-*O*-metilcitidilil-(5'→3')-2'-*O*-metilcitidilil-(5'→3')-2'-*O*-metiluridilil-(5'→3')-2'-*O*-metiluridilil-(5'→3')-2'-desoxi-2'-fluorocitidilil-(5'→3')-2'-*O*-

metilguanilil-(5'→3')-timidilil-(5'→3')-2'-*O*-metilguanilil-(5'→3')-2'-*O*-metiladenilil-(5'→3')-2'-*O*-metilcytidilil-(5'→3')-2'-*O*-metiluridilil-(5'→3')-2'-desoxicitidilil-(5'→3')-2'-*O*-metiluridilil-(5'→3')-2'-desoxiadenilil-(5'→3')-2'-*O*-metiladenilil-(5'→3')-2'-*O*-metil-*P*-tioguanilil-(5'→3')-2'-desoxi-*P*-tiocitidilil-(5'→3')-2'-*O*-metiladenosina

p.454 **surovatamigum #**

-456 surovatamig *Please note that the MedNet file has been updated*
surovatamig *Veuillez noter que le fichier MedNet a été mis à jour*
surovatamig *Tenga en cuenta que se ha actualizado el archivo MedNet*

p.485 **vensemaglutidum**

vensemaglutide *replace the chemical name and molecular formula by the following ones*

vensémaglutide *remplacer le nom chimique et la formule moléculaire par les suivants*

vensemaglutida *sustitúyase el nombre químico y la fórmula molecular por los siguientes*

N$^{2.2}$-{2-[(4*S*)-4-carboxy-4-(15-carboxypentadecanamido)butanamido]ethyl}-*N*$^{6.22}$-[(22*S*)-22,40-dicarboxy-10,19,24-trioxo-3,6,12,15-tetraoxa-9,18,23-triazatetracontan-1-oyl]-[**E^{5}>G^{1},R^{6}>G^{2},A^{8}>Aib^{4},K^{34}>R^{30}**]human glucagon-like peptide 1(5-37)

N$^{2.2}$-{2-[(4*S*)-4-carboxy-4-(15-carboxypentadécanamido)butanamido]éthyl}-*N*$^{6.22}$-[(22*S*)-22,40-dicarboxy-10,19,24-trioxo-3,6,12,15-tétraoxa-9,18,23-triazatétracontan-1-oyl]-[**E^{5}>G^{1},R^{6}>G^{2},A^{8}>Aib^{4},K^{34}>R^{30}**]peptide 1(5-37) apparenté au glucagon humain (GLP-1(5-37))

N$^{2.2}$-{2-[(4*S*)-4-carboxi-4-(15-carboxipentadecanamido)butanamido]etil}-*N*$^{6.22}$-[(22*S*)-22,40-dicarboxi-10,19,24-trioxo-3,6,12,15-tetraoxa-9,18,23-triazatetracontan-1-oil]-[**E^{5}>G^{1},R^{6}>G^{2},A^{8}>Aib^{4},K^{34}>R^{30}**]péptido 1(5-37) similar al glucagón humano (GLP-1(5-37))

$C_{214}H_{337}N_{49}O_{67}$

p.495 **zelebrudomidum**

zelebrudomide *replace the CAS registry number by the following one*

zélébrudomide *remplacer le numéro de registre du CAS par le suivant*

zelebrudomida *sustitúyase el número de registro del CAS por el siguiente*

3024312-52-2

ANNEX 1

PROCEDURE FOR THE SELECTION OF RECOMMENDED INTERNATIONAL NONPROPRIETARY NAMES FOR PHARMACEUTICAL SUBSTANCES[1]

The following procedure shall be followed by the World Health Organization (hereinafter also referred to as "WHO") in the selection of recommended international nonproprietary names for pharmaceutical substances, in accordance with resolution WHA3.11 of the World Health Assembly, and in the substitution of such names.

Article 1 - Proposals for recommended international nonproprietary names and proposals for substitution of such names shall be submitted to WHO on the form provided therefore. The consideration of such proposals shall be subject to the payment of an administrative fee designed only to cover the corresponding costs of the Secretariat of WHO ("the Secretariat"). The amount of this fee shall be determined by the Secretariat and may, from time to time, be adjusted.

Article 2 - Such proposals shall be submitted by the Secretariat to the members of the Expert Advisory Panel on the International Pharmacopoeia and Pharmaceutical Preparations designated for this purpose, such designated members hereinafter referred to as "the INN Expert Group", for consideration in accordance with the "General principles for guidance in devising International Nonproprietary Names for Pharmaceutical Substances", annexed to this procedure[2]. The name used by the person discovering or first developing and marketing a pharmaceutical substance shall be accepted, unless there are compelling reasons to the contrary.

Article 3 - Subsequent to the examination provided for in article 2, the Secretariat shall give notice that a proposed international nonproprietary name is being considered.

a) Such notice shall be given by publication in *WHO Drug Information*[3] and by letter to Member States and to national and regional pharmacopoeia commissions or other bodies designated by Member States.

i) Notice shall also be sent to the person who submitted the proposal ("the original applicant") and other persons known to be concerned with a name under consideration.

b) Such notice shall:

i) set forth the name under consideration;

ii) identify the person who submitted the proposal for naming the substance, if so requested by such person;

iii) identify the substance for which a name is being considered;

iv) set forth the time within which comments and objections will be received and the person and place to whom they should be directed;

v) state the authority under which WHO is acting and refer to these rules of procedure.

c) In forwarding the notice, the Secretariat shall request that Member States take such steps as are necessary to prevent the acquisition of proprietary rights in the proposed name during the period it is under consideration by WHO.

Article 4 - Comments on the proposed name may be forwarded by any person to WHO within four months of the date of publication, under article 3, of the name in *WHO Drug Information*.

[1] See Annex 1 in WHO Technical Report Series, No. 581, 1975. The original text was adopted by the Executive Board in resolution EB15.R7 and amended in resolutions EB43.R9 and EB115.R4.

[2] See Annex 2.

[3] Before 1987, lists of international nonproprietary names were published in the *Chronicle of the World Health Organization*.

Article 5 - A formal objection to a proposed name may be filed by any interested person within four months of the date of publication, under article 3, of the name in *WHO Drug Information.*

Such objection shall:

i) identify the person objecting;

ii) state his or her interest in the name;

iii) set forth the reasons for his or her objection to the name proposed.

Article 6 - Where there is a formal objection under article 5, WHO may either reconsider the proposed name or use its good offices to attempt to obtain withdrawal of the objection. Without prejudice to the consideration by WHO of a substitute name or names, a name shall not be selected by WHO as a recommended international nonproprietary name while there exists a formal objection thereto filed under article 5 which has not been withdrawn.

Article 7 - Where no objection has been filed under article 5, or all objections previously filed have been withdrawn, the Secretariat shall give notice in accordance with subsection (a) of article 3 that the name has been selected by WHO as a recommended international nonproprietary name.

Article 8 - In forwarding a recommended international nonproprietary name to Member States under article 7, the Secretariat shall:

a) request that it be recognized as the nonproprietary name for the substance; and

b) request that Member States take such steps as are necessary to prevent the acquisition of proprietary rights in the name and to prohibit registration of the name as a trademark or trade name.

Article 9
a) In the extraordinary circumstance that a previously recommended international nonproprietary name gives rise to errors in medication, prescription or distribution, or a demonstrable risk thereof, because of similarity with another name in pharmaceutical and/or prescription practices, and it appears that such errors or potential errors cannot readily be resolved through other interventions than a possible substitution of a previously recommended international nonproprietary name, or in the event that a previously recommended international nonproprietary name differs substantially from the nonproprietary name approved in a significant number of Member States, or in other such extraordinary circumstances that justify a substitution of a recommended international nonproprietary name, proposals to that effect may be filed by any interested person. Such proposals shall be submitted on the form provided therefore and shall:

i) identify the person making the proposal;

ii) state his or her interest in the proposed substitution; and

iii) set forth the reasons for the proposal; and

iv) describe, and provide documentary evidence regarding the other interventions undertaken in an effort to resolve the situation, and the reasons why these other interventions were inadequate.

Such proposals may include a proposal for a new substitute international nonproprietary name, devised in accordance with the General principles, which takes into account the pharmaceutical substance for which the new substitute international nonproprietary name is being proposed.

The Secretariat shall forward a copy of the proposal, for consideration in accordance with the procedure described in subsection (b) below, to the INN Expert Group and the original applicant or its successor (if different from the person bringing the proposal for substitution and provided that the original applicant or its successor is known or can be found through diligent effort, including contacts with industry associations).

In addition, the Secretariat shall request comments on the proposal from:

i) Member States and national and regional pharmacopoeia commissions or other bodies designated by Member States (by including a notice to that effect in the letter referred to in article 3(a), and

ii) any other persons known to be concerned by the proposed substitution.

The request for comments shall:

i) state the recommended international nonproprietary name that is being proposed for substitution (and the proposed substitute name, if provided);

ii) identify the person who submitted the proposal for substitution (if so requested by such person);

iii) identify the substance to which the proposed substitution relates and reasons put forward for substitution;

iv) set forth the time within which comments will be received and the person and place to whom they should be directed; and

v) state the authority under which WHO is acting and refer to these rules of procedure.

Comments on the proposed substitution may be forwarded by any person to WHO within four months of the date of the request for comments.

b) After the time period for comments referred to above has elapsed, the Secretariat shall forward any comments received to the INN Expert Group, the original applicant or its successor and the person bringing the proposal for substitution. If, after consideration of the proposal for substitution and the comments received, the INN Expert Group, the person bringing the proposal for substitution and the original applicant or its successor all agree that there is a need to substitute the previously recommended international nonproprietary name, the Secretariat shall submit the proposal for substitution to the INN Expert Group for further processing.
Notwithstanding the foregoing, the original applicant or its successor shall not be entitled to withhold agreement to a proposal for substitution in the event the original applicant or its successor has no demonstrable continuing interest in the recommended international nonproprietary name proposed for substitution.

In the event that a proposal for substitution shall be submitted to the INN Expert Group for further processing, the INN Expert Group will select a new international nonproprietary name in accordance with the General principles referred to in article 2 and the procedure set forth in articles 3 to 8 inclusive. The notices to be given by the Secretariat under article 3 and article 7, respectively, including to the original applicant or its successor (if not the same as the person proposing the substitution, and provided that the original applicant or its successor is known or can be found through diligent effort, including contacts with industry associations), shall in such event indicate that the new name is a substitute for a previously recommended international nonproprietary name and that Member States may wish to make transitional arrangements in order to accommodate existing products that use the previously recommended international nonproprietary name on their label in accordance with national legislation.

If, after consideration of the proposal for substitution and the comments received in accordance with the procedure described above, the INN Expert Group, the original applicant or its successor and the person bringing the proposal for substitution do not agree that there are compelling reasons for substitution of a previously recommended international nonproprietary name, this name shall be retained (provided always that the original applicant or its successor shall not be entitled to withhold agreement to a proposal for substitution in the event that the original applicant or its successor has no demonstrable continuing interest in the recommended international nonproprietary name proposed to be substituted). In such an event, the Secretariat shall advise the person having proposed the substitution, as well as the original applicant or its

successor (if not the same as the person proposing the substitution, and provided that the original applicant or its successor is known or can be found through diligent effort, including contacts with industry associations), Member States, national and regional pharmacopoeia commissions, other bodies designated by Member States, and any other persons known to be concerned by the proposed substitution that, despite a proposal for substitution, it has been decided to retain the previously recommended international nonproprietary name (with a description of the reason(s) why the proposal for substitution was not considered sufficiently compelling).

ANNEX 2

GENERAL PRINCIPLES FOR GUIDANCE IN DEVISING INTERNATIONAL NONPROPRIETARY NAMES FOR PHARMACEUTICAL SUBSTANCES[1]

1. International Nonproprietary Names (INN) should be distinctive in sound and spelling. They should not be inconveniently long and should not be liable to confusion with names in common use.

2. The INN for a substance belonging to a group of pharmacologically related substances should, where appropriate, show this relationship. Names that are likely to convey to a patient an anatomical, physiological, pathological or therapeutic suggestion should be avoided.

These primary principles are to be implemented by using the following secondary principles:

3. In devising the INN of the first substance in a new pharmacological group, consideration should be given to the possibility of devising suitable INN for related substances, belonging to the new group.

4. In devising INN for acids, one-word names are preferred; their salts should be named without modifying the acid name, e.g. “oxacillin” and “oxacillin sodium”, “ibufenac” and “ibufenac sodium”.

5. INN for substances which are used as salts should in general apply to the active base or the active acid. Names for different salts or esters of the same active substance should differ only in respect of the name of the inactive acid or the inactive base.
For quaternary ammonium substances, the cation and anion should be named appropriately as separate components of a quaternary substance and not in the amine-salt style.

6. The use of an isolated letter or number should be avoided; hyphenated construction is also undesirable.

7. To facilitate the translation and pronunciation of INN, “f” should be used instead of “ph”, “t” instead of “th”, “e” instead of “ae” or “oe”, and “i” instead of “y”; the use of the letters “h” and “k” should be avoided.

8. Provided that the names suggested are in accordance with these principles, names proposed by the person discovering or first developing and marketing a pharmaceutical preparation, or names already officially in use in any country, should receive preferential consideration.

9. Group relationship in INN (see General principle 2) should if possible be shown by using a common stem. The following list contains examples of stems for groups of substances, particularly for new groups. There are many other stems in active use.[2] Where a stem is shown without any hyphens it may be used anywhere in the name.

---

[1] In its Twentieth report (WHO Technical Report Series, No. 581, 1975), the WHO Expert committee on Nonproprietary Names for Pharmaceutical Substances reviewed the general principles for devising, and the procedures for selecting, INN in the light of developments in pharmaceutical compounds in recent years. The most significant change has been the extension to the naming of synthetic chemical substances of the practice previously used for substances originating in or derived from natural products. This practice involves the use of a characteristic “stem” indicative of a common property of the members of a group. The reason for, and the implications of, the change are fully discussed.
The guiding principles were updated during the 13th consultation on nonproprietary names for pharmaceutical substances (Geneva, 27-29 April 1983) (PHARM S/NOM 928 13 May 1983, revised 18 August 1983).

[2] A more extensive listing of stems is contained in the working document WHO/EMP/RHT/TSN/2018.1 which is regularly updated and can be requested from the INN Programme, WHO, Geneva.

Latin	English	
-acum	*-ac*	anti-inflammatory agents, ibufenac derivatives
-adolum	*-adol }*	analgesics
-adol-	*-adol-}*	
-astum	*-ast*	antiasthmatic, antiallergic substances not acting primarily as antihistaminics
-astinum	*-astine*	antihistaminics
-azepamum	*-azepam*	diazepam derivatives
bol	*bol*	steroids, anabolic
-cain-	*-cain-*	class I antiarrhythmics, procainamide and lidocaine derivatives
-cainum	*-caine*	local anaesthetics
cef-	*cef-*	antibiotics, cefalosporanic acid derivatives
-cillinum	*-cillin*	antibiotics, 6-aminopenicillanic acid derivatives
-conazolum	*-conazole*	systemic antifungal agents, miconazole derivatives
cort	*cort*	corticosteroids, except prednisolone derivatives
-coxibum	*-coxib*	selective cyclo-oxygenase inhibitors
-entanum	*-entan*	endothelin receptor antagonists
gab	*gab*	gabamimetic agents
gado-	*gado-*	diagnostic agents, gadolinium derivatives
-gatranum	*-gatran*	thrombin inhibitors, antithrombotic agents
gest	*gest*	steroids, progestogens
gli	*gli*	antihyperglycaemics
io-	*io-*	iodine-containing contrast media
-metacinum	*-metacin*	anti-inflammatory, indometacin derivatives
-mycinum	*-mycin*	antibiotics, produced by *Streptomyces* strains
-nidazolum	*-nidazole*	antiprotozoal substances, metronidazole derivatives
-ololum	*-olol*	β-adrenoreceptor antagonists
-oxacinum	*-oxacin*	antibacterial agents, nalidixic acid derivatives
-platinum	*-platin*	antineoplastic agents, platinum derivatives
-poetinum	*-poetin*	erythropoietin type blood factors
-pril(at)um	*-pril(at)*	angiotensin-converting enzyme inhibitors
-profenum	*-profen*	anti-inflammatory substances, ibuprofen derivatives
prost	*prost*	prostaglandins
-relinum	*-relin*	pituitary hormone release-stimulating peptides
-sartanum	*-sartan*	angiotensin II receptor antagonists, antihypertensive (non-peptidic)
-vaptanum	*-vaptan*	vasopressin receptor antagonists
vin-	*vin- }*	vinca-type alkaloids
-vin-	*-vin-}*	

ANNEXE 1

PROCEDURE A SUIVRE EN VUE DU CHOIX DE DENOMINATIONS COMMUNES INTERNATIONALES RECOMMANDEES POUR LES SUBSTANCES PHARMACEUTIQUES[1]

L'Organisation mondiale de la Santé (également désignée ci-après sous l'appellation « OMS ») observe la procédure exposée ci-dessous pour l'attribution de dénominations communes internationales recommandées pour les substances pharmaceutiques, conformément à la résolution WHA3.11 de l'Assemblée mondiale de la Santé, et pour le remplacement de telles dénominations.

Article 1 - Les propositions de dénominations communes internationales recommandées et les propositions de remplacement de telles dénominations sont soumises à l'OMS sur la formule prévue à cet effet. L'examen de telles propositions est soumis au paiement d'une taxe administrative destinée uniquement à couvrir les coûts correspondants assumés par le Secrétariat de l'OMS (« le Secrétariat »). Le montant de cette taxe est déterminé par le Secrétariat et peut être modifié de temps à autre.

[1] Voir annexe 1 dans OMS, Série de Rapports techniques, N° 581, 1975. Le texte original a été adopté par le Conseil exécutif dans sa résolution EB15.R7 et amendé dans ses résolutions EB43.R9 et EB115.R4.

Article 2 - Ces propositions sont soumises par le Secrétariat aux experts désignés à cette fin parmi les personnalités inscrites au Tableau d'experts de la Pharmacopée internationale et des Préparations pharmaceutiques, ci-après désignés sous l'appellation « le Groupe d'experts des DCI» ; elles sont examinées par les experts conformément aux « Directives générales pour la formation de dénominations communes internationales pour les substances pharmaceutiques » reproduites ci-après[1].La dénomination acceptée est la dénomination employée par la personne qui découvre ou qui, la première, fabrique et lance sur le marché une substance pharmaceutique, à moins que des raisons majeures n'obligent à s'écarter de cette règle.

Article 3 - Après l'examen prévu à l'article 2, le Secrétariat notifie qu'un projet de dénomination commune internationale est à l'étude.

a) Cette notification est faite par une insertion dans *WHO Drug Information*[2] et par l'envoi d'une lettre aux Etats Membres et aux commissions nationales et régionales de pharmacopée ou autres organismes désignés par les Etats Membres.

i) Notification est également faite à la personne qui a soumis la proposition (« le demandeur initial ») et à d'autres personnes portant à la dénomination mise à l'étude un intérêt notoire.

b) Cette notification contient les indications suivantes :

i) dénomination mise à l'étude;

ii) nom de l'auteur de la proposition tendant à attribuer une dénomination à la substance, si cette personne le demande ;

iii) définition de la substance dont la dénomination est mise à l'étude ;

iv) délai pendant lequel seront reçues les observations et les objections à l'égard de cette dénomination ; nom et adresse de la personne habilitée à recevoir ces observations et objections ;

v) mention des pouvoirs en vertu desquels agit l'OMS et référence au présent règlement.

c) En envoyant cette notification, le Secrétariat demande aux Etats Membres de prendre les mesures nécessaires pour prévenir l'acquisition de droits de propriété sur la dénomination proposée pendant la période au cours de laquelle cette dénomination est mise à l'étude par l'OMS.

Article 4 - Des observations sur la dénomination proposée peuvent être adressées à l'OMS par toute personne, dans les quatre mois qui suivent la date de publication de la dénomination dans *WHO Drug Information* (voir l'article 3).

Article 5 - Toute personne intéressée peut formuler une objection formelle contre la dénomination proposée dans les quatre mois qui suivent la date de publication de la dénomination dans *WHO Drug Information* (voir l'article 3).

Cette objection doit s'accompagner des indications suivantes :

i) nom de l'auteur de l'objection ;

ii) intérêt qu'il ou elle porte à la dénomination en cause ;

iii) raisons motivant l'objection contre la dénomination proposée.

Article 6 - Lorsqu'une objection formelle est formulée en vertu de l'article 5, l'OMS peut soit soumettre la dénomination proposée à un nouvel examen, soit intervenir pour tenter d'obtenir le retrait de l'objection. Sans préjudice de l'examen par l'OMS d'une ou de plusieurs appellations de

[1] Voir annexe 2.

[2] Avant 1987, les listes de dénominations communes internationales étaient publiées dans la *Chronique de l'Organisation mondiale de la Santé*.

remplacement, l'OMS n'adopte pas d'appellation comme dénomination commune internationale recommandée tant qu'une objection formelle présentée conformément à l'article 5 n'est pas levée.

Article 7 - Lorsqu'il n'est formulé aucune objection en vertu de l'article 5, ou que toutes les objections présentées ont été levées, le Secrétariat fait une notification conformément aux dispositions du paragraphe a) de l'article 3, en indiquant que la dénomination a été choisie par l'OMS en tant que dénomination commune internationale recommandée.

Article 8 - En communiquant aux Etats Membres, conformément à l'article 7, une dénomination commune internationale recommandée, le Secrétariat :
a) demande que cette dénomination soit reconnue comme dénomination commune de la substance considérée ; et
b) demande aux Etats Membres de prendre les mesures nécessaires pour prévenir l'acquisition de droits de propriété sur cette dénomination et interdire le dépôt de cette dénomination comme marque ou appellation commerciale.

Article 9 -
a) Dans le cas exceptionnel où une dénomination commune internationale déjà recommandée donne lieu à des erreurs de médication, de prescription ou de distribution ou en comporte un risque démontrable, en raison d'une similitude avec une
autre appellation dans la pratique pharmaceutique et/ou de prescription, et où il apparaît que ces erreurs ou ces risques d'erreur ne peuvent être facilement évités par d'autres interventions que le remplacement éventuel d'une dénomination commune internationale déjà recommandée, ou dans le cas où une dénomination commune internationale déjà recommandée diffère sensiblement de la dénomination commune approuvée dans un nombre important d'Etats Membres, ou dans d'autres circonstances exceptionnelles qui justifient le remplacement d'une dénomination commune internationale recommandée, toute personne intéressée peut formuler une proposition dans ce sens. Cette proposition est présentée sur la formule prévue à cet effet et doit s'accompagner des indications suivantes :

i) nom de l'auteur de la proposition ;

ii) intérêt qu'il ou elle porte au remplacement proposé ;

iii) raisons motivant la proposition ; et

iv) description, faits à l'appui, des autres interventions entreprises pour tenter de régler le problème et exposé des raisons pour lesquelles ces interventions ont échoué.

Les propositions peuvent comprendre une proposition de nouvelle dénomination commune internationale de remplacement, établie conformément aux Directives générales, compte tenu de la substance pharmaceutique pour laquelle la nouvelle dénomination commune internationale de remplacement est proposée.

Le Secrétariat transmet une copie de la proposition pour examen, conformément à la procédure exposée plus loin au paragraphe b), au Groupe d'experts des DCI et au demandeur initial ou à son successeur (s'il s'agit d'une personne différente de celle qui a formulé la proposition de remplacement et pour autant que le demandeur initial ou son successeur soit connu ou puisse être retrouvé moyennant des efforts diligents, notamment des contacts avec les associations industrielles).

De plus, le Secrétariat demande aux entités et personnes ci-après de formuler des observations sur la proposition :

i) les Etats Membres et les commissions nationales et régionales de pharmacopée ou d'autres organismes désignés par les Etats Membres (en insérant une note à cet effet dans la lettre mentionnée à l'article 3.a), et

ii) toutes autres personnes portant au remplacement proposé un intérêt notoire.

La demande d'observations contient les indications suivantes :

i) dénomination commune internationale recommandée pour laquelle un remplacement est proposé (et la dénomination de remplacement proposée, si elle est fournie) ;

ii) nom de l'auteur de la proposition de remplacement (si cette personne le demande) ;

iii) définition de la substance faisant l'objet du remplacement proposé et raisons avancées pour le remplacement ;

iv) délai pendant lequel seront reçus les commentaires et nom et adresse de la personne habilitée à recevoir ces commentaires ; et

v) mention des pouvoirs en vertu desquels agit l'OMS et référence au présent règlement.

Des observations sur la proposition de remplacement peuvent être communiquées par toute personne à l'OMS dans les quatre mois qui suivent la date de la demande d'observations.

b) Une fois échu le délai prévu ci-dessus pour la communication d'observations, le Secrétariat transmet les observations reçues au Groupe d'experts des DCI, au demandeur initial ou à son successeur et à l'auteur de la proposition de remplacement. Si, après avoir examiné la proposition de remplacement et les observations reçues, le Groupe d'experts des DCI, l'auteur de la proposition de remplacement et le demandeur initial ou son successeur reconnaissent tous qu'il est nécessaire de remplacer la dénomination commune internationale déjà recommandée, le Secrétariat soumet la proposition de remplacement au Groupe d'experts des DCI pour qu'il y donne suite.

Nonobstant ce qui précède, le demandeur initial ou son successeur n'est pas habilité à refuser son accord à une proposition de remplacement au cas où il ne peut être démontré qu'il porte un intérêt durable à la dénomination commune internationale recommandée qu'il est proposé de remplacer.

Dans le cas où une proposition de remplacement est soumise au Groupe d'experts des DCI pour qu'il y donne suite, le Groupe choisit une nouvelle dénomination commune internationale conformément aux Directives générales mentionnées à l'article 2 et selon la procédure décrite dans les articles 3 à 8 inclus. La notification faite par le Secrétariat en vertu de l'article 3 et de l'article 7, respectivement, y compris au demandeur initial ou à son successeur (si ce n'est pas la même personne que celle qui a proposé le remplacement et pour autant que le demandeur initial ou son successeur soit connu ou puisse être retrouvé moyennant des efforts diligents, notamment des contacts avec les associations industrielles), doit dans un tel cas indiquer que la nouvelle dénomination remplace une dénomination commune internationale déjà recommandée et que les Etats Membres peuvent souhaiter prendre des mesures transitoires pour les produits existants qui utilisent la dénomination commune internationale déjà recommandée sur leur étiquette conformément à la législation nationale.

Si, après examen de la proposition de remplacement et des observations communiquées conformément à la procédure exposée plus haut, le Groupe d'experts des DCI, le demandeur initial ou son successeur et l'auteur de la proposition de remplacement ne s'accordent pas sur le fait qu'il y a des raisons impératives de remplacer une dénomination commune internationale déjà recommandée, cette dernière est conservée (étant entendu toujours que le demandeur initial ou son successeur n'est pas habilité à refuser son accord à une proposition de remplacement au cas où il ne peut être démontré qu'il porte un intérêt durable à la dénomination commune internationale recommandée qu'il est proposé de remplacer). Dans un tel cas, le Secrétariat informe l'auteur de la proposition de remplacement, ainsi que le demandeur initial ou son successeur (s'il s'agit d'une personne différente de celle qui a formulé la proposition de remplacement et pour autant que le demandeur initial ou son successeur soit connu ou puisse être retrouvé moyennant des efforts diligents, notamment des contacts avec les associations industrielles), les Etats Membres, les commissions nationales et régionales de pharmacopée, les autres organismes désignés par les Etats Membres et toutes autres personnes portant un intérêt notoire au remplacement proposé que, malgré une proposition de remplacement, il a été décidé de conserver la dénomination commune internationale déjà recommandée (avec une brève description de la ou des raisons pour lesquelles la proposition de remplacement n'a pas été jugée suffisamment impérative).

ANNEXE 2

DIRECTIVES GENERALES POUR LA FORMATION DE DENOMINATIONS COMMUNES INTERNATIONALES APPLICABLES AUX SUBSTANCES PHARMACEUTIQUES[1]

1. Les dénominations communes internationales (DCI) devront se distinguer les unes des autres par leur consonance et leur orthographe. Elles ne devront pas être d'une longueur excessive, ni prêter à confusion avec des appellations déjà couramment employées.

2. La DCI de chaque substance devra, si possible, indiquer sa parenté pharmacologique. Les dénominations susceptibles d'évoquer pour les malades des considérations anatomiques, physiologiques, pathologiques ou thérapeutiques devront être évitées dans la mesure du possible.

Outre ces deux principes fondamentaux, on respectera les principes secondaires suivants :

3.Lorsqu'on formera la DCI de la première substance d'un nouveau groupe pharmacologique, on tiendra compte de la possibilité de former ultérieurement d'autres DCI appropriées pour les substances apparentées du même groupe.

4. Pour former des DCI des acides, on utilisera de préférence un seul mot. Leurs sels devront être désignés par un terme qui ne modifie pas le nom de l'acide d'origine : par exemple «oxacilline» et «oxacilline sodique», «ibufénac» et «ibufénac sodique».

5. Les DCI pour les substances utilisées sous forme de sels devront en général s'appliquer à la base active (ou à l'acide actif). Les dénominations pour différents sels ou esters d'une même substance active ne différeront que par le nom de l'acide inactif (ou de la base inactive).
En ce qui concerne les substances à base d'ammonium quaternaire, la dénomination s'appliquera de façon appropriée au cation et à l'anion en tant qu'éléments distincts d'une substance quaternaire. On évitera de choisir une désignation évoquant un sel aminé.

6. On évitera d'ajouter une lettre ou un chiffre isolé ; en outre, on renoncera de préférence au trait d'union.

7. Pour simplifier la traduction et la prononciation des DCI, la lettre « f » sera utilisée à la place de « ph », « t » à la place de « th », « e » à la place de « ae » ou « oe », et « i » à la place de « y » ; l'usage des lettres « h » et « k » sera aussi évité.

8. On retiendra de préférence, pour autant qu'elles respectent les principes énoncés ici, les dénominations proposées par les personnes qui ont découvert ou qui, les premières, ont fabriqué et lancé sur le marché les préparations pharmaceutiques considérées, ou les dénominations déjà officiellement adoptées par un pays.

9. La parenté entre substances d'un même groupe (voir Directive générale 2) sera si possible indiquée dans les DCI par l'emploi de segments-clés communs. La liste ci-après contient des exemples de segments-clés pour des groupes de substances, surtout pour des groupes récents. Il y a beaucoup d'autres segments-clés en utilisation active.[2] Les segments-clés indiqués sans trait d'union pourront être insérés n'importe où dans une dénomination.

---

[1] Dans son vingtième rapport (OMS, Série de Rapports techniques, N° 581, 1975), le Comité OMS d'experts des Dénominations communes pour les Substances pharmaceutiques a examiné les directives générales pour la formation des dénominations communes internationales et la procédure à suivre en vue de leur choix, compte tenu de l'évolution du secteur pharmaceutique au cours des dernières années. La modification la plus importante a été l'extension aux substances de synthèse de la pratique normalement suivie pour désigner les substances tirées ou dérivées de produits naturels. Cette pratique consiste à employer des syllabes communes ou groupes de syllabes communes (segments-clés) qui sont caractéristiques et indiquent une propriété commune aux membres du groupe des substances pour lequel ces segments-clés ont été retenus. Les raisons et les conséquences de cette modification ont fait l'objet de discussions approfondies.
Les directives ont été mises à jour lors de la treizième consultation sur les dénominations communes pour les substances pharmaceutiques (Genève, 27-29 avril 1983) (PHARM S/NOM 928, 13 mai 1983, révision en date du 18 août 1983).

[2] Une liste plus complète de segments-clés est contenue dans le document de travail WHO/EMP/RHT/TSN/2018.1 qui est régulièrement mis à jour et qui peut être demandé auprès du programme des DCI, OMS, Genève

Latin	Français	
-acum	*-ac*	substances anti-inflammatoires du groupe de l'ibufénac
-adolum	*-adol* }	analgésiques
-adol-	*-adol-* }	
-astum	*-ast*	antiasthmatiques, antiallergiques n'agissant pas principalement en tant qu'antihistaminiques
-astinum	*-astine*	antihistaminiques
-azepamum	*-azépam*	substances du groupe du diazépam
bol	*bol*	stéroïdes anabolisants
-cain-	*-caïn-*	antiarythmiques de classe I, dérivés du procaïnamide et de la lidocaïne
-cainum	*-caïne*	anesthésiques locaux
cef-	*céf-*	antibiotiques, dérivés de l'acide céphalosporanique
-cillinum	*-cilline*	antibiotiques, dérivés de l'acide 6-aminopénicillanique
-conazolum	*-conazole*	agents antifongiques systémiques du groupe du miconazole
cort	*cort*	corticostéroïdes, autres que les dérivés de la prednisolone
-coxibum	*-coxib*	inhibiteurs sélectifs de la cyclo-oxygénase
-entanum	*-entan*	antagonistes du récepteur de l'endothéline
gab	*gab*	gabamimétiques
gado-	*gado-*	agents diagnostiques, dérivés du gadolinium
-gatranum	*-gatran*	antithrombines, antithrombotiques
gest	*gest*	stéroïdes progestogènes
gli	*gli*	antihyperglycémiants
io-	*io-*	produits de contraste iodés
-metacinum	*-métacine*	substances anti-inflammatoires du groupe de l'indométacine
-mycinum	*-mycine*	antibiotiques produits par des souches de *Streptomyces*
-nidazolum	*-nidazole*	substances antiprotozoaires du groupe du métronidazole
-ololum	*-olol*	antagonistes des récepteurs β-adrénergiques
-oxacinum	*-oxacine*	substances antibactériennes du groupe de l'acide nalidixique
-platinum	*-platine*	antinéoplasiques, dérivés du platine
-poetinum	*-poétine*	facteurs sanguins de type érythropoïétine
-pril(at)um	*-pril(ate)*	inhibiteurs de l'enzyme de conversion de l'angiotensine
-profenum	*-profène*	substances anti-inflammatoires du groupe de l'ibuprofène
prost	*prost*	prostaglandines
-relinum	*-réline*	peptides stimulant la libération d'hormones hypophysaires
-sartanum	*-sartan*	antagonistes d'un récepteur de l'angiotensine II, antihypertenseurs (non peptidiques)
-vaptanum	*-vaptan*	antagonistes du récepteur de la vasopressine
vin-	*vin-* }	alcaloïdes du type vinca
-vin-	*-vin-* }	

ANEXO 1

PROCEDIMIENTO DE SELECCIÓN DE DENOMINACIONES COMUNES INTERNACIONALES RECOMENDADAS PARA SUSTANCIAS FARMACÉUTICAS[1]

La Organización Mundial de la Salud (OMS) seguirá el procedimiento que se expone a continuación tanto para seleccionar denominaciones comunes internacionales recomendadas para las sustancias farmacéuticas, de conformidad con lo dispuesto en la resolución WHA3.11, como para sustituir esas denominaciones.

Artículo 1 - Las propuestas de denominaciones comunes internacionales recomendadas y las propuestas de sustitución de esas denominaciones se presentarán a la OMS en los formularios que se proporcionen a estos efectos. El estudio de estas propuestas estará sujeto al pago de una tasa destinada a sufragar los costos de administración que ello suponga para la Secretaría de la OMS («la Secretaría»). La Secretaría establecerá la cuantía de esa tasa y podrá ajustarla periódicamente.

Artículo 2 - Estas propuestas serán sometidas por la Secretaría a los miembros del Cuadro de Expertos en Farmacopea Internacional y Preparaciones Farmacéuticas encargados de su estudio, en adelante designados como «el Grupo de Expertos en DCI», para que las examinen de conformidad con los «Principios generales de orientación para formar denominaciones comunes internacionales para sustancias farmacéuticas», anexos a este procedimiento.[2] A menos que haya poderosas razones en contra, la denominación aceptada será la empleada por la persona que haya descubierto o fabricado y comercializado por primera vez esa sustancia farmacéutica.

Artículo 3 - Tras el examen al que se refiere el artículo 2, la Secretaría notificará que está en estudio un proyecto de denominación internacional.

a) Esa notificación se hará mediante una publicación en *Información Farmacéutica OMS*[3] y el envío de una carta a los Estados Miembros y a las comisiones nacionales y regionales de las farmacopeas u otros organismos designados por los Estados Miembros.

i) La notificación será enviada también a la persona que haya presentado la propuesta («el solicitante inicial») y a otras personas que tengan un interés especial en una denominación objeto de estudio.

b) En esa notificación se incluirán los siguientes datos:

i) la denominación sometida a estudio;

ii) la identidad de la persona que ha presentado la propuesta de denominación de la sustancia, si lo pide esa persona;

iii) la identidad de la sustancia cuya denominación está en estudio;

iv) el plazo fijado para recibir observaciones y objeciones, así como el nombre y la dirección de la persona a quien deban dirigirse; y

v) los poderes conferidos para el caso a la OMS y una referencia al presente procedimiento.

---

[1] Véase el anexo 1 en OMS, Serie de Informes Técnicos, Nº 581, 1975. El texto vigente fue adoptado por el Consejo Ejecutivo en su resolución EB15.R7 y modificado en las resoluciónes EB43.R9 y EB115.R4..

[2] Véase el anexo 2.

[3] Hasta 1987 las listas de DCI se publicaban en la *Crónica de la Organización Mundial de la Salud*.

c) Al enviar esa notificación, la Secretaría solicitará de los Estados Miembros la adopción de todas las medidas necesarias para impedir la adquisición de derechos de patente sobre la denominación propuesta, durante el periodo en que la OMS la tenga en estudio.

Artículo 4 - Toda persona puede formular a la OMS observaciones sobre la denominación propuesta dentro de los cuatro meses siguientes a su publicación en *Información Farmacéutica OMS*, conforme a lo dispuesto en el artículo 3.

Artículo 5 - Toda persona interesada puede presentar una objeción formal a una denominación propuesta dentro de los cuatro meses siguientes a su publicación en *Información Farmacéutica OMS*, conforme a lo dispuesto en el artículo 3.
Esa objeción deberá acompañarse de los siguientes datos:

i) la identidad de la persona que formula la objeción;

ii) las causas que motivan su interés por la denominación; y

iii) las causas que motivan su objeción a la denominación propuesta.

Artículo 6 - Cuando se haya presentado una objeción formal en la forma prevista en el artículo 5, la OMS podrá reconsiderar el nombre propuesto o utilizar sus buenos oficios para intentar lograr que se retire la objeción. La OMS no seleccionará como denominación común internacional una denominación a la que se haya hecho una objeción formal, presentada según lo previsto en el artículo 5, que no haya sido retirada, todo ello sin perjuicio de que la Organización examine otra denominación o denominaciones sustitutivas.

Artículo 7 - Cuando no se haya formulado ninguna objeción en la forma prevista en el artículo 5, o cuando todas las objeciones presentadas hayan sido retiradas, la Secretaría notificará, conforme a lo dispuesto en el párrafo *a*) del artículo 3, que la denominación ha sido seleccionada por la OMS como denominación común internacional recomendada.

Artículo 8 - Al comunicar a los Estados Miembros una denominación común internacional, conforme a lo previsto en el artículo 7, la Secretaría:

a) solicitará que esta denominación sea reconocida como denominación común para la sustancia de que se trate; y

b) solicitará a los Estados Miembros que adopten todas las medidas necesarias para impedir la adquisición de derechos de patente sobre la denominación, y prohíban que sea registrada como marca de fábrica o como nombre comercial.

Artículo 9
a) En el caso excepcional de que, debido a su semejanza con otra denominación utilizada en las prácticas farmacéuticas y/o de prescripción, una denominación común internacional recomendada anteriormente ocasione errores de medicación, prescripción o distribución, o suponga un riesgo manifiesto de que esto ocurra, y parezca que tales errores o potenciales errores no sean fácilmente subsanables con otras medidas que no sean la posible sustitución de esa denominación común internacional recomendada anteriormente; en el caso de que una denominación común internacional recomendada anteriormente difiera considerablemente de la denominación común aprobada en un número importante de Estados Miembros, o en otras circunstancias excepcionales que justifiquen el cambio de una denominación común internacional recomendada, cualquier persona interesada puede presentar propuestas en este sentido. Esas propuestas se presentarán en los formularios que se proporcionen a estos efectos e incluirán los siguientes datos:

i) la identidad de la persona que presenta la propuesta;

ii)las causas que motivan su interés en la sustitución propuesta;

iii) las causas que motivan la propuesta; y

iv) una descripción, acompañada de pruebas documentales, de las otras medidas que se hayan adoptado con el fin de resolver la situación y de los motivos por los cuales dichas medidas no han sido suficientes.

Entre esas propuestas podrá figurar una relativa a una nueva denominación común internacional sustitutiva, formulada con arreglo a los Principios generales y que tenga en cuenta la sustancia farmacéutica para la que se proponga la nueva denominación común internacional sustitutiva.

La Secretaría enviará al Grupo de Expertos en DCI y al solicitante inicial o a su sucesor (en el caso de que sea una persona diferente de la que ha presentado la propuesta de sustitución y siempre que el solicitante inicial o su sucesor sean conocidos o puedan ser encontrados mediante esfuerzos diligentes, como el contacto con las asociaciones industriales) una copia de la propuesta, para que sea examinada de conformidad con el procedimiento descrito en el párrafo *b*) *infra*.
Además, la Secretaría solicitará observaciones sobre la propuesta:

i) a los Estados Miembros y a las comisiones nacionales y regionales de las farmacopeas u otros organismos designados por los Estados Miembros (ello se hará incluyendo una notificación a tal efecto en la carta a la que se refiere el párrafo *a*) del artículo 3), y

ii) a cualquier persona que tenga un interés especial en la sustitución propuesta.

Al solicitar que se formulen estas observaciones se facilitarán los siguientes datos:

i) la denominación común internacional recomendada que se propone sustituir (y la denominación sustitutiva propuesta, si se ha facilitado);

ii) la identidad de la persona que ha presentado la propuesta de sustitución (si lo pide esa persona);

iii) la identidad de la sustancia a la que se refiere la sustitución propuesta y las razones para presentar la propuesta de sustitución;

iv) el plazo fijado para recibir observaciones, así como el nombre y la dirección de la persona a quien deban dirigirse; y

v) los poderes conferidos para el caso a la OMS y una referencia al presente procedimiento.

Toda persona puede formular a la OMS observaciones sobre la sustitución propuesta dentro de los cuatro meses siguientes a la fecha en que se realizó la solicitud de observaciones.

b) Una vez agotado el mencionado plazo para la formulación de observaciones, la Secretaría enviará todos los comentarios recibidos al Grupo de Expertos en DCI, al solicitante inicial o a su sucesor, y a la persona que haya presentado la propuesta de sustitución. Si después de examinar la propuesta de sustitución y las observaciones recibidas, el Grupo de Expertos en DCI, la persona que haya presentado la propuesta de sustitución y el solicitante inicial, o su sucesor, están de acuerdo en la necesidad de sustituir la denominación común internacional recomendada anteriormente, la Secretaría remitirá la propuesta de sustitución al Grupo de Expertos en DCI para que la tramite.
No obstante lo anterior, el solicitante inicial o su sucesor no tendrán derecho a impedir el acuerdo sobre una propuesta de sustitución en el caso de que hayan dejado de tener un interés demostrable en la denominación común internacional cuya sustitución se propone.

En caso de que la propuesta de sustitución sea presentada al Grupo de Expertos en DCI para que la tramite, este grupo seleccionará una nueva denominación común internacional de conformidad con los Principios generales a los que se refiere el artículo 2 y al procedimiento establecido en los artículos 3 a 8 inclusive. En ese caso, en las notificaciones que la Secretaría ha de enviar con arreglo a los artículos 3 y 7, respectivamente, incluida la notificación al solicitante

inicial o a su sucesor (en el caso de que no sea la misma persona que propuso la sustitución y siempre que el solicitante inicial o su sucesor sean conocidos o puedan ser encontrados mediante esfuerzos diligentes, como el contacto con las asociaciones industriales), se indicará que la nueva denominación sustituye a una denominación común internacional recomendada anteriormente y que los Estados Miembros podrán, si lo estiman oportuno, adoptar disposiciones transitorias aplicables a los productos existentes en cuya etiqueta se utilice, con arreglo a la legislación nacional, la denominación común internacional recomendada anteriormente que se haya sustituido.

En caso de que, después de haber estudiado la propuesta de sustitución y los comentarios recibidos de conformidad con el procedimiento descrito anteriormente, el Grupo de Expertos en DCI, el solicitante inicial o su sucesor y la persona que haya presentado la propuesta de sustitución no lleguen a un acuerdo sobre la existencia de razones poderosas para sustituir una denominación común internacional recomendada anteriormente, esta denominación se mantendrá (siempre en el entendimiento de que el solicitante inicial o su sucesor no tendrán derecho a impedir el acuerdo sobre una propuesta de sustitución en el caso de que hayan dejado de tener un interés demostrable en la denominación común internacional cuya sustitución se propone). En ese caso, la Secretaría comunicará a la persona que haya propuesto la sustitución, así como al solicitante inicial o a su sucesor (en el caso de que no sea la misma persona que propuso la sustitución y siempre que el solicitante inicial o su sucesor sean conocidos o puedan ser encontrados mediante esfuerzos diligentes, como el contacto con las asociaciones industriales), a los Estados Miembros, a las comisiones nacionales y regionales de las farmacopeas o a otros organismos designados por los Estados Miembros y a cualquier otra persona que tenga interés en la sustitución propuesta, que, pese a la presentación de una propuesta de sustitución, se ha decidido mantener la denominación común internacional recomendada anteriormente (con una descripción de la o las razones por las que se ha considerado que la propuesta de sustitución no estaba respaldada por razones suficientemente poderosas).

ANEXO 2

PRINCIPIOS GENERALES DE ORIENTACIÓN PARA FORMAR DENOMINACIONES COMUNES INTERNACIONALES PARA SUSTANCIAS FARMACÉUTICAS[1]

1. Las denominaciones comunes internacionales (DCI) deberán diferenciarse tanto fonética como ortográficamente. No deberán ser incómodamente largas, ni dar lugar a confusión con denominaciones de uso común.

2. La DCI de una sustancia que pertenezca a un grupo de sustancias farmacológicamente emparentadas deberá mostrar apropiadamente este parentesco. Deberán evitarse las denominaciones que puedan tener connotaciones anatómicas, fisiológicas, patológicas o terapéuticas para el paciente.

Estos principios primarios se pondrán en práctica utilizando los siguientes principios secundarios:

3. Al idear la DCI de la primera sustancia de un nuevo grupo farmacológico, deberá tenerse en cuenta la posibilidad de poder formar DCI convenientes para las sustancias emparentadas que se agreguen al nuevo grupo.

4. Al idear DCI para ácidos, se preferirán las de una sola palabra; sus sales deberán denominarse sin modificar el nombre del ácido: p. ej. «oxacilina» y «oxacilina sódica», «ibufenaco» y «ibufenaco sódico».

[1] En su 20º informe (OMS, Serie de Informes Técnicos, Nº 581, 1975), el Comité de Expertos de la OMS en Denominaciones Comunes para las Sustancias Farmacéuticas revisó los Principios generales para formar denominaciones comunes internacionales (DCI), y su procedimiento de selección, a la luz de las novedades registradas en los últimos años en materia de compuestos farmacéuticos. El cambio más importante había consistido en hacer extensivo a la denominación de sustancias químicas sintéticas el método utilizado hasta entonces para las sustancias originadas en productos naturales o derivadas de éstos. Dicho método conlleva la utilización de una «partícula» característica que indica una propiedad común a los miembros de un grupo. En el citado informe se examinan en detalle las razones y consecuencias de este cambio.
Los Principios generales de orientación se actualizaron durante la 13ª consulta sobre denominaciones comunes para sustancias farmacéuticas (Ginebra, 27 a 29 de abril de 1983) (PHARM S/NOM 928, 13 de mayo de 1983, revisado el 18 de agosto de 1983).

5. Las DCI para las sustancias que se usan en forma de sal deberán en general aplicarse a la base activa o al ácido activo. Las denominaciones para diferentes sales o esteres de la misma sustancia activa solamente deberán diferir en el nombre del ácido o de la base inactivos.
En los compuestos de amonio cuaternario, el catión y el anión deberán denominarse adecuadamente por separado, como componentes independientes de una sustancia cuaternaria y no como sales de una amina.

6. Deberá evitarse el empleo de letras o números aislados; también es indeseable el empleo de guiones.

7. Para facilitar la traducción y la pronunciación, se emplearán de preferencia las letras «f» en lugar de «ph», «t» en lugar de «th», «e» en lugar de «ae» u «oe», e «i» en lugar de «y»; se deberá evitar el empleo de las letras «h» y «k».

8. Siempre que las denominaciones propuestas estén de acuerdo con estos principios, recibirán una consideración preferente las denominaciones propuestas por la persona que haya descubierto las sustancias, o que fabrique y comercialice por primera vez una sustancia farmacéutica, así como las denominaciones ya adoptadas oficialmente en cualquier país.

9. El parentesco entre sustancias del mismo grupo se pondrá de manifiesto en las DCI (véase el Principio 2) utilizando una partícula común. En la lista que figura a continuación se indican ejemplos de partículas para grupos de sustancias, en particular para grupos nuevos. Existen muchas otras partículas que se usan habitualmente.[1] Cuando una partícula aparece sin guión alguno, puede utilizarse en cualquier lugar de la palabra.

Latin	**Español**	
-acum	*-aco*	antiinflamatorios derivados del ibufenaco
-adolum	*-adol*)	analgésicos
-adol-	*-adol-*)	
-astum	*-ast*	antiasmáticos, sustancias antialérgicas cuya acción principal no es la antihistamínica
-astinum	*-astina*	antihistamínicos
-azepamum	*-azepam*	derivados del diazepam
bol	*bol*	esteroides anabolizantes
-cain-	*-caína-*	antiarrítmicos de clase I, derivados de procainamida y lidocaína
-cainum	*-caína-*	anestésicos locales
cef-	*cef-*	antibióticos, derivados del ácido cefalosporánico
-cillinum	*-cilina*	antibióticos derivados del ácido 6-aminopenicilánico
-conazolum	*-conazol*	antifúngicos sistémicos derivados del miconazol
cort	*cort*	corticosteroides, excepto derivados de prednisolona
-coxibum	*-coxib*	inhibidores selectivos de ciclooxigenasa
-entanum	*-entán*	antagonistas del receptor de endotelina
gab	*gab*	gabamiméticos
gado-	*gado-*	agentes para diagnóstico derivados de gadolinio
-gartranum	*-gatrán*	inhibidores de la trombina antitrombóticos
gest	*gest*	esteroides progestágenos
gli	*gli*	hipoglucemiantes,antihiperglucémicos
io-	*io-*	medios de contraste iodados
-metacinum	*-metacina*	antiinflamatorios derivados de indometacina
-mycinum	*-micina*	antibióticos producidos por cepas de *Streptomyces*
-nidazolum	*-nidazol*	antiprotozoarios derivados de metronidazol
-ololum	*-olol*	antagonistas de receptores β-adrenérgicos

[1] En el documento de trabajo WHO/EMP/RHT/TSN/2018.1, que se actualiza periódicamente y puede solicitarse al Programa sobre Denominaciones Comunes Internacionales, OMS, Ginebra, figura una lista más amplia de partículas.

-oxacinum	*-oxacino*	antibacterianos derivados del ácido nalidíxico
-platinum	*-platino*	antineoplásicos derivados del platino
-poetinum	*-poetina*	factores sanguíneos similares a la eritropoyetina
-pril(at)um	*-pril(at)*	inhibidores de la enzima conversora de laangiotensina
-profenum	*-profeno*	antiinflamatorios derivados del ibuprofeno
prost	*prost*	prostaglandinas
-relinum	*-relina*	péptidos estimulantes de la liberación de hormonas hipofisarias
-sartanum	*-sartán*	antihipertensivos (no peptídicos) antagonistas del
-vaptanum	*-vaptán*	antagonistas del receptor de vasopresina
vin-	*vin-)*	alcaloides de la vinca
-vin-	*-vin-)*	

Selected WHO publications of related interest

WHO Expert Committee on Biological Standardization. Sixty-seventh Report. WHO Technical Report Series, No. 1004, 2017

WHO Expert Committee on Drug Dependence. Thirty-ninth Report. WHO Technical Report Series, No. 1009, 2018

The Selection and Use of Essential Medicines. Report of the WHO Expert Committee, 2017 (including the 20th WHO Model List of Essential Medicines and the 6th WHO Model List of Essential Medicines for Children). WHO Technical Report Series, No. 1006, 2017

Quality assurance of pharmaceuticals 2018. WHO guidelines, good practices, related regulatory guidance and GXP training materials. (CD-ROM, USB and online)

WHO Expert Committee on Specifications for Pharmaceutical Preparations. Fifty-third Report. WHO Technical Report Series, No. 1019, 2019

International Nonproprietary Names (INN) for Pharmaceutical Substances. CD-ROM. 2017

The International Pharmacopoeia. Eighth edition 2018. CD-ROM. (CD-ROM, USB and online)

WHO Expert Committee on Biological Standardization. Guidelines on management of blood and blood components as essential medicines, 2016. Adopted by the Committee at its Sixty-seventh Meeting; published as Annex 3 to the WHO Technical Report Series, No. 1004, 2017

Council for International Organizations of Medical Sciences (CIOMS)

International Ethical Guidelines for Health-related Research Involving Humans. 2016 (e-training module about this guideline is available at https://cioms.ch/online-training/)

Drug-induced liver injury (DILI): Current status and future directions for drug development and the post-market setting. 2020

CIOMS Guide to Active Vaccine Safety Surveillance. 2017

CIOMS Guide to Vaccine Safety Communication. 2018

Evidence Synthesis and Meta-Analysis for Drug Safety. 2016

Development and Rational Use of Standardised MedDRA Queries (SMQs): Retrieving Adverse Drug Reactions with MedDRA. Second Edition. 2016

CIOMS e-publications are also available free at: https://cioms.ch/publications/

Further information on these and other World Health Organization publications can be obtained from:

WHO Press. World Health Organization
20 Avenue Appia, 1211 Geneva 27, Switzerland
http://www.who.int/bookorders
bookorders@who.int